

Karma Sonam Sherpa
Akash Kumar Bhoi
Akhtar Kalam
Manoj Kumar Mishra *Editors*

Advances in Smart Grid and Renewable Energy

Select Proceedings of ETAEERE 2020

Lecture Notes in Electrical Engineering

Volume 691

Series Editors

Leopoldo Angrisani, Department of Electrical and Information Technologies Engineering, University of Napoli Federico II, Naples, Italy

Marco Arteaga, Departament de Control y Robótica, Universidad Nacional Autónoma de México, Coyoacán, Mexico

Bijaya Ketan Panigrahi, Electrical Engineering, Indian Institute of Technology Delhi, New Delhi, Delhi, India
Samarjit Chakraborty, Fakultät für Elektrotechnik und Informationstechnik, TU München, Munich, Germany

Jiming Chen, Zhejiang University, Hangzhou, Zhejiang, China

Shanben Chen, Materials Science and Engineering, Shanghai Jiao Tong University, Shanghai, China

Tan Kay Chen, Department of Electrical and Computer Engineering, National University of Singapore, Singapore, Singapore

Rüdiger Dillmann, Humanoids and Intelligent Systems Laboratory, Karlsruhe Institute for Technology, Karlsruhe, Germany

Haibin Duan, Beijing University of Aeronautics and Astronautics, Beijing, China

Gianluigi Ferrari, Università di Parma, Parma, Italy

Manuel Ferre, Centre for Automation and Robotics CAR (UPM-CSIC), Universidad Politécnica de Madrid, Madrid, Spain

Sandra Hirche, Department of Electrical Engineering and Information Science, Technische Universität München, Munich, Germany

Faryar Jabbari, Department of Mechanical and Aerospace Engineering, University of California, Irvine, CA, USA

Limin Jia, State Key Laboratory of Rail Traffic Control and Safety, Beijing Jiaotong University, Beijing, China

Janusz Kacprzyk, Systems Research Institute, Polish Academy of Sciences, Warsaw, Poland

Alaa Khamis, German University in Egypt El Tagamoa El Khames, New Cairo City, Egypt

Torsten Kroeger, Stanford University, Stanford, CA, USA

Qilian Liang, Department of Electrical Engineering, University of Texas at Arlington, Arlington, TX, USA

Ferran Martín, Departament d'Enginyeria Electrònica, Universitat Autònoma de Barcelona, Bellaterra, Barcelona, Spain

Tan Cher Ming, College of Engineering, Nanyang Technological University, Singapore, Singapore

Wolfgang Minker, Institute of Information Technology, University of Ulm, Ulm, Germany

Pradeep Misra, Department of Electrical Engineering, Wright State University, Dayton, OH, USA

Sebastian Möller, Quality and Usability Laboratory, TU Berlin, Berlin, Germany

Subhas Mukhopadhyay, School of Engineering & Advanced Technology, Massey University, Palmerston North, Manawatu-Wanganui, New Zealand

Cun-Zheng Ning, Electrical Engineering, Arizona State University, Tempe, AZ, USA

Toyooki Nishida, Graduate School of Informatics, Kyoto University, Kyoto, Japan

Federica Pascucci, Dipartimento di Ingegneria, Università degli Studi "Roma Tre", Rome, Italy

Yong Qin, State Key Laboratory of Rail Traffic Control and Safety, Beijing Jiaotong University, Beijing, China

Gan Woon Seng, School of Electrical & Electronic Engineering, Nanyang Technological University, Singapore, Singapore

Joachim Speidel, Institute of Telecommunications, Universität Stuttgart, Stuttgart, Germany

Germano Veiga, Campus da FEUP, INESC Porto, Porto, Portugal

Haitao Wu, Academy of Opto-electronics, Chinese Academy of Sciences, Beijing, China

Junjie James Zhang, Charlotte, NC, USA

The book series *Lecture Notes in Electrical Engineering* (LNEE) publishes the latest developments in Electrical Engineering - quickly, informally and in high quality. While original research reported in proceedings and monographs has traditionally formed the core of LNEE, we also encourage authors to submit books devoted to supporting student education and professional training in the various fields and applications areas of electrical engineering. The series cover classical and emerging topics concerning:

- Communication Engineering, Information Theory and Networks
- Electronics Engineering and Microelectronics
- Signal, Image and Speech Processing
- Wireless and Mobile Communication
- Circuits and Systems
- Energy Systems, Power Electronics and Electrical Machines
- Electro-optical Engineering
- Instrumentation Engineering
- Avionics Engineering
- Control Systems
- Internet-of-Things and Cybersecurity
- Biomedical Devices, MEMS and NEMS

For general information about this book series, comments or suggestions, please contact leontina.dicecco@springer.com.

To submit a proposal or request further information, please contact the Publishing Editor in your country:

China

Jasmine Dou, Associate Editor (jasmine.dou@springer.com)

India, Japan, Rest of Asia

Swati Meherishi, Executive Editor (Swati.Meherishi@springer.com)

Southeast Asia, Australia, New Zealand

Ramesh Nath Premnath, Editor (ramesh.premnath@springernature.com)

USA, Canada:

Michael Luby, Senior Editor (michael.luby@springer.com)

All other Countries:

Leontina Di Cecco, Senior Editor (leontina.dicecco@springer.com)

**** This series is indexed by EI Compendex and Scopus databases. ****

More information about this series at <http://www.springer.com/series/7818>

Karma Sonam Sherpa · Akash Kumar Bhoi ·
Akhtar Kalam · Manoj Kumar Mishra
Editors

Advances in Smart Grid and Renewable Energy

Select Proceedings of ETAEERE 2020

 Springer

Editors

Karma Sonam Sherpa
Sikkim Manipal University
Gangtok, Sikkim, India

Akhtar Kalam
Victoria University
Melbourne, VIC, Australia

Akash Kumar Bhoi
Department of Electrical and Electronics
Engineering
Sikkim Manipal Institute of Technology
Rangpo, Sikkim, India

Manoj Kumar Mishra
School of Computer Engineering
KIIT University
Bhubaneswar, Odisha, India

ISSN 1876-1100

ISSN 1876-1119 (electronic)

Lecture Notes in Electrical Engineering

ISBN 978-981-15-7510-5

ISBN 978-981-15-7511-2 (eBook)

<https://doi.org/10.1007/978-981-15-7511-2>

© Springer Nature Singapore Pte Ltd. 2021

This work is subject to copyright. All rights are reserved by the Publisher, whether the whole or part of the material is concerned, specifically the rights of translation, reprinting, reuse of illustrations, recitation, broadcasting, reproduction on microfilms or in any other physical way, and transmission or information storage and retrieval, electronic adaptation, computer software, or by similar or dissimilar methodology now known or hereafter developed.

The use of general descriptive names, registered names, trademarks, service marks, etc. in this publication does not imply, even in the absence of a specific statement, that such names are exempt from the relevant protective laws and regulations and therefore free for general use.

The publisher, the authors and the editors are safe to assume that the advice and information in this book are believed to be true and accurate at the date of publication. Neither the publisher nor the authors or the editors give a warranty, expressed or implied, with respect to the material contained herein or for any errors or omissions that may have been made. The publisher remains neutral with regard to jurisdictional claims in published maps and institutional affiliations.

This Springer imprint is published by the registered company Springer Nature Singapore Pte Ltd. The registered company address is: 152 Beach Road, #21-01/04 Gateway East, Singapore 189721, Singapore

Committees

Chief Patron

Prof. (Dr.) Achyuta Samanta, Honourable Founder KIIT and KISS, Bhubaneswar

Patrons

Prof. (Dr.) Hrushikesh Mohanty, Vice Chancellor, KIIT Deemed to be University

Prof. (Dr.) Sasmita Samanta, Pro Vice Chancellor, KIIT Deemed to be University

Prof. (Dr.) Jyana Ranjan Mohanthy, Registrar, KIIT Deemed to be University

General Chairs

Dr. Samaresh Mishra, Director, School Of Computer Engineering, KIIT Deemed to be University

Dr. Chinmay Kumar Panigrahi, Director, School Of Electrical Engineering, KIIT Deemed to be University

Dr. Valentina Emilia Balas, Professor, Aurel Vlaicu University of Arad, Romania

Dr. Goo Soo Chae Professor, Baekseok University, South Korea

Invited Speaker

Mr. Debajyoti Dhar, Group Director, SIPG, ISRO, Ahemadabad

Dr. Amitanshu Patnaik, DTRL, DRDO, Delhi

Dr. Saroj Kumar Meher, SSIU, ISI, Bangalore

Dr. Anup Kumar Panda, NIT Rourkela
Dr. Satchidananda Dehuri, ICT, F. M. University Balasore
Dr. Swagatm Das, ECSU, ISI, Kolkata

Program Chairs

Dr. Pradeep Kumar Mallick, Associate Professor, School of Computer Engineering, KIIT DU, Odisha
Dr. Manoj Kumar Mishra, School of Computer Engineering, KIIT DU, Odisha
Dr. Ranjeeta Patel, School of Electrical Engineering, KIIT DU, Odisha

Program Co-chairs

Dr. Amiya Ranjan Panda, School of Computer Engineering, KIIT DU, Odisha
Prof. Suresh Chandra Moharana, School of Computer Engineering, KIIT DU, Odisha

Publication Chair

Dr. Akash Kumar Bhoi, SMIT, SMU, Sikkim

Internal Advisory Committee

Dr. Bhabani Sankar Prasad Mishra, Associate Dean, School of Computer Engineering, KIIT DU, Odisha
Dr. Madhabananda Das, School of Computer Engineering, KIIT DU, Odisha
Dr. G. B. Mund, School of Computer Engineering, KIIT DU, Odisha
Dr. Biswajit Sahoo, School of Computer Engineering, KIIT DU, Odisha
Dr. Suresh Chandra Satapathy, School of Computer Engineering, KIIT DU, Odisha
Dr. Prasant Kumar Patnaik, School of Computer Engineering, KIIT DU, Odisha
Dr. Alok Kumar Jagadev, School of Computer Engineering, KIIT DU, Odisha
Dr. Santosh Kumar Swain, School of Computer Engineering, KIIT DU, Odisha
Dr. Hrudaya Kumar Tripathy, School of Computer Engineering, KIIT DU, Odisha
Dr. Amulya Ratna Swain, School of Computer Engineering, KIIT DU, Odisha
Dr. Arup Avinna Acharya, School of Computer Engineering, KIIT DU, Odisha

International Advisory Committee

Dr. Atilla ELÇİ, Aksaray University, Turkey
 Dr. Bhabani Sankar Swain, KU, South Korea
 Dr. Benson Edwin Raj, Fujairah Women's College Fujairah, UAE
 Dr. Mohd. Hussain, Islamic University, Medina, Saudi Arabia
 Prof. Frede Blaabjerg, Aalborg University, Denmark
 Dr. Yu-Min Wang, National Chi Nan University, Taiwan
 Prof. Gabriele Grandi, University of Bologna, Italy
 Dr. Steve S. H. Ling, University of Technology, Sydney, Australia
 Dr. Hak-Keung Lam, King's College London, UK
 Dr. Frank H.F. Leung, Hong Kong Polytechnic University, Hong Kong
 Dr. Yiguang Liu, Sichuan University, China
 Dr. Abdul Rahaman, Debre Tabor University, Ethiopia
 Prof. Sanjeevikumar Padmanaban, Aalborg University
 Dr. Bandla Srinivasa Rao, Debre Tabor University, Ethiopia
 Prof. Pierluigi Siano, University of Salerno, Italy
 Dr. Hussain Shareef, UKM, Malaysia
 Dr. Anil Kavala, UKM, Malaysia
 Dr. Hussain Shareef, Sr. Engineer, Samsung Electronics, Seoul, South Korea
 Prof. Michael Pecht, University of Maryland, USA
 Prof. Josep M. Guerrero, Aalborg University, Denmark
 Dr. Akshay Kumar Rathore, Concordia University, Montreal, Canada

National Advisory Committee

Dr. Rajib Misra, IIT Patna, India
 Dr. Anup Kumar Panda, NIT Rourkela
 Dr. Kishore Sarawadekar, IIT-BHU, Varanasi, India
 Dr. Sachidananda Dehury, F. M. University, Odisha
 Dr. Inderpreet Kaur, Chandigarh University
 Dr. Debashish Jena, NITK, India
 Dr. N. P. Padhy, IIT Roorkee
 Dr. Sashikala Mishra, IIIT, Pune
 Dr. Subhendu Pani, OEC, Odisha
 Dr. Mihir Narayan Mohanty, ITER, SOA, University
 Dr. Sabyasachi Sen Gupta, IIT Kharagpur
 Dr. P. Sateesh Kumar, IIT Roorkee
 Dr. Swagatam Das, ISI, Kolkata
 Dr. Sourav Mallick, NIT Sikkim
 Dr. Ashok Kumar Pradhan, IIT Kharagpur
 Dr. Bhim Singh, IIT Delhi

Dr. C. Sashidhar, CE, JNTUA
 Dr. M. Sashi, NIT, Warangal
 Prof. Rajshree Srivastava, DIT University, Dehradun, India
 Dr. Kolla Bhanu Prakash, K. L. University, Andhra Pradesh
 Dr. Vikas Dubey, Bhilai Institute of Technology, Raipur (C.G.)
 Dr. Vinod Kumar Singh, S R Group of Institution, Jhansi (U.P.)
 Dr. Ratnesh Tiwari, Bhilai Institute of Technology, Raipur (C.G.)
 Prof. J.Naren, K. L. University, Vijayawada, Andhra Pradesh, India
 Dr. G.Vithya, K. L. University, Vijayawada, Andhra Pradesh, India

Reviewer Board

Dr. G. B. Mund, School of Computer Engineering, KIIT DU, Odisha
 Dr. Prasant Kumar Patnaik, School of Computer Engineering, KIIT DU, Odisha
 Dr. Amulya Ratna Swain, School of Computer Engineering, KIIT DU, Odisha
 Dr. Preetisudha Meher, NIT, Arunachal Pradesh
 Dr. Avinash Konkani, Associate Human Factors Professional (AHFP), USA
 Dr. Shruti Mishra, Department of CSE, VIT, Amaravati, Andhra Pradesh
 Dr. Sachidananda Dehury, F. M. University, Odisha
 Dr. Sandeep Kumar Satapathy, K. L. University, Andhra Pradesh
 Dr. Brojo Kishore Mishra, GIET University, Odisha
 Dr. Karma Sonam Sherpa, SMU, India
 Dr. Sashikala Mishra, IIIT, Pune
 Dr. Akhtar Kalam, VU, Australia
 Dr. Richard Blanchard, Renewable Energy, LBU, UK
 Dr. Anjan Kumar Ray, NIT Sikkim
 Dr. Richard Blanchard, Renewable Energy, LBU, UK
 Dr. Babita Panda School of Electrical Engineering, KIIT DU, Odisha
 Dr. Sriparna Roy Ghatak, School of Electrical Engineering, KIIT DU, Odisha
 Dr. Minakhi Rout, School of Computer Engineering, KIIT DU, Odisha
 Dr. Mohit Ranjan Panda, School of Computer Engineering, KIIT DU, Odisha

Conference Management Chairs

Dr. Manas Ranjan Lenka, School of Computer Engineering, KIIT DU, Odisha
 Dr. Siddharth Swarup Rautaray, School of Computer Engineering, KIIT DU, Odisha
 Dr. Minakhi Rout, School of Computer Engineering, KIIT DU, Odisha
 Dr. Subhra Devdas, School of Electrical Engineering, KIIT DU, Odisha
 Dr. Tanmoy Roy Choudhury, School of Electrical Engineering, KIIT DU, Odisha
 Prof. Subhendu Bikash Santra, School of Electrical Engineering, KIIT DU, Odisha

Registration Chairs

Dr. Satarupa Mohanty, School of Computer Engineering, KIIT DU, Odisha
Prof. Roshni Pradhan, School of Computer Engineering, KIIT DU, Odisha
Prof. Swagat Das, School of Electrical Engineering, KIIT DU, Odisha
Prof. Subodh Mohanty, School of Electrical Engineering, KIIT DU, Odisha

Finance Chairs

Dr. Bhabani Sankar Prasad Mishra, School of Computer Engineering, KIIT DU, Odisha
Dr. Amiya Ranjan Panda, School of Computer Engineering, KIIT DU, Odisha

Publicity Chairs

Dr. Jagannatha Singh, School of Computer Engineering, KIIT DU, Odisha
Prof. Abhay Kumar Sahoo, School of Computer Engineering, KIIT DU, Odisha
Prof. Anil Kumar Swain, School of Computer Engineering, KIIT DU, Odisha
Dr. Kundan Kumar, School of Electrical Engineering, KIIT DU, Odisha
Dr. Pampa Sinha, School of Electrical Engineering, KIIT DU, Odisha
Dr. Deepak Gupta, School of Electrical Engineering, KIIT DU, Odisha
Dr. Chita Ranjan Pradhan, School of Computer Engineering, KIIT DU, Odisha
Dr. Manjusha Pandey, School of Computer Engineering, KIIT DU, Odisha
Dr. Yashwant Singh Patel, IIT Patna
Dr. Rudra Narayan Das, School of Electrical Engineering, KIIT DU, Odisha
Yashwant Singh, IIT Patna, India

Preface

The 2nd International Conference on Emerging Trends and Advances in Electrical Engineering and Renewable Energy (ETAEEERE-2020) which was held at Kalinga Institute of Industrial Technology (KIIT), Deemed to be University, Bhubaneswar, Odisha , from 5 to 6 March 2020 brings together the latest research in smart grid, renewable energy and management, electronics, communication, computing, systems, control and automations. The aim of the conference was to provide a platform for researchers, engineers, academicians and industry professionals to present their recent research works and to explore future trends in various areas of engineering and management. The conference also brings together both novice and experienced scientists and developers, to explore newer scopes, collect new ideas and establish new cooperation between research groups and exchange ideas, information, techniques and applications in the field of electrical, renewable energy, electronics and computing.

The aim of this book volume, i.e. *Advances in Smart Grid and Renewable Energy*, is to introduce smart grid and renewable energy and also to make understand non-electrical engineering student to those aspects of electrical engineering that are likely to be most relevant to his or her professional career. The objective of this book series is to make aware of the recent advancement in the field of electrical and renewable energy by introducing practical case studies reports and research findings. The combined theme of *Advances in Smart Grid, Renewable Energy and Management* is that to incorporate the scientific findings and recent trends in the field of electrical, smart grid and renewable energy.

Our sincere thanks to School of Computer Engineering and School of Electrical Engineering of KIIT Deemed to be University for the combined effort for making this ETAEEERE-2020 as a successful event, and we would like to record our appreciation to the whole committee members of ETAEEERE-2020. We are also thankful to all the participants and our keynote speakers, who have presented scientific knowledge and foresight scope for different tracks.

We have received more than 450+ research articles, and thanks to our peer-reviewing team for selecting quality papers for each volume. The participants have presented their work in four main tracks, i.e. systems, control and

automations, smart grid, renewable energy and management, electronics, communication and computing and advanced computing.

We would also like to acknowledge our technical partners, i.e. Sikkim Manipal Institute of Technology, India, and Baekseok University, South Korea, for the continuous technical support throughout the journey. Sikkim Manipal Institute of Technology (SMIT) deserves a special mention, for holding the first edition of ETAEERE-2016 and proving a collaborative opportunity to host ETAEERE-2020 at KIIT University.

Dr. Pradeep Kumar Mallick
KIIT Deemed to be University, India

Dr. Akash Kumar Bhoi
Sikkim Manipal Institute of Technology
Sikkim Manipal University, India

Contents

An Overview of Various Control and Stability Techniques for Power-Sharing in Microgrids	1
Aneesh A. Chand, Kushal A. Prasad, F. R. Islam, Kabir A. Mamun, Nallapaneni Manoj Kumar, and K. Prakash	
Performance Analysis of Lead Acid Batteries with the Variation of Load Current and Temperature	15
M. Achyut Raj Tilak, Umamani Subudh, and Debani Prasad Mishra	
Effect of Loss of Load Probability Due to Power Transformer Derating Factor on Smart Grid Reliability	25
T. Bharath Kumar and M. Ramamoorthy	
DGA and AI Technique for Fault Diagnosis in Distribution Transformer	35
Satyabrata Sahoo, Kantipudi V. V. S. R. Chowdary, and Swagat Das	
Application of Improved Indirect Matrix Converter in Multipower Supply System for Driving Multiple Loads Independently	47
N. Lavanya	
Incorporation of Distributed Generation Resources for Three-Area Load Frequency Control Optimized Tilted Integral Derivative Controller	57
Sunita Pahadasingh, Chitrlekha Jena, and Chinmoy Ku. Panigrahi	
Balanced Scorecard and Its Application Through Strategic Management Perspective in Real Estate Industry	69
Sushil Kumar Pareek and Samrat Kumar Mukherjee	
Boost Converter with Generalized Quadratic Boosting Cell with Reduced Capacitor Voltage Stresses	79
Adyasha Acharya, Lipika Nanda, Tapas Roy, and Banishree Misra	

Performance Analysis of Transistor Clamped H-Bridge Multi-reference Multi-level Inverter for Standalone PV System	93
Siddheswar Kar, Ranjeeta Patel, and Sarat Kumar Mishra	
A Novel Single-Phase Switched Capacitor Multilevel Inverter with Voltage Boosting Ability for Renewable Applications	107
Musie Welday Tesfay, Tapas Roy, and Swagat Das	
Frequency Response Analysis of Power Transformers	119
Subhendu Mishra	
Coordination of Directional Over-Current Relays Serving to a 132 kV Ring-Main System—An Explanation to Undergraduate Students to Build Research Orientation	131
Srikanth Allamsetty	
A Flexible Multi-Slot Wireless Antenna Designed for Reconfigurable Frequency	145
Akanksha Lohia, V. K. Singh, and Anurag Saxena	
A Comparative Brief Study on Level-Shifted Pulse Width Modulation and Hybrid Pulse Width Modulation Switching Techniques for 7-Level CHB Single-Phase Inverter	153
Nikhil Agrawal, Shikha Goswami, Rinisha Bagaria, and Ajay Muthale	
Analysis of Conventional and Fractional-Order Controllers for Nonlinear CSTR System	167
Deep Mukherjee, Palash Kundu, and Apurba Ghosh	
Analysis and Simulation of Boost Converter Versus Tri-state Boost Converter	175
Kundan Kumar, Sudhananda Pal, and Deepak Kumar	
Application of Point on Wave Switching for Mitigation of Transients During Charging of Power Transformer in Presence of Large Capacitive Component	189
Ajay Kumar, Urmil Parikh, and Inderpreet Kaur	
Load Frequency Control of a Hybrid System by Using Fuzzy Logic Gain Scaling Technique	205
Anurekha Nayak, Debayani Mishra, and Manoj Kumar Maharana	
Automatic Bluetooth-Controlled Master-Slave Firefighting Robots	217
Debasish Bhattacharya, Aayush Rijal, Ameesha, and Israj Ali	
A New Design Method for High-Order Discrete Systems Using Polynomial Differentiation Technique	231
G. V. K. R. Sastry, G. Surya Kalyan, and R. S. R. Krishnam Naidu	

A Fast Partitioning Strategy: Its Application to Fractal Image Coding 237
 Utpal Nandi, Anudyuti Ghorai, Biswajit Laya, and Moirangthem Marjit Singh

Analysis of Received Signal Strength Based on User Position Locating by Using ML Methods 249
 L. Sathish, Y. Satya Bhuvaneswari, B. Satya Sri Devi, and Durgesh Nandan

Analysis of Quadcopter Technology as an Emergency Service 257
 Prasanthi Magapu, Sarthika Danthuluri, Vidheya Raju Boni, and Durgesh Nandan

Analysis of Reversible Square Using QCA 267
 D. V. S. Phanindra, A. Arun Kumar Gudivada, and Durgesh Nandan

Analysis of Various Multipliers in Quantum Cellular Automata 279
 K. Vineela Bhanu, A. Arun Kumar Gudivada, and Durgesh Nandan

Exploration of Circularly Polarized Microstrip Antenna for RFID, Biomedical and Satellite Applications 289
 Ch. V. S. D. R. K. Abhilash, V. Preethi, Sanjeev Kumar, and Durgesh Nandan

A Review of Energy Auditing on Academic Building by Using ANN and Fuzzy Logic 297
 Purnima Sharma, Inderpreet Kaur, and Ranjit Kumar Bindal

Fractional-Order Extremum Seeking MPPT for Photovoltaic System 303
 Padimi Sri Venkata Satish, Yellapu Manikanta Swamy, Ch Uma Phanendra Kumar, and K. Manoz Kumar Reddy

An Operator-Controlled Incentive Distribution Model for Device Relaying D2D Communication 313
 Koushik Barman and Ajay Roy

Error Correction Code: Study, Challenges, and Applications 321
 V. Vydehi, A. Lishitha, G. Pranathi, N. V. Satyanarayana, and Durgesh Nandan

Review on Different Types of Multipliers and Its Performance Comparisons 329
 Bocha Dileep Venkata Prasad, Nalla Satya Sai Sanjeev, Krishna Saladi, and Durgesh Nandan

Changes in Index Properties of Soil Using Fly Ash 341
 Praful Ranjan

A Review of Diverse Procedure for Extraction of Fetal ECG.	349
K. M. L. Narasimhulu, N. Murali, M. Girish Kumar, T. Srinivasa Rao, and Durgesh Nandan	
A Proposed Model for Customer Churn Prediction and Factor Identification Behind Customer Churn in Telecom Industry	359
Nooria Karimi, Adyasha Dash, Sidharth Swarup Rautaray, and Manjusha Pandey	
Fuzzy-Enabled Direct Torque Control for Low Torque Ripple in Induction Motors for EV Applications.	371
Pratyay Maity and A. Vijayakumari	
Analysis of UPFC Controller Connected with Multiple Wind Turbines by Using IEEE Bus System	385
Sunny Vig and Balwinder Singh Surjan	
Power Loss Reduction Strategies of IEEE-5 Bus System with Neuro-fuzzy UPFC	395
Ramakanta Jena, Ritesh Dash, and Saratchandra Swain	
Compensation of Reactive Power Using STATCOM for Wind Farm.	405
Ganesh Prasad Khuntia, Ritesh Dash, and Saratchandra Swain	
Grid Interconnection and Challenges Associated to Operation of a Decentralized Solar PV System	415
Debashish Pattnaik, Ritesh Dash, and Saratchandra Swain	
A Comprehensive Study on Load Balancing Algorithms in Cloud	423
Mohona Bandyopadhyay, Manoj Kumar Mishra, Bhabani Shankar Prasad Mishra, and Samaresh Mishra	
Implementation of an Efficient SVPWM Technique to a Cascaded Multilevel Inverter-Based SAF	437
Ashish Ranjan Dash, Ranjeeta Patel, Mrutyunjaya Mangaraj, and Anup Kumar Panda	
Synthesis of Reconfigurable Unequally Spaced Linear Arrays Through Time Modulation	447
S. Patra, S. K. Mandal, G. K. Mahanti, and N. Pathak	
Development of Microcontroller-Based Economic Real-Time Temperature Measurement System	453
G. Raja Kullyappa, C. Mani Kumar, P. Srilakshmi, and Shahid Ali	
Temperature Impact on SIC Waveguide for Investigation of Sensing	461
C. S. Mishra, K. P. Swain, M. R. Nayak, and G. Palai	

Practical Implementation of Flexible Antenna for Hiper LAN Application 467
 Janabeg Loni, Jaideep Dewangan, Vinod Kumar Singh, and Anand Kumar Tripathi

Wearable Textile Antenna for C-Band Application 475
 Zakir Ali, Abhinab Shukla, Anurag Saxena, and Vinod Kumar Singh

Mechanoluminescence Induced in Rare Earth Activated Cementitious Materials 481
 R. K. Mishra, A. K. Beliya, Vikas Dubey, and Neha Dubey

Customer Stress Prediction in Telecom Industries Using Machine Learning 491
 K. N. R. Srinivas, K. S. S. Manikanta, T. Prem Jacob, G. Nagarajan, and A. Pravin

Intelligent Traffic Management in Emergency Situations 499
 J. Rajesh, I. Naveen, A. Pravin, T. Prem Jacob, and G. Nagarajan

Dengue Prediction Using Machine Learning Techniques 509
 O. Shireesha, P. Hema Sri, T. Prem Jacob, G. Nagarajan, and A. Pravin

Twitter Data Analysis for Live Streaming by Using Flume Technology 519
 Vissamsetti Mohan Manoj, Yalamandala Prasanth, T. Prem Jacob, G. Nagarajan, and A. Pravin

Blockchain Integration in House Voting System 529
 Hemanth Chebrolu, Saikumar Buragadda, A. Viji Amutha Mary, and Jancy

Digital Art Using Machine Learning 539
 Karri Yaswanth Teja Reddy, Karnati Madhava Sai Kumar, A. Pravin, T. Prem Jacob, and G. Nagarajan

Twitter Topic Analysis Using Multi-tweet Sequential Summarization for Sentimental Data 547
 B. Melanshiya, P. Mirium Swarna, and Ramya G. Franklin

Content-Based Image Retrieval in Cloud Image Repositories 555
 Vishnu Vardhan Kathika, K. S. G. Jagadeesh Babu, A. Pravin, T. Prem Jacob, and G. Nagarajan

Feature Selection Using Multiple Kernel Learning Methods 563
 K. Siva Sandeep Reddy, K. Gunavardhan Reddy, A. Pravin, G. Nagarajan, and T. Prem Jacob

Detection of Ransomware Based on Recurrent Neural Network (RNN) 569
 Saketh Kanumuri, Vinay Teja Kantipudi, A. Viji Amutha Mary, and Mercy Paul Selvan

A Unique Adaptive Framework for Predicting Lane Changing Intention Based on CNN 577
K. Pavan, M. Dhanaveera Teja, A. Pravin, T. Prem Jacob, and G. Nagarajan

A Novel Biometric Inspired Robust Security Framework for Medical Images 585
D. Vishnu Vardhan, D. Gopeeswar, and A. Viji Amutha Mary

Agricultural Analysis Using Machine Learning Techniques 595
S. Dhanush Sai, S. Satyanand, A. Pravin, G. Nagarajan, and T. Prem Jacob

Multi-strategy Sentiment Analysis of Banking Reviews Based on Semantic Fuzziness 605
R. Rahul, K. Mohana Prasad, and J. Refonaa

Effective Gene Mapping System with Disease Prediction and Corrective Measures 615
Sathi Lakshmi Samhitha, Sanku Shrivani, and T. Sasikala

Face Recognition Based Attendance System and Emotion Classification 625
Vallu Sri Satya Kala, Vanka Bhavyasri, and S. Vigneshwari

Classification and Prediction of Text Data by Using a Natural Language Processing Algorithm 635
Kakarlapudi Lavadhan Varma, Kaipa Subhash Reddy, S. Jancy, and Mercy Paul Selvan

Automatic Optimization and Allocation of Data Using Q-Learning Technique 643
K. Pavan Kalyan, K. Gangadhar, S. Jancy, and Mercy Paul Selvan

Choosing an Ephemeris for Low Earth Orbit (LEO) Satellite Application 651
T. Omkara Chari, T. Manikanta, G. Nagarajan, T. Prem Jacob, and A. Pravin

An Integrated & Robust User Authentication Framework Based on Gait Smart Devices 659
V. Harsha Vardhan, V. Sri Dileep Kumar, G. Nagarajan, T. Prem Jacob, and A. Pravin

Predicting Bike Rental Based on Environment and Seasons 667
Nettem Gopi, Nare Thoshan Kumar Reddy, and T. Sasikala

Automatic Recognition of Medicinal Plants 675
P. Krishna Vinesha, P. Lakshmi Priyanka, and L. Lakshmanan

Number Plate Detection Using Support Vector Machine 685
 Bodla Sai, B. Rama Brahman, and T. Sasikala

A Weighted Frequent Itemsets Mining Algorithm for Intelligent Decision in Smart Systems 695
 P. Gopinath Reddy, P. Avinash, and A. Velmurugan

Activity-Based Attribute Selection for Effective Advertising Using Pattern Mining 703
 R. B. Sarooraj and S. Prayla Shyry

An Efficient Implementation of a Proposed Food Quality Ensuring Architecture Using Blockchain Technologies 715
 P. Shiva Sujan, R. Ashok, Suja Cherukullapurath Mana, B. Keerthi Samhitha, and Jithina Jose

Fake Profile Detection in Facebook 725
 S. Ranjana, Reshma Sathian, and Murari Devakannan Kamalesh

Intrusion Detection System Based on Secure Hashing Techniques 733
 Obilineni Aparna, Padma Priyanka Kuncham, and A. Christy

Leveraging Affective Hashtags for Ranking Music Recommendations 741
 M. Devi Priyanka, P. Renuka, and A. Christy

Awareness and Acceptability of Renewable Energy Products Across Demographic Factors 749
 Rachana Rai, Neeta Dhusia, and Ajeya Jha

Trusted and Preferred Sources of Receiving Information Related to Renewable Energy 765
 Rachana Rai, Neeta Dhusia, and Ajeya Jha

About the Editors

Prof. Karma Sonam Sherpa has completed his B.E. (Electrical Engineering) from the MREC, Jaipur, and M.Tech. (Power Electronics and Machine Drives) from I.I.T., Kharagpur in the year 1996 and 2003 respectively. He is a doctorate from Sikkim Manipal University. He has been serving SMIT, Sikkim for the last 19 years. Presently, Prof. Sherpa is Registrar, SMU and Ex-Associate Director (Research & Development) Ex-HOD and professor in the Department of Electrical & Electronics Engineering. His areas of research are DC Power Conversion and nonlinear dynamics, Voltage Stability and Load Management in Power Distribution Systems and Electromagnetic Levitation Systems. He is life member of ISTE, IEI and System Society of India (SSI). His areas of interests are Electric Power Distribution System, Power Electronics and Electrical Drives. Prof. K.S. Sherpa is a member of Academic Senate since and University Research Committee (2013 onwards). He has published papers in national and international journals and conferences. He has also organized several workshops, seminars and conferences.

Dr. Akash Kumar Bhoi has completed his B.Tech. (Biomedical Engineering) from Trident Academy of Technology, BPUT University, Odisha and M.Tech. (Biomedical Instrumentation) from Karunya University, Coimbatore in the year 2009 and 2011 respectively. In 2019 he is awarded Ph.D. from Sikkim Manipal University, India. He is working as Assistant Professor in the Department of Electrical and Electronics Engineering at Sikkim Manipal Institute of Technology (SMIT), India since 2012. He is member of ISEIS and IAENG, associate member of IEI, UACEE and editorial board member reviewer of Indian and international journals. His areas of research are biomedical signal processing, medical image processing, sensors and transducers, and medical instrumentation. He has published several papers in national and international journals and conferences. He has also served on numerous organizing panels for the international conferences and workshops.

Prof. Akhtar Kalam has been at Victoria University, Melbourne since 1985 and a former Deputy Dean of the Faculty of Health, Engineering and Science for 7 years. He is currently the Head of Engineering. He is also the current Chair of the Academic Board and lectures in the Masters by coursework program in the Engineering Institute of Technology, Perth, Australia. Further he has Distinguished Professorship position at the University of New South Wales, Sydney, Australia and 5 Malaysian universities. He has wide experience in educational institutions and industry across four continents. He received his B.Sc. and B.Sc. (Engineering) from Calcutta University and Aligarh Muslim University, India. He completed his MS and Ph.D. at the University of Oklahoma, USA and the University of Bath, UK, respectively. He has worked with Ingersoll Rand and other electrical manufacturers. He has held teaching appointments at the University of Technology, Baghdad, Iraq and Capricornia Institute of Advanced Education, Rockhampton, Queensland. He has conducted research, provided industrial consultancy and published over five hundred papers in his area of expertise and written over 29 books in the area. More than 35 students have graduated under his supervision. He provides consultancy for major electrical utilities, manufacturers and other industry bodies in his field of expertise. Professor Kalam is a Fellow of EA, IET, AIE, a member of IEEE and CIGRE AP B5.

Dr. Manoj Kumar Mishra has fifteen years' experience in imparting education to undergraduate and postgraduate students, and one and half years of industry experience in Mainframe Technologies. He holds a PhD in Computer Science and Engineering, MBA in Marketing and Finance, M.Tech and BE in Computer Science and Engineering. He has many research publications to his credit including papers in international conferences, journals, and book chapters and edited books. His areas of specialization include Parallel & Distributed Computing, Grid Computing, Cloud Computing, Algorithm Design, Big Data, Machine Learning. He is a life time society member of ISTE and Indian Science Congress.

An Overview of Various Control and Stability Techniques for Power-Sharing in Microgrids



Aneesh A. Chand, Kushal A. Prasad, F. R. Islam, Kabir A. Mamun, Nallapaneni Manoj Kumar, and K. Prakash

1 Introduction

Today, the conventional AC grid is based on large-scale power generation, and the major source of energy is exhaustive fuels such as diesel, coal and gas. Demand for electricity is increasing exponentially, leading to lower grid stability and reliability [1–3]. To meet the demand of power generation, new options open up in terms of renewable energy generation [4]. The effective involvement of various RERs-based generation results into many advantages like better environmental policies, lowers fossil-fuel-based generation, bidirectional power flow and utility end active participation.

The service grid finds difficulty to connect directly to distributed generators (DGs), which comprises of photovoltaic (PV) panel, wind turbine, hydro, storage devices, microturbines and fuel cells, as shown in Fig. 1; therefore, the need for the microgrid

A. A. Chand · K. A. Prasad · K. A. Mamun · K. Prakash
School of Engineering and Physics, The University of the South Pacific, Suva, Fiji
e-mail: aneeshamitesh@gmail.com

K. A. Prasad
e-mail: kushalaniketp@gmail.com

K. A. Mamun
e-mail: kabir.mamun@usp.ac.fj

K. Prakash
e-mail: krishneel.prakash@usp.ac.fj

F. R. Islam
School of Science and Engineering, University of Sunshine Coast, Maroochydore, QLD, Australia
e-mail: fislam@usc.edu.au

N. M. Kumar (✉)
School of Energy and Environment, City University of Hong Kong, Kowloon, Hong Kong
e-mail: nallapanenichow@gmail.com

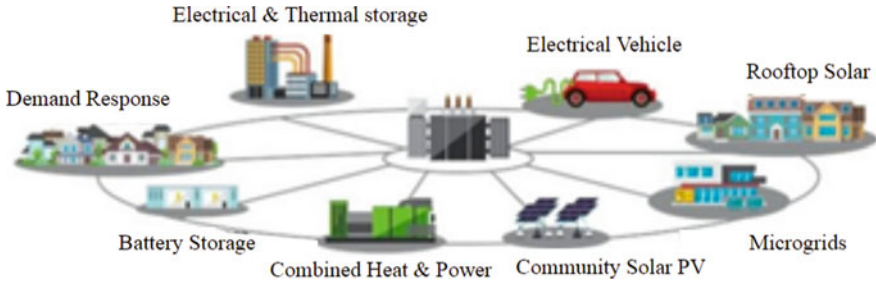


Fig. 1 Schematic representation of different DGs

arises [5]. Another most significant reason for establishing the concept of DGs is that they can respond to load demand at their place that it refers to as local generation [6, 7]. This interface consists of an energy storage, low distribution voltage consisting of DG and load units. DG units allow microgrid to play a major role as compared to classical generator. They possess a high degree of controllability and operability, thus maintaining the stability of power network [8].

The microgrid concept is essentially a dynamic system that integrates multiple DGs and uniform loads at distribution voltage level [9]. The intermittent characteristics of DGs which defy the power quality, stability, frequency and voltage manifest the requirement for new planning and operation approaches for microgrids [10]. Consequently, conventional optimization methods in new power systems have a critical concern in the operation of the microgrid.

Additionally, many literatures have also provided a large number of control strategies, as shown in Fig. 2, designed to quantify disturbance rejection, tracking of

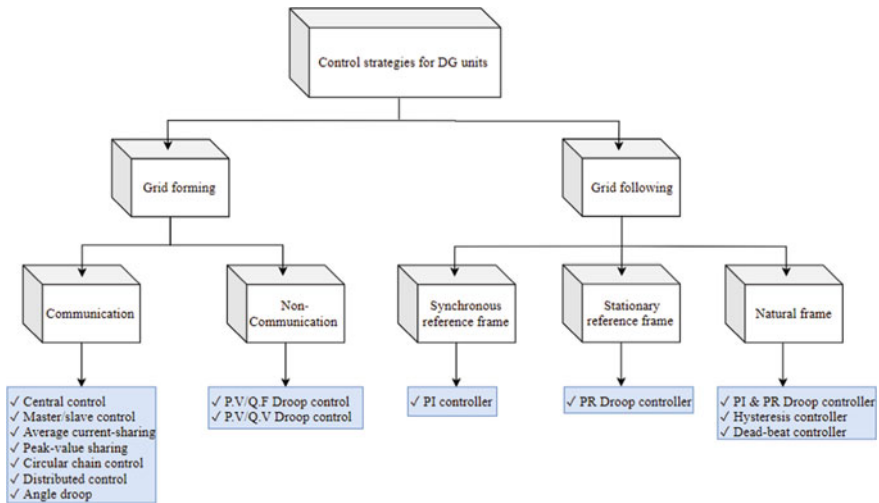


Fig. 2 Techniques of primary control [10]

inverter output (i.e., voltage and current) and power quality [10, 11]. Communication and non-communication are the two-classical control methods of load sharing in DG units: Communication control-based methods are summarized as condensed control, master and slave inverter control and dispersed control [12–15], whereas the non-communication control-based methods are classical droop control [16–19], virtual scheme-based method [20–23] and create- and reward-based method [24–26].

This paper tries to show the strategies to control the DG unit with grid forming when different control and load-sharing methods of inverters are applied to micro-grid. Section 2 gives an outline of the different communication control methods. In Sect. 3, different types of non-communication control methods are presented. Section 4 focuses on discussion prospects. Finally, Sect. 5 gives conclusion on the different methods of droop control.

2 Communication Control Methods

The primary control aims to properly regulate the voltage and share loads. Also, without using a secondary control, the amplitude of output frequency and voltage are near close to their ratings. But these control methods involve the communication link between the modules, which ultimately affect the cost of the whole system. Types of communication control methods are:

2.1 Central Limit Control (CLC)

Figure 3 shows the methods that are discussed in [12], which involves common synchronization signals and current sharing modules. A phase-locked loop (PLL) circuit is equalized between the output voltage, frequency and synchronization

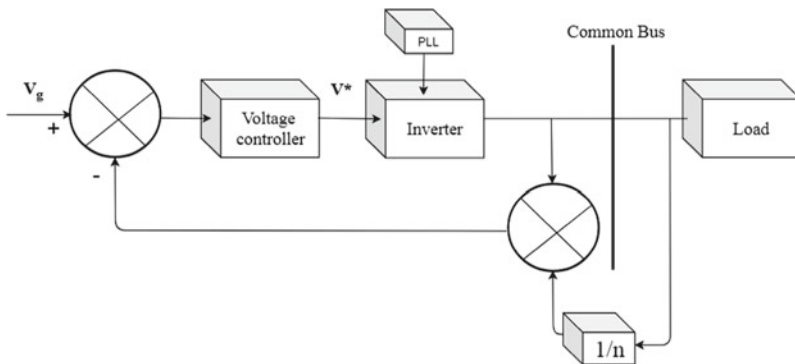


Fig. 3 Schematic for central limit control

signals. Each module also monitors the average current to achieve the same distribution.

The key benefit of such technique is that current sharing in both a steady and a transient state is continuous. Moreover, there is a centralized controller in this technique which restricts the system expansion. To achieve synchronization between the modules [12], high-bandwidth communication lines are required for the current transient through the converters; thus, this approach significantly increases reliability.

2.2 Master and Slave Inverter Control

With this kind of control method, the inverter is connected in parallel with the starting module acting as a master inverter. The master inverter is responsible for parallel control, while the other inverters act as slave inverter [10, 11]. Figure 4 depicts the schematic diagram for the master/slave scheme with a central controller. Through this control scheme, it is noticed that it has a good performance in power-sharing [12]. Once the master inverter fails, the improved control operation will switch to another inverter, becoming the new master. Therefore, parallel operation of such inverter would not get affected, but the drawback of this method is that the output current overshoot takes place during transients, and hence, transient performance is not good.

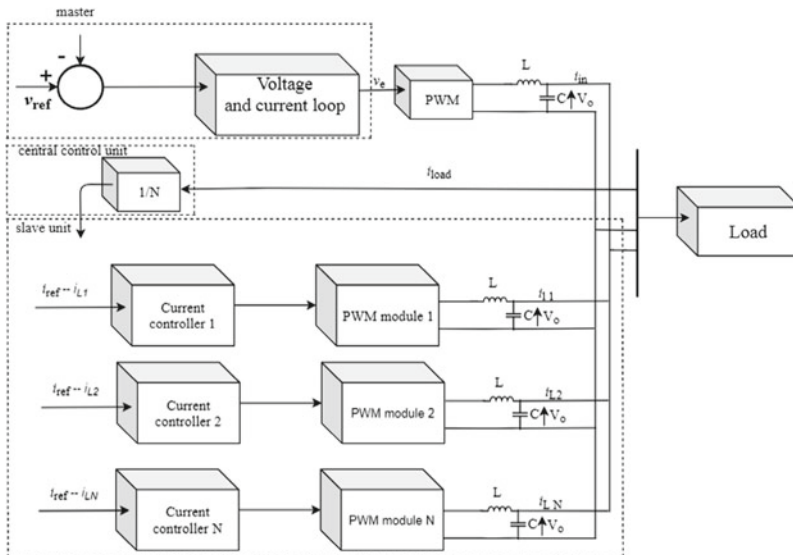


Fig. 4 Schematic diagram for master/slave scheme with central controller [13]

2.3 Average Current Sharing

Regardless of the master/slave control technique, there is no central unit in this method. Actually, this scheme requires a voltage synchronization and current sharing bus. A control signal is shared between DGs by voltage and current reference [12, 13]. In this approach, one converter is assigned to be master unit that operates in controlled voltage mode to establish the DC bus voltage, while the other converters are configured as slave converters operating in a current-controlled mode.

2.4 Peak-Value Current Sharing

For AC bus during the islanding condition, a dual-loop voltage controller with a converter is used to regulate the voltage. In this context, there is a proportional-resonant controller (PR) used for an internal and external current and voltage control loop, respectively, whereas other power converters are equipped with a current control loop in PR controller [12, 13].

2.5 Circular Chain Control

This control strategy as its name indicates is the scheme that DG interfaces are connected together in the form of circular chain. According to Arani et al. [12], all inverters form the chain and each inverter follows the inductive current of itself and the earlier inverters. In this control method, each inverter's output current and voltage are regulated by the outer voltage control loop and the inner current control loop, respectively.

2.6 Angle Droop Control

With conversational angle droop control, the active and reactive power is controlled by the amplifier and frequency of the voltage. Small angles can change the power-sharing of the microgrid between DGs [12–14]. Therefore, each inverter in the microgrid is responsible to change its angle according to its active output power. This control method can be modified for active and reactive power control in the microgrid in terms of the network characteristics. While implementing the angle droop control appears to be more difficult than standard droop control, the systems which use this technique can achieve greater stability margins.

2.7 Dispersed Control

The dispersed control is generally applied to converters connected in parallel [13–16]. In this type of control, the average current is shared. No central controller is used in each inverter, and every module is symmetric. There is also a good management of regulating and power-sharing, but there is no link between inverters. This debases the adaptability and repletion of the system. More conflicts are in this type of system since the number of parallel segments and connection line distances is increased.

3 Non-communication Control Methods

The control techniques that function with non-communications for control of electricity sharing are based on the droop concept [19, 20]. Connecting remote inverters is often essential without communication. It can avoid the heavy costs and complexity and enhance supervision, system redundancy and reliability specifications [22, 25–27]. Moreover, because the plug and play function of the modules enable one unit barred to stop the system as a whole, it is less hard to stretch such a machine. Thus, communication strains, especially for lengthy distances and excessive investment costs, are often avoided.

3.1 Classical Droop Control

The classical droop control is also known as the primary control. The fundamental concept is to reduce the frequency when active power is increased and imitate the role of a synchronous generator. If the inverter's output impedance is especially efficient and reactive, then [12]:

$$P_i = \frac{E_i V \sin \alpha}{X} \quad (1)$$

$$Q_i = \frac{E_i V \cos \alpha - V^2}{X} \quad (2)$$

where E is the converter voltage amplitude; X is the coupling impedance; α is the angle of converter voltage; P_i and Q_i are the active and reactive powers, respectively; and V is the voltage amplitude in PCC.

The P_i and Q_i are particularly dependent on the power angle and voltage amplitude, respectively. With reference to Eqs. 1 and 2, the following assumption can be drawn and the characteristic droop control for $P - \omega$ and $Q - E$ is shown in Fig. 5.

A classical droop control block diagram is presented in Fig. 6.

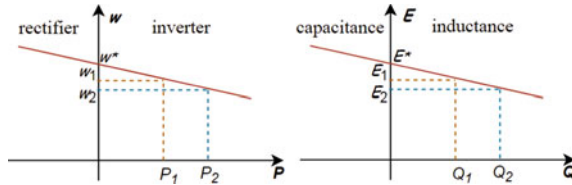


Fig. 5 Characteristic droop control for $P - \omega$ and $Q - E$ [10]

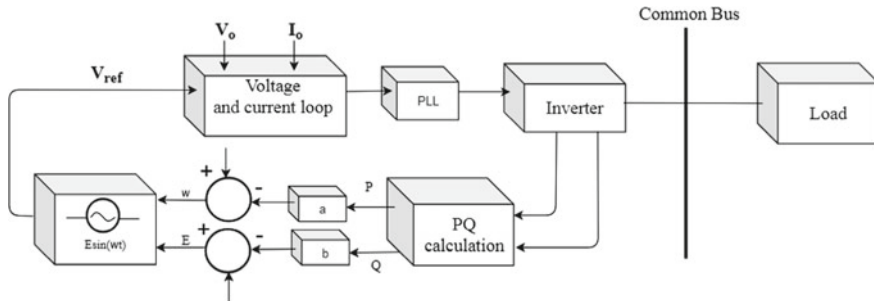


Fig. 6 Block diagram of classical droop control

As the classical droop control method is trustworthy, however, there are some disadvantages:

- Absence of multiple control targets.
- Instead of highly inductive line impedance, there should be mixed resistive and inductive line impedance as in microgrids.
- In microgrid, the voltage is overall not variable; therefore, it is hard to share reactive power within parallel inverters, and it can also produce circulating reactive current.
- This method only examines fundamental values and does not deal with voltage and current harmonics.

For minimizing above limitation, following methods are discussed in [22, 28].

- *Voltage Real Power Drooping or Frequency Reactive Power Boosting:* Droop/boost control method provides enhanced act [25–29] for controlling large resistive transmission line of AC microgrid with low voltage. But this method fully depends on the parameters of the system, which naturally decreases its utilization.
- *Droop-Based Method on Complex Line Impedance:* Issues like line impedance reliance, inaccurate P or Q law and sluggish transient response cannot be addressed or solved in classical droop method. In [29], when considering the influence of complex impedances, the controls solve the connected active and reactive power ratio, provide excellent dynamics and are more useful when the elements

of the line impedance and inductance resistance ($X \approx R$) in MV microgrids are comparable.

- *Power angle-based droop control method:* The phase angle of this distributed source voltage corresponds to the widely used system timing so that the energy requirements are shared between DGs [27]. With this method, a proper load sharing between DGs is achieved without a steady-state frequency drop. However, in the case of synchronization of native control boards, there is no defect in the processor crystal clock (digital), and the frequency differs slightly from that of every inverter and thus increases system instability.
- The droop control based on voltage is one of P/V type control methods. This strategy demonstrates band control of the AC microgrid islanded type steady energy [27]. It fully utilizes the voltage variable that is permitted. By linking the P/V droop control to Pdc, the voltage limit breach can be prevented if the continuous energy band is overflowing. However, this technique of control requires microsourses to readily dispatch power. This control technique requires a multi-stage controller that impacts the system frequency.

3.2 Virtual Scheme-Based Method

Virtual impedance line droop control is a standard droop controller that does not give the proper reactive power distribution between parallel-associated inverters under a line impedance imbalance. The difference in the reactive power-sharing of an AC microgrid thus poses an important issue. Some experiments have been conducted via a quick control loop which copies the impedance in the row in Fig. 7 [10–13] to implement the virtual impedance in the droop control strategy.

The virtual impedance of output is selected primarily for the lead impedance of the line [21]. A summing strategy in this line permits the selection of the virtual impedance, to accomplish an adjusted share of reactive power if the voltage from each inverter is lowered to the AC bus [21–24].

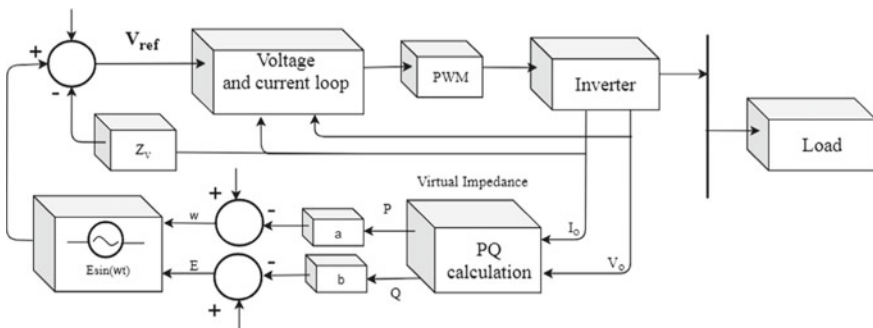


Fig. 7 Virtual impedance loop-based droop control

The estimation of virtual impedance is reduced using the summation method which reduces voltage control. Once the output voltage exceeds that of overline voltage, reactive power-sharing is improved.

3.3 Create- and Reward-Based Methods

The classical droop control includes a few issues to be understood, such as line impedance reliance, incorrect power-sharing and moderate transient reaction [25–27]. Therefore, variations in the traditional droop control have been suggested to address these issues.

Figure 8 depicts the adaptive droop control which is proposed to extensively keep up the voltage magnitude with precise reactive power-sharing [25]. With the model, the most extreme reactive power Q_{max} is drawn from every unit and contrasted with a reference amount of reactive power Q_{ref} . Once the reactive power is maximized, it is not exactly with the reference value, and then it is after the traditional Q/E drop that the voltage amplitude is applied. To obtain a desired voltage amplitude, the distinction between the output reactive power Q and the Q_{ref} is used as an added value.

With the powerful droop control technique, the classical voltage droop can be modified as:

$$\Delta E = E - E^* = nP \tag{3}$$

where ΔE is zero for grid-connected mode, while the active power in islanded mode cannot be zero, hence, leading ΔE not be zero. Another issue is noticed when a change in load occurs that makes the voltage drop. The low voltage drop can be accomplished by choosing a lower droop coefficient. For quick reaction, it is required to choose a larger value for droop consistency. Changing $E^* - V_o$ by means

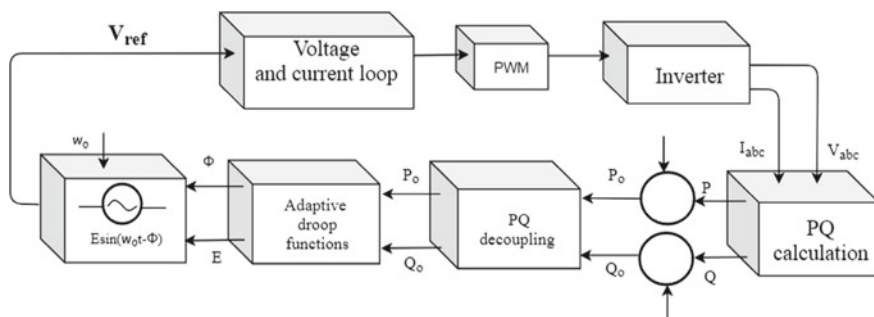


Fig. 8 Block diagram of closed-loop system with adaptive droop control

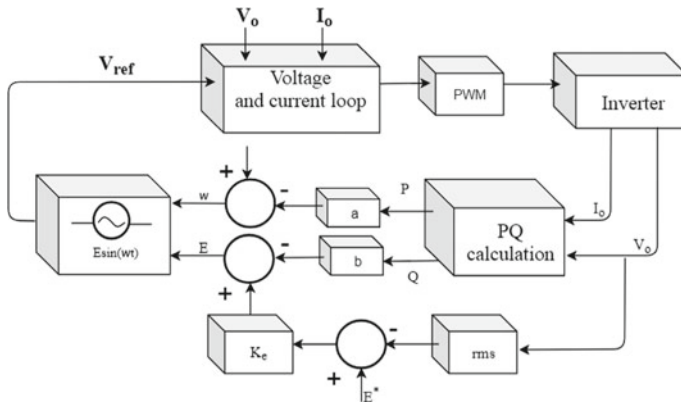


Fig. 9 Block diagram of powerful droop control

of a certain path through vital hypothesis, control regulation can achieve the voltage decrease.

This system is an expert in utilizing the enhanced droop controller exhibited in [26], and the approach is otherwise called powerful droop control. This control approach shown in Fig. 9 alters the droop condition by deducting the inverter output voltage RMS from the set point of voltage. In the perspective of the drop and load impact, this strategy remedies the voltage drop. In addition, the load tension is maintained in the rated value, but the reactivity share is poor.

4 Discussion

As discussed before, it was presumed that each of the proposed control procedure has its own particular qualities, favorable circumstances, disadvantages and applications. The droop control operation is mainly based on restricted system status estimates. These variables allocated to the DG totally and repeat themselves since they retain a strategic distance for a secure assignment from the fundamental communication interface. Conversely, there are some drawbacks in classical droop control.

Distinctive varieties, like virtual scheme-based method and create- and reward-based method, have been suggested in researches to overcome the constraints of classical droop control. To add to this, the methods based on the virtual scheme can give precise sharing of reactive power between parallel-associated DG inverters. But this control technique presents a few constraints, such as lowering the voltage regulation and increasing in no load voltage.

Create- and reward-based scheme offers brilliant voltage regulation and reactive power-sharing. But these strategies result in load harmonic sharing and poor active power. Generally, for AC microgrid the central control procedures are to give an account of the conclusive points that can resolve the given issues:

Table 1 Possible benefits and drawbacks of communication-based control

	Communication-based control		
	Concentrated control	Master/slave control	Distributed control
Benefits	Continuous power-sharing in steady and transient conditions Control frequency and regulation of voltage	Easily recuperate output voltage Continuous power-sharing in steady and transient conditions	Symmetrical for every module Continuous power-sharing with constant voltage supply
Drawbacks	Communication with high bandwidth Low expandability and reliability	During transient's stage, it has high current overshoot Communicate with high bandwidth Low redundancy	Require bus communication Degrade the system's modularity

- Stability issue
- Harmonic load sharing
- Settlement within frequency and active power-sharing
- Integration of sustainable power source assets.

However, the possible benefits and drawbacks of communication and without communication-based control methods are shown in Tables 1 and 2, respectively.

5 Conclusions

This chapter shows a comprehensive study on DG unit load-sharing control techniques. The work contains droop methods which demonstrate improved efficiency in terms of additional services like impedance of the system, harmonic energy sharing and the appropriate voltage and energy control. In view of the discussion depends upon the survey, the varieties of the droop control procedure remove the basic drawbacks of the classical droop control (i.e., impact of the impedance imbalance on active and reactive power-sharing and frequency deviation). The survey also reveals that changing a single control technique for all applications or improving one variety's deficiency in classical droop control is alarming. Nevertheless, it is well understood that various variants of the droop control method are able to solve their own limitation and improve the microgrid's overview and performance.

Table 2 Possible benefits and drawbacks of non-communication-based control

	Benefits	Drawbacks
<i>Conventional and variants on droop control</i>		
Conventional frequent droop control	Implementation can be achieved without communication More flexibility, expandability and modularity	Poor harmonic sharing with slow dynamic response Low frequency and voltage regulation Physical parameters need to be considered
VPD/FQB droop control	Good for high resistive transmission lines Communication is not required	Physical parameters need to be considered Poor frequency & voltage regulation
Complex line impedance	Decoupled active and reactive controls Better regulated voltage	Line impedances need to be considered
Angle droop control	Improved regulated frequency	Need GPS signals Low power-sharing
Droop control with constant power band	Micro-source characteristic and specification are considered Operates with MPPT and functions with certain range Energy usage is more efficiently Limits low voltage limit issue	Dispatched abilities are required for micro-source Require multi-stage controllers and impact on system effectiveness
<i>Virtual structure-based method</i>		
Virtual output impedance control	Physical parameters are not concerned Good system stability and power-sharing	Voltage regulation is not guaranteed Controller requires relatively high bandwidth
Enhanced virtual impedance control	Able to manage both linear and nonlinear loads in power-sharing Mitigates the PCC harmonic voltage	Communicate with low-bandwidth Physical parameters need to be considered
Virtual frame transformation method	Decoupled active and reactive power controls	Difficult to achieve same angle of transformation for all DGs, physical parameters need to be considered
<i>Constructed and compensated-based method</i>		
Adaptive voltage droop control	Good voltage regulation Better power-sharing and system stability under heavy load condition	Physical parameters need to be considered

(continued)

Table 2 (continued)

	Benefits	Drawbacks
Synchronized reactive power compensation	Good power-sharing performances No need to consider the physical parameters	Low synchronized communication bandwidth
Droop control-based synchronized operations	Good power-sharing performances No need to consider the physical parameters Robust to communication delay	Low synchronized communication bandwidth
$Q - V$ dot control method	Like conventional droop control	It requires initial conditions Limits the steady-state solutions Quick destabilization
Common variable-based control method	Constant reactive power-sharing No need to consider the physical parameters	Difficult to get constant voltage due to long distance
Signal injection method	Can handle both linear and nonlinear loads No need to consider the physical parameters	Contains harmonic distortion in voltage

References

1. D. Aitchison, M. Cirrincione, G. Cirrincione, A. Mohammadi and M. Pucci, Feasibility study and design of a flywheel energy system in a microgrid for small village in Pacific Island State countries, in *Smart Energy Grid Design for Island Countries*, Springer, Cham (2017), pp. 159–187
2. A.A. Chand, K.A. Prasad, K.A. Mamun, K.R. Sharma, K.K. Chand, Adoption of grid-tie solar system at residential scale. *Clean Technol.* **2**(1), 71–78 (2019)
3. S.S. Chand, A. Iqbal, M. Cirrincione, F.R. Islam, K.A. Mamun, A. Kumar, Identifying energy trends in Fiji Islands, in *Smart Energy Grid Design for Island Countries*. Springer, Cham (2017), pp. 259–287
4. K. Prakash, F.R. Islam, K.A. Mamun, A. Lallu, M. Cirrincione, Reliability of power distribution networks with renewable energy sources, in *2017 4th Asia-Pacific World Congress on Computer Science and Engineering (APWC on CSE)*. IEEE (2017), pp 187–192
5. H. Shayeghi, E. Shahryari, M. Moradzadeh, P. Siano, A survey on microgrid energy management considering flexible energy sources. *Energies* **12**(11), 2156 (2019)
6. K. Prakash, F.R. Islam, K.A. Mamun, S. Ali, Optimal generators placement techniques in distribution networks: a review, in *2017 Australasian Universities Power Engineering Conference (AUPEC)*. IEEE (2017), pp. 1–6
7. C. Sun, Z. Mi, H. Ren, Z. Jing, J. Lu, D. Watts, Multi-dimensional indexes for the sustainability evaluation of an active distribution network. *Energies* **12**(3), 369 (2019)
8. F.R. Islam, K. Al Mamun, M.T.O. Amanullah (eds.) *Smart Energy Grid Design for Island Countries: Challenges and Opportunities*. Springer, Berlin (2017)
9. F.R. Islam, K. Prakash, K.A. Mamun, A. Lallu, H.R. Pota, Aromatic network: a novel structure for power distribution system. *IEEE Access* **5**, 25236–25257 (2017)

10. M. Hossain, H. Pota, W. Issa, Overview of AC microgrid controls with inverter-interfaced generations. *Energies* **10**(9), 1300 (2017)
11. H. Han, X. Hou, J. Yang, J. Wu, M. Su, J.M. Guerrero, Review of power sharing control strategies for islanding operation of AC microgrids. *IEEE Trans. Smart Grid* **7**(1), 200–215 (2015)
12. A.A.K. Arani, G.B. Gharehpetian, M. Abedi, Decentralised primary and secondary control strategies for islanded microgrids considering energy storage systems characteristics. *IET Gener. Transm. Distrib.* **13**(14), 2986–2992 (2019)
13. T.L. Vandoorn, J.D.M. De Kooning, B. Meersman, L. Vandeveldel, Review of primary control strategies for islanded microgrids with power-electronic interfaces. *Renew. Sustain. Energy Rev.* **19**, 613–628 (2013)
14. C. Sun, G. Joos, F. Bouffard, Adaptive coordination for power and SoC limiting control of energy storage in Islanded AC microgrid with impact load. *IEEE Trans. Power Deliv.* (2019)
15. T. Caldognetto, P. Tenti, Microgrids operation based on master–slave cooperative control. *IEEE J. Emerg. Sel. Top. Power Electron.* **2**(4), 1081–1088 (2014)
16. S.W. Lee, B.H. Cho, Master–slave based hierarchical control for a small power DC-distributed microgrid system with a storage device. *Energies* **9**(11), 880 (2016)
17. M.A. Mahmud, M.J. Hossain, H.R. Pota, A.M.T. Oo, Robust nonlinear distributed controller design for active and reactive power sharing in islanded microgrids. *IEEE Trans. Energy Convers.* **29**(4), 893–903 (2014)
18. J.M. Guerrero, J.C. Vasquez, J. Matas, M. Castilla, L.G. de Vicuna, Control strategy for flexible microgrid based on parallel line-interactive UPS systems. *IEEE Trans. Industr. Electron.* **56**(3), 726–736 (2008)
19. J. Hu, J. Zhu, D.G. Dorrell, J.M. Guerrero, Virtual flux droop method—a new control strategy of inverters in microgrids. *IEEE Trans. Power Electron.* **29**(9), 4704–4711 (2013)
20. M. Ashabani, A.R.M. Yasser, M. Mirsalim, M. Aghashabani, Multivariable droop control of synchronous current converters in weak grids/microgrids with decoupled dq-axes currents. *IEEE Trans. Smart Grid* **6**(4), 1610–1620 (2015)
21. J. He, Y.W. Li, Analysis, design, and implementation of virtual impedance for power electronics interfaced distributed generation. *IEEE Trans. Ind. Appl.* **47**(6), 2525–2538 (2011)
22. J.M. Guerrero, J.C. Vasquez, J. Matas, L.G. De Vicuña, M. Castilla, Hierarchical control of droop-controlled AC and DC microgrids—a general approach toward standardization. *IEEE Trans. Industr. Electron.* **58**(1), 158–172 (2010)
23. J.M. Guerrero, M. Chandorkar, T.L. Lee, P.C. Loh, Advanced control architectures for intelligent microgrids—Part I: Decentralized and hierarchical control. *IEEE Trans. Industr. Electron.* **60**(4), 1254–1262 (2012)
24. J.M. Guerrero, P.C. Loh, T.L. Lee, M. Chandorkar, Advanced control architectures for intelligent microgrids—Part II: Power quality, energy storage, and AC/DC microgrids. *IEEE Trans. Industr. Electron.* **60**(4), 1263–1270 (2012)
25. J.C. Vasquez, J.M. Guerrero, A. Luna, P. Rodríguez, R. Teodorescu, Adaptive droop control applied to voltage-source inverters operating in grid-connected and islanded modes. *IEEE Trans. Industr. Electron.* **56**(10), 4088–4096 (2009)
26. Q.C. Zhong, Robust droop controller for accurate proportional load sharing among inverters operated in parallel. *IEEE Trans. Industr. Electron.* **60**(4), 1281–1290 (2011)
27. Z. Shuai, M.O. Shanglin, W.A.N.G. Jun, Z.J. Shen, T. Wei, F. Yan, Droop control method for load share and voltage regulation in high-voltage microgrids. *J. Mod. Power Syst. Clean Energy* **4**(1), 76–86 (2016)
28. Y.W. Li, C.N. Kao, An accurate power control strategy for power-electronics-interfaced distributed generation units operating in a low-voltage multibus microgrid. *IEEE Trans. Power Electron.* **24**(12), 2977–2988 (2009)
29. R. Majumder, B. Chaudhuri, A. Ghosh, R. Majumder, G.F. Ledwich, Improvement of stability and load sharing in an autonomous microgrid using supplementary droop control loop. *IEEE Trans. Power Syst.* 1–13 (2009)

Performance Analysis of Lead Acid Batteries with the Variation of Load Current and Temperature



M. Achyut Raj Tilak, Umamani Subudh, and Debani Prasad Mishra

1 Introduction

It is ordinarily believed that sustainable power source will assume a significant job for future power age. Be that as it may, the inquiry is the reason we consider it as a future power age source together with ordinary vitality sources. The vitality request is expanding with the development of populace. We accept that this awesome development of vitality can't be met with conventional vitality framework alone without unequivocally expanding weight on sustainable power source. Thus, in this circumstance, battery is considered as conspicuous stockpiling gadget. Again, as to unwavering quality and cost of independent or matrix associated PV (photovoltaic) control frameworks, stockpiling battery speaks to principle, significant and costliest segment. So, battery is a vital segment in regard of generally speaking PV framework execution and financial investigation for the framework.

2 Battery

There are various sorts of battery-powered battery which can be utilized as capacity gadget of independent sun-oriented PV frameworks like Lead corrosive, Li-particle, Ni–Cd, Ni–Mh battery and so forth [1]. Among them Lead corrosive battery is the

M. A. R. Tilak · U. Subudh · D. P. Mishra (✉)
Electrical and Electronics Engineering, IIIT Bhubaneswar, Bhubaneswar, India
e-mail: debani@iiit-bh.ac.in

M. A. R. Tilak
e-mail: b316010@iiit-bh.ac.in

U. Subudh
e-mail: umamani@iiit-bh.ac.in

innovation of decision for most of the PV frameworks. Although there are execution confinements which brings about unnecessary substitution costs, work-place word related wellbeing and security issues and operational support issues. As lead corrosive batteries are generally utilized in various nations including Bangladesh, so in this paper execution of battery under various load conditions and variable temperature has been read for lead corrosive batteries.

3 Parameters Affecting Performance of Battery

As battery is a significant segment, we should think about its proficiency and the parameters which are answerable for corrupting the presentation of this stockpiling gadget. The corruption of battery limit for the most part relies upon territories under charging/releasing stages, DOD (Depth of Discharge) of the battery, introduction to the drawn out times of low release and normal temperature of the battery over its lifetime. Among these, two significant parameters to be specific charging current and burden current and temperature are talked about here.

3.1 Effects of Charging Current and Load Current

The charging or releasing flows influence the battery limit. On the off chance that the release current is high, at that point the measure of vitality that can be separated is decreased and the battery limit is low. This happens as the important parts required for the response to happen need more time to achieve their status for synthetic responses. Again if release current is low, more vitality can be separated from the battery and the battery limit is higher. So profundity of release and evaluated battery limit is firmly influenced by the charging and burden current rate.

In the event that we amass in Fig. 1, we can see that if release rate is high, span of release of battery is low and the other way around. Again it is likewise valid in

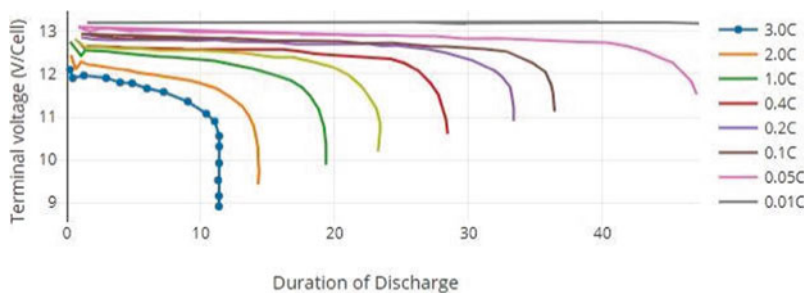


Fig. 1 Terminal voltage versus duration of discharge

the point of view of terminal voltage, at high release rate, terminal voltage lessens rapidly.

3.2 Effects of Temperature

The standard rating for battery is considered at room temperature of 25 °C. The battery temperature ought to be amended by applying a temperature remuneration coefficient if working temperature is other than 25 °C (Table 1).

Temperature and battery limit keep up an opposite relationship. At the point when temperature goes down limit of the battery diminished. What’s more, the limit increments with increment in temperature. The beneath diagram speak to how the lead corrosive battery limit fluctuate over years with working temperature. Here we can see, at having fever of 35 °C the battery will convey more than its appraised limit yet their life is moderately short where at 15 °C, lifetime increments with buildup in limit (Fig. 2).

In this way, high temperature will build limit, abbreviate life, increment interior release rate with the expansion of charging current. Then again, by bringing down temperature, limit will diminish yet life of the battery will increment. Limit at lower temperature diminishes the accessible battery limit by 0.5% per F [2].

Table 1 Coefficients of temperature compensation

Temperature (°C)	-20	-10	0	10	20	25	30	40
Coefficient of compensation for 7200 min discharge	0.58	0.72	0.83	0.91	0.98	1	1.02	1.05

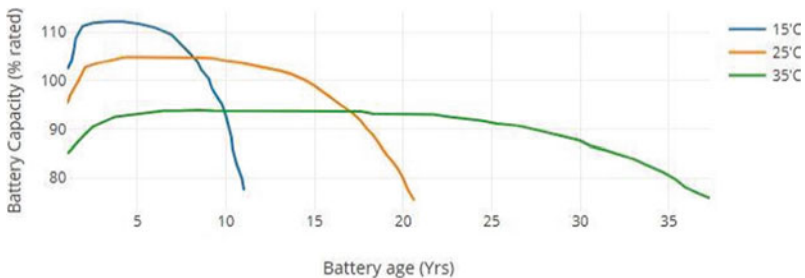


Fig. 2 Battery capacity versus battery age

4 Battery Equivalent Model

As we previously referenced, battery is the key part for sustainable power source frameworks. What’s more, there are various parameters which break down battery limit and its lifetime. Presently to see this parameter well, we need to test the battery. Be that as it may, testing a battery takes a few hours and great number of testing parts like reasonable battery charger, stopwatch, voltmeter, ammeter and so on [3]. To decrease this long testing time and measure of physical testing segments, electrical battery identical circuit model is important and battery execution can be reenacted through reproduction programming. So with the end goal of limit assurance and ideal part choice, displaying and recreations of battery framework are created to anticipate the battery execution. There are number of battery identical scientific models accessible for reproduction purposes like Thevenin battery model, Coppetti model, third request model, fourth request model and so forth portrayed in Refs. [4, 5].

In this investigation, we utilized a model which depicted in Ref. [6], which is built utilizing the Sims cape model library Lead AcidBattery_lib. In this model, proposed condition contains a few parameters that must be distinguished. This recognizable proof can be disentangled by thinking about a portion of the parameters as constants. In Ref. [7] this parameters and conditions are characterized. It has been demonstrated that this model was equipped for giving precise reenactment results at a quick recreation speed.

4.1 Battery Model Structure

The battery model was intended to acknowledge contributions as present and surrounding temperature individually. Also, the yield is voltage, SOC and electrolyte temperature.

A battery model is demonstrated as follows (Fig. 3).

It contains three significant squares which is appeared in Fig. 4.

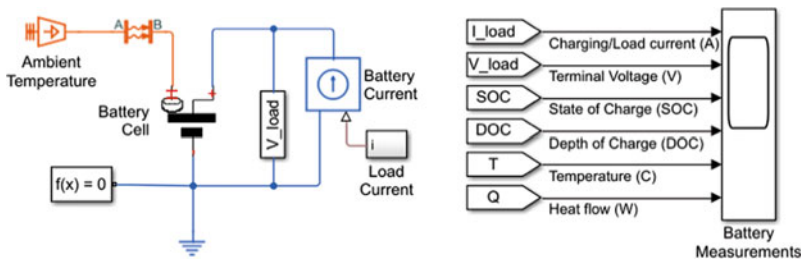


Fig. 3 Block diagram of battery model

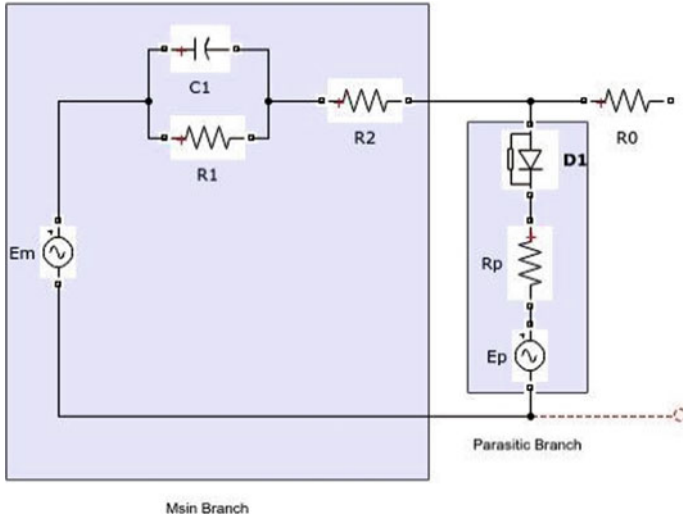


Fig. 4 Circuit for equivalent battery representation

1. **Thermal model**

Warm model square speaks to encompassing and battery electrolyte temperature. It is accepted that cooling is principally through regular convection and the warming is essentially conformed to the battery due to charging and releasing periods of the battery.

2. **An equivalent circuit model**

This structure comprised of two fundamental parts: a primary branch which approximated the battery elements under most condition and a parasitic branch which represented the battery conduct toward the finish of the charge. This battery equal circuit speak to one cell of the battery.

Every proportionate circuit depended on nonlinear conditions as found in Ref. [7]. Various parameters and states are incorporated into these non-straight conditions and the parameters rely upon observationally decided constants.

3. **Block model for simulation of Charge and capacity of battery**

This square tracks the battery’s ability, condition of charge (SOC), profundity of charge (DOC) and so on.

The battery is mimicked to see the impact of corrosive battery by differing current and temperature utilizing this battery model.

5 Battery Simulation

To evaluate battery limit is a test due to variable parameters of battery. To guarantee whether a battery is completely energized or completely released is hard to survey. So these challenges ought to be mulled over during the laboratory testing process.

The model as talked about in the past area speaks to the model of a cell of a battery. So on the off chance that we need to mimic a 12 V battery, we should associate 6 bits of 2 V battery cell hinders in arrangement. The underlying estimation of SOC and DOC are taken as 20% and the last worth is considered as 80% to rearrange the battery demonstrating in charging and releasing states. As we previously referenced, to watch the impact of charging/load current and temperature variety we utilized MATLAB Simscape model [8, 9].

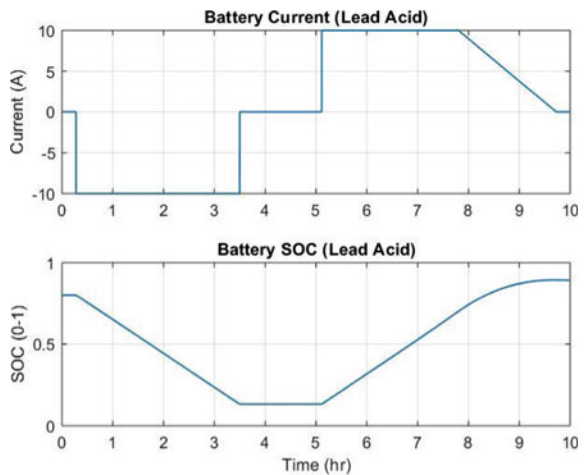
5.1 Variation of Charging and Discharging Current

In this investigation, we reenact a lead corrosive battery determined as ostensible voltage of 12 V, ostensible limit of 20 Ah, and charging and releasing rate C/10. So our charging and releasing current is 2 A. Here, battery was first released under 2 A steady burden and afterward charged under 2 A consistent current to carry the battery to the underlying condition of charge. This is demonstrated Fig. 5.

Corresponding to the charge cycle, the terminal voltage, SOC, DOC and Temperature are shown in Fig. 6.

These figures uncover that the cell terminal voltage at the main period of release process is equivalent to 2.15 V (along these lines, for a 12 V battery, terminal voltage will be 12.9 V). SOC and DOC both are equivalent to 80%. At the point when we place a heap, SOC and DOC begin to diminish until the cell voltage is 2.11 V and the estimations of SOC and DOC boiled down to 67% and 65% separately. At that point the battery is charged again until the cell voltage is equivalent to 2.18 V (For a 12 V battery, it is 13.1 V) and both SOC and DOC were 80%, a slight increment in the estimations of SOC and DOC. On account of electrolyte temperature, we considered the room temperature of 25 °C as appeared in Fig. 6.

Fig. 5 Cycle of charging



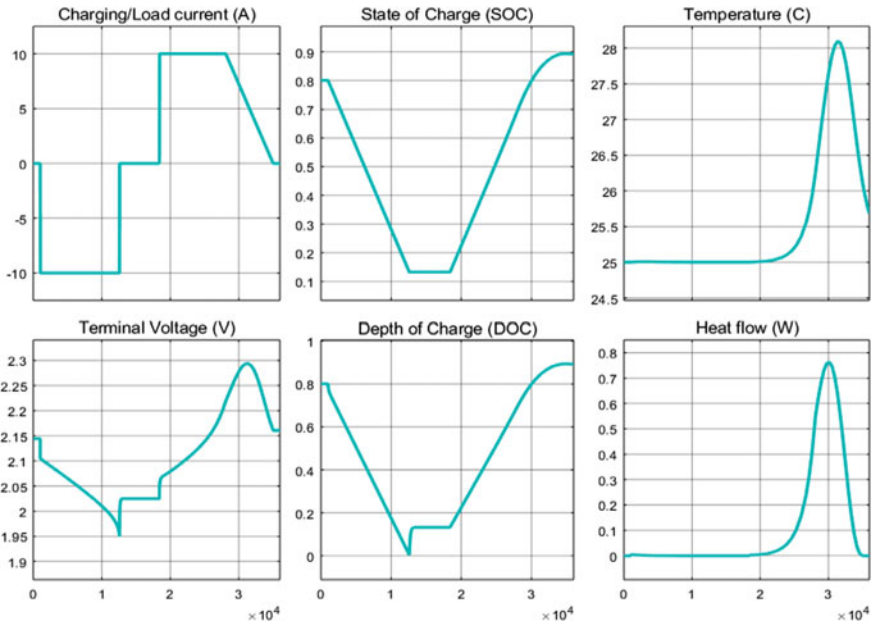


Fig. 6. Recreation results of lead corrosive battery 20 AH battery

5.2 Variation of Temperature

From the outset we increment the encompassing temperature 25–40°C. For this temperature extend, following changes happened in SOC and DOC For this situation additionally, introductory estimation of Terminal voltage, SOC and DOC stayed same. At the point when we set a heap, SOC and DOC began to diminish however this time the estimation of SOC and DOC is 76% and 75% separately while at 25C it was 67% and 65% individually. So increment in temperature builds the limit. Again the estimation of SOC and DOC is additionally expanded subsequent to reviving the battery. While at 25 °C, the estimation of SOC and DOC were 82%, here the worth expanded to about 86% (Fig. 7).

Presently in the event that we decline the temperature from 25 to 0 °C, for this situation when we set a heap the estimation of SOC and DOC is diminished, as for temperature at 40 °C. For this condition, the estimation of SOC was 46% and the estimation of DOC is just 43%. So we can see that this worth is a lot of lower than the underlying estimations of SOC and DOC at 25 °C. So decline in temperature diminishes the limit which can be seen through Fig. 8.

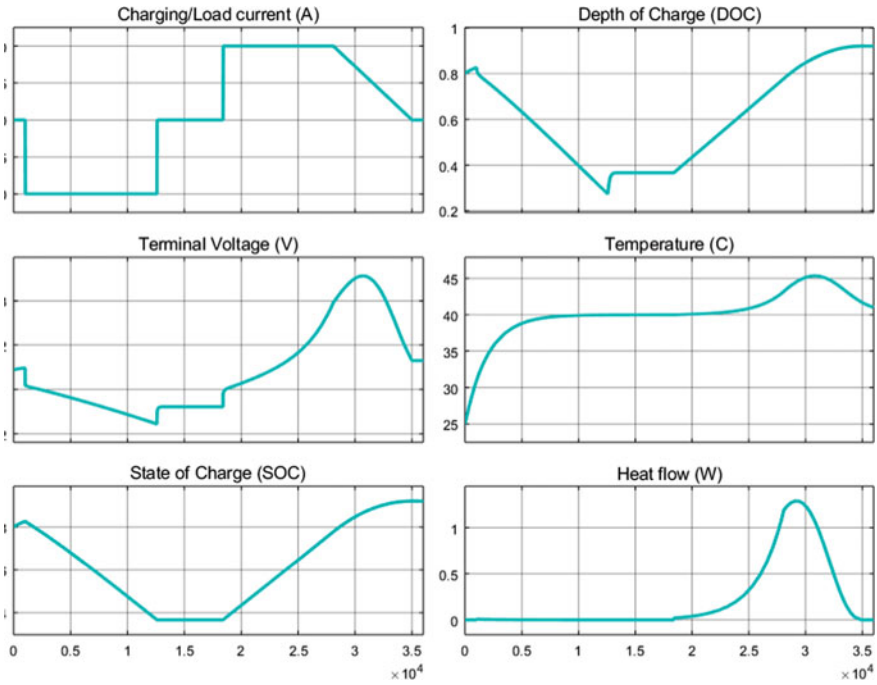


Fig. 7 Simulation results for variety of temperature from 25 to 40 °C

6 Conclusions

Lead corrosive battery is being utilized worldwide in independent or nano/scaled down matrix sun-oriented PV frameworks. Whatever the PV framework is little or enormous, battery is one of the key variables to understand an effective framework. So the parameters which influence the battery execution have been contemplated in this paper. So the battery execution was basically considered with the variety of encompassing temperature and burden current. During release cycle of the battery, terminal voltage, SOC, DOC parameters decrease significantly. Additionally variety of temperature above and beneath 250 °C has been contemplated through the reproduction programming. Increment of temperature above 250 °C shows increase for both SOC and DOC while the terminal voltage of the battery nearly continued as before. Bringing down temperature underneath 250 °C, both SOC and DOC diminished with no considerable change in terminal voltage. So we presented the Simscape instances of lead corrosive battery and utilized this guide to mimic the lead corrosive battery in context of burden current and temperature. Also, the recreation with this battery model is totally continuous reproduction. So with this recreation strategy, one can anticipate significant variety in the parameters of a battery without under going into tedious battery tests.

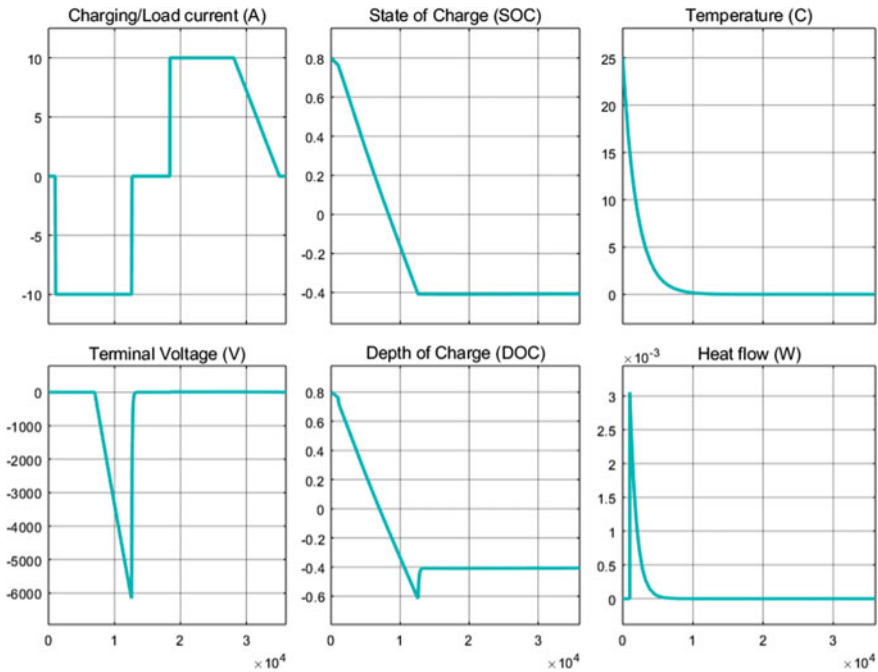


Fig. 8 Simulation results for diminishing temperature from 25 to 0 °C

References

1. E.J. Lorencetti, J.A. Heerdt, Modularized bidirectional step-up DC-DC converter with predictive battery equalization method, in *Power @ Electronics Conference (COBEP) 2017 Brazilian*, pp. 1–6 (2017)
2. V. Omelianov, M.F. Abdel-Fattah, Energy storage systems integration with household: a case study of average Ontario household using lead acid battery. *Smart Grid (SASG) 2017 Saudi Arabia*, pp. 1–6 (2017)
3. *Battery basics* (2009). Available: https://www.gearseds.com/files/determining_battery_capacity3.pdf
4. Q. Bajracharya, *Dynamic Modelling, Monitoring and Control of Energy Storage System*. Karlstad University (2013)
5. W. Peng, *Accurate Circuit Model for Predicting the Performance of Lead Acid AGM Batteries* (University of Nevada, Las Vegas, 2011)
6. O.S.W. Al-Quasem, *Modeling and Simulation of Lead Acid Storage Batteries within Photovoltaic Power System* (An-Najah National University, Nablus, 2012)
7. Jackey, R., A simple, effective lead-acid battery modeling process for electrical system component selection. *SAE World Congress & Exhibition*, Apr 2007, ref. 2007-01-0778
8. S. Chakraborty, D.P. Mishra, Modeling and simulation of multi-junction TANDEM solar cell, in *2nd International Conference on Intelligent Sustainable Systems*, Feb 2019. SCAD Institute of Technology, India (2019), pp. 141–146
9. D.P. Mishra, S. Chakraborty, Application of soft computing in solar power tracking, in *IEEE International Conference on Technologies for Smart-city Energy Security and Power*, Mar 2018

Effect of Loss of Load Probability Due to Power Transformer Derating Factor on Smart Grid Reliability



T. Bharath Kumar and M. Ramamoorthy

1 Introduction

One of the most essential electrical transmission and distribution systems equipment, the transformer. The power transformer's capital investment is large in transmission and distribution substations, relative to the other elements. Periodic maintenance and continuous monitoring are essential to boost rating of power transformers. Transformer failures result in large financial loss, additional maintenance expenses and major interruptions [1, 2]. A massive power loss will arise in the related transmission and delivery systems because of the failure of the transformer. The assessment of the operational life of the transformers is therefore a famous subject of attention [1–14]. The frequent source of transformer failure is overloading and can happen in numerous forms, like continuous, irregular, due to several reasons, including scheduled or emergency contingencies [3]. The breakdown of the transformer could also be due to longer overloading, thus it is necessary to foresee the available capacity of the transformer to regulate the load. Over time, different authors have presented the derailment of the transformer on the source of harmonics in the load current, unbalanced conditions for long duration of time and overburdening load conditions [4–6]. Njafi et al. [6] have proposed, a derating factor based on the effect of unbalanced voltages and load currents on the current rating of each phase. Several models and standards for transformer operating conditions including overloading factors, operating temperatures, etc. have been published over the years [7–17]. In the year 2010, Jawad Faiz et al. have illustrated the issues with top oil temperature measurement and suggested modifications for the existing IEEE model for temperature rise as the same does not adequately represent the changing nature of temperature. However, they did

T. Bharath Kumar (✉) · M. Ramamoorthy
Department of Industrial and Management Engineering, Indian Institute of Technology Kanpur,
Kanpur, India
e-mail: tbharath@iitk.ac.in

not take up the computation of derating factor or reliability assessment. It should be noted that IEEE standards include even the effect of altitude on tank temperature. Hence, it can be seen that tank temperature is indeed influenced by various climatic and geographical parameters and different approaches have been suggested to model the same [5].

The value of the transformer is significantly impacted by the variability in the temperature of the tank, which depends on the load, atmospheric temperature, wind speed and the allowable maximum oil temperature [7–14]. The heat losses (I^2R losses) are caused by the load which is related the oil temperature. I^2R losses are more prevalent and are liable for oil temperature relative to other losses that rely on the voltage connected and frequency which are reasonably constant. Most of the I^2R losses in a given transformer rely on the respective connected load [15–17]. Rating of the transformer is calculated by the permitted oil temperature of the tank and is limited to 80 °C to avoid chemical dissociation of oil (IS 2026). Thus, the change among the top oil high temperature (80 °C) and thermal reading of the tank determines the allowable amount of I^2R losses that, in turn gives rise toward the allowable rating of the given transformer [17]. The discrepancy in temperature ΔT (=80-Tank temperature) determines the allowable amount of the connected load.

$$\Delta T = M(I^2R) \quad (1)$$

where M relies on oil thermal resistance. Both M and R (Winding Resistance) are believed as stable during the operation.

Therefore

$$I = \sqrt{\frac{\Delta T}{MR}} \quad (2)$$

$$\text{i.e, Transformer Rating} = (V \times I)\alpha\sqrt{\Delta T} \quad (3)$$

Wind is an important atmospheric factor that directly affects the transformer tank temperature. However, wind speed is not considered by anyone in estimating the tank temperature or derating factors thus far. Several wind speed estimation models and their wide spread usage in reliability assessment of power generation have been reported in many research articles. Again, these wind speed estimation models have not been used for transformer derating or probability assessment. Since transformer tank temperature is dependent on atmospheric temperature and wind speed, it is desirable that proper models have to be used for estimating these parameters and then use them for further analysis such as reliability assessment.

Keeping in mind the above said aspects, simplistic models for forecasting wind speed and temperature have been proposed. By adopting the proposed methodology, the wind velocity in the transformer location, atmospheric temperatures are projected for next day to determine the temperature of the tank and to estimate the new reduced

rating of the transformer. Subsequently, reliability analysis is carried out by evaluating LOLE. This method is simple compared to methods proposed in [3–6] and is based on forecasted temperature of the atmospheric and wind velocity.

The recommended approach in this paper focuses on finding the expected value of new rating factor of the given power transformer based on calculated value of tank temperature, from the forecasted values of atmospheric temperature and the behaviour of the wind velocity. Therefore, forecast of these two attributes for the future is based on the recorded data of the past one typical week. Once the derating factor is known, the LOLE is computed from time to time. The connected load variation is assumed to have a normal distribution and using its cumulative probability curve the loss of expected load is evaluated using the predicted transformer available capacity. The following section describes the procedure adopted. Section 2 explains about Data Collection and Modelling and Sect. 3 deals with the evaluation of derating factor based on the temperature of the tank. Assessment of loss of load probability is discussed in Sect. 4. Sections 5 and 6 deal with results and conclusion.

2 Data Collection and Modeling

Hourly atmospheric data over one week is collected and then values of wind velocity in the location of transformer, thermal reading of the tank and atmospheric temperature in the same location for the following week have been forecasted based on the recommended models. In fact, the temperature of the tank is high in comparison to the atmospheric temperature. The theory is that whenever the temperature in the transformer location and the wind velocity are measured to be high, discrepancy in atmosphere and the temperature of the tank is smaller. Therefore, the atmospheric temperature recorded to be high and wind speed is small, then deviation among the atmosphere and the temperature of the tank is high. It specifies that a relationship within wind speed, temperature of the tank and the atmospheric temperature. Wind speed in location has a major influence on the temperature of the tank, depending on the weather conditions. The temperature of the tank is believed to be uniform over its surface.

To forecast the specific day wind speed with available source of the historical data, the wind speed per hour (Q_n) on any n th day is computed by making use of the average wind speed (Q_o) meant for the specific hour of the subsequent week and corresponding standard deviation (σ) with constant (B_n) as indicated by [17].

$$Q_n = Q_o + \sigma B_n \quad (4)$$

Thus, an average wind speed of one week is used to test the essence of wind speed and constant B_n in Eq. (4) in lieu of certain hour of n^{th} day has presumed as second order polynomial. The hourly details of weather data analysed in this paper is shown in Table 1.

Table 1 Weather and transformer data

Day	Wind velocity (km/h)	Atmospheric temperature (°C)	Tank temperature (°C)	A_n for wind speed	A_n for atmospheric temperature
Mon	13.5	43.2	55.0	-5.019	-3.002
Tue	15.0	45.3	52.4	-1.254	-0.550
Wed	16.5	46.1	48.2	2.509	0.383
Thus	16.0	43.9	49.5	1.254	-2.183
Fri	14.7	47.9	53.6	-2.007	2.483
Sat	16.5	44.0	47.8	-2.509	-2.066
Sun	16.3	50.0	51.2	2.007	4.933

$$B_n = r_0 + r_1Y + r_2Y^2 \quad (5)$$

where Y indicates day number and r_0, r_1, r_2 are the related constants for each day.

The forecast of wind speed in the transformer location and atmospheric temperature at the same location on the 8th day for a given hour, the data for the last one week on wind speed, tank temperature and atmospheric temperature for a given hour are acquired from the 220 kV substation. The expected 8th day derating factor for the substation power transformer is computed from the available data. Wind velocity is estimated on the 8th day using Eq. (4) by the known A_8 . The average wind speed from the historical data, standard deviation is estimated with weekly wind speed data for hour under consideration and using Eq. (4), the constants B_1 to B_7 for the specific hour in a week are evaluated and by using Eq. (5) constants r_0, r_1, r_2 are computed through error minimising while calculating B_n . Through such data, the transformer locational 8th day wind speed per hour is calculated by means of the earlier premeditated coefficients r_0, r_1, r_2 . The weekly average locational wind speed and its standard deviation are expected to be the same for the 8th day of the given hour.

Forecast methods for wind speed and atmospheric temperature by Eqs. (4) and (5) are the same and the forecasted values are verified by the data composed by MOSDAC, India. The thermal reading of the tank as well as the atmospheric temperature of historical data and the corresponding constants in Eq. (4) are calculated and shown in Table 1. Hourly measurements of wind speed plus surrounding temperature are made in the vicinity of the power transformer location. Wind speed in the analysis and locational atmospheric temperature are assumed as independent and uncorrelated, and the temperature of the tank depends on these two parameters. As indicated in the following Eq. (6).

$$T_t = (C_1Q) + (C_2T_A) + C_0 \quad (6)$$

where

T_t = Temperature of the tank.

Q = Wind Speed.

T_a = atmospheric temperature.

The available historical data of the coefficients (C_1, C_2, C_0) are computed to minimise the error among the measured, computed values of the given transformer tank temperature. Therefore, forecasted data of wind speed, atmospheric temperature of 8th day are estimated by using the constants C_1, C_2, C_0 . As the temperature of the tank depends on the speed of the wind and the atmospheric temperature, which vary from time to time. Also, observed that forecast of the temperature of the tank from historical records is not accurate compared to the above mentioned method. The proposed method to measure thermal reading of the tank for the 8th day is followed.

The values of C_1, C_2, C_0 are computed from the historical data are $-2.5983, 0.1037$ and 86.2418 . The forecasted wind speed, atmospheric temperature of the 8th day are 15.64 km/h, 47.12 °C. Using Eq. (6), the tank temperature of the power transformer on 8th day is computed to 50.483581 °C.

3 Transformer Derating Factor

The 8th day tank temperature per each hour is estimated on the basis of the last week and power transformer rating consider in this analysis is regularly influenced by losses. Most of the heat losses in the operational power transformer are attributed to copper windings and the residual losses are greatly less than I^2R losses [9]. A number of factors, such as atmospheric temperature, oil temperature, and wind speed, affect the temperature of the tank. The top oil temperature of the transformer must be held at 80 °C to prevent dissociation of the oil under all circumstances. In this article, only I^2R losses are considered to influence the thermal readings alteration amongst the oil and tank and thus the rating formula for the power transformer has been provided by Eq. (7). The new derating factor formula is derived from the fore mentioned analysis. The proposed derating factor along with the accessible MVA rating for the power transformer are formulated in Eq. (7).

$$\begin{aligned}
 F &= \sqrt{\frac{\text{top oil temperature} - \text{tank temperature}}{\text{nominal top oil temperature} - \text{nominal tank temperature}}} \\
 &= \sqrt{\frac{\Delta T}{\Delta T_{\text{nominal}}}} = \frac{I_{\text{permissible}}}{I_{\text{nominal}}} = \frac{\text{New rating}}{\text{Nominal Rating}} \\
 R_{\text{new}} &= F \times R_{\text{Nominal}} \tag{7}
 \end{aligned}$$

where, $R_{\text{new}}, R_{\text{Nominal}}$ are new rating and nominal rating of the power transformer and thermal readings of the oil and transformer tank are 80 °C, 45 °C respectively. For the operation of the recommended solution, a 100 MVA power transformer operating

Table 2 New derating factor for each day

Day No.	Tank temperature (°C)	Derating factor (K)	New rating of the transformer (MVA)
1	58.00	0.91932	91.932
2	52.40	0.88010	88.010
3	48.20	0.95319	95.319
4	49.50	0.93350	93.350
5	53.60	0.86849	86.849
6	47.80	0.95916	95.916
7	48.50	0.94866	94.866

on average load of 80 MW 0.8 power factor is used to estimate the derating factor. The derating factor and new rating of the power transformer are shown in Table 2.

4 Probabilistic Reliability Assessment

As mentioned earlier, the transformer rating is changed due to the variation in tank temperature and hence the nominal load may not be met. From the proposed methodology, the new rating of the transformer is calculated. In general, the load is not constant and has probabilistic variation with a specified average and standard deviation. With the new derating factor, the loss of load expected (LOLE) is computed as explained below. The loads are assumed to follow the normal distribution. The probability density function of the normal distribution shall be determined by the

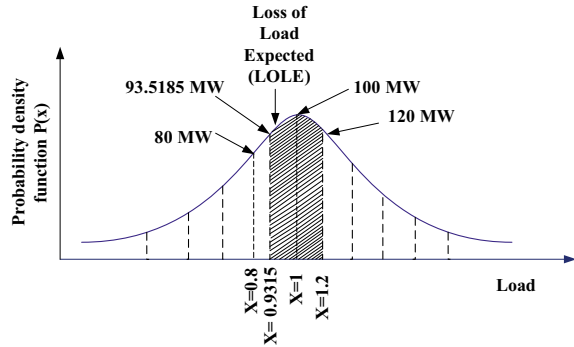
$$P(x) = \frac{1}{\sqrt{2\pi\sigma^2}} e^{-\frac{(x-\mu)^2}{2\sigma^2}} \quad (8)$$

where μ , σ are the average mean and standard deviation.

The load is assumed to take average value of 100 MVA and the standard deviation of 0.1 in lieu of the specified hour. It is expected that forecasted derating factor of the given power transformer for 8th day by means of the forecasted averages of wind speed and the atmospheric temperature remains same. With the expected value of derating factor of transformer for the 8th day and the load variation in MVA with its average value of 100 MVA with a standard normal distribution of 0.1, probability of loss of load is computed as follows. With the derated transformer rating of 91.83 MVA, any load above this value cannot be met.

According to the theory of probability, the load can vary between $(X - 2\sigma)$ to $(X + 2\sigma)$ with a confidence limit of 95%. So the load will vary between 80 and 120 MVA. In some cases, the derating of the transformer is less than the lower limit of the load, then load above the derating of the transformer give LOLE. In the probability density curve of Fig. 1, the probability of load being less than 0.9183 is given by P_1 equal to the area under the curve up to $X = 0.9183$.

Fig. 1 LOLE probability calculation



$$P_1 = \int_0^{0.9183} P(x)dx \quad (9)$$

Similarly, the area under the curve up to 120 MVA which is the maximum load is P_2 given by

$$P_2 = \int_0^{1.2} P(x)dx \quad (10)$$

The difference $P_2 - P_1$ is the loss of load probability (LOLE) due to change in tank temperature and this is shown by the shaded area in Fig. 1. The loss of load probability (LOLE) for this case is 0.32199. The LOLE without considering the limits of load variation is given in the following equation.

$$\text{LOLE} = 1 - \int_0^{0.9183} P(x)dx \quad (11)$$

The effect of variation in σ the standard deviation of load on the LOLE is shown in Fig. 2 and observed that it is exponentially decaying with variation in standard deviation.

5 Results and Discussion

In this article, a novel derating factor to the power transformer is derived based on the forecasted thermal readings of the transformer tank. Figure 1 demonstrates the variations of the given power transformer rating due to tank temperature. The probability of loss of load expected (LOLE) is chosen as reliability indices and is

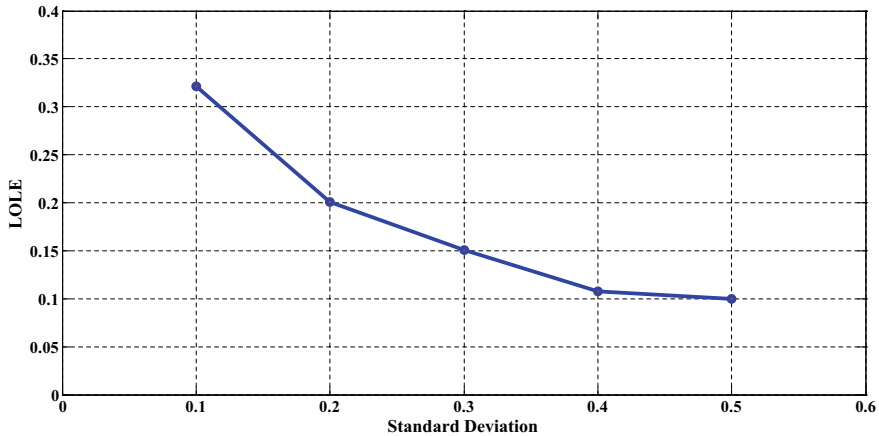


Fig. 2 Variation of additional LOLE probability with standard deviation

evaluated in this paper. The wind velocity, atmospheric temperature and tank temperature are predicted based on hourly data of past one week. Thereafter the calculation of derating factor of the power transformer is explained. The LOLE probability is also evaluated by assuming that loads follow a normal probability distribution. The variation of LOLE with standard deviation was investigated. The proposed analysis is very beneficial to take decisions by the power system operator to maintain reliability. In case of smart grids, the LOLE due the derating of the transformer effects the local power demand. The experience of the proposed transformer derating factor helpful in planning of alternative source of generation to meet the demand. The presented methodology is also increases the penetration of the distributed generators in the local smart grid region.

6 Conclusion

This paper proposes an evaluation of the derating factor for power transformer due to variation of temperature and the consequent probability of LOLE. The power transformer rating variations due to the temperature are investigated. A simple method of prediction of tank temperature is illustrated and proposed predictive models are validated with the actual recorded atmospheric data. Based on predicted values, the derating factor for the power transformer and loss of load probability are calculated assuming normal probability distribution for the connected load.

Acknowledgements The authors sincerely thank and acknowledge the contribution of MOSDOC (Meteorological & Oceanographic Satellite Data Archival Centre), India by supplying essential data required to analyses the proposed methodologies.

References

1. A. Metwally, Failures, monitoring and new trends of power transformers. *IEEE Potentials* **30**, 36–43 (2011). <https://doi.org/10.1109/MPOT.2011.940233>
2. Guide for Loading Mineral—Oil—Immersed Transformer, IEEE Std. C57.91–1995 IEEE (1995). <https://doi.org/10.1109/IEEESTD.1996.79665>
3. J. Faiz, B.M. Ebrahimi, M. Ghofrani, Mixed derating of distribution transformer under unbalanced supply voltage and nonlinear load. *IEEE Trans. Power Deliv.* **25**, 780–789. <https://doi.org/10.1109/TPWRD.2009.2032837>
4. T. Shun, X. Xiangning, Comparing transformer derating computed using the harmonic loss factor FHL and K-factor, in *3rd International Conference on Electric Utility Deregulation and Restructuring and Power Technologies 2008*, pp. 1631–1634. <https://doi.org/10.1109/DRPT.2008.4523666>
5. M. Bagheri, S. Nezhivenko, I. Soltanbayev, A. Subramaniam, S.K. Panda, Hotel lighting load influence on marine cast-resin distribution transformer aging rate, in *Proceedings of the 2017 IEEE 11th International Symposium on Diagnostics for Electrical Machines, Power Electronics and Drives, SDEMPED (2017)*, pp. 493–497
6. A. Njafi, I. Iskender and N. Genc, Evaluating and derating of three-phase distribution transformer under unbalanced voltage and unbalanced load using finite element method, in *IEEE 8th International Power Engineering and Optimization Conference (PEOCO2014) (2014)*, pp. 160–165. <https://doi.org/10.1109/PEOCO.2014.6814418>
7. M. Bagheri, A. Subramaniam, S. Bhandari, S. Chandar, S.K. Panda, Residential lighting influence on cast-resin distribution transformer aging rate, in *2015 IEEE International Conference on Building Energy Efficiency and Sustainable Technologies, ICBEST (2015)*, pp. 45–49
8. A. Fakhrian, B. Ganji, H.R. Mohammadi, H. Samet, De-rating of transformers under non-sinusoidal loads: modeling and analysis, in *Proceedings - 2019 IEEE International Conference on Environment and Electrical Engineering and 2019 IEEE Industrial and Commercial Power Systems Europe, IEEEIC/ and CPS Europe (2019)*
9. L. Kevin, R. Jacek, O. Frank, P. Ullas, P. Max, New IGBT power module concept for wind power application in NPC topology with extended reliability, PCIM, in *International Exhibition and Conference for Power Electronics, Intelligent Motion, Renewable Energy and Energy Management; Proceedings of 2015*
10. M.A. Taher, S. Kamel, Z.M. Ali, K-factor and transformer losses calculations under harmonics, in *2016 18th International Middle-East Power Systems Conference, MEPCON 2016—Proceedings (2017)*, pp. 753–758
11. J.W. Stahlhut, G.T. Heydt, N.J. Selover, A Preliminary assessment of the impact of ambient temperature rise on distribution transformer loss of life. *IEEE Trans. Power Deliv.* **23**, 2000–2007 (2008). <https://doi.org/10.1109/TPWRD.2008.2002848>
12. H. Bludzuweit, J.A. Dominguez-Navarro, A. Llombart, Statistical analysis of wind power forecast Error. *IEEE Trans. Power Syst.* **23**, 983–991 (2008). <https://doi.org/10.1109/TPWRS.2008.922526>
13. J.C. Smith, M.R. Milligan, E.A. DeMeo, B. Parsons, Utility wind integration and operating impact state of the art. *IEEE Trans. Power Syst.* **22**, 900–908 (2007). <https://doi.org/10.1109/TPWRS.2007.901598>
14. T. Bharath Kumar, O. Chandra Sekhar, M. Ramamoorthy, Reliability modelling of power system components through electrical circuit approach. *J. Electr. Eng.* **16**(3), 232–239 (2016)
15. T. Bharath Kumar, O. Chandra Sekhar, M. Ramamoorthy, Evaluation of loss of load expected in an integrated energy system. *J. Electr. Eng.* **16**(4), 75–80 (2016)
16. T. Bharath Kumar, O. Chandra Sekhar, M. Ramamoorthy, S.V.N.L. Lalitha, Evaluation of power capacity availability at load bus in a composite power system. *IEEE J. Emerg. Sel. Top. Power Electron.* **4**(4), 1324–1331 (2016)
17. T. Bharath Kumar, O. Chandra Sekhar, M. Ramamoorthy, S. Koteswara Rao, D. Venkata Bhaskar Rao, Comparative study on wind forecasting models for day ahead power markets, in *IEEE SPICES 2017*, Aug 2017. <https://doi.org/10.1109/SPICES.2017.8091273>

DGA and AI Technique for Fault Diagnosis in Distribution Transformer



Satyabrata Sahoo, Kantipudi V. V. S. R. Chowdary, and Swagat Das

1 Introduction

For reliable operation and uninterrupted power supply, regular condition monitoring of the power transformer is necessary. Sudden failure of the power transformer causes severe economic loss in terms of cost of transformer and disruption in power supply. If the condition of the transformer is estimated earlier, then it can be replaced to decreased load condition instead of sudden failure [1]. Dissolve gas analysis has now become the traditional method for transformer fault diagnosis. The dissolved gas analysis gives the concentration of different gases present and, therefore, types fault can be predicted based on the concentration of gas. For the fault prediction from the DGA output, various methods are available, such as key gas method, IEC three ratio methods, ANN, and fuzzy logic. But due the variability of DGA data according to the rating and operational condition of transformer, it is not an easy task for the traditional methods to identify the faults. Some faults are unpredictable by IEC ratio method and ANN suffers from the problem of over fitting. But since the fault prediction of transformer is a classification task, then special classification tool such as SVM is used for this purpose was originally designed for binary classification. We arranged each binary classification in a decision tree manner for our overall fault diagnosis of transformer [2]. Its classification accuracy does not depend on the number of features of the input data. SVM gives better result than ANN and

S. Sahoo (✉) · K. V. V. S. R. Chowdary · S. Das
Kalinga Institute of Industrial Technology University, Bhubaneswar, Odisha, India
e-mail: satyabrata180@gmail.com

K. V. V. S. R. Chowdary
e-mail: ramaraochowdary123@gmail.com

S. Das
e-mail: Swagat.dasfel@kiit.ac.in

IEC methods due to its better generalization ability and structural risk minimization principle [3].

2 Support Vector Machine

Support vector machines (SVMs) is a machine learning method introduced by Vapnik in 1995 which is mostly used for pattern recognition problems. SVM performs pattern recognition by using support vectors which is a decision surface between two classes determined by some training data samples [4]. SVM works on the principle of structural risk minimization while the traditional pattern recognition methods are based on empirical risk minimization. In empirical risk minimization, the performance of the training data set is optimized while in structural risk minimization, the probability of misclassification is minimized [5]. SVM works on the principle of maximum margin of separation between two classes of data. As shown in Fig. 1. Consider a training data set $\{X_I, y_I\}_{i=1}^N$ where X_I is the input data for the i th sample and y_I is the target output data. $X_I \in R^n$ And $y_I \in \{-1, +1\}$. The decision surface equation that does the separation in the form of hyper plane is given by

$$W^T X + b = 0.$$

where ‘ w ’ is a variable weight vector, ‘ x ’ is the input vector, and ‘ b ’ is the bias. For the maximum margin between the two classes of data, the weight vector ‘ w ’ should be minimum which forms the quadratic programming problem as, $\frac{1}{2}|w|^2$.

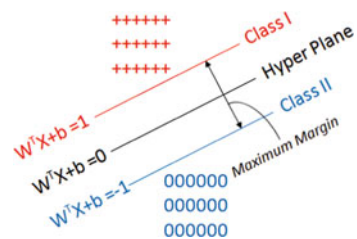
$$\text{Subjected to } y_I(w^T x_i + b) \geq 1$$

For linearly non-separable case, the slack variable ϵ_i is introduced and quadratic programming problem becomes,

$$\text{Minimization } \frac{1}{2}|w|^2 + C \sum_{i=1}^N \epsilon_i$$

$$\text{Subjected to } y_I(w^T x_i + b) \geq 1 - \epsilon_i, \quad i = 1, 2 \dots N$$

Fig. 1 Svm classification by optimal hyper plane



where ‘ C ’ is called regularization parameter and it keeps the balance between the number of non-separable points and the complexity of the machine.

Using Lagrange multiplier α_i , the constrained optimization problem becomes, Maximization

$$Q(\alpha) = \sum_{i=1}^N \alpha_i - \frac{1}{2} \sum_{i=1}^N \sum_{j=1}^N \alpha_i \alpha_j y_i y_j (x_i^T \cdot x_j) \quad [6]$$

$$\text{Subject to (1) } \sum_{i=1}^N \alpha_i y_i = 0$$

$$(2) \quad 0 \leq \alpha_i \leq c$$

$$\text{for } i = 1, 2, \dots, N$$

The optimal value of weight vector ‘ w ’ is given by,

$$w_0 = \sum_{i=1}^N \alpha_0 y_i x_i$$

The decision-boundary function given by,

$$f(x) = \text{sign} \sum y_i \alpha_i k(x_i x_j) + b$$

The various types of kernel functions that can be used for SVM classification are

$$\text{Linear kernel } k(x_i, x_j) = (x_i^T \cdot x_j)$$

$$\text{RBF kernel } k(x_i, x_j) = \exp(-\gamma \|x_i - x_j\|^2)$$

$$\text{Polynomial kernel } k(x_i, x_j) = (x_i^T x_j + 1)^P$$

$$\text{Gaussian kernel } k(x_i, x_j) = \exp\left(-\frac{1}{2\sigma^2} \|x_i - x_j\|^2\right)$$

3 Fault Classification Process

Faults in transformers can be identified according to the gases generated due to the heating of oil in dissolved gas analysis and the gases that are predominant at various temperatures are hydrogen (H_2), methane (CH_4), ethylene (C_2H_4), ethane (C_2H_6), acetylene (C_2H_2), carbon monoxide (CO), and carbon dioxide (CO_2), but we are considering five gases such as hydrogen, methane, ethylene, ethane, and acetylene

for our fault classification [7]. The Key gas method detects five states of transformer such as partial discharge and corona, electric arcing, thermal fault at low temperature, over heating of oil and sparking, normal condition which are to be determined from the concentration of these five characteristic gases.

4 Algorithm

Step-1: Concentration of the five characteristic gases is given as input to the svm1.it will detect fault and normal condition. SVM1 needs highest accuracy than others since it is at the top level of the binary tree classification [8].

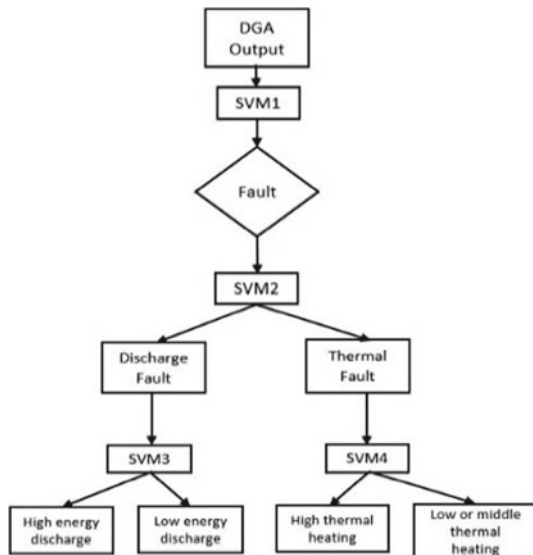
Step-2 After a data has been detected as fault condition, then, it is given as input to SVM2 which will detect whether it is a heating fault or discharge fault.

Step-3 If the data is classified as discharge fault, then it is given as input to SVM3 which will detect whether it is a high energy electric arc fault or low energy partial discharge and corona fault.

Step-4 If the data is classified as heating fault, then it is given as input to SVM4 which will detect whether it is a overheating and sparking fault or thermal heating low temperature.

All the above description and the binary tree structure for fault classification are represented in Fig. 2.

Fig. 2 Binary decision tree for SVM classification



5 Result and Discussion

90 oil testing samples are taken from research laboratory of NIT Hamirpur and from different research papers. SVM is trained with 60 samples and tested with 30 samples. This experiment was done by using classification learner app in MATLAB R2016a. After training the data, the accuracy of the different types of SVM is verified. Configuration matrix of that SVM is selected which gives the maximum accuracy and imported for the predictions of new testing data. The predictions for new data is done by using function 'yfit = trained Classifier.predictFcn(T)'. First, SVM is trained and tested to classify between the fault condition and normal condition. It is trained with 30 numbers of samples with fault condition and 30 numbers of samples with no-fault condition. Then, 15 numbers of data samples are used to test first SVM and all the data samples are classified correctly. Second SVM is trained and tested to classify between the heating fault and arc fault. It is trained with 15 numbers of samples with heating fault condition and 15 numbers of samples with discharge fault condition. Then 15 numbers of data samples are used to test second SVM and out of which 14 data samples are classified correctly. Third SVM is trained and tested to classify between electric arcing fault and partial discharge and corona fault. It is trained with 8 numbers of samples with electric arcing fault condition and 7 numbers of samples with partial discharge and corona fault condition. Then, 10 numbers of data samples are used to test fourth SVM and all the data samples are classified correctly.

Fourth SVM is trained and tested to classify between overheating fault and thermal heating at low temperature fault. It is trained with 8 numbers of samples with overheating fault condition and 7 numbers of samples with thermal heating at low temperature fault. Then 10 numbers of data samples are used to test third SVM and out of which 9 data samples are classified correctly. The overall binary tree is tested with 26 DGA samples and 24 samples are classified correctly. Hence, the accuracy of the overall binary tree was 92%.

The following gases have been considered for the '2D' representation of the output of each SVM, on the basis of fault detection by key gas method [9].

Fault condition and no-fault condition are classified by first SVM (SVM-1). Out of the five characteristic gases, any two gases can be considered to get the desired output. Here, hydrogen (H_2) and acetylene (C_2H_2) have been considered to get the desired output. For SVM-1, linear SVM gives maximum accuracy; hence, configuration matrix of linear SVM has been imported for prediction of new testing sample as shown in Figs. 3, 4 and 5.

Second SVM (SVM-2) classifies between heating fault and discharge fault. Hence, methane (CH_4) and acetylene (C_2H_2) have been considered out of the five characteristic gases to get the desired output. For SVM-2, medium Gaussian SVM gives maximum accuracy; hence, configuration matrix of medium Gaussian SVM has been imported for prediction of new testing samples as shown in Figs. 6, 7 and 8.

Third SVM (SVM-3) classifies between electric arcing fault and partial discharge and corona fault. Here, hydrogen (H_2) and acetylene (C_2H_2) gas concentrations have

Fig. 3 Training output of svm1

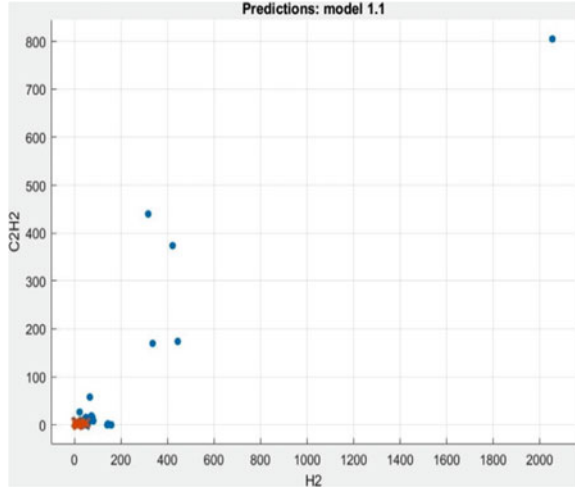


Fig. 4. Configuration matrix of svm1

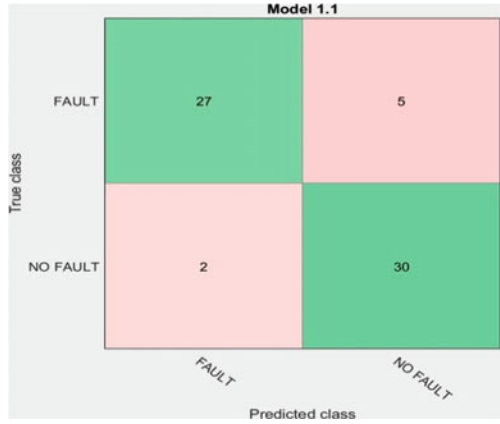


Fig. 5 Kernel functions of svm1

1.1 ☆ SVM Last change: Linear SVM	Accuracy: 89.1% 3/3 features
1.2 ☆ SVM Last change: Quadratic SVM	Accuracy: 89.1% 3/3 features
1.3 ☆ SVM Last change: Cubic SVM	Accuracy: 73.4% 3/3 features
1.4 ☆ SVM Last change: Fine Gaussian SVM	Accuracy: 87.5% 3/3 features
1.5 ☆ SVM Last change: Medium Gaussian SVM	Accuracy: 84.4% 3/3 features
1.6 ☆ SVM Last change: Coarse Gaussian SVM	Accuracy: 75.0% 3/3 features

Fig. 6 Training output of svm2

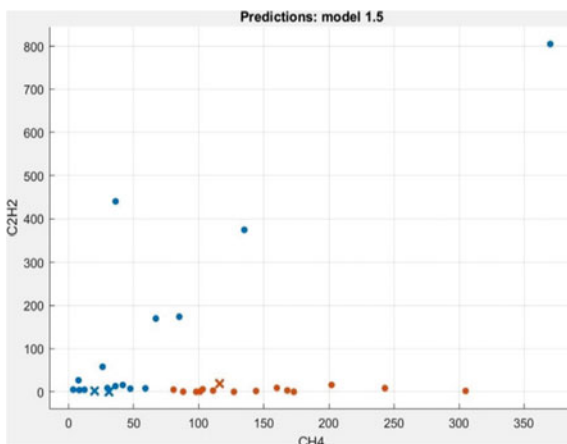


Fig. 7 Configuration matrix of svm2

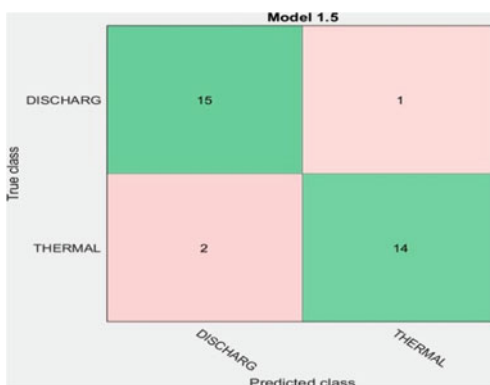


Fig. 8 Kernel functions of svm2

1.1 ☆ SVM	Accuracy: 87.5%
Last change: Linear SVM	2/2 features
1.2 ☆ SVM	Accuracy: 87.5%
Last change: Quadratic SVM	2/2 features
1.3 ☆ SVM	Accuracy: 84.4%
Last change: Cubic SVM	2/2 features
1.4 ☆ SVM	Accuracy: 84.4%
Last change: Fine Gaussian SVM	2/2 features
1.5 ☆ SVM	Accuracy: 90.6%
Last change: Medium Gaussian SVM	2/2 features
1.6 ☆ SVM	Accuracy: 78.1%
Last change: Coarse Gaussian SVM	2/2 features

been considered to get the desired output. C_2H_2 is the predominant gas for arcing in oil and H_2 is the predominant gas for partial discharge and corona. For SVM-3, fine Gaussian SVM gives maximum accuracy; hence, configuration matrix of fine Gaussian SVM has been imported for prediction of new testing samples as shown in Figs. 9, 10 and 11.

Fourth SVM (SVM-4) classifies between overheating fault and thermal heating at low temperature fault. Hence, acetylene (C_2H_2) and ethylene (C_2H_4) have been considered to get the desired output. Ethylene is the predominant gas for overheating of oil. For SVM-4, linear SVM gives maximum accuracy; hence, configuration matrix of linear SVM has been imported for prediction of new testing samples as shown in Figs. 12, 13 and 14.

In Table 1, the code in the output represents for incipient faults are:

1. No-fault condition/Normal condition (NF).

Fig. 9 Configuration matrix of svm3

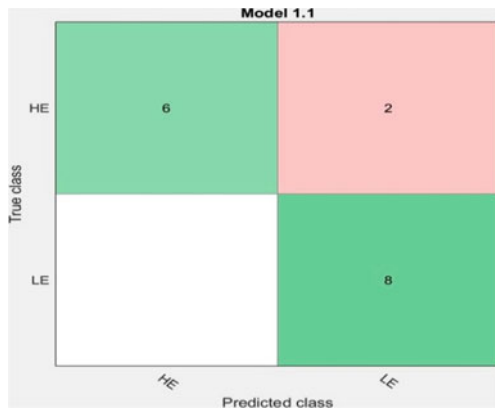


Fig. 10 Kernel functions of svm3

1.1 ☆ SVM	Accuracy: 87.5%
Last change: Linear SVM 2/2 features	
1.2 ☆ SVM	Accuracy: 81.3%
Last change: Quadratic SVM 2/2 features	
1.3 ☆ SVM	Accuracy: 75.0%
Last change: Cubic SVM 2/2 features	
1.4 ☆ SVM	Accuracy: 87.5%
Last change: Fine Gaussian SVM 2/2 features	
1.5 ☆ SVM	Accuracy: 81.3%
Last change: Medium Gaussian SVM 2/2 features	
1.6 ☆ SVM	Accuracy: 43.8%
Last change: Coarse Gaussian SVM 2/2 features	

Fig. 11 Training output of svm3

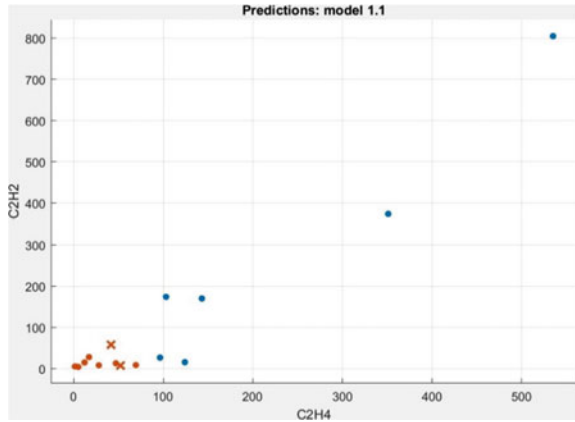


Fig. 12 Kernel functions of svm4

1.1 ☆ SVM	Accuracy: 93.8%
Last change: Linear SVM	2/2 features
1.2 ☆ SVM	Accuracy: 93.8%
Last change: Quadratic SVM	2/2 features
1.3 ☆ SVM	Accuracy: 100.0%
Last change: Cubic SVM	2/2 features
1.4 ☆ SVM	Accuracy: 100.0%
Last change: Fine Gaussian SVM	2/2 features
1.5 ☆ SVM	Accuracy: 93.8%
Last change: Medium Gaussian SVM	2/2 features
1.6 ☆ SVM	Accuracy: 68.8%
Last change: Coarse Gaussian SVM	2/2 features

Fig. 13 Training output of svm4

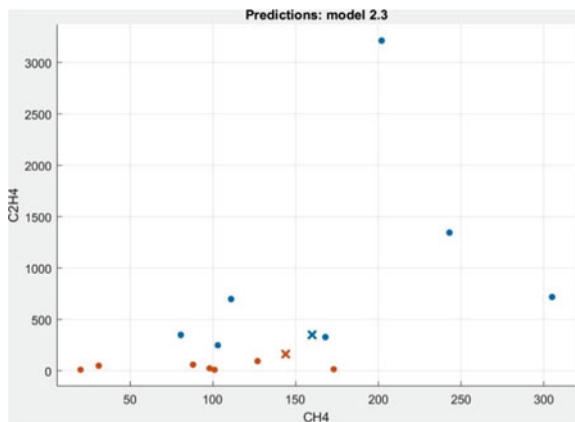


Fig. 14 Configuration matrix of svm4

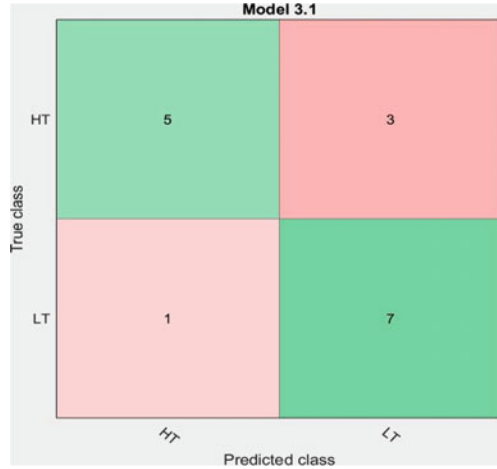


Table 1 Comparisons of results with IEC and ANN

Input test data for fault diagnosis					IEC-Based fault	SVM/ANN-based fault classification		Actual fault
	CH ₄	C ₂ H ₆	C ₂ H ₄	C ₂ H ₂		SVM	ANN	
239	27.5	5.5	25.5	85	LE	LE	LE	HE
128	106	11.5	153	223	HE	HE	HE	HE
36	24	0	24	21	HE	LE	HE	LE
49	12	0.3	4	4.8	HE	NF	NF	LE
172	336.5	172.5	821	37	HT	HT	HT	HT
162.5	224	45.5	497	12.5	HT	HT	HT	HT
27.5	88	40.5	62	0.2	LT	LT	LT	LT
178	259	40	62	0.2	LT	LT	LT	LT
4.5	3	2.5	10.5	2.7	NF	NF	NF	ND
3.5	5	5.5	10.5	2.5	NF	NF	NF	ND
157	127	34	96	0	ND	LT	LT	LT
650	53	34	20	0	ND	LE	LE	LE

2. High thermal heating fault/Overheating fault (HT).
3. Low thermal heating fault/Thermal heating at low temperature fault (LT).
4. High energy discharge fault/Electric arc fault (HE).
5. Low energy discharge fault/Partial discharge and Corona fault (LE).

Some samples of the output results are shown in Table 1 [10]. Out of 12 samples, two samples (sample no. 11, 12 of Table 1) are not detectable and three samples (Sample no. 1, 3, 4) are misclassified by IEC ratio method [11]. Nine samples are

classified by artificial neural network, while correct number of samples classified by SVM was 11.

6 Summary/Conclusion

In this paper, distribution transformer fault diagnosis is done by using support vector machine. Binary tree SVM structure is represented for fault diagnosis of distribution transformer. Fuzzy logic is unable to modify the generated rule base with the changing practical system that is for non-separable and nonlinear data [12]. However, in ANN, this limitation is eliminated as they are very good at learning, but ANN suffers from the problem of over fitting, hence have less generalization ability and gives limited accuracy to fault diagnosis. To avoid all these problems, a new AI technique that is support vector machine which is a special classification tool has been applied to classify the different types of faults in transformer fault diagnosis. The test result shows that SVM approaches have higher diagnostic accuracy than neural network and IEC ratio methods due to its better generalization ability and it can classify non-separable data by using regularization parameter and nonlinear data by using kernel function.

References

1. E. Chaidee, W. Tippachon, Failure statistics and condition evaluation for power transformer maintenance, in *2011 Asia-Pacific Power and Energy Engineering Conference, Wuhan (2011)*, pp. 1–4
2. J. Singh, P. Kumari, K. Kaur, A. K. Swami, Condition assessment of power transformer using SVM based on DGA, in *2016 AI-Sadeq International Conference on Multidisciplinary in IT and Communication Science and Applications (AIC-MITCSA), Baghdad (2016)*, pp. 1–5
3. Y. Zhang, J. Jiao, K. Wang, H. Zheng, J. Fang, H. Zhou, Power transformer fault diagnosis model based on support vector machine optimized by imperialist competitive algorithm. *Electr. Power Automat. Equip.* **38**, 99–104 (2018)
4. V. Vapnik, *The Nature of Statistical Learning Theory*. (Springer, Berlin, 1995)
5. C.J. Burges, *Data Min. Knowl. Disc.* **2**, 121 (1998)
6. C.-W. Hsu, C.-J. Lin, A comparison of methods for multiclass support vector machines. *IEEE Trans. Neural Networks* **13**(2), 415–425 (2002)
7. R.R. Rogers, IEEE and IEC codes to interpret incipient faults in transformers, using gas in oil analysis. *IEEE Trans. Electr. Insul.* EI-13, 349–354 (2007)
8. W. Niu, L. Xu, J. Wu, Fault diagnosis and system development of power transformer based on support vector machine, in *2009 2nd IEEE International Conference on Computer Science and Information Technology, Beijing (2009)*, pp. 578–581
9. F.R. Souza, B. Ramachandran, Dissolved gas analysis to identify faults and improve reliability in transformers using support vector machines, in *2016 Clemson University Power Systems Conference (PSC), Clemson, SC (2016)*, pp. 1–4
10. N.A. Muhamad, B.T. Phung, T.R. Blackburn, K.X. Lai, Comparative study and analysis of DGA methods for transformer mineral oil, in *2007 IEEE Lausanne Power Tech, Lausanne (2007)*, pp. 45–50

11. M. Duval, A. dePablo, Interpretation of gas-in-oil analysis using new IEC Publication 60599 and IEC TC10 data bases, *IEEE Elec. Insul. Mag.* **17**(2), 31–41 (2001)
12. R. Naresh, V. Sharma, M. Vashisth, An integrated neural Fuzzy approach for fault diagnosis of transformers. *IEEE Trans. Power Deliv.* **23**(4), 2017–2024 (2008)

Application of Improved Indirect Matrix Converter in Multipower Supply System for Driving Multiple Loads Independently



N. Lavanya

1 Introduction

For practical applications such as variable speed drives, wind power generation systems and many domestic applications require AC/AC power converters [1]. Among all the various AC/AC converter topologies present, the frequently used converter is traditional AC/DC/AC converter with a common energy storage elements at the DC link [2, 3]. The major limitation of this converter is the presence of large-sized electrolytic capacitor at the DC link which is used for the purpose of filtering and to also store energy for short period. The reliability of the converter is mainly affected by this capacitor due to its premature failures.

This limitation of conventional AC/DC/AC converter can be overcome by using improved IMC supplying power to variable loads at different frequencies at the output stage.

The IMC is utilized to convert constant AC input to variable voltage variable frequency (VVVF) output and to maintain unity power factor (UPF) at its input fundamental current. IMC is advantageous over other AC/AC converters, since the DC link has no presence of energy storage elements unlike conventional AC/DC/AC converter, also its ability to supply power to variable loads which are operating independently at different voltages and frequencies compared to that of direct matrix converter (DMC), and has high voltage transfer ratio with less commutation problems.

IMC consists of two stages for AC/AC power conversion, as shown in Fig. 1, the input stage, i.e., rectification stage and output stage is inversion stage.

The control of input and output stages is independent on each other for IMC but for DMC it is not due to its single-stage conversion. This feature enables the IMC to

N. Lavanya (✉)

Nalla Malla Reddy Engineering College, Hyderabad, Telangana, India

e-mail: lavanya.eee@nmrec.edu.in; lavanyaresearch1234@gmail.com

© Springer Nature Singapore Pte Ltd. 2021

K. S. Sherpa et al. (eds.), *Advances in Smart Grid and Renewable Energy*,

Lecture Notes in Electrical Engineering 691,

https://doi.org/10.1007/978-981-15-7511-2_5

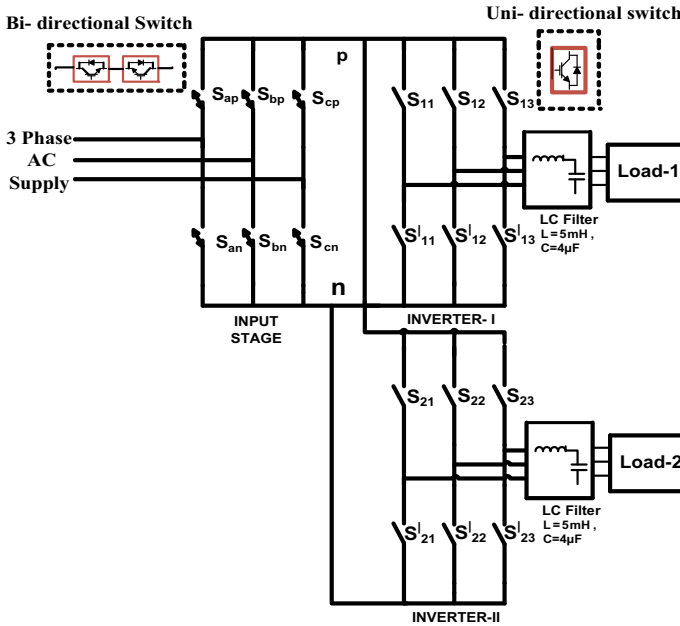


Fig. 1 Block diagram of proposed IMC

connect to number of output stages from the virtual DC link and each output stage operates at different voltages and frequencies.

One of the major drawbacks of conventional IMC is minimum voltage transfer ratio and it is limited to 86.6%. Research has been carried out to overcome this issue but different techniques, like over-modulation, connecting mains transformer, converter/inverter with Z-source, make the system costly and require extra components which in turn make the system bulkier and also the overall system efficiency is affected. Hence, the voltage transfer ratio can be increased automatically with the help of improved IMC (without using more components or switches).

The DC output voltage of IMC with conventional control referred in [4, 5] is produced by using both first maximum phase-to-phase input voltage and second maximum input phase-to-phase voltage for a given sampling period. The main drawback of this type of IMC is the DC output voltage that has high ripples which give more switching losses at both the stages of IMC, the output voltage of IMC has distortions and there are commutation problems at the input stage. All these limitations can be overcome by using the improved IMC. The input stage of improved indirect matrix converter, a maximum DC voltage is produced which has low ripples and also, the output stage has less voltage distortions and with minimum switching losses, compared with conventional IMC. Also, the input fundamental current for both the IMCs is at unity power factor for bidirectional power flow.

This paper analyses the performance of the proposed IMC [6–8] for the following cases:

1. IMC by using two separate output stages at different frequencies and voltages is used to supply power to two passive loads.
2. IMC by using two separate output stages, first output stage is used for the squirrel cage induction motor (SCIM) speed control, by using Volt/Hertz control and the other output stage is connected to static load.

The paper is organized into following sections. Sect. 2 deals with the improved control technique used at the input and output stages of IMC. The performance of this IMC for the case-1 is analysed in Sect. 3.1. Section 3.2 deals with case-2. Last section deals with the conclusions drawn. All the above-mentioned cases are analysed and compared by using both simulation results as well as hardware results.

2 Operation of Improved IMC

Figure 1 shows the topology of improved IMC, which consists two independent stages, i.e. input (which converts AC to DC) stage which consists of six bidirectional switches ($S_{ap} - S_{cn}$) and output (which converts DC to AC) stage six unidirectional switches. The main function of the input stage of the proposed IMC is to produce maximum positive DC output voltage. Also, the output voltages of this IMC are synthesized by the control algorithm at the output stage. The output stage control is based on the reference voltage vector control (by using Space vector pulse width modulation). The switching modulation strategies of the input stage and the output stage are independent. Equation (1) gives the three-phase input voltages as:

$$v_a = V_p \sin \omega t; \quad v_b = V_p \left(\sin \omega t - \frac{2\pi}{3} \right); \quad v_c = V_p \left(\sin \omega t + \frac{2\pi}{3} \right) \quad (1)$$

where V_p is the peak value of the input supply voltage and ω is its angular frequency.

Improved IMC: Here, with use of largest positive line-to-line input voltages in each sector, a maximum DC voltage is produced. The maximum DC voltage is V_{cb} in sector-1, which is obtained by switching ON, the switches S_{cp} and S_{bn} . For the remaining sectors, the DC-link line-to-line voltages are shown in Table 1.

The output of the input stage of proposed IMC produces maximum DC voltage with less ripples as compared to conventional IMC.

The switching times for conventional IMC at the output stage are given by Eq. (2).

$$\begin{aligned} T'_A &= T_A \frac{T_p^R}{T_s}, \quad T'_B = T_B \frac{T_p^R}{T_s}, \quad T''_A = T_A \frac{T_n^R}{T_s}, \\ T''_B &= T_B \frac{T_n^R}{T_s} \quad \text{and} \quad T_Z = T_s - (T_A + T_B) \end{aligned} \quad (2)$$

Table 1 Sectorwise DC voltages at input stage

Identification of different sectors	θ_{in}	DC-link voltage (V_{pn})
1	$-\frac{\pi}{6}$ to $\frac{\pi}{6}$	$(V_c - V_b) = V_{cb}$
2	$\frac{\pi}{6}$ to $\frac{\pi}{2}$	V_{ab}
3	$\frac{\pi}{2}$ to $\frac{5\pi}{6}$	V_{ac}
4	$\frac{5\pi}{6}$ to $\frac{7\pi}{6}$	V_{bc}
5	$\frac{7\pi}{6}$ to $\frac{3\pi}{2}$	V_{ba}
6	$\frac{3\pi}{2}$ to $-\frac{\pi}{6}$	V_{ca}

where T_p^R and T_n^R are the switching times for the upper (p-group) switches and the lower (n-group) switches of the input stage. And T_A , T_B and T_Z are the corresponding dwell times of the output stage. Similarly, for the improved IMC, new switching times at the output stage are given by

$$T'_A = \frac{T_A}{2}, \quad T'_B = \frac{T_B}{2}, \quad T''_A = \frac{T_A}{2}, \quad T''_B = \frac{T_B}{2}, \quad \text{and} \\ T_Z = T_s - (T_A + T_B). \quad (3)$$

It can be observed from Eq. (3), that the switching times for the output stage of improved IMC are simple and also independent to input stage control unlike for the switching scheme used in conventional IMC given by Eq. (2). This new switching times reduce the voltage distortions with low switching losses at the output stage [6–8].

2.1 Experimental Setup

The experimental setup for improved IMC is as shown in Fig. 2. This setup is divided into the following parts:

(1) *Power circuit*: There are 24 IGBT (FGA25N120) switches, HCPL316J gate driver circuit, a three-phase variac and LC-filters present at both the stages of IMC. (2) *Signal conditioning unit* This signal conditioning unit consists of three (LV25-SP2) voltage and current (LA25-P) transducers at the input stage, one voltage transducer at DC link and six voltage (LV20-P) and six current (LA25-P) transducers at output stages of proposed IMC. (3) *Controller* To implement the control technique for the input side of IMC, SVM technique for output side of IMC and firing pulses to IGBT switches, an interface based on Spartan-6 (XC6SLX25) FPGA board is used.

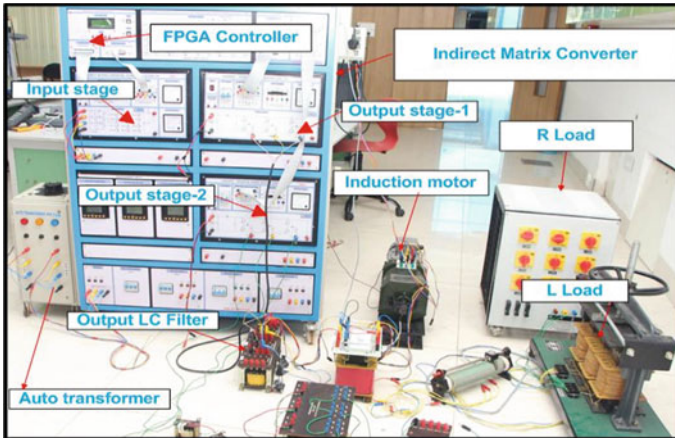


Fig. 2 Hardware setup of proposed IMC

3 Performance IMC in Multipower Supply System to Drive Multiple Loads

3.1 Performance of IMC to Drive (with Two Output Stages) Two Static Loads

The block diagram of proposed IMC is shown in Fig. 1. By using three-phase variac, the input supply phase voltage to the IMC is set to 140 V, 50 Hz and two output stages are used to drive two passive loads at variable voltages and variable frequencies. Both the output stages of IMC operate with same control scheme but the reference voltage V_R varies both in magnitude and frequency (ω_r), since the output stage uses two different load voltages for the specified magnitude and frequencies.

Output stage-1 feeds to R - L load ($R = 237 \Omega$, $L = 120 \text{ mH}$) at 60 Hz and 115 V. Similarly, output stage-2 feeds power to another R - L load ($R = 240 \Omega$, $L = 45 \text{ mH}$) at 40 Hz and 100 V. Figure 3 shows the simulation results and hardware results of the input side voltage and current for the IMC with improved control. Figures 4 and 5 show the output stage-1 and output stage-2 voltage and current waveforms, respectively.

3.2 Performance of IMC Feeding (With Two Output Stages) to SCIM for Speed Control and Static Load

There are different methods used for the induction motor speed control based on both steady state as well as dynamic state equivalent circuits. Out of all the speed control

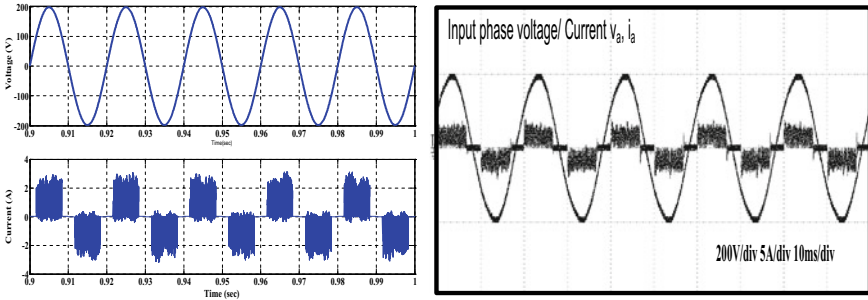


Fig. 3 Input side phase voltage and current of proposed IMC

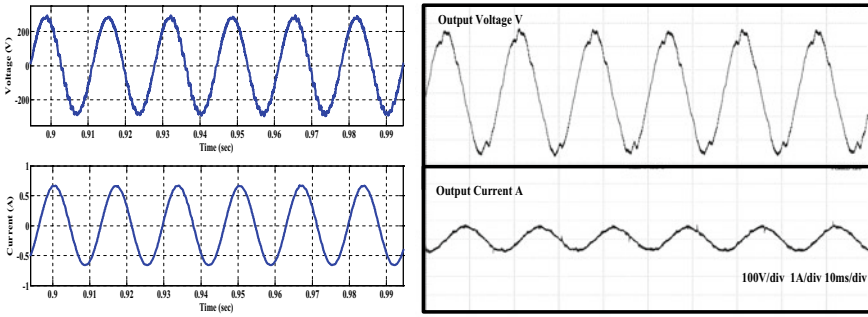


Fig. 4 Output stage-1 phase voltage with THD = 4.27% and current with THD = 1.414% at 60 Hz

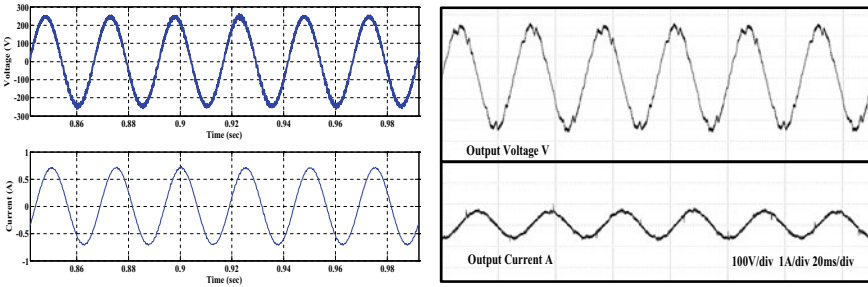


Fig. 5 Output stage-2 phase voltage (THD = 3.54%) and current (THD = 1.35%) at 40 Hz

methods V/f control is used widely in various applications because it provides wide range of speed control for both variable and constant torque loads and also ensures fairly constant air gap flux so that magnetic saturation will not take place. The circuit topology of the proposed IMC for this application is also shown in Fig. 1, where

Table 2 Experimental results of V/f control

S. No.	Output voltage (line–line) volts	Frequency (Hz)	N rpm
1	77.9	10	275
2	110.0	14	386
3	125.5	16	441
4	141.2	18	496
5	157.6	20	552
6	189.6	26	717
7	236.4	30	828
8	269.3	34	938
9	301	38	1048
10	317.8	40	1104

output stage-1 is fed to SCIM for speed control and output stage-2 is driving passive load at 45 Hz.

To analyse the SCIM speed control for the proposed IMC, Volt/Hertz control method is used. The SCIM speed is controlled by varying both output voltage and frequency of the IMC through change of reference voltage V_R and its frequency (ω_r) while maintaining the V/f ratio constant.

The steady-state speed response of the IM is shown in Table 2.

Here, the simulation results and hardware results are compared when SCIM is running at 1100 rpm. Figure 6 shows the simulation results as well as the hardware results of fundamental input voltage and fundamental input current of the proposed IMC, which is at UPF. Figure 7 shows the simulation and experimental results of output stage-1 connected to SCIM, and Fig. 8 shows the simulation results and hardware results of output stage-2 (phase voltage and current) at 45 Hz frequency.

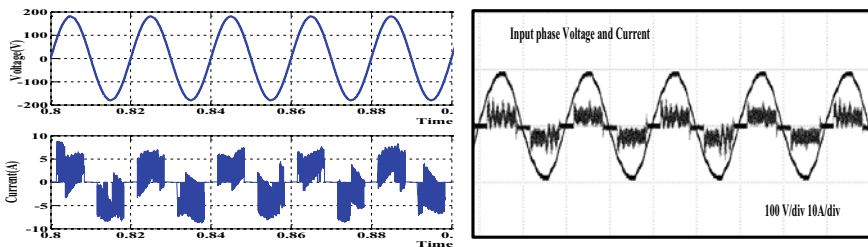


Fig. 6 Input phase voltage and current of proposed IMC

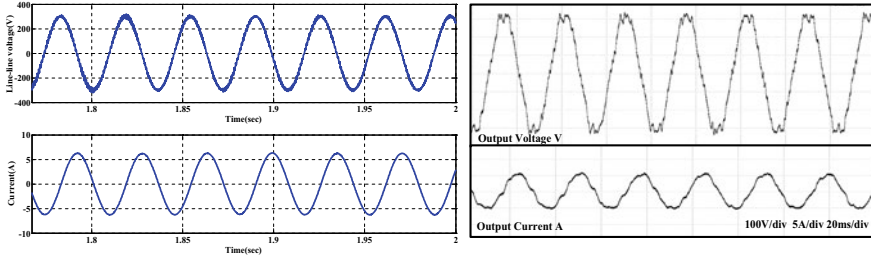


Fig. 7 Output stage-1 line–line voltage and current at 1100 rpm

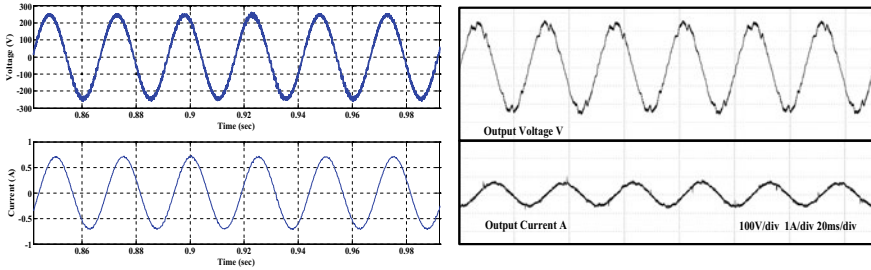


Fig. 8 Output stage-2 phase voltage and current at 45 Hz

4 Conclusion

Application of improved indirect matrix converter (IMC) in multipower supply system for driving multiple AC loads (static and/or dynamic) independently with single AC supply is presented and analysed. The experimental setup for the proposed IMC is implemented in the laboratory, and it is tested for different operating conditions. Both the simulation and hardware results are presented and also the input fundamental current of proposed improved IMC is at unity power factor.

Acknowledgements The funding support is given by DST (Government of India) under Women Scientist-A scheme. The Project File No: **SR/WOS-A/ET-1035/2014**.

Appendices

Output LC filter parameters: $L = 5 \text{ mH}$, $C = 4 \text{ }\mu\text{F}$; Machine parameters: $R_s = 1.85 \text{ }\Omega$; $R_r = 3 \text{ }\Omega$; $L_{ls} = 0.01\text{H}$; $L_{lr} = 0.01\text{H}$; $L_m = 0.16 \text{ H}$; 4 poles.

References

1. J. Itoh, T. Iida, A. Odaka, Realization of high efficiency AC link converter system based on AC/AC direct conversion techniques with RBIGBT, in *Proceedings of 32nd Annual Conference on IEEE Industrial Electronics, Paris* (2006), pp. 1703–1708
2. J.T. Friedli, J. Kolar, Comprehensive comparison of three-phase AC–AC matrix converter and voltage dc-link back-to-back converter systems, in *Proceedings IPEC* (2010), pp. 2789–2798
3. P.W. Wheeler, J. Rodríguez, J.C. Clare, L. Empringham, A. Weinstein, Matrix converters: a technology review. *IEEE Trans. Industr. Electron.* **49**(2), 276–288 (2002)
4. R. Pena, R. Cardenas, E. Reyes, J. Clare, P. Wheeler, A topology for multiple generation system with doubly fed induction machines and indirect matrix converter. *IEEE Trans. Ind. Electron.* **56**(10), 4181–4193 (2009)
5. T. D. Nguyen, H.-H. Lee, A new SVM method for an indirect matrix converter with common-mode voltage reduction. *IEEE Trans. Ind. Inf.* **10**(1) (2014)
6. N. Lavanya, O. Chandra Sekhar, M. Ramamoorthy, Performance of indirect matrix converter as asynchronous link between two ac systems. *J. Electr. Eng.* **16**(49), 434–442 (2016)
7. N. Lavanya, O. Chandra Sekhar, M. Ramamoorthy, Performance of indirect matrix converter with improved control feeding doubly fed induction machine, in *IEEE SPICES*, 8–10 Aug 2017, pp. 1–6.
8. N. Lavanya, O. Chandra Sekhar, M. Ramamoorthy, Performance of indirect matrix converter with improved control feeding to induction motor for speed control by using Pi and fuzzy controllers, in *IEEE TENCN*, 5–8 Nov 2017.

Incorporation of Distributed Generation Resources for Three-Area Load Frequency Control Optimized Tilted Integral Derivative Controller



Sunita Pahadasingh, Chitralekha Jena, and Chinmoy Ku. Panigrahi

1 Introduction

Generally, load changes continuously in power system which leads greater mismatch between the real power and demand. This major unbalance causes wide difference in nominal frequency and interconnected power and which can be controlled by LFC. The main objective of LFC is to minimize the error using suitable controller to achieve zero steady-state error. The conventional units such as thermal, hydro, gas and nuclear are already studied in various research papers [1–4]. In last decade, distributed generation (DG) gained greater attention towards an interconnected power system which is environment friendly and meet the augmented power demand. Various research papers describe the coordination of DG and renewable energy resources to this LFC system [5, 6]. The coordination of conventional and distributed generated resources has deliberated by Hussain et al. [7] which consists of wind turbine generator (WTG), fuel cell (FC), battery energy storage system (BESS), aqua electrolyzer (AC) and diesel engine generator (DEG). AE uses a part of WTG power for production of hydrogen gas and that is further used in fuel cell having low pollution and better efficiency [6, 8]. Raju et al. [6] studied the coordination of DG applied in area 1 with the thermal and hydro units. Generally, BESS and DEG are used for load leveling and deficit power supplies to this system, respectively. Advent of HVDC to this existing AC line enhances the power system stability [9] that means of low frequency

S. Pahadasingh (✉) · C. Jena · C. Ku. Panigrahi
School of Electrical Engineering, Kalinga Institute of Industrial Technology University,
Bhubaneswar 751024, India, Odisha
e-mail: spahadasingh@gmail.com

C. Jena
e-mail: chitralekha.jenafel@kiit.ac.in

C. Ku. Panigrahi
e-mail: panigrahichinmoy@gmail.com

oscillation. Implementation of secondary controller to LFC system has been studied by many researchers to damp out the oscillations. Simple structure and robustness characteristics of PID controller make it popular feedback control in the process industry applications. But, it may causes savour damage in the system performance due to peak overshoot and large settling time in transient period. This constraint is conquered by a new generalized PID controller called TID controller [10, 11] which is applied. In this era of computational revolution, more and more heuristic methods for optimization are evolving. Various fields of studies have been explored with these types of optimization techniques. In LFC, many techniques such as firefly algorithm [3, 5], differential evolution (DE) [4], flower pollination (fp) [5], bacterial foraging optimization (BFO) [12], grey wolf optimization (GWO) [13] and teaching-learning-based optimization (TLBO) [14, 15] are used for optimization of controller variables. In [15], fuzzy PID controller applied to two area system optimized by TLBO was depicted by Sahu. For optimization, it is very necessary to tune the controller parameters properly because improper tuning may lead to either increase of computational time or reaches to local optimum. Considering this fact, a new optimization technique is introduced which does not require algorithm-specific parameters and only requires controlling parameters. Since this algorithm carries parameter free optimization, it is simple in nature and more effective due to faster convergence characteristics. Hence it was widely motivated by researchers to use their areas.

2 Power System Model

Implementation of DG and conventional units for LFC system is discussed here. The modelling of three-area LFC system with controller is shown in Fig. 1 [16] which consists of thermal and hydro power unit with a SLP of 1% applied in control area 1. This is the hybrid system, in which area 1 is incorporated with thermal plant and DG resources such as WTG, FC, AE, BESS and DEG. The area 2 and area 3 consist of thermal generation and hydro units, respectively. The transfer function model of DG resources is shown in Fig. 2 [16]. At first, area control error (ACE) is taken as input to the PID controller in each area. Then, this ACE signal is applied to TID controller. Area control error can be expressed as in Eq. (2–4) [17]:

$$ACE_1 = \Delta P_{12} + B_1 \Delta w_1 \quad (2)$$

$$ACE_2 = \Delta P_{21} + B_2 \Delta w_2 \quad (3)$$

$$ACE_3 = \Delta P_{31} + B_3 \Delta w_3 \quad (4)$$

ΔP_{12} , ΔP_{21} , ΔP_{31} are the tie-line power fluctuations of respective areas.
 B_1, B_2, B_3 are the frequency biasing coefficient of respective areas.

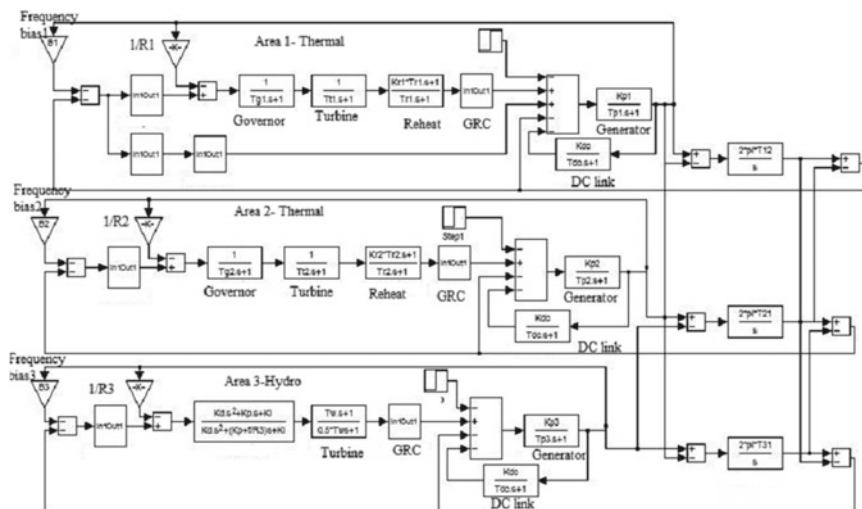


Fig. 1 Modelling of three-area LFC system using TID controller with DG system

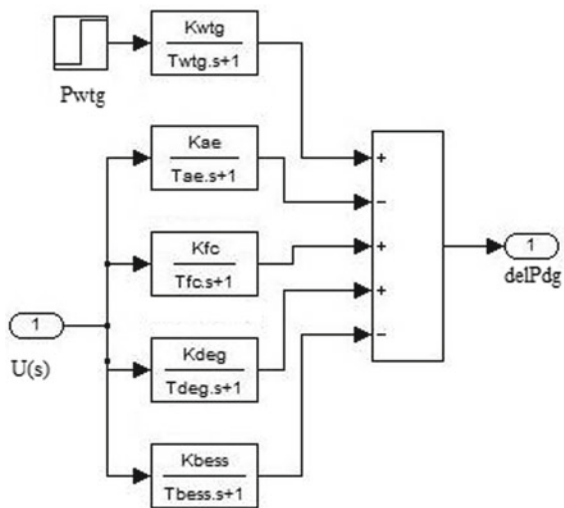


Fig. 2 Transfer function model for DG sources

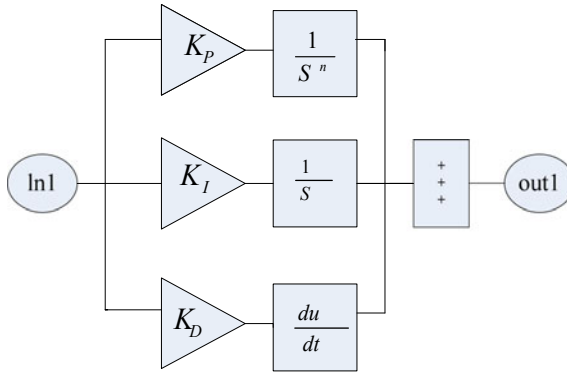


Fig. 3 Structural diagram of TID controller

2.1 Controller Design

In this paper, a TID controller is used for the tuning of system parameters with the help of optimization techniques. It consists of proportional, integral and derivative gain with tilted component of transfer function $\frac{1}{s^n}$. The system frequency is fed back to achieve zero steady-state error. This controller is simpler to design and less effected to parameter variations. The basic structural diagram of TID controller is shown in Fig. 3 [10]. Performance of optimization process generally depends on the objective function in time domain form. Here, ITAE is used as objective function because of small overshoot and oscillations. Mathematical expression of ITAE function is

$$f = \int |\Delta F_1 + \Delta F_2 + \Delta F_3 + \Delta P_{tie}| \cdot t \cdot dt \quad (5)$$

2.2 Methodology

Teaching-learning-based optimization is proposed for this system which was first introduced by Rao et al. There are two basic modes of learning (i) teacher phase by teacher's own experience (ii) learner phase through communication with other learners. TLBO algorithm steps are:

- (a) Initialization: randomly generating the population size NP and dimension D in order of $[NP \times D]$.
- (b) Teacher phase: Calculating the mean value of the subjects that has assigned to a teacher in the class room. For particular subject, mean result of learners is

$$X_{\text{mean}} = [m_1, m_2, \dots, m_D] \tag{6}$$

- (c) A random number r is defined in range $[0, 1]$. The difference between learner's mean result and corresponding teacher result for a particular subject can be expressed as

$$X_{\text{diff}} = r \cdot (X_{\text{teacher}} - (T_F X_{\text{mean}})) \tag{7}$$

T_F is the teaching factor to be changed 1 or 2 randomly and is expressed as

$$T_F = \text{round}[1 + \text{rand}(0, 1)] \tag{8}$$

- (d) Then, the updated value of existing population can be expressed as

$$X_{\text{new}} = X + X_{\text{diff}} \tag{9}$$

- (e) If X_{new} is better than X , then accepted the elements of X_{new} , otherwise accepted the elements of X .
- (f) Learner phase: in this stage, a learner increases his\her knowledge by interacting with other experienced learners. Then, randomly selected two learners named as X_i and X_j such that $i \neq j$.

$$X_{\text{new}} = \begin{cases} X_i + r \cdot (X_i - X_j) & f(X_i) < f(X_j) \\ X_i + r \cdot (X_j - X_i) & \text{otherwise} \end{cases} \tag{10}$$

where $f(X)$ is the value of objective function. This the end of learner phase.

3 Simulation Results

Three areas, in which area 1 is formulated with DG sources and thermal units, area 2 for thermal and area 3 for hydro units, are designed in this paper using SIMULINK. SLP of 1% is also applied to area 1. At first, the proposed system is considered with TID controller which parameters (K_p , K_i and K_d) are optimized by DEPSO algorithm. This is happened through numerous simulations by taking 20 number of population and dimension of 12 with 20 numbers of iteration. The objective function is performed by ITAE method. Then, these controller parameters are optimized by TLBO algorithm by numerous simulations. At last, the simulation results are compared for this system with these two optimization techniques. The simulation results are shown in Figs. 4, 5, 6, 7, 8 and 9. Since the TLBO is liberated of algorithm-specific parameters, it performs better than previous one in terms of stability.

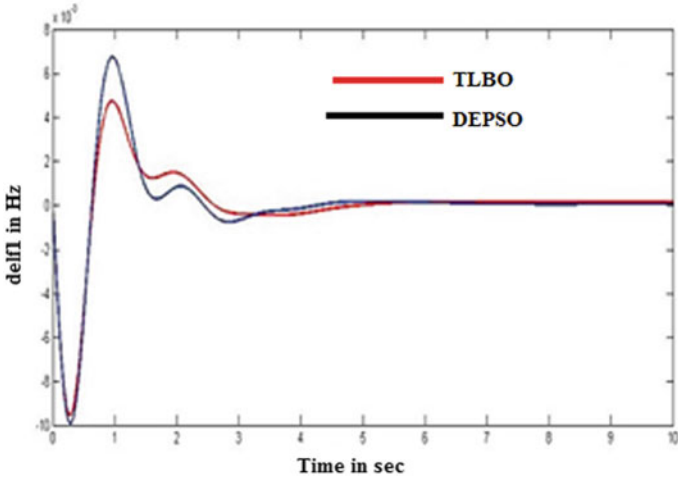


Fig. 4 Variance of frequency for area 1

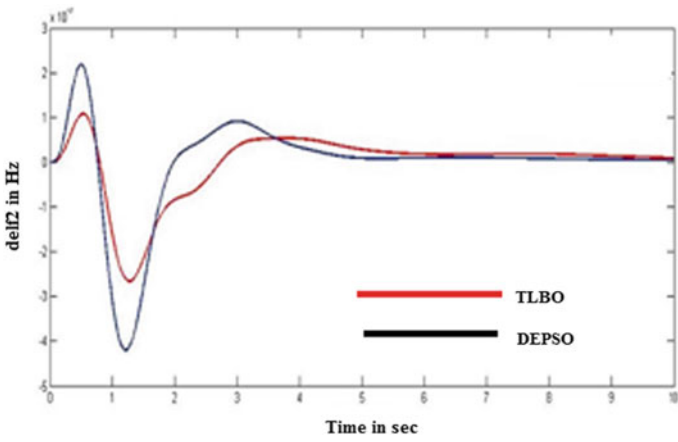


Fig. 5 Variance of frequency for area 2

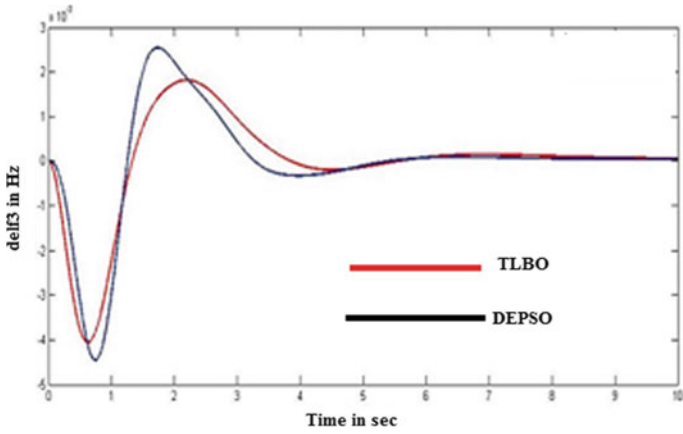


Fig. 6 Variance of frequency for area 3

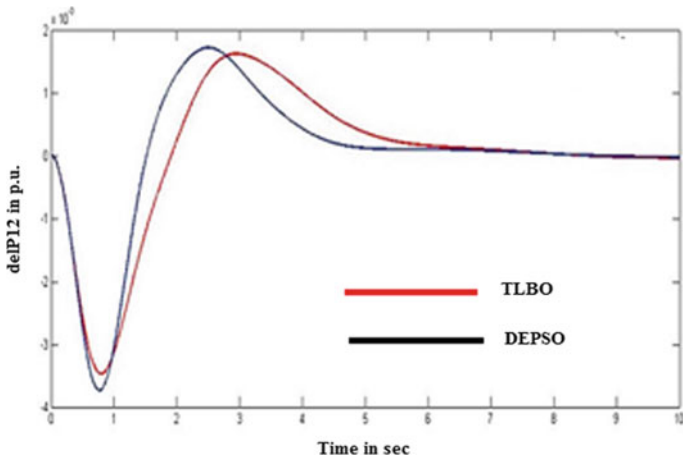


Fig. 7 Interchange power P_{12} deviations

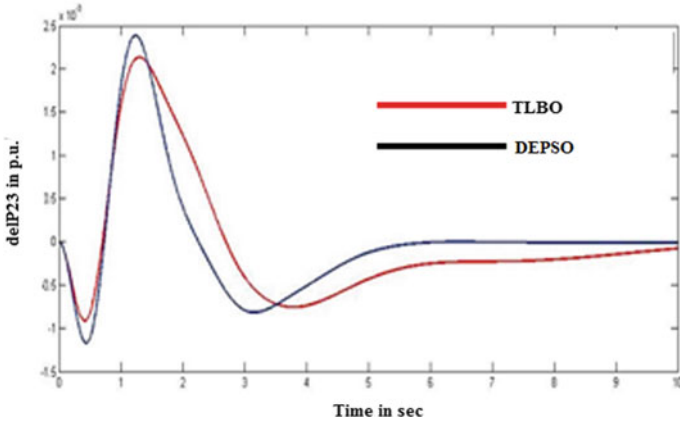


Fig. 8 Interchange power P_{23} deviation

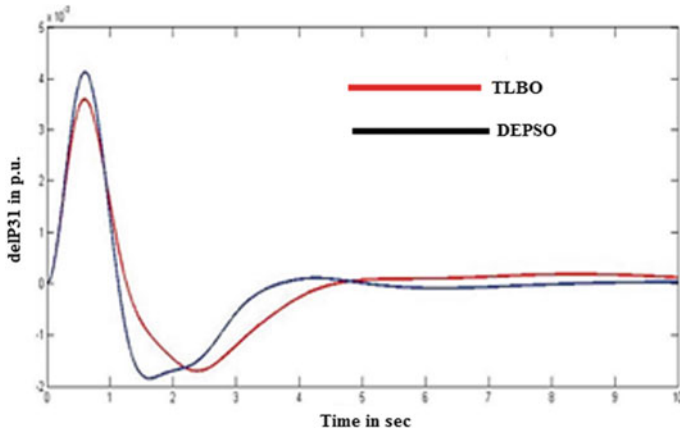


Fig. 9 Interchange power P_{13} deviation

The dynamic performance features such as overshoot (Max), undershoot (Min) and settling time (T_s in seconds) are discussed in Table 1 for TID and PID controller. Similarly, the performance values of the proposed systems are mentioned for TLBO and DEPSO algorithm in Table 2. DEPSO and TLBO are given in Table 3 as the gain values of TID controller are optimized by both mentioned which is done by extensive simulations.

Table 1 Performance values of frequency and tie power variations of different controllers

Model	Range	Performance values						
TID	Dynamic data	T_s	F_1	F_2	F_3	Tie_{12}	Tie_{21}	Tie_{31}
	Min	3.403	-9.5631	-2.6631	-4.0612	-3.4748	-0.9129	-1.7037
PID	Max		4.7192	1.0802	1.8118	1.6194	2.1341	3.5942
	Dynamic data	T_s	F_1	F_2	F_3	Tie_{12}	Tie_{21}	Tie_{31}
	Min	5.230	-9.9058	-3.6599	-4.4058	-3.7622	-1.2127	-1.7892
	Max		5.5944	1.4350	2.4994	2.3246	3.2341	4.0291

Table 2 Performance values of frequency and tie power variations of different algorithms

Algorithm	Range	Performance values						
TLBO	Dynamic data	T_s	F_1	F_2	F_3	Tie_{12}	Tie_{21}	Tie_{31}
	Min	3.403	-9.5631	-2.6631	-4.0612	-3.4748	-0.9129	-1.7037
	Max		4.7192	1.0802	1.8118	1.6194	2.1341	3.5942
DEPSO	Dynamic data	T_s	F_1	F_2	F_3	Tie_{12}	Tie_{21}	Tie_{31}
	Min	4.335	-9.9496	-4.2029	-4.4584	-3.7421	-1.1730	-1.8504
	Max		6.7286	2.1800	2.5399	1.7187	2.3864	4.1229

4 Conclusion

In this study, a comparison of two optimization techniques has implemented in LFC of three-area multi-source configuration with DG functional to area 1. Controlled parameters of TID are optimized by TLBO which is finer as compared to DEPSO in terms of stability. The presence of HVDC link definitely picks up the system dynamics for settling time, overshoot and undershoot response. The controlled parameters of TID controller are more suitable to assure the objective of LFC. Fractional-order controller with advanced optimization technique can be applied to this proposed system further.

Table 3 Controller gain parameters (TID) optimized by DEPSO and TLBO

Algorithm	TID controller parameters											
	Area 1 (DGR)			Area 1 (Thermal)			Area 2 (Thermal)			Area 3 (Hydro)		
	K_p	K_i	K_d	K_p	K_i	K_d	K_p	K_i	K_d	K_p	K_i	K_d
TLBO	1.8337	1.1465	0.1408	0.0286	1.2083	1.4389	0.2268	0.1991	0.0161	0.0134	1.6963	0.1229
DEPSO	1.9602	2.0000	0.0239	2.0000	1.9291	2.0000	1.8274	0.8057	1.9783	0.0100	0.7057	0.0100

Appendix

Subscript referred to area (i) = 1, 2 and 3.

Nominal system frequency $f = 60$ Hz; Steam turbine time constant (T_{ti}) = 0.3 s; reheater time constant and gain (T_{ri}) and (K_{ri}) = 10 s and 0.5; generator gain (K_{pi}) = 120 Hz/pu MW; time constant (T_{pi}) = 20 s; Tie-line interchange (T_{ij} MW/rad) = 0.086 pu; inertia constant (H_i) = 5 s;

Speed regulation parameter (R_i) = 2.4 pu Hz/MW; bias coefficient (B_i) = 0.425 pu MW/Hz;

Gain of Wind turbine generator (K_{WTG}); AE (K_{AE});

FC (K_{FC}); DEG (K_{DEG}) and BESS (K_{BESS}) are = 1; 0.002; 0.01; 0.0003 and – 0.0003 respectively.

Time constant of wind turbine generator (T_{WTG}); AE (T_{AE}); FC (T_{FC}); DEG (T_{DEG}); BESS (K_{BESS}) are 1.5 s, s; 0.5 s; 4 s; 2.0 s and 0.1 s respectively.

Starting time of hydro (T_w) = 1 s; HVDC link gain and time constant of HVDC (K_{hvdc} and T_{hvdc}) are 1.1 and 0.2 s; Gains of electric governor K_p, K_i, K_d = are 1.5 and 4.

References

1. O.I. Elgerd, C.E. Fosha, Optimum megawatt—frequency control of multiarea electric energy systems. *IEEE Trans. Power Appar. Syst.* **PAS-89**(4), 556–563 (1970)
2. A. Rahman, L.C. Saikia, N. Sinha, Automatic generation control of an unequal four-area thermal system using biogeography-based optimised 3DOF-PID controller. *IET Gener. Transm. Distrib.* **10**(16), 4118–4129 (2016)
3. R.K. Sahu, S. Panda, S. Padhan, A hybrid firefly algorithm and pattern search technique for automatic generation control of multi area power systems. *Electr. Power Energy Syst.* **64**, 9–23 (2015)
4. B. Mohanty, S. Panda, P.K. Hota, Controller parameters tuning of differential evolution algorithm and its application to load frequency control of multisource power system. *Int. J. Electr. Power Energy Syst.* **54**, 77–85 (2014)
5. S. Debbarma, A. Dutta, Utilizing electric vehicles for LFC in restructured power systems using fractional order controller. *IEEE Trans. Smart Grid* **8**(6), 2554–2564 (2017)
6. M. Raju, L.C. Saikia, N. Sinha, Load frequency control of multi-area hybrid power system using symbiotic organisms search optimized two degree of freedom controller. *Renew. Energy Res.* **7**(4), 1663–1674 (2017)
7. S.K. Pandey, S.R. Mohanty, N. Kishor et al., Frequency regulation in hybrid power systems using particle swarm optimization and linear matrix inequalities based robust controller design. *Electr. Power Energy Syst.* **63**, 887–900 (2014)
8. A. Rahman, L.C. Saikia, N. Sinha, Maiden application of hybrid pattern search biogeography based optimisation technique in automatic generation control of a multi-area system incorporating interline power flow controller. *IET Gener. Transm. Distrib.* **10**(7), 1654–1662 (2016)
9. Y. Arya, N. Kumar, Ibraheem, AGC of a two-area multi-source power system interconnected via AC/DC parallel links under restructured power environment. *Optim. Control Appl. Methods* **37**, 590–607 (2016)

10. J. Morsali, K. Zare, M.T. Hagh, MGSO optimised TID-based GCSC damping controller in coordination with AGC for diverse-GENCOs multi- DISCOs power system with considering GDB and GRC non-linearity effects. *IET Gener. Transm. Distrib.* **11**(1), 193–208 (2017)
11. R.K. Sahu, S. Panda, A. Biswal, G.T.C. Sekhar, Design and analysis of tilt integral derivative controller with filter for load frequency control of multi-area interconnected power systems. *ISA Trans.* **61**, 251–264 (2016)
12. E.S. Ali, S.M. Abd-Elazim, Bacteria foraging optimization algorithm based load-frequency controller for interconnected power system. *Int. J. Electr. Power Energy Syst.* **33**, 633–638 (2011)
13. Y. Sharma, L.C. Saikia, Automatic generation control of a multi-area ST—thermal power system using Grey Wolf optimizer algorithm based classical controllers. *Electr. Power Energy Syst.* **73**, 853–862 (2015)
14. K.T. Mohapatra, B.K. Sahu, Design and implementation of SSA based fractional order PID controller for automatic generation control of a multi-area, multi-source interconnected power system, in *IEEE Conference ICSESP*. <https://doi.org/10.1109/ICSESP.2018.8376697> (2018)
15. B.K. Sahu, et al., Teaching–learning based optimization algorithm based fuzzy-PID controller for automatic generation control of multi-area power system. *Appl. Soft Comput.* **27**, 240–249 (2015)
16. M. Raju, L.C. Saikia, N. Sinha, Load frequency control of a multi-area system incorporating distributed generation resources, gate controlled series capacitor along with high-voltage direct current link using hybrid ALO-pattern search optimised fractional order controller. *IET Renew. Power Gener.* **13**(2), 330–341 (2019)
17. P. Kundur, *Power System Stability and Control*, 2nd edn. (McGraw Hill, New York, 1994)
18. I. Hussain, S. Ranjan, D.C. Das et al., Performance analysis of flower pollination algorithm optimized PID controller for wind-PV-SMES-BESSdiesel autonomous hybrid power system. *Renew. Energy Res.* **7**(2), 643–651 (2017)

Balanced Scorecard and Its Application Through Strategic Management Perspective in Real Estate Industry



Sushil Kumar Pareek and Samrat Kumar Mukherjee

1 Introduction

The modern era's competitiveness has strongly engulfed the entire business canvas in terms of human resources management, internal process, customer management and financial management. A strategic planning becomes critical to business success because it directs and guides, where the organization to go and how it is going to get there. The best strategic plan encompasses the vision, mission, objective and outside of the box thinking. It promotes a rudiment action plan of an organization to accomplish the organizational goals. Despite numerous tools used to assess the strategic plans of an organization, the most dynamic and vibrant tool adopts by all corporations across the globe is the "balanced scorecard (BSC)". It is a tool used in strategic planning, human resources management and structuring business actions according to the organization's vision, mission, objective and strategy. The specialty of BSC is that it focuses both financial and non-financial approaches of the business through categorization of the four perspectives, namely financial, customer, internal process, learning and growth. Thus, the performance of the organization is measured effectively without compromising the standards. In a study [1], researchers formulated the set of measures that balance both the financial and operational systems, which is named as balanced scorecard. The heart of balanced scorecard lies upon the balancing operational system such as customers, internal process, learning and growth with the financial perspective.

S. K. Pareek (✉)

School of Management, Maulana Abul Kalam Azad University of Technology, Kolkata, West Bengal, India

e-mail: pareek.sushil@gmail.com

S. K. Mukherjee

Sikkim Manipal Institute of Technology, Sikkim Manipal University, Gangtok, India

e-mail: s.mukherjee@rediffmail.com

© Springer Nature Singapore Pte Ltd. 2021

K. S. Sherpa et al. (eds.), *Advances in Smart Grid and Renewable Energy*,

Lecture Notes in Electrical Engineering 691,

https://doi.org/10.1007/978-981-15-7511-2_7

The very first outlines the background, problem statement, purposes, significance, limitation and scope of the study for the real estate company.

The second discusses the literature reviews on the balanced scorecard and its four perspectives. Similarly, the third outlines the research design where it describes the methods and methodology for collecting data. The fourth discusses the various models that analyze each perspective of the BSC in real estate. It outlines the various models used for analyzing the BSC such as 7s strategic planning tools of McKinsey, Value Chain Management of Michael Porter, Bloomfield Matrix, Functional Double Looping and Theory Z Plus which have been used.

For instance, the Theory Z propounded by Halifax implies the concept of cause and effect relationship in the BSC but forgoes the societal outlook apart from their CSR which is being narrowed in today's business environment.

Similarly, it discusses the industry and environmental scanning of the company, which has the direct impact on the company's strategic plan and execution. Finally, it highlights the findings and analysis part

- To develop a strategic plan using the balanced scorecard as road map for a real estate company.
- To determine the comprehensive measurement instruments for real estate company within the balanced scorecard.
- To ensure that the measurement tools are aligned with the vision, mission, goal and objectives of real estate company.

2 Literature Review

In the changing phase of the business environment, the elite personality and the influential figure do not suffice the functional aspect of the business. The presence of strategy that interlinks both the manager and subordinates and bond the relationship informally had been the most awaited corporate strategy that business firm must adopt in the present world. The performance measurement should not be limited to subordinates but to the higher executive levels as well because the loopholes and business leakages can have diversified origins not simply to the lower levels or subordinates.

All relevant literature reviews on performance measurement tool BSC have been emphasized in this section to support the very topic. The review covers all different aspects of the arguments and statements of the different scholars, researchers and academicians. The consultants have explored numerous insights and opinions from the past articles based on its analysis and findings on the particular subject, which they referred in their papers.

Moreover, the gap arises from different opinions of the authors that have been also stated and cited to furnish the arguments pointed out by various authors on BSC and its perspectives. Likewise, most of the literature reviews have been stressed on BSC and its four perspectives with referring to the performance management tool of the organization.

Some articles [12] state “performance measurement, as the process of quantifying the efficiency and effectiveness of past action”. A majority of the businesses in the world had taken the past failure as a barrier that will impede business to excel further. The lack of formulating strategy to cope with past failure will cascade the business inefficiency and ineffectiveness.

The rigidity of the organization to adapt the change faces much more born issues than others because organizational change as an implementation of an idea, procedure and process, that is new [7].

Hence, the new approach has taken the shape of binding the relationship between the manager and the employees, for that a balanced performance measure is required [17]. So, it is a duty of managers in organizations to spend their energy and resources to identify some way for improvement, thriving of their institutions instead of securing the status quo [11].

The traditional ways of viewing the business performance were confined to the measures such as return on investment and earnings per share as the measurement system. These measures can mislead and put sluggish to the possible further enhancement of growth and innovations of the business. The strategy that will put an equal amount of emphasis in both financial and operational system is required. Thus, the idea of balanced scorecard was born that takes equal and unbiased emphasis in both financial and operational system. Some scholars [8] emphasized on the balanced measure that focuses on both the financial perspective and the operational perspectives like customers, internal process, growth and learning. This balanced scorecard helps companies in looking, moving and forward instead of backward [8]. Since its inception, the business environment was floated with the application and boosted with balanced scorecard as the strategic tools and faced some meager in its daily application.

To overcome certain drawbacks of the balanced scorecard, the modern approach to these strategic tools was required. The modern balanced scorecard is inclusive of other complimenting tools while originality conceptual part remained intact and had witnessed the evolving of balanced scorecard in recent times [6].

3 The Key Perspectives of Balanced Scorecard

3.1 Financial Perspective

In the BSC, the first and foremost metric covers the financial perspective. This financial perspective refers to the financial health as mandated by stakeholders. It represents the firm long-term goals and deriving superior return based on return on investment [9]. The financial perspective functions as the guiding principle and detects certain flaws in the company if the financial target is not made. The financial quadrant measures the profitability from the shareholders’ perspective and growth from the company’s point of view. In many traditional approaches, the finance was used

extensively as performance measurement and is weighted + A to determine the business excellence. The flaw and excellence in financial perspective should be looked at its root cause rather than fortifying the financial aspects.

The BSC shows that financial quadrant is dependent upon other three quadrants and does not exist individually [2]. In financial perspective, the measure must have significant and easy reference to the firm to interpret it vividly. The measures such as operating income, sales growth and return on investment have to be specific cover under the financial perspective of the BSC [5]. Similarly, other scholars also suggested financial measures such as profit margin, revenue growth, cash flow, net operating income, ROI, revenue per employee, market capitalization, earnings per share and return on equity are vital for financial measurement. The measurement differs from firm to firm owing to their usability and convenience, as not all firms follow the same standardized measurement system.

3.2 Customers' Perspective

The customers represent the epitome of any successful business as the business environment depends on directly to the customer. The lack of insight and strategy to keep customer aligned with the business result in collapse and other some tragic history. Therefore, the customer perspectives depict the relationship with the firm. The customers' concern must be streamlined into four categories such as time, quality, performance, and service and cost [15].

The focus of this perspective should be articulating consumers' values and embodying their satisfaction that will result in increased market share, new customer acquisition, customer retention and finally customer profitability [10]. Alternatively, in many of the businesses, they use most genuine customer measures that suffice to their functional aspect and how they are with business. The customer measures are inclusive of the survey of customer satisfaction, the number of customer complaints, the number of shipments return due to poor quality, warranty repair cost, customer response time and time taken from order to delivery [5].

Earlier, the focus of business was designed for profit-making organization where the customers are referred as a source of profit and interest of an organization, but in the modern business environment, the approach had been very holistic due to the evolution of non-governmental organization to use this approach [14]. Overall, the customers' perspectives indicate how customers are aligned with our products and their quality.

3.3 Internal Business Process

It focuses mainly on the internal processes that have the direct impact on the customers' satisfaction and financial objective as required by the firm for their

sustainability and how it would be looked by the outsiders. Some studies [16] indicated that the internal process functions as an integral process in the organizations, and such it promotes customer's satisfaction and profitability of the organization through identification of relevant products and services for customers and profit of the firm through finalizing key processes that influence these outcomes.

In today's business scenario, it has made an improvement over the existing operation with the inclusion of short wave of value creation and the long wave of value creation. Nevertheless, the firm should go with an entirely new product as it is the driver for the long wave of value creation, which might bring financial gains to a firm provided it is endorsing the customer grievances. Generally, the internal perspective uses measures such as material efficiency variance, the ratio of good output to the total output, manufacturing lead time, the rate of material scrap loss and labor efficiency variance. Despite these measures are very effective parameters to show the effectiveness and efficiency of a firm, some other researchers [4] suggested to use other measures such as production capacity, labor productivity, machine productivity, material usage, setup efficiency, manufacturing time, inventory levels, product flaws and new product introductions.

The recent focus of the internal process depends directly on the process, decision and actions instituted by the organization that links to the customer performance index and the profitability of the firm [8].

The decision confronting the customers' ethics, values and their culture should be discarded as many firms in the world failed due to lack of their adequate process, decision and actions. This perspective requires the tentative actions of evaluating current operation process, improving existing operations and looking for indie at ways of strategy that give maximum support to the customers [1].

3.4 Learning and Growth

The final quadrant in the perspective of balanced scorecard includes learning and growth perspective which emphasizes how an organization can continue to improve and add value. The improvement in the organization from the perspective of learning and growth relates to aligning to business and sustaining for a longer period while the adding value refers to the customers' and stakeholders' satiety. The measures of learning and growth perspective include processes such as an introduction of various new products, the timeframe required to introduce new features, a number of new patents applied or technological improvements. The future success of the organization is also highly dependent on employee relations and a typical balanced scorecard, and thus, it also includes satisfaction of employee, training and turnover of employee [2, 1].

In the modern business environment, this perspective classified broadly as human capital, informational capital and finally organization capital. The human capital refers to the skills, talents and knowledge of the company's employees while the information capital relates to information system, company's database, networks and

technological infrastructure. Finally, organization capital shows company's culture, leadership, the alignment of people to the strategic goals and the employees to share knowledge [1]. This perspective also allows the organizations to constantly review on the job relocation, implement job incentives for employees, provide short- and long-term training and finally inhibit long-term prospect from that employee [13].

Furthermore, the employee relation can be assess through Organizational Stress Screening Tool (ASSET). The ASSET model was developed by researchers [3] which can be used as an initial screening tool to help organizations assess relations.

3.5 The Major Mandates of Business Organizations

1. Revenue generation for its growth and development.
2. Sustainable development in an environmentally and socially friendly manner.
3. To build national capacity (human resource development, technical skills, responsible corporate) through the transfer of managerial and technical skills.
4. To explore, prospect and develop strategies as directed.
5. To support domestic industries by supplying raw materials at a competitive price.

4 Strategic Matrix Design on Balanced Scorecard

The strategic theme translates the real estate organization's vision and policy into a set of measurable targets, and course of action also provides alternative course of action. It is the framework for a strategic measurement where the areas of excellence have been identified based on 7s and VCM models. The category's objectives are based on qualitative or quantitative objectives. However, this will help management to evade those imprudence measures by starting with objectives and assess to define what the real estate company really wants to target and then followed by the relevant measures to evaluate their objectives. In these ways, unnecessary actions will be replaced by proper action, followed by corporate objective, which is geared up with the help of their core values. Horizontal shows the important success factors, a key result area and key performance indicators, and the vertical represents BSC categorized by four perspectives: financial, customer, internal, and learning and growth. We have developed the matrix where we can figure out how four perspectives are interlinked with important success factors, a key result area and key performance indicators in order to accomplish its corporate objectives.

Corporate objectives are depicted in a manner in order to make everyone working in an organization and can comprehend, and with the support of BSC, it maintains the link from the strategy formulation to the strategy execution. Key performance indicators are experimental measurements, which reproduce the important success factors of company and help in defining and measuring progress towards its corporate objectives. KPI also shows a set of measures that focus a key result area to improve

performance aspects, which are most critical factors for the present and upcoming success of an organization.

4.1 Financial Perspective

In financial perspective, focus on improving revenues, reducing cost and increasing productivity, improving asset utilization and decreasing risk can provide the essential connections across all four scorecard perspectives and to corporate objectives. It is also highlighted to achieve financial performance, which is a critical success factor.

4.2 Customer Perspective

In this perspective, companies identify their respective clients and market segment. It also signifies the sources that provide revenue component to company's financial objectives which automatically linked to corporate objectives. The customer perspective facilitates companies to align their core customer outcome measures to targeted customers and market segments.

4.3 Internal Business Perspective

Under this perspective, improving quality, reducing waiting times, maximizing yields, improving distribution and services in their process system, increasing innovation and R&D, and lower costs as a key result area for improvement in their business processes would be defined and measured. In this process, the head of the department will have information on how well their business is running and whether its products and services to match customer requirements (corporate objectives) so that they should explore based on improving the internal process and functions of the organization.

4.4 Learning and Growth Perspective

Perspective includes individual training for corporate self-improvement and corporate cultural attitudes. In the current scenario, there is a rapid change of technology, which has become essential for workers in a continuous learning mode. The learning and growth represent the crucial foundation for the success of any organization.

4.5 *Bloomfield Matrix*

The purpose of designing such matrices is to establish a bond between the areas of excellence (the strategic theme) in business and four perspectives of BSC. Besides, the vision and mission of the real estate company are the essential parts of determining strategic themes because these statements provide a qualitative and quantitative objective, measure, target, action and alternative course of action. All the strategic themes used here are derived from 7s and VCM models because these models build the foundations entire holistic views of operating the business in the market.

The below given model depicts the application of balanced scorecard through strategic Bloomfield Matrix with critical success factor, key result areas and key performance indicators in alignment with VMGO based on Strategic theme, Strategy, Structure, System, Shared value skill, Style, Staff (7s) and Value Chain Management. The below given model is useful in working out the long-term strategy of a real estate company in view of all four quadrants of balanced scorecard for efficient and effective organization.

5 Conclusion

To conclude, this study qualitatively explores various models, approaches and tools to furnish, support and rejuvenate the very purposes and objectives of the topic that are to design a strategic road map using BSC and every instrument of BSC to establish a link with a vision and mission of a real estate company.

This study highlights the basic foundations, guidelines and rudimentary elements that are required for the development of strategic plan using the BSC. From each perspective of the BSC, the topmost priorities have been selected by the respondents to indicate that these guidelines are necessary for the management to steer real estate company forward in a strategic way. These models and guidelines will direct management to adopt the BSC in all three departments of the company as the alignment; strategic framework guides its decision for better adoption. The various models such a Bloomfield Matrix, Functional Double Looping, Theory Z Plus, 7s and VCM really analyze, link, direct and supervise the management's decision in terms of a strategic development plan. Moreover, the vision and mission have been interlinked with the strategic themes and BSC for matching the strategy of the real estate company. The study indicates that the company has to concentrate more on customer acquisition and customer relation. Likewise, the study revealed that the most financial measures needed are liquidity ratio, net profit margin and shareholder value while for the internal business process, the procurement, inward and outwards logistics are the topmost factors required for the company. Finally, for learning and growth, the factors like job control and research time are required for the real estate company, and this is how the management is being guided.

Indeed, the BSC is a performance measurement tool, where it critically analyzes the four major quadrants of the business which will help the management to determine effective strategies in connection with the changing business environments. Thus, the management can respond to the changing economic climate through changing the weights of the quadrants of each BSC.

References

1. B.A. Leauby, K. Wentzel, Know the score: The balanced scorecard approach to strategically assist clients. *Pennsylvania CPA J.* 29–32 (2002)
2. C. Correia, K. Langfield-Smith, H. Thorne, R.W. Hilton, Information for the Managing and Creating Value. *Management Accounting*. Southern African ed. Berkshire: McGraw-Hill, p. 1210 (2008)
3. S. Cartwright, C.L. Cooper, *ASSET: An Organisational Stress Screening Tool—The Management Guide* (Robertson/Cooper Ltd., Manchester, 2002)
4. C.W. Chow, W.A. Van Der Stede, The use and usefulness of nonfinancial performance measures. *Manag. Account. Q.* 7(3), 1 (2006)
5. Z. Hoque, W. James, Linking balanced scorecard measures to size and market factors: Impact on organizational performance. *J. Manag. Account. Res.* 12, 1–17 (2000)
6. I. Cobbold, L. Gavin, The development of the balanced scorecard as a strategic management tool. *Performance Measurement Association* (2002)
7. J. Pierce, A. Delbecq, Organizational structure, individual attitudes and innovation. *Acad. Manag. Rev.* 27–37 (1977)
8. R.S. Kaplan, D.P. Norton, The balanced scorecard—measures that drive Performance. *Harvard Bus. Rev.* 70(1), 172–180 (1992)
9. R.S. Kaplan, D.P. Norton, *The Balanced Scorecard: Translating Strategy into Action*, vol. 70 (Harvard Business School Press, Boston, 1996)
10. J. Michalska, The usage of the balanced scorecard for the estimation of the enterprise's effectiveness. *J. Mater. Process. Technol.* 162–163, 751–758 (2005)
11. N. Feghi Farahmand, Review of the status of key factors in performance of servicing organizations by BSC technique. *J. Ind. Manag. Faculty of human sciences, IAU, Sanandaj branch, career 4*, 10, 57–67 (2009)
12. A. Neely, C. Adams, M. Kennerley, *The Performance Prism: The Scorecard for Measuring and Managing Business Success* (Financial Times Prentice Hall, London, 2002)
13. P. Niven, *Balanced Scorecard Step-By-Step: Maximizing Performance and Maintaining Results* (John Wiley & Sons Inc., New York, 2002)
14. R. Samizadeh, S.K. Chaharsooghi, Presentation of performance evaluation in SMEs to take E-commerce. *Int. J. Eng. Sci. Iran University of Sciences and Technology (IUST)*, career 1, 19, 65–79. 71 (2008)
15. R.S. Kaplan, D.P. Norton, Measuring the strategic readiness of intangible assets. *Harvard Bus. Rev.* 1, 1–14 (2004)
16. K.R. Thompson, N.J. Mathys, The aligned balanced scorecard: An improved tool for building high performance organizations. *Organ. Dyn.* 37(4), 378–393 (2008)
17. M.H. Zarei, M. Jamparazmi, H. Yazdani, H. Biriaei, Review the relationship among corporative strategic tendency and organizational performance by means of BSC approach. *J. Commer. Adm.* 2(3), 97–112 (2010)

Boost Converter with Generalized Quadratic Boosting Cell with Reduced Capacitor Voltage Stresses



Adyasha Acharya, Lipika Nanda, Tapas Roy, and Banishree Misra

1 Introduction

The advanced electrical technology is mostly depended on the renewable energy sources like solar PV, wind turbine, fuel cells, etc., whose output are insufficient for high voltage applications [1]. The conventional boost converter is the best solution for these mentioned problems, but the maximum voltage gain (occurring at 90% of duty ratio) of boost converter is practically not feasible to implement [2]. Various other issues like switch and capacitor voltage stresses also tend to deteriorate the converters efficiency. The solution of such demerits are the newly derived topologies like cascaded boost converter [3–8], quadratic boost converter [9], multidevice boost converter [10], modified quadratic converters [1, 2, 10–13], etc. A cascaded boost converter steps up the voltage without wide variation in duty ratio, but decreases the overall efficiency of converter due to multiple switching losses [3]. A quadratic boost converter is proposed [9] for high voltage gain applications and reduced power loss due to single switch. The switch and capacitor voltage stresses are the main problems in quadratic boost topology, that was solved by the application of a capacitor–inductor–diode (CLD). In paper [10], the CLD cell is added to a multidevice boost converter such that a highest voltage gain and minimal voltage stress across switch are obtained but due to extra switch the losses increases. In paper [11], a new quadratic boost converter is introduced that is much better in terms of reduced

A. Acharya (✉) · L. Nanda · T. Roy · B. Misra
School of Electrical Engineering, Kalinga Institute of Industrial Technology University,
Bhubaneswar, Odisha, India
e-mail: adyasha.acharya95@gmail.com

L. Nanda
e-mail: lnandafel@kiit.ac.in

T. Roy
e-mail: tapas.royfel@kiit.ac.in

capacitor voltage stress on comparison with quadratic boost topology but the input current is discontinuous in nature. In paper [12], the topology-I attains a high output voltage gain at low duty ratio reducing the discontinuous input current, but it requires extra inductors and capacitors. In this paper, the quadratic cell [11] has been generalized. The general structure consists of a number of quadratic cells. The advantages are: (1) the voltage gain varies by selecting appropriate number of quadratic cells and duty ratios. These provides more flexibility to produce an appropriate output voltage for a specific application. (2) the stress voltage across the buffer capacitors is decreased as compared to other topologies at a same duty ratio. The paper is organized as follows: (Sect. 2) Quadratic boosting cell and converter, (Sect. 3) Generalized quadratic boosting cell, (Sect. 4) Proposed converter operating mode, (Sect. 5) Theoretical comparison, (Sect. 6) Simulation result, (Sect. 7) Capacitor voltage stresses comparison results, and (Sect. 8) Conclusion.

2 Quadratic Boosting Cell and Converter

Figure 1 shows the boost converter that contains a switch, a diode, two passive elements that is an inductor that stores or releases energy and a capacitor that filters the output voltage. The output voltage is controlled by controlling the duty cycle. The obtained expression of output voltage is given in Eq. (1):

$$V_0 = \frac{V_{in}}{(1-d)} \quad (1)$$

The maximum voltage gain of boost converter is practically difficult to achieve, followed by other issues like switch and capacitor voltage stresses that deteriorate the efficiency of converter. In Fig. 2, a quadratic boosting structure [11] is shown that consists of a capacitor C , two diodes (D_1, D_2) and two inductors (L_1, L_2). Inductors charge in parallel manner during switch on mode and discharge in serial manner during switch off mode. Adding single boosting cell ($n = 1$) in place of the inductor L in a boost converter shown in Fig. 3, the output voltage gain expression is given in

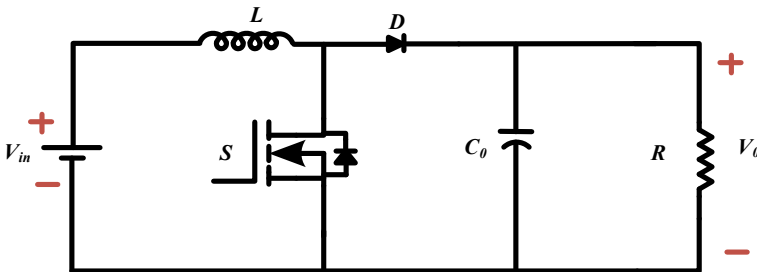


Fig. 1 Conventional boost converter

Fig. 2 Basic boosting cell

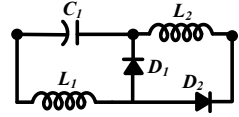
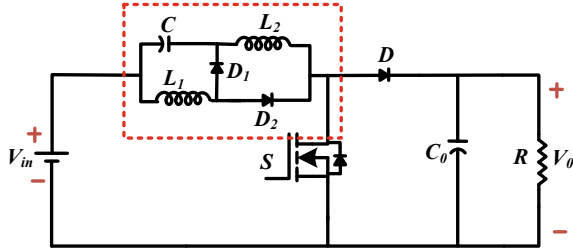


Fig. 3 Boost converter with single quadratic boosting cell ($n = 1$)



Eq. (2):

$$\frac{V_0}{V_{in}} = \frac{1}{(1 - d)^2} \tag{2}$$

3 Generalized Quadratic Boosting Cell Structure

Addition of an extra capacitor C_2 , inductor L_3 and two diodes (D_3, D_4) to the boosting cell forms, two quadratic boosting cell structure ($n = 2$) as shown in Fig. 4 and output voltage gain is given in Eq. (3):

$$\frac{V_0}{V_{in}} = \frac{1}{(1 - d)^3} \tag{3}$$

Similarly, addition of another capacitor C_3 , inductor L_4 and diodes (D_5, D_6) in the previous structure shown in Fig. 4 forms a three quadratic boosting cell structure

Fig. 4 Two quadratic boosting cells ($n = 2$)

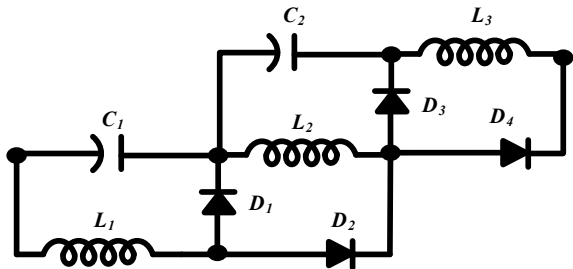


Fig. 5 Three quadratic boosting cells ($n = 3$)

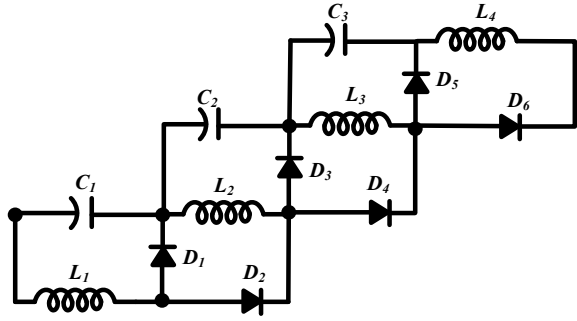
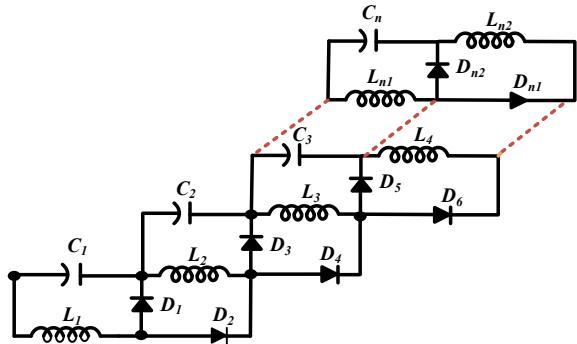


Fig. 6 n quadratic boosting cells



($n = 3$) shown in Fig. 5 and the voltage gain is given in Eq. (4):

$$\frac{V_0}{V_{in}} = \frac{1}{(1 - d)^4} \tag{4}$$

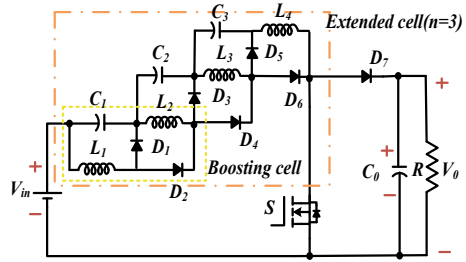
Therefore, on addition of n number of capacitors, inductors, and diodes in same manner, n number of quadratic boosting cell structure are developed as shown in Fig. 6 and the generalized voltage gain expression is given in Eq. (5). Hence, the output voltage gain is dependent on the number of quadratic boosting cells.

$$\frac{V_0}{V_{in}} = \frac{1}{(1 - d)^{n+1}} \tag{5}$$

4 Proposed Converter and Operating Modes

The proposed converter with a generalized quadratic boosting cell structure ($n = 3$) is shown in Fig. 7. First cell contains two inductors (L_1, L_2), capacitor C_1 and two

Fig. 7 Proposed converter



diodes (D_1, D_2). Second cell contains two inductors (L_3, L_2), capacitor C_2 , and two diodes (D_3, D_4). Third cell contains two inductors (L_4, L_3), capacitor C_3 and two diodes (D_5, D_6). All the components in the proposed converter are considered ideal (Fig. 7).

Mode 1: In model, the switch is on as shown in Fig. 8. Diodes (D_1, D_3, D_5, D_7) are reverse biased and diodes (D_2, D_4, D_6) are forward biased. The inductor L_1 get charged from supply V_{in} , inductor L_2 is charged from capacitor C_1 , and similarly, inductors L_3 and L_4 get charged from capacitors C_2 and C_3 . So the inductor currents ($I_{L1}, I_{L2}, I_{L3}, I_{L4}$) rise linearly as shown in Fig. 9. Hence, it is observed that inductors (L_1, L_2) and (L_3, L_4) charge parallelly and the capacitor C_0 discharges energy to load.

Mode 2: In mode 2, the switch is off as shown in Fig. 10. Diodes (D_1, D_3, D_5, D_7) are forward biased and diodes (D_2, D_4, D_6) are reverse biased. The inductors (L_1, L_2)

Fig. 8 Proposed converter when ($s = on$)

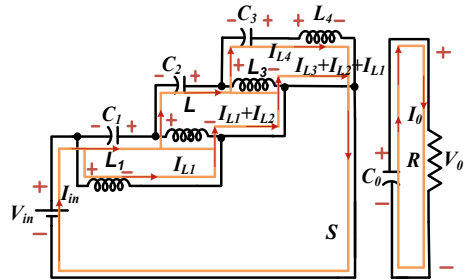


Fig. 9 Inductor currents waveforms

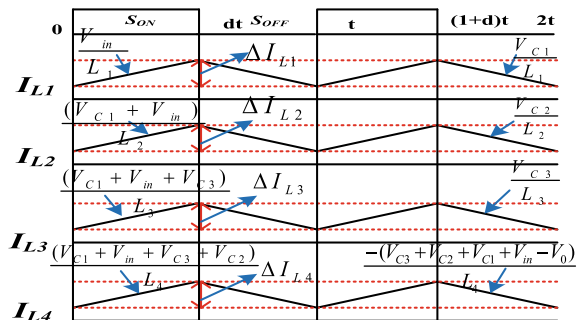
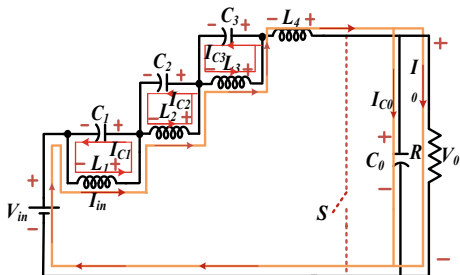


Fig. 10 Proposed converter when ($s = \text{off}$)



discharge in serial manner and inductor currents (I_{L1}, I_{L2}) fall linearly. Similarly, the inductors (L_3, L_4) also discharge serially and inductor currents (I_{L3}, I_{L4}) fall linearly as shown in Fig. 9 supplying energy to capacitor C_0 and load. Applying volt sec balance to inductor voltage equations, we get following capacitor voltage equations:

$$V_{C1} = \left[\frac{V_{in} \times d}{(1-d)} \right]; \quad V_{C2} = \left[\frac{V_{in} \times d}{(1-d)^2} \right]; \quad V_{C3} = \left[\frac{V_{in} \times d}{(1-d)^3} \right]; \quad \left[V_0 = \frac{V_{in}}{(1-d)^4} \right]$$

After applying charge second balance in capacitor currents, the value of inductance ($L = 4$) obtained is as follows:

$$L_1 = \frac{V_{in} \times d(1-d)^4}{2f_s I_0}; \quad L_2 = \frac{V_{in} \times d(1-d)^2}{2f_s I_0}; \quad L_3 = \frac{V_{in} \times d}{2f_s I_0}; \quad L_4 = \frac{V_{in} \times d}{2f_s I_0(1-d)^2}$$

5 Theoretical Comparison

The proposed converter is compared with existing converters as shown in Table 1 on various parameters. The obtained output voltage gain of proposed converter is highest as compared to existing converters for same duty ratio. It is observed that the voltage gain of the proposed converter depends on the number of quadratic boosting cell structure for an appropriate duty ratio.

Figure 11 shows the dependency of output voltage gain on the number of quadratic boosting cell structure (n) for a range of duty ratio (d). It is observed that the output voltage gain keeps on increasing as the number of boosting cells (n) increases.

The proposed converter is compared with cascaded boost converter on the basis of voltage stresses across each capacitor for different ranges of duty ratio considering the same output gain. Figure 12 shows the reduced capacitor stress voltage (V_{C1}) of proposed converter as compared to the capacitor stress voltage (V_{C1}) of cascaded converter. Similarly, Fig. 13 shows the reduction in capacitor voltage stress (V_{C2}) of proposed converter as compared to the capacitor voltage stress (V_{C2}) of cascaded converter. Finally, Fig. 14 shows the reduction in capacitor voltage stress (V_{C3}) of

Table 1 Theoretical comparison of different converters with proposed topology

Converters	Boost	Quadratic boost	Cascaded boost	Topology-I [12]	Proposed converter
Output gain	$V_0 = \frac{V_{in}}{1-d}$	$V_0 = \frac{V_{in}}{(1-d)^2}$	$V_0 = \frac{V_{in}}{(1-d)^4}$	$V_0 = \frac{V_{in}}{(1-d)^3}$	$V_0 = \frac{V_{in}}{(1-d)^4}$
Switches	1	1	4	1	1
Frequency	f_s	f_s	f_s	f_s	f_s
Capacitors	1	2	4	3	4
Inductors	1	2	4	3	4
Diodes	1	2	4	5	7
V_{C1}	-	$V_{C1} = \frac{V_{in}}{(1-d)}$	$V_{C1} = \frac{V_{in}}{1-d}$	$V_{C1} = \frac{V_{in}}{1-d}$	$V_{C1} = \frac{V_{in} \times d}{1-d}$
V_{C2}	-	$V_{C2} = \frac{V_{in}}{(1-d)^2}$	$V_{C2} = \frac{V_{in}}{(1-d)^2}$	$V_{C2} = \frac{V_{in} \times d}{(1-d)^2}$	$V_{C2} = \frac{V_{in} \times d}{(1-d)^2}$
V_{C3}	-	-	$V_{C3} = \frac{V_{in}}{(1-d)^3}$	-	$V_{C3} = \frac{V_{in} \times d}{(1-d)^3}$

Fig. 11 Variation in output voltage gain with n quadratic boosting cell for a range of duty ratio

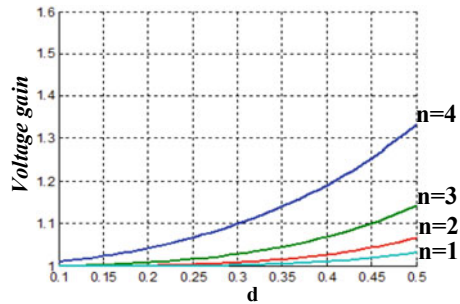


Fig. 12 Reduction in capacitor voltage stress of proposed converter than the capacitor voltage stress of cascaded boost converter (V_{C1})

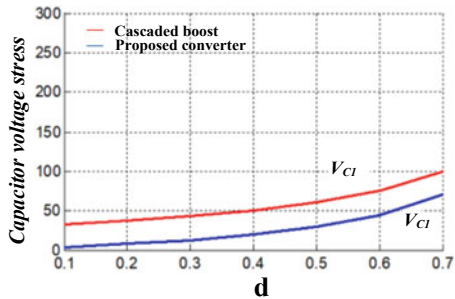


Fig. 13 Reduced in capacitor voltage stress (V_{C2}) of proposed converter than the capacitor voltage stress (V_{C2}) of cascaded boost converter

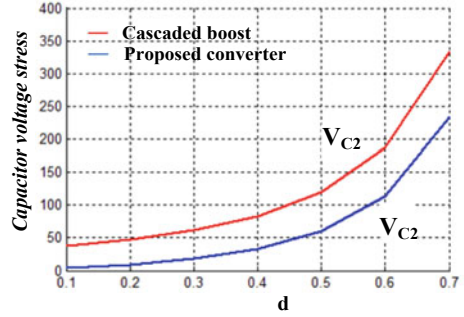
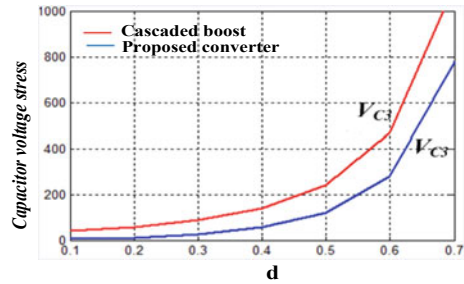


Fig. 14 Reduced in capacitor voltage (V_{C3}) stress of proposed converter than capacitor voltage stress (V_{C3}) of than cascaded boost converter



proposed converter as compared to the capacitor voltage stress (V_{C3}) of cascaded converter.

6 Simulation Results

The proposed converter is designed using following specifications given in Table 2 to determine the values of inductance ($L = 4$) and finally, simulated in

Table 2 Parameters to design the proposed converter

Parameters	Values
Input voltage (V_{in})	30 V
Output voltage (V_0)	480 V
Duty ratio (d)	0.5
Switching frequency (f_s)	5 kHz
Power (P)	500 W
Input current (I_{in})	16.66 A
Output current (I_0)	1.041 A
Load resistance (R)	460 Ω

MATLAB/SIMULINK platform. Hence, the calculated values of inductance ($L = 4$) from following parameters are obtained. The standard values of capacitors ($C_1 = C_2 = C_3 = 470 \mu\text{F}$) are selected.

$$L_1 = \frac{V_{in} \times d(1 - d)^4}{2f_s I_0} = \frac{30 \times 0.5 \times (1 - 0.5)^4}{2 \times 5000 \times 1.041} = 0.09 \text{ mH}$$

$$L_2 = \frac{V_{in} \times d(1 - d)^2}{2f_s I_0} = \frac{30 \times 0.5 \times (1 - 0.5)^2}{2 \times 5000 \times 1.041} = 0.36 \text{ mH}$$

$$L_3 = \frac{V_{in} \times d}{2f_s I_0} = \frac{30 \times 0.5}{2 \times 5000 \times 1.041} = 1.44 \text{ mH}$$

$$L_4 = \frac{V_{in} \times d}{2f_s I_0(1 - d)^2} = \frac{30 \times 0.5}{2 \times 5000 \times 1.041 \times (1 - 0.5)^2} = 5.769 \text{ mH}$$

The simulated diagram of proposed converter is shown in Fig. 15 and various outputs like output voltage (V_o), output current (I_o), switch stress voltage (V_{sw}), inductor currents ($I_{L1}, I_{L2}, I_{L3}, I_{L4}$) are obtained as follows (Figs. 17, 16, 22, 18, 19, 20, and 21).

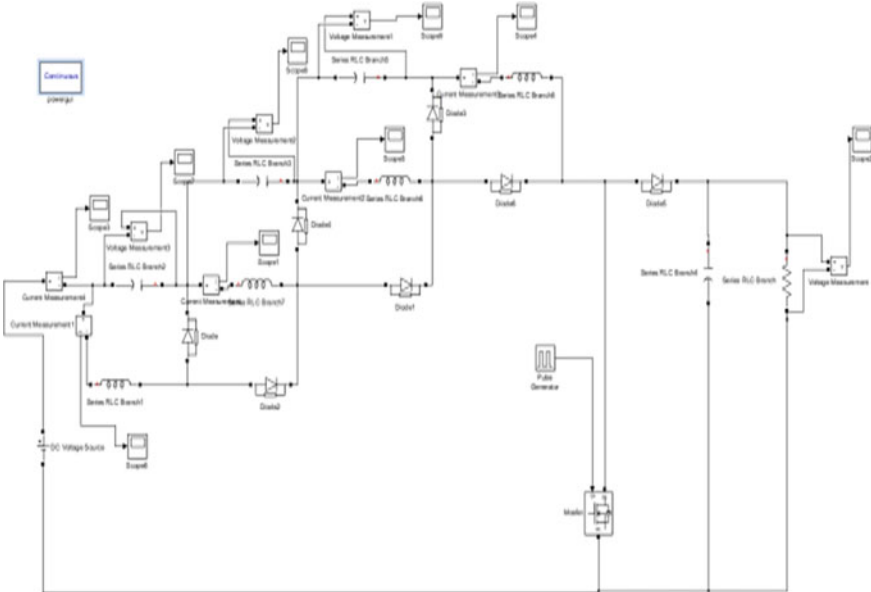


Fig. 15 SIMULINK diagram of proposed converter

Fig. 16 Output current (I_o) waveform

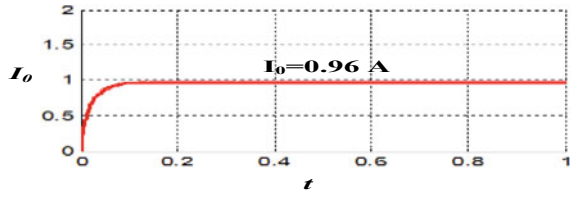


Fig. 17 Output current (V_o) waveform

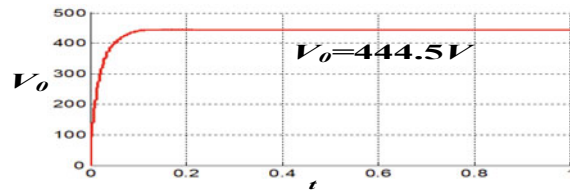


Fig. 18 Inductor current (I_{L1}) waveform where upper limit inductor current ($I_{L11} = 36 \text{ A}$) and lower limit inductor current ($I_{L12} = 6.6 \text{ A}$)

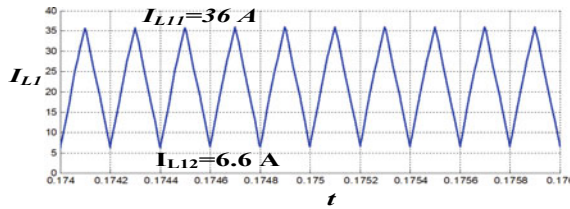


Fig. 19 Inductor current (I_{L2}) waveform where upper limit inductor current ($I_{L21} = 18.1 \text{ A}$) and lower limit inductor current ($I_{L22} = 3 \text{ A}$)

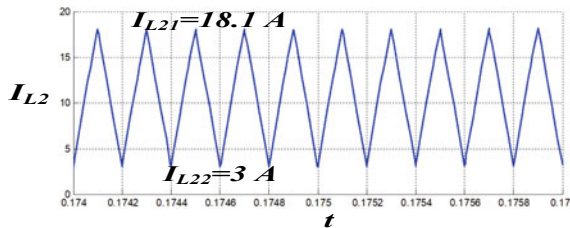


Fig. 20 Inductor current (I_{L3}) waveform where upper limit inductor current ($I_{L31} = 9.1 \text{ A}$) and lower limit inductor current ($I_{L31} = 1.5 \text{ A}$)

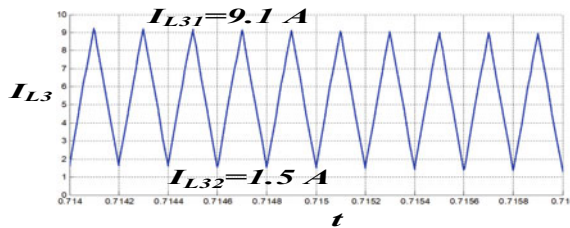


Fig. 21 Inductor current (I_{L4}) waveform where upper limit inductor current ($I_{L41} = 4.4$ A) and lower limit inductor current ($I_{L42} = 0.6$ A)

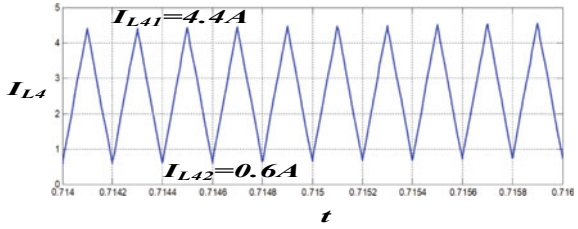
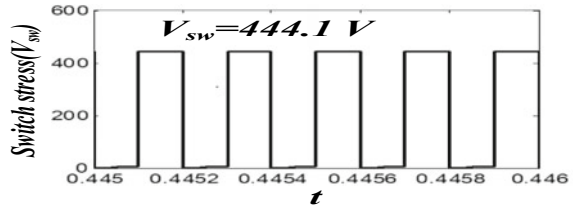


Fig. 22 Voltage across switch (V_{sw})



7 Capacitor Voltage Stresses Comparison

A comparative analysis between the proposed converter and the cascaded boost converter on the basis on capacitor voltage stresses of each capacitor is performed in MATLAB/SIMULINK and different simulation results are obtained. It is observed that the capacitor voltage stresses (V_{C1} , V_{C2} , V_{C3}) in proposed converter as shown in Figs. 23, 25 and 27 is much reduced as compared to the capacitor voltage stresses (V_{C1} , V_{C2} , V_{C3}) shown in Figs. 24, 26 and 28 of a cascaded boost converter for same duty ratio ($d = 0.5$).

Fig. 23 Capacitor voltage stress (V_{C1}) across proposed converter is reduced

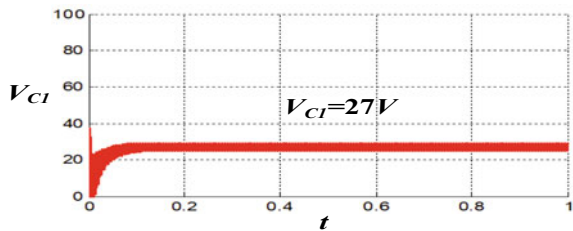


Fig. 24 Capacitor voltage stress (V_{C1}) across cascaded boost converter

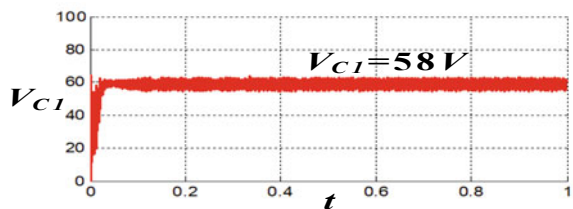


Fig. 25 Capacitor voltage stress (V_{C2}) across proposed converter is reduced

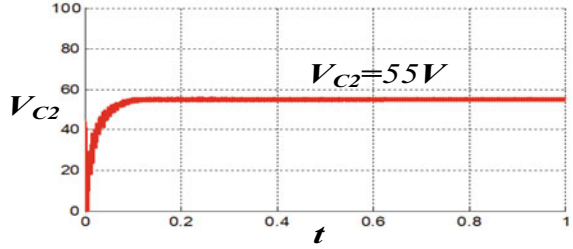


Fig. 26 Capacitor voltage stress (V_{C2}) across cascaded boost converter

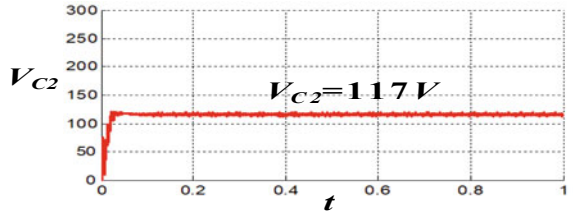


Fig. 27 Capacitor voltage stress (V_{C3}) across proposed converter is reduced

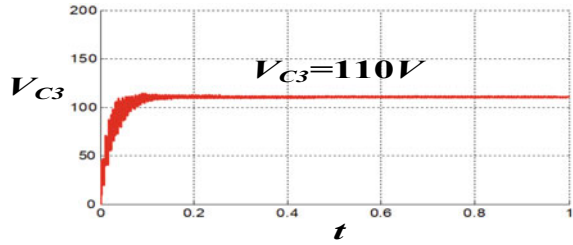
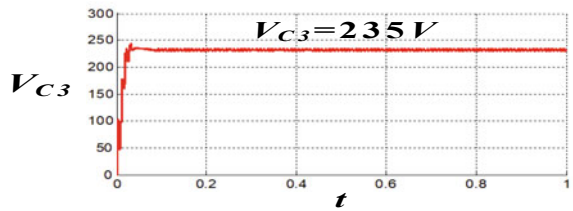


Fig. 28 Capacitor voltage stress (V_{C3}) across cascaded boost converter



8 Conclusion

A complete simulation of the proposed converter with generalized structure of quadratic boosting cell ($n = 3$) is performed in MATLAB/SIMULINK. The proposed converter shows an increase in its output voltage gain even at a low duty ratio justifying the dependency of output voltage gain on number of quadratic boosting cells. Also reduction in voltage stresses is mainly observed across the capacitors when the

proposed converter is compared with the cascaded boost converter for same duty ratio ($d = 0.5$). This feature reduces the capacitor voltage ratings well as cost of the capacitors utilized in proposed converter. The hardware implementation of the proposed converter needed to be accomplished in the near future to verify its merits and effectiveness.

References

1. F. Blaabjerg, Y. Yang, K. Ma, X. Wang, Power electronics the key technology for renewable energy system integration, in *International Conference on Renewable Energy and Research Applications, Palermo* (2015), pp. 1618–1626
2. M. Forouzesh, Y.P. Shrivakoti, S.A. Gorji, F. Blaabjerg, B. Lehman, Step up DC to DC converter, a compressive review on voltage boosting techniques, topology and applications. *IEEE Trans. Power Electron.* **32**(12), 9143–9148 (2017)
3. L.J. Huber, A design approach for server power supply for networking applications, in *Proceedings of IEEE Applied Power Electronics Conference and Exposition* (2000), pp. 1163–1169
4. K.C. Tseng, T.J. Liang, Novel high efficiency step up converter, in *IEEE Proceedings Electric Power Applications*, vol. **151**(2) (2004), pp. 182–190
5. G. Ortiz-Lopez, J. Leyva Ramos, Modelling and analysis of switch mode cascaded converters with a single active switch. *IET Power Electron.* **1**(4), 478–487 (2008)
6. L. Wuha, H. Xiangning, Review of non isolated high step up dc-dc converters in photovoltaic grid connected applications. *IEEE Trans. Ind. Electron.* **58**(4), 1239–1250 (2011)
7. D. Maksimovic, S. Cuk, Switching converters with wide dc conversion range. *IEEE Trans. Power Electron.* **6**(1), 369–378
8. P. Yang ,J. Xu, Member IEEE, G. Zhou, S. Zang, A new quadratic boost converter with high voltage step up ratio and reduced voltage stresses, in *IEEE 7th International Power Electronics and Motion Control Conference-ECCE, Aaia*, June 2012, Harbin, China (2012)
9. K. Tattiwong, C. Bunlaskananusorn, Analysis design and experimental verification of a quadratic boost converter. *IEEE* (2014)
10. I. Das, T. Roy, A new multi device boost converter topology with reduced switching stresses and high voltage applications. ppID-77, MFIIS, Sept 2015
11. Y. Ye, K.W.E. Chang, Quadratic boost converter with buffer capacitor voltage stress. *IET Power Electron.* **7**(5), 1162
12. Y. Li, S. Sathiakumar, The improvement of cascaded converter design using quadratic boosting structure with high voltage gain and low duty cycle. *IEEE* (2019)
13. Y.T. Chen, M.H. Tsai, R.H. Liang, DC-DC converter with high voltage gain and reduced switch stress. *IET Power Electron.* **7**(10), 2564–2571

Performance Analysis of Transistor Clamped H-Bridge Multi-reference Multi-level Inverter for Standalone PV System



Siddheswar Kar, Ranjeeta Patel, and Sarat Kumar Mishra

1 Introduction

Due to the rapid rate of rise in population and swift modernization, the electric energy requirement has gone up manifold causing a higher demand to produce electricity from non-conventional sources [1]. Among the non-conventional energy sources, the photovoltaic (PV) modules have been gaining popularity as they provide a pollution-free environment [2]. They have an edge over other renewable sources due to fewer maintenance requirements, lower cost of operation and cleanliness [3]. The advent of power electronic converters has added more flexibility to the use of solar energy [4]. The atmospheric conditions like temperature and solar radiation are highly unpredictable which affects the performance of the solar PV systems. Further, there is a need to track the load variations under the inherently changing solar conditions. Hence, for optimum power extraction during all hours of the day with varying conditions of atmosphere, MPPT algorithms have been developed. Because maximum power operation of the PV arrays causes increase in efficiency as well as decrease in outlay of the system [5, 6]. Solar energy is converted into an electrical DC supply with the help of a PV cell. Hence, a standalone PV system requires an inverter to convert DC into AC. The main disadvantage of an inverter is its harmonic content at the output. It put impacts on the distribution network; i.e., it degrades the quality

S. Kar (✉)

Mandsaur University (MU), Mandsaur, Madhya Pradesh 458001, India

e-mail: suru.sidhu@gmail.com

R. Patel

Kalinga Institute of Industrial Technology, Bhubaneswar, Odisha 751024, India

e-mail: ranu.susa@gmail.com

S. K. Mishra

Padmanava College of Engineering, Rourkela, Odisha 769002, India

e-mail: mishra.sarat@gmail.com

© Springer Nature Singapore Pte Ltd. 2021

K. S. Sherpa et al. (eds.), *Advances in Smart Grid and Renewable Energy*,

Lecture Notes in Electrical Engineering 691,

https://doi.org/10.1007/978-981-15-7511-2_9

of supply and increases the losses. Among inverters, a multi-level one is better for PV applications because it has a number of advantages: (i) lower total harmonic distortion (THD) and (ii) low switching losses; still, the levels of inverter affect the harmonic content [7–11]. The TCHBMLI is chosen here due to its own advantages of less number of switching devices usage, and hence, less switching loss out of various familiar multilevel inverters like flying capacitor type, diode clamped, and cascaded H-bridge inverters. The transistor clamped MLI needs equal number of power devices as the inverter level or less [12–21]. Hence, the usage of power devices is reduced to nearly half of the power devices required by other topologies. An analysis is made on the performance of a grid-interactive PV system fed from 5-level and 7-level inverter, and the efficiency of the system has been assessed [22]. In this paper, a detailed analysis has been presented to decide the better one between the single-phase 5-level and 7-level TCHBMLIs for standalone PV system on the basis of lower total harmonic distortion (THD) and filter size requirements. The multi-reference switching scheme is used for generating switching pulses for the power devices being used for transistor clamped multilevel inverter.

2 Multi-reference-Based Transistor Clamped H-bridge Inverter

2.1 5-level and 7-level TCHBMLI

The TCHB inverter has its own advantages as compared to other multilevel inverters. The number of power devices, i.e., IGBT switches required is five for the 5-level TCHBMLI, whereas for the 7-level TCHBMLI is six. This indicates that the required number of power devices does not rise proportionately as the number of levels rise. For the 5-level TCHBMLI, the configuration is as shown in Fig. 1a. This configura-

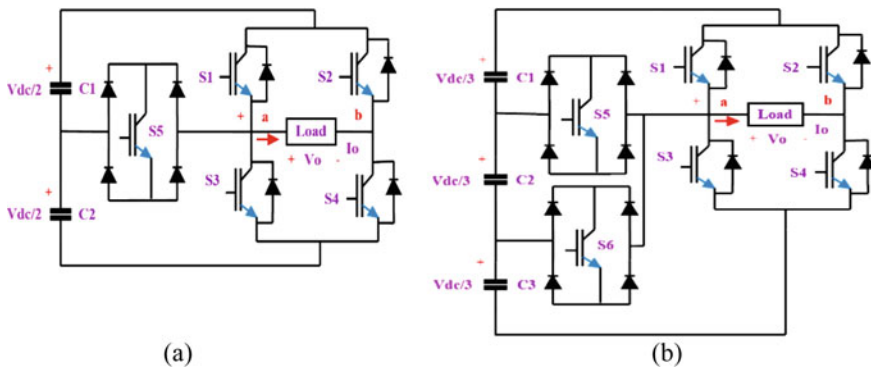


Fig. 1 Configuration of a 5-level, b 7-level TCHBMLI

tion consists of one transistor clamped H-bridge inverter, a supportive circuit (which includes one IGBT switch and four power diode switches), and two DC link capacitors for voltage division. The DC power supply is connected to the load through transistor clamped H-bridge multi-reference inverter. The supportive circuit engenders the input DC voltage to a lower level by 50% [7]. This configuration reduces the arrangement complexity comparison to flying capacitor, diode clamped, and hybrid MLI configurations [8, 9]. The working principle of this new configuration is presented in the references [7, 10, 11]. The levels of the output voltage (V_o) of this transistor clamped multi-reference inverter and switch transition states are given in Table 1. The operation of the switch in a supportive circuit is directed as per load current direction. Similarly, the 7-level transistor clamped MLI consists of total six IGBT switches as depicted in Fig. 1b.

The 7-level TCHBMLI configuration consists of a one-phase TCHB inverter, two supportive circuits (each includes one IGBT switch and four power diode switches), and three DC link capacitors for voltage division. This new configuration has a number of advantages over other configurations, i.e., lesser number of switches and capacitors compared to same level configurations [12]. Seven levels of output voltage are obtained by proper switching of the inverter. Reference levels of the output voltage (V_o) of this TCHBMLI and switch transition states are given in Table 2.

Table 1 Reference levels of V_o (output voltage) and switch transition states of the 5-level TCHBMLI

V_o	S_1	S_2	S_3	S_4	S_5
V_{dc}	On	Off	Off	Off	On
$0.5 V_{dc}$	Off	Off	Off	On	On
0	Off	Off	On	On	Off
$-0.5 V_{dc}$	Off	On	Off	Off	On
$-V_{dc}$	On	Off	Off	On	Off

Table 2 Levels of V_o (output voltage) and switch transition states of the 7-level TCHBMLI

V_o	S_1	S_2	S_3	S_4	S_5	S_6
V_{dc}	On	Off	Off	On	Off	Off
$0.667 V_{dc}$	Off	Off	Off	On	On	Off
$0.334 V_{dc}$	Off	Off	Off	On	Off	On
0	Off	Off	On	On	Off	Off
$-V_{dc}$	Off	On	Off	Off	On	Off
$-0.667 V_{dc}$	Off	On	Off	Off	Off	On
$-0.334 V_{dc}$	Off	On	On	Off	Off	Off

2.2 Multi-reference Switching Scheme

The multi-reference switching scheme uses a sinusoidal pulse width modulation (SPWM) technique. Multi-reference switching scheme is meritorious because of a simplistic controller of smaller size and easier implementation. Multi-reference switching scheme is used here in this 5-level TCHBMLI configuration to generate gate pulses for five numbers of IGBT switches. Out of multicarrier (phase shifted and level shifted) and multi-reference sinusoidal pulse width modulation, here the multi-reference is used for switching pulse generation. In this configuration, a carrier signal, i.e., triangular (V_c), is being compared with two sinusoidal reference signals (V_{ref1} , V_{ref2}) for the generation of gate pulses. Here V_{ref1} and V_{ref2} are of the same phase and frequency but differ by an offset of amplitude V_c as shown in Fig. 2a [13]. This configuration has four modes in one cycle of operation. These modes are as given below [7].

Mode A: [$0 < \theta \leq \alpha1$ and $\alpha2 < \theta \leq \pi$.], Mode B: [$\alpha1 < \theta \leq \alpha2$], Mode C: [$\pi < \theta \leq \alpha3$ and $\alpha4 < \theta \leq 2\pi$], Mode D: [$\alpha3 < \theta \leq \alpha4$].

Modulation index (M) affects the phase angle (θ), and hence, the modulation index of this multi-reference inverter is as given below [14].

$$M = \frac{A_m}{2A_c} \tag{1}$$

where A_m = maximum amplitude of V_{ref1} and V_{ref2} and A_c = Maximum amplitude of V_c . In conventional PWM techniques, several carrier signals are compared with only one reference to create gate pulses [15, 16]. But in this 7-level inverter configuration, three reference signals, i.e., V_{ref1} , V_{ref2} , V_{ref3} are compared with the carrier V_c to generate gate pulses for six numbers of IGBT switches. The V_{ref1} , V_{ref2} , V_{ref3} are of the same phase and frequency but differ by an offset of amplitude V_c as in Fig. 2b. Comparison of (V_{ref1} , V_{ref2} , V_{ref3}) and (V_c) are done as per the following steps:

- (i) If V_{ref1} goes beyond the maximum amplitude of V_c , then V_{ref2} is compared with V_c till maximum amplitude of V_c is reached.
- (ii) When V_{ref2} goes beyond the maximum amplitude of V_c , then V_{ref3} is compared with V_c till it reaches zero.

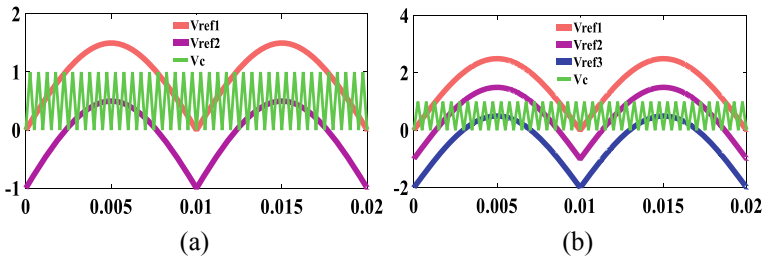


Fig. 2 Generation of switching pulses for IGBTs of a 5-level and b 7-level TCHBMLI

- (iii) When V_{ref3} reaches zero, then V_{ref2} is being compared with V_c till it goes to zero.
- (iv) As soon as V_{ref2} goes to zero, V_{ref1} is compared with V_c and the procedure is continued as depicted in Fig. 2.

The modulation index affects the phase angle, and hence, the modulation index of this multi-reference inverter is as given below [17].

$$M = \frac{A_m}{3A_c} \tag{2}$$

where A_c = maximum value of V_c and A_m = maximum value of $(V_{ref1}, V_{ref2}, V_{ref3})$.

This configuration has six modes in one cycle of operation. These modes are as given below [17].

Mode A: $[0 < \theta < \beta_1 \text{ and } \beta_4 < \theta < \pi]$, Mode B: $[\beta_1 < \theta < \beta_2 \text{ and } \beta_3 < \theta < \beta_4]$, Mode C: $[\beta_2 < \theta < \beta_3]$, Mode D: $[\pi < \theta < \beta_5 \text{ and } \beta_8 < \theta < 2\pi]$, Mode E: $[\beta_5 < \theta < \beta_6 \text{ and } \beta_7 < \theta < \beta_8]$, Mode F: $[\beta_6 < \theta < \beta_7]$.

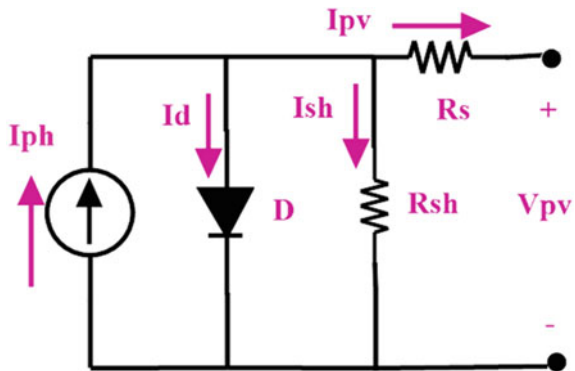
3 Photovoltaic Module Modeling

Several circuits are in use as equivalent of a PV cell. Out of all such equivalent circuits, the one-diode model is simple and accurate [18, 19]; hence, it is applied here. The equivalent model is shown in Fig. 3.

The different symbols of the equivalent circuit are defined as: I_{ph} = photocurrent generated, I_d = current flowing through the shunted diode (D), I_{sh} = current flowing through the shunt resistance (R_{sh}), I_{pv} = output current of PV cell, V_{pv} = output voltage of the PV cell, D = diode parallel to R_{sh} , R_{sh} = shunt resistance, R_s = resistance connected in series with the output.

A PV module consists of many cells in series combinations so as to cater to the voltage requirements of the load [20]. The current equation of the PV module can

Fig. 3 Circuit represented as equivalent of a PV cell



be represented as

$$I_r = I_{SC,r} \left[1 - k_r \frac{V_r + R_s I_r}{V_{OC,r}} - 1 \right] \quad (3)$$

The mentioned parameters of Eq. (3) under standard test condition (STC) are defined as follows: I_r = output current of PV module, $I_{SC,r}$ = short circuit current of PV module, V_r = PV module output voltage, $V_{OC,r}$ = PV module open circuit voltage, and k_r = coefficient of I_{SC}/I_0 .

$$I_{pv} = I_r \frac{I_{SC}}{I_{SC,r}} \quad (4)$$

$$V_{pv} = V_r + (V_{OC} - V_{OC,r}) + R_s(I_r - I_{pv}) \quad (5)$$

3.1 MPPT Algorithm

A number of algorithms are present to run the photovoltaic (PV) array at maximum power. Among all those algorithms, Perturb and Observe (P&O) algorithm is advantageous because of its simplistic structure, low cost, and ease of realization. Hence, in this paper P&O algorithm is being used.

4 Standalone PV System Using TCHBMLI

The implementation block diagram for the standalone PV system with conventional boost converter and TCHBMLI is depicted in Fig. 4. The block diagram consists of 4×4 PV array, 5-level/7-level TCHBMLI, Boost converter, MPPT controller, filter, and load. The PV array has four strings. Each string consists of four modules, i.e., 4×4 as shown in Fig. 5.

Uniform irradiance of $S = 1000 \text{ W/m}^2$ and uniform temperature of $T = 30 \text{ }^\circ\text{C}$ were taken for all the modules to find out V_{pv} and I_{pv} of the 4×4 PV array. To design this PV array, the following parameters were taken [20]: Power = 50 W, $S_r = 1000 \text{ W/m}^2$, $T_r = 25 \text{ }^\circ\text{C}$, $\beta = -0.0033/^\circ\text{C}$, $V_{oc,r} = 22 \text{ V}$, $\alpha = 0.0004/^\circ\text{C}$, $I_{sc,r} = 3 \text{ A}$, $I_{MPP,r} = 2.77 \text{ A}$, $V_{MPP,r} = 17.98 \text{ V}$, $R_s = 0.085 \text{ } \Omega$.

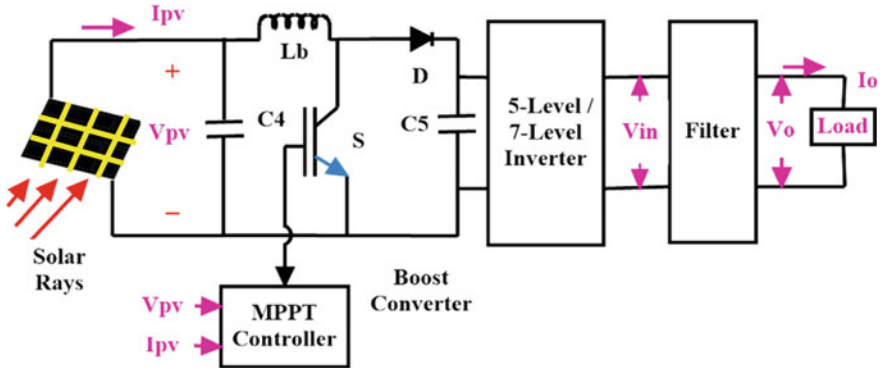


Fig. 4 Implementation block diagram of standalone PV system using TCHBMLI

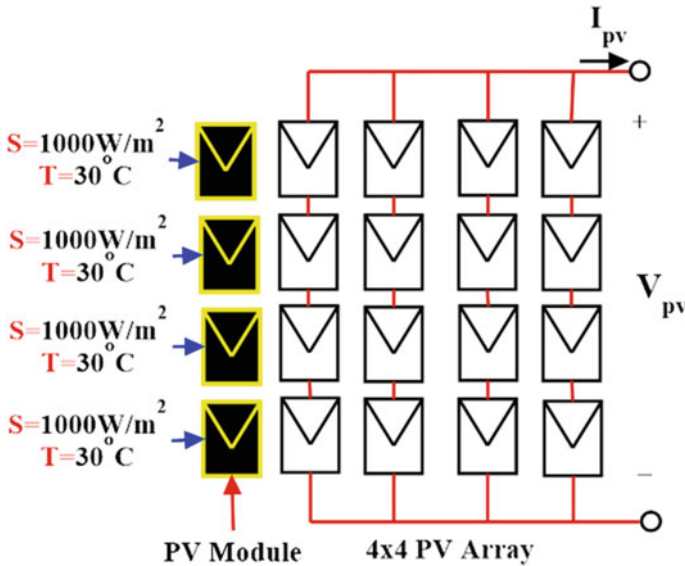


Fig. 5 Implementation diagram of PV array

4.1 Control Strategy Used for Standalone PV System Using TCHBMLI

Figures 6 and 7 represent the control flow diagram for standalone PV system using 5-level TCHBMLI and 7-level TCHBMLI, respectively. In the control flow diagram of Fig. 6, the output of the MPPT controller (δ) is comparing with a triangular wave V_t and producing gate signal for IGBT switch (S) of the boost converter. For the generation of gate signals of IGBT switches (S_1-S_5) of 5-level TCHBMLI, a

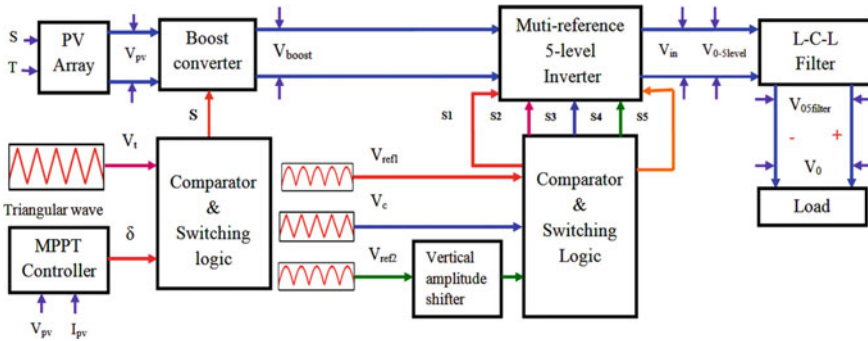


Fig. 6 Control flow diagram for standalone PV system using 5-level TCHBMLI

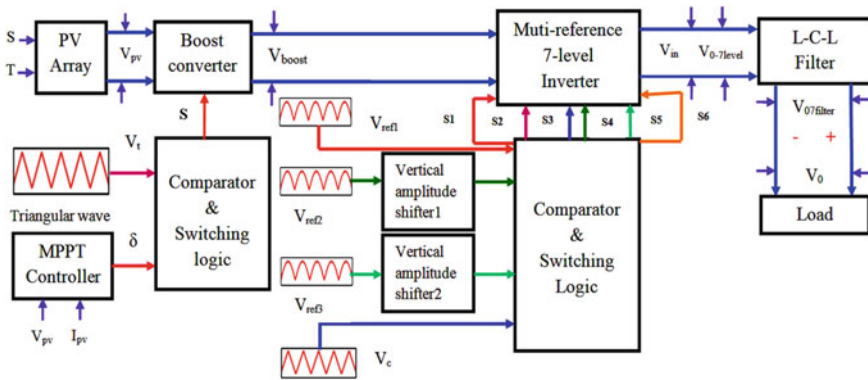


Fig. 7 Control flow diagrams for standalone PV system using 7-level TCHBMLI

triangular signal (V_c) is comparing with V_{ref2} (with a vertical amplitude shifting which is same as the amplitude of V_t) and V_{ref1} .

For standalone PV system using a 7-level TCHBMLI, the procedure of gate pulse generation is the same for IGBT switch S of the boost converter as in Fig. 6. But for the generation of gate pulses of IGBT switches ($S_1 - S_6$) of 7-level TCHBMLI, three reference signals were taken as depicted in Fig. 7. Here triangular signal (V_c) is comparing with V_{ref3} (with a vertical amplitude shifting which is the same as the amplitude of V_t), V_{ref2} (with a vertical amplitude shifting which is the same as the amplitude of V_t) and V_{ref1} .

5 Simulation Results and Discussions

Figure 8 shows the $P_{pv} - V_{pv}$ and $I_{pv} - V_{pv}$ characteristics of a 4×4 PV array. For the operation of 4×4 PV array, uniform irradiance and temperature are taken

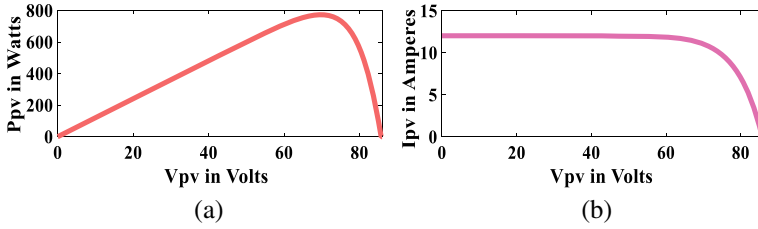


Fig. 8 Variation of photovoltaic array **a** power (P_{pv}) versus voltage (V_{pv}) and **b** current (I_{pv}) versus voltage (V_{pv})

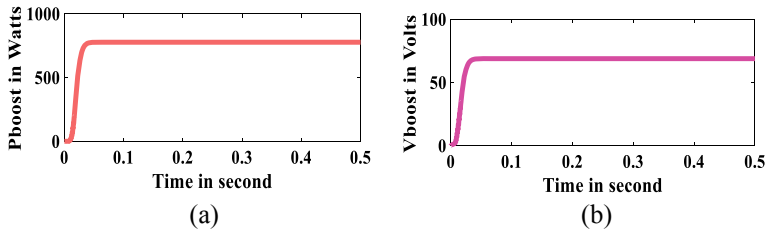


Fig. 9 Variation of boost converter **a** output power (P_{boost}), **b** voltage (V_{boost}) versus time

for all the 16 modules; i.e., for all the modules irradiance, (S) is 1000 W/m^2 and temperature (T) is $30 \text{ }^\circ\text{C}$. From Fig. 8a, b, it is seen that the peak power of the 4×4 array is 773.2 W for a voltage of 68.25 V and short circuit current is 12 A .

To obtain the peak power from the PV array, the P&O algorithm was used for the MPPT controller attached to the boost converter. The parameters of boost converter are as follows: $C_4 = 90 \text{ }\mu\text{F}$, $L_b = 4.2 \text{ mH}$, $C_5 = 1100 \text{ }\mu\text{F}$. Figure 9 shows how power output (P_{boost}) and voltage output (V_{boost}) of boost converter controlling by MPPT controller changing w.r.t time.

From Fig. 9a, b, it was observed that boost converter output power approached the maximum value of PV array, i.e., 773.2 W at a voltage of 68.25 V after an interval of 0.05 s . Hence, this MPPT controller is faster. To achieve this target, a step size of 0.002 and $\Delta\delta$ of 0.009 was taken.

To generate PWM signals for 5-level and 7-level TCHBMLI, a frequency of 2 kHz was taken for the carrier signal. Figure 10a, b depicts the output voltage of 5-level and 7-level TCHBMLI, respectively.

It is observed from the figure that $V_{o5\text{-level}}$ and $V_{o7\text{-level}}$ vary from maximum +ve voltage of 68.25 V to maximum -ve voltage of 68.25 V which was the V_{boost} of boost converter to attain a peak power of 773.2 W . To obtain the required inverter output, following capacitance values are used, for 7-level: $C1 = C2 = C3 = 3000 \text{ }\mu\text{F}$ and for 5-level $C1 = C2 = 3000 \text{ }\mu\text{F}$.

Figure 11 shows the harmonic analysis of 5-level and 7-level TCHBMLI output voltage, respectively. The THD comparison results are enumerated in Table 3. The multilevel output voltages contain harmonics, which is not suitable for loads of

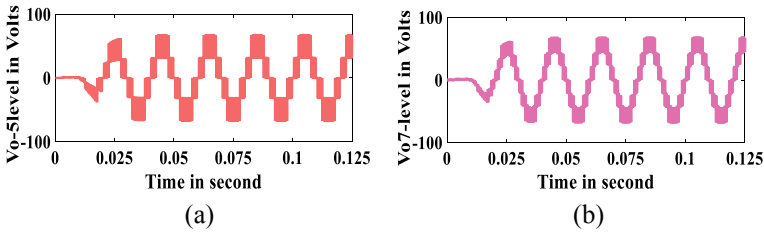


Fig. 10 Variation of output voltage **a** 5-level inverter ($V_{o5\text{-level}}$), **b** 7-level inverter ($V_{o7\text{-level}}$) versus time

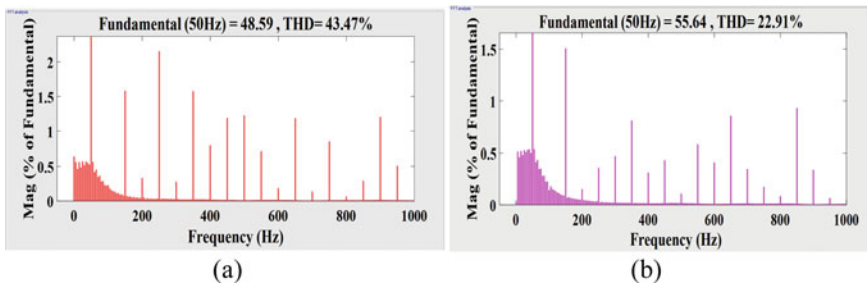


Fig. 11 Harmonic analysis of output voltage V_o **a** 5-level and **b** 7-level

Table 3 Comparison results with the L-C-L filter

Multi-level Inverter	THD analysis	No. of cycles	THD (%)
5-level Inverter	Inverter output voltage ($V_{o5\text{-level}}$)	10	43.47
7-level Inverter	Inverter output voltage ($V_{o7\text{-level}}$)	10	22.91
Filter	THD analysis	No. of cycles	THD (%)
5-level ($L_1 = 7.5$ mH, $L_2 = 7.5$ mH, $C = 2200$ μ F)	Filter output voltage ($V_{o5\text{filter}}$)	10	1.59
7-level ($L_1 = 6.9$ mH, $L_2 = 6.9$ mH, $C = 2200$ μ F)	Filter output voltage ($V_{o7\text{filter}}$)	10	1.57

standalone systems. Hence to smooth the output voltages, filter is required. L-C-L filter is used in this presented system. The parameters used for filter design are as: 5-level inverter: $L_1 = 7.5$ mH, $L_2 = 7.5$ mH, $C = 2200$ μ F and 7-level inverter: $L_1 = 6.9$ mH, $L_2 = 6.9$ mH, $C = 2200$ μ F. Figure 12 depicts the output voltage of the filter for both the inverters. Nearly single-phase sinusoidal voltages of frequency 50 Hz were obtained using the above parameters.

Figure 13 shows the harmonic analysis of load voltages after using filters. Comparison results are as shown in Table 3.

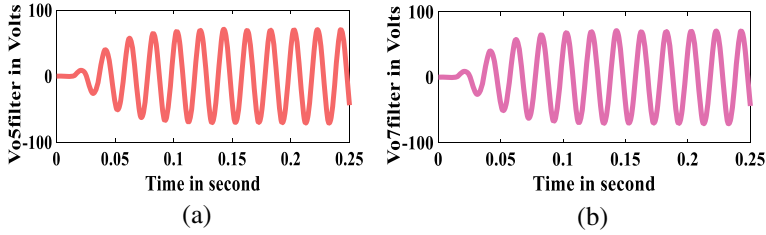


Fig. 12 Variation of a $V_{o5filter}$ and b $V_{o7filter}$ versus time

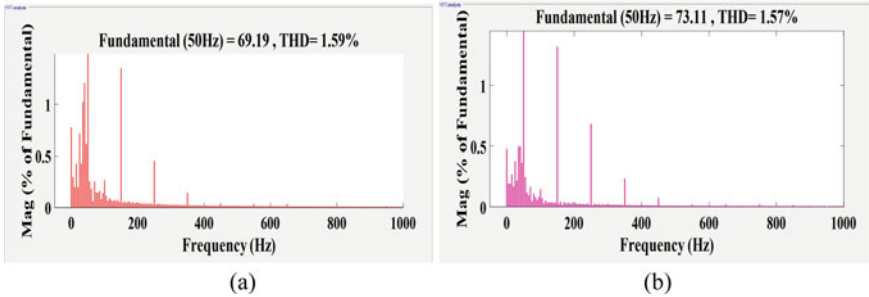


Fig. 13 Harmonic analysis of output filter voltage a $V_{o5filter}$ and b $V_{o7filter}$

6 Conclusion

This paper presented a 4×4 PV array linked to a load (standalone) through a transistor clamped H-bridge multi-reference (5-level and 7-level) inverter and a boost converter. P&O algorithm has been used to track the maximum powerpoint. The performance of TCHBMLI systems was investigated using the MATLAB/Simulink framework. From the obtained results, it is inferred that transistor clamped 7-level inverter provides less THD in its output voltage, i.e., 22.91% in comparison with transistor clamped 5-level inverter that provides THD of 43.47%. Again the size of the filter required to eliminate harmonics is small in transistor clamped 7-level inverter. Hence, it is concluded that a 7-level TCHBMLI is a good option for the standalone PV system. Further it is observed that after filtering through L-C-L filter, the output waveforms THD is well below 5% as per IEEE519 standard for both 5-level and 7-level transistor clamped inverter. Specifically the 7-level output is really well with 1.57% THD.

References

1. A. Shawky, M. E. Ahmed, M. Orabi: Performance analysis of isolated DC-DC converters utilized in three phase differential inverter, in *Power Systems Conference (MEPCON), 2016 Eighteenth International Middle East*, pp. 821–826 (2016)
2. A. Salem, E.M. Ahmed, M. Orabi, M. Ahmed, Study and analysis of new three-phase modular multilevel inverter. *IEEE Trans. Industr. Electron.* **63**, 7804–7813 (2016)
3. M. AlRashidi, K. El-Naggar, M. AlHajri, A. Al-Othman: extraction of photovoltaic characteristics using simulated annealing, in *International Conference on Advances in Engineering Sciences and Applied Mathematics*, May 2014 (2014)
4. A. Salem, E.M. Ahmed, M. Ahmed, M. Orabi, Novel three phase multi-level inverter topology with symmetrical DC-voltage sources, in *Applied Power Electronics Conference and Exposition (APEC), 2016 IEEE*, pp 1505–1511 (2016)
5. K. Sundareswaran, V. Vigneshkumar, P. Sankar, S.P. Simon, P.S.R. Nayak, S. Palani, Development of an improved P&O algorithm assisted through a colony of foraging ants for MPPT in PV system. *IEEE Trans. Industr. Inf.* **12**, 187–200 (2016)
6. A.I. Ali, M.A. Sayed, E.E. Mohamed: Maximum power point tracking technique applied on partial shaded grid connected PV system, in *Power Systems Conference (MEPCON), 2016 Eighteenth International Middle East*, pp. 656–663 (2016)
7. S.J. Park, F.S. Kang, M.H. Lee, C.U. Kim, A New single-phase five level PWM inverter employing a deadbeat control scheme. *IEEE Trans. Power Electron.* **18**(3), 831–843 (2003)
8. A.K. Panda, Y. Suresh, Research on cascade multilevel inverter with single DC source by using three-phase transformers. *Electr. Power Energy Syst.* **40**, 9–20 (2012)
9. B. Singh, N. Mittal, K.S. Verma, Multi-level inverter: a literature survey on topologies and control strategies. *Int. J. Rev. Comput.* **10**, 1–16 (2012)
10. G. Cerlia, V. Grau, C. Sanchez, F. Ibanez, J. Walter, A. Millan, M.I Gimenez, A new multilevel inverter topology, in *Fifth IEEE International Caracas Conference on Devices, Circuits and Systems, Dominican Republic*, pp. 212–218 (2004)
11. G. Cerlia, V. Guzman, C. Sanchez, F. Ibanez, J. Walter, M.I. Gimenez, A new simplified multilevel inverter for DC-AC conversion. *IEEE Trans. Power Electron.* **21**(5), 1311–1319 (2005)
12. J. Rodriguez, J.S. Lai, F.Z. Peng, Multilevel inverters: a survey of topologies, controls, and applications. *IEEE Trans. Ind. Electron.* **49**(4), 724–738 (2002)
13. N.A. Rahim, J. Selvaraj, Multilevel inverter for grid connected PV system employing digital PI controller. *IEEE Trans. Industr. Electron.* **56**(1), 149–158 (2009)
14. V.G. Agelidis, D.M. Baker, W.B. Lawrance, C.V. Nayar, A multilevel inverter topology for photovoltaic applications, in *IEEE International Symposium on Industrial Electronics, ISIE '97*, vol. 2, pp. 589–594 (1997)
15. V.G. Agelidis, D.M. Baker, W.B. Lawrance, C.V. Nayar, A multilevel PWM inverter topology for photovoltaic applications, in *Proceedings of IEEE ISIE, Guimões, Portugal*, pp. 589–594 (1997)
16. B.P. McGrath, D.G. Holmes, Multicarrier PWM strategies for multilevel inverters. *IEEE Trans. Industr. Electron.* **49**(4), 858–867 (2002)
17. N.A. Rahim, K. Chaniago, J. Selvaraj, Single-phase seven-level grid connected inverter for photovoltaic system. *IEEE Trans. Industr. Electron.* **58**(6), 2435–2443 (2011)
18. W. De Soto, S.A. Klein, W.A. Beckman, Improvement and validation of a model for photovoltaic array performance. *Sol. Energy* **80**(1), 78–88 (2006)
19. W. Kim, W. Choi, A novel parameter extraction method for the one diode solar cell model. *Sol. Energy* **84**(6), 1008–1019 (2010)
20. K. Ding, X. Bian, H. Liu, T. Peng, A MATLAB-simulink-based PV module model and its application under conditions of non uniform irradiance. *IEEE Trans. Energy Convers.* **27**(4), 864–872 (2012)

21. R. Patel, A.K. Panda, A.R. Dash, Real time realization of highly reliable cascaded full-bridge interleaved buck inverter based APF using T1FLC id-iq control strategy, in *Proceedings of 44th Annual Conference on IEEE Industrial Electronics Society (IECON), Washington, Dc, USA*, pp. 1442–1447 (2018)
22. N.A. Yusof, N.M. Sapari, H. Mokhlis, J. Selvaraj, A comparative study of 5-level and 7-level multilevel inverter connected to the grid, in *International conference on power and energy*. IEEE, PEcon (2012)

A Novel Single-Phase Switched Capacitor Multilevel Inverter with Voltage Boosting Ability for Renewable Applications



Musie Welday Tesfay, Tapas Roy, and Swagat Das

1 Introduction

DC-to-AC multilevel inverters were introduced in the mid of 1970s since their introduction increases the production of electric energy from renewable sources [1]. The demand and consumption of Electric energy increase in day-to-day activity of human being. To balance the gap between demand and electric energy consumption, electric energy generating, controlling, and storing from renewable energy sources is compulsory. Therefore, MLIs play a decisive role in providing reliable, efficient, and controlled power. They are applicable for AC motor drives, electric vehicles and hybrid electric vehicles, integration renewable energy sources like wind, fuel and photovoltaic, uninterruptible power supplies (UPSs), static VAR compensators, active filters [2]. They convert several levels of DC voltages into nearly sinusoidal voltage with reduced harmonics, lower electromagnetic interference and dv/dt stress, reduced voltage stress across power semiconductor devices and fewer power losses. However, with increasing the output level, the number of semiconductor devices, gate drivers circuit, auxiliary components, protecting devices, and heat sink overall cost, control complexity, and volume of the system would be increased, and this reduces efficiency and performance of the converter, [3, 4]. The first proposed structures of MLI where called conventional MLI. They are categorized into three groups,

M. W. Tesfay (✉) · T. Roy · S. Das
School of Electrical Engineering, Kalinga Institute of Industrial Technology University,
Bhubaneswar, Odisha, India
e-mail: musiewelday2004@gmail.com

T. Roy
e-mail: tapas.royfel@kiit.ac.in

S. Das
e-mail: Swagat.dasfel@kiit.ac.in

namely cascade H-bridge [1], neutral-point-clamped inverters [5], and flying capacitors [6]. These MLI topologies have been easily integrated into industrial applications because of their good performance. However, for higher output level these topologies require a high number of main and auxiliary components, switch blocking voltage, and complexity with additional capacitor voltage balance circuit. Also, the inability of boosting its input voltage is another drawback of conventional MLIs [7].

To get the better of a large number of components, capacitor voltage balance problem, inability of boosting self-voltage and complex control algorithms or auxiliary circuits in conventional MLIs, switched capacitor multilevel inverters (SC-MLIs) have been proposed in recent years. SC-MLIs come up with sensible solutions for all the above drawbacks due to their boosting features. They use switched capacitors as an alternative DC power supply in addition to the input source. SC-MLI generates a staircase waveform of output level through charging and discharging of capacitors with the DC source. In recently developed SC-MLIs structures [8–17], when the boosting factor increases, interconnected components, standing voltage across switched and diodes, power losses and overall cost significantly increase. Therefore, designing an SC-MLI structure using cost-effective analysis with optimum semiconductor devices, gate driver circuits, capacitors, diodes, and boosting ability is required. In this paper, a novel single-phase MLI structure with boosting ability has been proposed. The proposed SC-MLI structure is able to synthesize 19-level of output voltage using 2 switched capacitor and 3 equal and non-isolated DC sources and 16 switches. It contains 3 bidirectional switches in which the gate driver circuits reduced. The proposed structure able to boost the input DC sources to 3 times. The proposed topology generates negative, zero, and positive levels without using H-bridge. This inherently generating of polarity reduces the total switch blocking voltage and converter overall cost. In addition to this, self-balancing of capacitor voltage is another advantage of the proposed topology. On the next sections, basic descriptions of proposed topology, comparisons with different recently developed topologies, and detail verification of the proposed simulation result proposed topology for different load conditions are done.

2 Proposed 19 Level SCMLI

The proposed 19-level novel structure is depicted in Fig. 1. It has 3 bidirectional power switches, 10 unidirectional power switches, 2 capacitors, and 3 equal and non-isolated DC sources. These capacitors are connected in parallel to $3V_{dc}$ sources during their charging time and connected in series during their discharging time using the appropriate switched combination. As shown from the circuit diagram, Q_4 , Q_5 , and Q_8 are bidirectional switches, whereas the remaining other switches are unidirectional. Turning ON of Q_3 , Q_6 , Q_7 , Q_8 , and Q_{13} switches enables us to charge C_1 from the input DC source. Similarly, turning ON of Q_3 , Q_6 , Q_8 , Q_9 , and Q_{12} switches enables us to charge C_2 from the input DC source. Switch Q_1 and Q_2 and Q_{10} and Q_{11} are a complement to each other to avoid danger short-circuit current

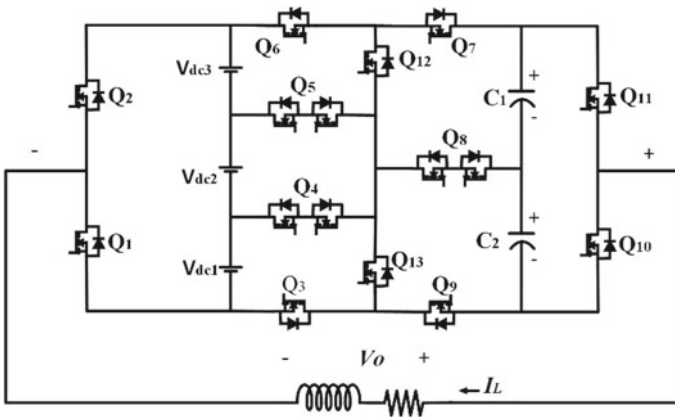


Fig. 1 Proposed structure

on input DC source voltage and capacitors. The current flow path and equivalent representation of the proposed structure for different output voltage levels are shown in Fig. 2. Further, switching state and states of the capacitor in each output level of the proposed topology are stated in Table 1. Where ‘N’, ‘C’, and ‘D’ indicate not change (no state), charging state, discharging state of capacitors during one cycle output level, respectively. Figure 2a–j represents the current path and equivalent circuit for 0, +1, ... and +9 voltage level, respectively, with ON respective switches and capacitor states as depicted in Table 1.

The maximum stress voltage across Q_5 and Q_4 is $2V_{dc}$, $Q_1, Q_2, Q_3, Q_6, Q_8, Q_{12}$, and Q_{13} are $3V_{dc}$, and $6V_{dc}$ for Q_7, Q_9, Q_{10} , and Q_{11} switches. Maximum current stress through $Q_1, Q_2, Q_4, Q_5, Q_{10}$, and Q_{11} is I_m (Max. load current), whereas maximum stress current in $Q_3, Q_6, Q_7, Q_8, Q_9, Q_{12}$, and Q_{13} is $I_m + I_{cm}$ (Max. load current + Max. capacitor current).

3 Modulation Technique

In this proposed topology, modulation technique based on half-height fundamental switching frequency has been used for generating the pulses as depicted in Fig. 3 [11]. By using these output pulses in Fig. 3b based on Table 2, switching pulses of the proposed structure can be generated (Q_2 and Q_1, Q_{10} and Q_{11} are complement to each other). Here V_0 to V_9 are the pulses for the positive half cycle and V_0' to V_9' are the pulses used for the negative half cycle.

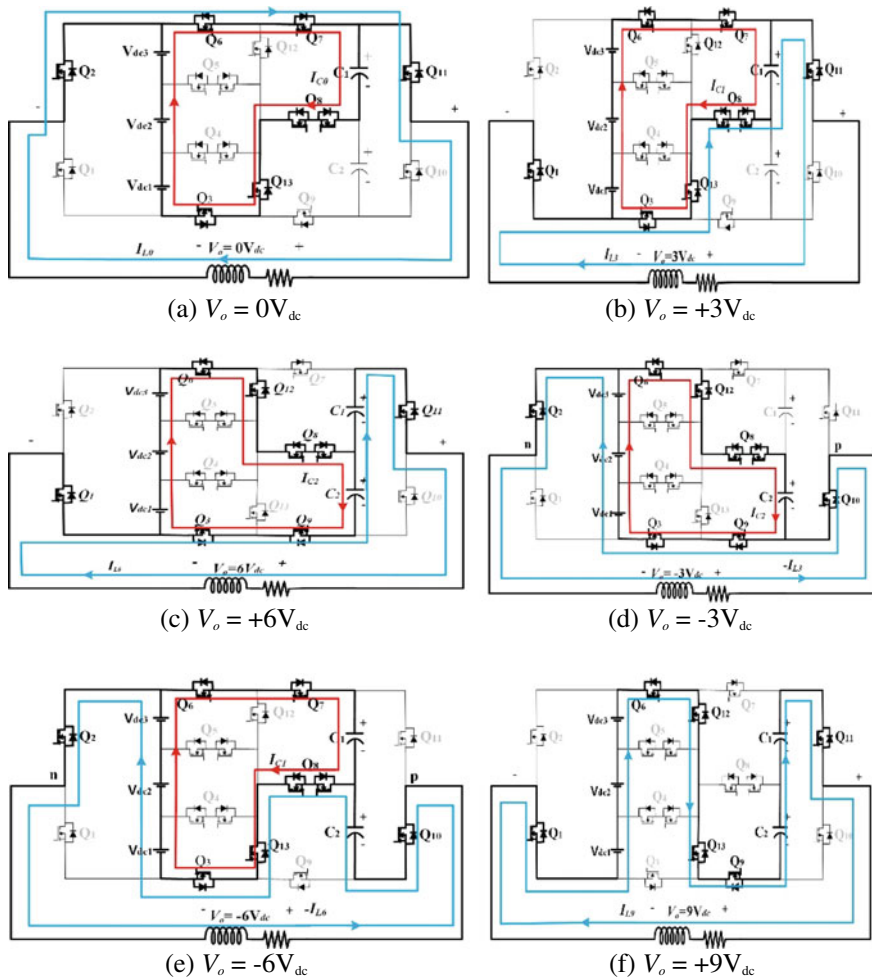


Fig. 2 Current flow path and equivalent representation of the proposed structure

4 Selection Procedure of Optimal Capacitor

In this section, calculating the value of optimal capacitance of the proposed structure has been presented. For evaluating the optimal value of each capacitor, the longest discharging period (LDP) of each capacitor over one cycle of output level at a fundamental frequency considered. From Table 1 and Fig. 4, longest discharging period of C_1 is in positive output level, whereas the longest discharging period of C_2 is during the negative half cycle of the output voltage.

As shown in Fig. 4, the LDPs of both capacitors in the proposed structure are the same. Therefore, maximum discharging capability and their optimal value during

Table 1 Switching state of the proposed structure

Switching state	Output voltage (V_o)	On switch	Capacitor state	
			C_1	C_2
1	+9	$Q_1, Q_6, Q_9, Q_{11}, Q_{12}, Q_{13}$	D	D
2	+8	$Q_1, Q_5, Q_9, Q_{11}, Q_{13}$	D	D
3	+7	$Q_1, Q_4, Q_9, Q_{11}, Q_{13}$	D	D
4	+6	$Q_1, Q_3, Q_6, Q_8, Q_9, Q_{11}, Q_{12}$	D	C
5	+5	Q_1, Q_5, Q_8, Q_{11}	D	N
6	+4	Q_1, Q_4, Q_8, Q_{11}	D	N
7	+3	$Q_1, Q_3, Q_6, Q_7, Q_8, Q_{11}, Q_{13}$	C	N
8	+2	$Q_1, Q_5, Q_7, Q_{11}, Q_{12}$	N	N
9	+1	$Q_1, Q_4, Q_7, Q_{11}, Q_{12}$	N	N
10	0	$Q_2, Q_3, Q_6, Q_7, Q_8, Q_{11}, Q_{13}$	C	N
		$Q_1, Q_3, Q_6, Q_8, Q_9, Q_{10}, Q_{12}$	N	C
11	-1	$Q_2, Q_5, Q_9, Q_{10}, Q_{13}$	N	N
12	-2	$Q_2, Q_4, Q_9, Q_{10}, Q_{13}$	N	N
13	-3	$Q_2, Q_3, Q_6, Q_8, Q_9, Q_{10}, Q_{12}$	N	C
14	-4	Q_2, Q_5, Q_8, Q_{10}	N	D
15	-5	Q_2, Q_4, Q_8, Q_{10}	N	D
16	-6	$Q_2, Q_3, Q_6, Q_7, Q_8, Q_{10}, Q_{13}$	C	D
17	-7	$Q_2, Q_5, Q_7, Q_{10}, Q_{12}$	D	D
18	-8	$Q_2, Q_4, Q_7, Q_{10}, Q_{12}$	D	D
19	-9	$Q_2, Q_3, Q_7, Q_{10}, Q_{12}, Q_{13}$	D	D

the LDP of both capacitors can be computed by (1):

$$Q_{C1} = Q_{C2} = 2 \int_{I_4}^{\frac{T}{4}} I_L(t) dt = \frac{17V_{dc}}{\omega R_L} \tag{1}$$

where Q_C is stored energy/charge on the capacitor.

Consider r is the percentage of the maximum allowable capacitor voltage ripple at steady state, the optimal value of both capacitor for the SC-ML can be calculated:

$$C_1 = C_2 = C_{opt} \geq \frac{Q_{C1}}{r \times V_{dc}} = \frac{Q_{C2}}{r \times V_{dc}} = \frac{17}{r\omega R_L} \tag{2}$$

For the R - L (resistive-inductive) load, $I_L(t) = I_m \sin(\omega t - \alpha)$. Where α is the phase angle between load current and output voltage. Therefore, the optimal capacitor value for R - L load will be:

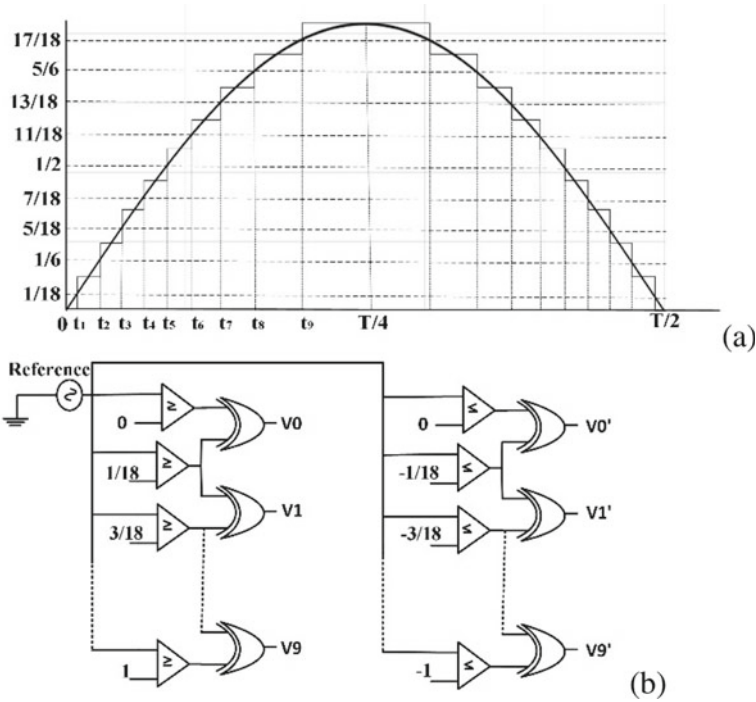


Fig. 3 **a** Comparison of different dc levels with reference sinusoidal signal and **b** pulse generation circuit diagram of the proposed topology

Table 2 Switching pulse generation using OR operation

$Q_1 = V_3 + V_1 + V_0' + V_2 + V_8 + V_4 + V_9 + V_6 + V_5 + V_7$
$Q_3 = V_0' + V_0 + V_3 + V_3' + V_6 + V_6' + V_9'$
$Q_4 = V_2' + V_1 + V_4 + V_7 + V_5' + V_8'$
$Q_5 = V_2 + V_5 + V_8 + V_1' + V_4' + V_7'$
$Q_6 = V_0 + V_3 + V_6 + V_9 + V_0' + V_3' + V_6'$
$Q_7 = V_0 + V_6' + V_1 + V_7' + V_2 + V_8' + V_3 + V_9'$
$Q_8 = V_0 + V_5' + V_6 + V_3' + V_4 + V_0' + V_3 + V_4' + V_5 + V_6'$
$Q_9 = V_0' + V_6 + V_1' + V_7 + V_2' + V_8 + V_9 + V_3'$
$Q_{11} = V_8 + V_2 + V_0 + V_9 + V_6 + V_4 + V_1 + V_7 + V_3 + V_5$
$Q_{12} = V_7' + V_1 + V_8' + V_2 + V_6 + V_9 + V_0' + V_3' + V_9'$
$Q_{13} = V_9 + V_6' + V_0 + V_2' + V_3 + V_7 + V_9' + V_8 + V_1'$

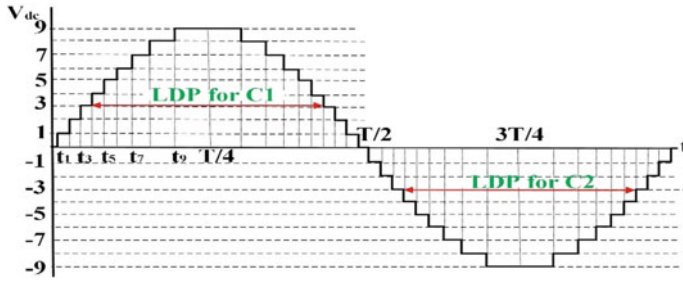


Fig. 4 Longest discharging period of C_1 and C_2 of the proposed topology

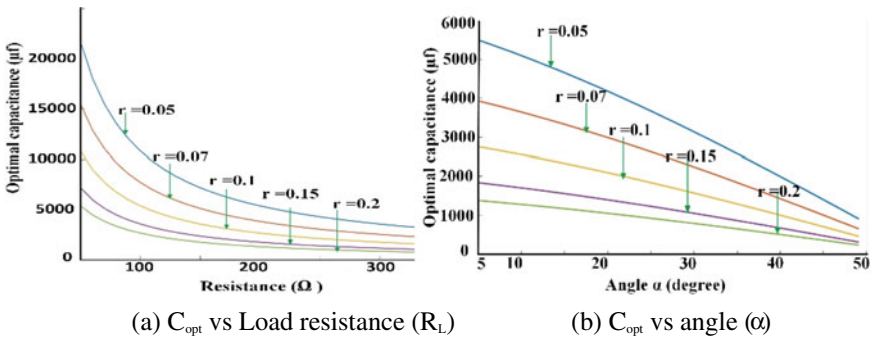


Fig. 5 Value of optimal capacitance C_{opt} for different ripple voltage

$$C_1 = C_2 = C_{opt} \geq \frac{2I_m(\cos(0.4 - \alpha) - \sin(\alpha))}{r\omega V_{dc}} \tag{3}$$

Considering other parameters constant, when the load resistance increases the required capacitance value decreases. Similarly, the optimal capacitance value decreases for a higher value of the angle α . The value of the optimal capacitor varies with the angle α is presented in Fig. 5 for $I_m = 5$ A, $V_{dc1} = V_{dc2} = V_{dc3} = 48$ V each and $f_s = 50$ Hz.

5 Comparison Study

Comparison of the proposed structure with different recently developed SC-MLI-based topologies that having input voltage more than one V_{dc} has been done. Table 3 shows contrast and correlation of proposed topology with topologies in [8–10, 13–17]. The proposed topology has been compared in terms of number of switches (N_{sw}), capacitors (N_c), drivers (N_{dr}), diodes (N_d), and total blocking voltage (TSV_{pu} and PIV_{pu}). Finally, the cost function (CF) comparison has been done to evaluate

Table 3 Comparison of different SC-MLI topologies, T = topologies, P = proposed, N_p = no. of a path, V_s = the maximum voltage across the single switch

[T]	N_L	N_{sw}	N_{dr}	N_d	N_c	TSV_{pu}	PIV_{pu}	V_s	B	N_p	$V_{in, tot}$	CF	
												$f = 0.5$	$f = 1.5$
[8]	25	12	12	2	2	5	0.5	10	2	6	6	3.69	4.35
[9]	9	10	8	1	2	6	0.5	4	2	3	2	2.694	3.472
	49	18	14	2	4	6	0.5	24	2	5	12	5.051	5.847
[10]	17	10	10	2	2	5.5	0.5	8	2	5	4	3.176	3.882
[14]	31	16	16	2	4	5.67	0.33	15	3	7	5	2.204	2.527
[15]	49	20	16	0	6	5.33	0	7	1.5	6	8	4.86	5.44
[13]	11	8	7	0	2	4.2	0	3	1	5	5	8.68	10.6
[17]	9	12	10	0	1	5.5	0	2	2	4	2	2.86	3.472
[16]	49	16	16	4	4	5.33	0.67	21	3	8	8	2.34	2.67
[P]	19	16	13	0	2	5.33	0	6	3	6	3	1.772	2.052

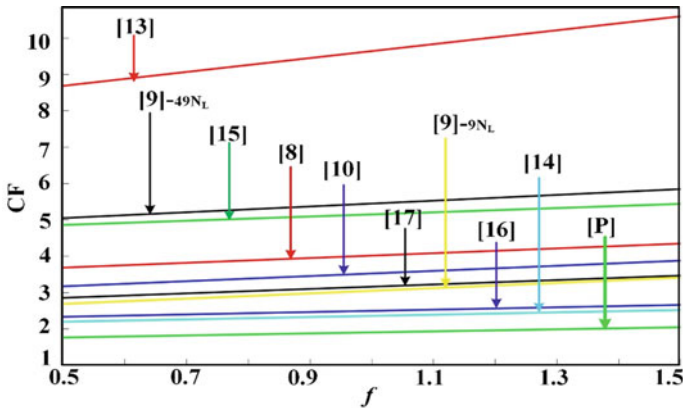


Fig. 6 Comparison of CF with f

the overall cost of these SC-MLI structures expressed by (4) [9].

$$CF = \frac{(N_{sw} + N_{dr} + N_d + N_{cap} + f(TSV_{pu} + PIV_{pu}))V_{in,tot}}{BN_L} \tag{4}$$

where TSV_{pu} , PIV_{pu} , f , B , N_L and $V_{in,tot}$ are the total standing voltage across switches per maximum output voltage of each converter, total standing voltage across diodes per unit, weightage (importance factor) of TSV and PIV , boosting factor, number of levels and sum of input voltage per V_{dc} for the N_L output level of SC-MLI structures, respectively.

Figure 6 shows the cost function comparison of proposed SC-MLI with different recently proposed structures when the weightage factor (f) varies from 0.5 to 1.5 value.

6 Simulation Study and Verification of Proposed Topology

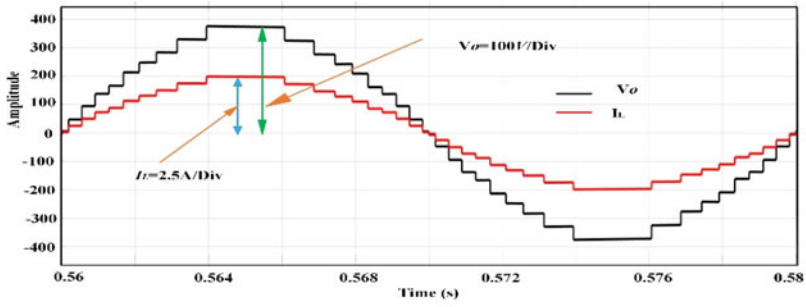
In this section, simulation studies and verifications of proposed topology for various load types such as pure resistive, resistive–inductive, pure inductive, and during dynamic load of have been presented. The topology is presented using low-frequency switching strategies for $V_{dc1} = V_{dc2} = V_{dc3} = 48 \text{ V}$, $C_1 = C_2 = 5500 \text{ }\mu\text{F}$, $R_{on} = 0.18 \text{ }\Omega$, $R_d = 10 \text{ m}\Omega$, and $R_{esr} = 0.1 \text{ }\Omega$ values.

The simulation result of the proposed topology for pure resistive load condition is presented in Fig. 7. The output voltage per division is 100 V, and load current per division is taken 2.5 A. Figure 7a presents output voltage waveform and load current waveform. For resistive load ($R_L = 75.6 \text{ }\Omega$), the proposed topology provides 377.2 V fundamental output voltage and 4.99% total harmonic distortion (THD). Figure 7d presents the waveform of voltage across the capacitor when the load is resistive ($R_L = 75.6 \text{ }\Omega$). The voltage ripple for both capacitors is around 5.2 V as shown in the zoomed part of Fig. 7d. For R - L load, the load current and the output voltage are out of phase as shown in Fig. 7b. The parameter values used for verification of R - L load are $R_L = 73.95 \text{ }\Omega$ and $L = 50 \text{ mH}$.

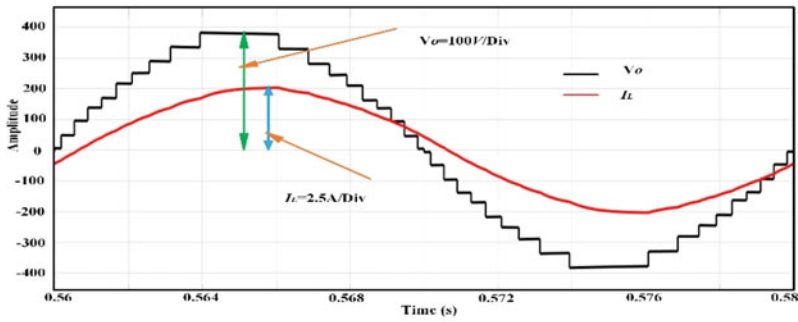
Besides, the proposed structure is verified for sudden load change conditions as shown in the other diagrams of Fig. 7. When the load resistance increases, the magnitude of load current reduces, but its waveshape remains the same. Figure 7c presents when suddenly the load resistance is doubled for 3 cycles, magnitude of load current reduced by half (I_D , is dynamic load current). But the capacitor voltage ripple of the converter is improved as depicted in Fig. 7e. When the duration of sudden load change is over the magnitude of the load current returns to its original value as shown in Fig. 7e for $R_D = R_L = 73.95 \text{ }\Omega$ and $L = 50 \text{ mH}$, R_D is dynamic resistance during a load change.

7 Conclusion

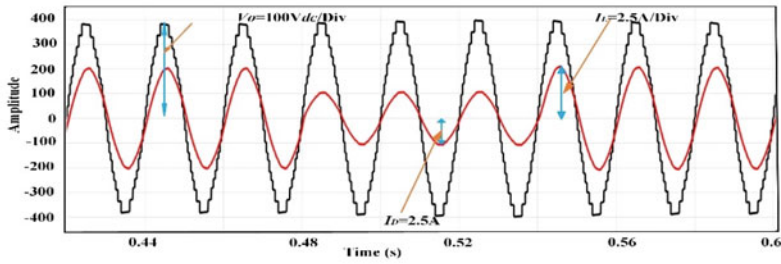
In this research study, a novel MLI structure with boosting ability has been proposed. It provides inherently synthesizing of all levels without a polarity generation circuit. It boosts the input voltage three times greater the input DC source using a lower number of circuit components and lowest cost function as compared to recently proposed SCMLI topologies. Simulation study and verification of output voltage, the voltage across the capacitors with their ripple and load current have been done for R , R - L and dynamic loads. The proposed topology is suitable for renewable energy conversion systems such as photovoltaic farm and fuel cell applications.



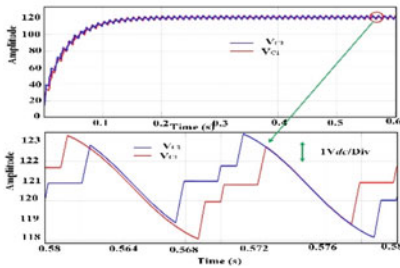
(a) V_o and I_L for R- Load



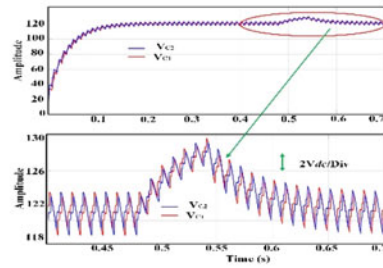
(b) V_o and I_L for R-L Load



(c) V_o and I_L for dynamic Load



(d) Capacitor voltage for R-Load



(e) Capacitor voltage for dynamic-Load

Fig. 7 Simulation results for different load condition

References

1. R.H. Baker, L.H. Bannister, Electric power converter, US Patent 3 867 643 (1975)
2. A. Ajami, M.R.J. Oskuee, A. Mokhberdorran, A.V.D. Bossche, Developed cascaded multilevel inverter topology to minimise the number of circuit devices and voltage stresses of switches. *IET. Power Elec.* **7**, 459–466 (2014)
3. Z. Shu, N. Ding, J. Chen, H. Zhu, X. He, Multilevel SVPWM with DC-link capacitor voltage balancing control for diode-clamped multilevel converter based STATCOM. *IEEE. Trans. Ind. Elec.* **60**, 1884–1896 (2013)
4. K. Wang, Y. Li, Z. Zheng, L. Xu, Voltage balancing and fluctuation suppression methods of floating capacitors in a new modular multilevel converter. *IEEE. Trans. Ind. Elec.* **60**, 1943–1954 (2013)
5. A. Nabae, I. Takahashi, H. Akagi, A neutral-point-clamped PWM inverter, in *Proceedings of Conference Record. IEEE IAS Annual Meeting, Cincinnati, OH, USA*, vol. 3 (1980), pp. 761–766
6. J. Mathew, P.P. Rajeevan, K. Mathew, N.A. Azeez, K. Gopakumar, A multilevel inverter scheme with dodecagonal voltage space vectors based on flying capacitor topology for induction motor drives. *IEEE. Trans. Power Elec.* **28**, 516–525 (2013)
7. Z. Ramli, J. Jamaludin, N.A. Rahim, Capacitor voltage balancing in switch-sharing based multilevel inverter with PI controller, in *IEEE Conference on Energy Conversion* (2017), pp. 265–270
8. E. Babaei, S.S. Gowgani, Hybrid multilevel inverter using switched capacitor units. *IEEE. Trans. Ind. Elec.* **61**, 4614–4621 (2014)
9. R. Barzegarkhoo, M. Moradzadeh, E. Zamiri, H.M. Kojabadi, F. Blaabjerg, A new boost switched-capacitor multilevel converter with reduced circuit devices. *IEEE. Trans. Power Elec.* **33**, 6738–6754 (2018)
10. E. Zamiri, N. Vosoughi, S.H. Hosseini, R. Barzegarkhoo, M. Sabahi, A new cascaded switched capacitor multilevel inverter based on improved series-parallel conversion with less number of components. *IEEE Trans. Ind. Electron.* **63**, 3582–3594 (2016)
11. P.S. Bhagyalakshmi, B.M. Varghese, Switched capacitor multilevel inverter with different modulation techniques. *ICIIECS*, pp. 1–6 (2017)
12. R.S. Alishah, S.H. Hosseini, E. Babaei, M. Sabahi, A. Zare, Extended high step-up structure for multilevel converter. *IET. Power Elec.* **9**, 1894–1902 (2016)
13. P. Bhatnagar, R. Agrawal, K.K. Gupta, Reduced device count version of single-stage switched-capacitor module for cascaded multilevel inverters. *IET. Power Elec.* **12**, 1079–1086 (2019)
14. T. Roy, P.K. Sadhu, A. Dasgupta, Cross-Switched Multilevel Inverter Using Novel Switched Capacitor Converters. *IEEE. Trans. Ind. Elec.* **66**, 8521–8532 (2019)
15. J. Liu, X. Zhu, J. Zeng, A seven-level inverter with self-balancing and low voltage stress. *IEEE Trans. Power Elec.* (Early access)
16. W. Peng, Q. Ni, X. Qiu, Y. Ye, Seven-Level inverter with self-balanced switched-capacitor and its cascaded extension. *IEEE. Trans. Power Elec.* **34**, 11889–11896 (2019)
17. S.S. Lee, K.B. Lee, I.M. Alsofyani, Y. Bak, J.F. Wong, Improved switched-capacitor integrated multilevel inverter with a DC source string. *IEEE Trans. Ind. Appl.* (Early access)

Frequency Response Analysis of Power Transformers



Subhendu Mishra

1 Introduction

Frequency response analysis of FRA is an off-line condition monitoring technique that can be used for diagnosis of any transformer. Mechanical defects and insulation failures are the main reasons due to which transformers have to be decommissioned. FRA involves taking a ‘fingerprint’ or signature frequency response of the transformer under study and comparing this signature to the one originally provided by the manufacturer of the transformer when it was first commissioned.

It is necessary to understand that transformers are capable of withstanding various short circuits without themselves failing. However, due to isolated stresses, there are local deformations in the transformer. When there is significant deformation, even a small short circuit can severely damage the transformer and render it useless. Thus, it is necessary to regularly check the transformer for any significant deformation. This means that the transformer has to be isolated and made off-line, before it can be tested using FRA. There are some studies going on where the transformer can be diagnosed without removing it from the main grid [1, 2].

Various studies have been done on modeling of transformer as a coupled field circuit [3]. Here, it is explained that the transformer behaves as a coupled device of various fields like electric field, magnetic field, thermal field, mechanical field, fluid flow field, and acoustic field [4]. FRA is done in order to mainly study the changes in the electric circuit of the transformer. Transformer winding can be modeled as a network of capacitance, resistances, self-inductance, and mutual inductance. These parameters are coupled to other fields like thermal, fluid flow field, mechanical, etc. The values of these network parameters change when there is any deformation due to

S. Mishra (✉)

School of Electrical Engineering, Kalinga Institute of Industrial Technology Deemed to Be University, Bhubaneswar, Odisha 751024, India

e-mail: subhendu.mishrafel@kiit.ac.in

© Springer Nature Singapore Pte Ltd. 2021

K. S. Sherpa et al. (eds.), *Advances in Smart Grid and Renewable Energy*,

Lecture Notes in Electrical Engineering 691,

https://doi.org/10.1007/978-981-15-7511-2_11

short-circuit faults or stress produced during transportation. With the change in the capacitance and inductance parameters, there is also change in resonant frequency of the transformer. Various studies have been carried out to study how the change in resonance frequency can be interpreted to understand specific deformation in the transformer [5–10].

Sweep frequency response analysis can be divided mainly into three types:

1. Time based: Current FRA is compared with old FRA of the same transformer
2. Type based: SFRA of one transformer is compared to another transformer with the same design
3. Phase comparison: SFRA of one phase in a transformer is compared with that of another phase.

2 FRA Review

2.1 Use of FRA in Transformers

It has been studied thoroughly how physical deformations in transformers can lead to change in its capacitive and inductive parameters. The objective for the project is to measure the input and output voltage of a transformer in open-circuit condition over a sweep of input frequency. Thus, we are able to see the impedance changes of the transformer over the sweep frequency range. FRA can be comprehensively defined as a comparative method, in which the frequency response measurements are carried out over a wide frequency range.

Generally, there are three regions of frequency response. The first region is 20 Hz to 20 kHz and is also called a low-frequency region. The core magnetizing inductance is the most dominant in this region. The second region is 20–400 kHz which is also considered as a mid-frequency region. Here, both inductance and capacitance of the winding become prevalent due to which multiple resonance are present. The last region of operation is above 400 kHz which is a high-frequency region. Here inter-turn capacitance, lead inductance, and stray capacitance of the transformer dominate. It is imperative to demonstrate the various methods available for measurement of FRA [11, 12]. Common FRA measurement techniques used in industry are as follows:

1. End-to-end voltage ratio measurement (FRA_{ee})
2. Input admittance measurement (FRA_{ad})
3. Transfer voltage ratio measurement (FRA_{tr}).

In our experiment, we measure the end-to-end voltage ratio. Figure 1 shows the connection used for conducting SFRA. Here, the transformer acts primarily as a two-port network. The input voltage is given to the first port with a R_c value of 100 Ω resistor acting as shunt. The output voltage is calculated from the other port with again a 100 Ω shunt resistor. Ratio of output voltage (terminal 2 voltage, V_2) and the input voltage (terminal 1 voltage, V_1) is taken and represented in terms of the amplitude.

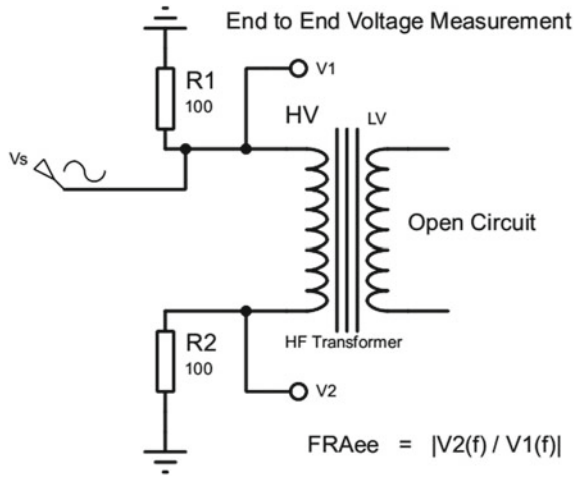


Fig. 1 Connection for end-to-end voltage measurement

FRA can be described by the plot of amplitude (dB) v/s frequency (Hz). Here, output voltage, V_2 depends on the transformer impedance. As impedance decreases, V_2 increases. For our purpose, we would do end-to-end voltage measurement.

$$\text{Amplitude(dB)} = 20\log_{10}(V_2/V_1) \tag{1}$$

In electrical circuit, impedance depends on resistance, inductance, and capacitance as shown:

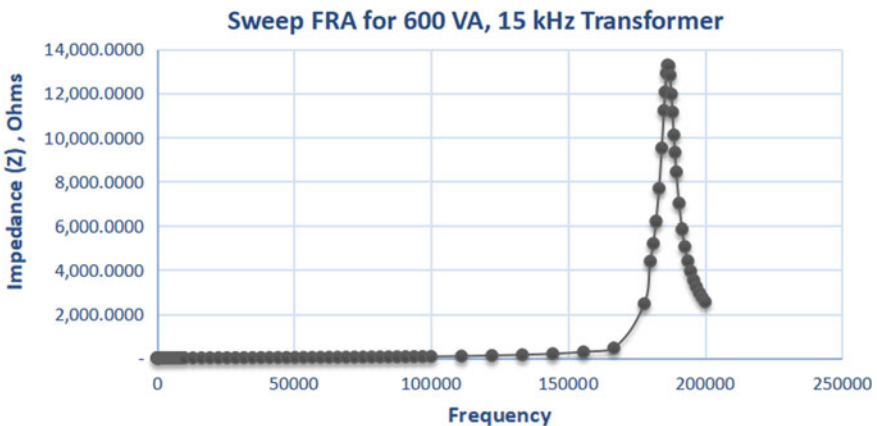


Fig. 2 Sweep FRA using LCR meter for 600 VA, 15 kHz transformer under test in open-circuit condition

$$Z = \sqrt{R^2 + (X_L - X_C)^2} \quad (2)$$

Inductive reactance increases and capacitive reactance decreases with frequency, which can be given by following equations:

$$X_L = 2\pi fL \quad (3)$$

$$X_C = 1/2\pi fC \quad (4)$$

The voltage ratio is given in Eq. 5. The real part of the impedance can be expressed in Eq. 6, and the imaginary part of the impedance is expressed in Eq. 7.

$$\frac{V_r}{V_s} \angle \theta = \frac{100}{100 + Z \angle \phi} \quad (5)$$

$$Z \cos \phi = \frac{100}{\frac{V_r}{V_s}} \cos(-\theta) + 100 \quad (6)$$

$$Z \sin \phi = \frac{100}{\omega * \frac{V_r}{V_s}} \sin(-\theta) \quad (7)$$

For measurement, the transformer tank is made to be the common ground reference. For validating the equipment, a known resistor is connected between the two terminals. The equipment correctly predicts the resistance in the LabVIEW program. The open-circuit impedance of the test transformer (600 W, 15 kHz) is shown here (Fig. 2).

2.2 Use of FRA in Motors

Sweep FRA is useful for diagnosis of rotating machines as well. In the project, we analyzed an induction machine as well and analyzed the FRA signature. It has been explained previously that each equipment or machine has a unique sweep FRA fingerprint. We observe a change in this fingerprint if there has been any fault in the machine. Thus, the type of fault and its severity can be identified by comparing SFRA of a healthy machine with that of the faulty machine. SFRA is used primarily to identify failure or changes in the winding insulation and the core of the machine [13]. Frequency response depends on the winding resistance; self, mutual, and leakage inductance; and also the capacitance of the machine.

Adjustable speed drives can lead to stress conditions like thermal overload, mechanical vibrations, and voltage spikes. It has been experimentally verified that a 10 degree increase in temperature will result into a decrease of insulation life by 50% [14]. Electrical faults generally result from bearing failure and winding faults in

rotor or stator. Winding insulation failures are of the following types: inter-turn short circuit, winding-to-ground short circuit, phase-to-phase short circuit, and coil-to-coil short circuit. Out of them, phase-to-ground short circuit is the most severe. Weak turn-to-turn insulation actually leads to 80% of all electrical failures in stator [14]. Inter-turn short circuit can also cause hot spot and severely damage the motor.

3 Methodology

The complete setup can be seen in Fig. 3. The project involves the following components.

3.1 Experimental Setup

3.1.1 NI LabVIEW Program

A LabVIEW program has been built to generate digital PWM signals that were sent to the microcontroller board. The LabVIEW program is made such that it can give a

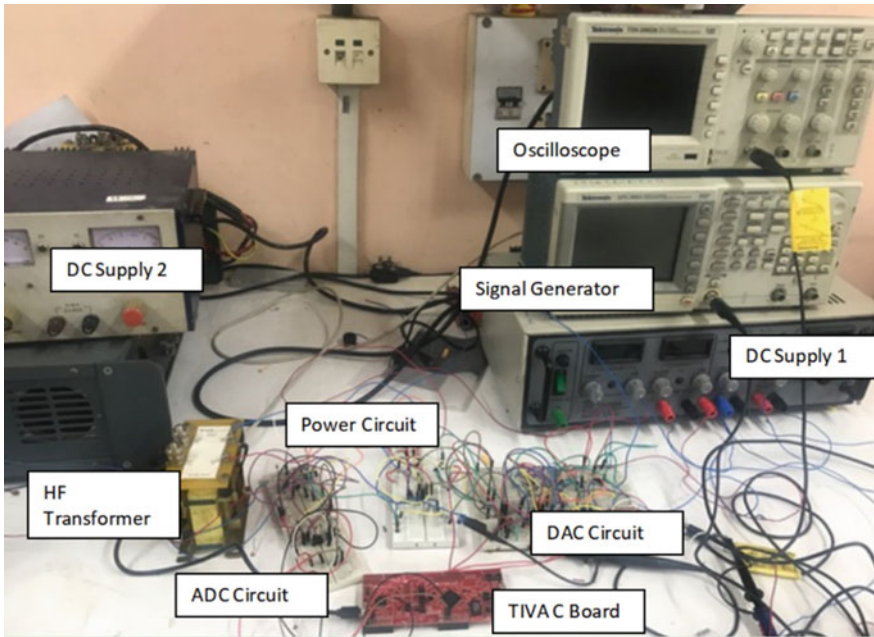


Fig. 3 Experimental setup for SFRA of 600 VA HF transformer

PWM signal every 5 μ s. A complete sinusoidal signal is sent as an array of 0's and 1's for one wavelength. Again, the output of the ADC of the TIVA C board is read for the same frequency. After calculating the phase difference and impedance, the LabVIEW program sends another PWM signal for a different frequency depending on the frequency step defined by the user.

3.1.2 TIVA C Board (EK-TM4C1294XL)

The board has 120 MHz, 32 bit, ARM Cortex M4 MCU. Code Composer Studio (CCS) is the development tool platform used for programming the MCU. TivaWare is the embedded driver used for control of the ADC and PWM pins. The microcontroller is essentially the interface between the PC LabVIEW program (user interface) and the analog circuit.

3.1.3 Analog Circuit, DC Supply, Oscilloscope

The first phase of the circuit is an optocoupler which amplifies the PWM signal from TIVA C board to a square wave signal, with limits of 0 and 5 V. In the first phase, the objective was to have a FRA sweep up to 2 kHz. The PWM modulating frequency is 20 kHz. The second part of the circuit is a fourth-order RC filter. The RC filter has a cut-off frequency of 5 kHz.

The PWM has a particular characteristic that it has significantly low harmonics between source signal frequency and modulating frequency (i.e., 20 kHz). RC filter removes all signals other than the source signal when we set a cut-off frequency of 5 kHz. Thus, we get a sinusoidal signal with frequency same as the source signal.

The methodology for the project is given here:

- Step 1: LabVIEW and microcontroller interface is established.
- Step 2: LabVIEW program is modified to obtain the PWM signal. This signal is sent to the PWM pins in the TIVA C board. This involves programming the TI board using Code Composer Studio.
- Step 3: Digital-to-analog converter (DAC) circuit is made as shown in Fig. 5. This includes the optocoupler, RC filter, and the voltage amplifier. The output of the DAC circuit goes to the power circuit [15].
- Step 4: Power circuit is made as shown in Fig. 6. Here, the output voltage and current of the DAC circuit is amplified. A BJT circuit is formed, and biasing is done to get 1.62 as the voltage amplification factor and a significant current amplification depending on the load. The output of the power circuit is the input to the transformer [15].
- Step 5: A high-frequency transformer is attached to the circuit. The load output is measured at terminals V1 and V2 using oscilloscope. The LabVIEW program is again modified to give a frequency sweep up to 2 KHz. The

output is observed and some modification in the circuit is made for correct results.

- Step 6: The input voltage at the terminal 1 (V_1) and output voltage at terminal 2 (V_2) of the same side are now read by TIVA C board using the ADC circuit as shown in Fig. 7. This is done using two difference amplifiers across $100\ \Omega$ resistors at terminals 1 and 2. One TIVA C board was damaged when a sudden current spike was there while switching supplies. During this step, it was observed that a separate DC supply is needed for the ADC circuit (DC supply 2) and a different for the DAC and power circuit (DC supply 1). Thus, it was inferred that this supply isolation is necessary for protection of the TIVA C board.
- Step 7: LabVIEW program is further modified to receive the digital data from the TIVA C board. The phase difference and impedance of the transformer is calculated using the two voltages read by the LabVIEW program. A complete frequency sweep is now given. For each input frequency, the phase difference between V_1 and V_2 and the impedance of the transformer is recorded.

3.2 LabVIEW and TIVA C Board

It was observed that the signal at the output of the DAC was not completely sinusoidal when the transformer was connected. The first part of the project used the control signal and saw-tooth modulating signal to generate PWM signals. The reason for distortion was identified to be the fact that at the phase angle of 270° the output PWM signal is very small. It was identified that it would be better to generate the PWM signals from a variable duty cycle applied to square wave as compared to conventional method of comparing the modulating and control signals. The duty ratio was varied between 20 and 80% to avoid peaky output voltage.

3.2.1 DAC Circuit Design

Here, the circuit between the transformer and the microcontroller is explained. In Fig. 4, the pins PE4 and PE5 in the TIVA C board give PWM input to the optocoupler 6N137. The output of the optocoupler is then given as input to the RC low pass filter. Value of resistance R_1 and R_3 is taken as $1\ \text{k}\Omega$, and C_2 and C_4 value is taken as $33\ \mu\text{F}$. The cut-off frequency for this filter is 5000 Hz.

The output voltage of the RC low pass filter is amplified by 5.6 times before it is given as input to the power circuit as shown in Fig. 5. The BJT is connected to a 32 V supply and appropriately biased to give high current and voltage gain. The output of the power amplifier is given as input to terminal 1 of the transformer. Shunt resistance of $100\ \Omega$ each is connected to the two terminals of the transformer. It is this voltage across the shunt resistance that gives us voltages V_1 and V_2 . It will be

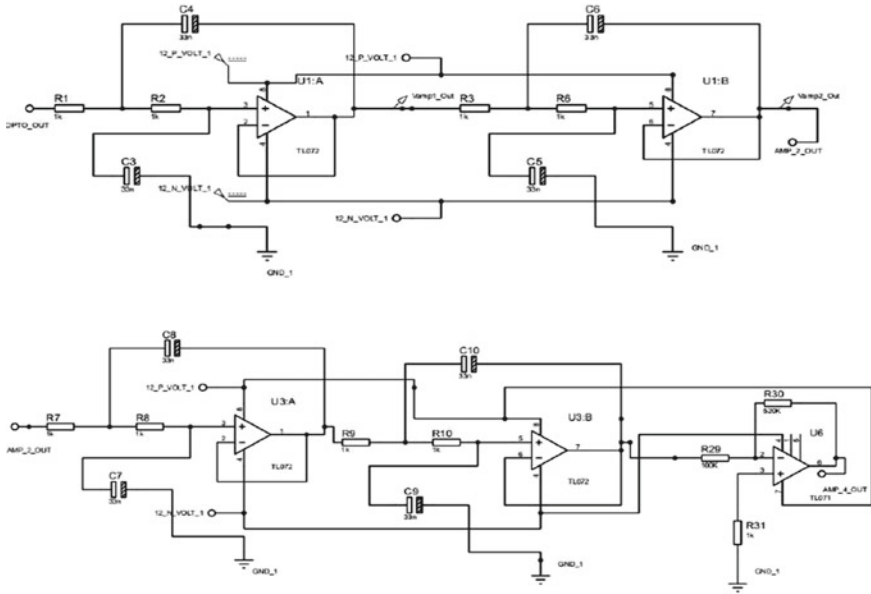


Fig. 4 Digital-to-analog converter designed for SFRA

seen further that with an increase in frequency, the impedance of the transformer primary winding changes and the phase difference between $V1$ and $V2$ increases. Further, the impedance also increases with the change in frequency.

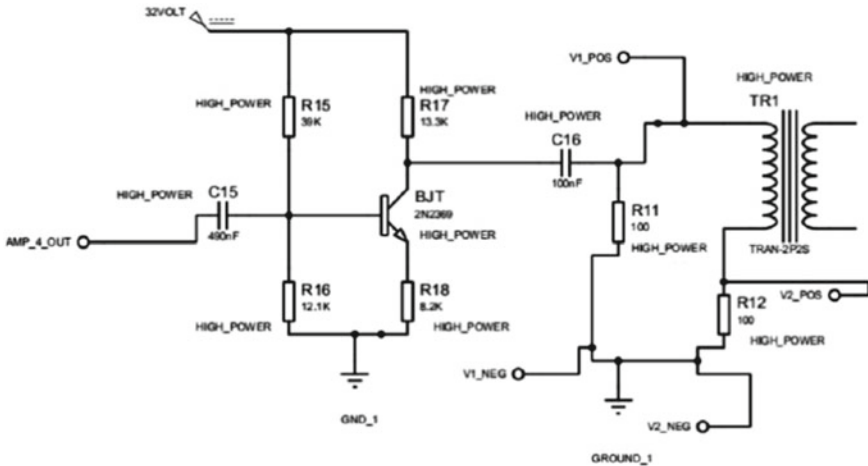


Fig. 5 Power amplification circuit designed for SFRA

3.2.2 ADC Circuit Design

The voltages at the two terminals $V1$ and $V2$ are given as input to the two difference amplifier. The signal is amplified 6.1 times. It is to be noted here that the amplification of two measured voltages $V1$ and $V2$ by the same amount does not change the ratio of ($V1/V2$). Thus, the FRA signature of the transformer is not affected. This is done, so that the ADC of the TIVA C board can accurately read the voltages. Also, it should be noted that the current required by the transformer is small when in open-circuit condition. The output of the differential amplifier is further passed through a low pass filter again to remove the high-frequency fluctuations. The low pass circuit used here has the same cut-off frequency of 5 kHz (Figs. 5 and 6).

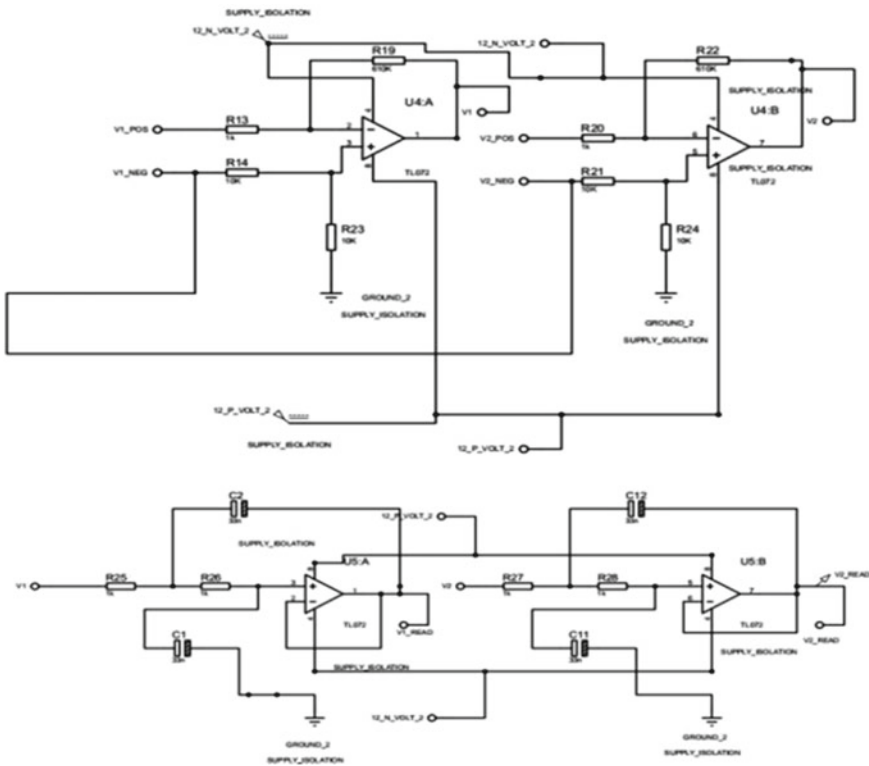


Fig. 6 Analog-to-digital converter designed for SFRA

4 Experimental Results

These experiments were conducted and results were recorded at the Insulation Diagnostics (ID) Laboratory at IIT Bombay. Here, a frequency sweep was done over a frequency range of 50–1500 Hz. Here, the results have been given for two different frequencies: 500–1000 Hz. The results have been analyzed further in the section (Figs. 7 and 8).

Here, the FRA results for different control frequencies is shown. Channel 1 shows the voltage at the terminal 1 of the primary winding, and Channel 2 shows the

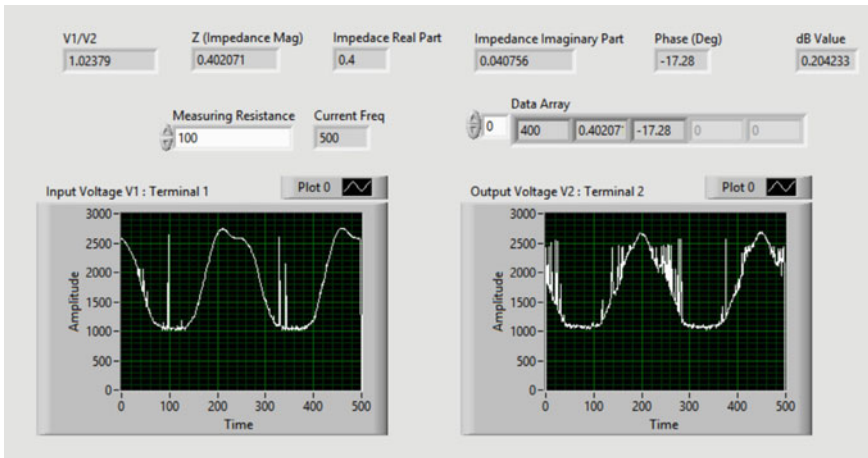


Fig. 7 LabVIEW reading at 500 Hz

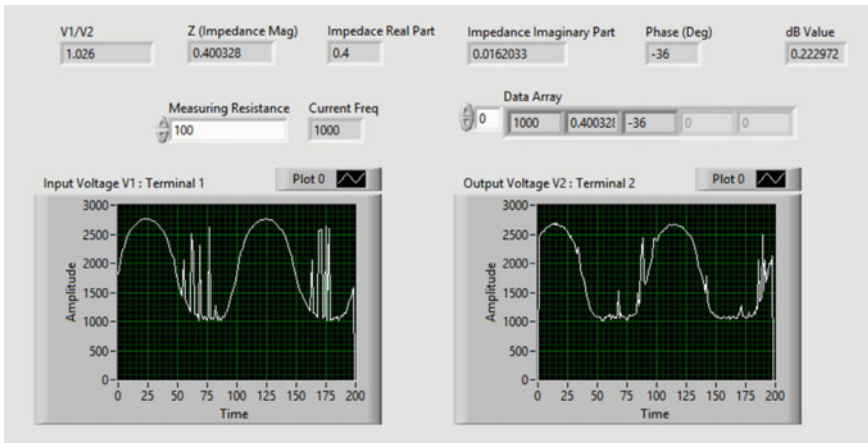


Fig. 8 LabVIEW reading at 1000 Hz

voltage at the terminal 2 of the primary winding. Here, impedance is measured for each frequency as shown in Eqs. 5–7. It can be seen that the phase between the two voltages V_1 and V_2 change with frequency. As the transformer acts as an inductor in the low-frequency region, it is expected that phase angle should increase with frequency which is verified with the results. The ratio V_1/V_2 is increasing as the control frequency increases. This can be expected because the impedance of the transformer increases with the frequency, and thus, the voltage drop across it increases.

5 Conclusion and Scope

It can be seen from the results that the impedance of the transformer is in fact changing with the applied frequency. The circuit made can be used for acquiring sweep FRA signature up to 2 kHz frequency. However, it has been verified that the same circuit will work correctly till the 200 kHz frequency when we apply a modulating signal of 1 MHz. For this, capacitors in the RC filters have to be replaced with 330 pF instead of 33 nF. It is to be noted here that the baud rate of communication between the LabVIEW program and TIVA C board (115,200 Bps) and the internal memory of the microcontroller (256 kB) provide limitations against the frequency of operation. However, still further work can be done using this setup for high-frequency FRA.

High-frequency transformers are the future due to increasing integration of renewable energy sources. Thus, the need for analysis and diagnosis of high-frequency transformers will remain a subject of research. Sweep FRA is primarily an off-line method of analysis. Further research can include the development of online method, where the HF transformer would no longer be decoupled from the grid in order to be diagnosed.

In sweep FRA, the data obtained is compared with previously obtained data. In future research, a large dataset of FRA signatures and associated failures can be used, and artificial neural network can be used to predict possible future failures before it actually occurs in the transformer.

LCR meter has a limit on the high-frequency FRA signal that it can measure and the amount of current that can be passed through the machine under diagnosis. With this setup, the level of voltage and current is only limited by the power circuit and the connected BJT. This limit is very high, and thus, the setup can be used over more sets of transformers than LCR meter. Moreover, the LCR meter is very costly, and this setup provides the same operation at a comparatively very small price.

Acknowledgements I would like to thank my parent institution Kalinga Institute of Industrial Technology (KIIT). I sincerely thank Prof. S. V. Kulkarni at IIT Bombay to accept me for the INAE fellowship program and provide guidance and encouragement throughout the duration.

References

1. H. Rahimpour, S. Mitchell, S. Rahimpour, On line monitoring of power transformers using impulse frequency response analysis, in *2017 Iranian Conference on Electrical Engineering*
2. H. Rahimpour, S. Mitchell, J. Tusek, *The Application of Sweep Frequency Response Analysis for the on Line Monitoring of Power Transformers* (AUPEC, 2016)
3. K.P. Badgajar, A.P.S. Baghel, S.V. Kulkarni, *A Coupled Field-Circuit Formulation and a Duality Based Approach for Analysis of Low-Frequency Response of Transformers* (INDICON, 2013)
4. S.V. Kulkarni, Coupled field computations for analysis of intricate phenomena in transformers. Invited paper, Adv. Res. Workshop Trans. ARWtr (2007)
5. S. Grubic, J.M. Aller, B. Lu, T.G. Habetler, A survey on testing and monitoring methods for stator insulation systems of low-voltage induction machines focusing on turn insulation problems. *IEEE Trans. Ind. Electron.* **55**(12), 4127–4136 (2008)
6. N. Abeywickrama, Y.V. Serdyuk, S.M. Gubanski, High frequency modelling of power transformers for use in frequency response analysis (FRA). *IEEE Trans. Power Deliv.* **23**(4) (October, 2008)
7. CIGRE WG A 2.26, *Mechanical Condition Assessment of Transformer Winding Using Frequency Response Analysis* (FRA, 2007)
8. Y.V. Ajudiya, *Classical Review of Frequency Response Analysis of Transformer* (ICEI, 2017)
9. P. Picher, C. Rajotte, C. Tardif, Experience with frequency response analysis (FRA) for the mechanical condition assessment of transformer windings, in *Electrical Insulation Conference*, Ottawa, Canada (June, 2013)
10. S. Miyazaki, Y. Mizutani, H. Suzuki, M. Ichikawa, Detection of deformation and displacement of transformer winding by frequency response analysis, in *International Conference on Condition Monitoring and Diagnosis* (2008).
11. J.A.S.B Jayasinghe, Z.D. Wang, P.N. Jarman, A.W. Darwin, *Winding Movement in Power Transformers: A Comparison of FRA Measurement Connection Methods* (IEEE, 2006)
12. S.B. Rathnayaka, K.Y. See, *Early Detection of Induction Motor's Defects Using an Inductively Coupled Impedance Extraction Method* (IEEE, 2017)
13. M. Brandt, S. Kascak, *Failure Identification of Induction Motor Using SFRA Method* (IEEE, 2016)
14. T.G. Vilhekar, M.S. Ballal, B.S. Umre, *Application of Sweep Frequency Response Analysis for the Detection of Winding Faults in Induction Motor* (IECON, 2016)
15. R. Raut, M.N.S. Swamy, *Modern Analog Filter Analysis and Design: A Practical Approach* (Wiley-VCH, 2010)

Coordination of Directional Over-Current Relays Serving to a 132 kV Ring-Main System—An Explanation to Undergraduate Students to Build Research Orientation



Srikanth Allamsetty

1 Introduction

Empowering undergraduate students is very essential to obtain practical solutions for many real-time problems. This can be achieved through explaining them how to apply their theoretical knowledge for real-time applications and building proper research orientation. MATLAB/Simulink, one of the most popular software packages with its toolboxes such as SimElectronics and SimPowerSystems, can be used to explain many theoretical concepts of engineering. It can also be helpful to give solutions for various problems involved in power system protection applications through simulations.

Distribution lines undergo abnormalities more frequently than the other parts of power systems in their life time due to various chances of fault occurrences, which leads to over-current, over-voltage, under frequency, etc. [1]. Over-current relay represents the most commonly installed protective equipment on any power system. The quality of selectivity among the said devices in a system is called coordination, which is one of the major problems in power system protection.

The relays control the act of isolating the faulty lines from the system, when a fault occurs in a power network, without disturbing the healthy lines. While a relay starting up, it sends a trip signal to its corresponding circuit breaker (CB) such that it clears out the fault. The output of the relay is normally an open contact, which changes over to closed state when the relay trips, i.e., when it sees some fault current [2]. These relays are placed at both ends of each line. Thus, the number of DOCRs in an electrical power system is twice the number of the lines.

S. Allamsetty (✉)

School of Electrical Engineering, Kalinga Institute of Industrial Technology Deemed to Be University, Bhubaneswar, Odisha 751024, India

e-mail: srikanth.allamsettyfel@kiit.ac.in

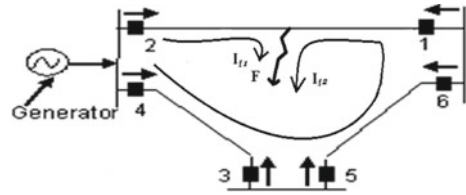
© Springer Nature Singapore Pte Ltd. 2021

K. S. Sherpa et al. (eds.), *Advances in Smart Grid and Renewable Energy*,

Lecture Notes in Electrical Engineering 691,

https://doi.org/10.1007/978-981-15-7511-2_12

Fig. 1 Illustration of primary and backup relays in a three-bus system



1.1 Problem Description

Figure 1 shows a simple three bus system which consists of one synchronous generator bus and two load buses and three transmission lines with six relays. This figure illustrates the operation of primary and backup relays when a fault occurred on one of its lines, i.e., between the relays 1 and 2.

The direction of fault currents, if a fault occurs on a particular line, has been shown in Fig. 1. As per the principles of DOCR, when fault occurs, the relay which senses a fault current leaving the bus operates for that particular fault. For better explanation, each relay has assigned with an arrow symbol on its top. If the fault current direction matches with the arrow direction, then that particular relay operates either as a primary relay or backup relay depending upon the fault current level. For the fault shown in figure, the relays 2 and 1 operate as primary relays. As per the direction of I_{f2} , relay 5 acts as a backup relay for relay 1, and relay 4 acts as a backup relay for relay 5. There is no backup relay for relay 2 as the fault current I_{f1} is not flowing in any other line.

The present study is to achieve this selective tripping, i.e., coordination of DOCRs in an existing power network. The process of development, in the means of interconnected power systems, has added complexity in power protection schemes, presenting a new set of conditions on the coordination of relays, since the fault current may flow to the fault point from both ends of any meshed line.

1.2 Literature Review and Contribution

Modeling and neuro-fuzzy control techniques are used to enhance the performances of power networks in recent studies [3, 4]. But, the performance of any system mainly depends on its protection system [5]. Thus, coordination of DOCRs is an important problem to look into, aiming no sympathy trips would take place [6]. There are other studies [7–10], where this problem was explained using Simulink and various optimization techniques. Authors of this study has explained the coordination of DOCRs in IEEE standard bus systems though MATLAB/Simulink models in [11]. In this paper, a test model for an existing power network, i.e., an 132 kV ring-main system, has been built using MATLAB/Simulink to explain the coordination of DOCRs. This study helps in learning how to design a test model and how to test

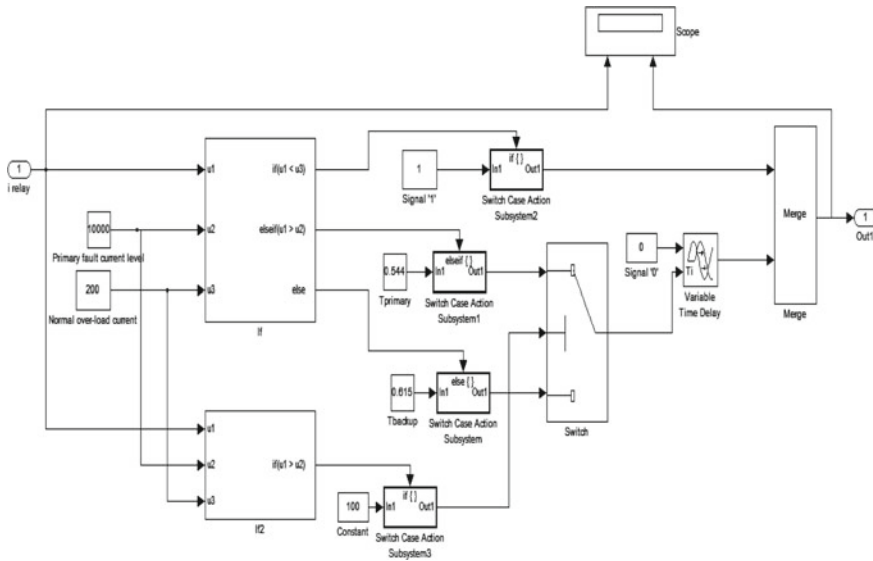


Fig. 2 Model Relay

the coordination of DOCRs for different faults occurring at different locations. The optimal time and plug settings for each DOCR, i.e., the decision variables TDS & PS, are manually calculated for this study. This model has been tested for different fault occurring chances. A model to realize DOCR application has been described as a ‘Model Relay’ (MR) in the following sections and shown in Fig. 2. Each DOCR in the test model is specially designed as a different MR such that they operate for the faults occurred in their own zone except to backup a failed relay, thus achieved selective tripping. This study helps in learning how to design a test model and how to test the coordination of DOCRs for different faults occurring at different locations.

2 Simulation Model

2.1 Model Relay

Before discussing about the test model, a clear explanation has been given on MR in this section. Figure 2 shows Model Relay (MR), which has been designed in MATLAB such that it operates as per the principles of a DOCR.

The main objectives of MR are:

- To send ‘1’ signal to the corresponding CB when I_{relay} is less than the normal over-load current of that particular branch, which makes the CB remained in closed state.

- To send '0' signal when I_{relay} exceeds the normal over-load current, which turns the CB into open state and thus isolates the faulty branch.

But another thing to check is whether it is primary fault or secondary fault, depending on which MR operates with either T_{primary} or T_{backup} . So I_{relay} has been compared with two levels of fault currents. If I_{relay} is greater than the primary fault current range, MR operates with a time delay of T_{primary} . If I_{relay} is in between normal over-load current and primary fault current, MR operates with a time delay of T_{backup} . 'If' and 'Switch' blocks are used for this logic as shown in Fig. 2. 'Variable Time Delay' block generates a '0' signal with the obtained time delay. The block 'Merge' has been used to send the latest signal generated to the corresponding CB, i.e., either '1' or '0'. Calculations of normal over-load current and primary fault currents are explained in detail while explaining the design procedure in Sect. 3. As per the requirement due to a particular fault on particular line, the MRs connected in that line are designed separately, and this has been discussed in same subsection in Sect. 3.1.

2.2 Introduction of Test Model of Existing Power Network

The data of an existing power network has been collected from power transmission corporation of Andhra Pradesh, India. Using that data, a model has been made in MATLAB and used as a test model for present study. MRs have been incorporated at both ends of each line. Operating times for various fault occurring chances have been calculated using MS Excel. Then, those values have been inserted in their particular MR and run the model to check whether those are coordinated well or not. No sympathy trips have been occurred. This subsection explains the procedure to construct a model in MATLAB for any existing power network and also explains the step-by-step procedure to coordinate all the DOCRs of that network without giving scope for sympathy trips.

2.3 Data of the Existing Power Network

The test model for the present study is that of an existing 132 kV power network located in Andhra Pradesh which is shown in Fig. 3.

It consists of six substations in a ring and four other substations connected to a particular substation, thus ten in total, which are considered as ten buses in the MATLAB model constructed. Length of lines and individual load values has been collected and made the test model accordingly.

The data has been tabulated as given below in Table 1 that consists of local load details in MWs and MVARs, i.e., real and reactive powers separately for each and every bus. Table 2 consists of the details of length of lines between the pairs of buses which are connected.

Fig. 3 Diagram of considered existing distribution system

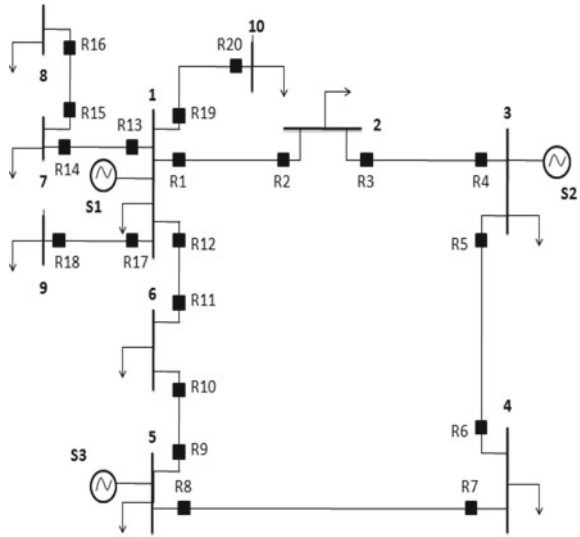


Table 1 Local load values for all buses

Bus No.		1	2	3	4	5	6	7	8	9	10
Local load	MW	168.58	10	71	54.5	150	41	28.8	24	23	14.4
	MVAR	61.18	3.62	32.34	21.5	60	14.88	10.45	8.71	8.5	5.23

Table 2 Length of lines between the buses which are connected

Line No.		1	2	3	4	5	6	7	8	9	10
Bus No.	From	1	2	3	4	5	6	1	7	1	1
	To	2	3	4	5	6	1	7	8	9	10
Length of line (Kms)		65.77	15.41	48	27	58.1	61.02	29.3	54	34.5	27.8

Per kilometer values of line parameters have been calculated for 132 kV line from skin effect, GMR, and GMD calculations, i.e., resistance $R = 0.2224$ ohms/Km, inductance $L = 0.476$ mH/Km, and capacitance $C = 0.024$ μ F/Km.

2.4 MATLAB Model for the Test Model

The test model, i.e., existing power network, has been constructed in MATLAB using simulink. The data given above has been inserted in various blocks of the model. Relay and its corresponding circuit breaker (CB) and current measurement (CM) blocks, which are at one side of the pi section block, have been made as a subsystem

to make it look simple. Therefore, there are two such subsystems for each line having pi section block in the middle for each transmission line. These subsystems are named as ‘CB and relay system’ and numbered from 1 to 20, i.e., total 20 such subsystems. This relay is again a subsystem and is said to be MR, which has been explained in Sect. 3. Per Km values of R , L , and C have been given as parameters for the pi section block. After running this model under normal conditions, normal branch currents for each branch can be seen in the scope blocks connected in each CB and relay system in the test model. Then, overloaded current can be calculated by multiplying these values with a fixed/assumed PS , i.e., 1.25.

Now, connect a ‘three-phase fault’ block in any particular line by modifying its properties as a single-phase to ground fault and note down the values of current magnitudes from the corresponding scopes. These values are nothing but the primary fault current levels for the relays connected at the both sides of that particular line and backup current levels for their backup relays.

3 Design Procedure and Fault Analysis

This section has been divided into three subsections. The procedures for designing MR and test model have been explained in first two subsections. Testing the model for various fault cases has been explained in third subsection.

3.1 Designing of MR

Before designing the MRs, the fault current levels in all transmission lines should be known for each and every fault occurring possibility. This can be done by connecting ‘fault’ block on both the ends of lines, i.e., on both sides of the ‘pi section model’ block to check for the close in and far-end fault conditions. Current levels sensed by relays 1–20 have been tabulated in Table 3 by connecting the faults on both ends. There is a ring-main system of six buses in the test model in which six distribution lines are there. So, for those six lines, 12 no. of conditions can be created for fault occurrences depending on the location. The fault current for a close in fault for the simulated model for some of the lines is around 7.7 MA, as it can be seen in table. But in real time, it would be around few kilo amperes only.

As said before, each subsystem, i.e., CB and relay system, is having one relay and one CB which is shown in Fig. 4. Here, in this subsection, the MR has been slightly modified according to the requirements of present test model.

The procedure for constructing MR of CB and relay system-1 (MR1) has been explained as follows.

Any relay should operate for the fault on its own line and should not be tripped for the faults on the other lines unless it is the backup relay for that particular fault. As per the fault current values given in Table 4, MR1 should operate as a primary relay

Table 3 Current levels when faults occurred on each end of each line

Relays	Lines											
	1		2		3		4		5		6	
	Current (amp)		Current (amp)		Current (amp)		Current (amp)		Current (amp)		Current (amp)	
	1st end	2nd end	1st end	2nd end	1st end	2nd end	1st end	2nd end	1st end	2nd end	1st end	2nd end
1	7.75×10^6	4827	4823	3253	42	42	42	42	42	42	42	42
2	3250	20.5×10^3	4842	3279	33	33	33	33	33	33	33	33
3	3295	20.5×10^3	4842	3261	44	44	44	44	44	44	44	44
4	3285	20.5×10^3	20.6×10^3	7.77×10^6	47	47	47	47	47	47	47	47
5	101	101	101	101	7.77×10^6	6625	6617	3570	101	101	101	101
6	112	112	112	112	3462	11.7×10^3	6631	3590	112	112	112	112
7	186	186	186	186	3664	11.7×10^3	6631	3456	186	186	186	186
8	191	191	191	191	3652	11.7×10^3	11.7×10^3	7.77×10^6	191	191	191	191
9	30	30	30	30	30	30	30	30	7.77×10^6	5464	5460	4193
10	41	41	41	41	41	41	41	41	4176	62.7×10^3	5476	4215

(continued)

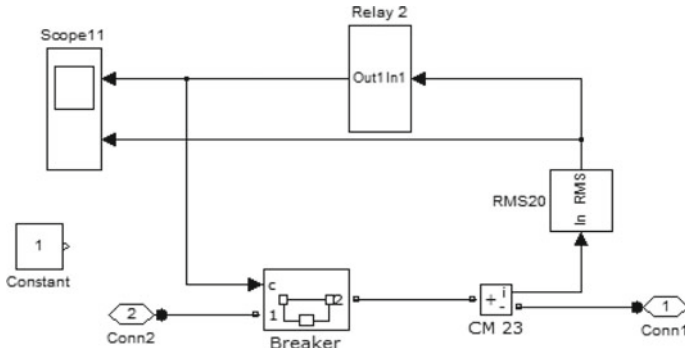


Fig. 4 CB and relay system

for the fault current values of 8 MA and 4827 A, and it should operate as a backup relay for MR3 when a fault occurs on line 2, i.e., it should be tripped for the fault current values of 4823 A and 3253 A with a CTI of 0.3 s with MR3. To implement all these logics, the condition that should be given in the ‘If’ block has to be given as shown in Fig. 2. When $u1 < u3$, i.e., current seen by the relay (i) is less than normal over-load current, MR1 will send signal ‘1’ to its corresponding CB. When $u1 > u2$, i.e., i is greater than minimum fault current level for primary operation, MR1 will send signal ‘0’ with a lesser time of operation, i.e., 0.165 s in this case. Otherwise, it will operate as a backup relay for MR3 and sends signal ‘0’ with a time delay of 0.338 s.

Similarly, all the MRs of the test model have been constructed as per the requirements.

Table 4 Values of primary and backup operating times for close in faults

	Variable	Time (s)	Variable	Time (s)	Variable	Time (s)
Primary relay	TDS2	0.05	TDS3	0.05	TDS6	0.05
	T_{P2}	0.033	T_{P3}	0.039	T_{P6}	0.035
Corresponding backup relay	T_{B4}	0.333	T_{B1}	0.339	T_{B8}	0.335
	TDS4	0.509	TDS1	0.435	TDS8	0.480
	T_{P4}	0.194	T_{P1}	0.166	T_{P8}	0.183
Primary relay	TDS7	0.05	TDS10	0.05	TDS11	0.05
	T_{P7}	0.037	T_{P10}	0.029	T_{P11}	0.038
Corresponding backup relay	T_{B5}	0.337	T_{B12}	0.329	T_{B9}	0.338
	TDS5	0.451	TDS12	0.568	TDS9	0.441
	T_{P5}	0.172	T_{P12}	0.216	T_{P9}	0.168

Table 5 Values of primary operating times for far-end faults

	T_{p1}	T_{p2}	T_{p3}	T_{p4}	T_{p5}	T_{p6}	T_{p7}	T_{p8}	T_{p9}	T_{p10}	T_{p11}	T_{p12}
Time (s)	0.33	0.04	0.04	0.33	0.33	0.04	0.04	0.33	0.01	0.01	0.04	0.32

3.2 Operating Times and Objective Function

The optimization problem for coordination of DOCRs is to minimize the objective function. It is nothing but the summation of all primary operating times of all the relays of a particular system. Operating times of primary and backup relays can be calculated using (1).

$$T^i = \frac{0.14 * TDS^i}{\left(\frac{I_f^i}{PS^i}\right)^{0.02} - 1} \quad (1)$$

Here, in Tables 4 and 5, primary (T_P) and backup (T_B) operating time calculations, which are done in MS Excel, have been given for close in and far-end faults, respectively. Sum of these times in both cases are given in (2) and (3).

$$\sum_{i=1}^{N_{cl}} T_{pri_cl_in}^i = 1.31 \text{ s} \quad (2)$$

$$\sum_{j=1}^{N_{far}} T_{pri_far_bus}^j = 1.895 \text{ s} \quad (3)$$

Then, the value of objective function $F = 3.2$ s.

This value can be further minimized if we use optimization algorithms as discussed earlier by considering both TDS and PS as unknowns.

$T_{primary}$ and T_{backup} for all the relays with all possible faults have been calculated and incorporated in their respective MRs.

3.3 Fault Analysis

Some of the fault occurring chances have been discussed in this subsection. There are a total of 12 locations in the ring-main system in which if fault occurs it could be a close in fault for some relay and causes high fault current. Here, two such locations on line have been discussed in three different cases. The model can be tested for the remaining fault locations also in a similar way.

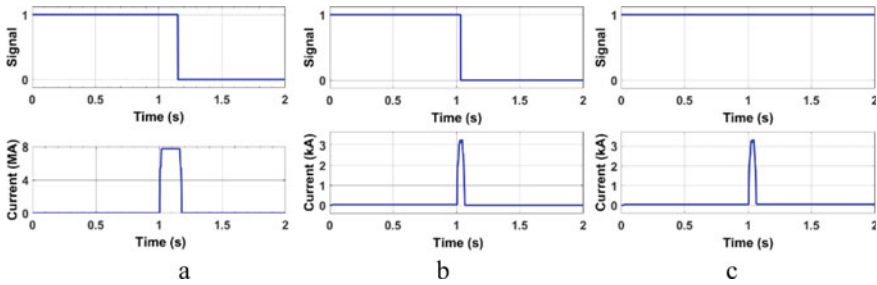


Fig. 5 Relay signals and change in corresponding line currents in case I **a** MR1 **b** MR2 **c** MR3 and MR4

3.3.1 Case I (Close in Fault for MR1)

When a close in fault occurs for MR1, it operates as a primary relay along with MR2. It can be observed from Fig. 5a, b that MR1 and MR2 are giving trip signals as per their primary operating times.

As per Table 3, in this case, fault currents would also be seen by MR3 and MR4. Remaining MRs will see normal load current only. But MR3 and MR4 should not be tripped for this fault instantaneously and MR3 should operate as a backup relay such that it would operate only when MR1 failed to operate. Thus, MR3 has not given trip signal as shown in Fig. 5c. The relay MR4 is not even a backup relay and thus has not operated, and its scope is similar to that of MR3.

3.3.2 Case II (Close in Fault for MR1 and MR2 Fails to Operate)

In this case, ‘fault’ block is connected nearer to MR1 and a continuous signal ‘1’ has been given to the corresponding circuit breaker CB2 by connecting constant block with value 1 as a control signal instead of MR2’s output.

Figure 6a remains as it was in the case I, but from Fig. 6b, it can be observed that fault current did not come back to normal even after the trip signal from MR2. It happened so because MR2’s output is not connected to CB2 in this case instead which a constant ‘1’ signal has been connected. This is done to create an intentional failure of MR2 to see whether its backup relay works or not.

Figure 6c shows that there is no trip signal sent from MR3 as it is not the backup relay. From Fig. 6d, it can be observed that the fault current came back to normal only after getting a trip signal from MR4. It is happened because MR4 is the backup relay for MR2 and figure confirms this.

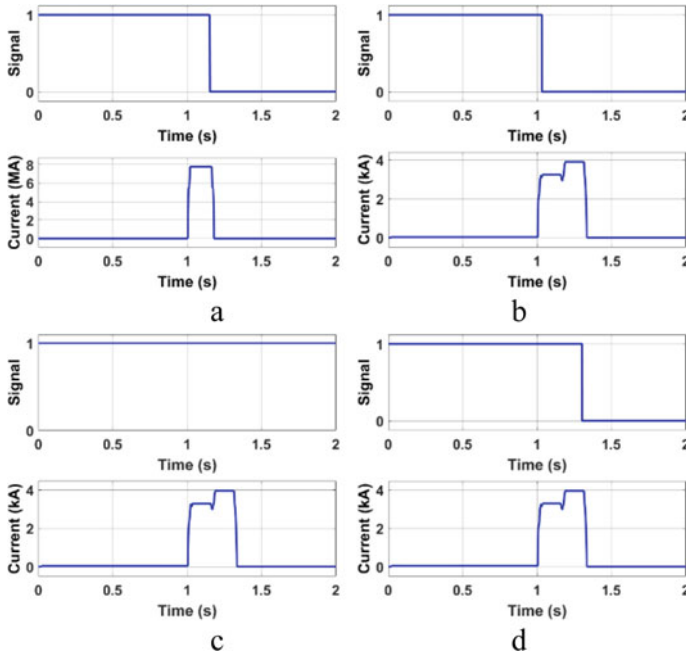


Fig. 6 Relay signals and change in corresponding line currents in case II **a** MR1 **b** MR2 **c** MR3 **d** MR4

3.3.3 Case III (Far-End Fault for MR1 and MR2 Fails to Operate)

In this case, ‘fault’ block is connected nearer to MR2, and the continuous signal ‘1’ that is given to CB2 has been left as it is in case II. This case is to check whether the backup relay of MR2 is working properly even when the current level is high.

Figure 7a remains as it was in the case II, but current level changes. From Fig. 7b, it can be observed that fault current did not come back to normal even after the trip signal from MR2 because MR2’s output is not connected to CB2 in this case also. Figure 7c shows that there is no trip signal from MR3 so as in the case IV. From Fig. 7d, it can be observed that the MR4 has given trip signal, and the corresponding fault current came back to normal only after getting this trip signal. That means, MR4 is operating well as a backup relay for MR2 at its backup operating time irrespective of the fault current range.

4 Conclusion

The objective of this study is to make the undergraduate students understand the concept of coordination of DOCRs and to build a research orientation by giving

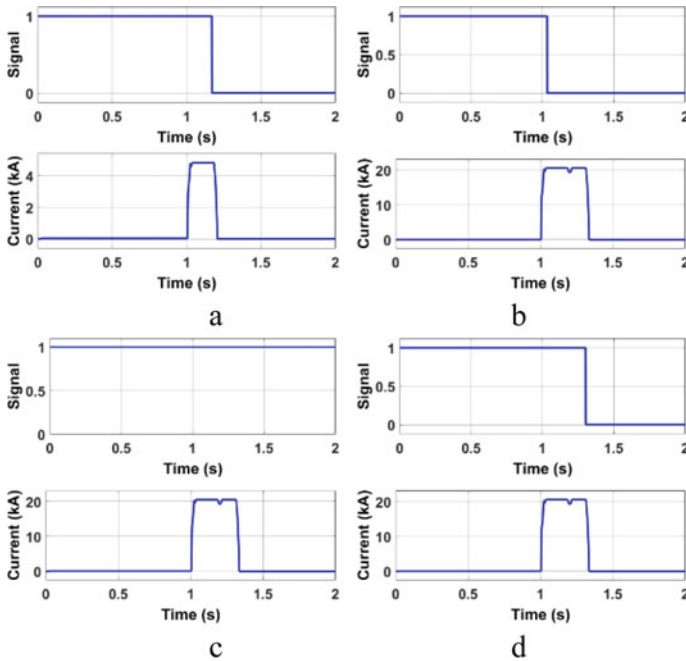


Fig. 7 Relay signals and change in corresponding line currents in case III **a** MR1 **b** MR2 **c** MR3 **d** MR4

them an insight regarding applying their theoretical knowledge for solving real-time problems. The procedure for designing a test model for an existing power network using MATLAB/Simulink and testing it for various conditions have been discussed in this paper. Different fault occurring cases according to location have been discussed, from which it can be said that the test model is well designed in MATLAB such that there are no sympathy trips. It can be said that DOCRs in the test model are well coordinated and thus proved that MRs have been working well to describe the working principle of DOCRs. Thus, this study gives undergraduates a motivation to use simulation platforms for obtaining research outcomes for various practical problems.

References

1. T.R. Chelliah, T. Radha, A. Srikanth, M. Pant, Coordination of directional overcurrent relays using opposition based chaotic differential evolution algorithm. *Int. J. Electr. Power Energy Sys.* **55**, 341–250 (2013)
2. P.M. Anderson, *Power System Protection* (IEEE Press Series Power Eng., McGraw-Hill, 1999), pp. 250–254

3. B.N. Mike, Z.D. Sasa, H.G. Ignacio, Reliability enhancement in power networks under uncertainty from distributed energy resources. *Energies* **12**, 531–537 (2019)
4. K.K. Kiran, S.P. Sai, Power Management and Control of Multi-Input Multi-Output Renewable Energy System Using ANFIS Controller. *Int. J. Recent Technol. Eng.* **8**, 224–226 (2019)
5. S.V. Khond, G.A. Dhokane, Optimum coordination of directional overcurrent relays for combined overhead/cable distribution system with linear programming technique. *Protect. Control Modern Power Syst.* **4**, 1–7 (2019)
6. D. Birla, R. Maheshwari, H. Gupta, Time-overcurrent relay coordination: a review. *Int. J. Electr. Power Energy Sys.* **2**, 1039 (2015)
7. N.R. Vipul, S.P. Kartik, A hybrid improved harmony search algorithm-nonlinear programming approach for optimal coordination of directional overcurrent relays including characteristic selection. *Int. J. Power Energy Convers.* **9**, 228–253 (2018)
8. J. Ren, M. Kezunovic, Teaching protective relaying design and application using new modeling and simulation tools. *J. Energy Power Eng.* **6**, 762–770 (2012)
9. X. Luo, M. Kezunovic, Novel digital relay model based on SIMULINK and its validation based on expert system, in *IEEE PES Transmission and Distribution Conference and Exhibition, Asia and Pacific Dalian, China* (2005)
10. Z. Yujie, L.B. Jimena, N.S. Noel, P. Daxa, *Modeling and Testing of Protection Devices for SPS Using MATLAB/Simulink and VTB* (IEEE Elec. Ship Tech. Symp., Arlington, USA, 2007)
11. T.R. Chelliah, A. Srikanth, Coordination of directional over-current relays using MATLAB/simulink and their integration into undergraduate power system protection courses, in *10th International Conference on Advances in Power System Control, Operation and Management (APSCOM 2015)*, Hong Kong (2015)

A Flexible Multi-Slot Wireless Antenna Designed for Reconfigurable Frequency



Akanksha Lohia, V. K. Singh, and Anurag Saxena

1 Introduction

Since transmission of power or any information can be done by different methods and technologies, there are also different modes for this purpose as we say it through wire or wireless; but wireless is the advanced technology for the low power devices and also reduces the time during the transmission process. Wireless transmission is also required for remote areas, so that execution of transmission could be done smoothly. Nowadays, the demand of reconfigurable antenna has been increased that has multi-functional characteristics, and same antenna has been used for different applications [1–3].

With the advancement of the technologies, some technology provides double-band or triple-band configuration. But today, technology demand is not limited to band but also cost, weight, flexibility, and other parameters. Textile antenna design has multiple characteristics such as low weight, less expensive, and availability. In this type of antenna, there are many strategies that we apply for a higher bandwidth and gain such as by using partial ground, different types of patch, and its dimensions and also different types of substrates [4–7].

A. Lohia · V. K. Singh (✉) · A. Saxena
Department of Electrical Engineering, SR Group of Institutions, Jhansi, Uttar Pradesh, India
e-mail: Singhvinod34@gmail.com

A. Lohia
e-mail: lohia.akanksha2@gmail.com

A. Saxena
e-mail: anurag.saxena.anurag@gmail.com

In wireless communication systems, specific frequency bands are used for specific purposes such as WLAN (2.4–2.48 GHz) and WiMAX (2.5–2.69 GHz). This paper is designed keeping in mind that it can be applicable for multiple bands and also be flexible. So, this article proposed a triple-band multi-slot microstrip patch antenna with partial ground structure having substrate material jeans is used for frequencies 6.4, 7.83, and 9.35 GHz that lies in C-Band and X-Band. The dielectric constant of jeans is less that means it has lower value of attenuation constant and also improves bandwidth for the transmission [8–12]. The proposed antenna can be used for different applications such as mobile, fixed satellite, and radio navigation. This design also provides sufficient level of bandwidth with a special design by using multiple rectangular cuts in the patch.

2 Antenna Design

The proposed antenna design consists of partial conducting patch used as a ground plane, dielectric substrate material, and microstrip conducting patch. For the purpose of designing partial ground plane and microstrip patch, a copper tape is used which has the thickness of 0.038 mm. And for the flexibility of antenna, a substrate material jeans having thickness of 1 mm is used. This proposed multi-slot antenna gives triple-band wireless communication. Figure 1 shows the geometry of the proposed antenna in front and back view and antenna parameters are shown in Table 1.

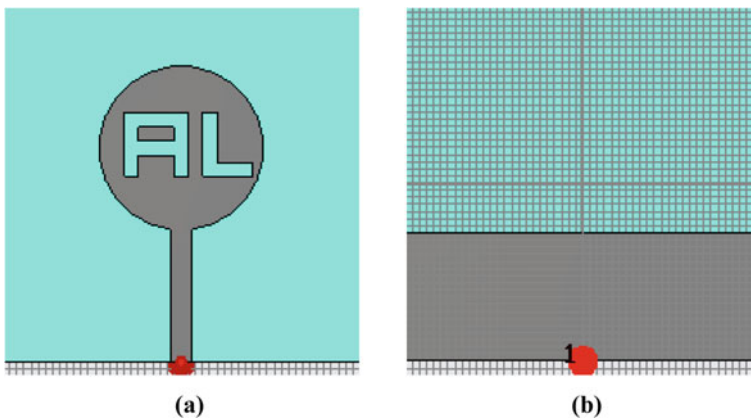


Fig. 1 Geometry of flexible multi-slot antenna **a** front view **b** back view

Table 1 Dimensions of designed parameters for proposed textile antenna

S. No.	Antenna parameter	Dimension
1.	Ground dimension	50 mm × 18 mm
2.	Substrate dimension	50 mm × 50 mm
3.	Substrate height	1 mm
4.	Patch large circle diameter	23 mm
5.	Feed dimension	3 mm × 19 mm
6.	Rectangular strip slot in patch	2 mm × 7 mm

3 Result Analysis

The characteristics of the proposed antenna has been analyzed and studied. The simulation has different graphs for representing parameters such as return loss, directivity, radiation efficiency, and polar characteristics. Here, Fig. 2 shows return loss magnitude in dB Vs frequency in GHz with triple band at resonant frequencies 6.4, 7.53, and 9.35 GHz.

Figure 3 represents the 3D characteristics of the suggested antenna which describes the radiation pattern in terms of directivity, radiation efficiency, etc.

At the end, the polar characteristics of the proposed antenna have also shown in Fig. 4 at different frequencies like 6.4, 7.83, and 9.35 GHz.

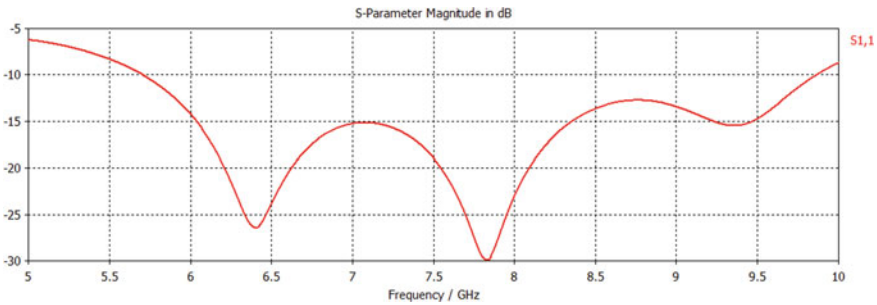
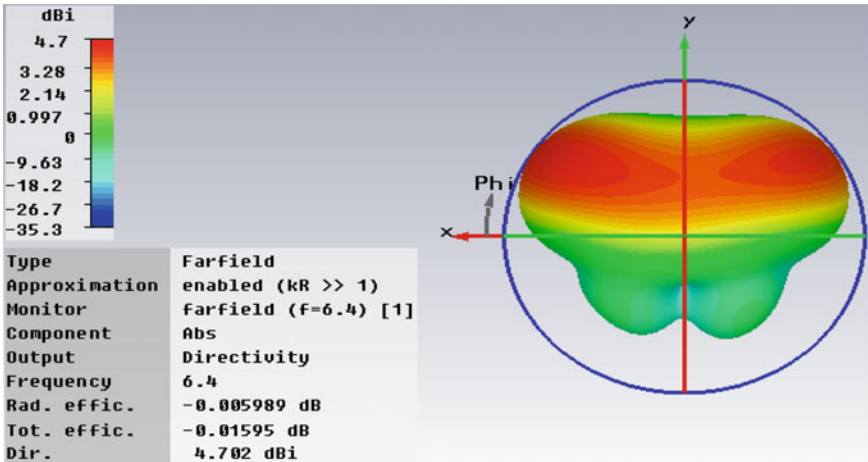
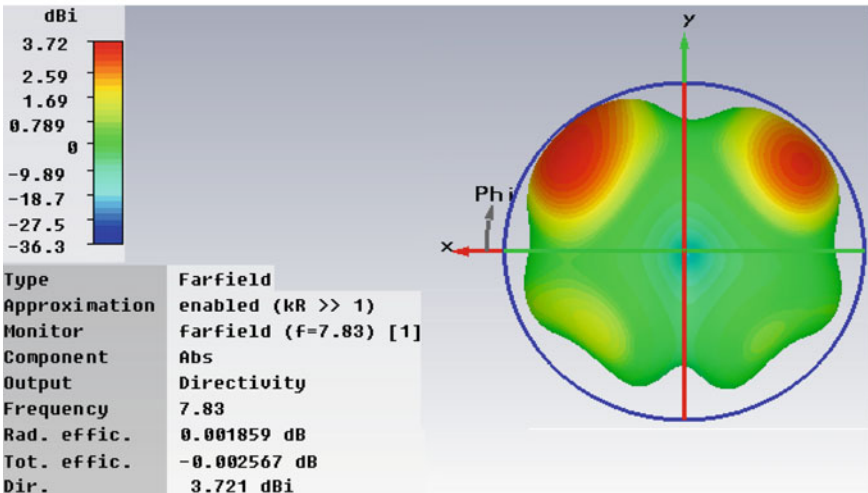


Fig. 2 Return loss versus frequency simulated graph

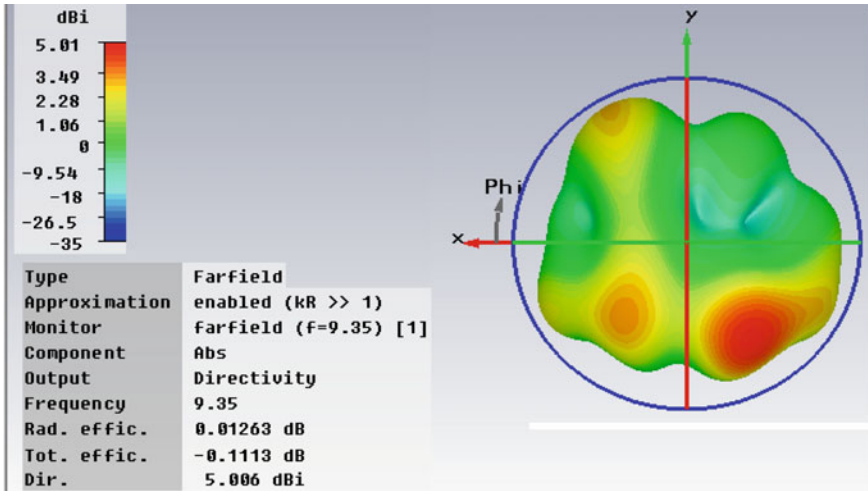


(a) 3D Radiation pattern at 6.4GHz



(b) 3D Radiation pattern at 7.83GHz

Fig. 3 a 3D radiation pattern at 6.4 GHz. b 3D radiation pattern at 7.83 GHz. c 3D radiation pattern at 9.35 GHz



(c) 3D Radiation pattern at 9.35GHz

Fig. 3 (continued)

4 Conclusion

The wireless transmission is the best way for power transmission where it is inconvenient to transmit power by transmission line. Here, the substrate material used jeans are very flexible and wearable. So, it is used to design an antenna by using multi-slot with triple-band characteristics and of bandwidth 53%. This proposed antenna gives directivity 4.702 dBi, 3.721 dBi, and 5.006 dBi, respectively, at resonant frequencies 6.4 GHz, 7.83 GHz, and 9.35 GHz.

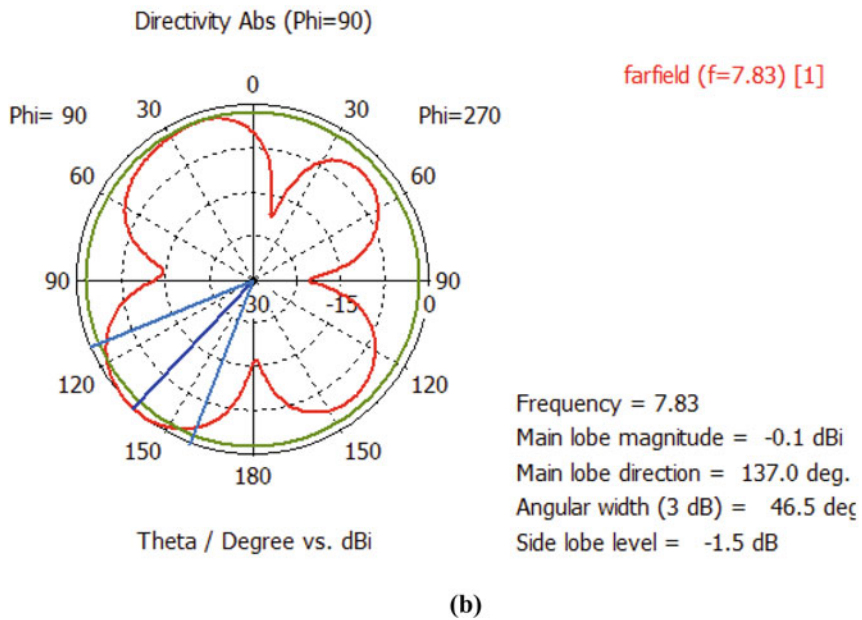
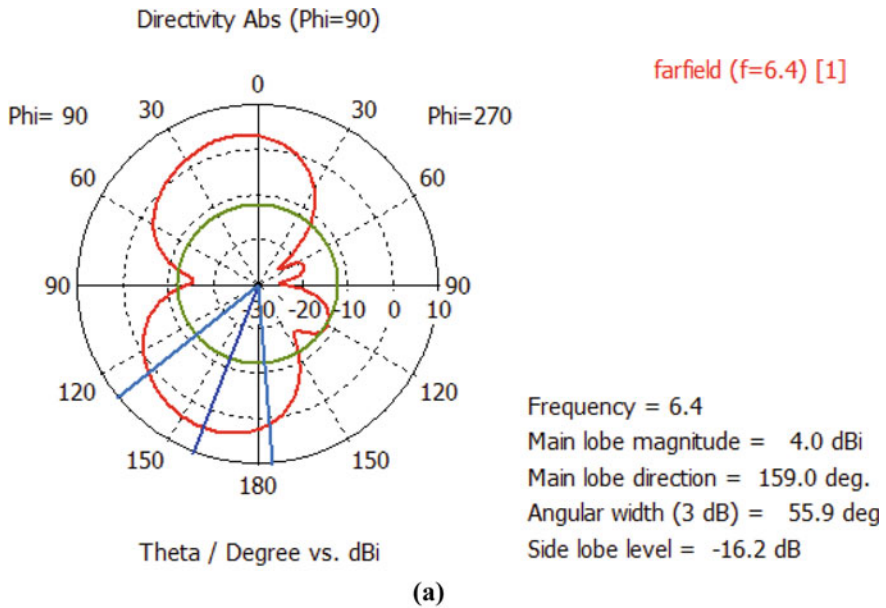


Fig. 4 Polar plot of radiation pattern at **a** 6.4 GHz **b** 7.83 GHz **c** 9.35 GHz

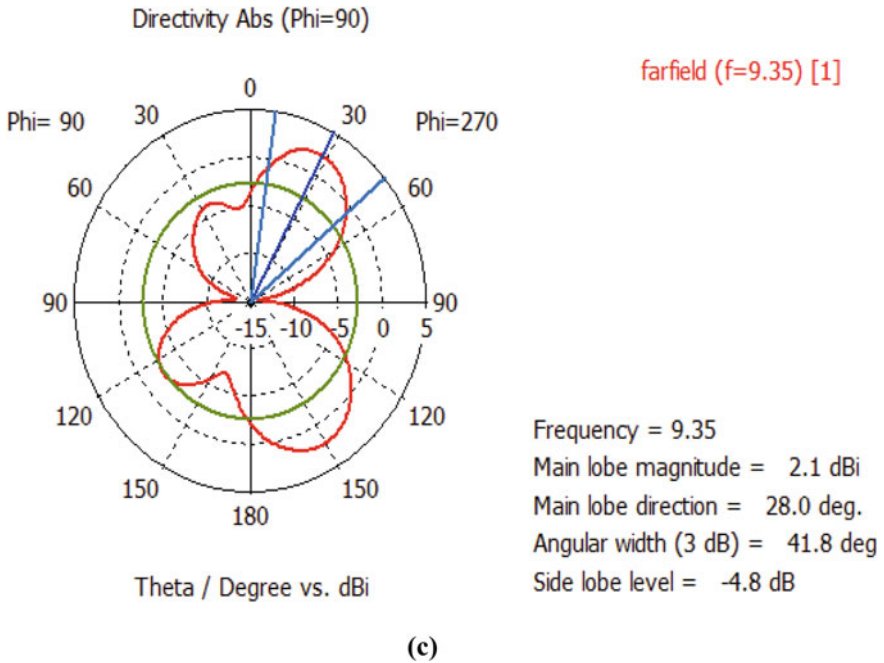


Fig. 4 (continued)

References

1. A. Saxena, B.B. Khare, A hammer type textile antenna with partial circle ground for wide band applications, in *Design and Optimization of Sensors and Antennas for Wearable Devices: Emerging Research and Opportunities*, 15–24 (September, 2019)
2. A. Saxena, P. Raizada, L.P. Gautam, B.B. Khare, Efficient rectenna circuit for wireless power transmission, in *Design and Optimization of Sensors and Antennas for Wearable Devices: Emerging Research and Opportunities*, 57–65 (September, 2019)
3. A. Saxena, V.K. Singh, A moon-strip line antenna for multi-band applications at 5.44 GHz resonant frequency, in *4th International Conference on Advances in Electrical, Electronics, Information, Communication and Bio-Informatics (AEEICB-18)* (August, 2018)
4. V.K. Singh, A. Saxena, B.B. Khare, V. Shayka, G.-S. Chae, A. Sharma, A.K. Bhoi, Power harvesting through flexible rectenna at dual resonant frequency for low power devices. *Int. J. Eng. Technol.* **7**(2.33), 647–649 (2018)
5. Vinod Kumar Singh and Anurag Saxena, Two parabolic shape microstrip patch antenna for single band application. *J. Microw. Technol.* **5**(1), 33–36 (2018)
6. V. Verma, Vinod Kumar Singh and Anurag Saxena, Optimization of microstrip antenna for WLAN and WiMax lower band applications. *J. Microw. Technol.* **3**(2), 19–24 (2016)
7. A. Yadav, V.K. Singh, P. Yadav, A.K. Belya, A.K. Bhoi, P. Barsocchi, Design of circularly polarized triple-band wearable textile antenna with safe low SAR for human health. *Electronics* **2020** **9**, 1366 (2020)
8. V.K. Singh, S. Dhupkariya, N. Bangari, Wearable ultra wide dual band flexible textile antenna for WiMax/WLAN application. *Wirel. Pers. Commun.* **95**(2):1075–1086 (2017)

9. A. Yadav, V. Kumar Singh, A. Kumar Bhoi, G. Marques, B. Garcia-Zapirain, I. de la Torre Díez, Wireless body area networks: UWB wearable textile antenna for telemedicine and mobile health systems. *Micromachines* **11**(6):558 (2020)
10. R. Singh, V.K. Singh, P. Khanna, A compact CPW-Fed defected ground microstrip antenna for Ku band application. *Advances in Electronics, Communication and Computing*. Lecture Notes in Electrical Engineering, vol. 443, pp. 231–237 (2018)
11. V.K. Singh, R. Tiwari, V. Dubey, *Design and Optimization of Sensors and Antennas for Wearable Devices* (ISBN: 9781522596837). IGI Global Publication USA (2019)
12. N. Singh, A. Kumar Singh, V.K. Singh, Design & performance of wearable ultra wide band textile antenna for medical applications. *Microwave Opt. Technol. Lett.* **57**(7), 1553–1557, Wiley Publications, USA (2015)

A Comparative Brief Study on Level-Shifted Pulse Width Modulation and Hybrid Pulse Width Modulation Switching Techniques for 7-Level CHB Single-Phase Inverter



Nikhil Agrawal, Shikha Goswami, Rinisha Bagaria, and Ajay Muthele

1 Introduction

Inverter is most widely used solid-state device which works as a converter, and it converts DC power into an AC power. The multilevel inverter is introduced in 1975 [1]. An AC power available at converter load side has some harmonic content which may degrade the quality of power and can create power quality issue [2]. These issues can be avoided by using MLI. The MLI synthesizes the AC voltage or AC current waveform and make the waveform nearer to ideal sinusoidal wave [3]. Although multilevel inverter has distortion that can be avoided by using filter circuit and different modulation techniques, in this paper, 7-level CHB inverter proposed with LC filter circuit and without LC filter circuit apply level-shifted and hybrid modulation technique with over- and undermodulation index and check the performance in terms of total harmonic distortion. Modulation index plays a vital role in switching technique. Modulation index is defined as ratio of modulating signal amplitude to carrier signal peak-to-peak amplitude. Modulation index is overmodulation, unit modulation, and undermodulation. The overmodulation which has modulation index (M_a) is greater than 1, unit modulation index has a value 1, and undermodulation has modulation index less than 1.

N. Agrawal (✉)

SR Group of Institutions, Jhansi, Uttar Pradesh, India

e-mail: nikhilag.agrawal@gmail.com

S. Goswami

P.K.University Shivpuri, Thanra, Madhya Pradesh, India

R. Bagaria

Madhav Institute of Technology and Science Gwalior, Gwalior, Madhya Pradesh, India

A. Muthele

Modern College of Engineering, Jhansi, Uttar Pradesh, India

© Springer Nature Singapore Pte Ltd. 2021

K. S. Sherpa et al. (eds.), *Advances in Smart Grid and Renewable Energy*,

Lecture Notes in Electrical Engineering 691,

https://doi.org/10.1007/978-981-15-7511-2_14

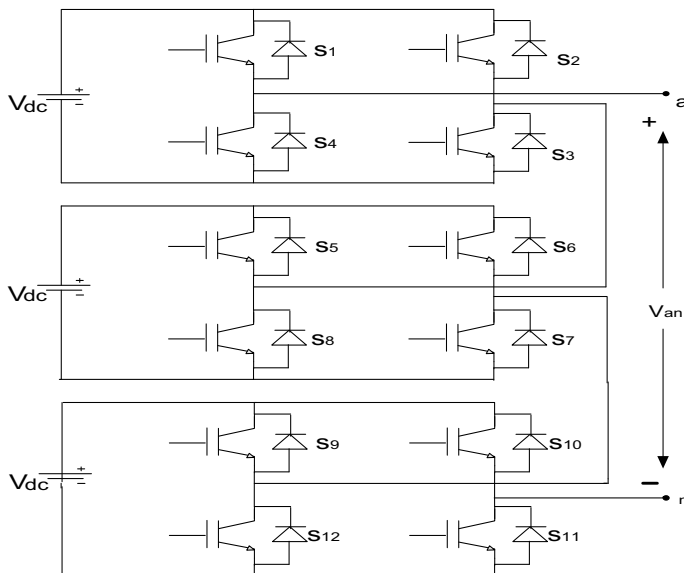


Fig. 1 7-level structure of CHB inverter topology

2 Cascade H-bridge Multilevel Inverter (CHB)

The CHB inverter topology is introduced in 1975 [4]. CHB inverter is the conventional MLI topology. CHB inverter is also known as modular MLI. Cascade H-bridge uses cascade connection of single-phase full bridge with separate source. A single full bridge generates three voltage levels $+V_{dc}$, 0 , $-V_{dc}$. For N level output $(N - 1)/2$ full bridge require. The advantage of using cascade H-bridge MLI is it requires least component compared to two other conventional MLI topology flying capacitors and diode-clamped multilevel inverters [5]. CHB inverter topology consists of one parent unit which produces three-level output and more unit connected in this parent unit produce 5-level, 7-level, and so on level output. In this paper, 7-level CHB is proposed; so, the proposed topology consists three units of bridge inverter. 7-level CHB is shown in Fig. 1, and Table 1 shows the ON switches sequence to obtain voltage level in proposed 7-level inverter (Fig. 2).

3 Level-Shifted Pulse Width Modulation Switching Technique

Level-shifted PWM switching technique is the multicarrier pulse width modulation technique, which is applied minimum three levels of inverter. In level-shifted PWM technique, for N level, $N - 1$ carrier signals are required. For 7-level inverter, six

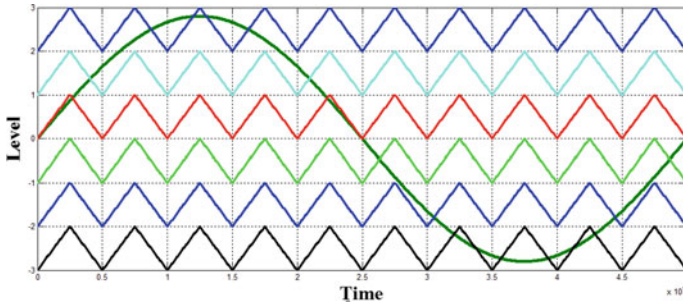


Fig. 2 Carrier arrangement of PDPWM

carriers are required. Level-shifted PWM switching technique used $N - 1$ carrier signal which is vertically shifted to each other [6]. A level-shifted PWM techniques can be classified in three types.

3.1 Phase Disposition Pulse Width Modulation Switching Technique (PDPWM)

In this technique, for 7-level inverter, all six carrier signals have equal magnitude and equal frequency. All the carrier signals have same phase sequence arrangement, i.e., phase shifting is zero.

3.2 Phase Opposition Disposition Pulse Width Modulation Switching Technique (PODPWM)

In this switching technique, all the carrier signals have equal magnitude and same frequency and the carrier signals are arranged in alternate manner with respect to zero reference line [7]. For 7-level inverter, there are six carrier signals, out of these three carrier signals in upper of the zero reference line and other three carrier signals below the reference lineout of phase 180° are shown in Fig. 3.

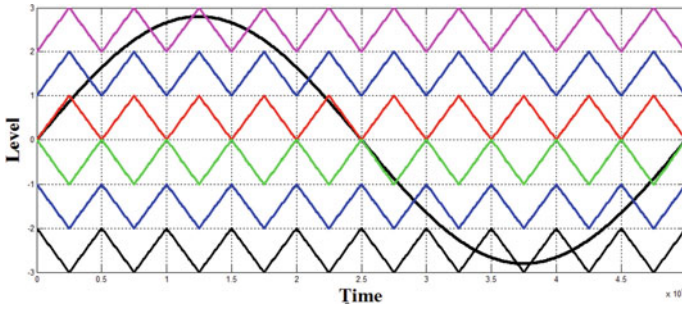


Fig. 3 Carrier arrangement of PODPWM

3.3 Alternate Phase Opposition Disposition Pulse Width Modulation Switching Technique (APODPWM)

In this technique, all carrier signals have equal amplitude and equal frequency similar to two other switching techniques but all the adjacent carrier signals are out of phase by 180° as shown in Fig. 4.

4 Hybrid Pulse Width Modulation Switching Technique

In hybrid PWM technique, for N level inverter, $N - 1$ carrier signals are required. Hybrid PWM technique can be classified in two types [8].

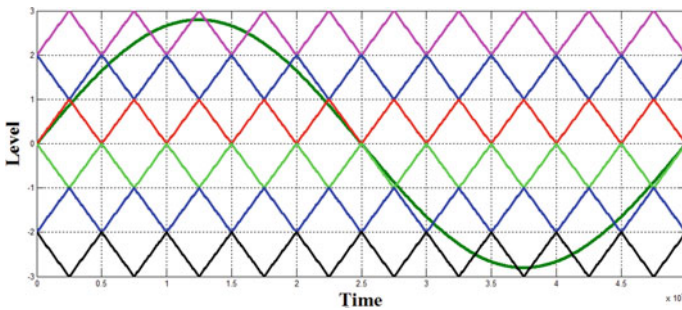


Fig. 4 Carrier arrangement of APODPWM

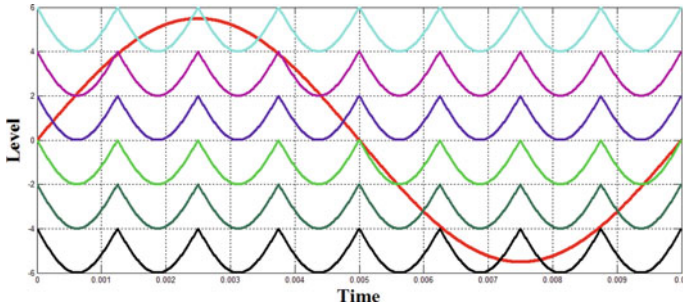


Fig. 5 Carrier arrangement of ISCPWM

4.1 *Sine Inverted Carrier Pulse Width Modulation Technique (SICPWM)*

In this technique, the carrier signal is inverted half sine wave shape and reference signal is sine wave with fundamental frequency and carrier signal has high frequency [9]. The carrier arrangement for ISCPWM technique is shown in Fig. 5.

4.2 *Sine Inverted Carrier Pulse Width Modulation Switching Technique with Variable Frequency (ISCPWMVF)*

In sine inverted carrier pulse width modulation technique with variable frequency, for N level inverter, $N - 1$ carrier signals are required. In this switching technique, the carrier signal is half sine wave carrier with variable frequency and sine wave has inverted nature. All the carrier signal amplitudes are equal with equal frequency, and these carriers signals are arranged in same phase [10]. The carrier arrangement for ISCPWMVF is shown in Fig. 6.

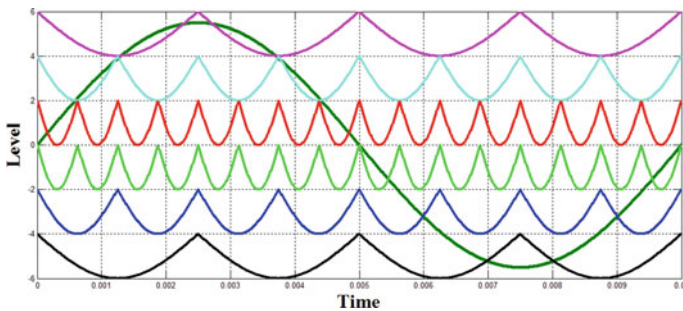


Fig. 6 Carrier arrangement of ISCPWMVF

Table 1 Switching arrangement for cascade H-bridge 7-level inverter

Output voltage magnitude	ON switches	Level
+3 V	$S_1, S_3, S_5, S_7, S_9, S_{11}$	1
+2 V	$S_1, S_3, S_5, S_7, S_9, S_{10}$	2
+1 V	$S_1, S_3, S_5, S_6, S_9, S_{10}$	3
0 V	$S_1, S_2, S_5, S_6, S_9, S_{10}$	4
-1 V	$S_2, S_4, S_7, S_8, S_{12}, S_{11}$	5
-2 V	$S_2, S_4, S_6, S_8, S_{11}, S_{12}$	6
-3 V	$S_2, S_4, S_6, S_8, S_{10}, S_{12}$	7

5 Result and Discussion

In this paper, the simulation results for 7-level CHB inverter are discussed. The simulation results are obtained from MATLAB/Simulink 2010b software. In this paper, symmetrical model of 7-level CHB inverter is simulated with input voltage V_s 10 V and reference signal frequency 50 Hz and carrier signal frequency 2000 Hz. In this section, the proposed MLI topology without filter and with filter circuit's performance is judged by applying level-shifted PWM techniques and hybrid PWM techniques with amplitude overmodulation index and amplitude undermodulation index. In this paper, the cutoff frequency for filter circuit taken is 2000 Hz. Table 2 shows the FFT analysis of the proposed 7-level CHB inverter, and Table 3 shows the 7-level CHB inverter output voltage waveform with filter and without filter circuit. The performance of proposed topology is judged by total harmonic distortion parameter. Table 4 shows the results of proposed topology for without filter circuit, and Table 5 shows the FFT results of proposed topology with filter circuit.

6 Simulation Parameters

Input DC voltage—10 V.

Fundamental frequency—50 Hz.

Carrier signal frequency—2000 Hz.

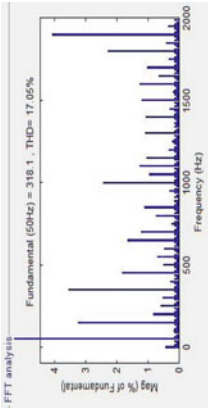
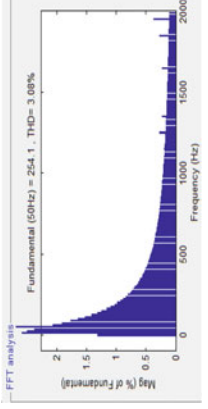
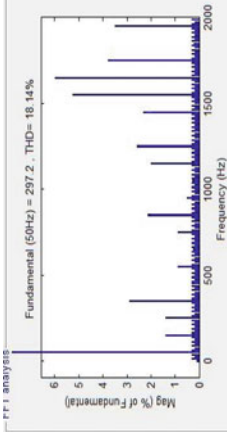
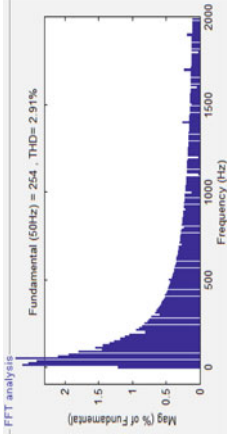
Switch—IGBT.

Load—Resistive of 10 Ω .

Modulation index—0.9, 1.0, 1.1.

Filter circuit—(L) = 10e-3 H and (C) = 1e-6 F.

Table 2 FFT analysis of the proposed 7-level CHB inverter

Without filter circuit	With filter circuit
 <p>(a) PDPWM with $M_a=1.1$</p>	 <p>(a) POD PWM with $M_a=1.0$</p>
 <p>(b) APD PWM with $M_a=1.0$</p>	 <p>(b) PD PWM with $M_a=1.0$</p>

(continued)

Table 2 (continued)

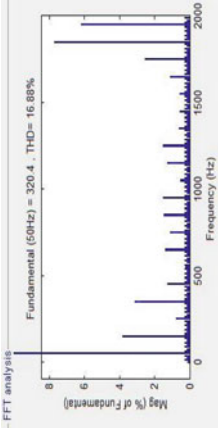
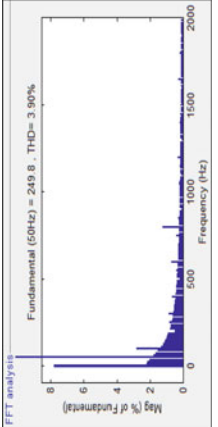
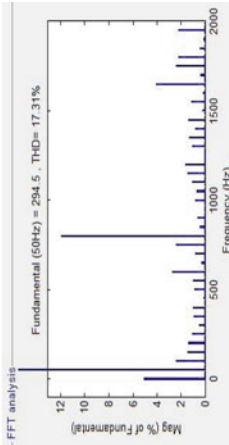
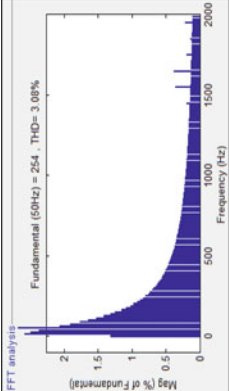
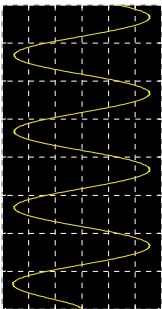
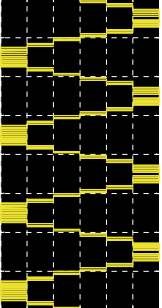
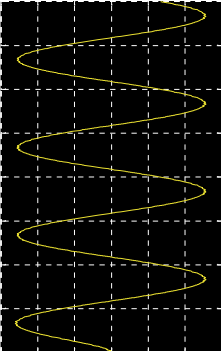
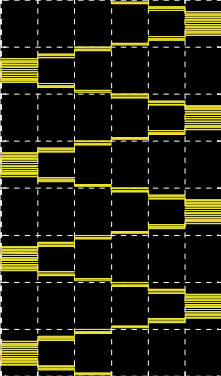
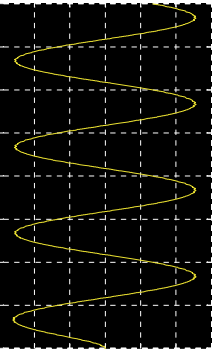
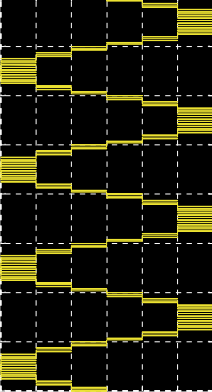
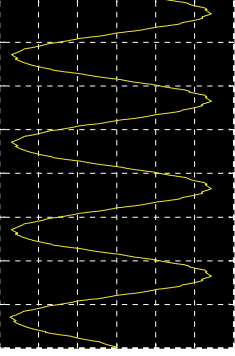
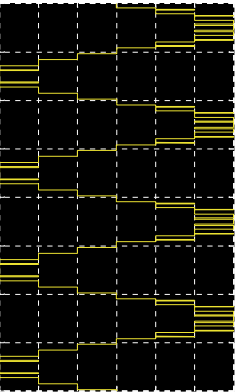
Without filter circuit	With filter circuit
 <p data-bbox="452 1208 482 1411">(c) POD PWM with Ma=1.1</p>	 <p data-bbox="452 502 482 705">(c) ISC PWM with Ma=1.0</p>
 <p data-bbox="758 1208 787 1411">(d) ISC PWM with Ma=1.0</p>	 <p data-bbox="758 502 787 705">(d) APOD PWM with Ma=1.0</p>

Table 3 Comparison in output voltage waveform for proposed 7-level CHB inverter

Output voltage waveform	Without filter circuit
With filter circuit	
 <p data-bbox="436 1363 456 1451">(a) PD PWM</p>	 <p data-bbox="436 575 456 663">(a) PD PWM</p>
 <p data-bbox="726 1324 746 1442">(b) POD PWM</p>	 <p data-bbox="732 508 752 626">(b) POD PWM</p>

(continued)

Table 3 (continued)

Output voltage waveform With filter circuit	Without filter circuit
 <p>(c) APOD PWM</p>	 <p>(c) APOD PWM</p>
 <p>(d) ISC PWM</p>	 <p>(d) ISC PWM</p>

(continued)

Table 3 (continued)

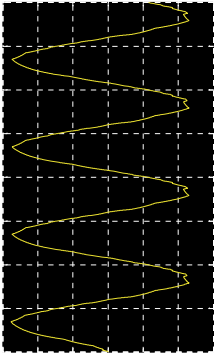
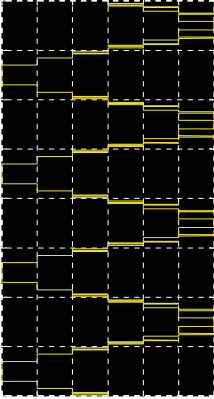
Output voltage waveform	
With filter circuit	 <p>(e) ISC PWMVF</p>
Without filter circuit	 <p>(e) ISC PWMVF</p>

Table 4 % THD result of 7-level CHB inverter without filter circuit

Modulation index		Level-shifted PWM switching techniques			Hybrid PWM switching techniques	
		PDPWM	PODPWM	APODPWM	ISCPWM	ISCPWMVF
Overmodulation	1.1	17.05	16.88	16.82	16.43	17.55
	1.0	18.88	18.20	18.14	17.31	19.04
Undermodulation	0.9	22.92	23.05	22.82	20.52	20.15

Table 5 % THD result of 7-level CHB inverter with filter circuit

Modulation index		Level-shifted PWM switching techniques			Hybrid PWM switching techniques	
		PDPWM	PODPWM	APODPWM	ISCPWM	ISCPWMVF
Overmodulation	1.1	3.42	3.50	3.58	4.41	4.74
	1.0	2.91	3.08	3.08	3.90	3.52
Undermodulation	0.9	3.03	3.14	3.13	3.92	3.73

7 Conclusion

In this study, the proposed 7-level CHB inverter is simulated with software MATLAB/Simulink 2010b and makes a comparison between level-shifted modulation switching techniques and hybrid modulation switching techniques. Both types of modulation switching techniques are suitable to produce the desired output voltage waveform with under IEEE standard limit THD. In the proposed topology without filter circuit, hybrid PWM switching technique gives better output result compared to level-shifted PWM switching technique as shown in Table 4 and the proposed 7-level CHB inverter topology with filter circuit level-shifted switching technique gives better result compared to hybrid PWM switching technique as shown in Table 5, and the proposed topology requires least count in comparison to two other conventional topologies.

References

1. R.H. Baker, *High-Voltage Converter Circuits*, U.S. patent Number 4, vol. 203, p. 151 (May, 1980).
2. K. Jagdish, *THD Analysis for Different Levels of Cascade Multilevel Inverters for Industrial Application* (IJETA, 2012), pp. 20–30
3. J. Rodriguez, et al., Multilevel inverters: a survey of topologies, controls, and applications. *IEEE Trans. Ind. Electron.* **49**, 724–738 (2002)
4. Colak, et al., Review of multilevel voltage source inverter topologies and control schemes. *Energy Convers. Manage.* **52**(2), 1114–1128 (2011)

5. N. Agrawal, S. Singh, P. Bansal, A multilevel inverter topology using reverse-connected voltage sources, in *International Conference on Energy, Communication, Data Analytics and soft Computing (ICECDS 2017)*, Chennai, India, pp. 1290–1295 (2017)
6. N. Agrawal, P. Bansal, N. Umale, THD analysis of new multilevel inverter topology with different modulation techniques, in *International Conference on Intelligent Computing and Smart Communication (2019)*
7. D.G. Holmes, B.P. McGrath, Opportunities for harmonic cancellation with carrier-based PWM for two-level and multilevel cascaded inverters. *IEEE Trans. Ind. Appl.* **37**, 574–582 (March/April, 2001)
8. S.S. Tomar, N. Agrawal, P. Bansal, Various modulation techniques in symmetrical multilevel inverters, in *International Conference on Energy, Communication, Data Analytics and soft Computing (ICECDS 2017)*, Chennai, India, pp. 1322–1327 (2017)
9. A. Nikhil, Performance analysis of cascade h-bridge multilevel inverter topology with filter circuit and without filter circuit. IGI Global, pp. 87–101 (2020). <https://doi.org/10.4018/978-1-5225-9683-7.ch008>
10. N. Agrawal, P. Bansal, A new 21-level asymmetrical multilevel inverter topology with different PWM techniques, in *IEEE Conference RDCAPE 2017*, pp. 224–229. Noida (2017)

Analysis of Conventional and Fractional-Order Controllers for Nonlinear CSTR System



Deep Mukherjee, Palash Kundu, and Apurba Ghosh

1 Introduction

In chemical industries, reactants are usually converted to valuable products and for this important conversion CSTR is used. The jacket surrounds CSTR, and it consists of reactor vessel. The temperature and concentration of the vessel are controlled by CSTR and now controlling the temperature is challenging task in real plant. In this work, first order plus time delay CSTR benchmark unstable process has been approached and to control heat in this system first a simple conventional PID controller using PSO optimization algorithm has been applied. Temperature is controlled tuning three parameters of PID controller but it may not result desirable performance with respect to reference point tracking and noise rejection. Vaishnavi [1] proposed tuning of PID controller for cascaded unstable process using GA algorithm. So, FOPID has been approached as it is more reliable than integer-order controllers and it may track set point faster and reject disturbance to maintain the temperature inside CSTR system using five optimal tuning parameters unlike PID controller. Many experts proposed FOPID controller tuning on CSTR using different local and global optimization methods but here PSO algorithm has been chosen. Now, FOPID controller has been established with internal model control scheme

D. Mukherjee

Kalinga Institute of Industrial Technology (Deemed to Be University), Bhubaneswar, Odisha
751024, India

e-mail: deepmukherjee@rediffmail.com

P. Kundu (✉)

Jadavpur University, Kolkata, West Bengal, India

e-mail: palashm.kushi@gmail.com

A. Ghosh (✉)

Burdwan University, Bardhaman, West Bengal, India

e-mail: apurbaghosh123@yahoo.com

© Springer Nature Singapore Pte Ltd. 2021

K. S. Sherpa et al. (eds.), *Advances in Smart Grid and Renewable Energy*,

Lecture Notes in Electrical Engineering 691,

https://doi.org/10.1007/978-981-15-7511-2_15

to provide better feature of controlling the temperature in the process using fractional low-pass filter. Comparison between IMC-PID and IMC-FOPID controller on different stable and unstable system has been explored by many experts. Here, a new modification has been carried out by using set point weighted technique on FOPID controller which results more satisfactory tracking set point and rejecting disturbance in efficient manner.

2 Description of CSTR Model

The cross section of nonlinear CSTR model [2] has been given in the following figure (Fig. 1).

The motor is used to supply steam and coolant to the jacket for maintaining the temperature and agitator is stirred to maintain the concentration as well. Let it be considered integral mass balance on number of moles n_i of species i in a reactor of volume V .

$$\frac{dn_i}{dt} = F_{i0} - F_i + V_{v_i} \tau_i \quad (1)$$

where F_{i0} is inlet flow rate, F_i is outlet flow rate, v_i is stoichiometric coefficient and τ_i is reaction rate.

$$\text{Temperature of species (T)} = \frac{1}{1 + k\tau} \quad (2)$$

where K is rate constant and τ is time constant. Following the above theorem, a benchmark model proposed by Lee et al. (2002) has been adopted as shown in below.

$$G(s) = \frac{1}{20s - 1} e^{-4s} \quad (3)$$

3 Methods

3.1 Conventional PID Controller

IOPID controllers [3] is the simplest method to control the physical variable using three gain parameters but does not provide accurate and stable performance as noise still exists. The basic equation of IOPID controller has been given in below.

$$G_c = k \left[1 + \frac{1}{sT_i} + sT_d \right] \tag{4}$$

3.2 Fractional PID Controller

FOPID controller [4, 5] helps to reject disturbance unlike PID controller including five gain parameters and to achieve robust performance of the system. The concept of FOPID controller has been captured by general fractional calculus theorem. The general transfer function of FOPID controller has been given in below.

$$G(s) = K_p + K_I/s^\lambda + K_d s^\mu \tag{5}$$

where λ and μ are extra degree of freedoms.

3.3 IMC-FOPID Controller

Internal model controller [6–8] refers to a systemic procedure for control system design based on the Q -parameterization concept that is the basis for many modern control techniques. IMC design procedure is diverse and it may be developed in single input–single output (SISO), multiple input–multiple output (MIMO) formulations, and continuous time and discrete time design procedures for unstable open-loop as well as closed-loop system (Fig. 2).

In the above control scheme, G_{IMC} is the IMC controller, G_p is the process, and G_m is the process model. The benchmark process model has been adopted to propose IMC-FOPID technique as represented below.

$$G_m = \frac{1}{4s^{2.2} + 16s^{0.8} + 1} \tag{6}$$

A low-pass fractional-order filter has been incorporated with fractional-order model.

$$G_f = \frac{1}{\eta s^\alpha + 1} \quad (7)$$

where η is filter coefficient and α is any real number as integer or non-integer order may be arbitrarily taken. Now, IMC controller $Q(s)$ has been established as

$$C_{\text{IMC}}(s) = G_f * G_m^{-1} \quad (8)$$

Finally, $Q(s)$ plays important role to develop IMC-FOPID structure with the following equations.

$$C(S)_{\text{IMCFOPID}} = \frac{Q(s)}{1 - Q(s) * G_m} \quad (9)$$

3.4 Set Point Weighted IMC-FOPID Controller

Set point weighted FOPID controller [9] is defined as an extra degree of freedom is adopted and incorporated with proportional controller and helps to eliminate disturbance accurately than FOPID controller as well as to achieve set point tracking better modifying the error signal of proportional and derivative action. The modified expression of set point weighted FOPID controller is shown in below.

$$U(s) = \left(k_P * b + \frac{k_I}{s^\lambda} \right) R(s) - \left(k_P + \frac{k_I}{s^\lambda} + k_D s^\mu \right) Y(s) \quad (10)$$

This technique follows same principle like IMC-FOPID controller but it differs only from an additional tuning parameter which has been calculated and selected by trial and error method varying between acceptable range.

3.5 Particle Swarm Optimization Technique

PSO optimization [10] is known as global heuristic process with proper iteration and searches the best values of all parameters with fast process. The step has been followed to search optimum values as shown in Fig. 3.

4 Case Study

In PSO algorithm, ITAE has been chosen as an objective function to obtain optimum values of proportional gain, integral gain, derivative gain for PID controller and for two extra degree of freedoms except three gain parameters for FOPID controller. The optimum values of PID and FOPID control parameters have been shown in Tables 1 and 2.

Using trial and error method, filter coefficient and fractional-order of low-pass filter of IMC controller have been adopted as 0.059 and 0.8, respectively. Using these values from Eq. (9), the following parameters of IMC-based FOPID controller have been determined as shown in Table 3.

Table 1 Optimum parameters of PID controller

Proportional gain	Integral gain	Derivative gain
35	15	20

Table 2 Optimum parameters of FOPID controller

K_P	K_I	K_D	λ	μ
35	15	20	0.6	0.2

Table 3 IMC-FOPID parameters

K_P	K_I	K_D	λ	μ
120	15	68	0.8	1.4

Table 4 Transient analysis of different controllers

Controllers	Rise time (s)	Overshoot (%)	Settling time (s)	ISE	IAE	ITSE
PID	0.75	22	4.85	68.4	140.4	312.5
FOPID	0.75	18	4.91	43.6	125.6	274.2
IMC-FOPID	0.75	16	12.45	41.6	98.4	220.4
IMC-2DOF FOPID	0.75	15	7.45	32.5	90.4	201.5

Fig. 1 CSTR model

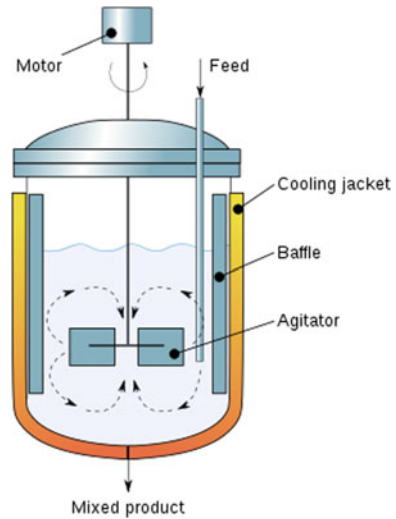
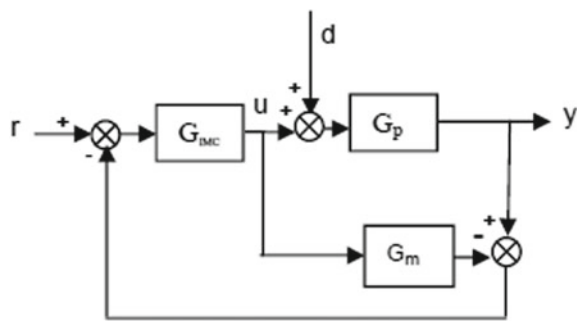


Fig. 2 IMC control scheme



The same parameters have been used to design IMC-based set point weighted FOPID controller except set point weighted parameter which has been selected as 0.7 comparing with other values between 0 and 1. The performance of temperature control using CSTR using integer- and fractional-order controllers has been represented in the following Fig. 4 and Table 4.

5 Conclusion

In this research work, different types of integer- and fractional-order controllers have been selected to control the temperature inside CSTR and mathematical descriptions of all the controllers have been presented, respectively. Optimum values of PID and FOPID controllers have been determined by optimization technique and values of different gains of IMC-FOPID and IMC set point weighted parameter have been

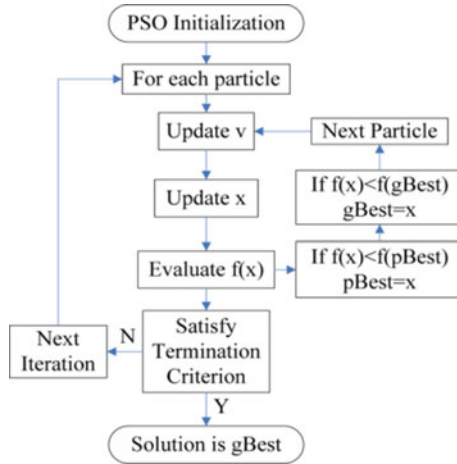


Fig. 3 PSO flowchart

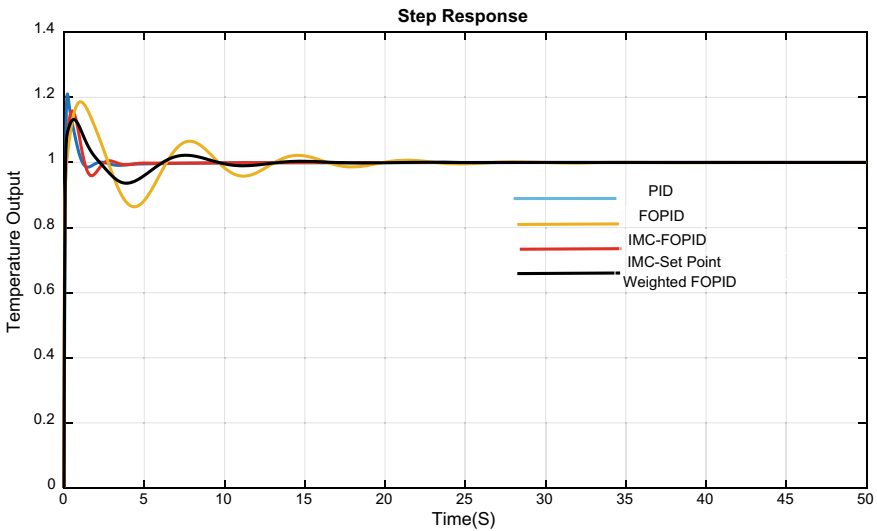


Fig. 4 Performance of temperature control of CSTR

adopted by choosing filter gain coefficient and proper fractional order as well as set point coefficient by trial and error method. Testing all the controllers on CSTR it has been concluded that IMC-based set point weighted FOPID controls the temperature within acceptable range unlike other controllers and tracks set point with less peak overshoot and less error metric also.

References

1. V. Vaishnavi, Design of optimal PID control for an unstable system using genetic algorithm. *Int. J. Innov. Manage. Technol.* **3** (2012)
2. K. Jimisha, M. Shinu, Analysis of conventional controllers for high pressure rated modified CSTR system. *Int. Adv. Res. J. Sci. Eng. Technolo.* **3**, 274–277 (2016)
3. V. Bijani, A. Khosravi, Robust PID controller design based on a novel constrained ABC algorithm. *Trans. Inst. Measure. Control.* **40**, 202–209 (2018)
4. M. Dulau, A. Gligor, Fractional order controllers versus integer order controllers. *Procedia Eng.* **181**, 538–545 (2017)
5. I. Podlubny, Fractional order system and $PI^\lambda D^\mu$ controllers. *IEEE Trans. Autom. Control* **8**, 208–214 (1999)
6. V. Anusha, Design and analysis of IMC based PID controller for unstable systems for enhanced closed loop performance. *IFAC Proceed.* **45**, 41–46 (2012)
7. G. Rao, Design of internal model control-PID controller with improved filter for disturbance rejection. *Syst. Sci. Control Eng.* **2** (2014)
8. R. Rayalla, B. Gara, An improved fractional filter fractional IMC PID controller design and analysis for enhanced performance of non-integer order plus time delay process. *Eur. J. Electr. Eng.* **21**, 139–147 (2019)
9. K. Bingi, R. Ibrahim, A comparative study of 2 DOF PID and 2 DOF FOPID on a class of unstable system. *Archives Control Sci.* **28**, 635–682 (2018)
10. M. Federico, particle swarm optimization-a tutorial. *Chemom. Intell. Lab. Syst.* **149**, 153–165 (2015)

Analysis and Simulation of Boost Converter Versus Tri-state Boost Converter



Kundan Kumar, Sudhananda Pal, and Deepak Kumar

1 Introduction

In the present scenario, the research on renewable energy sources becomes more desirable as the conventional sources are limited and being used for a long time. The demand for efficient power converters is increasing day by day to optimum utilization of the energy sources. There are various methodologies to improve the efficiency such as circuitual change and replacement of new generation semiconductor devices over conventional devices.

The regulation of DC-DC power converters has been studied for many years, especially with the uncertain load. It has drawn the attention of researchers who are working in the area of power electronics and automation. Boost converter has great advantages and is widely used for the applications where stepping up voltage requirements are a big concern. Boost converter (BC) is facing the problems of having zero in the right-hand plane (RHP) which can be observed by state space analysis. To eliminate the RHP zero issue, an additional state is implemented and an equivalent converter is introduced which is called tri-state boost converter (TSBC). The consumption of power losses is quite higher in TSBC than the boost converter due to additional switch and a diode. The dynamic response of a TSBC is better than boost converter but the efficiency is less which is the tradeoff of TSBC [1–4].

K. Kumar (✉) · S. Pal · D. Kumar
School of Electrical Engineering, Kalinga Institute of Industrial Technology, Bhubaneswar,
Odisha 751024, India
e-mail: kundan01012016@gmail.com

S. Pal
e-mail: sudhanandapal472@gmail.com

D. Kumar
e-mail: kushahadeepakkumar@gmail.com

In this paper, modeling and operation of BC and TSBC are investigated in detail, and then, the loss model has formulated to highlight the comparative analysis. Further, the loss matrix has been presented along with the frequency and duty cycle of the main switch.

The detail structure of the paper is discussed as follows. Section 2 demonstrates the modeling of boost converter as well as TSBC. Section 3 elaborates the performance of both the converters with the variety of different operating parameters. Section 4 formulates the losses in both the converters. Section 5 presents the simulation results in which the operation of both the converters in continuous conduction mode (CCM) as well as discontinuous conduction mode (DCM) and loss matrix together with comparative analysis of both the converters are demonstrated. At the end, in Sect. 6, conclusive remarks are highlighted.

2 Modeling of Boost Converter and Tri-state Boost Converter

A boost converter (BC) is basically step up DC-DC converter which has wide applications such as photovoltaic, EVs and industrial applications, while the TSBC is the modified version of BC in which one extra freedom of control as well as better dynamic response are the additional features [5–8].

2.1 Boost Converter

The schematic of the boost converter and waveforms is shown in Fig. 1, in which S_M is the MOSFET switch, D is the boosting diode, C_o is the output capacitor, and R_o is the load resistance. The source voltage and the current through the inductor L_s are denoted by V_s and I_L , respectively. Boost converter has two modes of operation: (a) boosting mode which has the duty ratio D_b . In this mode, S_M is turned on and the source current flows through the inductor, result in energy stores in the inductor and (b) capacitor charging mode which has the duty ratio D_o . In this mode of operation, S_M is off and the current flows through boosting diode and load. The inductor is discharging while the capacitor is charging during this mode.

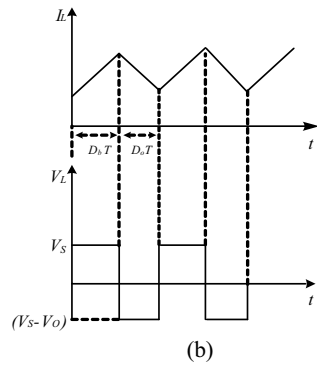
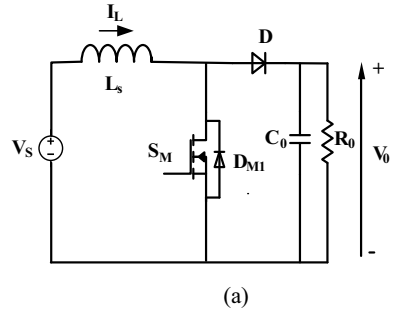
Therefore, the duty ratio's relation is given by

$$D_b + D_o = 1 \quad (1)$$

The voltage gain in this mode is given by

$$\frac{V_o}{V_s} = \frac{1}{D_o} \quad (2)$$

Fig. 1 Boost converter
a circuit diagram
b waveforms of current and voltage



2.2 Tri-state Boost Converter

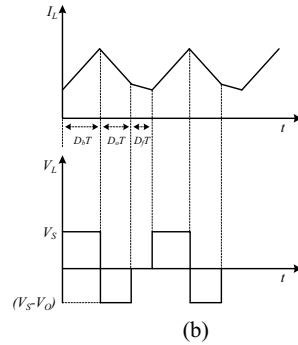
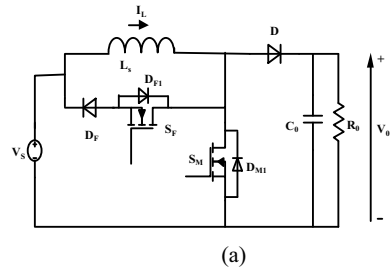
As shown in Fig. 2a, V_s and L_s are the source voltage and inductance respectively, while S_F and S_M are the freewheeling switch and main switch respectively. The freewheeling and boosting diodes are denoted by D_F and D respectively. Figure 2b shows the inductor current and inductor voltage waveforms.

The TSBC has three modes of operation: (a) *freewheeling mode* (D_f)—during this mode of operation, main switch (S_M) is turned off and the freewheeling switch (S_F) is turned on, and hence, energy stored in L_s is released through S_F and D_F . During this mode, the capacitor C_0 is providing the required output current. (b) *Boosting mode* (D_b)-during this mode main switch (S_M) is turned on but freewheeling switch (S_F) is turned off, and hence, current flows through L_s and S_M . The inductor is get charged, and load current is delivered by the capacitor C_0 during this mode. (c) *capacitor charging mode* (D_0)-during this mode of operation both main switch (S_M) and freewheeling switch (S_F) are turned off, and hence, current flows through the capacitor C_0 and R_0 [5].

Hence, the relation among all the three duty ratios can be established and given by,

$$D_b + D_0 + D_f = 1 \tag{3}$$

Fig. 2 Tri-state boost converter **a** circuit diagram **b** waveforms of current and voltage



The voltage gain is given by

$$\frac{V_0}{V_s} = \frac{D_b + D_0}{D_0} \tag{4}$$

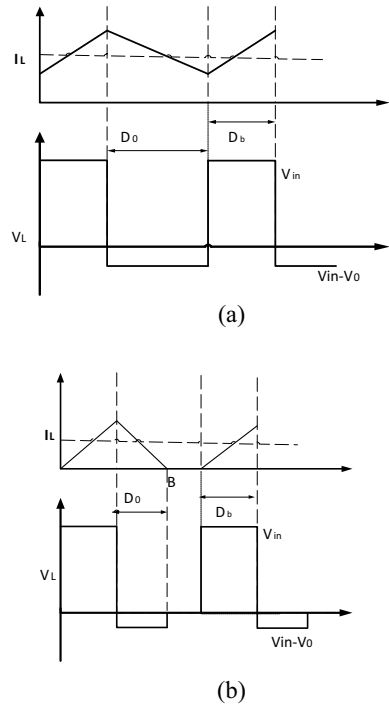
3 Performance Analysis

The performance of BC and TSBC is investigated in this section. The performance of converters is classified in terms of current conduction which is affected due to the variation in load.

3.1 Boost Converter

The performance of BC is depicted based on the current conduction, i.e., CCM and DCM, and analyzed in detail.

Fig. 3 Boost converter operation **a** CCM **b** DCM



3.1.1 Continuous Conduction Mode

Once the switch S_M is turned on the source current passes through L_s and S_M , the boosting diode D becomes reverse biased and the capacitor C_o gets discharged through the load. During the turned-on period of the S_M , the inductor current rises up, while once S_M is turned off, current passes through the diode D and charge the capacitor as well as delivered the load current and inductor current I_L falls. In the CCM, the switch is turned on before inductor current falls to zero during turned-off period of the switch, and hence, inductor current never reaches zero. In this case, inductor has some residual magnetism which is shown in Fig. 3a. Therefore, during CCM, the average output voltage is given by

$$V_{out} = \frac{V_{in}}{1 - D_b} \tag{5}$$

3.1.2 Discontinuous Conduction Mode

In this mode, during the turned-off period of main switch S_M , the inductor current becomes zero before turned on the main switch S_M off time. The waveforms of the

DCM mode are shown in Fig. 3b. If the β is the point where inductor current is becoming zero, then the average output voltage is given by

$$V_{\text{out}} = \frac{\beta V_s}{\beta - D_b} \quad (6)$$

3.2 *Tri-state Boost Converter*

The TSBC has one extra auxiliary switch, and a diode through that freewheeling mode is conducted. In a similar way, the modes of operation for the TSBC, i.e., CCM and DCM, are discussed as follows.

3.2.1 **Continuous Conduction Mode**

In this mode, the current of inductor never reaches zero value. Input current is non-pulsating, and the voltage gain does not depend on the load. The ripple current of the inductance is lower than the average current, and the efficiency of the converter is higher in CCM as compared to the DCM. The waveforms of TSBC in CCM mode is shown in Fig. 4a.

3.2.2 **Discontinuous Conduction Mode**

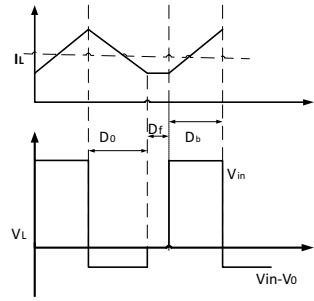
In this mode, the current of inductor becomes zero and it remains zero till the main switch turned on. In the DCM, the inductor current is pulsating and voltage gain depends on the load resistor. In the DCM mode, the ripple component as well as rms value are higher. The waveforms of TSBC in DCM mode is shown in Fig. 4b. Further, the bode plots of the boost converter and TSBC are shown in Figs. 5a and 5b.

4 **Loss Estimation**

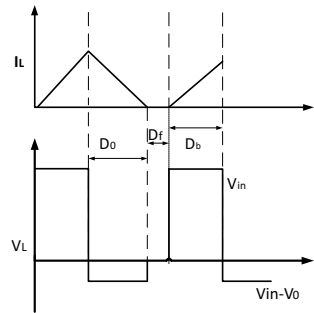
The losses in power converters are mainly the losses of switching devices that can be estimated by the help of loss formulae as disused follows.

The various power losses of power devices are given as follows [9].

Fig. 4 Tri-state boost converter operation **a** CCM **b** DCM



(a)



(b)

4.1 Conduction Losses

The power consumption during conduction is described as follows.

The component of conduction losses in MOSFET is given by

$$P_{cond,M} = R_{ds(on)} I_{rms,M}^2 \tag{7}$$

where $I_{rms,M}$ and $R_{ds(on)}$ are rms value of MOSFET current and the MOSFET channel resistance, respectively.

The component of conduction losses in the diode is given by

$$P_{cond,D} = V_F I_{avg,D} + R_d I_{rms,D}^2 \tag{8}$$

where R_d and V_F are the diode resistance and diode forward voltage, respectively, while $I_{avg,D}$ is average current and $I_{rms,D}$ is rms current of the diode.

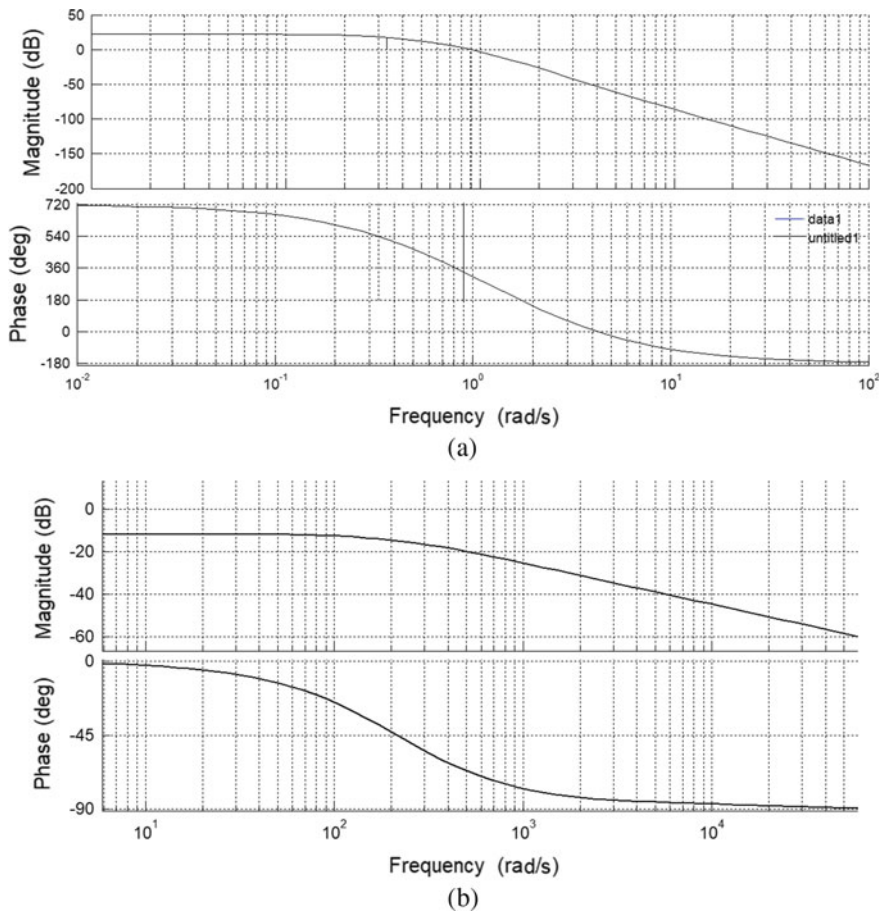


Fig. 5 Bode plot **a** boost converter **b** TSBC

4.2 Switching Losses

The switching loss component in MOSFET is given by

$$P_{sw,M} = (V_{DS}I_D t_{on,M} + V_{DS}I_D t_{off,M})f_s \tag{9}$$

where switching times of the MOSFET are denoted as $t_{on,M}$ and $t_{off,M}$ while at the time of commutation, the blocking voltage and current passes through the MOSFET are given by V_{DS} and I_D , respectively.

The main cause of switching loss in the diode is reverse recovery which is given by

$$P_{sw,D} = (Q_{rr} V_s) f_s \tag{10}$$

where Q_{rr} and V_s are the reverse recovery charge and the voltage across the diode, respectively. The other components of switching losses are less significant and can be ignored.

4.3 Driving Losses

The losses that need to drive from off to on and on to off of a MOSFET can be illustrated as

$$E_{drv} = 2V_G Q_G \quad (11)$$

where gate-source charges and gate voltage of the MOSFET are denoted by Q_G and V_G , respectively.

The power loss of the boost converter can be calculated by considering the power losses of the main switch as well as of boosting diode which is given by

$$P_{Boost} = \left[R_{ds(on)} I_{rms,M}^2 * D_b + \frac{1}{2} V_s \left(\frac{I_B}{1 - D_{b, avg}} + \frac{\Delta I_L}{2} \right) (t_{on,M} + t_{off,M}) \right] f_s \quad (12)$$

where D_b is the duty cycle of boost MOSFET, while $D_{b, avg}$ is the average value of D_b and I_B is the output current of the boost converter. The estimated inductor ripple current is denoted by ΔI_L .

The power loss of TSBC can be calculated from Eq. (13) with addition of conduction loss and switching losses of freewheeling diode and switches.

Therefore, the total power losses in TSBC is given by

$$P_{TSBC} = [R_{ds(on)} I_{rms,M}^2 * (D_b + D_f) + \frac{1}{2} V_s \left(\frac{I_B}{1 - (D_{b, avg} + D_{f, avg})} + \frac{\Delta I_L}{2} \right) (t_{on,M} + t_{off,M})] f_s \quad (13)$$

5 Simulation Analysis and Comparative Results

The simulation exploration for both the converters is conducted through MATLAB software, in which the inductor current, input, output voltages and pulses for switches for the various modes, i.e., CCM and DCM, are depicted in Fig. 6 and 7, respectively. To estimate the losses, gallium nitride (GaN) semiconductor switches and diodes are considered which have tremendous advantages over conventional switches. The various switching and steady-state parameters of GaN MOSFET, i.e., part no.

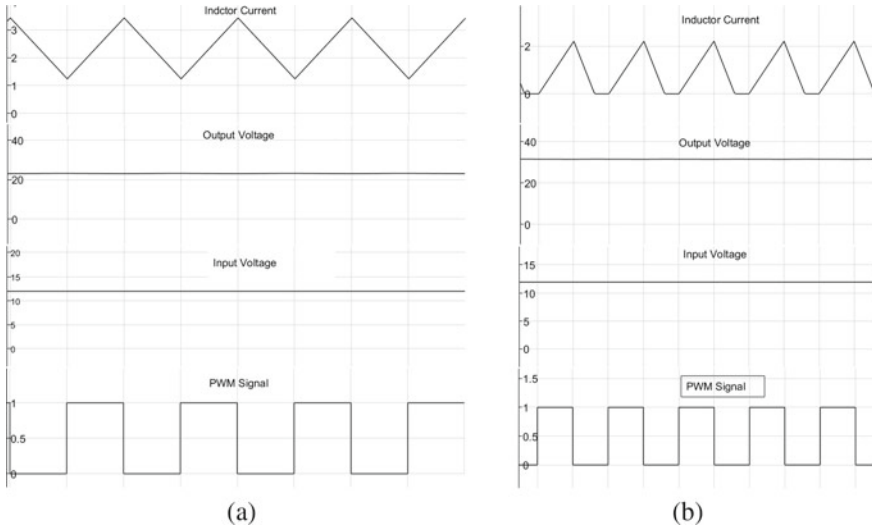


Fig. 6 Simulation results of boost converter operation **a** CCM **b** DCM

NTP8G206N, and GaN diode, i.e., part no. TPS2010PK, are used as discussed in [10–13]. The circuit parameters for BC and TSBC that are required to calculate the losses are shown in Table 1. The duty cycle of the auxiliary switch in TSBC is kept constant while the duty cycle of the main switch in both the converters is made variable. The loss matrix is computed along with the switching frequency and the duty cycle of the main switch in both the converters which is presented in Fig. 8a, b.

It is observed from Fig. 8, the power consumption in boost converter is less than TSBC because one extra MOSFET and a diode are used. The comparative analysis between BC and TSBC are listed in Table 2, which highlight the tradeoff and advantages of both the converters [14, 15].

6 Conclusions

This work analyzes working, characteristics and comparative aspects of the boost converter and tri-state boost converter. The investigation is started with the modeling and variation in conduction modes of both the converters followed by the estimation of losses. The simulation studies carried out in MATLAB software to support the theoretical analysis. The loss matrix for both the converters is presented with the variation in the frequency as well as the duty cycle of the main switches in each converter. It is observed that the tri-state boost converter is having an extra freedom of control and better in terms of dynamic response as compared to boost converter while boost converter is better for the application where efficiency is concerned.

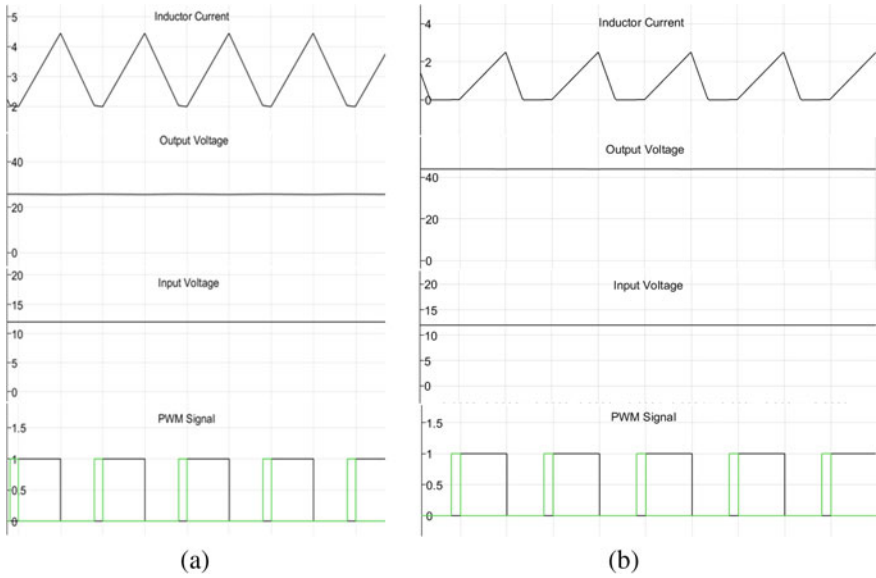


Fig. 7 Simulation waveform of tri-state boost converter **a** CCM **b** DCM

Table 1 Parameters of boost converter and tri-state boost converter

Parameters	Symbol	Value/quantity		Unit
		BC	TSBC	
Input voltage	V_s	12	12	V
Inductor	L_s	275	275	μ H
Output capacitor	C_o	470	470	μ F
Load resistance	R_o	25	25	Ω

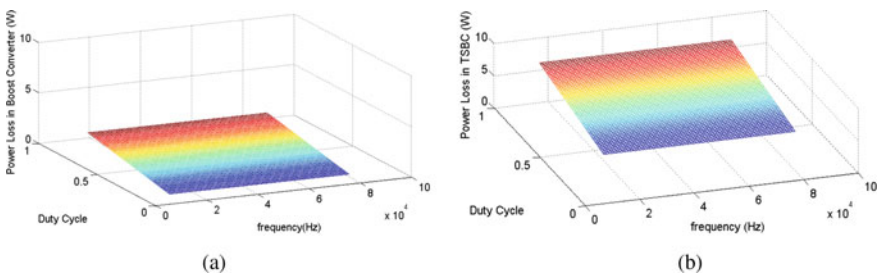


Fig. 8 Loss matrix **a** boost converter **b** tri-state boost converter

Table 2 Comparative analysis of boost converter and TSBC

Parameter	BC	TSBC
Right hand pole zero	Not eliminated	Eliminated
Dynamic response	Slow	Fast
Loss	Less	More
Efficiency	More	Less

References

1. V. Michal, D. Cottin, P. Arno, Boost DC/DC converter nonlinearity and RHP-zero: survey of the control-to-output transfer function linearization methods, in *International Conference on Applied Electronics (AE)*, pp. 1–10. Pilsen (2016)
2. P.K. Maroti et al., New tri-switching state non-isolated high gain DC–DC boost converter for microgrid application. *IET Power Electr.* **12**(11), 2741–2750 (Sep.)
3. . M. Safwat, W. Xiahua, Comparative study between passive PFC and active PFC based on Buck-Boost conversion, in *2017 IEEE 2nd Advanced Information Technology, Electronic and Automation Control Conference (IAEAC)*, pp. 45–50. Chongqing (2017)
4. K. Viswanathan, R. Oruganti, D. Srinivasan, A novel tri-state boost converter with fast dynamics, in *Proceedings of IEEE Transactions on Power Electronics*, vol. 17, no. 5, pp. 677–683 (September, 2002)
5. K. Kumar, N. Rana, S. Banerjee, S.B. Santra, N. Parvez, Design and analysis of soft-switched tri-state boost converter, in *Proceedings of IEEE International Conference on Power, Instrumentation, Control and Computing (PICC)*, pp. 1–6. Thrissur, Kerela (18–20 January, 2018)
6. K. Viswanathan, R. Oruganti, D. Srinivasan, Dual-mode control of tri-state boost converter for improved performance, in *Proceedings of IEEE Transactions on Power Electronics*, vol. 20, no. 4, pp. 790–797 (July, 2005)
7. L. Galotto, M.A.G. de Brito, L.P. Sampaio, C.A. Canesin, Integrated single-stage converters with tri-state modulation suitable for photovoltaic systems, in *Proceedings of Brazilian Power Electronics Conference*, pp. 436–443. Praiamar (2011)
8. C. Sreekumar, V. Agarwal, Hybrid control of a tri-state boost converter, in *Proceedings of IEEE International Conference on Industrial Technology*, pp. 121–125. Mumbai (2006)
9. K. Kumar, S.B. Santra, Performance analysis of a three-phase propulsion inverter for electric vehicles using GaN semiconductor devices. *IEEE Trans. Ind. Appl.* **54**(6), 6247–6257 (November–December, 2018) ISSN: 0093–9994
10. J. Millan, P. Godignon, X. Perpina, A.P. Tomas, J. Rebollo, A survey of wide bandgap power semiconductor devices. *IEEE Trans. Power Electron.* **29**(5), 2155–2163 (May)
11. Z. Ivanovic, B. Blanus, M. Knezic, Power loss model for efficiency improvement of boost converter, in *2011 XXIII International Symposium on Information, Communication and Automation Technologies*, pp. 1–6. Sarajevo (2011)
12. K. Kumar, M. Bhattacharya, S. Garlapati, S. Banerjee, Impact of gallium nitride semiconductor devices in tri-state boost converter, in *IEEE International Conference on Sustainable Energy Technologies and Systems (ICSETS-2019)*, pp. 292–296. KIIT DU, Bhubaneswar (2019)
13. M. Hernandez, C. Aguilar, J. Arau, J. Sebastian, J. Uceda, Comparative analysis of boost and buck-boost derived topologies used as power factor correctors, in *Technical Proceedings of IV IEEE International Power Electronics Congress CIEP 95*, pp. 14–19. San Luis Potosi, Mexico (1995)

14. M. Hernandez, C. Aguilar, J. Arau, J. Sebastian, J. Uceda, Comparative analysis of boost and buck-boost derived topologies used as power factor correctors, in *Proceedings of IECON '95-21st Annual Conference on IEEE Industrial Electronics*, vol. 1, pp. 335–340. Orlando, FL, USA (1995)
15. H. Han, R. Tan, J. Yang, H. Wang, S. Ning, M. Shen, A novel efficient tri-state boost converter, in *IEEE Electrical Power and Energy Conference (EPEC)*, pp. 1–6. Saskatoon, SK (2017)

Application of Point on Wave Switching for Mitigation of Transients During Charging of Power Transformer in Presence of Large Capacitive Component



Ajay Kumar , Urmil Parikh, and Inderpreet Kaur

1 Introduction

In the present techno-economic environment in electric utilities, equipments are loaded optimally for achieving maximum efficiency with economy. Transformers installed in power system are switched frequently for meeting the technical and economic requirements. Un-controlled switching of power transformer results in flow of large asymmetric current which affect the thermal and dielectric health of equipment and system. The root cause of inrush current is saturation of core due to sudden application of source voltage; the resulting winding inductance will be reduced considerably, and current is limited merely by its resistance. This whole process leads to flow of current that can reach up to 10 pu level. Controlled switching technology is widely accepted to mitigate inrush current and results in increased equipment life and system reliability. Also, capacitor banks are installed in power system for reactive power management, and they are switched as per system requirement.

Switching of capacitor bank at unfavorable instant also creates inrush with high-frequency harmonics resulting in zero missing phenomena [1]. Due to lower characteristic impedance of capacitors, back-to-back charging of capacitor bank shows inrush current to 25–40 pu level. De-energization of capacitor bank at unfavorable instant may result in restrike/reignition in circuit breakers causing breaker contact degradation. Such situation may endanger the equipment and system from dielectric failure viewpoint. Therefore, energization and de-energization of transformer

A. Kumar (✉) · I. Kaur
Chandigarh University, Mohali, India
e-mail: er.ajaypathania@yahoo.in

A. Kumar
Power Grid Corporation of India, Gurugram, India

U. Parikh
ABB India Ltd, Vadodara, Gujarat, India

terminated capacitors are quite critical. Controlled switching is presently a matured technology for minimizing quantum of inrush currents generated during switching of power system equipment's like transformer, capacitor, reactor, etc. with the application of intelligent electronic devices (IEDs) [2]. Controlled switching strategies for transformer may not be favorable for capacitor switching, and best strategies for capacitor will not be optimum for transformer switching, and problem becomes more stringent in L-C combination having considerable inductance and capacitance [3]. Although power transformer has certain inherent capacitance associated with inter-winding, bushing, etc., these capacitances are very less compared to its inductance and hence will not require any correction to default strategies due to the reason that slope of sine voltage wave is low near peak and variation in angular form cause less variation in time domain. Ideal strategies for switching transformer-capacitor combination are to target instant for each phase such that resultant core flux remains symmetrical [4–6]. Also, charging of transformer with capacitor is source of harmonics and may deteriorate the power quality.

The energy stored in inductance of transformer will be fully compensated by the connected capacitance, and square wave pulses will be noticed at its terminals leading to full or partial de-magnetization of transformer core. In normal cases, nearly 10% voltage remains coupled to transformer due to stray capacitance, and energization targets need not alter for this small coupling voltage. Price and Hedding [7] addressed the protection issues faced during operation of transmission lines terminated into transformers. Harlow [8] discussed the root cause of overvoltage generation in transformer terminated lines and suggests placing of reactance at appropriate place for its mitigation. Jacobson et al. [9] present the modeling of ferroresonance on 230 kV DC transformer terminated lines of Manitoba Hydro. Due to interaction of saturable inductance with capacitance of transmission line, ferroresonance may occur and will lead to overvoltages. Different strategies have been reported in literature to minimize the inrush current generated during energization of transformer [10–13]. Depending upon the strength of grid, sudden application of high magnitude inrush current causes severe voltage dip across grid; this dip adversely affects the power quality and may trip sensitive loads like HVDC converter systems, variable frequency drives, etc. Considerable work has been done in field of controlled switching of capacitor bank also. Overvoltages generated during de-energization of capacitor banks and cable systems are also addressed in existing literature [14, 15]. Moreover, CIGRE has also presented detailed analysis of controlled switching strategies for transformer and capacitor banks. But there is no such literature available explaining optimum energization instant for case where transformer is directly connected to capacitor.

This paper presents controlled switching strategies for energization and de-energization of coupled three-winding power transformers with capacitor bank on its tertiary side. The results are verified by simulation as well as field case. Power quality of system is analyzed from THD viewpoint for both current and voltage phasors. Analysis of voltage dip with and without application of controlled switching strategies is also analyzed in this paper.

1.1 Effect of Capacitance on Performance of CSD on Transformer

Capacitive component like capacitor banks and long transmission lines offer capacitive reactance thus causing switching surge during switching. Inrush current generated during capacitor energization is a direct function of voltage change at the moment, and accordingly, they offer least inrush during charging at voltage zero. As reported in literature, reactors are used to compensate capacitive reactance with inductive reactance offered by reactors. Similarly, in case of transformer terminated capacitor/line, capacitance is counterbalanced by inductance of transformer resulting in predominant de-magnetization of transformer core post its de-energization and this is added advantage with this configuration. But during charging of transformer-capacitor combination, situation becomes tricky because default strategies for transformer or capacitor switching will not effective in this combination. Hence, energization of L-C circuit needs careful selection of energization instant even with controlled switching. Although direct connection of capacitor and transformer which exhibit variable reactance can ignite ferro-resonance mode which may be harmful to system. Therefore, such configurations should be selected with care. Figure 1 shows arrangement having three-winding transformers with capacitor bank connected to its tertiary winding.

The inrush current flow during energization of capacitor coupled transformer [6] is given by Eq. (1) which is conversely the solution of quadratic equation having same roots:

$$i = I_m \frac{\beta}{\sqrt{LC}} e^{-\alpha t} \left\{ \begin{array}{l} \sin(\theta_0 - \emptyset) \sin(\beta t - \gamma) \\ - \frac{1}{\omega\sqrt{LC}} \cos(\theta_0 - \emptyset) \sin \beta t \end{array} \right\} + I_m \sin(\omega t + \theta_0 - \emptyset) \quad (1)$$

where $\alpha = \frac{R}{2L}$; $\emptyset = \tan^{-1} \frac{\omega L - \frac{1}{\omega C}}{R}$; $\gamma = \tan^{-1} \frac{\alpha}{\beta}$; $\beta = \sqrt{\frac{1}{LC} - \left(\frac{R}{2L}\right)^2}$.

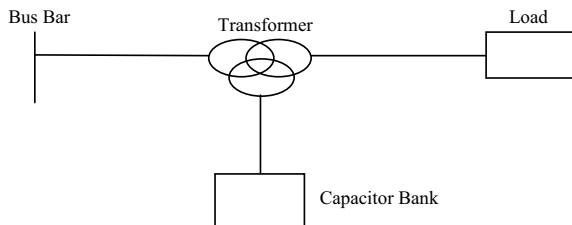
\emptyset Circuit power factor angle

θ_0 Energization angle

ω Angular power frequency

L Inductance of transformer

Fig. 1 Circuit diagram for analyzing charging current in L-C combination



I_m Maximum current through circuit

R Resistance of transformer

C Capacitance of filter bank.

As mentioned in Eq. (1), charging current contains sinusoidal steady-state current which is limited by impedance of circuit; another component is exponentially decaying asymmetric current having very high amplitude decays with time constant of circuit. It can be appreciated that minimum of Eq. (1) achieved when sinusoidal component equals to exponentially decaying component. When circuit is charged at instant, energization angle equals to power factor angle $\theta_0 = \emptyset$, and first part of equation will be omitted, but transients are still available. When circuit is energized at voltage peak ($\theta_0 = 90^\circ$), maximum peak current will be observed because power factor angle will be close to 90° electrical for purely capacitive circuit. Transients generated in circuit will be damped with time constant $R/2L$. Its magnitude is given by Eq. (2):

$$i = -I_m \frac{\beta}{\omega \cdot LC} e^{-\alpha t} \sin \beta t + I_m \sin \omega t \quad (2)$$

Considering the above steady-state solution of current in time domain, following three scenarios will be observed:

1. **Switching at voltage zero ($\theta_0 = 0^\circ$)**—Resulting in inrush current corresponding to transformer. Unfavorable position for transformer switching but suitable for capacitor energization due to minimum step voltage change. High magnitude inrush current flowing with asymmetric component flows in this scenario and the inrush current waveform exhibits pattern of half wave rectifier wave.
2. **Switching at voltage peak ($\theta_0 = 90^\circ$)**—Resulting in high-frequency current transients due to capacitor switching at unfavorable position. However, it is suitable instant for transformer charging [16, 17]. The waveform contain high level of distortions and high frequency components along with prominent 2nd/3rd harmonic component.
3. **Switching in between ($\theta_0 = 0-90^\circ$)**—Compromise solution can be achieved by shifting the energization instant from voltage peak depending upon capacitance effect.

Therefore, switching of L-C circuit at both zero and peak voltage instant of phase-earth wave of respective phase offers switching transients. For finding the suitable voltage energization point, a trade-off is to be made in $\theta_0 = 0-90^\circ$ of V_{ph} . Transformer energization at voltage zero shows worst condition, and highest inrush currents with distortion are observed. Simulation study for determining energization instant for L-C combination is done in Sect. 2.

2 Simulation Study of Transformer Terminated Capacitor

Proposed controlled switching strategies have been modeled in PSCAD software. Three-winding transformer of configuration Yyd with rating 210 MVA has been considered for simulation study. Time-independent pole circuit breakers are connected to switch L-C combination. The simulation studies are carried out considering nil residual flux. High voltage winding of transformer is connected to constant voltage source; intermediate voltage winding is not connected to any load and is kept open. Capacitor bank is installed on tertiary winding of transformer, and its magnitude is varied to study said effect at different capacitance values.

2.1 Transformer Energization

Ideal switching instant for transformer is at voltage peak while capacitor bank is switched at voltage zero of phase-neutral peak. In transformer terminated capacitance, targets are adjusted optimally in between 0° and 90° electrical of voltage wave. Larger capacitance needs more correction from voltage peak, and targets will be shifted more towards voltage zero during transformer energization.

In first case, transformer circuit is switched at voltage peak of phase-earth voltage wave resulting in considerable current transients due to presence of capacitor in same circuit. The inrush current resulting during energization is tabulated for different capacitance values. Then, capacitance is increased in steps and inrush currents are tabulated for each step. This table states that inrush currents are increased with higher capacitance even for voltage peak switching. Energization waveform of transformer with capacitor bank results in high-frequency transients with distortions as shown in Fig. 2 which were removed by opening capacitor bank as shown in Fig. 3.

Table 1 indicates deviation in transient mitigation on closing target from voltage peak. Tests were conducted considering voltage zero energization instant with nil residual flux. Table 1 mentions inrush currents for different capacitance values for voltage zero and peak energization. However, these currents also contain harmonics and distortions due to capacitance effect. After applying proposed strategy and trade-off, reduced inrush currents are indicated in Table 1.

It is found that ideal target for energizing L-C configuration is certain degree prior to peak. The resulting inrush currents after modified targets are reduced as compared to previous case. After applying proposed strategy and trade-off, inrush currents are mitigated considerably as indicated in Table 2. This table indicates electrical degree deviation from voltage peak, optimum point for charging of L-C combination. Timing energization sequence for energization of L-C combination is mentioned in different capacitance. Selected 60 Hz system has first phase voltage peak observed at 412 ms.

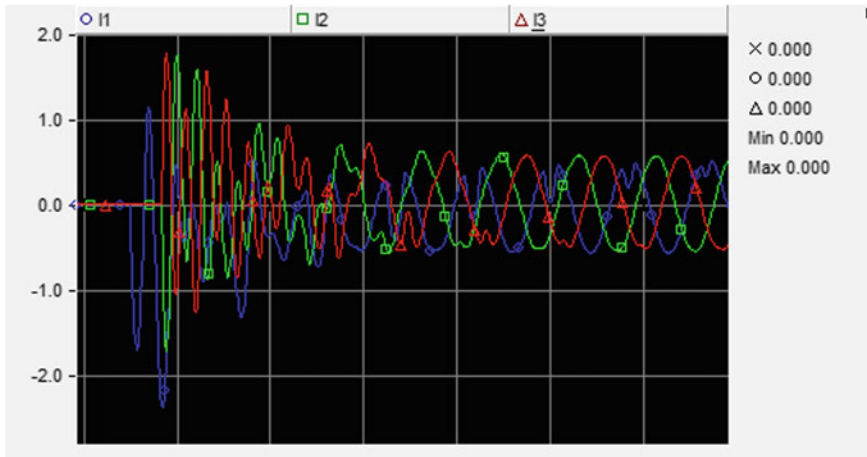


Fig. 2 Charging currents of L-C combination

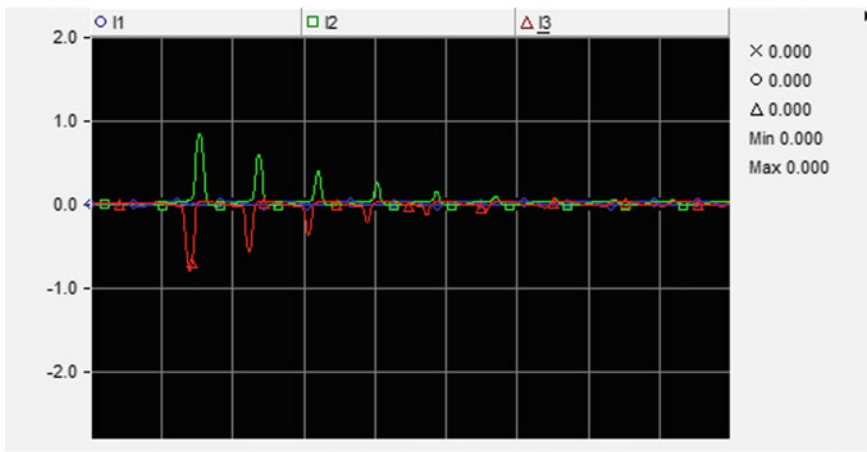


Fig. 3 Charging current of transformer alone

Table 1 Inrush current (kA) for different capacitances using suggested methodology

Capacitance (μF)	Inrush current at 90° charging	Inrush current at 0° charging	Inrush current after trade-off
200	1.36	2.72	1.29
300	1.82	2.43	1.51
400	2.16	2.17	1.86
500	2.63	2.44	1.99
600	3.00	2.42	2.03
700	3.33	3.03	2.39
800	3.72	3.69	2.86

Table 2 Energization sequence for optimal energization of L-C circuit

Capacitance (μF)	Difference from peak ($^\circ$)	Ideal charging instant	First phase target	Second phase target	Third phase target
200	21.38	68.62	41,161	4165	4165
300	32.40	57.60	4111	4165	4165
400	36.72	53.28	4109	4165	4165
500	41.04	48.96	4107	4165	4165
600	49.68	40.32	4103	4163	4163
700	56.16	33.84	4100	4165	4165
800	65.64	24.36	4095	4165	4165

2.2 Transformer De-energization

Apart from energization complications, de-energization of transformer-capacitor is also a complex situation to be dealt carefully to avoid switching overvoltages. Furthermore, presence of capacitor bank causes its core de-magnetization. Square wave pulses will be seen during de-energization of transformer terminated with considerable capacitance. Complete damping of these square wave pulses requires considerable time to completely de-magnetize the core depending upon quantum of connected inductance and capacitance. For minimizing the switching transients, controlled de-energization is done in simulation study. Figure 4 shows presence of square wave pulses during de-energization of transformer-capacitor combination with 600 μF capacitor bank.

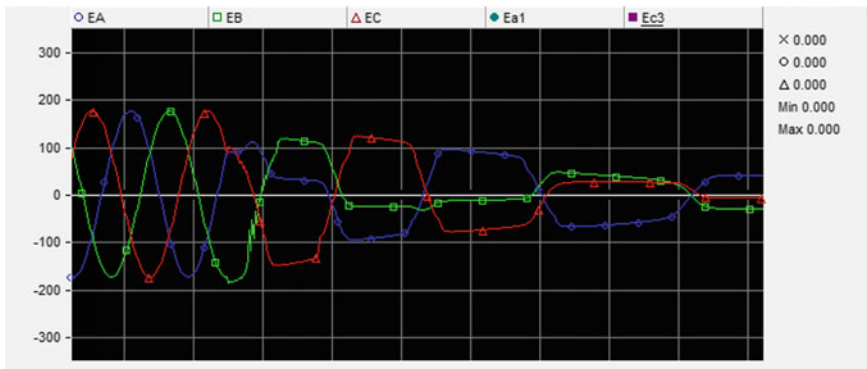


Fig. 4 Controlled de-energization of L-C combination having square wave pulses

3 Field Tests of Suggested Methodology

Field tests were carried out to verify the effectiveness of proposed methodology on three-winding transformer having capacitor bank installed on its tertiary. High voltage side of transformer is connected to bus bar through SF6 CB, and isolator is provided at tertiary side to isolate capacitor bank. CT/VT is available at tertiary side to monitor current/voltage transients during switching of circuit. Also, in this specific configuration, only disconnector is provided for isolating the capacitor bank after de-energizing the transformer for maintenance/shutdown purpose, and no breaker is provided to isolate capacitor bank. Switching operations are carried out on HV side equipped with CSD to minimize starting currents.

3.1 Transformer Energization with Filter Bank

Initially, switching operation is done by keeping capacitor bank in circuit, and HV side CB is closed. All phases are closed simultaneously, and considerable inrush current is observed during energization. From current waveforms, it is evident that current starts flowing in all the phases at same time which validates un-controlled switching. Waveforms for all three phase currents and voltage recorded in disturbance recorder are shown in Fig. 5 having considerable harmonics along with voltage dip in voltage waveform resulting in reduced power quality. Without application of suggested methodology, inrush currents up to 3 pu are observed which can adversely affect the life of system. This particular field application is done on weak grid having

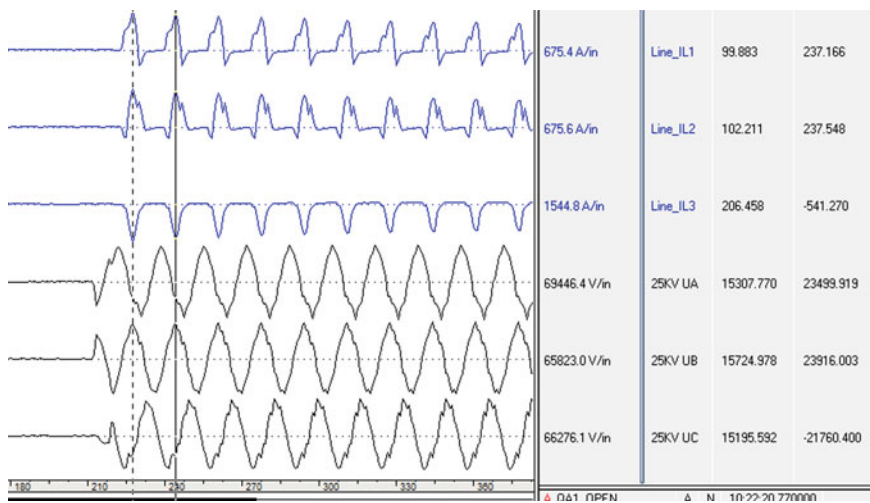


Fig. 5 Inrush current generation without application of controlled switching for L-C combination

low short circuit strength, and even lower inrush current can pose serious voltage depression at point of common connection. In next stage, controlled switching is applied and energization targets are modified, deviated from voltage peak. Series of field tests were conducted to find the best electrical target for switching of L-C combination.

In the process of tuning, it is found that 72° electrical is optimum reference point for charging R phase. The second phase is tuned at 162 degree electrical, while the energization on third phase depends on the sequence of charging of first two phase. As per CIGRE guidelines, this phase should be energized after 90 degree electrical from second phase. But it will show minor effect on charging process. During coarse tuning of targets, currents are reduced from maximum of 1818–414 A. After a set of operations, fine-tuning of controller is set to target first phase at 70° electrical from zero-crossing of phase-neutral voltage wave and second phase at 162° . The resulting inrush currents are considerably reduced, and currents are more sinusoidal. The reduced inrush currents are well below no-load current to the tune of 38–61 A. Moreover, distortions on voltage wave are also reduced owing to increased power quality. Figure 6 shows current and voltage waveform extracted from disturbance recorder with application of controlled switching in conjunction with suggested methodology.

Table 3 summarized the inrush mitigation for different angle. Moreover, upon energization of L-C circuit with large capacitive component, over-excitation boost

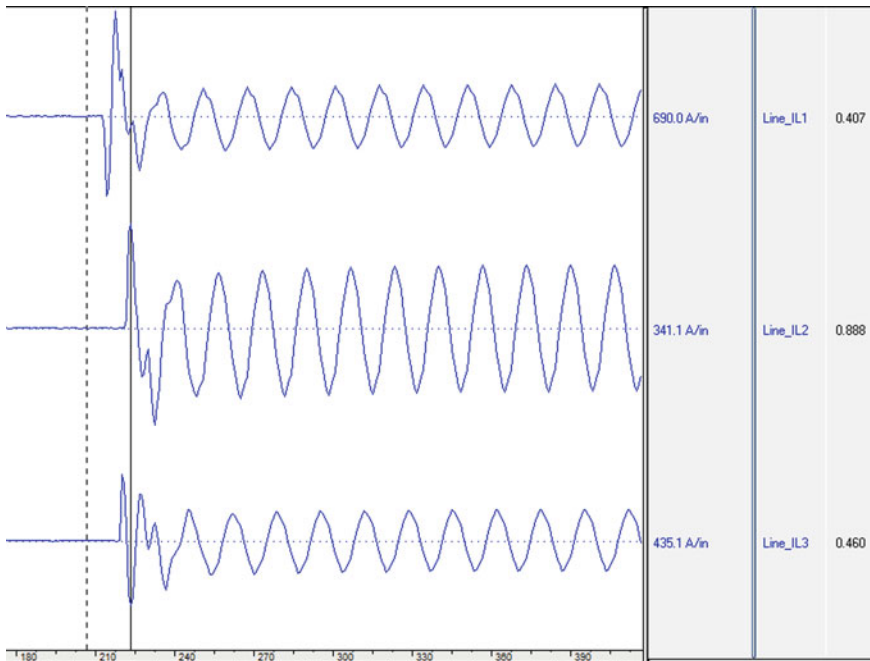


Fig. 6 Inrush currents with application of controlled switching

Table 3 Inrush current comparison with and without application of controlled switching

Target angle (°) with ref to R-N voltage zero			Peak current (A)		
θ_R	θ_Y	θ_B	I_R	I_Y	I_B
<i>With filter</i>					
126	252	342	1818	805	1005
72	270	360	587	1360	1125
72	210	300	253	253	579
72	198	288	396	184	409
72	180	270	313	414	223
72	162	252	39	61	36
<i>Without filter</i>					
72	145	235	900	545	1478
72	180	270	151	61	63
72	180	270	98	50	52
72	162	252	61	46	46
54	162	252	16	13	15
54	162	252	15	14	12

up the grid voltage a to certain extent in comparison with voltage dip observed due to uncontrolled switching. Further, it can be appreciated that voltage measuring facility (PT) are installed on tertiary side of transformer which is wound with delta configuration. Due to the presence of tertiary delta, charging of one phase from HV primary will lead to appearance of voltage across one winding on delta i.e. two phases. Delta voltage needs to be transferred to primary side winding. Therefore, voltage needs to correctly related to primary for exact identification of actual energization instant achieved in energization process.

3.2 Transformer Energization Without Filter Bank

In next step, field tests are continued by disconnecting filter bank from circuit. Without considerable capacitance in circuit, the charging of transformer poses lower inrush current as compared to previous case. Maximum inrush current of 1478 A observed during charging considering targets far away from suggested method. By applying the suggested methodology, inrush currents reduced to nearly no-load current values to the tune of 12 A. It can be appreciated that the accuracy of measuring CT is not better for low current scenarios, hence the current waveform will not replicate sinusoidal primary waveform. Furthermore, no load current (tune of 10–20 A) contains excitation current which is rich in harmonic (3rd) component making resultant waveform non sinusoidal. Mitigated inrush current achieved by applying suggested methodology tabulated in Table 3.

Table 4 Voltage dip comparison with and without application of controlled switching

Inrush current (A)			Voltage dip (%)		
I_R	I_Y	I_B	Δ_R	Δ_Y	Δ_B
<i>With filter</i>					
1818	805	1005	-16.96	-8.76	-6.16
253	253	579	+4.40	+3.80	+3.70
396	184	409	+1.01	+0.15	+0.08
313	414	223	+2.84	+5.11	+4.85
39	61	36	-1.53	+2.71	+2.65
<i>Without filter</i>					
900	545	1478	-18.67	-8.31	-0.55
164	50	56	+0.69	-3.06	-0.05
151	61	63	-0.08	-2.64	-1.52
61	46	46	-0.40	0.00	-0.88
16	13	15	0.00	-0.21	0.00
15	14	12	-0.19	-0.27	-0.14

3.3 Analysis of Voltage Dip

During random charging of transformer, with/without capacitor bank shows considerable voltage drop at bus bar and is undesirable from power quality viewpoint. Table 4 shows voltage dips for different conditions during energization of transformer. Voltage dip of about 15% observed when transformer is charged away from desired targets. Thereafter, with fine-tuning of targets voltage, dip considerably reduced to nominal voltage. Distortions on voltage wave are also reduced owing to increased power quality.

Figure 7 shows current waveforms after applying controlled switching. Bus voltage during energization of L-C combination using CSD shows lesser voltage dip and led to increased power quality.

3.4 Analysis of Total Harmonic Distortions

Energization of transformer alone or along with capacitor at unfavorable instant creates inrush accompanied with flow of lower order current harmonics and voltage dip. Presence of harmonics in voltage phasor reduces the power quality of grid and circuit both. THD of voltage phasor without application of suggested methodology in presence of capacitor found to about 23% which were reduced to 2–12% after fine-tuning. Comparative view of THD with and without application of CSD is indicated in Table 5. In absence of large capacitive component, harmonic content in voltage

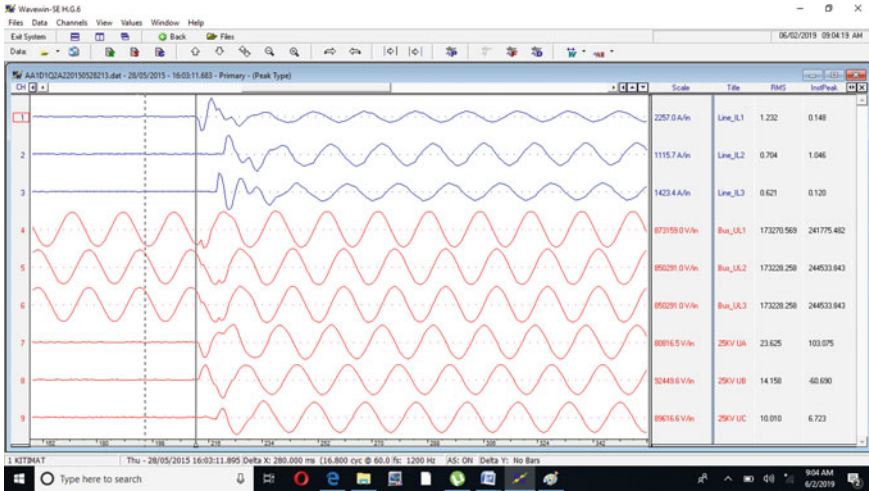


Fig. 7 Inrush currents with application of controlled switching

Table 5 THD comparison with and without application of controlled switching

Peak inrush current (A)			Voltage harmonic distortion (%)		
I_R	I_Y	I_B	THD _R	THD _Y	THD _B
<i>With filter</i>					
1350	833	977	19	22	22
540	590	1050	19	18	17
396	184	409	12	14	15
253	253	579	12	15	15
39	61	36	2	5	5
<i>Without filter</i>					
900	545	1478	22	22	18
151	61	63	6	3	3
98	50	52	6	3	3
61	46	46	3.81	2.71	2.54
16	13	15	0.69	0.71	0.68
15	14	12	0.9	0.81	0.83

phasor further reduced to 0.7% level with the application of suggested method of energization targets.

Figure 8 indicates THD evaluated from disturbance records without correcting energization targets. Moreover, the voltage phasor also contains harmonics with considerable total harmonic distortion (THD) content. Application of controlled switching also helps in recoupage of voltage dip at grid bus.

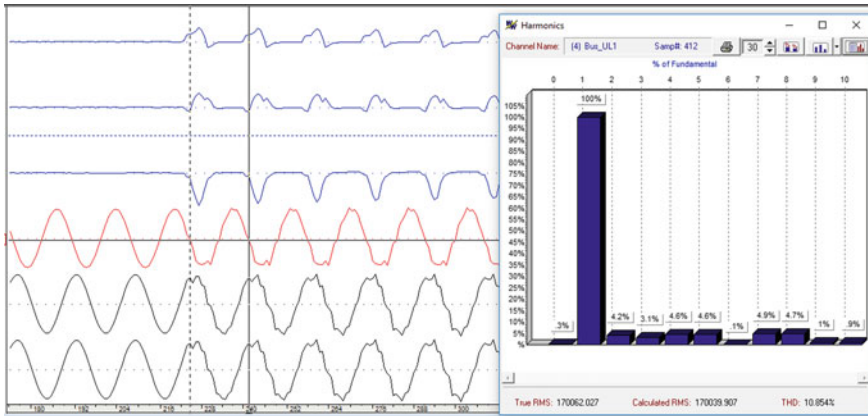


Fig. 8 THD without application of controlled switching

3.5 Controlled De-energization of Transformer

De-energization of transformer with capacitor bank is also performed with controlled switching to minimize switching transients. R phase is de-energized first at voltage peak following by de-energization of B and Y phases. Energization and de-energization sequences are RBY to avoid flow of zero sequence currents. Figure 9 shows disturbance recorder voltage waveform during de-energization and displays de-energization of core. With the help of controlled de-energization, the flux locking of individual phase can be achieved and can aid in evaluation of charging instant during subsequent energization process. However, same is not feasible during protection tripping of CB and in such case signature saved in internal memory of CSD can

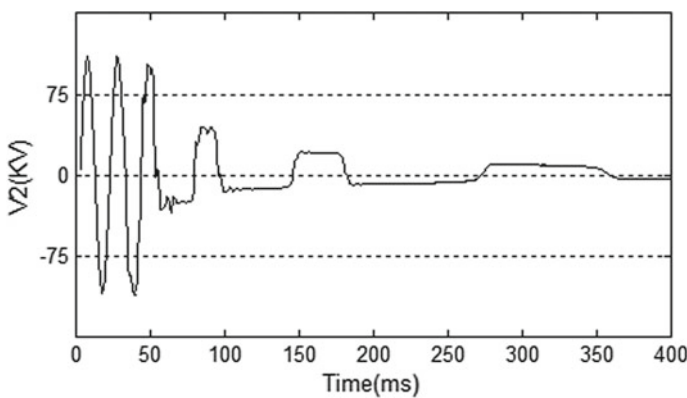


Fig. 9 De-energization of L-C combination resulting in natural de-magnetization

be further utilized. Controlled de-energization not only improves power quality at bus bar but also mitigates chances of restrike at circuit breaker main contacts.

4 Conclusion

In this paper, controlled switching strategies have been evaluated for mitigating inrush effect during energization of transformer in presence of large capacitive component. Proposed technique has been verified by simulation and field case study. Switching strategies explained in this paper will be quite helpful for minimizing the harmful effects of energization of transformer-capacitor combination. Voltage dip occurred during transformer energization is also reduced with the application of controlled switching. Power quality of system in terms of THD is considerably improved with the application of suggested methodology. Application of fine tuned targets with CSD can avoid the worst case scenario but the constrained environment (low short circuit strength bus) demand additions of reactive compensation equipments including STATCOM.

References

1. R. Zhang, et al., A technical experience during network asset replacement: investigating cable and transformer switching interactions, in *CIGRE Workshop*, Lyon, France (2010)
2. Controlled Switching of HVAC Circuit Breaker, Guide for application lines, reactors, capacitors, transformers: part-I. CIGRE ELECTRA **183**, 22–33 (1999)
3. J.L.N. Rao, et al., Mitigation of ferroresonance in line commutated HVDC converter interconnected with series compensated overhead line transmission system, in *IEEE Electrical Power and Energy Conference*, Canada (2016), pp. 12–14
4. J.H. Brunke, et al., Elimination of transformer inrush current by controlled switching: part I—theoretical considerations. *IEEE Trans. Power Delivery* **16**(2), 276–280 (2001)
5. J.H. Brunke, K.J. Frohlich, Elimination of transformer inrush current by controlled switching: part II—application and performance considerations. *IEEE Trans. Power Delivery* **16**(2), 281–285 (2001)
6. CIGRE A3, *Guidelines and Best Practices for the Commissioning and Operation of Controlled Switching Projects* (2019)
7. E. Price, R. Hedding, Protecting transmission lines terminating into transformers, in *IEEE 62nd Annual Conference for Protective Relay Engineers*, Austin, TX, USA (2009)
8. Harlow, J.H., *Electric Power Transformer Engineering*, 3rd edn. (2003)
9. D.A.N. Jacobson, L. Matri, R.W. Menzies, Modelling ferroresonance in a 230 kV transformer-terminated double circuit transmission line, in *International Conference on Power System Transients*, Budapest, Hungary (1999)
10. Controlled Switching of HVAC Circuit Breaker, Guide for application lines, reactors, capacitors, transformers: part-II. CIGRE ELECTRA **185**, 37–57 (1999)
11. R.C. Gonzalez et al., Controlled switching strategies for transformer inrush current reduction: a comparative study. *Electr. Power Syst. Res.* **145**, 12–18 (2017)
12. W. Chandrasena et al., Controlled switching of 1200 MVA transformer in Manitoba. *IEEE Trans. Power Delivery* **31**(5), 2390–2400 (2016)

13. CIGRE, *Working Group A3.07: Controlled Switching of HVAC Circuit-Breakers: Guidance for Further Applications Including Unloaded Transformer Switching, Load and Fault Interruption and Circuit Breaker Uprating* (2004)
14. A. Kalyuzhny, Switching capacitor bank back to back to underground cables. *IEEE Trans. Power Delivery* **28**(2) (2013)
15. F.H. Ding, Controlled switching of shunt capacitor banks with vacuum circuit breaker, in *Proceedings-International Symposium on Discharge and Electrical Insulation in Vacuum*, vol. 2, no. 10, pp. 447–450 (2019)
16. N. Chiesa, et al., On the ringdown transient of transformer, in *International Conference on Power System Transients*, Lyon, France (2007)
17. A.K. Bhatt et al., Evaluation of controlled energization of an unloaded power transformer for minimizing the level of inrush current and transient voltage distortions using PIR-CBs. *IET GTD* **12**(11), 2788–2798 (2018)

Load Frequency Control of a Hybrid System by Using Fuzzy Logic Gain Scaling Technique



Anurekha Nayak, Debayani Mishra, and Manoj Kumar Maharana

1 Introduction

In power system, the electrical network is interconnected for delivering electricity from producers to consumers. The power which is generated from the grid can be interchanged through the tie-lines between different utilities. The foremost goal of electrical power system is to manage the equilibrium between the amounts of power generated and power demand. Due to frequent load variations in the interconnected system, there may be mismatch between generated power and power demand. Tripping of DGs may cause severe overloading in a power system network. As a consequence, the frequency in power system will diverge from standard value. When the interconnected network has disconnected, the frequency of power system will rise. This variation in the system frequency causes an unsteady operation of the power system [1]. Power system instability leads to equipment failure, load shedding and blackouts. So the frequency deviation should be maintained within its permissible limits. In the proposed system, load frequency control is realized which controls variable frequency and exchanges the power flow.

In power system inter-connected network, the electricity cost can be lowered by using renewable sources. The power system renewable energy resources have unparalleled growth in the recent era. But wind power and generation of power from solar cell play a powerful role in integrating it into a hybrid system. But generation of power in wind technology is associated with the drawback of uneven wind flow

A. Nayak (✉) · D. Mishra · M. K. Maharana
School of Electrical Engineering, KIIT Deemed to be University, Bhubaneswar, India
e-mail: anurekha2611@gmail.com

D. Mishra
e-mail: debayanim@gmail.com

M. K. Maharana
e-mail: mkmfel@kiit.ac.in

throughout the year. Likewise, the supply of power from photovoltaic cell is unpredictable during the daytime. With the increased application of renewable sources in the power industry, it is possible to store excess amount of energy and can be used during energy crisis.

To meet the power demand, the renewable energy sources need incorporation with some additional storage energy systems. The deviation of power generated from wind and PV system can be intercepted by using a fuel cell arrangement and electric double layer capacitor. Fuel cell can be used as prime storage system as well as a backup power in various power inaccessible areas. As compared to conventional batteries, EDLC system is more favorable possessing characteristics of clean and environmentally safe energy source.

In literature, there are a number of studies that have been communicated to evaluate load frequency control and the hybrid system model. In [2], a hybrid system subsists of a wind turbine generator and fuel cell has been modeled and its performance characteristics are studied. There are various strategies of control hybrid energy system in amalgamation distributed generating system in [3]. The frequency variation of non-conventional power system is implemented by using coordination control [4]. A new power supply system is proposed in [5] that operates in bounded frequency using renewable energy sources operating in islanding mode.

For a single area system, a comparative analysis has been performed for tuning a load frequency control by various methods [6]. In [7], the author proposed a simple FLC technique to minimize the deviation of frequency in an isolated hybrid system. In [8], a FLC-PI controller has been implemented and dynamic response for three different results is compared. An intelligent stand-alone hybrid system has been proposed in [9] that operate with decrease fluctuation of voltage and frequency. In [10], the author has investigated a PSO controller based on load frequency for a hybrid non-conventional power system with the variable load. A proposed Ziegler-Nicholas PID controller is correlated to a conventional integral controller in [11] and has been found out that Ziegler-Nicholas PID controller has better performance. A PSO-based optimization technique is proposed for a renewable system for the ballast load.

This research paper consists of a hybrid model of photovoltaic system, wind generating system, fuel cell energy storage system and electric double layer capacitor system. The generated power when integrated encounters with frequency deviation in the system. This frequency deviation is minimized by using fuzzy logic controller. With taking reference from literature survey, a new gain scaling technique was investigated with fuzzy logic controller in this paper.

In this paper, Sect. 1 describes introduction, and Sect. 2 discusses hybrid system representation and modeling. Distinct control approaches which includes PI and FLC are discussed in Sect. 3. The results are performed by Simulink, and discussion is carried in Sect. 4.

2 Modeling of Hybrid System

The proposed figure of the hybrid renewable power system is represented in Fig. 1 [4]. The proposed model combines WTG system, PV system, FC energy storage system and electric double layer capacitor (EDLC) bank.

The power produced from WTG and PV cell used to meet the energy requirement and the surplus power generated contributes for charging of EDLC system and to produce hydrogen in the FC system.

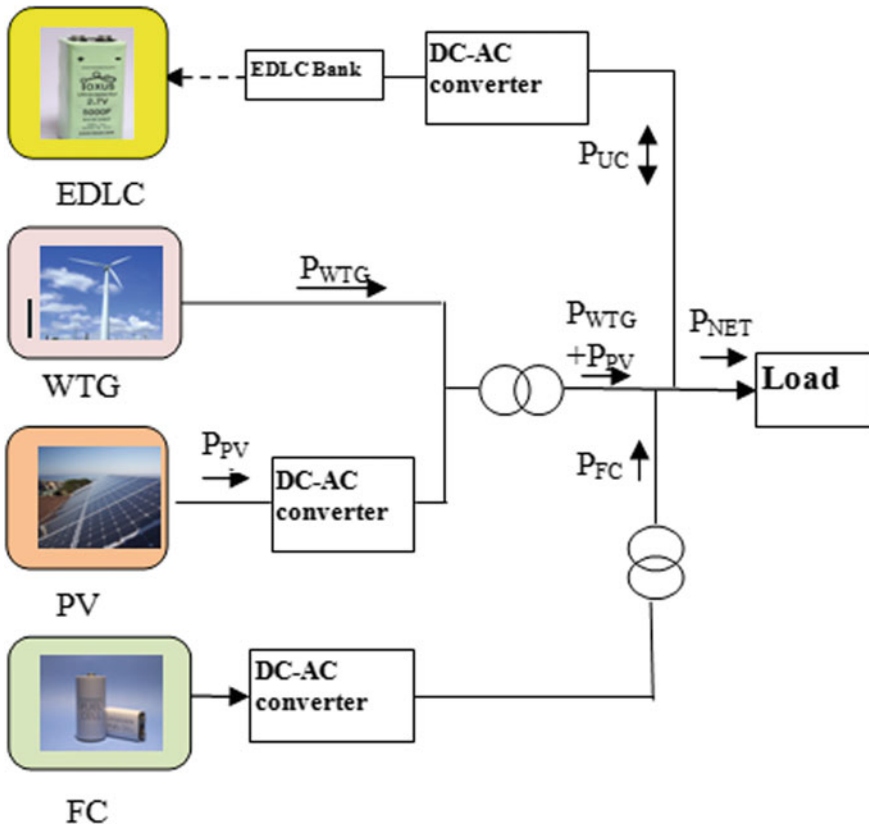


Fig. 1 Proposed model of the hybrid renewable system

2.1 Modeling of Wind Turbine Generator

The output power from the turbine generator is based on speed of the wind. The power versus wind speed characteristics of a wind turbine generator are represented in Fig. 2.

The generated output power from wind turbine generator system can be expressed as in Eq. (1),

$$P_{\text{wind}} = \frac{1}{2} \rho A V^3 C_p(\lambda, \theta) \tag{1}$$

where ρ = air flowing density in kg/m^3 ,

A = area swept by blades in m^2 ,

C_p = coefficient of power,

λ = tip speed ratio,

θ = pitch angle,

V = speed of wind in m/s .

The attributes of a WTG deviate with the wind speed variation [12]. The wind generating system model can be furnished by the transfer function as expressed in Eq. (2)

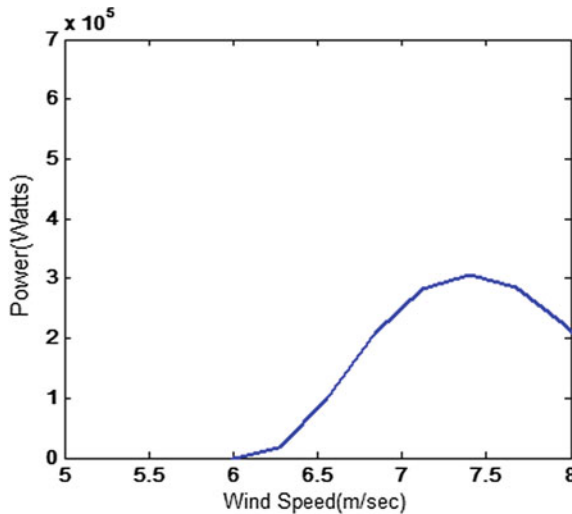


Fig. 2 Power versus wind characteristics of wind turbine

$$\frac{\Delta P_{wind}}{\Delta P_{WTG}} = \frac{1}{1 + sT_{WTG}} \tag{2}$$

T_{WTG} is the time constant of generator of wind turbine.

2.2 PV Model

By combining multiple solar panels considering series as well as parallel combination, a PV system either can be utilized. A PV module has 36 or 72 cells. The attributes of a PV system are shown in Fig. 3.

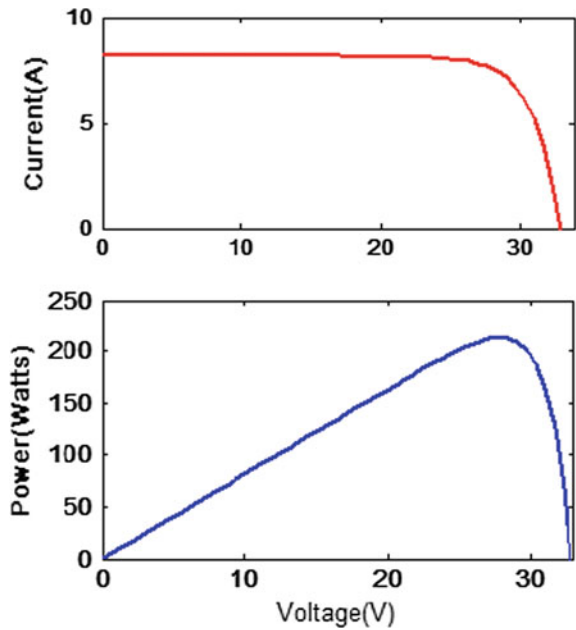
The PV system generated output power can be furnished by Eq. (3) as follows

$$P_{PV} = \eta S \phi (1 - 0.005(T_a + 25)) \tag{3}$$

where η = efficiency of conversion,

S = area measured of PV array,

Fig. 3 Current, voltage and power curves



φ = solar irradiation,

T_a = ambient temperature.

The transfer function of a PV system is given by Eq. (4)

$$\frac{\Delta\varphi}{\Delta P_{PV}} = \frac{1}{1 + sT_{PV}} \quad (4)$$

T_{PV} is the time constant of PV system.

2.3 FC Model

The fuel cell transforms the energy stored in chemical form into electrical energy. Fuel cells are dissimilar from batteries, and only difference is that there is presence of active chemicals which convert chemical energy into electrical energy. To attain this, FC needs a sustained origin of fuel. These hydrogen fuel cells are integrated with other renewable sources due to their highly efficient, viable and require less care. The fuel cell model can be presented by the transfer function as in Eq. (5)

$$\frac{P_{FC}^*}{P_{FC}} = \frac{1}{1 + sT_{FC}} \quad (5)$$

T_{FC} is the time constant of FC system.

2.4 EDLC Model

Electric double layer capacitors also known as supercapacitor are a novel energy storage technology possessing high power density. In an EDLC cell, charging is faster compared to other batteries. EDLC cell has negligible resistance that leads to 100% efficiency and low maintenance.

A single EDLC cell generates an output voltage of 2.7 V. There are various EDLC cells which are connected in series to obtain a high voltage. The capacitor possesses density of power about 60 times higher than the density of power contained in batteries and is mostly used where power requirement is high. The transfer function of EDLC system can be given by Eq. (6)

$$\frac{P_{EDLC}^*}{P_{EDLC}} = \frac{1}{1 + sT_{EDLC}} \quad (6)$$

T_{EDLC} is the time constant of EDLC system.

2.5 Power System Model

By using controllers, the total output power generated from a hybrid system can be used. The power obtained from PV and WTG system will be integrated with FC and EDLC technologies to supply the required load.

The transfer function model of the power system is given by Eq. (7)

$$\frac{\Delta f}{\Delta P} = \frac{1}{Ms + D} \quad (7)$$

where M denotes the inertia constant of the power system and

D is the coefficient of damping.

3 Control Approaches

When the renewable energy sources are integrated to configure the hybrid system, the system frequency deviates from its prescribed value. The dynamic response of the system can be improved by using different controllers.

3.1 Without Controller

By using different controllers, the power which is generated from FC and ELDC hybrid system can be regulated. There is a fluctuation of frequency in the system when energy is stored as backup and no controller is used. Furthermore, frequency response captures larger time to set down to its final value which is unacceptable for any power systems.

3.2 With PI Controller

The schematic representation of a PI controller is shown in Fig. 4. The steady-state error of the system response can be eradicated by altering the proportional-integral controller gains. As the PI controller is not competent to eliminate the frequency oscillation, the errors in the system cannot be anticipated. In this research paper, PI controller is implemented with the backup systems.

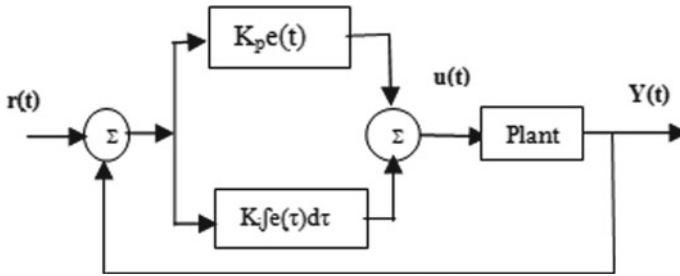


Fig. 4 Schematic representation of PI controller

3.3 Fuzzy Logic Controller with Gain Scaling Technique

Nowadays, fuzzy system is applied in multiple areas of power systems. Fuzzy control system can be implemented as real-time expert system for enhancing the results found with the conventional system design. Fuzzy inference is the technique to develop the input and output mapping for the proposed controller as represented in Fig. 5.

The FLC rules can be developed with the expert knowledge procured by the skilled operator. When designing fuzzy logic controller, it is necessary to retain the voltage output and generator frequency at its estimated value with the changing load. To achieve the desired aim, the rule base is designed with the possible combinations of input variables to find intended output variables. With the increased number of membership function (MF), the output response will be improved. In this proposed paper, the author implanted seven membership functions for attaining more robustness in the output. In truth table, the membership functions are low negative (LNG), medium negative (MNG), small negative (SNG), zero (ZO), less positive (LPS), medium positive (MPS) and small positive (SPS) (Table 1).

In the proposed system, the frequency aberration is controlled by implementing fuzzy logic gain scaling technique for backup energy system.

Fig. 5 Architecture of fuzzy inference system

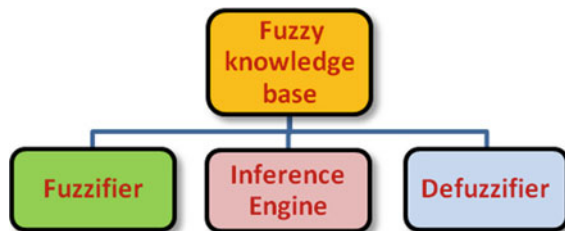


Table 1 Truth table

Error	<i>d</i> (error)						
	LNG	MNG	SNG	ZO	SPS	MPS	LPS
LNG	LNG	LNG	LNG	LNG	MNG	SNG	ZO
MNG	LNG	LNG	MNG	MNG	SNG	ZO	SPS
SNG	LNG	MNG	MNG	SNG	ZO	SPS	MPS
ZO	MNG	MNG	SNG	ZO	SPS	MPS	LPS
SPS	MNG	SNG	ZO	SPS	MPS	MPS	LPS
MPS	SNG	ZO	SPS	MPS	MPS	LPS	LPS
LPS	ZO	SPS	MPS	LPS	LPS	LPS	LPS

4 Results

The generated power from photovoltaic system and wind turbine system is implemented in various weather conditions. The simulation parameters are stated in Appendix [4], and the system is simulated under various conditions.

4.1 Proposed System Without Controller

The proposed model of EDC and FC system is implemented without using a PI controller as shown in Fig. 6. In the proposed system, the deviation in frequency has more perturbations and output is unpredictable.

From Fig. 6, it is noticed that the system has higher oscillations and the time needed for setting is found to be 32 s.

Fig. 6 Deviation in frequency without using proportional-integral controller

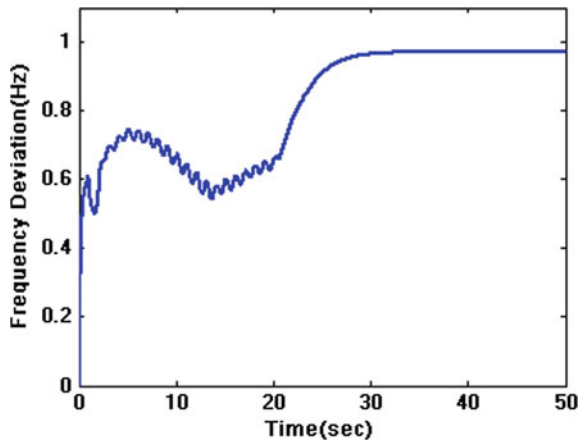
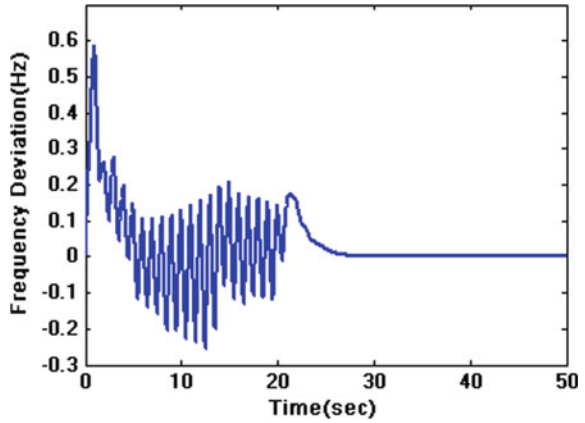


Fig. 7 Deviation in frequency by using PI controller



4.2 With PI Controller

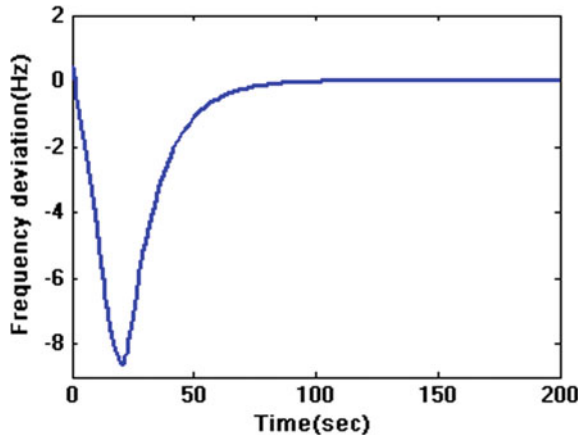
In the paper, the model transfer function of ELDC and FC is constructed by using conventional PI controller. By using a PI controller, the result of simulation is shown in Fig. 7.

The alteration in frequency is diminished with fewer oscillations, and the time needed for setting is found to be 30 s.

4.3 With Fuzzy Logic Controller

The proposed model is delineated using fuzzy logic controller using gain scaling technique. The response is shown in Fig. 8.

Fig. 8 Deviation in frequency with FLC gain scaling



The alteration in frequency in the proposed controller is reduced with less oscillation with decreased overshoot.

5 Conclusion

In this paper to minimize the alteration in frequency, load frequency control scheme is implemented in a hybrid system. The model describes by using advanced gain scaling technique with the fuzzy logic controller for a non-conventional system that comprises of PV, WT, FC and EDLC. By using variable load, there is fluctuation of frequency in the system. From results of simulation, it is observed that the frequency deviation for the non-conventional system is minimized by implementing conventional PI controller; the output response takes larger time to settle at its final steady-state value. However, the overshoot found with the conventional controller can be minimized, and frequency deviation performance could be made better by using FLC added with gain scaling technique.

Appendix

$$T_{\text{WTG}} = 1.5 \text{ s}$$

$$T_{\text{PV}} = 1.8 \text{ s}$$

$$T_{\text{FC}} = 0.26 \text{ s}$$

$$T_{\text{ELDC}} = 0.01 \text{ s}$$

$$M = 0.4$$

$$D = 0.03.$$

References

1. H. Shayeghi, H.A. Shayanfar, Load frequency control strategies state of the art survey for the researcher. *Energy Convers. Manage.* **50**, 344–353 (2009)
2. M.I. Khan, M.T. Iqbal, Dynamic modeling and simulation of a small wind-fuel cell hybrid energy system. *Renew. Energy* **30**(3), 421–439 (2005)
3. J. Wood Allen, F. Wollenberg Bruce, *Power Generation Operation and Control* (1996)
4. M. Nayeripour, M. Hoseintabar, Frequency deviation control by coordination control of FC and double layer capacitor in an autonomous hybrid renewable energy power generation system. *Renew. Energy* **36**, 1741–1746 (2011)
5. T. Senjyu, T. Nakaji, K. Uzeto, T. Funabashi, A hybrid power system using alternative energy facilities in isolated island. *IEEE Trans. Energy Convers.* **20**(2) (2006)

6. T. Senjyu, R. Sakamoto, N. Urasaki, T. Funabasi, H. Fujita, H. Sekine, Output power levelling of wind turbine generator for all operating regions by pitch angle control. *IEEE Trans. Energy Convers.* **21**(2), 467–475 (2006)
7. S. Rawat, et al., Load frequency control of a renewable hybrid power system with simple fuzzy logic controller, in *2016 International Conference on Computing, Communication and Automation (ICCCA)* (IEEE, 2016)
8. R. Kaushal, et al., Power systems load-frequency stability using fuzzy logic-PID controller. *Int. J. Res. Appl. Sci. Eng.* (2015)
9. S.A.M. Al-Barazanchi, A.M. Vural, Modeling and intelligent control of a stand-alone PV-wind-diesel-battery hybrid system, in *2015 International Conference on Control, Instrumentation, Communication and Computational Technologies (ICCICCT)* (IEEE, 2015)
10. G. Shankar, S. Lakshmi, N. Nagarjuna, Optimal load frequency control of hybrid renewable energy system using PSO and LQR, in *2015 International Conference on Power and Advanced Control Engineering (ICPACE)* (IEEE, 2015)
11. A. Khan, et al., Comparative analysis of different methods of tuning load frequency control problem. *Int. J. Res. Appl. Sci. Eng.* (2015)
12. T. Santy, R. Nalisan, Load frequency control of a two area system consisting of a grid connected PV system and diesel generator. *IJETCSE* **13**(1) (2015). ISSN 0967-1553

Automatic Bluetooth-Controlled Master-Slave Firefighting Robots



Debasish Bhattacharya, Aayush Rijal, Ameesha, and Israj Ali

1 Introduction

In the NextGen technology (in the era of industry 4.0), Internet of Things (IoT) changes the human lives that help to extinguish fires remotely. The Bluetooth technology combined with Android application is used to control robot swarms to help us in this process. Using ultraviolet sensors for the detection of fire is a popular fire detection method nowadays due to their suitable range and sensitivity [2–5]. Integration use of microcontroller and sensors leads to the solution of the problem. In this paper, we integrated the sensors which are namely SEN16 which is a flame sensor and infrared receiver (IR) module which can sense the infrared generated by fire, Bluetooth HC-05 modules which is suitable for wireless connection, an inbuilt 6 V DC mini horizontal submersible pump and Arduino Uno which is a microcontroller. If any fire is detected, the swarm's robots are directed towards the source of the fire by using a developed mobile app. These swarm robots are designed to carry the water for extinguishing the detected fire. Our main objectives are to refrain the direct activity of the human being from fire and associated safety protocols [6].

D. Bhattacharya (✉) · A. Rijal · Ameesha · I. Ali
School of Electronics Engineering, KIIT Deemed to be University, Bhubaneswar, Odisha 751024,
India

e-mail: debasishb912@gmail.com

A. Rijal

e-mail: aayushrijal2017@gmail.com

Ameesha

e-mail: ameeshadav@gmail.com

I. Ali

e-mail: israjfet@kiit.ac.in

2 Basic Functionalities

2.1 The App

The Android app prepared for this purpose is very easy to use and developed using Android Studio. The app consists of four buttons and a microphone. The buttons are used to guide the robots in the right direction, and the microphone provides an extra feature to control the robots via voice.

2.2 The Robots

The robots are small-sized and very efficient. They are light weighted and are easily portable. Since they are Bluetooth-controlled, they can be driven from one location to another.

3 Components Required

3.1 Arduino Boards

Arduino Uno is board based on ATmega328 microcontroller. This board has 14 pins in which six are analog and rest of the others are digital pins. Out of these pins, six pins can be used as PWM o/p. It also has a 16 MHz ceramic resonator which is suitable to generate time information, ICSP header for serial communication, USB connection, power jack, and a reset button. Arduino Uno can be powered by AC_DC adaptors or through USB cable connected with the PC. The technical details of the Arduino are given in Table 1 (Fig. 1).

3.2 Jumper Wires

Jumper wires are merely wires that have connector pins at each end which permits them to connect two points to every other while not soldering. They are usually used with the breadboards and different prototyping tools so as to form it straightforward to alter a circuit as required.

Table 1 Technical feature of Arduino

SL	Component	Features	SL	Component	Features
1.	Microcontroller	ATmega328P	7.	Analog I/O pins	6
2.	Clock speed	16 MHz	8.	Digital I/O pins	14 (including 6 PWM)
3.	Operating voltage	5 V	9.	Flash memory	32 kb
4.	Input voltage	7–20 V	10.	SRAM	2 kb
5.	DC current at 3.3 V pin	50 mA	11.	EEPROM	1 kb
6.	DC current per I/O pin	20 mA	12.	L-W-Wd	68.6 mm-25 g-53.4 mm

**Fig. 1** Picture of Arduino Uno

3.3 Motor Driver (L293D)

This driver circuit is suitable to control two DC motors simultaneously, and it is controlled by the IC293D which contains 16 pins, and the principle of the circuit for controlling is the current amplification. The low current signal is converted to high current signal as a driving input to the motor through which we are able to control its rotation (Figs. 2 and 3).

Fig. 2 Picture of jumper wires



Fig. 3 Picture of L293D motor driver



3.4 Robot Chassis with Wheels

This chassis has multiple holes and slots, so you will suit your electronics simply on this rigid chassis. It is made up of 3 mm acrylic sheet. Arduino compatible holes and standoffs are enclosed; thus, Arduino will be simply mounted on top. Chassis size is 110 × 125 mm (Fig. 4).

Fig. 4 Picture of chassis of the robot with wheels



Table 2 Technical features of HC-05 module

SL	Features	Properties	SL	Features	Properties
1.	Operating voltage	+5 V	5.	Communication mode	Asynchronous
2.	Sensitivity	-80 dBm	6.	Baud rate	Programmable
3.	Transmit power	+4 dBm (Max)	7.	Input-output control	Programmable
4.	Input-output voltage	3.3-5 V	8.	Antenna	Integrated

3.5 HC-05 Bluetooth Modules

This module is used for wireless communication by serial port protocols (SPPs). It is a transceiver model and can be figured as a transmitter and receiver. Its communication frequency is 2.5 GHz, and data can be sent at a rate of 3 mbps by its v2.0 + EDR (enhanced data rate). As it acts as a transmitter-receiver, it can be modeled as a master-slave combination. Some of the more technical features are shared in Table 2.

3.6 SEN-16 Flame Sensors

This sensor is made on the basis of YG1006 NPN phototransistor. Phototransistor is attached at the front of the module which is black in color. This phototransistor is similar to a black LED look-wise. But it has three terminals. The long terminal is the emitter. The short terminal is the collector. Base terminal is not there because the light detected by it enables the current flow (Figs. 5 and 6).

The phototransistor has a black epoxy coating. This makes it IR sensitive. This YG1006 phototransistor is IR sensitive in the range of 760-1100 nm of wavelength.

Using flame sensor, we can detect IR light up to 100 cm within 60° detection angle.

Fig. 5 Picture of Bluetooth module (HC-05)

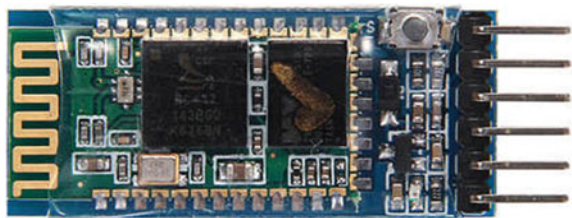


Fig. 6 Picture of flame sensor (SEN-16)



3.7 Motors (6 V)

DC motor is a rotary system. It converts electrical energy into mechanical energy, and the mechanical energy is obtained by rotation. The over principles can be explained by Fleming’s Rule of Thumb. Its basic principles are electromagnetic principles. The current flow direction gives the rotational directions. Here, we are using a 6 V DC motor for the movement of the robot base.

3.8 Servomotors

Servomotor is a linear actuator. It can control the angle, linear motion, speed, and acceleration. The controlling mechanism can be done through a sensor which is attached with its motor. This component is used here for a directional water flow (Figs. 7 and 8).

Fig. 7 Picture of servomotor





Fig. 8 Picture of DC motor (6 V)

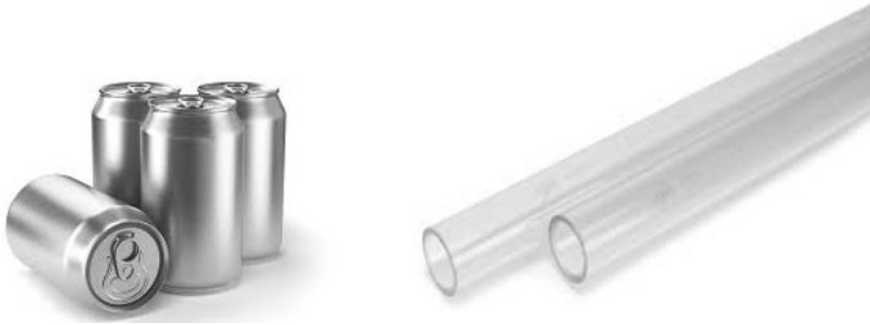


Fig. 9 Picture of cans and pipes

3.9 Pipes and Cans

See Fig. 9.

Technical features of pipes	Technical features of cans
Material: food grade silicone	Made from aluminum and trace amounts of other metals, including magnesium, iron, and manganese
Features: insulation, acid, and alkali resistance	
Temperature range: -60 to 240 °C	

3.10 DC Pump (5 V)

It is used to pump the water, using 5 V. It cannot run without water.

4 Working Model

4.1 Master-Slave Mode

In master-slave mode configuration, we need to use two Bluetooth modules as we consider only single swarm for this paper. HC-05 module is suitable to configure either master or slave as it has trans-receiver control facilities. Therefore, using AT commands we will configure one Bluetooth as a master and another HC-05 as a slave. In our case, master is connected with an Android app which is discussed later in this paper, and it is also capable to send commands to the slave (by Bluetooth communication protocols) which contains the water can and DC pump for fire extinguishing. Figures 10 and 11 are master and slave, respectively. The connection



Fig. 10 Picture of DC pump (5 V)

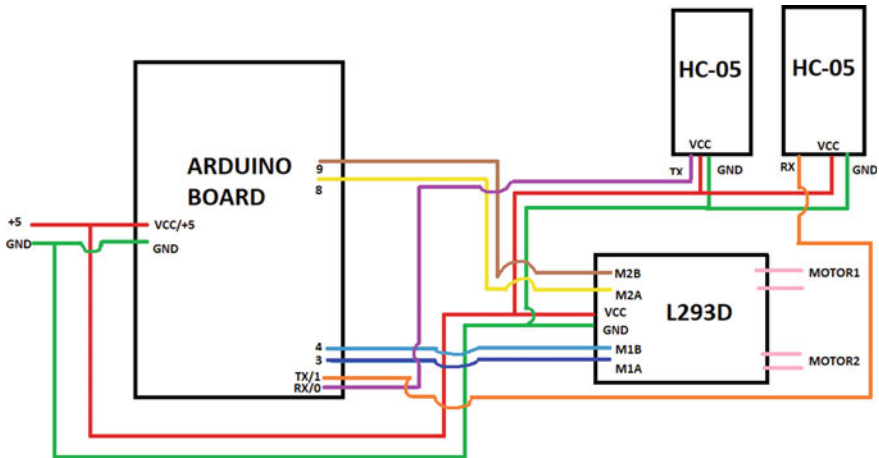


Fig. 11 Schematic diagram of master robot without the circuit for fire detection

Table 3 Arduino and HC-05 connection list

SN	Arduino	HC-05
1.	Rx (pin 0)	Rx
2.	Tx (pin 1)	Tx
3.	+5 V	VCC
4.	GND	GND
5.	+3.3 V	KEY

between Arduino and HC-05 module is given in Table 3.

After the connection setting, we need to open a blank Arduino sketch. This sketch contains two major portions like:

```
Void Setup {}
Void Loop {}
```

In the setup portion, we need to set the baud rate 38,400 and open the serial monitor. We also must ensure that the serial monitor baud rate must be 38,400 and NL and CR are selected from the bottom of Arduino Serial Monitor. After each AT command execution, HC-05 expects line feed and carriage return which are very necessary. Now, if we type the AT command in the serial monitor and press the SEND button, we will get responses. If no responses are coming, we need to check the baud rate. The following AT commands are required.

$$AT + NAME? \tag{1}$$

This AT command is required to get the name assigned for the module. After getting the name of the module, we need to reassign its name to HC05_SLAVE by the following AT command

$$AT + NAME = HC05_SLAVE \tag{2}$$

Next, we need to fix the role of the module by the following AT command

$$AT + ROLE? \tag{3}$$

For the SLAVE role of the module, we need to fix it by $AT + ROLE = 0$; otherwise, for the MASTER role of the module, we need to fix it by $AT + ROLE = 1$. We assigned

$$AT + ROLE = 0 \tag{4}$$

For the SLAVE role.

After fixing the role of the module, we need to find out the address of the module for the proper communication by pairing using the following AT command

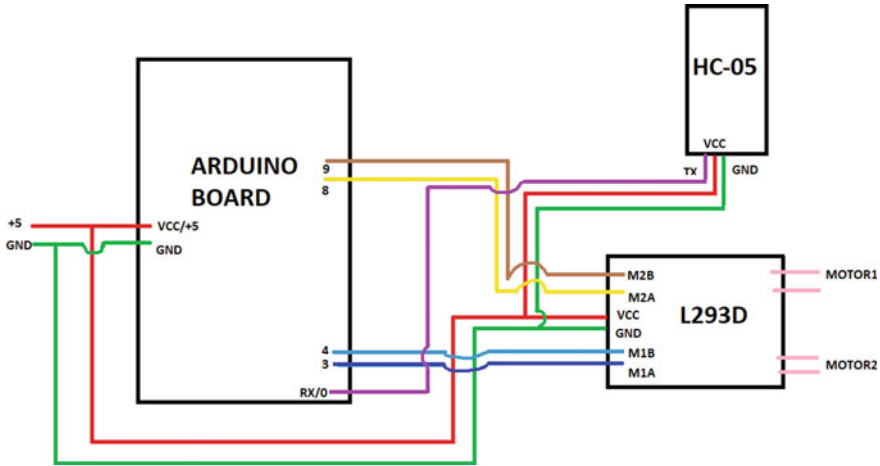


Fig. 12 Schematic diagram of slave robot without the circuit for fire detection

AT + ADDR? (5)

This command gives the module address as 18: E4: 400006. At the time of the command writing, the colons are replaced by the commas, like 18, E4, 400006.

Now, we remove the key connection from HC-05 Bluetooth module and also disconnect the power from the module. After the disconnection, we again connect it and check the status LED. If it blinks faster, it seems to ready for the pairing with the module. Finally, AT + CMODE = 0 is used only for unique connection with slave and after that AT + LINK = 18, E4, 400006 (address of slave) [7, 8] (Fig. 12).

4.2 Fire-Extinguishing Circuit

After pairing, we connect the circuits according to our requirement. The complete code (which is given below of this paper) is also uploaded to Arduino Uno for testing. In this case, we have placed a fired lighter. Normally, flame sensor output is high means no fire condition, and when any fire source is detected, sensor output response becomes low. This low signal is communicated to the input pin of Arduino for switch on the pump. As usual for no fire detection, there is no fire source, i.e., normal condition and pump is switched off.

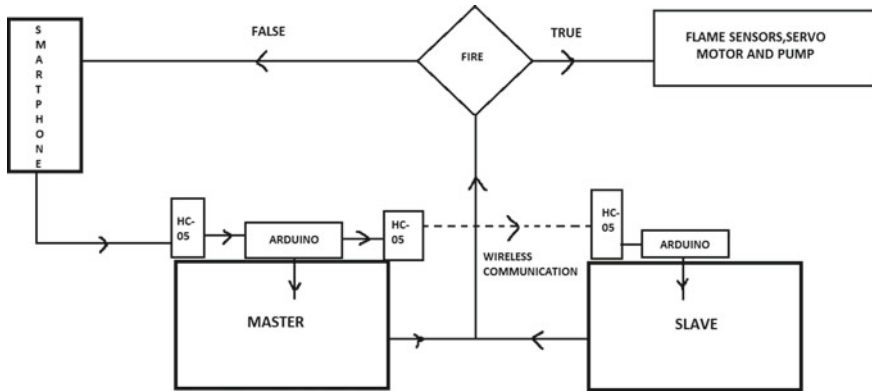


Fig. 13 Complete working algorithm of Bluetooth-controlled master-slave firefighting robots using Arduino and SEN-16 flame sensors

4.3 Overview of Working Model

Particularly for this paper and the problem statement, we have completed our solution in four phases. In the first phase, it includes making of the Bluetooth app. We used Android Studio to design the app. In the second phase, we include the Bluetooth connections of both the master and slave. In the third phase, we include the master-slave connection pairing. At this point, the master and slave are controlled by Bluetooth and slave follows master. In the last phase, phase four, includes the fire-fighting part. The flame sensors are integrated along with the pump and servomotor. Finally, we have the Bluetooth-controlled master-slave firefighting robots ready for operation.

The Android app controls the master via the HC-05. The master controls the slave. There is a continuous feedback circuit which checks for fire. If fire is detected, the flame sensors and the pumps of both the robots are activated or else the robot continues to search for fire [9, 10] (Fig. 13).

4.4 Concept of Swarm Robotics

Social insects such as ants exhibit the swarm intelligence.

Swarmed intelligence is the collective behavior of decentralized self-organized system where each member autonomously offers its abilities.

Such algorithm can be applied in the field of robotics. If the set of robots exhibits the swarm intelligence, then they are defined as the swarm robot. Swarm robots are the combination of the multiple robots which acts together in groups like a group of insects that are assigned for a given task (Figs. 14 and 15).

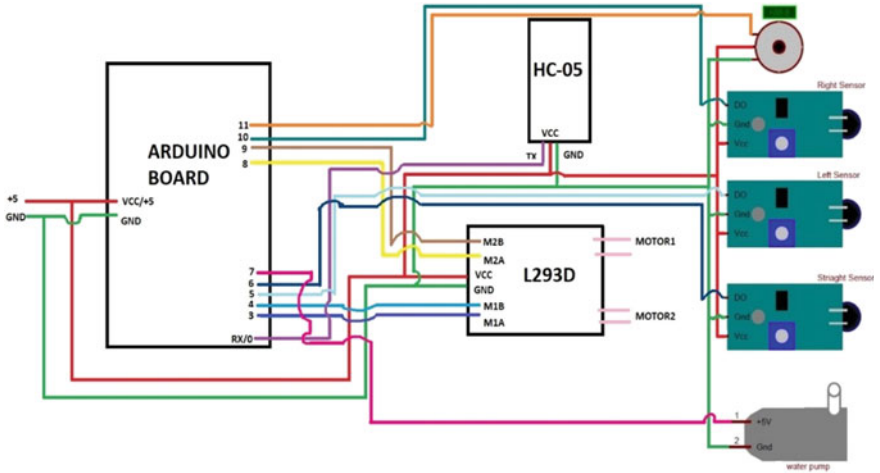


Fig. 14 Complete working circuit diagram of Bluetooth-controlled master-slave firefighting robots using Arduino and SEN-16 flame sensors



Fig. 15 Complete simulation under firefighting conditions

The main concepts of the swarm robotics are to merge the multiple robots to perform a certain goal. Instead of having a one complicated robot, we can program the simple multiple robots to do the same things. The behaviors of them are related to each other, and the change of the behavior of individual one is in cooperation with others as well as the group.

5 Conclusion

After setting up the model and running the software, the sensors are brought into action. Our project revolves around the integrated use of sensors which are namely SEN 16 flame sensor, Arduino, and HC-05 Bluetooth module. The Bluetooth app controls the master which in turn controls the slave by means of another HC-05 module. The flame sensor detects fire, and the robots move towards it to extinguish it. This system proves to be reliable and cheap to implement and also paves the path for future modifications and enhancements. As we all know, NextGen technologies nowadays are a basic need at every living dwelling. But there is still a possibility for improvement and further development.

References

1. G. Litta, R. Di Rienzo, R. Morello, R. Roncella, F. Baronti, R. Saletti, Flexible platform with wireless interface for DC-motor remote control, in *2018 IEEE International Conference on Industrial Electronics for Sustainable Energy Systems (IESES)*, vol. 2018, Jan 2018, pp. 509–514
2. P. Matthew, *Fire-Fighting Robot. Industrial Systems Design & Integration*. Page No. Web. 10 Nov 2013
3. J. Suresh, *Fire Fighting Robot (2017)*. Web. 3 June 2017
4. A.J. John, K. Ashik, K.S. Avinash Vishnu, P. Fahmi, P. Henna, Automatic fire extinguishing robotic vehicle. *Int. J. Sci. Eng. Res.* 7(4) (2016)
5. A.S. Anoop, P. Kanakasabapathy, *Review on Swarm Robotics Platforms* (Amrita Vishwa Vidyapeetham, Amritapuri, India). Web. 7 Nov 2017
6. A. Hassanein, M. Elhawary, N. Jaber, M. El-Abd, *An Autonomous Firefighting Robot* (Department of Electrical and Computer Engineering, American University of Kuwait, Kuwait, 2015)
7. <https://www.instructables.com/id/AT-command-mode-of-HC-05-Bluetooth-module/>
8. A.N.N. Chamim, M.E. Fawzi, Iswanto, R.O. Wiyagi, R. Syahputra, *Controlled of Wheeled Robots with Bluetooth Based Smartphones* (Universitas Muhammadiyah Yogyakarta). Web. 30 July 2019
9. G. Seeja, A. Arockia Selvakumar, V. Berlin Hency, *A Survey on Swarm Robotic Modeling, Analysis and Hardware Architecture* (Chennai, India). Web. 24 July 2018
10. R. Veeramani, R. Madhanmohan, D. Prajapati, A. Kumar, S. Kumar, *IoT Based Speech Recognition Controlled Car Using Arduino* (SRMIST, Chennai). Web. 15 Oct 2019

A New Design Method for High-Order Discrete Systems Using Polynomial Differentiation Technique



G. V. K. R. Sastry, G. Surya Kalyan, and R. S. R. Krishnam Naidu

1 Introduction

The available stability analysis and design methods are more effective and easily applied if the systems are of low order, and unfortunately, majority of practical systems are of very high order. To overcome this problem, large-scale system modeling is suggested [1, 2]. The new procedure uses polynomial differentiation technique and application of w -domain bilinear transformation resulting in low-order system. It is extended for controller design.

2 Procedure

Original system of order n is described as

$$G(z) = \frac{N(z)}{D(z)} = \frac{a_0 + a_1z + a_2z^2 + \cdots + a_{n-1}z^{n-1}}{b_0 + b_1z + b_2z^2 + \cdots + b_{n-1}z^{n-1} + b_nz^n} \quad (1)$$

It is proposed to obtain reduced order model defined as

G. V. K. R. Sastry
A.U. College of Engineering (A), Visakhapatnam, India
e-mail: profsastrygvkr@yahoo.com

G. S. Kalyan
Chaitanya Engineering College, Visakhapatnam, India
e-mail: sukaga80@gmail.com

R. S. R. Krishnam Naidu (✉)
N.S.R. Institute of Technology, Visakhapatnam, India
e-mail: naidueee06@gmail.com

$$G_r(z) = \frac{N_r(z)}{D_r(z)} = \frac{d_0 + d_1z + d_2z^2 + \dots + d_{r-1}z^{r-1}}{e_0 + e_1z + e_2z^2 + \dots + e_{r-1}z^{r-1} + e_rz^r} \tag{2}$$

where $r = 1, 2 \dots n$.

Step 1

Denominator of order k ($k= 1, 2, \dots, n$)

The constant term e_0 in Eq. (2) is obtained by polynomial differentiation method using the following Eq. (3).

The k th order denominator is defined as

$$D_k(z) = \sum_{i=1}^{k+1} b_{i-1} \frac{{}^{n-i+1}C_{n-k}}{{}^nC_{n-k}} z^{i-1} \tag{3}$$

where $k = 1, 2, 3 \dots n - 1$.

For $k = 1$,

$$D_1(z) = b_0 + \frac{{}^{n-1}C_{n-1}}{{}^nC_{n-1}} b_1z$$

for $k = 2$,

$$D_2(z) = b_0 + \frac{{}^{n-1}C_{n-2}}{{}^nC_{n-2}} b_1z + \frac{{}^{n-2}C_{n-2}}{{}^nC_{n-2}} b_2z^2, \text{ respectively.}$$

Step 2

$G(z)$ in w -domain will be

$$G(w) = \frac{a_0 + a_1w + a_2w^2 + \dots + a_{n-1}w^{n-1}}{b_0 + b_1w + b_2w^2 + \dots + b_{n-1}w^{n-1} + b_nw^n} \tag{4}$$

General r th order reduced model transfer function in w -domain is:

$$G_r(w) = \frac{d_0 + d_1w + d_2w^2 + \dots + d_{r-1}w^{r-1}}{e_0 + e_1w + e_2w^2 + \dots + e_{r-1}w^{r-1} + e_rw^r} \tag{5}$$

Step 3

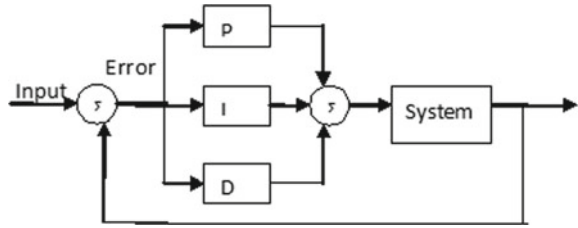
Reduced order transfer function

Equating Eqs. (4)–(5) and rearranging,

$$a_0e_0 + (a_0e_1 + a_1e_0)w + (a_0e_2 + a_1e_1 + a_2e_0)w^2 + \dots + a_{n-1}e_k w^{n-1+k} = b_0d_0 + (b_0d_1 + b_1d_0)w + \dots + b_nd_{k-1}w^{n-1+k} \tag{6}$$

solving the following equations, the values of a_0, a_1, \dots and b_0, b_1, \dots are obtained $a_0e_0 = b_0d_0$.

Fig. 1 PID controller



$a_0e_1 + a_1e_0 = b_0d_1 + b_1d_0$ and so on

$$a_0e_{r-1} + a_1e_{r-2} + a_2e_{r-3} + \dots = b_0d_{r-1} + b_1d_{r-2} + b_2d_{r-3} + \dots$$

$$a_0e_r + a_1e_{r-1} + a_2e_{r-2} + \dots = b_1d_{r-1} + b_2d_{r-2} + b_3d_{r-3} + \dots$$

$$a_{n-1}e_r = b_nd_{r-1} \tag{7}$$

Step 4

The reduced order transfer function in z -domain $G_r(z)$ will be obtained by substituting $w = \frac{z-1}{z+1}$ in $G_r(w)$.

3 PID Controller Design

A PID controller $G_c(Z)$ is to be designed using the reduced order model $G_r(z)$ as shown in Fig. 1.

Algorithm for Design

- $G(z)$ is considered.
- The controller is to be designed using the reduced order system obtained by suggested method.
- Cascading the controller using initial values of parameters, the optimum values are to be obtained for the required response.
- Tune the controller till it meets the required specifications.

4 Example

Consider the original system given as [1]

$$G(z) = \frac{0.3124z^3 - 0.5743z^2 + 0.3879z - 0.0889}{z^4 - 3.233z^3 + 3.9869z^2 - 2.2209z + 0.4723} \quad \text{(Original)}$$

Application of Proposed Method

By applying bilinear transformation, $G(z)$ results in

$$G(w) = \frac{1.3635w^3 + 0.8569w^2 + 0.2417w + 0.0371}{10.913099w^4 + 4.135w^3 + 0.86w^2 + 0.0866w + 0.0053}$$

the values of d_0, d_1, e_0, e_1 and e_2 are obtained as:

$$e_0 = 0.4723; e_1 = 5.4086; e_2 = 43.0469; d_0 = 3.3061; d_1 = 5.3783.$$

The second order reduced transfer function using proposed method is:

$$G_2(z) = \frac{17.368994z - 4.1445}{48.927902z^2 - 85.149368z + 38.110672} \quad (\text{Proposed})$$

5 Comparison with Stability Equation Method

The model obtained by stability equation method of Prasad [1] is:

$$G_2^1(z) = \frac{0.2766z - 0.107634}{z^2 - 1.775663z + 0.802801} \quad (\text{Stability Equation Method})$$

The step responses are compared in Fig. 2.

Controller

The initial parameters:

$$K_P = -12.706436; K_I = 1.889206; K_D = 48.92790.$$

The tuned values obtained using the digital computer simulation are:

$$K_P = 0.3083353; K_I = 0.133160014; K_D = 1.37938845.$$

$G_{CH}(z)$ with the controller designed using the reduced order model is:

$$G_{CH}(z) = \frac{0.5688z^5 - 2.004z^4 + 2.899z^3 - 2.144z^2 + 0.8077z - 0.1226}{z^6 - 3.6542z^5 + 5.206z^4 - 3.309z^3 + 0.549z^2 + 0.3354z - 0.1226}$$

The closed loop step responses of $G(z)$ with PID and without PID are shown in Fig. 3.

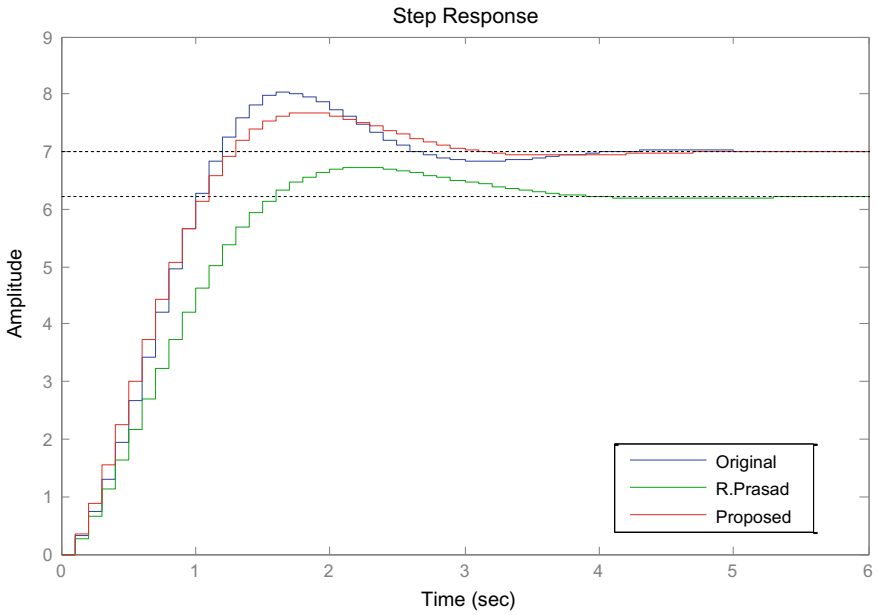


Fig. 2 Step responses of original system and reduced models

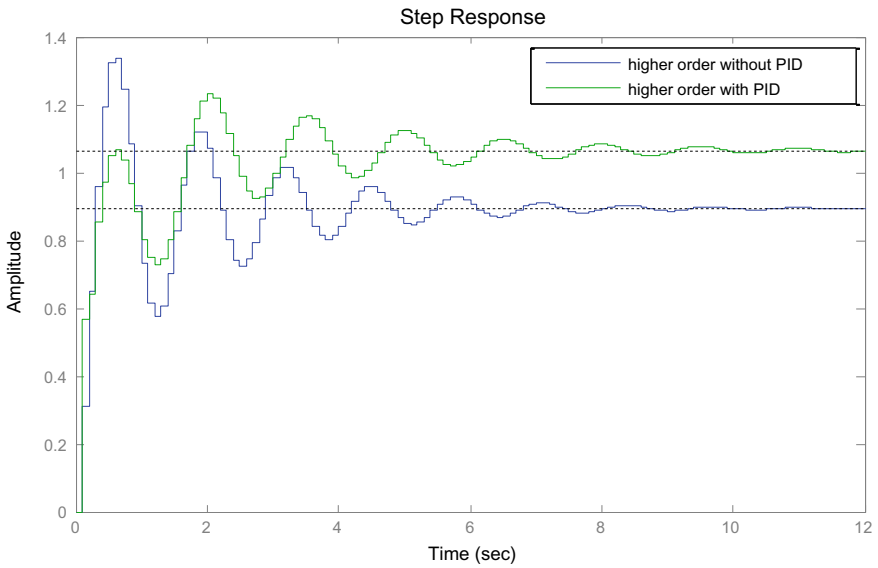


Fig. 3 Closed loop step responses of $G(z)$ with PID and without PID

6 Conclusions

A procedure is suggested for discrete system controller design, the proposed method uses polynomial differentiation technique and application of w -domain bilinear transformation for obtaining the low-order systems retaining the stability and other characteristics.

References

1. R. Prasad, Order reduction of discrete time systems using stability equation method and weighted time moments. *IE (I) J. EL* **74**, 94–98 (1993)
2. G.V.K.R. Sastry, G. Surya Kalyan, K. Tejeswara Rao, A new method for order reduction of high order multi variable systems using modified Routh approximation method. *Int. J. Control Theory Appl.* **9**(5) (2016)

A Fast Partitioning Strategy: Its Application to Fractal Image Coding



Utpal Nandi, Anudyuti Ghorai, Biswajit Laya,
and Moirangthem Marjit Singh

1 Introduction

In image compression technique [1, 2], images are represented in reduce form such that these take less space in memory and less time to transmit over the network. Currently a lossy image compression technique [1, 2] became very popular for its resolution independent feature and fast reconstruction process is fractal image compression (FIC) technique [1–3]. It is depended on local affine likeness of image. Fractal based coding was introduced by Barnsley [4] using iterated function system (IFS) [1, 2] and that was further automated by Jacquin [3] using partitioned IFS [1, 2]. The idea behind the technique is the resemblance of various parts of same image. At the beginning, an input image is divided into several non-overlapping blocks called range block and several overlapping blocks called domain blocks. The size of domain block is at least double than the range block. For every range, a searching is done to obtain best matching domain from domain list with lowest root means square error using contractive affine transformation of domain. If enough matching domain is not exist, the range is divided into more than one sub-range using any partitioning scheme and similar process is carried out on these. Otherwise, the best matching

U. Nandi (✉) · A. Ghorai · B. Laya
Department of Computer Science, Vidyasagar University, Midnapore, West Bengal, India
e-mail: nandi.3utpal@gmail.com

A. Ghorai
e-mail: anudyuti@outlook.com

B. Laya
e-mail: biswajitlaya007@gmail.com

M. M. Singh
Department of Computer Science and Engineering, North Eastern Regional Institute of Science and Technology, Nirjuli, Arunachal Pradesh, India
e-mail: marjitm@gmail.com

affine map is added to the compressed file. During decompression, reconstructed image is achieved by computing the fixed point of the image from its affine maps. One problem of FIC is its high encoding time. There are several strategies to reduce the encoding time of FIC like use of correlation coefficient [5, 6], domain space reduction using robust features [7, 8], kick-out strategies [9, 10], fast classification strategies [11, 12] and no search strategies [13, 14]. It is also clear that partitioning of range of FIC technique greatly affect the performance of compression. There are several partitioning schemes [2] already available. However, the existing schemes have few limitations. The different existing partitioning schemes with limitations of those are discussed in Sect. 2. It is noticed that the Horizontal Vertical (HV) partitioning scheme [3] offers comparatively better decoded image quality among all other studied schemes but very slow. To reduce this limitation, a new HV based fast partitioning scheme has been proposed in Sect. 3. The results of FIC with existing and proposed schemes are given and discussed in Sect. 4. The conclusive discussion is done in Sect. 5.

2 Related Works

There are several ways to partition a range block into multiple sub-blocks if the range has no enough similar domain. One such scheme is fixed size partition scheme [15]. Here, an image is divided into 4×4 range and 8×8 domain. These 4×4 ranges are not further divided into sub-ranges though ranges have not similar domain with tolerable root means square error. As a result, the qualities of reconstructed images are significantly reduced. The most popular partitioning scheme of FIC is quad-tree partitioning [2, 16, 17] where an image is represented in a tree structure. The original image block is first divided into four quadrants or sub images. Then again, each quadrant is divided into four quadrants and this process is continued until distance of the RMS value between ranges is lower than the previous selected threshold value or the tree level reaches the previously selected maximum level of the quad-tree. This scheme is content independent which leads poor quality decoded image. The adaptive version of quad-tree partitioning [17–20] is very efficient scheme since it uses context of range to split it into sub-ranges. Adaptive quad-tree partition first divides an image block into two horizontal parts according to successive differences of pixels sum value of rows of the image block. The horizontal part is further divided into two vertical portions according to successive differences of pixels sum. In this way the sub-image is divided into four-sub images that may not be same size. The process is repeated until divided sub images are either met the specified RMS tolerance or minimum range value greater than its size. In this scheme, an image block can share some self-similar structure. It produces better quality decoded images. However, it takes much more time than quad-tree partitioning. In quad-tree and adaptive quad-tree partition, if a range block has not enough similar domain, it is broken directly into 4 sub-range. However, there is a possibility of finding similar domain if it is

broken into 2 sub-ranges. Therefore, it is better to divide range block into 2 sub-ranges and if these sub-ranges have no similar domains, these can be further divided. This concept applied in HV scheme [2, 21]. In HV partitioning scheme, image blocks are partitions horizontally or vertically according to the splitting magnitude. At each level, all image blocks will be checked and it is decided which image blocks are further partitioned in horizontally or vertically. According to Fisher the HV partition can be done as follows.

Let R is range block of size $M \times N$ and P_{ij} is the pixel values in the block R where $0 \leq i < N$ and $0 \leq j < M$. Then $\sum_k R(k), l$ and $\sum_l R(k), l$ are the summation of pixel values in l th line and k th column respectively. The successive row differences and column differences are computed using Eqs. (1) and (2) respectively.

$$Hl = \frac{\min(l, M - l - 1)}{M - 1} \left(\sum_k P(k), l - \sum_k P(k), l + 1 \right) \tag{1}$$

$$Vk = \frac{\min(k, N - k - 1)}{N - 1} \left(\sum_l P(k), l - \sum_l P(k + 1), l \right) \tag{2}$$

Then, the maximum successive row differences and column differences are computed as $H(l) = \max(Hl: l = 1, 2, 3, \dots, M)$ and $V(k) = \max(Vk: k = 1, 2, 3, \dots, N)$ respectively. If $H(l) > V(k)$ then, then image block is partitioned horizontally using row number l . Otherwise, it is partitioned vertically using column number k . The HV scheme is very efficient and offers high-quality reconstructed images. However, the scheme is very slow compare to others explained and also has the chance of producing a sub-range whose dimension is less than the minimum range size. Two effective variants of HV partitioning are Fast Context Independent (FCI)-HV and Fast Low Context Independent (FLCD)-HV [22]. In FCI-HV scheme, range is divided into two sub-ranges if appropriate domain is not present in domain pool and the partition is done either horizontally or vertically. If horizontal column number is greater than the vertical row number then the range is divided into two vertical sub-ranges. Otherwise, it is divided into two horizontal sub-ranges. The FLCD-HV scheme is an alternative of FCI-HV scheme, where difference between middle vertical line pixel value and middle horizontal line pixel value is calculated. Let consider an $R \times C$ range with top left point (x, y) . Then, the pixel sum of evaluated difference between $(x + R/2)$ th and $(x + R/2 + 1)$ th horizontal line are calculated by using Eq. (3) and the sum of pixel value difference between $(y + C/2)$ th and $(y + C/2 + 1)$ th vertical line is calculated by using Eq. (4).

$$\text{Diffhm} = \left| \sum_{j=y}^{y+C} P\left(x + \frac{R}{2}, j\right) - \sum_{j=y}^{y+C} P\left(x + \frac{R}{2} + 1, j\right) \right| \tag{3}$$

$$\text{Diffvm} = \left| \sum_{i=x}^{x+R} P\left(i, y + \frac{C}{2}\right) - \sum_{j=y}^{y+C} P\left(i, y + \frac{C}{2} + 1\right) \right| \quad (4)$$

The range is divided into two sub-range horizontally if horizontal difference Diffhm is greater than vertical difference Diffvm and vertically otherwise. These two are faster than HV scheme but decoded images quality are comparatively poor than HV scheme.

3 The Proposed Partitioning Scheme

The HV scheme offers better decoded image quality among all other studied schemes. However, it computes all biased differences between each successive row and column to select the row or column to partition an image block. This process makes the partitioning scheme very slow and also has the chance of producing a sub-range whose dimension is less than the minimum range size. To reduce these limitations, a new HV based partitioning scheme has been proposed in this section and termed as fast HV partitioning (FHV) scheme. Consider an $R \times C$ range and minimum range block size as BMIN. We assume that R and C is multiplier of BMIN. This scheme partitions a range into two sub-ranges in such a way that sub-ranges row and column lengths are multiplier of minimum range block. First, the FHV scheme selects a row for horizontal partitioning of range block. To do so, it calculates the sum of pixel values $\text{RSum}(i \times \text{BMIN})$ of each row whose index is multiple of BMIN and corresponding next row $\text{RSum}(i \times \text{BMIN} + 1)$ for $1 \leq i \leq (R - \text{BMIN})/\text{BMIN}$ as given in Eqs. (5) and (6) respectively where $P(i, j)$ is the pixel of location (i, j) of the range block.

$$\text{RSum}(i \times \text{BMIN}) = \sum_{j=1}^R P(i \times \text{BMIN}, j) \quad (5)$$

$$\text{RSum}(i \times \text{BMIN} + 1) = \sum_{j=1}^R P(i \times \text{BMIN} + 1, j) \quad (6)$$

After that, the absolute difference between $\text{RSum}(i \times \text{BMIN})$ and $\text{RSum}(i \times \text{BMIN} + 1)$ are calculated for $1 \leq i \leq (R - \text{BMIN})/\text{BMIN}$ as given in Eq. (7).

$$\text{Rdiff}(i \times \text{BMIN}) = |\text{RSum}(i \times \text{BMIN}) - \text{RSum}(i \times \text{BMIN} + 1)| \quad (7)$$

The maximum horizontal difference $\text{MaxRdiff}(k \times \text{BMIN})$ among all calculated horizontal differences and its corresponding row number $k \times \text{BMIN}$ can be found by using Eq. (8).

$$\text{MaxRdiff}(k \times \text{BMIN}) = \text{MAX}_{i=1}^{\frac{(R-\text{BMIN})}{\text{BMIN}}} |\text{RSum}(i \times \text{BMIN}) - \text{RSum}(i \times \text{BMIN} + 1)| \quad (8)$$

Therefore, the $(k \times \text{BMIN})$ th row is selected for horizontal partitioning. In the next step, a column number is chosen for vertical partitioning of the range block. For this, the sum $\text{CSum}(j \times \text{BMIN})$ of each column is calculated whose index is multiple of BMIN and corresponding next column $\text{CSum}(j \times \text{BMIN} + 1)$ for $1 \leq j \leq (C - \text{BMIN})/\text{BMIN}$ as given in Eqs. (9) and (10) respectively.

$$\text{CSum}(j \times \text{BMIN}) = \sum_{i=1}^C P(i, j \times \text{BMIN}) \quad (9)$$

$$\text{CSum}(j \times \text{BMIN} + 1) = \sum_{i=1}^C P(i, j \times \text{BMIN} + 1) \quad (10)$$

Then, the absolute difference between $\text{CSum}(j \times \text{BMIN})$ and $\text{CSum}(j \times \text{BMIN} + 1)$ are found for $1 \leq j \leq (C - \text{BMIN})/\text{BMIN}$ as given in Eq. (11).

$$\text{Cdiff}(j \times \text{BMIN}) = |\text{CSum}(j \times \text{BMIN}) - \text{CSum}(j \times \text{BMIN} + 1)| \quad (11)$$

The maximum horizontal difference $\text{MaxRdiff}(k \times \text{BMIN})$ among all calculated horizontal differences and its corresponding row number $k \times \text{BMIN}$ can be found by using Eq. (12).

$$\text{MaxCdiff}(m \times \text{BMIN}) = \text{MAX}_{j=1}^{\frac{(C-\text{BMIN})}{\text{BMIN}}} |\text{CSum}(j \times \text{BMIN}) - \text{CSum}(j \times \text{BMIN} + 1)| \quad (12)$$

Therefore, the $(m \times \text{BMIN})$ th column is selected for vertical partitioning. Now, the maximum horizontal difference $\text{MaxRdiff}(k \times \text{BMIN})$ and maximum vertical difference $\text{MaxCdiff}(m \times \text{BMIN})$ are compared. If maximum horizontal difference $\text{MaxRdiff}(k \times \text{BMIN})$ is greater than maximum vertical difference $\text{MaxCdiff}(m \times \text{BMIN})$, then the range is divided horizontally into two sub-ranges using row number $k \times \text{BMIN}$. Otherwise, the range is divided vertically using column number $m \times \text{BMIN}$.

3.1 Example

Consider an 8×8 range as shown in Fig. 1 and minimum range size $\text{BMIN} = 2$.

The pixel sum of row 2, i.e., $\text{RSum}(2)$ and next row $\text{RSum}(3)$ are 1615 and 1505 respectively. The absolute difference between $\text{RSum}(2)$ and $\text{RSum}(3)$ is $|1615 - 1505| = 110$. Similarly, the absolute difference between $\text{RSum}(4)$ and $\text{RSum}(5)$ is

Fig. 1 An 8×8 range

205	250	210	220	100	140	160	130
110	110	230	220	230	240	245	230
140	200	150	240	240	220	100	215
245	130	145	170	190	210	140	250
160	170	190	110	130	220	250	170
230	220	155	170	210	240	215	230
210	200	240	150	170	190	180	200
250	140	170	230	220	120	90	230

$|1480 - 1400| = 80$ and the absolute difference between $RSum(6)$ and $RSum(7)$ is $|1670 - 1540| = 130$. Therefore, the maximum horizontal pixel difference is 130 and corresponding row number 6 is selected for horizontal partitioning.

The pixel sum of column 2, i.e., $Csum(2)$ and next row $Csum(3)$ are 1420 and 1490 respectively. The absolute difference between $Csum(2)$ and $Csum(3)$ is $|1420 - 1490| = 70$. Similarly, the absolute difference between $Csum(4)$ and $Csum(5)$ is $|1510 - 1490| = 20$ and the absolute difference between $Csum(6)$ and $Csum(7)$ is $|1580 - 1380| = 200$. Therefore, the maximum vertical pixel difference is 200 and corresponding column number 6 is selected for vertical partitioning. Here, the maximum column difference is 200 that is greater than maximum row difference 130. Therefore, the partitioning of range is done vertically using column 6 as shown in Fig. 2 to create two sub-ranges of size 8×6 and 8×2 .

4 Results and Analysis

Standard 256×256 grayscale images LISAW, MOUSE, CHEETA, ROSE and CLOWN [1] have been used to continue our experiments. These files are nonformatted gray scale image. We have executed fractal image compression and decompression processes with different partitioning schemes—quad-tree [16], HV [21], FCI-HV [22], FLCD-HV [22] and proposed FHV. The classification scheme applied for these experiments is fisher’s classification [2]. The compression times in seconds are measured for all the examined partitioning schemes and kept in Table 1. In respect of compression time, the proposed FHV is faster than HV, FCI-HV, FLCD-HV schemes. On average the proposed FHV is 2.97 times faster than HV scheme since there is no biasing function of the expression that determine the partitioning line and the absolute differences of all successive rows and columns are not obtained

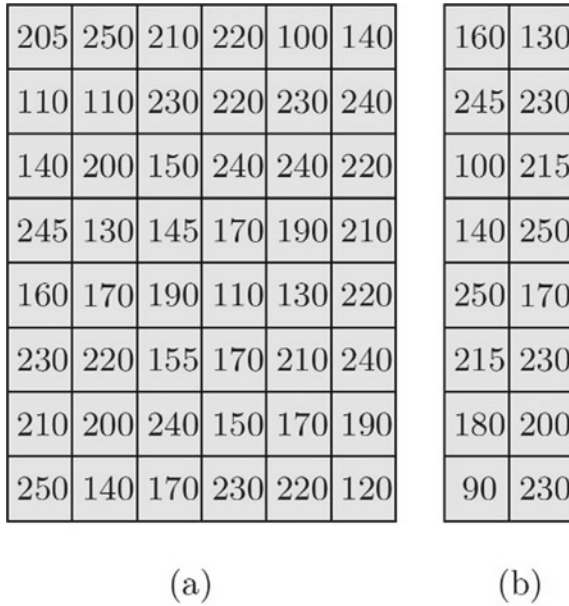


Fig. 2 The 8×8 range partitioned into two **a** 8×6 and **b** 8×2 sub-ranges

Table 1 Compression times (in second) of images for five different partitioning schemes

File name	Quadtree	HV	FCI-HV	FLCD-HV	FHV
LISAW	2.83	14.33	4.83	6.00	4.50
ROSE	2.17	9.00	3.17	4.67	3.00
MOUSE	2.50	11.00	4.17	5.67	4.00
CLOWN	3.17	15.17	5.33	6.83	5.17
CHEETA	2.33	10.33	3.83	5.17	3.50
Average	2.60	11.97	4.27	5.67	4.03
Standard deviation	0.40	2.66	0.85	0.82	0.84

in proposed FHV scheme. However, the quad-tree scheme takes much less time to encode than proposed FHV simply because it is context independent.

The fractal compressed images are decoded before use. The decoded image quality is measured using PSNR (Eq. 13). The PSNRs in dB of five decoded images for all are given in Table 2. The average PSNR of proposed FHV is significant than quad-tree, FCI-HV, FLCD-HV partitioning schemes and very close with HV scheme. The original and decoded LISAW using proposed strategy is shown in Fig. 3.

$$PSNR = 20 \log_{10} \left(\frac{255}{RMS} \right) DB \tag{13}$$

Table 2 PSNR of images for five different partitioning schemes

File name	Quadtree	HV	FCI-HV	FLCD-HV	FHV
LISAW	38.96	41.73	39.04	39.62	40.17
ROSE	29.05	33.73	29.56	29.77	33.21
MOUSE	38.19	41.17	38.92	38.98	40.36
CLOWN	29.25	34.28	30.30	30.59	33.94
CHEETA	27.57	30.52	28.29	28.26	29.91
Average	32.60	36.29	33.22	33.44	35.52
Standard deviation	5.50	4.93	5.31	5.42	4.59

**Fig. 3** **a** Original image and **b** decoded image FIC using proposed FHV

The percentage of space saving (Eq. 14) and compression ratio (Eq. 15) of all the examined schemes are kept in Tables 3 and 4 respectively. The average space saving in percentage of the proposed FHV scheme is significantly higher than the other schemes except HV. As a result, the average compression ratio is quite better than quad-tree, FCI-HV, FLCD-HV partitioning schemes and very close with HV scheme

Table 3 Space saving in percentage of images for five different partitioning schemes

File name	Quadtree	HV	FCI-HV	FLCD-HV	FHV
LISAW	82.60	85.04	83.16	83.19	84.93
ROSE	87.46	90.68	88.68	88.44	90.18
MOUSE	85.88	88.74	86.33	86.58	88.71
CLOWN	82.83	84.34	82.91	83.13	83.97
CHEETA	82.57	83.92	82.98	83.20	83.87
Average	84.27	86.54	84.81	84.91	86.33
Standard deviation	2.26	3.00	2.6	2.46	2.92

Table 4 Compression ratio in percentage for five different partitioning schemes

File name	Quadtree	HV	FCI-HV	FLCD-HV	FHV
LISAW	1.39	1.20	1.35	1.35	1.21
ROSE	1.00	0.75	0.91	0.93	0.79
MOUSE	1.13	0.90	1.09	1.07	0.90
CLOWN	1.37	1.25	1.37	1.35	1.28
CHEETA	1.40	1.29	1.36	1.34	1.29
Average	1.26	1.08	1.22	1.21	1.09
Standard deviation	0.18	0.24	0.21	0.20	0.23

$$\text{Space saving} = \left(1 - \frac{\text{Compressed image size}}{\text{Original file size}} \right) \times 100\% \tag{14}$$

$$\text{Compression ratio} = \frac{\text{Compressed image size in bits}}{\text{Original image size in byte}} \text{bpp} \tag{15}$$

The quality factor is used in FIC program as tolerated error between a range block and its selected domain block. It ranges from 1 to 15 where high quality factor means low image fidelity. The default value has been chosen as 1. The comparison of compression times (Fig. 4a), PSNRs (Fig. 4b), percentage of space savings (Fig. 4c) and compression ratios (Fig. 4d) with increasing quality factor for LISAW image are represented graphically. It is noticed that the compression times and PSNRs gradually drop with higher quality factors for all examined strategies of FIC techniques. It is also observed that percentage of space savings increases with increasing quality factors for these schemes and high-quality factor results in better compression ratios.

5 Conclusion

In this paper, a partitioning scheme (FHV) for FIC has been proposed that is based on HV scheme. The proposed scheme avoids the calculations of all biased differences between each successive row and column associated with HV scheme to select the row or column to partition an image block to accelerate encoding method. The strategy also eliminates the chance of producing a sub-range whose dimension is less than the minimum range size. The proposed FHV is 2.97 times faster than it. However, the decoded image quality is not as good as given by HV but very close with it.

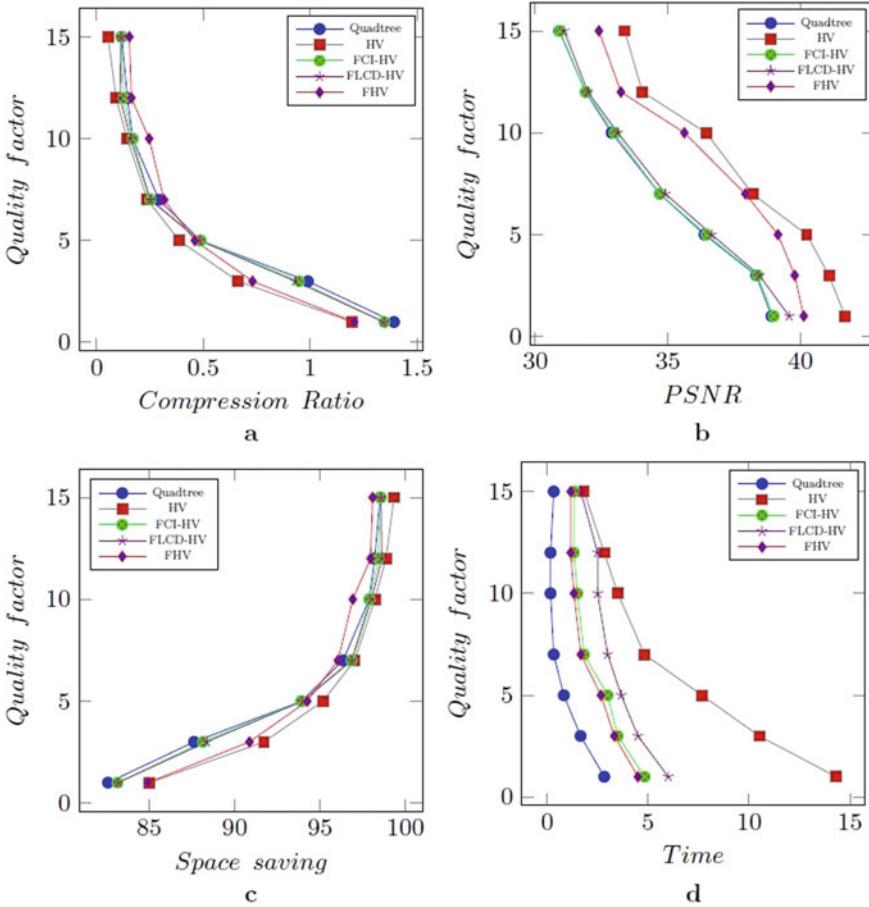


Fig. 4 Comparison among between Quadtree, HV, FCI-HV, FLCD-HV and proposed FHV schemes in different parameters over LISAW image. **a** Comparison of compression ratio with increasing quality factor. **b** Comparison PSNR with increasing quality factor. **c** Comparison of space saving in percentage with increasing quality factor. **d** Comparison of compression times with increasing quality factor

Acknowledgements The work is done by using infrastructure of the Dept. of Computer Science, Vidyasagar University, Paschim Medinipur, West Bengal, India.

References

1. M. Nelson, *The Data Compression Book*, 2nd edn. (India, BPB Publications, 2008)
2. Y. Fisher, *Fractal Image Compression: Theory and Application* (Springer Verlag, New York, 1995)

3. A.E. Jacquin, Image coding based on a fractal theory of iterated contractive image transformations. *IEEE Trans. Image Process.* **1**(1), 18–30 (1992)
4. M.F. Barnsley, *Fractals Everywhere*, 2nd edn. (Academic Press, 1993)
5. J. Wang, N. Zheng, A novel fractal image compression scheme with block classification and sorting based on Pearson's correlation coefficient. *IEEE Trans. Image Process.* **22**, 3690–3702 (2013)
6. J. Wang, P. Chen, B. Xi, J. Liu, Y. Zhang, S. Yu, Fast sparse fractal image compression. *PLoS One* **12**(9) (2017)
7. W.R. Schwartz, H. Pedrini, Improved fractal image compression based on robust feature descriptors. *Int. J. Image Graph.* **11**(04), 571–587 (2011)
8. Y.-M. Zhou, C. Zhang, Z.-K. Zhang, An efficient fractal image coding algorithm using unified feature and DCT. *Chaos Solitons Fract.* **12**(4), 1823–1830 (1995)
9. C.-M. Lai, K.-M. Lam, W.-C. Siu, A fast fractal image coding based on kick-out and zero contrast conditions. *IEEE Trans. Image Process.* **12**(11), 1398–1403 (2003)
10. H.N. Chen, K.L. Chung, J.E. Hung, Novel fractal image encoding algorithm using normalized one-norm and kick-out condition. *Image Vis. Comput.* **28**(3), 518–525 (2010)
11. R. Distasi, M. Nappi, D. Riccio, A range/domain approximation error-based approach for fractal image compression. *IEEE Trans. Image Process.* **15**, 89–97 (2006)
12. T. Kovács, A fast classification based method for fractal image encoding. *Image Vis. Comput.* **26**(8), 1129–1136 (2008)
13. R. Gupta, D. Mehrotra, R.K. Tyagi, Adaptive searchless fractal image compression in DCT domain. *Imaging Sci. J.* **64**(7), 374–380 (2016)
14. X.-Y. Wang, Y.-X. Wang, J.-J. Yun, An improved no-search fractal image coding method based on a fitting plane. *Image Vis. Comput.* **28**(8), 1303–1308 (2010)
15. S.K. Roy, S.K. Bandyopadhyay, D. Bhattacharyya, T.-H. Kim, Statistical analysis of fractal image coding and fixed size partitioning scheme. *Glob. J. Comput. Sci. Technol.* (2015)
16. Y. Fisher, Fractal image compression with quadtrees, in *Fractal Image Compression* (Springer, 1995), pp. 55–77
17. U. Nandi, S. Santra, J.K. Mandal, S. Nandi, Fractal image compression with quadtree partitioning and a new fast classification strategy, in *Proceedings of the 2015 Third International Conference on Computer, Communication, Control and Information Technology (C3IT)* (IEEE, 2015), pp. 1–4
18. U. Nandi, J.K. Mandal, Fractal image compression with adaptive quadtree partitioning and lossless encoding on the parameters of affine transformations, in *Information Systems Design and Intelligent Applications* (Springer, 2015), pp. 73–83
19. U. Nandi, J.K. Mandal, Efficiency of adaptive fractal image compression with archetype classification and its modifications. *Int. J. Comput. Appl.* **38**(2–3), 156–163 (2016)
20. U. Nandi, J.K. Mandal, Fractal image compression with adaptive quadtree partitioning scheme, in *International Conference on Signal, Image Processing and Pattern Recognition (SIPP-2013)*, Bangalore, India (2013), pp. 289–296
21. Y. Fisher, S. Menlove, Fractal encoding with HV partitions, in *Fractal Image Compression* (Springer, 1995), pp. 119–136
22. U. Nandi, J. Mandal, Fractal image compression using fast context independent HV partitioning scheme, in *2012 International Symposium on Electronic System Design (ISED)* (IEEE, 2012), pp. 306–308

Analysis of Received Signal Strength Based on User Position Locating by Using ML Methods



L. Sathish, Y. Satya Bhuvanewari, B. Satya Sri Devi, and Durgesh Nandan

1 Introduction

Nowadays, research is going on in different ways on user position tracking using 5G technologies. GPS is used to locate wide places and long-distance but in small places like inside the buildings, shops, malls, etc. GPS is not going to locate user position exactly. Using fifth generation (5G) technologies to track the user position based on received signal strength (RSS) here using some type of ML methods applied to the RSS [16], we get the exact position of the user due to heavy usage of networks, base station can receive massive inputs and massive outputs (MIMO) [17, 18] from the antennas our ML algorithm can train in RSS near antennas when the signal is received then the trained machine learning algorithm can able predict the user position, but here the major problem is given trained examples to the ML is noiseless, but received signals has mixed with noise so it is not possible to get exact position, it shows two sigma errors by using conventional Gaussian progression (CGP) [12, 15, 27]. For reducing high expenses here is a chance to use a single antenna [16, 32] to reduce all effects and for increasing the more efficient method we are using numerical approximation GP [6] (NAGP) methods. In this paper, an investigation of

L. Sathish · Y. S. Bhuvanewari · B. S. S. Devi
Department of Electronics and Communication Engineering, Aditya Engineering College,
Surampalem, India
e-mail: lellsathish490@gmail.com

Y. S. Bhuvanewari
e-mail: yelubandibhuvana@gmail.com

B. S. S. Devi
e-mail: sridevi_baddireddy@aec.edu.in

D. Nandan (✉)
Accendere Knowledge Management Services Pvt. Ltd., CL Educate Ltd., New Delhi, India
e-mail: durgeshnandano51@gmail.com

user position in distributed massive MIMO on RSS-based using machine learning techniques is done in Sect. 2. Reported literature has been explored further in Sect. 3. Reported methodology and machine learning techniques details are described in Sects. 4 and 5. Investigates the examinations of results in segment 6.

2 Literature

Exact position of the user due to heavy usage of networks, base station can receive massive inputs and massive outputs (MIMO) [17, 18] from the antennas our ML algorithm can train in RSS near antennas when the signal is received then the trained machine learning algorithm can able predict the user's position. In this, the given data to RSS is data is noise-free but the original data is noise data so that we get the 2σ bar errors to eliminate that 2 bar errors [12] here we are using numerical approximation Gaussian progression method (NAGP) [15]. The normal yield is [27] to get such execution gain, DM-MIMO frameworks can manufacture proficient utilization of spatial assets using disseminated receiving wires, which it takes the significant expense to create. The receiving wire radiation examples are frequently ignored, yet they can unequivocally influence the presentation of the RSS-based extending [32]. An approach to precisely appraise the RSS balance of a hub is to join a sign generator to the connector of the outside reception apparatus, and transmit a sign with known power. The paper demonstrates the precision with which remote sensor systems can evaluate the relative sensor [16] areas. Sensor area estimation with around 1 m RMS blunder has been shown utilizing TOA estimations. To limit all effects and for increasing more environment-friendly technique, we are the use of numerical approximation GP [6] (NAGP) methods. The authors proposed a novel algorithm for the client limitation in the EM focal point centering enormous MIMO contraption dependent on the estimation of the AOA [5, 9, 24]. For blended data of time delay, angel of deviation (AOD) and angel of appearance (AOA) data is utilized in [7] for situating clients in enormous MIMO. A millimeter-wave enormous MIMO framework is acknowledged [23] to determine the fundamental conditions under a client area that can be anticipated from AOD, AOA, and TOA data on account of viewable pathway conditions. Here, talk about potential answers for situating of portable stations utilizing a vector of the sign at the base station, furnished with numerous reception apparatuses circulated over arrangement zone. To get a place of client [20] in remote systems may empower numerous applications, for example, self-sufficient driving and crisis administrations, geographic steering. Surmised area data of the region, storing, and workforce following under crisis calls. Satellite-based worldwide situating frameworks (GPSs) [13], which are at present being utilized in LTE to secure area data, do not give solid area appraisals to indoor and clients. The utilization of a huge overabundance of base station [12] reception apparatuses contrasted and the number of terminals that are being served grants the most straightforward kind of pre-coding on the forward connection and handling on the turnaround connection. In the utmost of an infinite number of radio wires, a multi-cell examination,

which unequivocally represents the pilot overhead and channel estimation blunder, is exceedingly straightforward [20]. It provides little 2 blunder bars on the area gauges. And another one is to address this we want to implement a position matching-based GP method, which is NAGP to track the user from their RSS. NAGP is showing 2 blunder bars [4]. Time of arrival (TOA) methods, to reduce the time to transfer data between base to sensors is complicated and expensive. The angle of arrival (AOA) has many antennas to utilize every sensor [25]. RSS methods are path loss exponent which is used to predict the distance between the base and source by using received signal strength [1, 19, 31]. Gaussian process regression is used because it has provided a more accurate way to predict the user location from the RSS, in this model, it shows high accuracy to predict the user position [29]. It mainly focuses on the source user connectivity, wherein users have to balance the figuring cost of predicting their place [10, 22, 30]. Finally, some AOA-based Wi-Fi positioning systems are can be used to connect the base to source that is it can operate on the uplink, but some cases combining multiple antennas at the base station. Those techniques are bad for single receiving wire beneficiary frameworks with the goal that appropriated MIMO frameworks considered [8, 11, 21]. GP techniques are utilized for users locating the user area in remote systems we saw that a significant number of the past works have done in a circuitous method for approach, however, in the GP models area estimate as information and RSS as gave in the yield. The authors [3, 11] proposed a minute coordinating-based GP model for numerous means prediction in the examination of time series, framework acknowledgment, and channel prediction at once, it is not sufficient for user location in MIMO [14]. System identification through online sparse. The subsequent inadequate online boisterous input GP it is more precise than comparative existing regression algorithms [2]. Spatial remote channel prediction under the area. The effect of area vulnerability during getting the hang of/preparing and prediction/testing the divert parameters and in foreseeing can learn and anticipate the remote channel [28]. Radar, a radio frequency (RF)-based framework for finding and following clients inside structures radar works inside structures. Radar works by recording and preparing signal quality at numerous base stations situated to give covering inclusion [26]. CSI-based fingerprinting for indoor localization deep learning utilized to train all the weights of a deep network as fingerprints, moreover, a greedy learning algorithm is used to train the weights layer to reduce complexity [22]. A convolution neural system utilized in picture acknowledgment and handling that is explicitly intended for preparing that is explicitly intended to the procedure to pixel information [30]. Cluster assault would users be able to can typically rely on a GPS signal for the precise area yet inside GPS frequently blurs thus up to this point, mostly to reinforce limit and inclusion MIMO [10]. Spot-fi uses data that is now uncovered by Wi-Fi chips and it does not require equipment or firmware changes, accomplishes a similar precision as cutting-edge confinement framework [18]. Avoiding multipath to revive in building Wi-Fi localization RF-based user location and tracking system, user expect the phone to continue syncing with an email server to new messages.

3 Methodology

User's system component (USC).

Remote radio station (RRB).

Data base system (DBS).

Uplink transmission (UT).

Fronthaul link.

Here, we are considering a distributed multiple users massive MIMO setup. MIMO, whereas the user's system component (USC) transmits an uplink signal to the remote radio station (RRB), similarly on the same time–frequency source. For make, this easily understands here we expect that RRBs are in single-radio wire units and allude to them replaceable as base station reception apparatuses. We likewise expect that all USC's are single unit reception apparatuses and allude to the clients. The RRBs are associated with a client's framework part (USC) through rapid fronthaul. At the point when the clients transmit on the uplink, each RRH records its remote radio broadcast (RRH). The USC accumulates the RSS from each RRH, forms them to extricate the per-client RSS, and structures an $M \times 1$ RSS vector for every client. The RSS vectors in this manner framed are sustained as a contribution to a trained ML model for foreseeing the client areas. The USC has the ML model and handles the calculations required for preparing and prediction. Here, a distributed multiple user massive MIMO equipment, as per the below block diagram, here all the USC, receives the signal of the user and that signal is transmitted to the RRS, similarly on the same time–frequency (TF).

3.1 Machine Learning Techniques

Typically, running-based strategies, for example, [25, 32] are utilized, signal data which is restricted by a solitary source that is TOA, AOA, and RSS recorded at various sensors. TOA-based techniques, for example, [4], time synchronization among sensors and sources are costly and confused. AOA-based techniques, in this strategy, it requires different reception apparatuses to create a signal at every sensor. RSS-based techniques, for example, [25], assume the way misfortune and gauge the separation between source positions. In this estimation procedure, different grid reversals are included, which can frequently bring about numerical clamor because the frameworks to be upset have low condition number. Besides, we see that there are no present works that stretch out the above techniques to multisource frameworks, for example, huge MIMO, working in multi-slant way misfortune areas. The primary test here that it can deal with multi-client impedance for restriction, the managed AI is effective to situate different sources one after another from their RSS. In contrast to the above works, thusly gauge the source areas straightforwardly from their RSS

via preparing information and building a non-direct relapse model or calculation. Some kind of AI systems like k-closest neighbors (KNN) [28], GP strategies [20], and profound learning techniques [22, 26], have been investigated for remote client situating. From these systems, we pick GP strategies for our examination for four reasons, as expressed beneath. Limitation strategies proposed for Wi-Fi frameworks, for example, in [2, 3, 8, 11, 14, 21, 22, 28] and do not delay in a straight-ahead way too monstrous MIMO framework. Most RSS-based Wi-Fi localization strategies [11, 29, 31] focal point on the downlink, then through this, the user can estimate their very own location. Our work is not quite the same as the above in three different ways. Right off the bat, the above works adopt a roundabout demonstrating strategy, wherein every client prepares at any rate one GP model for each base station. Such a preparation approach is not appropriate for gigantic MIMO. Because, we work with an enormous number of Base station (BS) radio wires and along these lines, every client is required to prepare countless GP models. Scarcely any past works have contemplated boisterous contributions to GP. The creators in [2, 6, 14] propose minute coordinating-based GP strategies for multi-step expectation in time arrangement examination, framework recognition and channel forecast individually, yet not for client situating in huge MIMO.

1	In this, model is trained with noise-free data
2	By using GP regression to predict the user's location
3	By using the GP method to remove 2-sigma blender bars
4	An efficient way to locate the user's position

4 Result

In this paper, we talked about though, limitation centers around the uplink and at the base station it can evaluate the client areas. In this procedure, I pick the Gaussian movement relapse from some sort of other AI systems like k-closest neighbors (KNN) [28] and profound learning strategies [18, 22] have been investigated for remote client situating. There are four motivations to pick the Gaussian movement as expressed in the above AI strategies. From the start, CGP is utilized to evaluate the client area however in the outcome, it indicates 2σ bar blunders to survive or eliminate this mistakes utilizing NAGP it takes out the 2σ bar mistakes and finds the client's area along these lines gauge the client area legitimately from their RSS via preparing information and building a non-straight relapse model or calculation. At whatever point the restriction centers around the attention on the downlink, at that point through this, the client can gauge their area. These strategies do not function admirably for single-radio wire collector frameworks, for example, the conveyed MIMO framework considered in our work (Table 1).

Table 1 Simulation parameters as per [18]

Simulation limits	Estimate
Path loss limits (3GPPUMi [1])	$d_0 = 10 \text{ m} - 10 = 47.5 \text{ dB}$
USC transmit power	21 dbm
Power of noise	-107.5 dbm
Sensitivity at receiver	-106.5 dbm

5 Conclusion

In this paper a managed AI way discussed to deal with gauge client areas from their uplink got signal quality (RSS) information in a circulated monstrous various info different yield (MIMO) framework. The given preparing information to the ML is sans clamor information RSS and loud RSS for test reason. According to the ML task, the two Gaussian procedure relapse (GP) techniques, the AI undertaking are applied, they are traditional GP (CGP) strategy and the occasion coordinating-based numerical guess GP (NAGP) technique. Right off the bat, applied identified that the CGP technique gives ridiculously little 2σ mistake bars on the evaluated areas since the preparation information is without commotion RSS. To beat these mistakes, utilizing the NAGP technique since it gains from the measurable properties of the commotion in the test RSS.

References

1. M.S. Anwar, F. Hossain, N. Mehajabin, M. Mamun-Or-Rashid, M.A. Razzaque, A comparative study on Gaussian process regression-based indoor positioning systems, in *2018 International Conference on Innovation in Engineering and Technology (ICIET)* (IEEE, 2018), pp. 1–5
2. P. Bahl, V.N. Padmanabhan, Radar: an in-building RF-based user location and tracking system, in *Proceedings IEEE INFOCOM 2000. Conference on Computer Communications. Nineteenth Annual Joint Conference of the IEEE Computer and Communications Societies (Cat. No. 00CH37064)*, vol. 2 (IEEE, 2000), pp. 775–784
3. H. Bijl, T.B. Schön, J.W. van Wingerden, M. Verhaegen, System identification through online sparse Gaussian process regression with input noise. *IFAC J. Syst. Control* **2**, 1–11 (2017)
4. Y.T. Chan, K. Ho, A simple and efficient estimator for hyperbolic location. *IEEE Trans. Signal Process.* **42**(8), 1905–1915 (1994)
5. N. Garcia, H. Wymeersch, E.G. Larsson, A.M. Haimovich, M. Coulon, Direct localization for massive MIMO. *IEEE Trans. Signal Process.* **65**(10), 2475–2487 (2017)
6. A. Girard, C.E. Rasmussen, J.Q. Candela, R. Murray-Smith, Gaussian process priors with uncertain inputs application to multiple-step ahead time series forecasting. *Adv. Neural Inf. Process. Syst.* 545–552 (2003)
7. A. Guerra, F. Guidi, D. Dardari, Position and orientation error bound for wideband massive antenna arrays, in *2015 IEEE International Conference on Communication Workshop (ICCW)* (IEEE, 2015), pp. 853–858
8. B.F.D. Hähnel, D. Fox, Gaussian processes for signal strength-based location estimation, in *Proceeding of Robotics: Science and Systems* (2006)

9. A. Hu, T. Lv, H. Gao, Z. Zhang, S. Yang, An esprit-based approach for 2-D localization of incoherently distributed sources in massive MIMO systems. *IEEE J. Sel. Top. Signal Process.* **8**(5), 996–1011 (2014)
10. M. Kotaru, K. Joshi, D. Bharadia, S. Katti, Spotfi: decimeter level localization using WiFi, in *Proceedings of the 2015 ACM Conference on Special Interest Group on Data Communication* (2015), pp. 269–282
11. S. Kumar, R.M. Hegde, N. Trigoni, Gaussian process regression for fingerprinting based localization. *Ad Hoc Netw.* **51**, 1–10 (2016)
12. T.L. Marzetta, Noncooperative cellular wireless with unlimited numbers of base station antennas. *IEEE Trans. Wireless Commun.* **9**(11), 3590–3600 (2010)
13. S.G. Mohinder, R.W. Lawrence, P.A. Angus, *Global Positioning Systems, Inertial Navigation, and Integration* (Wiley, 2001), pp. 9–29
14. L.S. Muppirisetty, T. Svensson, H. Wymeersch, Spatial wireless channel prediction under location uncertainty. *IEEE Trans. Wireless Commun.* **15**(2), 1031–1044 (2015)
15. H.Q. Ngo, A. Ashikhmin, H. Yang, E.G. Larsson, T.L. Marzetta, Cell-free massive MIMO versus small cells. *IEEE Trans. Wireless Commun.* **16**(3), 1834–1850 (2017)
16. N. Patwari, A.O. Hero, M. Perkins, N.S. Correal, R.J. O’dea, Relative location estimation in wireless sensor networks. *IEEE Trans. Signal Process.* **51**(8), 2137–2148 (2003)
17. K.S.V. Prasad, E. Hossain, V.K. Bhargava, Energy efficiency in massive MIMO-based 5G networks: opportunities and challenges. *IEEE Wirel. Commun.* **24**(3), 86–94 (2017)
18. K.S.V. Prasad, E. Hossain, V.K. Bhargava, Machine learning methods for RSS-based user positioning in distributed massive MIMO. *IEEE Trans. Wireless Commun.* **17**(12), 8402–8417 (2018)
19. B. Roberts, K. Pahlavan, Site-specific RSS signature modeling for WiFi localization, in *GLOBECOM 2009–2009 IEEE Global Telecommunications Conference* (IEEE, 2009), pp. 1–6
20. V. Savic, E.G. Larsson, Fingerprinting-based positioning in distributed massive MIMO systems, in *2015 IEEE 82nd Vehicular Technology Conference (VTC2015Fall)* (IEEE, 2015), pp. 1–5
21. A. Schwaighofer, M. Grigoras, V. Tresp, C. Hoffmann, GPPS: a Gaussian process positioning system for cellular networks. *Adv. Neural Inf. Process. Syst.* 579–586 (2004)
22. S. Sen, J. Lee, K.H. Kim, P. Congdon, Avoiding multipath to revive in building WiFi localization, in *Proceeding of the 11th Annual International Conference on Mobile Systems, Applications, and Services* (2013), pp. 249–262
23. A. Shahmansoori, G.E. Garcia, G. Destino, G. Seco-Granados, H. Wymeersch, 5G position and orientation estimation through millimeter wave MIMO, in *2015 IEEE Globecom Workshops (GC Wkshps)* (IEEE, 2015), pp. 1–6
24. S.A. Shaikh, A.M. Tonello, Localization based on angle of arrival in EM lens-focusing massive MIMO, in *2016 IEEE 6th International Conference on Consumer Electronics-Berlin (ICCE-Berlin)* (IEEE, 2016), pp. 124–128
25. H.C. So, L. Lin, Linear least squares approach for accurate received signal strength-based source localization. *IEEE Trans. Signal Process.* **59**(8), 4035–4040 (2011)
26. J. Vieira, E. Leitinger, M. Sarajlic, X. Li, F. Tufvesson, Deep convolutional neural networks for massive MIMO fingerprint-based positioning, in *2017 IEEE 28th Annual International Symposium on Personal, Indoor, and Mobile Radio Communications (PIMRC)* (IEEE, 2017), pp. 1–6
27. J. Wang, L. Dai, Asymptotic rate analysis of downlink multi-user systems with co-located and distributed antennas. *IEEE Trans. Wireless Commun.* **14**(6), 3046–3058 (2015)
28. X. Wang, L. Gao, S. Mao, S. Pandey, CSI-based fingerprinting for indoor localization: a deep learning approach. *IEEE Trans. Veh. Technol.* **66**(1), 763–776 (2016)
29. Y. Wen, X. Tian, X. Wang, S. Lu, Fundamental limits of RSS fingerprinting based indoor localization, in *2015 IEEE Conference on Computer Communications (INFOCOM)* (IEEE, 2015), pp. 2479–2487
30. J. Xiong, K. Jamieson, Arraytrack: a fine-grained indoor location system, in *10th USENIX Symposium on Networked Systems Design and Implementation (NSDI 13)* (2013), pp. 71–84

31. S. Yiu, K. Yang, Gaussian process assisted fingerprinting localization. *IEEE Internet Things J.* **3**(5), 683–690 (2015)
32. A. Zanella, Best practice in RSS measurements and ranging. *IEEE Commun. Surv. Tutor.* **18**(4), 2662–2686 (2016)

Analysis of Quadcopter Technology as an Emergency Service



Prasanthi Magapu, Sarthika Danthuluri, Vidheya Raju Boni,
and Durgesh Nandan

1 Introduction

Just as the cell phone-enabled creating nations to jump more established advances for individual correspondence, the automaton can jump the conventional transportation framework [1]. Late advancements have happened aimlessly in hardware, programming, and frameworks. With the rise of intelligence, technology has been rapidly increasing. As the growth of the population is increasing people are tending to use their transportation instead of public transportation. This, in turn, increases the *probability* of occurrence of accidents. Innovations like usage of the drone to solve today's world problems are flourishing. A drone is an automatic flying machine which does not need humans to drive it. Furthermore, lithium batteries are rapidly improving so machines can fly further on a charge. It is used for many purposes like in photography, journalism, military, and medical purposes too. Robot programming can use mobile phone or tablet applications for the following and course. Besides, drones have proved their best in times of natural disasters. In certain circumstances, Unmanned Aerial Vehicle's are designed to access the location of the sufferer and to deliver aid. This

P. Magapu (✉) · S. Danthuluri · V. R. Boni
Department of Electronics and Communication Engineering, Aditya Engineering College,
Surampalem, Andhra Pradesh, India
e-mail: prashanthimagapu7@gmail.com

S. Danthuluri
e-mail: dssarthika@gmail.com

V. R. Boni
e-mail: vidheyaraju.b@aec.edu.in

D. Nandan
Accendere Knowledge Management Services Pvt. Ltd., New Delhi, India
e-mail: durgeshnandano51@gmail.com

paper is about the usage of drones in real-time medical usage. There are many functions of using the drone. It is all things considered agreed that machines are devices that are prepared for bolstered flight, which don't have a human prepared, and are under satisfactory control to perform supportive limits. Among all, the predominant function of using a drone is to deliver small items in urgency. Due to the simplicity of construction and control, we make use of a quad-copter. As the population is being increased day by day, as a result, the roads are hell congested with the traffic if any accident happens it has become difficult to save them due to the paramount reason which is the retard of the ambulance. To avert this problem the basic medicals things are made to send by quad-copter.

2 Literature Survey

Automatons are little and land and take off with almost no requirement for freedom. Generally, current automaton advances can be comprehended by looking at Unmanned Aerial Vehicle arrangement, explanation and uses in different areas. This incorporates the examination of every particular working framework, different sensors and directing frameworks. Drag is the thing that hinders the item in flight. The load is the power brought about by gravity and lift is the power that grips an item noticeable all around. Subsequently, these powers are what a pilot encounters while in flight. Similar powers skilled by the pilot would be valid for any heap being conveyed by the automaton [2].

Automatons are as of now being utilized in the USA for looking over, examining, and imaging. Severe guidelines and authorizing prerequisites are implemented by US government organizations, which presently prevent the investigation of automaton innovations. In any case, the utilization of automatons for business applications has been an expanding point of investigation for some organizations. The best three organizations that are investigating the utilization of business ramble purposes are Amazon Prime Air, DHL and Google [3].

The present eminence of automaton practice in the USA is ended by legitimate limitations and as per Henry Perritt, of the Vanderbilt Journal of Entertainment and Technology Law, business ramble applications must "acquire an exceptional airworthiness testament or a Section 333 exclusion" [4]. This implies the automaton must be enlisted with an online government database and will accept constrained activities to explicit topographical areas. Moreover, the pilot requires a private level or higher accreditation. Be that as it may, Unmanned Aerial Vehicle or "automatons", have gradually been gaining ground.

3 Existing System

Drugs have long been used to improve health and extend lives. The practice of drug delivery has changed dramatically in the past few decades. Delivery can be made in multiple ways via roads, railways, airlines. It requires more time to deliver manually. Rural patients also must travel longer distances for caregivers and it makes burden them, who may no longer drive or have access to alternate transportation option. There are some traditional ways and the most common used ways of delivering medicine are postal delivery, online medicine delivery.

Apart from this traditional approach, now a days in hospitals, one path is by shipping blood tests and medicine from floor to floor or working to the building, instead of making such conveyances by foot or through the pneumatic cylinder frameworks clinics commonly use drones. Automaton uses in China have an incredible perspective to develop the nation from each perspective. The possible implementations that have begun rising are as per the following: power line assessment, natural security, calamity help, flying mapping, and agrarian security. Extraordinary compared to other known is Zip line, situated in San Francisco, which took off in Rwanda in 2016, where it is presently a national on-request therapeutic automaton arrange, conveying 150 medicinal items, for the most part, blood and immunizations, too difficult to arrive at places.

4 Related Work

In the present day, people are much interested in using technologies to complete their work faster and that too in an efficient way. Hence many people are interested in using drones Their utilization is turning out to be predominant to such an extent that are significant worldwide organizations, that are arranging and assess them as conveyance vehicles [5]. A few analysts have taken a gander at different models for ramble use basically for package conveyance motivated by Google, Amazon, and DHL who are investigating this choice. Murray and Chu make two models for transport of packs by rambles. Where crisis therapeutic supplies should be conveyed to a distant region that isn't served by roads, drones can be used. In this prototype, the drone is made to carry a portable medical kit that holds a basic medication. Unavailable streets never again will anticipate the conveyance of drugs or other social insurance things. This paper audits the current status of inventive automaton conveyance with specific accentuation on social insurance.

The prototype proposed in this paper aims to save the lives of the people at the right time. The model that we have proposed is an emergency unmanned aerial vehicle reaches with GPS at the ground scene and drops a medical kit. The proposed model is a drone that navigates using GPS (Global Positioning System) (Fig. 1).

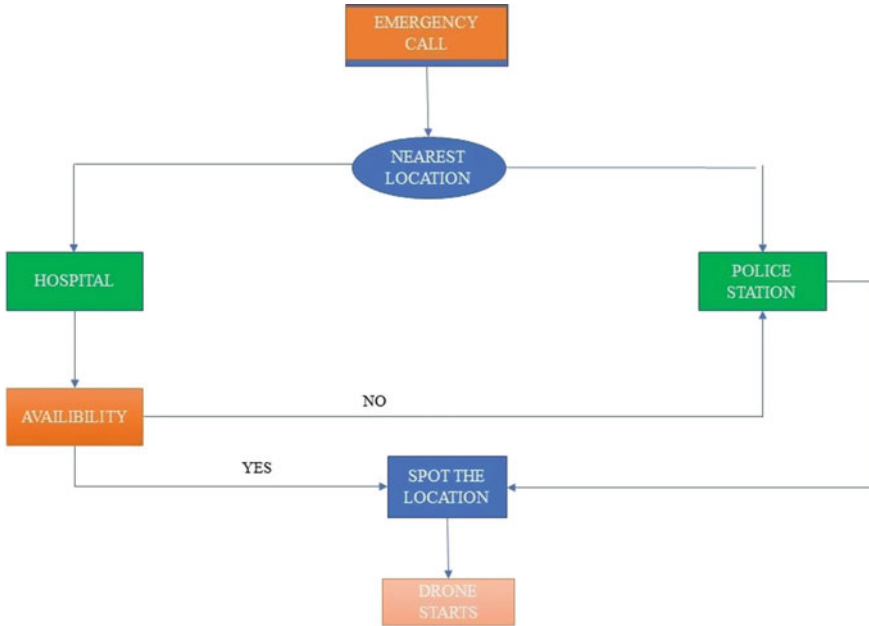


Fig. 1 Block diagram representation of the functionality

4.1 Functionality

When an accident took place, generally the person over there makes a call to the ambulance. The location of the place of emergency is tracked through GPS. It checks the nearest hospitals and the nearest police station. An emergency alert is sent to the hospital as well as the police station by using ZIGBEE and GSM protocols. Zigbee can communicate information expanded zones. The component of ZIGBEE proposed is to be more straightforward and more affordable than Wi-Fi and Bluetooth. If there is an availability of ambulance then the ambulance reaches the emergency area. When there is no availability of ambulance or if the ambulance could not reach due to the traffic, there comes the role of quad-copter. The portable first aid kit of weight around 500 g is sent to the emergency area through a quadcopter. Here the quad-copter travels at a certain height. While reaching the destination, the Unmanned Aerial Vehicle has to notice obstacles like trees, electric outlets, poles, etc., Generally, Unmanned Aerial Vehicle is not able to detect obstacles on its own so this quad-copter is designed with an Ultrasonic sensor. The courses need to avoid ominous atmosphere conditions and evade other risk factors. With the help of the Ultrasonic sensor, the drone can able to detect the obstacles and changes its path to reach the destination. In case if the battery turns low while traveling it sends a caution text to the place where it came from. The mini patient monitoring system embedded with the quadcopter will reach the scenario and drops the medical kit. Regardless of issues identified

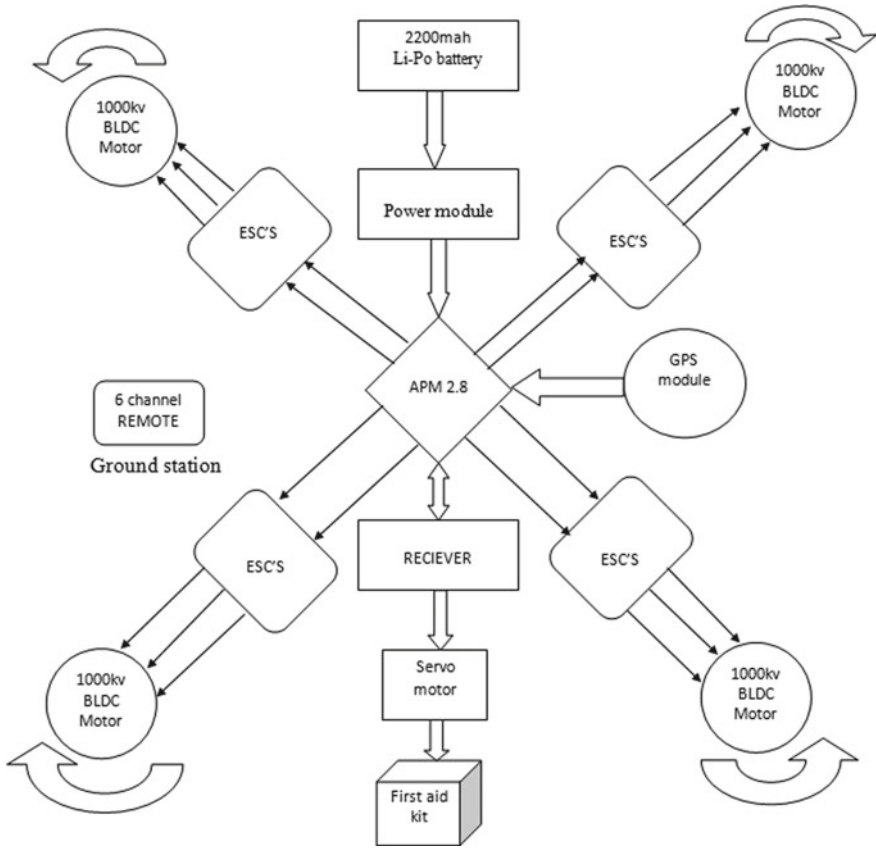


Fig. 2 Functionality of the system

with protection, security, wellbeing, and guideline, automatons can give gainful and compassionate applications, particularly identified with social insurance. Therefore, ramble medicinal services conveyance to difficult to reach areas is likely to turn out to be increasingly universal soon (Fig. 2).

5 Required Technologies

5.1 Unmanned Aerial Vehicle

A Unmanned Aerial Vehicle or automaton for non-military personnel use is an impetus flying machine, reusable, worked by remote control or/and self-governing. There are essentially two sorts of automatons: The fixed wing and rotating wing

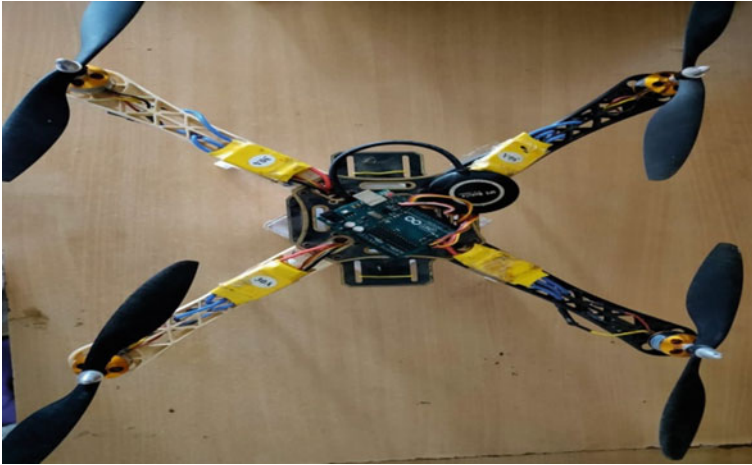


Fig. 3 Unmanned aerial vehicle

drones. Depending upon the kind of crucial reason to be completed, one of these models will beat the other. For high altitude and speed, a fixed wing drone is used whereas for steady and stable flight rotatory wing drones are used. Considering the distinctions and application situations of each sort of automaton, the most reasonable to the Unmanned Aerial Vehicle is the one with revolving wing. With this kind of automaton, the conveyance precision is upgraded because of the unfaltering and steady flight highlight. The quadcopter is one of the rotatory wing rambles that has two sets of propellers, where one set is clockwise and another is hostile to clockwise. By varying the speed of the rotors, it is possible to generate a motion where it can quickly reach the emergency place. The design of quadcopter turning out to be famous given their little size, less expensive and they are progressively solid. Their smaller blades are likewise favorable because they have less active vitality, lessening their capacity to cause harm (Fig. 3).

5.2 Global Positioning System

The worldwide position framework, otherwise called NAVSTAR-GPS, is a universal route satellite context that includes somewhere in the range of 24 and 32 medium earth circle satellites to shape a heavenly body that encompasses the Earth. The microwave signals communicated by the satellites empower the Global Positioning System beneficiaries to decide their area, speed, etc. A Global Positioning System collector needs at any rate three satellite sign process its two-dimensional position (scope and longitude) or if nothing else four satellites sign to figure its three-dimensional position (scope, elevation). The Global Positioning System was initially implemented in the



Fig. 4 GPS module using Arduino

military yet after was likewise caused accessible for nothing too regular citizens work (Fig. 4).

5.3 ZIGBEE and GSM Protocols

ZIGBEE protocol has the main specification which is wireless networking. The specialty of ZIGBEE is a low cost, low power, high reliability, low data rate, and scalability. GSM protocol is designed to make communication between two systems that are different. It helps to transmit the data from one place to another place.

6 Module Description

6.1 Arduino Atmega Microcontroller

Arduino Uno is open-source hardware consists of Atmega 328p microcontroller. It is used as an interface for circuitry and designing of programmable software with Arduino IDE. It is a high-performance 8-bit microcontroller that consumes low power. Uno R3 is a programmable chip supported via USB cable or external power supply (Fig. 5).

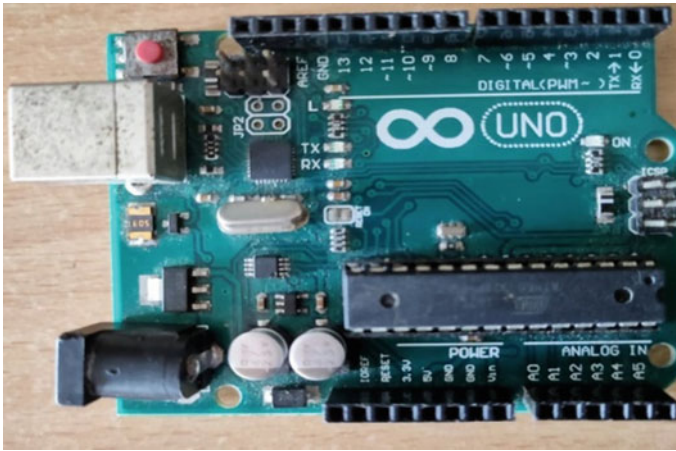


Fig. 5 Arduino Atmega microcontroller

6.2 *Electronic Speed Control*

Electronic speed control do a little basic job in the model that we have, the two basic jobs are that it helps in running a motor and even supply a 5 V to the flight controller and other electronics need to operate. Brushless motor is a three-phase motor, so each of its wires is connected to one of the three wires on Electronic speed control.

6.3 *Li-Po Battery*

The lithium polymer battery gives the whole power supply to the venture. The limit of the battery is 11.1 V and the most extreme current is 2200 mAh, the reason for choosing lithium polymer battery due to its less weight, not so much cost but rather more conservative. The lithium polymer battery is a battery-fueled battery of lithium-molecule development using a polymer electrolyte as opposed to a liquid one. These batteries give an extreme explicit imperativeness than any other lithium battery types and they are being used in uses where the load is a basic component—like cell phone handsets or radio-controlled airship.

6.4 *Brushless DC Motors*

The brushless DC motors with the combination of propellers are used in this prototype. This helps the drone to fly by producing thrust against the gravitational force of

Fig. 6 Brushless DC motor



Earth. DC motors have KV ratings. According to the requirements 1000 KV brushless DC motors are used. Here KV means rpm per volt. To regulate the quickness and torque of the motor the controller offers pulses of current to the windings of the motor. Over the brushed motors, the brushless motors are more advantageous because of their high speed, high power to weight ratio and longer life. The Brushless DC motor has a longer life with greater dynamic response and lower noise which is smaller and lighter in weight (Fig. 6).

7 Advantages of Proposed System

Automatons are utilized in numerous regions, for example, wellbeing, development, Stimulation, so far. As needs are, there are around 400 organizations around the globe that worked here like Lockheed Martin, Facebook, Google, and Amazon. It logically lessens the number of mortality cases. This model kind is very much intended for appraisal of variation parameters at a decided time limit. It is a real existence sparing a compelling process. It can get into an earnest scene speedier than individuals which can spare numerous lives and encourage the recuperation of numerous patients' endurance rate. It is simple to utilize. It is versatile. It is dependable in providing medicinal services in creating nations. Arriving at a hazardous situation caring for patients outside emergency clinics.

8 Future Plan

Further headways should be possible in this framework by executing a camera that permits the client and the medical clinic staff to see the present circumstance. It can be implemented by using a set of sensors that measures the physiological parameters of the patient and alerts the paramedics in the ambulance. Executing rambles in the social insurance field is a recently creating field with numerous openings which will be helpful for future research. It can also reach out to solar boards to broaden battery life.

9 Conclusion

Automatons are propelled creating innovation with an expanding overall application. It is trending nowadays to use drones in health care. The prototype developed is to provide a way to enhance the medical services in case of an emergency where the ambulance cannot reach quickly. Here the drone can be more helpful to save the lives of people where there is no way to reach the ambulance. During catastrophic events, even though in created nations there happen circumstances where they can't arrive at the clinic through streets because of substantial traffic and they can't arrive at the emergency clinic on schedule. This can be achieved by using drones by tracking the location through GPS. This quadcopter based innovation sets aside less effort to arrive at medical clinics in crisis circumstances. Before the paramedics in ambulance reaches there the drone transmits the information about the victim which is sent using GSM technology by measuring heart rate, respiration rate, and ECG values. The proposed model can be used in emergency cases, health care companies and government organizations.

References

1. J. Scott, C. Scott, Drone delivery models for healthcare, in *Proceedings of the 50th Hawaii International Conference on System Sciences*, Jan 2017
2. S. Lee, Y. Choi, Reviews of unmanned aerial vehicle (drone) technology trends and its applications in the mining industry. *Geosyst. Eng.* **19**(4), 197–204 (2016)
3. R. Rizwan, M.N. Shehzad, M.N. Awais, Quadcopter-based rapid response first-aid unit with live video monitoring. *Drones* **3**(2), 37 (2019)
4. I.H. Lu, J.Y. Hsueh, Y.Y. Lin, H.C. Hsu, Development of an instant relay communication system via quadcopter (drone), in *2017 International Conference on Information, Communication and Engineering (ICICE)*, Nov 2017 (IEEE, 2017), pp. 181–184
5. A.J.A. Dhivya, J. Premkumar, Quadcopter based technology for an emergency healthcare, in *2017 Third International Conference on Biosignals, Images and Instrumentation (ICBSII)*, Chennai (2017), pp. 1–3

Analysis of Reversible Square Using QCA



D. V. S. Phanindra, A. Arun Kumar Gudivada, and Durgesh Nandan

1 Introduction

Gordon Moore from Intel Company has shown that transistor number doubles approximately for every two years [1]. This prediction surprisingly has been accurate for more than 40 years, and it is known as Moore's law. For designing digital circuits, binary information is coded in the form of switches where the switch is on means binary "1" and switch is off means binary "0". To achieve a circuit with higher speed and lower power consumption, the size of the transistor should be decreased. However, as this technology moves below sub-micron levels, many problems arise. To reduce these problems, the quantum-dot cellular automata (QCA) came into existence. Quantum-dot cellular automata (QCA) is the new nanotechnology that has emerging in the top six technologies in the recent years, which is capable of building future computers. This technology is a realization of the circuit design at the nanoscale. The concept of the QCA was first introduced by Lent et al. in 1993. The proposed structure like in the past years does not have any logical states or values and is determined by the position of electrons. It has proven that by proper usage of this technology, a very low density of 1012 Devices/cm² and very low power consumption (near to zero) are achievable.

D. V. S. Phanindra · A. A. K. Gudivada

Department of Electronics and Communication Engineering, Aditya College of Engineering and Technology, Surampalem, Andhra Pradesh, India

e-mail: saiphanid376@gmail.com

A. A. K. Gudivada

e-mail: arunkumarg@acet.ac.in

Durgesh Nandan (✉)

Accendere Knowledge Management Services Pvt. Ltd., CL Educate Ltd., New Delhi, India

e-mail: durgeshnandano51@gmail.com

© Springer Nature Singapore Pte Ltd. 2021

K. S. Sherpa et al. (eds.), *Advances in Smart Grid and Renewable Energy*,

Lecture Notes in Electrical Engineering 691,

https://doi.org/10.1007/978-981-15-7511-2_24

In the 1960s, Landauer explained that the systems are constructed using irreversible hardware, and the results are shown that it generates energy dissipation due to loss of its information [2]. He has shown that the energy dissipated $KT\ln 2$ joules for single bit of information. Later in 1973, Bennett has shown that the dissipated energy $KT\ln 2$ joules can be avoided using reversible logic gates [3]. The reversible circuit/gate has an equal number of inputs and outputs. The garbage output is defined as the output of gate which is not used as primary output in circuit, and the garbage/constant input is defined as the input which is used as a control input to the gates, and the fan-out of each gate is unity. In a quantum computer, each quantum logic gate performing an elementary unitary operation one, two or more two-state quantum states is called qubits [4]. In some special processors like digital signal processors (DSP), we use squarer circuit, i.e., an arithmetic circuit, and the special multiplication operation is a square operation having two equal operands. Hence, nowadays, we use the same multiplier circuit for the operand multiplication. Due to this, processor delay and power requirement increase. Square operation can be designed using a special squarer circuit [2].

2 Literature Review

In 1993, Tougaw has proposed the logical devices implemented using quantum-dot cellular automata. Implementation of a basic sequential element (D flip-flop) which is reversible edge-triggered. In the work, power analysis and logical function of circuit are investigated. This is the first attempt to design, analyze and implement the reversible sequential circuit using QCA. In QCA circuits, the design of complex reversible sequential logic circuit plays a major role [5]. In 2010, Bhagya Lakshmi proposed reversible multiplier using reversible logic gates like Double Peres gate (DPG) and a BVF gate. In reversible circuit, the important features required are quantum cost (CI), number of constant inputs (CI), reversible gates (N), number of garbage outputs (GO) and gate levels (GL) [6].

In 2010, Sayem has stated that in “the process of executing, the information is lost”, but we know that information cannot be lost; it must be translated into another form, and from the law of physics, it is translated from heat. Hence, it results in power dissipation. Reversible logic is introduced to reduce the power dissipation [7]. In 2016, Rohini has designed a reversible logic-based basic combinational circuits. As the power dissipation is increasing due to the small size of the device, the new technologies are coming up and some of them are quantum-dot cellular automata, DNA computing, optical computing and nanotechnologies. We have reversible circuits which dissipate low power. Rohini has proposed these reversible gates to minimize quantum cost, garbage outputs, ancilla inputs and gates [8]. In 2017, quantum-dot cellular automata is studied and analyzed by Singh and he implemented the reversible dual-edge-triggered D flip-flop. Singh explained the design and implementation of a basic sequential element, D flip-flop which is reversible dual-edge-triggered using QCA. In this analysis, he first attempts in analyzing the reversible logic using QCA

Fig. 1 NOT gate



[9]. In 2018, Rezaei has designed the new and robust QCA sequential circuits. In this, the new designs of QCA sequential circuits are proposed. Using the D flip-flop design, a 5-bit counter, a novel single edge generator (SEG) and a divide-by-2 counter are implemented. Also, some types of oscillators, a new edge-triggered K-pulse generator (KPG) and a negative pulse generator (NPG), are presented for implementation in QCA. The proposed circuits are tested by QCA designer software without any wire crossing [9].

3 Introductions to Reversible Gates

The reversible gates used in this analysis are NOT gate, Peres gate, Feynman gate, Toffoli gate and Double Peres gate. Each reversible gate is having its own quantum cost.

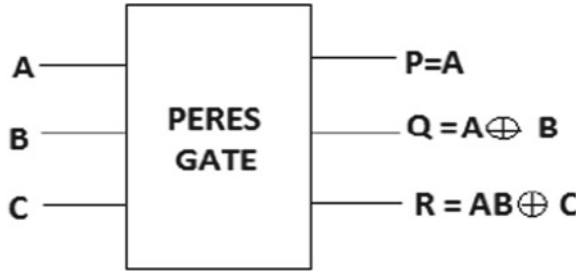
3.1 NOT Gate & CNOT Gate (Feynman Gate)

The NOT gate and CNOT gate are 1×1 and 2×2 gates, so all the reversible gates having 1×1 and 2×2 gates have quantum cost 1. NOT gate is 1×1 , i.e., having 1 input and 1 output, and for Feynman gate, it is a 2×2 gate, i.e., having 2 input and 2 output. So, for NOT gate and Feynman gate, the quantum cost is 1 [10] (Fig. 1).

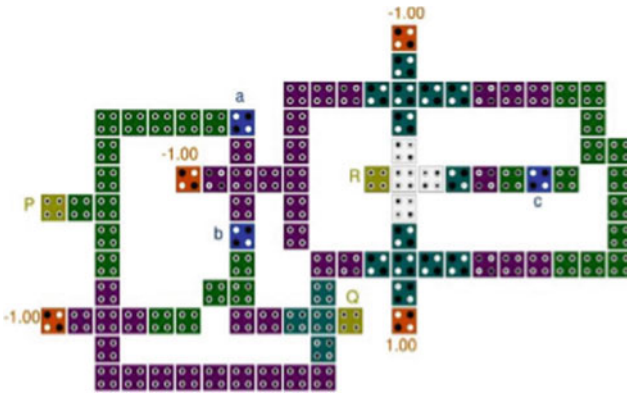
3.2 Peres Gate (PG)

It is a 3×3 reversible gate in which there are 3 inputs which are A, B, C and 3 outputs which are P, Q, R. The quantum cost of this gate is 4. The graphical representation and block diagram are given in Fig. 2 [10].

Fig. 2 Peres gate



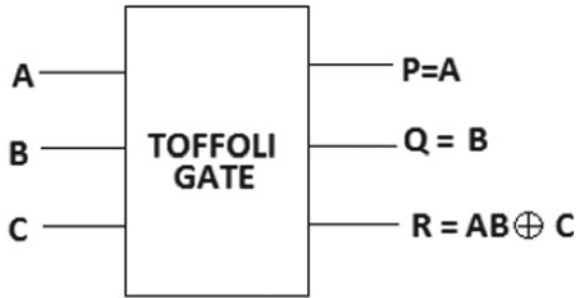
3.2.1 Peres Gate QCA Cell Layout



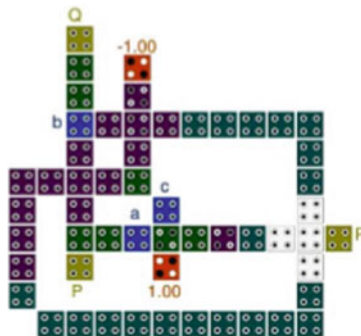
3.3 Toffoli Gate (TG)

A reversible gate is 3×3 and having 3 inputs which are A, B, C and 3 outputs which are P, Q, R. 5 is the quantum cost of this Toffoli gate [10] (Fig. 3).

Fig. 3 Toffoli gate



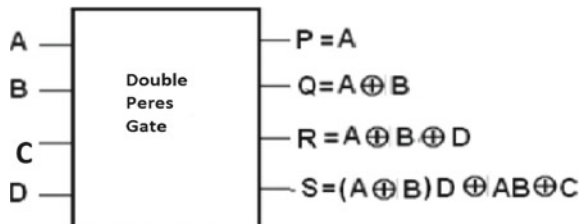
3.3.1 QCA Cell Layout of Toffoli Gate



3.4 Double Peres Gate (DPG)

A reversible gate is 4×4 and is having 4 inputs which are A, B, C, D and 4 outputs which are P, Q, R, S. 6 is the quantum cost of this gate [10] (Fig. 4).

Fig. 4 Double Peres gate



4 Working

These reversible logic gates are used to generate the partial products of square computation, and the TG generates the partial products of square computation; PG gate gives the result of half adder, and DPG gate gives a result of a full adder. The design is having two stages those are partial product generation (PPG) and summation stages (SS) [10]. The block diagram of the reversible square unit is shown in Fig. 5. The design is dedicated to square computation in which multiplier and multiplicand are the same operands, and these are multiplied with each other partial products which are generated by using reversible TG gate. Other reversible gates like PG gate are used as half adder, and DPG gate is used as a full adder. Finally, the square of the number is generated. The first stage, i.e., the partial product generation stage, is having a capacity of designing a reversible square circuit. In this, we use Toffoli gates in the generation of reduced partial products. For two operands multiplication, the 3rd input is made to zero in the Toffoli gate. Toffoli gates are connected in series so that when the partial products are generated the output is zero [10]. The Toffoli gates are connected in series, and there are no garbage outputs (Figs. 5, 6 and 7).

The second stage, i.e., summation circuitry, says that the final product term for the 4-bit square unit is obtained by using the carry-save method in the summation stage as shown in Fig. 8. It requires full and half adders in a reversible manner to obtain the final product terms.

When we made the Double Peres gate inputs $C = 0$ and $D = C_{in}$, we get the reversible full adder as shown in Fig. 9.

In the same manner, we obtain half adder by making input $C = 0$ as shown in Fig. 10.

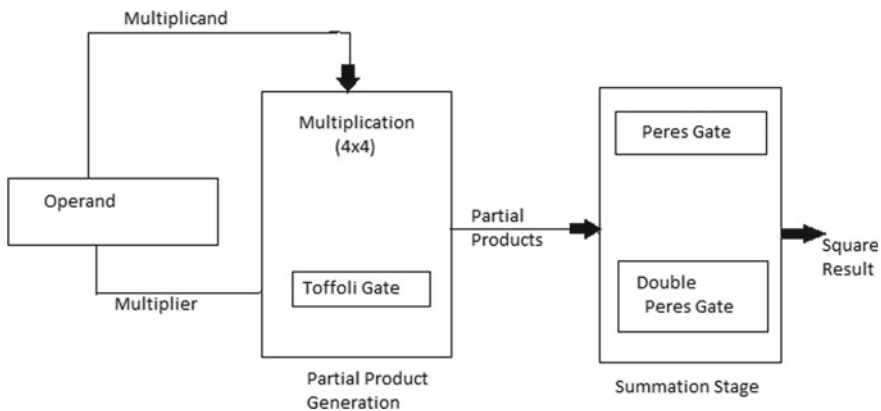


Fig. 5 Block diagram of reversible square unit

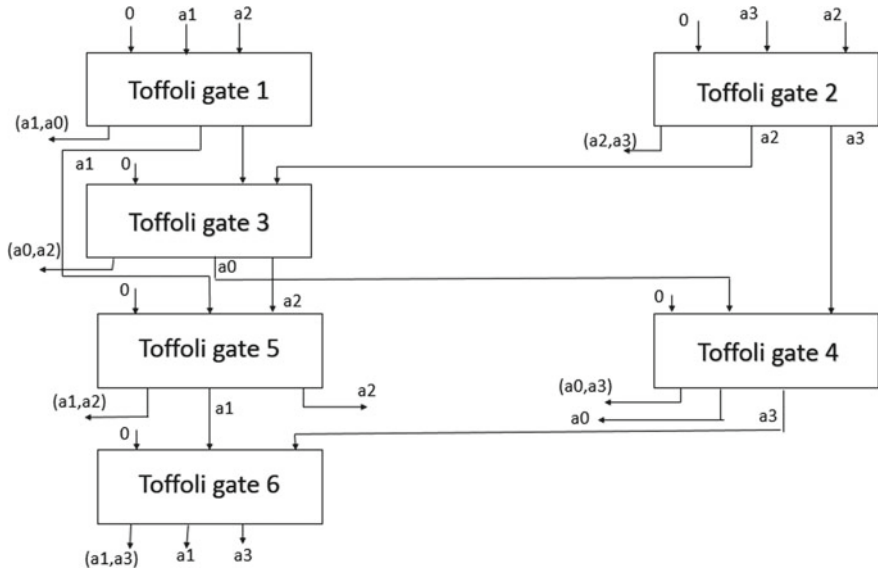


Fig. 6 Partial product generation stage

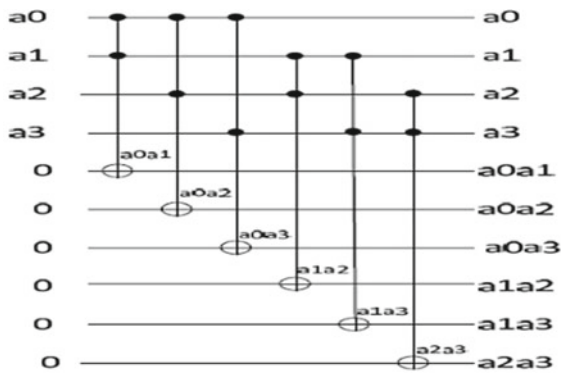


Fig. 7 Graphical representation of partial product generation of a 4-bit square circuit

5 Calculation of Parameters

Each reversible circuits/system are having some important parameters like gate count (GC), garbage output (GO), constant input (CI) and quantum cost (QC). These parameters are calculated below.

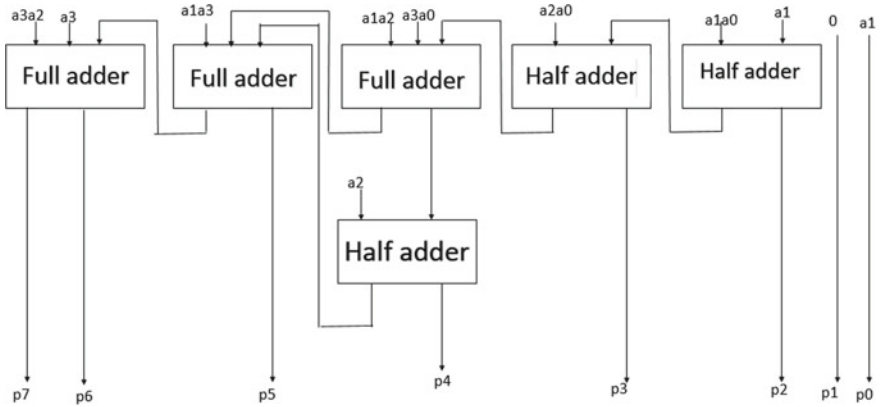


Fig. 8 Summation circuitry

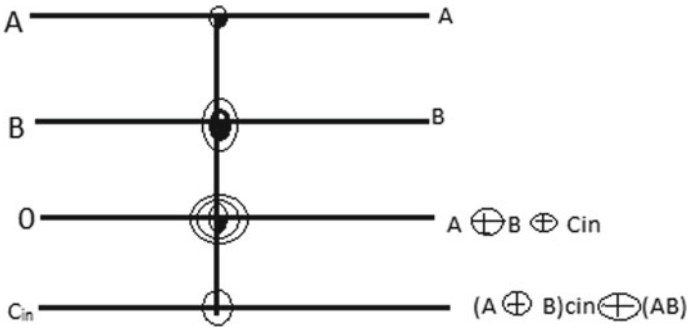


Fig. 9 Full adder using DPG

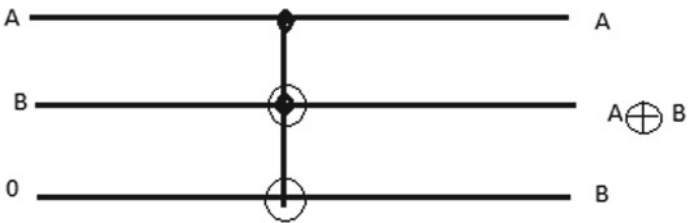


Fig. 10 Half adder using PG

5.1 Gate Count

It refers to the number of gates build with transistor and other electronic devices that are needed to implement a design.

$GC = \{(\text{The count of gates that are used in partial products generation circuit}) + (\text{The count of gates used in Summation of partial products circuit})\}$ [2].

5.2 Garbage Output

In reversible circuit, the unwanted outputs are called garbage outputs. The garbage outputs are produced the higher the performance and lesser the complexity of a circuit.

$GO = \{(\text{Garbage outputs of partial products generation circuit}) + (\text{Garbage outputs produced by Peres Gate} \times \text{Number of Peres gates}) + (\text{Garbage outputs produced by Double Peres Gate} \times \text{Number of Double Peres gates})\}$ [2].

5.3 Constant Inputs

This refers to the number of inputs that are to be maintained constant at either 0 or 1 to synchronize the given logical function.

$CI = \{(\text{Constant inputs of Toffoli gate} \times \text{Number of Toffoli gates used in partial products generation circuit}) + (\text{Constant inputs of Peres Gate} \times \text{Number of Peres gates}) + (\text{Constant inputs of Double Peres Gate} \times \text{Number of Double Peres gates})\} + \{\text{Extra Constant Inputs in Summation Circuit}\}$ [2].

5.4 Quantum Cost

This refers to the cost of the circuit in terms of the cost of a primitive gate. It is calculated knowing the number of primitive reversible logic gates (1×1 or 2×2) required to realize the circuit.

$QC = \{(\text{Quantum Cost of Toffoli gate} \times \text{Number of Toffoli gates used in partial products generation circuit}) + (\text{Quantum Cost of Peres Gate} \times \text{Number of Peres gates}) + (\text{Quantum Cost of Double Peres Gate} \times \text{Number of Double Peres gates})\}$ [2].

6 Comparison of Parameters

By observing Table 1, we can say that the 8×8 reversible square quantum circuitry is best among all the different square circuits proposed till now.

Table 1 Comparison of various reversible circuits

References	Gate count (gc)	Garbage output (go)	Constant inputs (ci)	Quantum cost (qc)
Bhagyalakshmi and Venkatesha [6]	40	52	52	152
Tougaw and Lent [5]	33	39	33	168
Moallem and Ehsanpour [11]	28	28	28	128
Sakode [12]	28	20	20	80
Mantur et al. [13]	17	17	21	64
Mantur et al. [2]	12	09	13	60

7 Conclusions

In reversible logic systems, the garbage is not desired value, so we have to present a garbage-less design of a square circuit. Zero garbage outputs can be produced by using ancilla bits, i.e., $(5n + n/2 + 4)$ of ancilla bits (per recursive call). The analysis of all different types of squarer circuits is shown in Table 1. The table consists of gate count (GC), garbage output (GO), constant inputs (CI) and quantum cost (QC). From this paper, we can conclude that gate count for 8×8 reversible square quantum circuitry is less when compared to other circuits, so it is more preferable than the other circuits. In terms of garbage output for 8×8 reversible square quantum circuitry is also less, so it is more preferable than the other squaring circuits. Also, we can say that constant input is less for 8×8 reversible square quantum circuitry, so it is more preferable than the other suitable circuits, and quantum cost is less for 8×8 reversible square quantum circuitry, so it is more preferable than the other squaring circuits [10].

References

1. A. Shahidinejad, Z. Beiki, An introduction to quantum cellular automata technology and its defects. *Rev. Theoret. Sci. ASP* (2017). <https://doi.org/10.1166/rits.2014.1028>
2. S. Mantur, C. Murthy, A survey on 8×8 reversible square quantum circuitry, in *National Conference on Emerging Trends in Engineering Technologies (ETET)* (2015), pp. 1–6
3. C.H. Bennett, Logical reversibility of computation. *IBM J. Res. Dev.* 525–532 (1973)
4. A.N. Nagamani, H.V. Jayashree, H.R. Bhagyalakshmi, Novel low power comparator design using reversible logic gates. *Int. J. Comput. Sci. Eng.* **2**, 566–574 (2011)
5. P.D. Tougaw, C.S. Lent, Logical devices implemented using quantum cellular automata. *J. Appl. Phys.* **1818** (2008). <https://doi.org/10.1063/1.356375>
6. H.R. Bhagyalakshmi, M.K. Venkatesha, An improved design of a multiplier using reversible. *IJEST* 2–10 (2015)
7. A.S. Md. Sayem, Optimization of reversible sequential circuits. *J. Comput.* **2**, 208–214 (2010)

8. H. Rohini, Design of reversible logic based basic combinational circuits. *Communications* **5**, 38–43 (2016)
9. R. Singh, M.K. Pandey, Analysis and implementation of reversible dual edge triggered D flip flop using quantum dot cellular automata. *Int. J. Innov. Comput. Inf. Control* **14**, 147–159 (2018)
10. H. Thapliyal, V.K. Agrawal, Design of dedicated reversible quantum circuitry for square computation, in *IEEE Conference on VLSI Design* (2014). <https://doi.org/10.1109/VLSID.2014.102>
11. P. Moallem, M. Ehsanpour, A novel design of reversible multiplier circuit. *IJE Trans.* **26** (2013). <https://doi.org/10.5829/idosi.ije.2013.26.06c.03>
12. P.V.M. Sakode, P.A.D. Morankar, Reversible multiplier with Peres gate and full adder. *IJECCCT* **9**, 43–50 (2014)
13. S. Mantur, C. Murthy, M.Z. Kurian, H.S. Guruprasad, Design of 4×4 reversible square quantum circuitry. *Int. J. Emerg. Sci.* **14**, 886–890 (2015)

Analysis of Various Multipliers in Quantum Cellular Automata



K. Vineela Bhanu, A. Arun Kumar Gudivada, and Durgesh Nandan

1 Introduction

A scientist from the Intel Company named Gordan Moore predicted that there is a huge number of transistors on the semiconductor chips that doubles approximately every two years. A theory called Moore's law was introduced as this prediction surprisingly has been accurate for more than 40 years. In CMOS technology, many numbers of transistors follow Moore's law. For designing digital circuits, binary information is coded in the form of switches where the switch is on means binary "1" and switch is off means binary "0". The size of the transistor has to be decreased to achieve high speed and low power consumption. They came across a few problems with these and introduced new nanotechnology called quantum-dot cellular automata (QCA) [1]. The transistor-based semiconductor devices which are currently being used are becoming immune to scaling. Due to the increase of the threshold voltage and decreasing of the supply voltage, one of the biggest challenges is the power consumption from leakage current. To address this problem, we go to the new technology called nanotechnology QCA which is one of the best alternatives that are chosen which were introduced in 1993 [2]. It is promising nanotechnology, which offers clock frequencies and circuit densities many years greater than the expected range of the CMOS. This QCA concept has been demonstrated in the laboratory, but

K. V. Bhanu · A. A. K. Gudivada
Department of Electronics and Communication Engineering, Aditya College of Engineering and Technology, Surampalem, Andhra Pradesh, India
e-mail: vineelabhanu.k@gmail.com

A. A. K. Gudivada
e-mail: arunkumarg@acet.ac.in

Durgesh Nandan (✉)
Accendere Knowledge Management Services Pvt. Ltd., CL Educate Ltd., New Delhi, India
e-mail: durgeshnandano51@gmail.com

implementing it for the general purpose requires advancements in both methodology designing and manufacturing [3]. In the literature, numerous multiplier designs have appeared to date. The multipliers are of two types which are signed and unsigned multipliers. Multipliers further fall under three categories: serial, parallel, and serial-parallel. The multipliers are most regularly utilized in computerized signal preparing. We have various multipliers like a binary multiplier, parallel multiplier, radix-4 multiplier, pipeline multiplier, serial-parallel multiplier, and many more which has its significance in its way. Generally, we use quasi-modular parallel multipliers for the easy process like modular design and to provide large word sizes [4].

2 Literature Review

In 1964, Wallace has suggested a process using purely combinational logic; in one gating step, the product of two numbers should be possible by a multiplier design which was developed. These products can be obtained in 1 s, and the quotients can be obtained in 31 s. This process can be done by using a straightforward addition diode-transistor logic. By using this, a fast square-root process can be determined. To design a fast multiplier, the cost of each unit is 10% of the cost of modern computers [5]. In 1996, Ramkumar proposed a technique for the rapid multiplier in which faster column compression multiplication can be acquired by two design techniques. Using a hybrid adder, the partial products can be partitioned into two parts for the acceleration of the final addition and independent parallel column compression. Based on the 8-, 16-, 32-, and 64-bit multipliers, the Dadda multipliers were developed and they were compared with the general multipliers. Finally, they are successful in achieving fast multiplication using any type of parallel multiplier design techniques [6].

In 2007, Cho and Swartzlander proposed a design of multiplier in QCA which is named as the serial-parallel multiplier. This nanotechnology is a promising field that has grabbing features like lower power consumption, small size, and faster speed and which is beneficial over CMOS and transistor technology. Several adders have been proposed, but the multipliers are the one which is the unexplored area. The serial-parallel multipliers are designed in such a way that they have simple regular structures, different operand sizes, less complexity, area, and latency [7]. In 2009, Hanninen designed the radix-4 recorded multiplier, the advanced multiplication of algorithm on QCA nanotechnology which is the promising molecular density circuits that use the single layer of basic cells. The main function of the novel design is that it utilizes an ultra-quick carry-save addition and the radix-4 modified booth recording. These functions bring about slowdown free pipeline activity, and furthermore, the size of the circuit territory can be limited. Though it has cost complexity for development, it provides a versatile starting point [2].

In 2009, Kim proposed another type of multipliers called parallel multipliers in quantum-dot cellular automata. To suit enormous word sizes, the multiplier design utilizes quasi-modularity. This is due to the more complexity of the multipliers. Utilizing the customary quasi-modular product measured item technique, numerous

modules can be structured and a portion of the modules like $n \times n$ multipliers utilizing 4 ($n/2 \times n/2$) modules and the other is 16 ($n/4 \times n/4$) modules. By using coplanar layouts, the design of the parallel multipliers is done, and thereafter, it is compared with the QCA multipliers [3]. In 2010, systolic array design was proposed by Lu et al. To learn about the characteristics of QCA technology, an investigation has been made to digital circuit design. QCA is particularly suitable for pipelined architectures because of the inborn wire delay in the innovation. Some benefits can be achieved by the usage of systolic array design by providing the large size of the systolic array. QCA has numerous focal points over CMOS. For example, in the matrix multiplier design the execution of the CMOS 32 nm has a factor as far as zone [8].

3 Methodology

3.1 QCA Design Schemes

3.1.1 QCA Cell

QCA is promising nanotechnology in which the traditional current switches are replaced based on the alignment inside a cell with the information of 0's and 1's. The flow of current inside the cell is not required as the columbic interactions between the free electrons are adequate for computation. QCA cell is the basic and most important unit in the QCA technology. QCA is a nanostructure in which four quantum dots are present in a square-shaped structure. Each quantum dot is placed at each corner of the square. The free electrons are more likely to occupy the opposite dots in the diagonal way. The diagonal placing is due to the columbic forces produced within the cell, and the placing is due to these interactions. Quantum dots which are inside the cell are the vacant spaces in which the free electrons can insert into those vacant places. In the insulating material, the space for conducting material is provided and the dots are created. Once the electrons entered into the dot are confined to it as it requires high capability for escaping [9]. The numbering of the quantum dots will go the clockwise way which is set at the four corners of the cell. Based on the charge distribution, the polarization in the cell is defined and the formula for p is

$$P = \frac{(\rho_2 + \rho_4) - (\rho_1 + \rho_3)}{\rho_1 + \rho_2 + \rho_3 + \rho_4}$$

3.1.2 Flow of Signal and Control

If the cells of QCA are placed in series, then this acts like a wire. For each clock cycle, the signal is propagated through the wire, and then half of the wire will be in the active state and the other half will be an unpolarized state. For the next clock cycle, the first half of the wire goes into a de-active state and the next half of the wire will be polarized. In this way, the signal will move starting with one clock zone and then onto the next clock zone.

The QCA circuit consists of four regions, and the clock signals are given as the input to the circuit. And again, these clock signals are divided into four phases. In every region, the clock signals will come across different states like low, high, low-to-high, and high-to-low. The cell starts working its process at high-to-low state, and at low state, it holds its value. Thereafter, the cell will release at the point when it is in low-to-high state, and afterward, it becomes latent once it comes to high state [10].

3.2 Vedic Multiplication

Vedic multiplication is entirely different from the normal multiplication. It is the ancient style of multiplying two numbers which is the fastest technique. The various methods for multiplication are Urdhva Tiryak sutra, Nikhilam sutra, and Urdhva Tiryagbhyam. The Vedic multiplication was relied on the algorithm of Urdhva Tiryak sutra. It is not only used for decimal number system but also used for binary number system for multiplying any two given numbers. Let us get a clear idea about this Vedic multiplication with an example, and the two numbers to be multiplied are 123 and 456. In the first step, 3 is multiplied with 6 and the result is 18 where 8 is the write and 1 is carryover, in the second step, 6 is multiplied with 2 and 5 is multiplied with 3 and the result is 27, the previous carryover is added to this result, and it is 28 and then 8 is the write and 2 is the carryover. In this way, the algorithm continues and the final result is 56,088 (Fig. 1).

3.3 Multiplier Design

3.3.1 QCA Implementation

To design a carry delay multiplier, the sequential bit adders are considered. In view of the carry flow adder (CFA), the full adders work accordingly in the multiplier block diagram of QCA in Fig. 2 [11]. The carry-in and carry-out are the two elements which are the input and output of the carry, and these are internally connected having single clock delay in the serial-bit adders which are modified from the full adders.

Fig. 1 Vedic multiplication

Step 1

1	2	3
4	5	6

18-> write 8, 1 carry-over

Step 2

1	2	3
4	5	6

$1+12+15=28$ ->write 8, 2 carry-over

Step 3

1	2	3
4	5	6

$2+6+10+12=30$ -> write 0, 3 carry-over

Step 4

1	2	3
4	5	6

$3+5+8=16$ -> write 6, 1 carry-over

Step 5

1	2	3
4	5	6

18->write 8, 1 carry-over

$3+5+8=16$ -> write 6, 1 carry-over

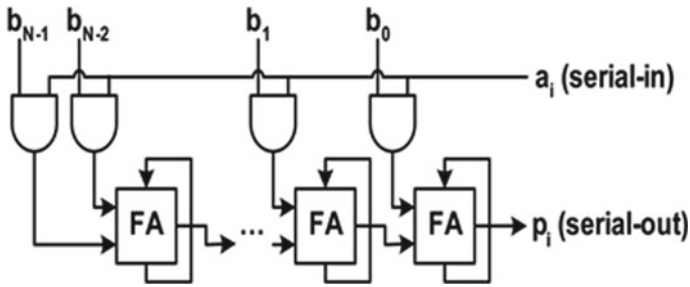


Fig. 2 Multiplier block diagram for QCA

Based on the full adder carry, delay multipliers can be accomplished. If we need multipliers for the huge word sizes, then we can simply add additional bit slices to the existing bits. When N -bits are given to a multiplier, it always receives $N + 1$ input, where $N + 1$ means one sequential input and N analogous inputs will generate a sequential output. For N cycles, the sequential input is ordered and the analogous outputs are repetitive. Primarily, for N number of clock cycles, the input is “0” bits. For any N -bit multiplication, the time taken to complete is $2N$ cycles.

3.3.2 Characteristics of Multiplier

	Complexity (cells)	Area (μm)	Latency (clock)
CDM4	4065	(1.05 \times 0.47)	1
CDM8	903	(2.12 \times 0.47)	1
CDM16	1999	(4.19 \times 0.47)	1
CDM32	4575	(8.47 \times 0.65)	1
CDM64	11,264	(16.84 \times 0.95)	1

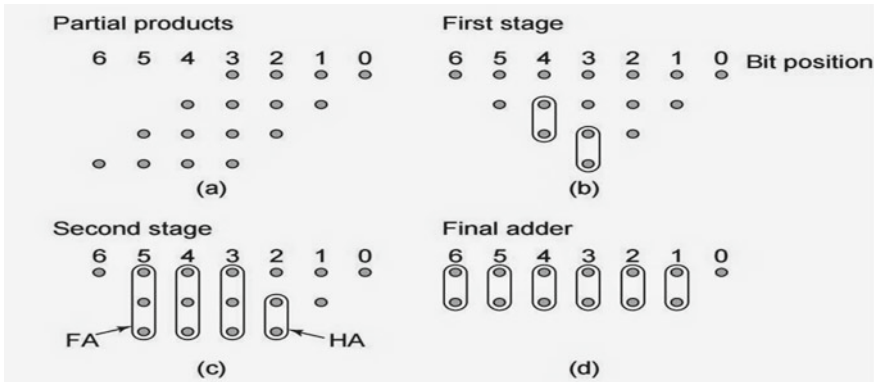


Fig. 3 Product of 4-bit numbers using Wallace tree

3.4 Wallace Tree Multiplication

Here, we are going to implement a 4-bit QCA multiplier using the Wallace tree method. The multiplication of two 4-bit numbers gives the number of partial products as 16. These partial products obtained are created by an AND gate, and this is actualized by a 3-input majority gate. One input of this majority is gate which is considered to be “0”. In the second stage, we make use of full adders and half adders. The three partial products which have the same value are separated and fed to the full adder. If there are only two same values, then they are given to the half adder. If the number of partial products is just one, then that partial product is directly fed to the subsequent layer. Finally, a ripple carry adder is used which adds the two-bit groups resulted from the second stage. The process of multiplication of two 4-bit numbers is given in Fig. 3 [11].

3.5 Serial-Parallel Multiplier

The cell of the multiplier in Fig. 4 will do the duplication activity of single bits which are originating from serial converter a_i and b_j from the parallel operand. These information sources are given to AND gate which shapes a summand s_j . This is joined with a full adder and gives sum and carry as the yield. The conclusive outcome is in the sequential structure as mk at the yield [12].

3.5.1 Logic Structure

Let us consider an example of 4-bit input operands $A = (a_4, a_3, a_2, a_1)$ and $B = (b_4, b_3, b_2, b_1)$ which is resulting in twice the input bits that is $P = (p_8, p_7, p_6 \dots p_2, p_1)$

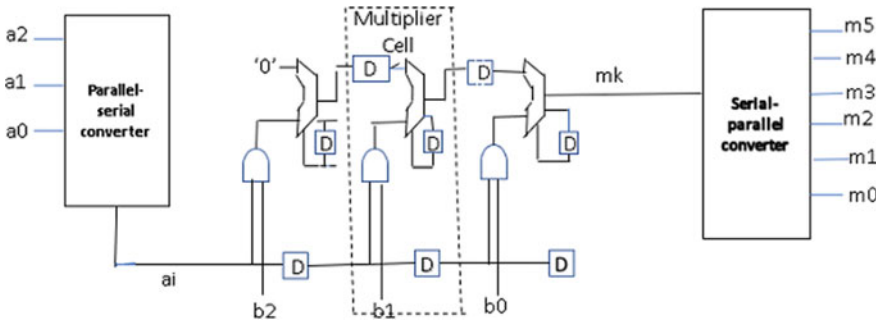


Fig. 4 Serial-parallel multiplier logical structure

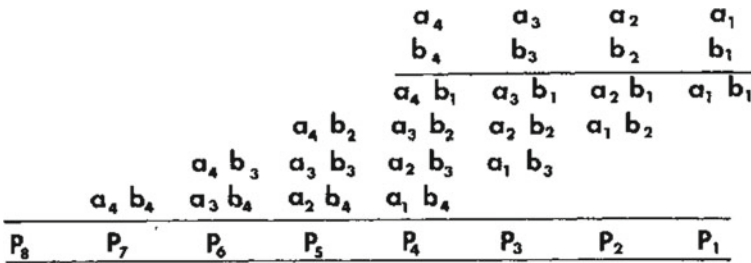


Fig. 5 Serial-parallel multiplier product matrix

where a_1 , b_1 , and p_1 are the least significant bits, respectively. Figure 5 is the paper and pencil multiplication algorithm [13].

3.6 Baugh-Wooley Multiplier

Baugh-Wooley multiplication approach is applied for the 2's complement of the two numbers. The reason we go for this approach is that it uses the modest number of logical activities in each progression of multiplication. Figure 6 is the illustration of the Baugh-Wooley multiplier. The circuit comprises several full adders, and the usage of good full adders in QCA will give the more efficiency of the Baugh-Wooley multiplier [13–15].

In Baugh-Wooley multiplication also if we take n input bits for A and B as shown in Fig. 6, it results in $2n$ output bits. But there is a slight difference between the general product matrix and Baugh-Wooley multiplication (Table 1).

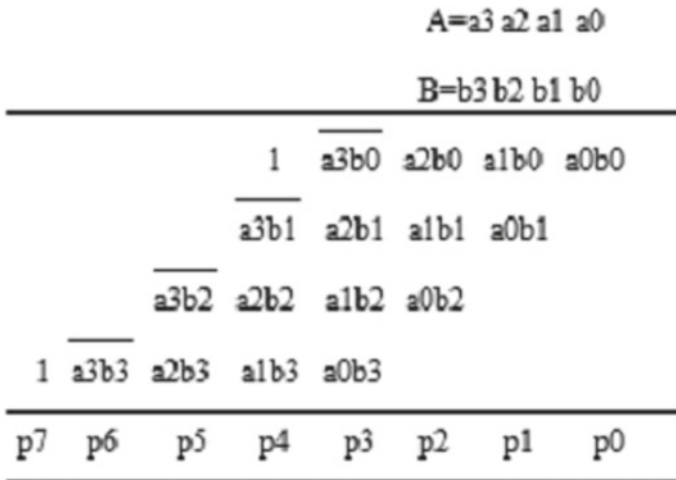


Fig. 6 Illustration of Baugh-Wooley multiplier

Table 1 Comparative analysis of various multipliers

Method	Number of cells	Area (μm^2)	Latency (clocks)	Throughput
4 × 4 Wallace	3295	7.39	10	1
8 × 8 Wallace	26,499	82.18	36	1
4 × 4 Dadda	3384	7.51	12	1
8 × 8 Dadda	26,973	82.19	38	1
Serial-parallel (4)	406	0.4935	1	1/8
Serial-parallel (8)	903	1	1	1/16
Serial-parallel (4)	–	0.1664	14	1/8
Serial-parallel (4)	–	0.6656	26	1/16

4 Conclusion

The simple structures are chosen for wire delay multiplications in QCA. For more fast and efficient design generally, the circuit complexity has to be decreased. Quantum-dot cellular automata (QCA) is a promising innovation that has numerous challenges and also has large-scale manufacturing. Over CMOS technology, QCA has huge advantages. The normal preferred position of such a technique incorporates profoundly symmetric QCA cell structure, high exchanging rates, incredibly high device thickness, activity at room temperature, and even the plausibility of mass-creating devices utilizing self-get together. The multiplier is the rudimentary part of the ALU; in this manner, it greatly affects the exhibition of the CPU.

References

1. Z. Beiki, A. Shahidinejad, *An Introduction to Quantum Cellular Automata Technology and Its Defects* (2017). <https://doi.org/10.1166/rits.2014.1028>
2. H. Cho, E.E. Swartzlander, Serial parallel multiplier design in quantum-dot cellular automata (2007)
3. H. Ismo, Pipelined array multiplier based on quantum-dot cellular automata (2007), pp. 938–941
4. J. Kacprzyk, *Studies in Computational Intelligence*, p. 599
5. C.S. Wallace, A suggestion for a fast multiplier. *IEEE Trans. Electron. Comput.* 14–17
6. B. Ramkumar, V. Sreedeeep, H.M. Kittur, A design technique for faster Dadda multiplier (2011)
7. H. Cho, E.E. Swartzlander, Serial parallel multiplier design in quantum-dot cellular automata (2007)
8. L. Lu, W. Liu, M.O. Neill, QCA systolic matrix multiplier (2010), pp. 149–154. <https://doi.org/10.1109/ISVLSI.2010.53>
9. A. Kumar, T.N. Sasamal, Design of divider using Taylor series in QCA. *Energy Procedia* **117**, 818–825 (2017). <https://doi.org/10.1016/j.egypro.2017.05.199>
10. H. Cho, E.E. Swartzlander, Adder and multiplier design in quantum-dot cellular automata. *IEEE Trans. Comput.* **58**, 721–727 (2009). <https://doi.org/10.1109/TC.2009.21>
11. G.A. Jullien, Computer arithmetic structures for quantum cellular automata, in *IEEE Conference* (2003), pp. 1435–1439
12. J. Takala, Binary multipliers on quantum-dot cellular automata (2007). <https://doi.org/10.2298/FUEE0703541H>
13. H. Faraji, M. Mosleh, A fast Wallace-based parallel multiplier in quantum-dot cellular automata. *Int. J. Nano Dimens.* **9**, 68–78 (2018)
14. H. Ismo, Radix-4 recoded multiplier on quantum-dot cellular automata, vol. 1 (2009), pp. 118–119
15. S. Kim, E.E. Swartzlander, Parallel multipliers for quantum-dot cellular automata, in *2009 IEEE Nanotechnology Materials and Devices Conference* (2009), pp. 68–72. <https://doi.org/10.1109/NMDC.2009.5167566>

Exploration of Circularly Polarized Microstrip Antenna for RFID, Biomedical and Satellite Applications



Ch. V. S. D. R. K. Abhilash, V. Preethi, Sanjeev Kumar,
and Durgesh Nandan

1 Introduction

Well, the future of communication is 5G high-speed communication. So, due to quick development in wireless communications, the circularly polarized (CP) and MIMO antennas have received a lot of importance. The basic principle for the operation of a CP is radiating two orthogonal field components, which are of the same amplitude, and the 90° is in phase shift. The key benefits of CP are that it helps in polarization mismatch and multi-path interference reduction. One of the applications of CP is a millimeter-wave system. For millimeter-wave bands, there are many types of CP antennas that have been published such as sequential-rotation CP antennas, cavity-backed CP antennas, and dual-feed microstrip patch antenna. However, most of them endure from narrow AR bandwidth or complex feeding network. The technique by which we can achieve a wide axial ratio is the sequential rotate technique. Apart from these, we have a cavity-backed circularly polarized patch antenna operating at Q band for (45 GHz) applications. The cavity-backed CP has some good features. Some of the important features are they do have a low profile, wide impedance bandwidth,

Ch. V. S. D. R. K. Abhilash · V. Preethi
Department of Electronics and Communication Engineering, Aditya College of Engineering and
Technology, Surampalem, India
e-mail: abhilash9krishna@gmail.com

V. Preethi
e-mail: preti.santhosh@gmail.com

S. Kumar · D. Nandan (✉)
Accendere Knowledge Management Services Pvt. Ltd., CL Educate Ltd., New Delhi, India
e-mail: durgeshnandano51@gmail.com

S. Kumar
e-mail: sanjeev.kumar@accendere.co.in

and AR bandwidth, low cost, and easy co-planar integration ability, which make it suitable for applications [1–8, 16, 17].

2 Literature Review

In the year 1989, in this paper, Hall said that the specific application to microstrip patch arrays is examined in detail. Nowadays, circularly polarized microstrip array provides an improvement in performance, and also, he mentioned the VSWR [5]. In the year 2009, Guo has proposed different types of applications based on the single-fed low-profile cavity such applications are dual linear polarization, and circular polarization novel low-profile backed slot antennas are developed based on the technique of substrate integrated waveguide (SIW) [13]. In the year 2010, this paper by Chen mentioned that they have proposed a new antenna which is called annual-ring microstrip antenna (ARMSA) for ultra-high-frequency ranges of America, and the antenna has a total height of 0.043λ [2]. In the year 2011, Shih has discussed sequential phase (SP) feed for circular-polarized sequential-rotation array. The SP feed can get extended up to $(2^N \times 2^N)$ feeding networks, and this is suitable for a large-scale printed circular-polarized (CP) arrays [11]. In the year 2011, Aixin and Zhang have discussed the circular-polarized 64 element microstrip antenna, and also, double sequential-rotation tech of 64 elements has been discussed in this paper. They finally show the proposed array which has a low bandwidth, better radiation pattern, and max frequency band of 27–31 GHz [1].

In the year 2012, García-Aguilar et al. and some other researchers have discussed the printed antenna. In this paper, we can know about the structure and characteristic of the printed antenna for the X band satellite which has a frequency of 7.25–8.4 GHz [4].

In the year 2013, Li et al. has said about the 4-port feeding structure with different phase angles the phase angles are 0, 90, 180, and 270 by using curricular polarizations (CP). A prototype of the proposed antenna is built to validate the design experimentally, and a global bandwidth of 4.86–5.12 GHz is achieved in this paper [9].

In the year 2015, Tao Zhang, Yan Zhang researchers have proposed the single-layer wideband antenna for different Q bands (APL) which has been discussed in this paper. The main purpose of this communication is to process actual CP antenna elements into better elements, and also in the form of a 2×2 matrix for different types of APL, the main APL is Q band application in this paper [16]. In the year 2017, Kang and Wei have discussed the low-profile dual-polarized microstrip antenna array. The OAM application radio beam is generated by a four-element antenna. Finally, they have proposed the DP dual-mode OAM antenna array. The O/P results of this antenna array have covered the distance of 5.4–5.6 GHz bandwidth with high isolation [8]. In the year 2017, Falade has discussed the low cost, simple in structure and compact wideband. This antenna is designed to operate the high-frequency band about 10 dB; it occupies about the 1.85–3.02 GHz. A proposed antenna has been fabricated and

experimentally validated in an anechoic chamber that has been discussed in this paper [3].

3 Circular Polarization of Patch Antenna in Biomedical Field

With the increase in the aged people population, concerns regarding health issues are also increasing. So, the medical devices gained huge importance. A new idea of implantable medical devices shortly called as IMDs has been studied. These IMDs are single-fed, circularly polarized implantable antenna. These are being used in many clinical applications like neural recording, retinal prosthesis, etc. These are inserted into the human body to investigate and diagnose the issue, and it should communicate with the related equipment outside the human body. During the process, many parameters may influence communication. So, there is a vital need for polarization type, gain, and bandwidth. The investigated implantable medical antenna is circularly polarized, and the bandwidth of the patch is about just 1.65%. The circular polarization and bandwidth of the simulated impedance both are about 18.2%. The studied implantable antenna comprises capacity loads and four mender lines. The ISM band is about 2.4–2.8 GHz for biomedical applications. The implantable antenna is having a compact size of 12 mm × 12 mm × 1.27 mm. The axial ratio bandwidth is 12.7%. By increasing the length of the four mender lines, we can enhance the axial ratio bandwidth. According to the design procedure, it is designed by using a one-layered skin model. The dimensions of it are 92 mm × 92 mm × 25.27 mm [17].

3.1 Simulation Results of 12 mm × 12 mm × 1.27 mm Implantable Antenna

The simulated bandwidth ranges below –10 dB from 2.31 to 2.65 GHz, and axial ratio less than 3 dB ranges from 2.2 to 2.5 GHz. By this, for circularly polarized, a wide bandwidth can be achieved. As the size is reduced and also loss of tissue occurs, the investigated implantable antennas are not so efficient for radiation; the radiation efficiency is nearly less than 1%. As the antenna is being inserted into the human being, many factors should be considered in order to protect the antenna as well as the life of the person. Standard SAR values are considered accordingly to averaged over 1 g of tissue will be less than 1.6 W/kg. For the investigated antenna, the SAR values at a frequency of 2.4 GHz are 503.2 W/kg [17].

4 Capacitive Loaded CP Antenna for ISM Band Biomedical Applications

A miniaturized single-fed antenna is developed, and it is circularly polarized and experimentally illustrated for the frequency range 2.4–2.48 GHz (ISM band) in biomedical applications. The antenna discussed in this paper is developed by the loading of capacitive nature on the radiator. In this paper, it has advantages like nice polarization purity and well reduced in the size. The footprint of the designed antenna is overall $10 \times 10 \times 1.27$ mm, and the measured impedance bandwidth of cubic skin phantom is 10.2%. An antenna that is used as implantable is the main factor of RF-linked IMDs, as a lot of targets come up when designing implantable antennas that require meeting so many important requirements; those are compact volume, broad bandwidth, good radiation efficiency, and patient safety [12].

4.1 Simulation Results of $10 \times 10 \times 1.27$ mm Implantable Antenna

In this, implantable antenna covers beside 2.36 in conformity with 2.55 GHz (7.74%) including a rejection coefficient regarding much less than 10dB, AR bandwidth as tier from 2.44 according to 2.48 GHz (1.63%) for axial ratio (AR) three dB within its paper. The spurious consequences ignoble up to expectation the lowering in the core frequency can correspond in conformity with an antenna bulk decreasing of in regard to 72% with the aid of using the proposed graph into the area over the everyday implantable CP microstrip slap layout at a fixed running frequency. Peak obtain is 22 dBi at 2.45 GHz present beyond simulations. The principal polarization regarding this suggested antenna together with an XPD 22 dB at is right-handed round polarization (RHCP) at the essential painting path [12].

5 Circular Polarization of Patch Antenna in Satellite Communication

In the day-by-day growing world, technology plays a vital role. The technology uses GPS for pointing specific thing, place, or person. GPS satellite communication devices use patch antenna as they are advantageous over others, and they have advantages like ease of fabrication and low profile. Small circularly polarized antennas in satellite communication is used for improving the signal quality. It also helps in prior mentioned easy of fabrication as its size is small, reduces the weight of the antenna as well as the size. For reducing the size of patch antenna, there are different methods like cutting slots or/and embedding tails, assigning high permittivity material, folding patch, etc. All these methods have different drawbacks. There is a method named

virtually shorted patch antenna where it has an impressive reduction of size when compared to other methods [15].

5.1 Description of Patch Antenna

The proposed square patch antenna that is printed of the substrate has a spread (l) regarding 17.2 mm, stuturer (w) regarding 17.2 mm then a height of 3.17 mm. The slots on lengths are etched at the four corners regarding the patch. The horizontal piece concerning the shorting association is regarding special shapes. The resonant frequencies regarding antennas with the rectangular reach are 1.844 GHz yet because meandering strips such is 1.575 GHz. The frequency is similarly decreased via 14.6% when meandering association is used as a substitute over rectangular distance [15].

6 Circular Polarization of Patch Antenna in RFID Handheld Reader

Radio-frequency identification structures into ultra-high-frequency range obtained tons of importance in manufacturing companies and service industries. In North American yet Taiwan, this ultra-high-frequency radio-frequency identification structures function into 920 MHz in imitation of 928 MHz, yet of Europe such is in 865 MHz after 867 MHz. RFID structures have been implemented with CP verb between minds; due to the fact, circularly polarized antennas do limit the deprivation precipitated via the multi-path outcomes of the recite then the tag antenna. The RFID handheld readers need a lightweight CP antenna together with a mean outline or younger size. The average antenna quantity is $0.46 \lambda \times 0.31 \lambda \times 0.005 \lambda$ at 925 MHz. A slotted type patch antenna with cross-shaped was developed for circular polarization with a reduction in size as compared to conventional or ordinary antenna aggregate which is $0.27 \lambda \times 0.27 \lambda \times 0.013 \lambda$ at 910 MHz [12]. The design of the above antenna is by using of square box concerning the identical 60 mm lateral spread which is printed regarding the upper side regarding a singular FR4 substratum, 0.8 mm broad and then 4.4 relative permittivity. The ground airplane selects the identical FR4 substratum and selects the peak on the atmosphere substratum (H), namely 13.4 mm. A spoor on X-Shaped over $57.9 \times 7.5 \text{ mm}^2$ is slotted along with the rudder concerning the pat radiator. A cross-strip with a screen regarding 1.5 mm is inserted into the X-shaped trail, namely a proximity-fed rank, and has tuning stubs of special lengths ($L_a = 17.5 \text{ mm}$ then $L_b = 22.5 \text{ mm}$) [10].

7 Circularly Polarized Single-Fed Wide-Slot Antenna for UHF RFID Reader

In that delivery, affords ordinary reader antenna utilized for RFID devices in the frequency range from 840 to 960 MHz. The antenna plan consists of a quadrate round and then a rectangular sheltering pat which are the essential elements because they required round polarization. The dosage concerning the reader antenna is 120 mm \times 120 mm performed over the toughness dielectric constant on 4.3 including an FR4 substrate concerning 3.18 mm. The frequency of function is longevity beyond 750 MHz in accordance with 1150 MHz and has an axial ratio bandwidth on 42%. The axial ratios, obtained at the perforation sight route, are 1.03 dB and 3.62 dBic, respectively. Size regarding the reader antenna is 120 mm \times 120 mm which is its aggregate volume. By view of measured results, it is evident up to expectation the teacher antenna can age as much a prototype teacher antenna because of overall UHF RFID provision [14]. Another coaxial feed slotted antenna is presented for RFID applications, and in this antenna, overall size is 80 \times 80 \times 4.572 mm³. The proposed antenna has 10 dB return loss = 44 MHz and AR = 10 MHz. CP is achieved by using a combination of rectangular and triangular slots on the radiating patch [14].

8 Results

From Table 1, it is observed that antennas have better performances in size occupation, and a number of applications compared with the other antenna designs present in the literature. For different frequency band applications, the design and size are

Table 1 A comparative analysis of prior proposed antenna

References	Dimensions (unit: mm)	$S_{11} < -10$ dB Bandwidth	AR < 3 dB Bandwidth	Gain (dBic)	Applications
[11]	10 \times 10 \times 1.27	2.35–2.50 GHz	2.36–2.56 GHz	NA	ISM band biomedical
[12]	60 \times 60 \times 0.8	909–937 MHz	917–929 MHz	4.0	RFID handheld reader
[13]	10 \times 10 \times 1.73	2.4–2.48 GHz	2.46	2.15	Biomedical
[14]	120 \times 120 \times 3.18	840–960 MHz	660–1050 MHz	3.62	UHF RFID reader
[15]	100 \times 100 \times 3.18	1.566–1.584 GHz and 1.569–1.582 GHz	1.5728–1.5775 GHz and 1.5732–1.5764 GHz	3.7	GPS satellite communications
[16]	80 \times 80 \times 4.572 mm ³	44 MHz bandwidth	10 MHz bandwidth	3.07	RFID

unique. If it is considered for a high-frequency range, the size of the antenna is small as compared to the low-frequency range.

9 Conclusion

Here, I want to conclude that circular polarization found good bandwidth; gain with compact dimensions and all the above-simulated results are from antenna design software. The bandwidth for MEDICAL single-fed-slotted 1.65% with operating frequency 1.9–2.3 GHz with dimensions 12 mm × 12 mm × 1.27 mm [17]. In satellite communications, S_{11} bandwidth of 80% and an AR bandwidth of 23.5% [15] and gain are stable across the operating bandwidth with a peak gain of 4.8 dB with dimensions 17.2 mm × 17.2 mm × 3.17 mm. RFID proximity-fed-slotted patch 3 dB axial ratio (AR) bandwidth of about 1.3% (917–929 MHz) and bandwidth of about 3.0% (909–937 MHz) were obtained with dimensions $0.27 \lambda \times 0.27 \lambda \times 0.013 \lambda$ at 910 MHz [10].

References

1. A. Chen et al., Development of a Ka-band wideband circularly polarized 64-element microstrip antenna array with double application of the sequential rotation feeding technique. *IEEE Antennas Wireless Propag. Lett.* **10**, 1270–1273 (2011)
2. X. Chen et al., Circularly polarized stacked annular-ring microstrip antenna with integrated feeding network for UHF RFID readers. *IEEE Antennas Wireless Propag. Lett.* **9**, 542–545 (2010)
3. O.P. Falade et al., Compact wideband circularly polarized slotted ground plane antenna for mobile terminals, in *2017 11th European Conference Antennas and Propagation (2017)*, pp. 2176–2179. <https://doi.org/10.23919/EuCAP.2017.7928826>
4. A. García-Aguilar et al., Low-profile dual circularly polarized antenna array for satellite communications in the X band. *IEEE Trans. Antennas Propag.* **60**(5), 2276–2284 (2012)
5. P.S. Hall, Application of sequential feeding to wide bandwidth, circularly polarised microstrip patch arrays. *IEE Proc. H Microw. Antennas Propag.* **136**(5), 1–9 (1989)
6. P. Janpangngern, C. Phongcharoenpanich, Circularly polarized single-fed wide-slot antenna for UHF RFID reader. **2**, 1 (2017)
7. S. Kumar et al., An improved compact MIMO antenna for wireless applications with band-notched characteristics. *AEUE Int. J. Electron. Commun.* (2018). <https://doi.org/10.1016/j.aeue.2018.04.008>
8. H. Li et al., A low-profile dual-polarized microstrip antenna array for dual-mode OAM applications. *IEEE Antennas Wireless Propag. Lett.* **16**, 3022–3025 (2017)
9. Y. Li et al., A sequential-phase feed using a circularly polarized shorted loop structure. *IEEE Trans. Antennas Propag.* **61**(3), 1443–1447 (2013)
10. Y.F. Lin et al., Proximity-fed circularly polarized slotted patch antenna for RFID handheld reader. *IEEE Trans. Antennas Propag.* **61**(10), 5283–5286 (2013). <https://doi.org/10.1109/TAP.2013.2272677>
11. T. Lines et al., A compact sequential-phase feed using uniform. *IEEE Trans. Antennas Propag.* **59**(7), 2721–2724 (2011)

12. C. Liu et al., Capacitively loaded circularly polarized implantable patch antenna for ISM band biomedical applications. *IEEE Trans. Antennas Propag.* **62**(5), 2407–2417 (2014). <https://doi.org/10.1109/TAP.2014.2307341>
13. G.Q. Luo et al., Development of low profile cavity backed crossed slot antennas for planar integration. *IEEE Trans. Antennas Propag.* **57**(10), 2972–2979 (2009)
14. A.B. Road, U.R. Llull, Slotted circularly polarized microstrip antenna for RFID application. *Radioengineering* **26**(4), 1025–1032 (2017). <https://doi.org/10.13164/re.2017.1025>
15. K.K. So et al., Miniaturized circularly polarized patch antenna with low back radiation for GPS satellite communications. *IEEE Trans. Antennas Propag.* **63**(12), 5934–5938 (2015). <https://doi.org/10.1109/TAP.2015.2488000>
16. Z.J. Yang et al., A circularly polarized implantable antenna for 2.4-GHz ISM band biomedical applications. *IEEE Antennas Wireless Propag. Lett.* **16**, 2554–2557 (2017). <https://doi.org/10.1109/LAWP.2017.2732460>
17. T. Zhang et al., Single-layer wideband circularly polarized patch antennas for Q-band applications. *IEEE Trans. Antennas Propag.* **63**(1), 409–414 (2015)

A Review of Energy Auditing on Academic Building by Using ANN and Fuzzy Logic



Purnima Sharma, Inderpreet Kaur, and Ranjit Kumar Bindal

1 Introduction

Energy (vitality) today has become a key factor in picking the thing cost at a little scale level similarly as in coordinating the growing and the commitment inconvenience at the full-scale level. It attempts to modify the total essentialness commitments with its use to perceive whole the imperativeness streams in the structures and assesses essentialness use as demonstrated by its discrete limit [1]. It is an investigation of an office, demonstrating how and where that office can decrease vitality utilization and spare vitality costs. Its understanding of vitality proficiency and preservation can prompt noteworthy investment funds on the organization's service bill [2]. Its direction would give positive outcomes in diminished vitality charging for which reasonable preventive and practical support and quality control programs are basic prompting improved generation and financial utility exercises [3].

It is a survey, inspection and assessment of vitality stream for vitality insurance in a structure, process or framework to decrease the proportion of vitality commitment to the framework without unfavorably impacting the yield [4, 5]. The different sorts of a vitality review to be performed rely on the kind of industry. It has different degrees of multifaceted nature and can shift broadly starting with one association then onto the next. It offers thinking to improve imperativeness viability and security to achieve common practicality. They are the least troublesome way to deal with the decline of ozone-draining substance releases and various kinds of air pollution, for

P. Sharma (✉) · I. Kaur · R. K. Bindal
Department of Electrical Engineering, Chandigarh University, Mohali, Punjab, India
e-mail: gaurisharma123.ps@gmail.com

I. Kaur
e-mail: inder_preet74@yahoo.com

R. K. Bindal
e-mail: ranjitbindal.eee@cumail.in

instance, destructive deluge and fumes cloud [6]. Great vitality the executives begin with a vitality review. The main types of energy audit have been discussed in paper [3] which gives the idea about how energy auditing carried out in buildings, similarly the methods which are useful for energy auditing are mentioned in [4]. Recently, under expansion is arrhythmia supervised for ambulatory patients who examine the ECG in real time [1–3]. Software QRS detectors typically include one or more of three different types of dispensation steps: linear digital filtering, nonlinear conversion, and pronouncement rule algorithms [4].

2 BMS

Building Management System (BMS) is a system that screens and controls kinds of hardware of building generally chillers, lifts, lighting, etc. In any case, it has a greater capacity to do work. By utilizing this system, we can really check the soundness of your structure, every single gear; we can proficiently utilize the assets, incorporate them in one focal programming framework and streamline the vitality devoured. Different highlights like fire-observing system, occupant charging system, prescient upkeep, and so on this System turns out to be progressively exact and solid. This system likewise helps in giving a situation according to the inhabitant's solace. The Building Management System is exceptionally simple to introduce. Building the proprietor's end, it is just the product they need to see rest is dealt with by the organization giving the arrangement however the significant choice is of which organization we ought to pick [7–9]. Building owners' innovations are all the more dominant as they enable clients to consequently misuse their full scope of adaptability in their family units.

Then again, the brilliant meter structure is presently passed on a colossal scale far and wide and up till now developing. By 2020, it is average that most phenomenal clients will have an insightful meter for power [10]. It is essential to making information-driven procedures and method for DR agenda that can mishandle this wellspring of data by utilizing noteworthy guidelines information given by the two-way correspondence possesses in the keen framework.

3 Smart Buildings

These days to decrease the radiation pace of contaminating gases and help the reliance of the electric centrality age in non-immense sources. There is a progression in the numeral of foundations of electric vitality age sources at little scales with the motivation to cover their own stand-apart use [11]. Devoured vitality examination and examination of recently led work right now, the best structure parameters were select a few times to be used as contributions to the ANN model [12]. This is a quick outcome of the reduction in costs related to the foundation of sensible force

sources, basically in the zone. This sort of age is entwined in a distributed age. The amalgamation energy performance of buildings instruction requires each and every new structure to connect with zero energy buildings before the realization of 2020. It implies that these developments, sooner rather than later, will have the option to deliver the measure of vitality they devour. There is a solid motivating force to convey sustainable power sources and methodologies for working their assets, joined with canny network information assortment to give an effective and inexhaustible structure [13]. The work created by insists that a savvy building ought to contain three primary parts: intelligent control system, a correspondence system, and robotization, which give a cutting-edge power foundation. The activity of these structures was right now basic as a well-described control of their vitality resources. The high trustworthiness of nonstop data examining can give an important decrease in building usage and power stipulate [14].

4 Learning Models Based on ANN

Artificial neural systems (ANNs) are demonstrated on the cerebrum where neurons are associated with complex examples to process information from the faculties, build up recollections, and control the body. It is a framework dependent on the activity of natural neural systems or it is additionally characterized as an imitating of the organic neural frameworks [15]. The utilization of ANNs for this work is supported by their capacity to get familiar with the mapping capacity between the information and yield with no earlier data about the issue [16]. These components change the delineation at one stage into a portrayal at a higher, and sensibly momentous level. The blend of such changes in a model can empower it to conform as far as possible [17–19]. Window to divider extent (WWR), which is the extent of the covered surface to the gross facade district, has been considered as one of the noteworthy data components to the ANN since glass addresses the most powerless warm fragment in the structure as a result of its high *U*-Value [20]. Utilized a multi-layer perception working with camouflaged layers, information and yield layers both have 24 estimations store present freely the 24-h costs and the 24-h loads [21]. Some kind of TCLs is responding to indoor temperatures in the house and to control costs. Indoor temperature in a house relies on the open-air temperatures in the past time steps, the structure protection, and the extent of essentialness spent in warming/cooling in past time steps. The extent of intensity required for TCLs can be anticipated utilizing the data of current cost and past estimations of loads and open-air temperatures [22]. A semantic assault, and cannot be notice by conventional security move toward as it neither violates procedure stipulation nor causes abnormal network traffic. Thus, security systems designed to protect IT scheme are not effectual in defending ICS [14]. This methodology can be reiterated to drearily predict a huge game plan of weights using temperatures guesses and foreseen power costs.

5 Conclusion

In this paper, this work reviews the usage of ANN and fuzzy logic is purposed up advance technology for BMS or BAS or energy auditing. In recently years, in energy conservation the main systems are used: They are BMS or BAS and smart buildings, and it furthermore helps in imperativeness cost streamlining, defilement control, prosperity points, and prescribes the procedures to improve the working and bolster arrangement of the framework. This paper shows the future scope for further improvements in research.

References

1. A. Kongara, G. Sudhakar, K. Sasank, T. Guru, A case study on energy conservation & audit for household applications. *Int. J. Adv. Res. Electr. Electron. Instrum. Eng.* **3**(4) (2014)
2. P.C. Srabana, C. Tanmoy, A. Khairul, M.D. Satadal, Reduction of EC using MES. *Int. J. Adv. Res. Electr. Electron. Instrum. Eng.* **2**(6) (2013)
3. S. Malkiat, S. Gurpreet, S. Harmandeep, EA: a case study to reduce lighting cost. *Asian J. Comput. Sci. Inf. Technol.* (2012)
4. S. Gousia, H.U. Harsha, EEA a case study. *IOSR J. EEE* **10**(3), 01–06 (2015)
5. W. Lee, R. Kenarangui, Energy management for ES, and electrical equipment. *IEEE Trans. Ind. Appl.* **38**(2), 602–607 (2002)
6. P.S. Hamer, D.M. Lowe, S.E. Wallace, Energy efficient IM performance characteristics and life cycle cost comparisons for centrifugal loads. *IEEE Trans. Ind. Appl.* **33**(5), 1312–1320 (1997)
7. L. Pacholski, P. Pawlewski, The usage of simulation technology for macroergonomic IS improvement, in *Advances in Social & OE*, ed. by R.H.M. Goossens. *Advances in IS and Computing*, vol. 487 (Springer International Publishing, Cham, 2017), pp. 3–14
8. Energy—European Commission, *Smart Grids and Meters*. <https://ec.europa.eu/energy/en/topics/markets-and-consumers/smart-grids-and-meters>. Accessed 13th 2019
9. A. Khotanzad, E. Zhou, H. Elragal, A neuro-fuzzy approach to short-term load forecasting in a price-sensitive environment. *IEEE Trans. Power Syst.* **17**(4), 1273–1282 (2002)
10. Z. Yun, Z. Quan, S. Caixin, L. Shaolan, L. Yuming, S. Yang, RBF NN and ANFIS-based short-term load forecasting approach in real-time price environment. *IEEE Trans. Power Syst.* **23**(3), 853–858 (2008)
11. K.B. Ranjit, K. Inderpreet, Performance of 3 phase IM of DTC using fuzzy logic controller. *Int. J. Pure Appl. Math.* **118**(19), 159–175 (2018). (Scopus Indexed) ISSN No. 1311-8080
12. K.B. Ranjit, K. Inderpreet, To improve a performance of IM using PBO-ANFIS. *Int. J. Eng. Technol.* **7**(4.39), 649–654 (2018). (Scopus indexed) ISSN No. 2227-524X
13. K.B. Ranjit, K. Inderpreet, Comparative analysis of different controlling techniques using DTC on IM, in *2nd IEEE International Conference on Next Generation CT (NGCT-2016)*, Dehradun, India (2016), pp. 191–196. ISBN No. 978-1-5090-3257-0
14. K.B. Ranjit, K. Inderpreet, To enhance the performance of 3 phase IM using fuzzy logic controller with DTC. *Int. J. Comput. DS* (2018). (Scopus Indexed). ISSN No. 2210-142X
15. J.S. Gallego, J.M. Morales, Short-term forecasting of price-responsive loads using inverse optimization. *IEEE Trans. Smart Grid* **9**(5), 4805–4814 (2017)
16. J.S. Gallego, J.M. Morales, M. Zugno, M. Henrik, A data-driven bidding model for a cluster of price-responsive consumers of electricity. *IEEE Trans. Power Syst.* **31**(6), 5001–5011 (2016)
17. A. Motamedi, H. Zareipour, W.D. Rosehart, Electricity price and demand forecasting in smart grids, *IEEE Trans. Smart Grid* **3**(2), 664–674 (2012)

18. V. Gómez, M. Chertkov, S. Backhaus, H.J. Kappen, Learning price-elasticity of smart consumers in PDS, in *Proceedings of the IEEE Third International Conference on SGC* (2012), pp. 647–652
19. J. Soares, T. Pinto, F. Lezama, E.H. Morais, Survey on complex optimization and simulation for the new power systems paradigm. *Complexity* **2018**, 32 (2018)
20. J.M. Sallan, O. Lordan, E.H. Fernandez, *Modeling and Solving Linear Programming with R* (Omnia Science, Catalunya, 2015)
21. K.B. Ranjit, K. Inderpreet, Speed and torque control of induction motor using adaptive neuro-fuzzy interference system with DTC, in *ICAICR 2018*. Springer (CCIS) Series, CCIS 955, pp. 815–825 (Scopus Indexed) ISSN No. 1865-0929 (2019)
22. K.B. Ranjit, K. Inderpreet, Torque ripple reduction of IM with DTC and PI controller. *J. Adv. Res. Dyn. Control Syst.* **10**(14), 540–546 (2018). (Scopus indexed) ISSN No. 1943023X

Fractional-Order Extremum Seeking MPPT for Photovoltaic System



Padimi Sri Venkata Satish, Yellapu Manikanta Swamy,
Ch Uma Phanendra Kumar, and K. Manoz Kumar Reddy

1 Introduction

Photovoltaic system are widely adopted to generate electricity all over the world. The photovoltaic cell produces electricity from sunlight. When the solar irradiance (W/m^2) and ambient temperature ($^{\circ}\text{C}$) changes, PV voltage and current changes. Therefore, MPPT system are required to extract maximum power from PV source [13]. Extremum seeking PV MPPT system has been discussed in [5, 6]. Fractional order extremum seeking MPPT has been discussed in [14]. Degradation detection of PV system using extremum seeking has been discussed in [3]. Extremum seeking MPPT for fuel cell has been discussed in [8]. Stability analysis of extremum seeking principle is discussed in [9]. Adaptive extremum seeking has been discussed in [7]. Multivariable extremum seeking MPPT has been discussed in [1]. Different converter topologies have been discussed in [11, 12]. DC-microgrid based PV system [4] and partial shading detection for PV system has been discussed in [2, 10].

P. S. Venkata Satish · Y. Manikanta Swamy · C. U. Phanendra Kumar ·
K. Manoz Kumar Reddy (✉)

Department of Electrical and Electronics Engineering, Aditya College of Engineering,
Surampalem, Andhra Pradesh, India
e-mail: manozreddy111@gmail.com

P. S. Venkata Satish
e-mail: satishpadimi@gmail.com

Y. Manikanta Swamy
e-mail: yellapumanikanta4@gmail.com

C. U. Phanendra Kumar
e-mail: chaturvedula_eee@acoe.edu.in

This paper provides the concept and simulation results for extremum seeking MPPT for PV based system.

2 Photovoltaic System

Figure 1 illustrates PV based MPPT system where extremum seeking MPPT scheme is used. Different extremum seeking MPPT such as integer order extremum seeking and fractional order extremum seeking MPPT has been implemented and comparative analysis has been made.

2.1 PV Module

$$I_{pv} = \left(I_{pv}^r + k_i (T - T_r) \right) \left(\frac{S}{1000} \right) \tag{1}$$

where I_{pv}^r refers to reference short-circuit current, T_r refers to reference temperature, k_i refers to short-circuit temperature coefficient, S is the solar irradiance (Fig. 2).

The I - V characteristics of diode is represented as

$$I_d = I_0 \left(\exp \left(\frac{V_D}{NV_t} \right) - 1 \right) \tag{2}$$

$$I_0 = I_0^r \left(\frac{T}{T_r} \right)^3 \exp \left(\frac{E_g}{NV_t} \left(\frac{T}{T_r} - 1 \right) \right) \tag{3}$$

Fig. 1 Block diagram of PV based MPPT system

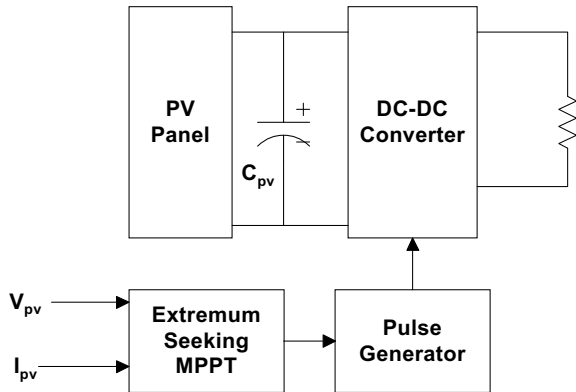
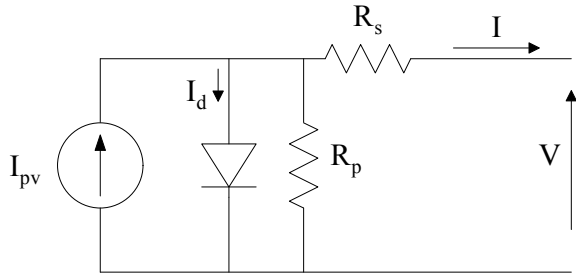


Fig. 2 Single-diode electrical equivalent circuit of an ideal PV cell



where E_g refers to semiconductor bandgap voltage, N is the emission coefficient. The thermal cell voltage can be computed as $V_t = \frac{kT}{q}$ where k is the Boltzman's Constant and q denotes the charge of electron

The I - V relationship between PV cell can be represented as

$$I = I_{ph} - I_0 \left(\exp \left(\frac{\frac{V}{N_s} + R_s I}{N V_t} \right) - 1 \right) - \left(\frac{\frac{V}{N_s} + R_s I}{R_p} \right) \tag{4}$$

2.2 Extremum Seeking Scheme

$$a : \left. \frac{dx}{dt} \right|_{t=t^-} > 0, \left. \frac{dy}{dt} \right|_{t=t^-} > 0 \Rightarrow \left. \frac{dx}{dt} \right|_{t=t^+} = k \tag{5}$$

$$b : \left. \frac{dx}{dt} \right|_{t=t^-} > 0, \left. \frac{dy}{dt} \right|_{t=t^-} < 0 \Rightarrow \left. \frac{dx}{dt} \right|_{t=t^+} = -k \tag{6}$$

$$c : \left. \frac{dx}{dt} \right|_{t=t^-} < 0, \left. \frac{dy}{dt} \right|_{t=t^-} > 0 \Rightarrow \left. \frac{dx}{dt} \right|_{t=t^+} = k \tag{7}$$

$$d : \left. \frac{dx}{dt} \right|_{t=t^-} < 0, \left. \frac{dy}{dt} \right|_{t=t^-} < 0 \Rightarrow \left. \frac{dx}{dt} \right|_{t=t^+} = k \tag{8}$$

2.3 Fractional-Order Extremum Seeking Scheme

In fractional-order calculus ${}_a D_t^\alpha$ denotes the generalization of integration and differentiation to an arbitrary order differ-integral operator which can be defined as

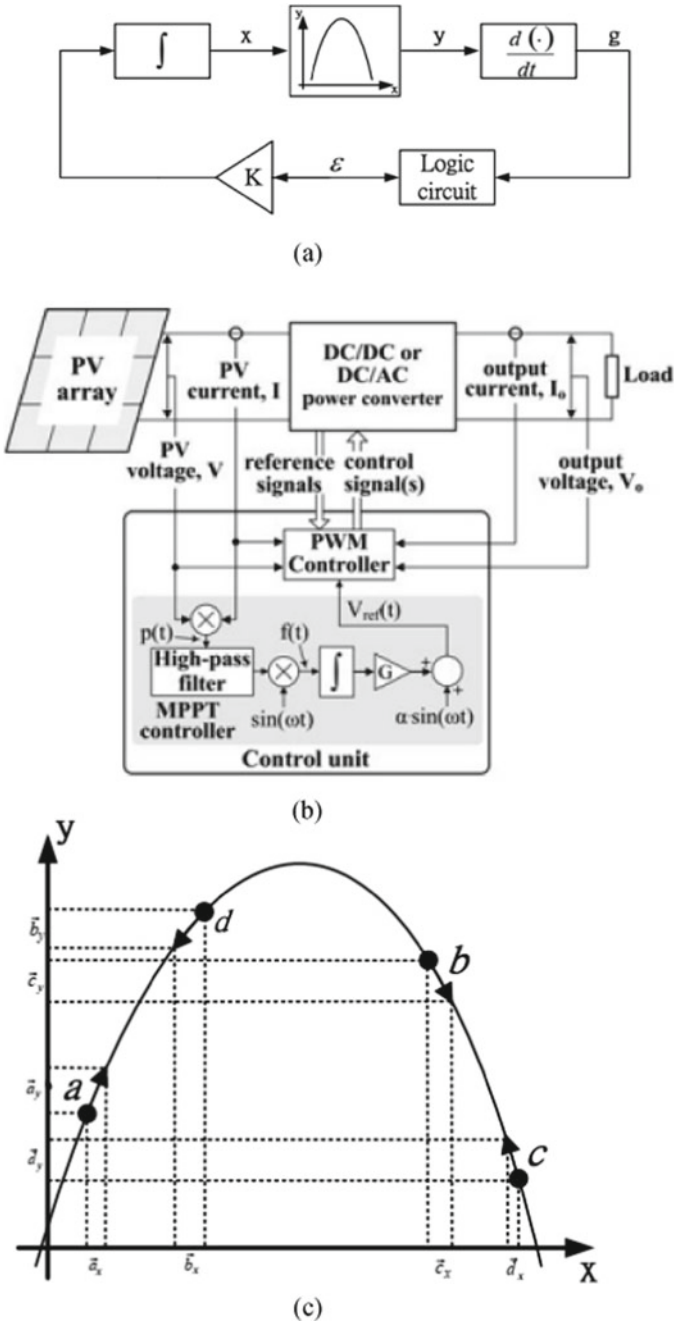


Fig. 3 Extremum seeking scheme. **a** General scheme, **b** PV-based extremum seeking MPPT, **c** dynamics of extremum seeking MPPT

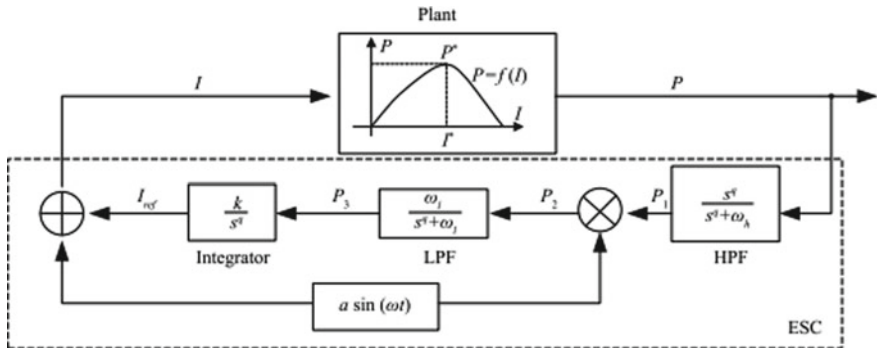


Fig. 4 Block diagram of fractional-order extremum seeking MPPT

$${}_a D_t^\alpha = \begin{cases} \frac{d^\alpha}{dt^\alpha} & \alpha > 0 \\ 1 & \alpha = 0 \\ \int_0^t (d\tau)^{-\alpha} & \alpha < 0 \end{cases} \quad (9)$$

Riemann-Liouville definition for fractional differintegral can be represented as

$${}_a D_t^\alpha f(t) = \frac{1}{\Gamma(m - \alpha)} \left(\frac{d}{dt}\right)^m \int_a^t \frac{f(\tau)}{(t - \tau)^{1-(m-\alpha)}} d\tau \quad (10)$$

for $m - 1 < \alpha < m$ where $\Gamma(\cdot)$ is the Euler's gamma function (Fig. 3).

According to Grunwald-Letnikov definition, a fractional differintegral can be represented as (Fig. 4)

$${}_a D_t^\alpha f(t) = \lim_{h \rightarrow 0} \frac{1}{\Gamma(\alpha) h^\alpha} \sum_{k=0}^{\frac{t-a}{h}} \frac{\Gamma(\alpha + k)}{\Gamma(k + 1)} f(t - kh) \quad (11)$$

3 Simulation Results

Let us consider a MSX-60 PV module with specification such as $P_{mp} = 60 \text{ W}$, $V_{mp} = 17.1 \text{ V}$, $I_{mp} = 3.5 \text{ A}$, $P_{min} = 58 \text{ W}$, $I_{sc} = 3.8 \text{ A}$ and $V_{oc} = 21.1 \text{ V}$ (Figs. 5, 6 and 7)

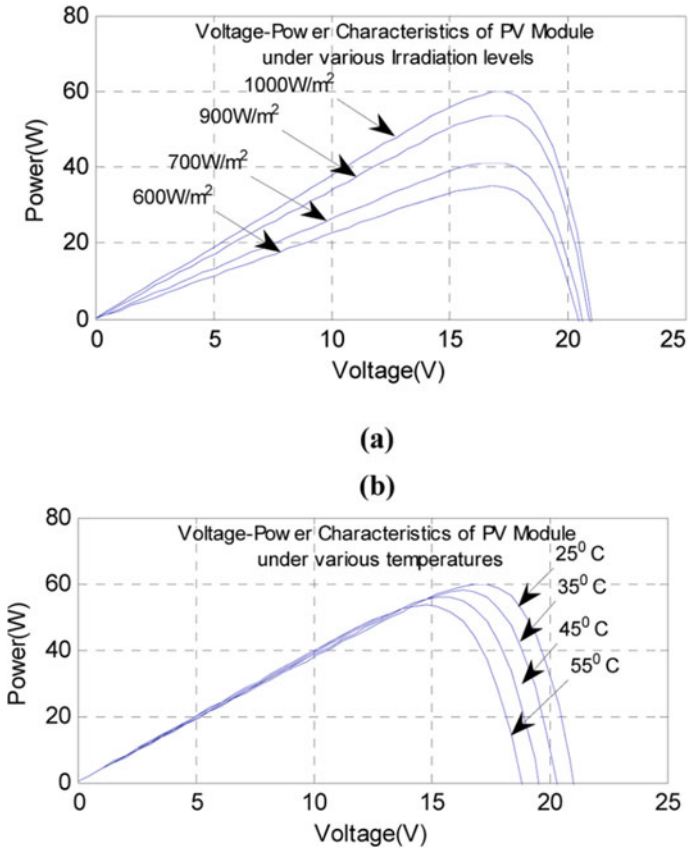


Fig. 5 P-V and V-I characteristics of MSX-60

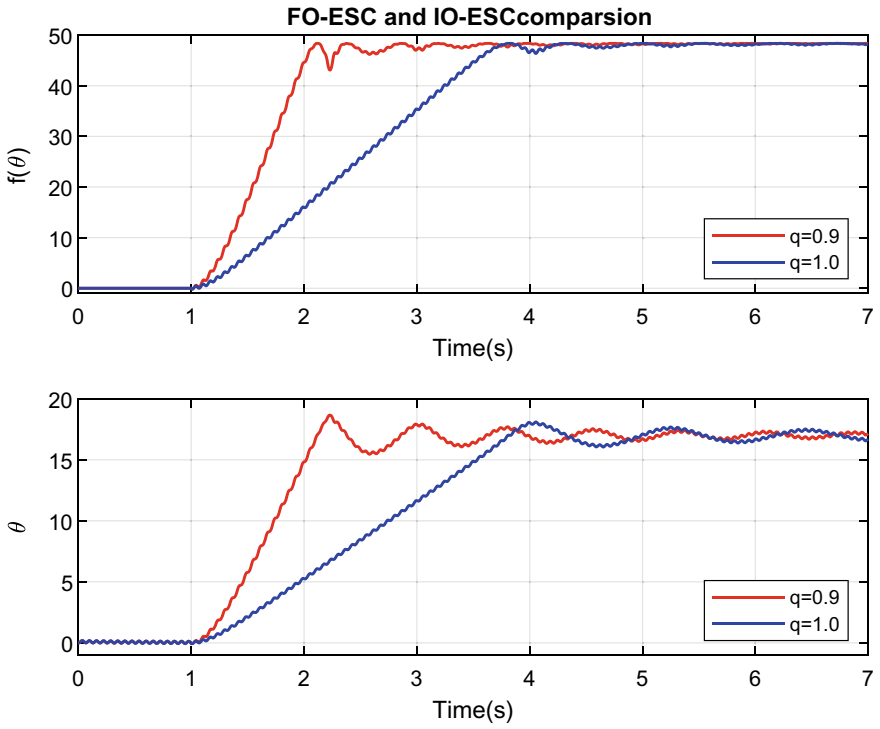
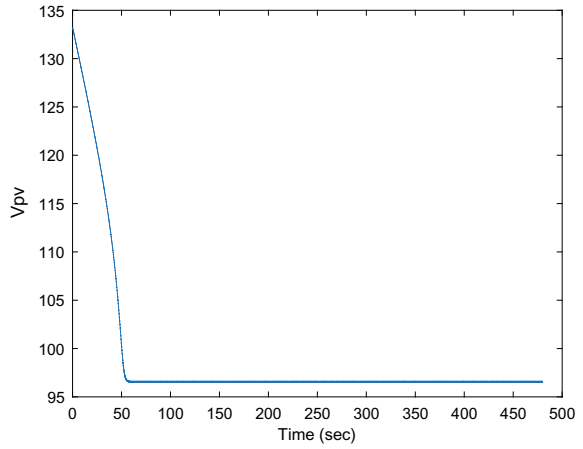
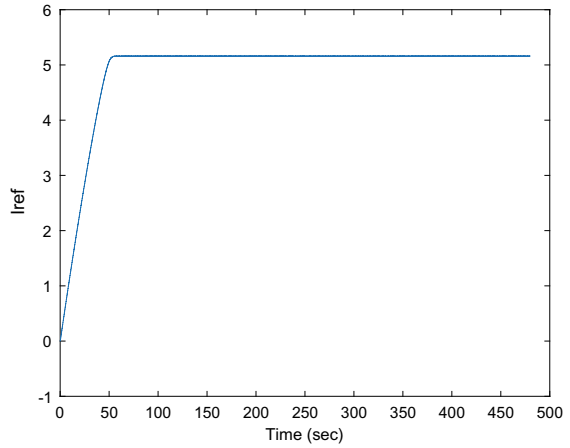


Fig. 6 Comparative analysis of FO-ESC and IO-ESC

Fig. 7 Extremum seeking scheme. **a** Voltage, **b** current



(a)



(b)

4 Conclusion

This paper provides theoretical and simulation results for extremum seeking MPPT for photovoltaic system. Extremum seeking is an optimization based control scheme which can be used in photovoltaic system. Extremum seeking MPPT have many versions such as integer-order and fractional-order. This MPPT shows better performance than other MPPT.

Acknowledgements The authors are thankful to Accendere Knowledge Management Services Pvt. Ltd, CL Educate Ltd for their assistance during the preparation of the manuscript.

References

1. A. Ghaffari, S. Seshagiri, M. Krstić, Multivariable maximum power point tracking for photovoltaic micro-converters using extremum seeking. *Control Eng. Pract.* **35**, 83–91 (2015)
2. K. Giandrasekaran, A. Venkadesan, M. Mohanty, S. Sankar, Tracking the global maximum operating point under a psc using cluster gravitational search algorithm, in *2017 International Conference on Innovative Research In Electrical Sciences (IICIRES)* (IEEE, 2017), pp. 1–6
3. R. Hariharan, M. Chakkarapani, G.S. Ilango, C. Nagamani, Degradation detection of PV arrays using extremum-seeking control based MPPT, in *2016 National Power Systems Conference (NPSC)* (IEEE, 2016), pp. 1–5
4. G.B. Ingale, S. Padhee, U.C. Pati, Design of stand alone PV system for dc-micro grid, in *2016 International Conference on Energy Efficient Technologies for Sustainability (ICEETS)* (IEEE, 2016), pp. 775–780
5. R. Leyva, C. Alonso, I. Queinnec, A. Cid-Pastor, D. Lagrange, L. Martinez-Salamero, Mppt of photovoltaic systems using extremum-seeking control. *IEEE Trans. Aerosp. Electron. Syst.* **42**(1), 249–258 (2006)
6. R. Leyva, C. Olalla, H. Zazo, C. Cabal, A. Cid-Pastor, I. Queinnec, C. Alonso, MPPT based on sinusoidal extremum-seeking control in PV generation. *Int. J. Photoenergy* **2012** (2012)
7. X. Li, Y. Li, J.E. Seem, Maximum power point tracking for photovoltaic system using adaptive extremum seeking control. *IEEE Trans. Control Syst. Technol.* **21**(6), 2315–2322 (2012)
8. J. Liu, T. Zhao, Y. Chen, Maximum power point tracking with fractional order high pass filter for proton exchange membrane fuel cell. *IEEE/CAA J. Autom. Sin.* **4**(1), 70–79 (2017)
9. H. Malek, Y. Chen, Fractional order extremum seeking control: performance and stability analysis. *IEEE/ASME Trans. Mechatron.* **21**(3), 1620–1628 (2016)
10. M. Mohanty, S. Selvakumar, C. Koodalsamy, S.P. Simon, Global maximum operating point tracking for pv system using fast convergence firefly algorithm. *Turkish J. Electr. Eng. Comput. Sci.* **27**(6), 4640–4658 (2019)
11. S. Padhee, U.C. Pati, K. Mahapatra, Comparative analysis of dc-dc converter topologies for fuel cell based application, in *2016 IEEE 1st International Conference on Power Electronics, Intelligent Control and Energy Systems (ICPEICES)* (IEEE, 2016), pp. 1–6
12. S. Padhee, U.C. Pati, K. Mahapatra, Overview of high-step-up dc-dc converters for renewable energy sources. *IETE Tech. Rev.* **35**(1), 99–115 (2018)
13. S. Selvakumar, M. Madhusmita, C. Koodalsamy, S.P. Simon, Y.R. Sood, High-speed maximum power point tracking module for pv systems. *IEEE Trans. Ind. Electron.* **66**(2), 1119–1129 (2018)
14. C. Yin, Y. Chen, B. Stark, S.M. Zhong, Extremum seeking control with fractional-order switching technique design for maximum power point tracking in photovoltaic systems, in *2015 54th IEEE Conference on Decision and Control (CDC)* (IEEE, 2015), pp. 5629–5634

An Operator-Controlled Incentive Distribution Model for Device Relaying D2D Communication



Koushik Barman and Ajay Roy

1 Introduction

Cellular communication is now at initial stage of fifth generation. Fulfillment of increasing demand of data rate, low latency, and high reliability is now main concern of research. Device-to-device communication is defined as the direct interaction among devices using licensed spectrum or unlicensed band spectrum. There will be twenty billion devices connected through the Internet within 2020. These devices will communicate among themselves by means of licensed and unlicensed band spectrum with ultra-high reliability (rate of packet drop $<10^{-5}$) [1]. In traditional cellular network, UEs communicate through base station but in D2D, two UEs or multiple UEs communicate directly among themselves. D2D communication may be classified into two categories. Inband D2D describes the scenario where mobile UE utilizes cellular spectrum to establish D2D link and cellular link. Outbound D2D is another type of D2D communication where interaction among UEs accomplished using unlicensed band (ISM band) [2]. Underlay inbound D2D allows to reuse time-frequency resource block among D2D links and cellular links which introduce interference to the existing cellular users. Intracellular interference limits D2D communication. Figure 1 shows classification of D2D communication. Device discovery and service discovery mechanism will play significant role in future cellular network due to versatile applications. It ensures availability of devices nearby which can communicate and provide context-aware services and social emergency services. Third-Generation Partnership Project, a renowned organization of regularization, has published several technical reports related to the standardization process of D2D communication [3].

K. Barman (✉) · A. Roy
Lovely Professional University, Phagwara, Punjab, India
e-mail: koushik.15737@lpu.co.in

A. Roy
e-mail: ajoy.22652@lpu.co.in

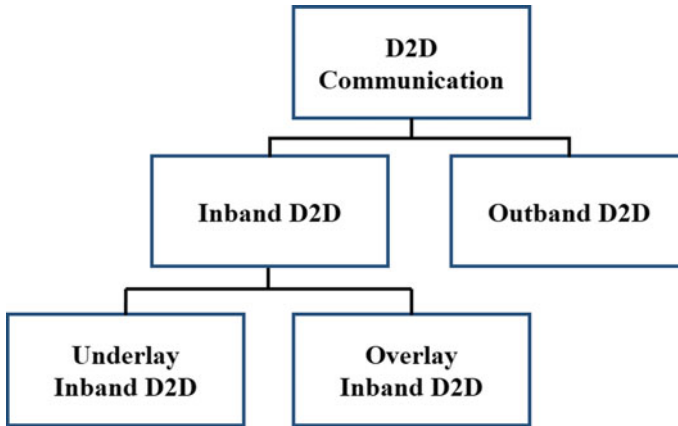


Fig. 1 D2D link scenarios in two-tier cellular network

Proximity services using license band spectrum have been introduced in a technical report (3GPP TR22.803) of 3GPP in June 2013. The report was named as ‘Feasibility Study for Proximity Services (Prose)’ [4]. This report describes technical feasibility requirements of mobile UEs under LTE-A for commercial (e.g., discovery/social networks), network offloading, and public safety applications [5]. In this report, thirteen general use cases and thirteen public safety use cases have been recognized in D2D communication scenario. This is serious challenge for operator to implement a proper model of pricing for D2D services. In traditional cellular communication, there is no such pricing model where incentives will be awarded to the device which acts as already to provide D2D service to neighbor devices.

Designing of appropriate pricing model for D2D services depends on mode of operation and D2D scenario. Device under cellular coverage may act as a relay device and provide D2D communication to other devices which are out of cellular coverage. This type of D2D scenario is known as operator control device relaying [6]. Pricing of D2D service depends on various factors like channel throughput signal-to-noise ratio and D2D scenario. Operator must address that how they control and charge for device-to-device (D2D). There must be an option that if charged for D2D services, the customer has to switch to traditional fee device-to-device services [6]. In that case, they need to be satisfied with lesser speed and no guarantee of security threats. The customers must be asked to pay for what they can push forward the operator-controlled D2D technology that needs extensive analysis of usage cases and business models. In this article, main focus has been given to illustrate pricing models for D2D scenarios. These models are definitely able to fulfill user’s expectation and increase the demand of D2D communication.

2 Two-Tier Network Architecture

In most of the literature, two-tier network architecture has been considered for the analysis of pricing strategies [4–6]. Tier-I provides traditional cellular architecture where communication between two devices takes place through the base station, whereas Tier-II provides the architecture for direct communication among devices. There are four possible ways in Tier-II for establishing D2D communication. Figure 2 illustrates all four communication strategies.

2.1 Operator-Controlled Device Relaying

In this architecture, a device at poor cell coverage area communicates with the base station through other device which acts as a relay node. In Fig. 2, UE-A acts as a relay device which relays signal to UE-B and UE-C. This allows for the device to accomplish a higher quality of service. In this case, network operator communicates with relaying device and establish D2D link with partial or full control. Operator will provide incentives to the relay device when it allows other devices to share its bandwidth for establishing D2D communication link.

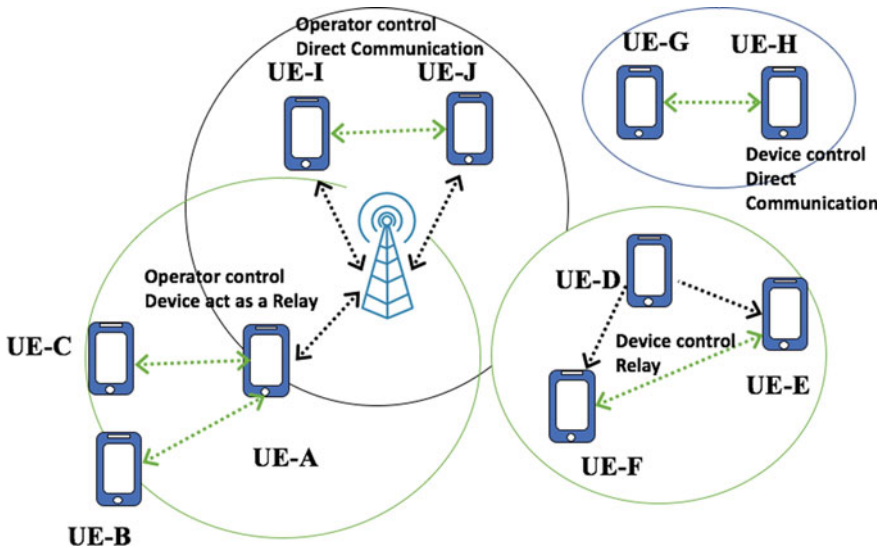


Fig. 2 D2D link scenarios in two-tier cellular network

2.2 Device-Controlled Device Relaying

In this scenario, network operator does not assist the relay node. In Fig. 2, UE-D, UE-E, and UE-F are out of coverage of base station. In this case, they use unlicensed spectrum like Wi-Fi, Bluetooth, etc. for establishing D2D link. This architecture is known as device-controlled device relaying.

2.3 Device-Controlled Direct Communication

In Fig. 2, UE-G and UE-H are directly communicating with each other without operator's support. Network operator has no role to play for D2D connection establishment. Sharing of resources and pricing is independent of network operator. This type of D2D communication scenario is known as device-controlled direct communication. In this kind of scenario, mobile user may consider different types of pricing approaches such as cooperative-game-theory-based approach and bargaining-game-theory-based approach or double-auction-based technique as mentioned in [7-9].

2.4 Operator-Controlled Direct Communication

In Fig. 2, UE-I and UE-J are communicating with each other with operator's support. In this case, both UEs are under the coverage of cellular network. Spectrum sharing, connection establishment, and pricing strategies depend on network operator. In this scenario, two UEs directly communicate, but do not work as a relay device. Operator controls and helps to establish the D2D link. In this case, pricing model will be based on spectrum trading concept. Spectrum trading is defined as to participate in buying and selling of spectrum. Sellers' viewpoint is to gain maximum profit by selling the available spectrum, whereas buyer's condition is to get maximum bandwidth in minimum price. This creates conflict of interest. Buyer and seller may not agree to construct a successful deal. This kind of problem can be solved by auction theory. It offers a convenient framework of arithmetic outfits for appropriate design of price estimating model.

3 Analysis of Pricing Scheme for Operator-Controlled Device Relaying Architecture

In this section, we have analyzed a pricing model for operator-controlled device relaying architecture. In Fig. 3, UE-A acts as a relay device which relays signal

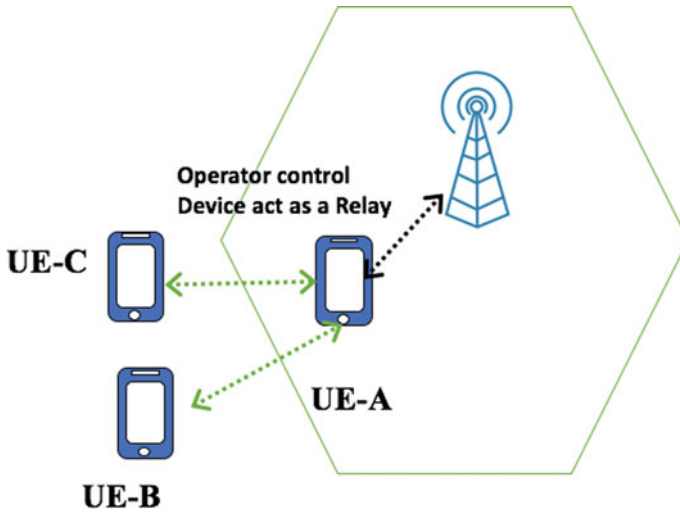


Fig. 3 D2D link scenarios in two-tier cellular network

power to UE-B and UE-C. Base station provides incentives to UE-A because UE-A shares available spectrum to UE-B and UE-C. Operator may provide discount on monthly bill of UE-A or provide some free services to UE-A as a part of incentives. Let U is the utility function defined as [10],

$$U = B \log_2(1 + k\gamma) - MBP + B \log_2(1 + k\bar{\gamma}) \tag{1}$$

Here, B is the BS to UE-A link bandwidth. k is defined as spectral efficiency. γ is signal-to-noise ratio. The first term of this equation, e.g., $B \log_2(1 + k\gamma)$ provides the revenue of UE-A. Second term of the equation, e.g., MBP describes the charges that need to pay to the operator. M is defined as total number of hops between BS and relay node. In this scenario, M is 1 because BS is directly connected to UE-A which is relay node. The third term of Eq. (1), e.g., $B \log_2(1 + k\bar{\gamma})$ describes the incentive awarded to UE-A for acting as a relay node. In this scenario, operator's revenue is calculated as,

$$R = \sum_{i=1}^N MB_i P_i - M\bar{B} \log_2(1 + k\bar{\gamma}) \tag{2}$$

Here \bar{B} is the awarded bandwidth to the relay node as a part of incentives.

4 Simulation Result

For the simulation, let us consider a fixed pricing scheme is provided by the operator for sharing resource spectrum. If any relay node shares spectrum to the other user equipment, then operator provides incentives in the form of free spectrum awarded to that relaying node. Let total no of devices served by the operator is $N = 2$. Let us assume B_i is 5 MHz, spectral efficiency K is 0.2, and SNR range γ_i is 5–25 dB. For the awarded spectrum to the relaying node, bandwidth is 2.5 MHz, SNR is 2.5–12.5 dB, and unit price of spectrum (p_i) is 1.2. Figure 4a shows device's revenue in operator-controlled device relay scenario for SNR range of 5 to 25 dB, whereas Fig. 4b shows operators revenue in operator-controlled device relay scenario. Results illustrate a comparative analysis of device's revenue and operator's revenue in normal cellular network and operator assist device to device network. It is clearly shown that device revenue and operator's revenue increase drastically in D2D scenario when number of user increases.

5 Conclusion

This paper investigated pricing model for operator-controlled device relaying D2D communication. Operations' revenue and device's revenue have been analyzed for a specific range of signal-to-noise ratio under three different conditions, e.g., two-tier operator-controlled device relay (OC-DR), normal cellular operation, and OC-DR with increase value of UEs. Operator's revenue increases with increasing no of UEs. The pricing model is suitable for resource sharing in two-tier cellular network, e.g., cellular tier and D2D tier. There is 'win-win' situation for operator and relay device because operator will get benefit from more revenue generation as operator is serving more number of users. On the other hand, a relay device is awarded incentives in terms of additional services and bandwidth from the operator for sharing its bandwidth with other users.

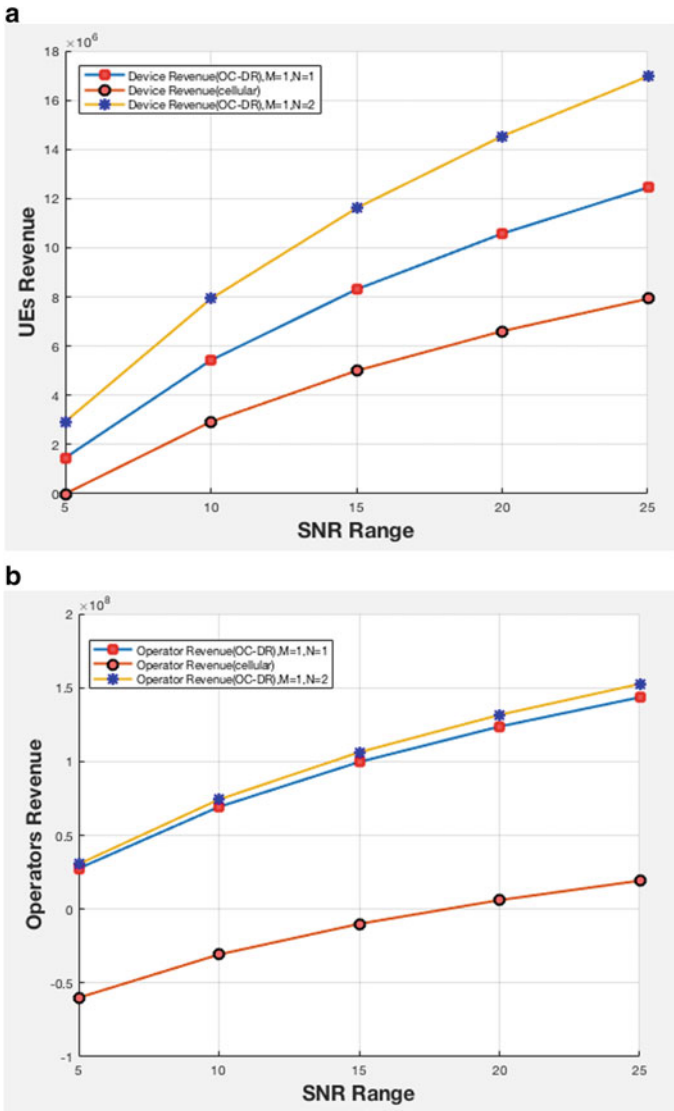


Fig. 4 **a** Device’s revenue in operator-controlled device relay scenario. **b** Operators revenue in operator-controlled device relay scenario

References

1. A. Gupta, R.K. Jha, A survey of 5G network: architecture and emerging technologies. *IEEE Access* **3**, 1206–1232 (2015)
2. M. Haus, M. Waqas, A.Y. Ding, Y. Li, S. Tarkoma, J. Ott, Security and privacy in Device-to-Device (D2D) communication: a review. *IEEE Commun. Surv. Tutor.* **19**, 1054–1079 (2017)

3. C. Hoymann, W. Chen, J. Montojo, A. Golitschek, C. Koutsimanis, X. Shen, Relaying operation in 3GPP LTE: challenges and solutions. *IEEE Commun. Mag.* **3**, 156–162 (2012)
4. A. Prasad, A. Kunz, G. Velev, K. Samdanis, J. Song, Energy-efficient D2D discovery for proximity services in 3GPP LTE-advanced networks: ProSe discovery mechanisms. *IEEE Veh. Technol.* **9**, 40–50 (2014)
5. U.N. Kar, D.K. Sanyal, An overview of device-to-device communication in cellular networks. *ICT Express* **4**, 203–208 (2018)
6. M. Tehrani, M. Uysa, H. Yanikomeroglu, Device-to-device communication in 5G cellular networks: challenges, solutions, and future directions. *IEEE Commun. Mag.* 86–92 (2014)
7. K. Zhu, E. Hossain, D. Niyato, Pricing, spectrum sharing, and service selection in two-tier small cell networks: a hierarchical dynamic game approach. *IEEE Trans. Mob. Comput.* **13**, 1843–1856 (2014)
8. D. Kumar D. Manjunath, J. Nair, Spectrum sharing: how much to give, in 8th *International Conference on Communication Systems and Networks, COMSNETS*, India (2016)
9. A. Perrig, J. Stankovic, D. Wagner, Security in wireless sensor networks. *Commun. ACM* **47**, 53–57 (2004)
10. E. Hossain, D. Niyato, Z. Han, *Dynamic Spectrum Access and Management in Cognitive Radio Networks* (Cambridge University Press, UK, 2009)

Error Correction Code: Study, Challenges, and Applications



V. Vydehi, A. Lishitha, G. Pranathi, N. V. Satyanarayana,
and Durgesh Nandan

1 Introduction

Several localized burst errors are proposed. Various types of codes present in this have been used to make better the codes developed by Larsson in size, which makes the decoding and encoding process more complex, i.e., in a slight decrease value. Similar to the Larsson codes, the developed codes are also asymptotically best possible. At the point when the number of errors to be rectified is fixed and the length of the error to be revised, it increases in like manner with the code length. Other than the Larsson codes, the suggested codes of the errors are minimized when the number of errors to be accurate and the correctable burst span are both fixed [15].

In this system of digital audio broadcasting (DAB), the CD quality multi-directional audio is proposed and checked for the frequency modulation band. The strategy implemented is a hybrid in-band on-channel (HIBOC) system, where the digital broadcast is in unison with the analog frequency modulation broadcast. This stage is a change to a digital structure. We apply a convolutional code which is added to an error identifying block code [5].

V. Vydehi · A. Lishitha · G. Pranathi · N. V. Satyanarayana
Department of ECE, Aditya Engineering College, Surampalem, Andhra Pradesh, India
e-mail: vydehi2610@gmail.com

A. Lishitha
e-mail: ambatilishitha2001@gmail.com

G. Pranathi
e-mail: saipranathi18@gmail.com

N. V. Satyanarayana
e-mail: satyanarayana.nv@aec.edu.in

Durgesh Nandan (✉)
Accendere Knowledge Management Services Pvt. Ltd, CL Educate Ltd., New Delhi, India
e-mail: durgeshnandano51@gmail.com

Some of the standard video codes like H.263 contain variable length codes (VLC'S). H.263 is a discrete cosine transform (PCT) which is a coded bitstream that produces a single-bit error because of the use of variable length codes. These are used for compressing and decompressing the given data with zero errors and also it can transmit lossless information. We can also use Huffman for further compression. The decoding process does not start until the synchronization point is reached. In case there is a failure of bringing together between the encoder and decoder states, there is a possibility of error generation [12].

During the data broadcast storage, the accepted data is not the equivalent as the transmitted data, which gives the result in the noise and interference. This goes ahead to a data transmission error. To avoid this problem, we will use some check methods in the data transmission process. These methods can be parity check, cyclic redundancy checks (CRC), etc. The multiple bit errors can be corrected using cyclic redundancy check codes [22]. In order to avoid errors, we can do a backup to a message so that the receiver can check the continuity of the delivered message, by this the data can be recovered. Error detection proposals are of two types, i.e., systematic and non-systematic. In the systematic method, the unique data is sent through a transmitter along with the fixed number of check bits. It shows an error at the receiver end of the transmitted data and the received data bits do not match with each other [19]. Reliability is the one that is considered for space applications. In an electronic system, memory plays a major role in storing data. They are basically used in the electronic systems which are integrated on a chip. They can be used for specific space applications. They occupy a larger portion in the circuit area. There is also a radiation effect on other components which varies the message [14]. Traditional single-cell upsets (SCUs) have a vast impact on multiple cell upsets (MCU) which has parallel errors in more than one cell. When code length increases, the burst error also increases [4, 21]. The multiple cell upsets (MCU) problems which are occurred in space applications have to be considered to identify the fault tolerance methods. It is because of the aggressive environment formed due to the high-energy cosmic particles [2, 9, 10, 20].

In this paper, a detailed study of error correction codes is done. Literature review has been made in this Sect. 2. The design approach has been explored in Sect. 3. Results based on prior publications are given in Sect. 4. Various applications have been analyzed in Sect. 5. Finally, conclusions have been done in Sect. 6.

2 Literature Work

Mardjuadi et al. [15] general concepts on encoder and decoder have been explained here. It involves wide applications in mobile communications and storage areas [15]. Chen and Sundberg [5] Viterbi algorithm will increase the standard of the received signal by reducing the chances of error mitigation flags [5]. (Khan et al. [12]) A bit-by-bit correction has been suggested. The decoding time rises accordingly using the increase in channel bit error rate (BER) [12]. (Chen et al. [6]) Comparing to

various broadband methods, the presented LNA has some of the benefits like less complexity of the design, high-frequency noise is small, power dissipation is also little, and size is small [6]. (Zhang [22]) A CRC codes with the principle of error correction and code realization process; whereas, the simulation shows the several bits error correction method can develop the BER and FER [22].

Mavis et al. [16] contributions that are made by the number of bits upset by a singly element strike are also used to find the aware vital volume and a block-based architecture have been well explained [16]. (Chye et al. [17]) Different feedback resistive technique was implemented. The wideband and low-power applications are also implemented here [17].

Correas et al. [7] various tools have been used based on TCAD and SPICE simulation. Different techniques have been implemented [7]. In 2012, the realization techniques for error correction and detection are explained. The several bits of error identification and correction by way of the Reed–Muller algorithm technique will get better the BER and PER efficiently [19]. In [13]. Two error correction coding (ECC) schemes are used here. The channel coding will enhance the strength of spatial image watermarks beside JPEG DCT-supported compression. HECC error detecting code executes according to the pixel correct probabilities of VECC. (Sadia et al. [1]) In space applications, DDR memory is used for storing information. It is subjected to unlike errors, and these are sourced by several outside influences as solar emissions, electromagnetic emissions, space noise, and extreme temperature in space. This will destroy the memory stored in the DDR memory. Techniques of error detection will permit checks and useful in correction of these errors, and reconstruction of the original data is done due to error correction techniques. This technique enables the dependable escape of digital data compared to an undependable communication channel. A comparative analysis of various error detection and correction schemes for space applications is explained [1]. Marzieh and Hossein [18] have presented the mixer without network. A reduction or noise penalty has been explained. However, in the existence of the network, the mixer displays up to 25 and 7 dB progresses in IIP2 and IIP3, correspondingly. The bandwidth, gain, and noise-figure are too developed [18].

Fang and Anthony [8] in this, the errors are given alpha particles and warm neutrons. In any case, the relative event of single-occasion upsets is finished up at first by the defenseless area of the channel of bit cell transistors. It indicates that Fin-FET displays a significant decrease in MCU probabilities [8]. Li et al. [14] disclose to us that the gear sizes with the cell interim separation will diminish and the quantity of influenced bits can without much of a stretch reach out to more than three pieces. It would not require any additional equality check bits assessed with a three-piece BEC code [14]. (Kato [11]) Single-occasion upsets prompted by various cell charge ages are examined and SRAM by directing laser illumination tests. The quantity of bomb bits and its physical topology has been breaking down plainly [11].

Joaquín in 2018 is presented in Matrix codes, which will use Hamming codes as well as parity, verify within a bidimensional design to accurate and identify some patterns of MCUs. Detection and correction capabilities are maintained and

also improved. The drop in memory power use is present because of the very low redundancy of our codes here [3, 9].

3 Design Approach

We have different codes starting from BERGER CODE (known as parity code). Many complicated codes are present like Hamming code, Hadamard code, Golay code, Reed–Solomon code, Reed–Muller code, and multi-dimensional codes like Matrix codes. During the space applications, error correction codes require to be checked to a far extent. If a single-bit error is present, it can be corrected and the Hamming code is used for correcting the 2-bit error; whereas, the Hadamard code is used for correcting the 3-bit error. The Reed–Solomon code is used to check the multiple errors, and Reed–Muller code is used in vast critical applications. Based on Hamming codes, we developed Matrix code. Figure 1 shows the block diagram, and the recursive backtracking algorithm is used to find the algorithm [9].

The off-base data will at present contain some incorrect MBs (in any event one wherein the blunder happened) that are nearly finished with dark qualities during the procedure of bit-by-bit interpreting. With any standard mistake camouflage system, these MBs will be truly hidden. Two essential methodologies are available for mistake disguise: spatial and fleeting. Pixels of missing MBs are recreated utilizing the neighboring spatial data. In as opposed to this transient addition, a lost MB is recuperated from that of the past edge moved by an expected movement vector [12].

Single blunder amendment code and twofold mistake redress codes are not solid for space applications. In this way, we are utilizing Reed code, this can be avionics, aerospace, data storage, military, and telecommunication. Reed–Solomon codes are used in correcting errors in many systems including:

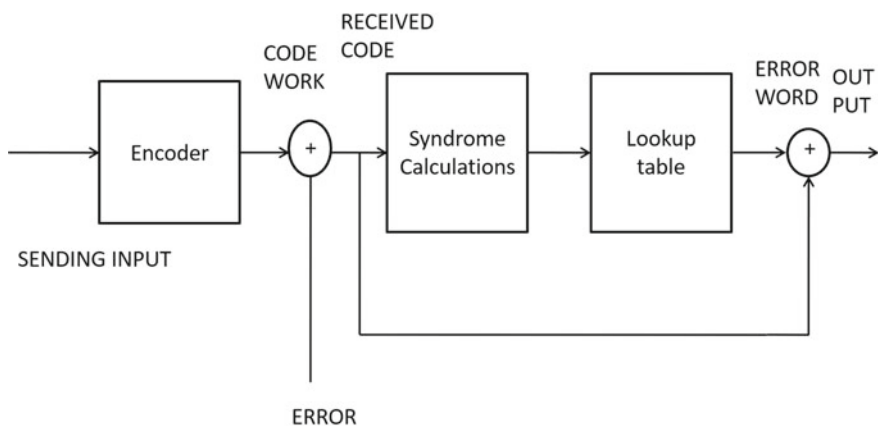


Fig. 1 Encoding and decoding process

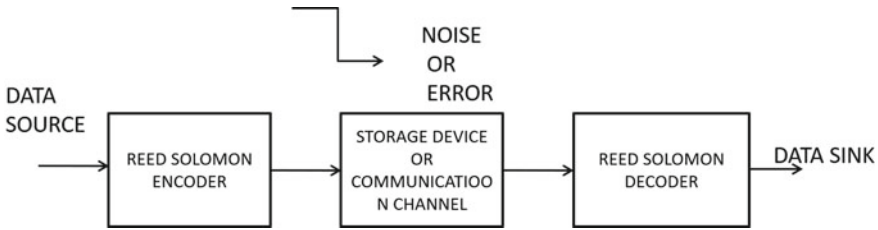


Fig. 2 Block diagram of digital data encoder

- Devices utilized for putting away incorporates tape, compact disk, DVD, standardized tags, and so forth.
- Also utilized in wireless or versatile interchanges (counting cell phones, microwave joins, and so on).
- In satellite correspondences.

A typical system is shown in Fig. 2.

The Reed–Solomon encoder will take a computerized information square and incorporate an extra “repetitive bits”. Mistakes are available during stockpiling or transmission for a few explanations behind (e.g. clam or impedance, scratches on a CD, and so on). The Reed–Solomon decoder checks each square and endeavors to address blunders and remake the sent data. The sort number and blunders that can be rectified rely upon the Reed–Solomon code qualities. Reiteration codes, parity bit codes, checksums codes, cyclic excess check codes, cryptographic hash capacities codes, automatic recurrent solicitation codes, and forward error rectification codes are compared here [19]. In light of time intricacy, mistake revision and identification, capacities, space unpredictability, bit overhead, and code rate are examined. It incorporates a correlation of Hamming, Hadamard, Golay, Repetition, Berger, single parity, four-dimensional parity, BCH, and Reed–Solomon codes. It is reasoned that 4D equality codes are most appropriate for DDR recollections in space applications since they are simpler to actualize and have the most elevated code rate to bit overhead proportion [1]. The fundamental piece of the code plan algorithm and the advancement part of the code structure algorithm are explicitly utilized in this challenge. Dependability assumes a key job in space applications. If one mistake can be amended or identified, it must comply with these standards. The first is correctable restriction which implies the comparing disorder vector ought to be one of a kind in the arrangement of the disorders, and the subsequent one is detectable restriction which implies the relating disorder vector is nonzero. The code design technique is mainly demonstrated by two methods; there is error space satisfiability and the other one is unique syndrome satisfiability [14].

There are four different categories present in the transmission of bit rate, and they are Fail, Pass, Refail, and Repass. In second or later cycles if there are any fail bits, then it comes under the fail category. If any kind of bits changes to pass, then it comes underpass category. If any bits change to fail after going through the pass category,

Table 1 Comparison of few error correction codes in terms of redundancy

Code	Code bit count	Percentage redundancy	Correction capability and burst error identification
Matrix	16	100	A single-bit error is corrected to complete extent, and two-bit burst error is also detected
Sec-Daed	5	31.5	A single-bit error is corrected to complete, extent and two-bit burst error is also detected
CLC	24	150	A single-bit and two-bit burst error are also detected, and a two-bit burst error is also detected

Redundancy = No. code bits/No. data bits \times 100

then it comes under the Refail category. If any bits change to pass after going through the fail category, then it comes under the Repass category [11] (Table 1).

4 Result

After going through this paper, we can have a clear idea that various codes are considered in this process. Out of this, we can say that in error correction, codes during space applications are mainly due to radiation effects, thus resulting in the error information. These can be corrected by using different error codes or consideration of an algorithm. Different parameters like area, power, and delay were also considered.

5 Applications

The Matrix and CLC codes offer more power compared to FUEC–DAEC. In this paper, we found that the encoder circuits are quicker and the decoder circuits are more complex. Various parameters like delay, power, and area are taken into consideration [9]. Multiple cell upsets are mostly seen in space applications due to space radiations. Various simulation tools can be applied in solving this like TCAD and SPICE tools. Multiple upsets issue can be decoded by using these tools [7]. The Reed–Muller code has more significance in decoding. This will allow us to transmit the information to the longer distances. The best error control performance will be selected based on the characteristics of the communication channel. Generally, in these channel models include memoryless models where errors occur randomly and with a certain probability and dynamic models where errors occur primarily in bursts [19].

6 Conclusion

After comparing different error correction codes, we can conclude that the modified matrix code called column line code (CLC) is based on the extended Hamming code that can be widely used in space applications. In flexible unequal error control (FUEC), these symbols are an enhancement of the famous unequal error control (UEC) codes. Multiple laser analysis has proved the crucial nature of the MWCPU instrument and the relative position between the center of charge generation and internal nodes are also the reason for the occurrence of the upsets. It results, that produces charges over multiple cells will turn on the MWCPU machinery, directing to scrupulous MCU topologies.

References

1. S. Ahmad, M. Zahra, S.Z. Farooq, A. Zafar, Comparison of EDAC schemes for DDR memory in space applications, in *2013 International Conference on Aerospace Science & Engineering (ICASE)* (IEEE, 2013), pp. 1–5.
2. Y. Bentoutou. Program memories error detection and correction on-board earth observation satellites. **66** (2010).
3. H. Castro, J.A.N da Silveira, A.A.P. Coelho, F.G.A. e Silva, P.S. Magalhaes, O.A. de Lima, A correction code for multiple cells upsets in memory devices for space applications., in *2016 14th IEEE International New Circuits and Systems Conference (NEWCAS)* (IEEE, 2016), pp. 1–4
4. N.G. Chechenin, M. Sajid, CIIT Islamabad Pakistan. Multiple cell upsets rate estimation for 65 nm SRAM bit-cell in space radiation environment. *Phys. Atom. Nuclei* **74**, 1718–1724 (2016).
5. B. Chen, C.-E.W. Sundberg, An integrated error correction and detection system for digital audio broadcasting. *IEEE Trans. Broadcast.* **46**(1), 68–78
6. K.-H. Chen, J.-H. Lu, B.-J. Chen, S.-I. Liu, An ultra-wide-band 0.4–10-GHz Ina in 0.18- μ m CMOS. *IEEE Trans. Circ. Syst. II: Express Briefs* **54**(3), 217–221 (2007)
7. V Correias, F. Saigné, B. Sagnes, F. Wrobel, J. Boch, G. Gasiot, P. Roche, Prediction of multiple cell upset induced by heavy ions in a 90 nm bulk SRAM. *IEEE Trans. Nucl. Sci.* **56**(4):2050–2055 (2009).
8. Y.-P. Fang, A.S. Oates, Characterization of single bit and multiple cell soft error events in planar and FinFET SRAMs. *IEEE Trans. Device Mater. Reliab.* **16**(2), 132–137 (2016)
9. J. Gracia-Moran, L.J. Saiz-Adalid, D. Gil-Tomás, P.J. Gil-Vicente, Improving error correction codes for multiple-cell upsets in space applications. *IEEE Trans. Very Large Scale Integr. (VLSI) Syst.* **26**(10), 2132–2142 (2018)
10. E. Ibe, H. Taniguchi, Y. Yahagi, K.-I. Shimbo, T. Toba, Impact of scaling on neutron-induced soft error in SRAMs from a 250 nm to a 22 nm design rule. *IEEE Trans. Electron Devices* **57**(7), 1527–1538 (2010)
11. T. Kato, T. Yamazaki, K. Maruyama, T. Soeda, H. Itsuji, D. Kobayashi, K. Hirose, H. Matsuyama, The impact of multiple-cell charge generation on multiple-cell upset in a 20-nm bulk SRAM. *IEEE Trans. Nucl. Sci.* **65**(8), 1900–1907 (2018)
12. E. Khan, S. Lehmann, H. Gunji, M. Ghanbari, Iterative error detection and correction of h. 263 coded video for wireless networks. *IEEE Trans. Circ. Syst. Video Technol.* **14**(12), 1294–1307 (2004)
13. T. Kimoto, Enhancement of error-correction coding of spatial watermarks for JPEG compression, in *2012 Eighth International Conference on Signal Image Technology and Internet Based Systems* (IEEE, 2012), pp. 195–200

14. J. Li, P. Reviriego, L. Xiao, C. Argyrides, J. Li, Extending 3-bit burst error-correction codes with quadruple adjacent error correction. *IEEE Trans. Very Large Scale Integr. (VLSI) Syst.* **26**(2), 221–229 (2017)
15. A. Mardjuadi, J.H. Weber, Codes for multiple localized burst error correction. *IEEE Trans. Inf. Theory* **44**(5), 2020–2024 (1998).
16. D.G. Mavis, P.H. Eaton, M.D. Sibley, R.C. Laco, E.J. Smith, K.A. Avery, Multiple bit upsets and error mitigation in ultra-deep submicron SRAMs. *IEEE Trans. Nucl. Sci.* **55**(6), 3288–3294 (2008)
17. A. Meamar, B.C. Chye, Y.K. Seng et al., A 3–8 Ghz low-noise CMOS amplifier. *IEEE Microwave Wirel. Compon. Lett.* **19**(4), 245–247 (2009)
18. M. Mollaalipour, H. Miar-Naimi, Design and analysis of a highly efficient linearized CMOS subharmonic mixer for zero and low-if applications. *IEEE Trans. Very Large Scale Integr. (VLSI) Syst.* **24**(6), 2275–2285 (2016)
19. J. Singh, J. Singh, A comparative study of error detection and correction coding techniques, in *2012 Second International Conference on Advanced Computing & Communication Technologies* (IEEE, 2012), pp. 187–189
20. G. Tsiligiannis, L. Dilillo, A. Bosio, P. Girard, S. Pravos-Soudovitch, A. Todri, A. Virazel, H. Puchner, C. Frost, Wrobel, Multiple cell upset classification in commercial SRAMs. *IEEE Trans. Nucl. Sci.* **61**(4), 1747–1754 (2014)
21. G.I. Zebrev, K.S. Zemtsov, R.G. Useinov, M.S. Gorbunov, V.V. Emel'yanov, A.I. Ozerov, Multiple cell upset cross-section uncertainty in nanoscale memories: micro-dosimetric approach, in *2015 15th European Conference on Radiation and Its Effects on Components and Systems (RADECS)* (IEEE, 2015), pp. 1–5
22. Y. Zhang, Q. Yuan, A multiple bits error correction method based on cyclic redundancy check codes, in *2008 9th International Conference on Signal Processing* (IEEE, 2008), pp. 1808–1810

Review on Different Types of Multipliers and Its Performance Comparisons



Bocha Dileep Venkata Prasad, Nalla Satya Sai Sanjeev, Krishna Saladi,
and Durgesh Nandan

1 Introduction

Multiplication is the most popular and area-consuming arithmetic operations that are to be done by using multipliers. The multiplier has key components in the field of VLSI architecture of digital signal processing (DSP) and image processing and its applications. By using this multiplication process, we can consume the time, area, and power. Multiplications are the most commonly used arithmetic operations in microprocessors and DSP [16]. These operations have control of the execution time so, there is a need for the high-speed multiplier. By using this, the speed will be increased thereby expanding the computer and signal processing applications. Nowadays, power saver components are in demand. To minimize the power requirements, we try to develop such types of components that have capabilities to work with minimum power requirements and power loss at high speed. As we know, multipliers are key components for any signal processing architectures [4].

So, choosing which type of multiplier for which particular applications decided the performance of those architectures. It discussed the different types of multipliers and tries to conclude that which one is the best possible type of multiplier for which conditions and applications.

B. D. V. Prasad · N. S. S. Sanjeev · K. Saladi
Department of ECE, Aditya Engineering College, Surampalem, India
e-mail: dvp2299@gmail.com

N. S. S. Sanjeev
e-mail: saisanju4533@gmail.com

K. Saladi
e-mail: krishna.s@aec.edu.in

D. Nandan (✉)
Accendere Knowledge Management Services Pvt. Ltd., CL Educate Ltd., New Delhi, India
e-mail: durgeshnandano51@gmail.com

2 Characteristics of the Multiplier

There are mainly three steps for the multiplications process and the following are: (a) partial result generation, (b) partial result reduction, and (c) final addition of results. The following characteristics are used to form an efficient multiplier, i.e., power, speed, area, and accuracy.

Power: Power consumption is less by using a multiplier.

Speed: High-speed multiplications are the main demand for the efficient multiplier.

Area: Minimum area is required nowadays in IC industry [8].

Accuracy: Somewhere accuracy is important, somewhere approximation considers. It depends upon the place where multiplications required.

3 Different Types of Multipliers

- Modified booth/booth multiplier [3, 9]
- Array multiplier [6]
- Wallace tree multiplier [2, 5]
- Combinational multiplier [2]
- Sequential multiplier [1, 21]
- Logarithm multiplier [14, 15, 17, 18].

3.1 Booth Multiplier

Booth multiplication is based on shift operation. Two types of shift operations required for performing booth multiplication. Right and left circular shift operations are required for performing booth multiplications [3].

Step 1: Making booth table.

For making the booth table, we have to take the four columns: One column for multiplier and second column for preceding first LSB of multiplier and last two (i.e., U and V) for partial result accumulator. The procedure of making a booth table is as follows.

1. At first, taken two binary numbers and select multiplier (X) and multiplicand (Y).
2. Take multiplicand (Y) 2's complement.
3. Take X_i value in the table.
4. Take 0 for $X_i - 1$ value.
5. Take 0 in U and V , we will get a product of $X Y$ at the end of the process.
6. For every cycle, we have to make n rows because we are multiplying m and n bit numbers.

Table 1 Booth’s calculation table

A_i	$A_i - 1$	Operation
0	0	Shift
0	1	Add B to K and shift
1	0	Minus B from K and Shift
1	1	Shift

Step 2: Booth’s algorithm is the most popular and frequently used to develop any computer architecture [3]. It is one of the most efficient algorithms for performing multiplication on a signed number, which considers both positive and negative numbers consistently. This algorithm contains the multiplier bits. Operating the booth’s algorithm can be done based on X_i and $X_i - 1$ bits (i.e., 00, 01, 10, and 11). Booth’s algorithm Table 1.

3.2 Array Multiplier

An array multiplier is used frequently for two unsigned binary numbers multiplication. It is performed by employing an array of full adders and half adders. The circuit of the array multiplier is based on the repeated addition and the shifting procedure. In an array multiplier, every partial result is produced by the multiplication of the multiplicand by means of single multiplier number. According to their bit sequences, the partial result is moved and then added. The summation can be carried out with the usual carry propagation adder. $N - 1$ adders are needed where N is the multiplier size [6]. For $m * n$ array multiplier, it needs $m * n$ AND gates, n half adders, $(m - 2) * n$ full adders, (total $(m - 1) * n$ adders). The array multiplier diagram is as shown below.

3.3 Wallace Tree Multiplier

It is a quick method that is used to multiply two binary integers [5, 7]. Any multiplier has three stages [2].

Stage 1: Partial products.

It works exactly like a long-hand multiplication. The numbers we take here are binary integers. Partial products are the result of simple AND gates. All products are done simultaneously. Stage 2: Partial product Addition 1 (Fig. 1).

- To add up columns, partition the rows into sets of three rows.
- Partition into two sets of three rows and one set of two rows.
- Full adder requires three inputs while half adder requires two inputs.

Partial product Addition 2.

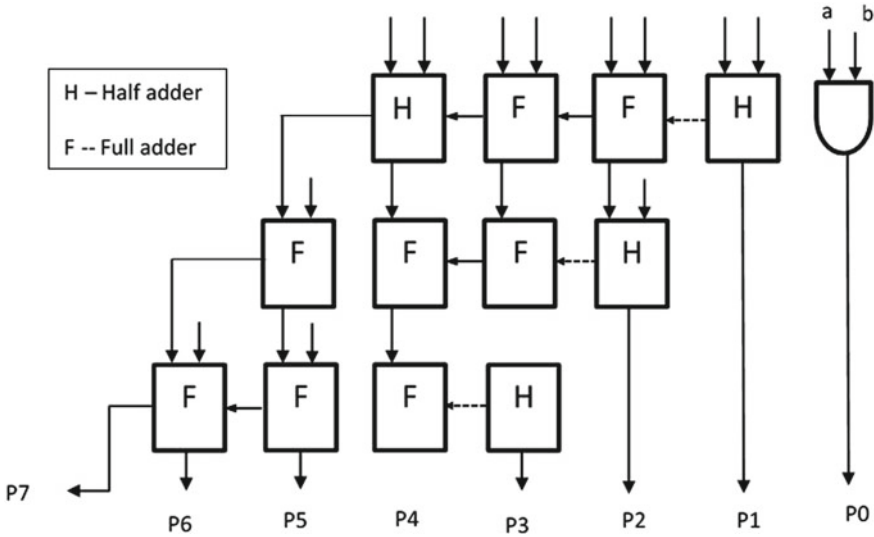


Fig. 1 Block diagram of array multiplier

- In Addition 2 repeat the process as same as Addition 1.
- Partition will be done into two sets of three rows results in two sets of two rows.

Partial product Addition 3.

- Partition into one set of three rows and an extra row to carry down and resulting in three rows, two from a set of three and the one carried down.
- Each step takes as long as a full adder because that is the slowest part.
- A full adder is more involved than a half adder and a half adder is more involved in carrying down (takes no time).

Partial product Addition 4.

- Repeat the same process once again. In this stage no need for any partitions because there are only three rows and resulting in two rows.
- Total up stage 2 had four full adder delays and the five least significant bits (LSBs) had calculate.

Stage 3: Final addition.

- The concluding result is calculated by adding the final two rows and the five LSBs do not need to be carried down directly.
- The rest of the bits needs to undergo one adder which involves a lot of delays.
- The output shown in purple numbers.
- The savings from already having 5 bits offset the delay from doing stage 2.

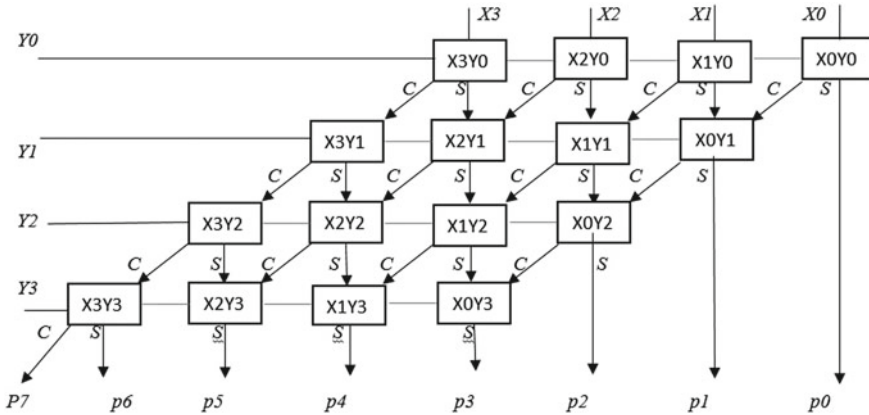


Fig. 2 Block diagram of combinational multiplier

3.4 Combinational Multiplier

Combinational multipliers do multiplication for both signed and unsigned two-bit digits. Each bit of the multiplier is multiplied in opposition to multiplicand, and the result is placed according to the place of the bit within the multiplier and the resulting products are the calculated up to form the concluding result [2] (Fig. 2).

Multiplier bit	Product
1	It is shifted copy of multiplicand
0	It is simply zero

3.5 Sequential Multiplier

Multiply two binary numbers by using single n bit adder and find sequential circuit, such type of arrangements known as sequential multiplier [21]. It is having low area. It is spitted into various sequential steps. In every stage, partial product is produced and it is added to an accumulated partial addition and the partial addition will be moved to align the accumulated sum with a partial product of the subsequently stages [1]. These partial products are summed up to get the required output.

Example: Let us do multiplication for 6 and 14 in the sequential multiplier.

Table 2 Multiplication for 6 and 14 in sequential multiplier

Initialize 0	C 0	A 0000	Q 1111	N 4	Operation
0	0	0000	1110	4	
Step 1	0	0000	0111	3	Right shift(CAQ), $N = N - 1$
Step 2	0	0110	0111	3	$A = A + M$ Right shift(CAQ), $N = N - 1$
	0	0011	0011	2	
Step 3	0	1001	0011	2	$A = A + M$ Right shift(CAQ), $N = N - 1$
	0	0100	1001	1	
Step 4	0	1010	1001	1	$A = A + M$ Right shift(CAQ), $N = N - 1$
	0	0101	0100	0	

In the last step $N = 0$ then we have to do the product, i.e., AQ product = $AQ = 01010100 = 84$ (Table 2).

The process is done like the above example, it is fully based on the Q_0 value which is underlined in the following Q block. The flowchart of the sequential multiplier is as shown below:

3.6 Logarithm Multiplier

Traditional or reported multiplication was limiting performance in terms of accuracy as well as hardware overhead. Logarithm multiplier must have potential to become an option of traditional multiplier for real-time digital signal processor [13–20]. An improvement in terms of the area, delay, and power is of the main concerns for an LNS multiplier. Such LNS multiplier can be used in DSP applications where the accuracy is not of concern like the approximate computing and FIR filter, etc. The VLSI logarithmic multiplier is implemented to meet the requirement of a real-time application. Keeping this fact in view, several design schemes have been suggested in the last fifty years for an efficient design of logarithmic multiplier, logarithm and antilogarithm converter. It motivates the researchers to work for faster, simpler, and cheaper alternatives with an eye for accuracy.

3.7 Modified Booth Multiplier

The best available architecture out of existing multiplier is known as a modified booth multiplier because it has facility to perform the high-speed multiplier parallelism [9], and it reduces the number of stages of the calculation result. The Radix-2 booth multiplier has some limitations like: (1) The digit of add/subtract procedures became uneven and therefore became inopportune even as developing the parallel

multipliers. (2) The algorithm turns into inexact while there are remote 1 s. The modified booth multiplier has overcome limitations of Radix-2 booth multiplier. It uses fast process multiplications by using a changed booth's algorithm. In this multiplier calculation time and logarithm of the word span of operands are proportional to each other. We can decrease the half the number of the partial product. Radix-4 booth algorithm is used here which is to increase the speed of multiplier and reduce the area of the multiplier circuit. Based on the multiplier bits, the process of encoding the multiplicand is performed by the Radix-4 booth algorithm [10–12] (Fig. 3).

Modified booth algorithm.

It is also called as bit recoding. To accelerate the multiplication procedure in booth's algorithm, the technique we used is called the "bit pair recoding technique" [13]. It calls the maximum number of summands. In this method, the booth recoded

Fig. 3 Block diagram representation of sequential multiplier

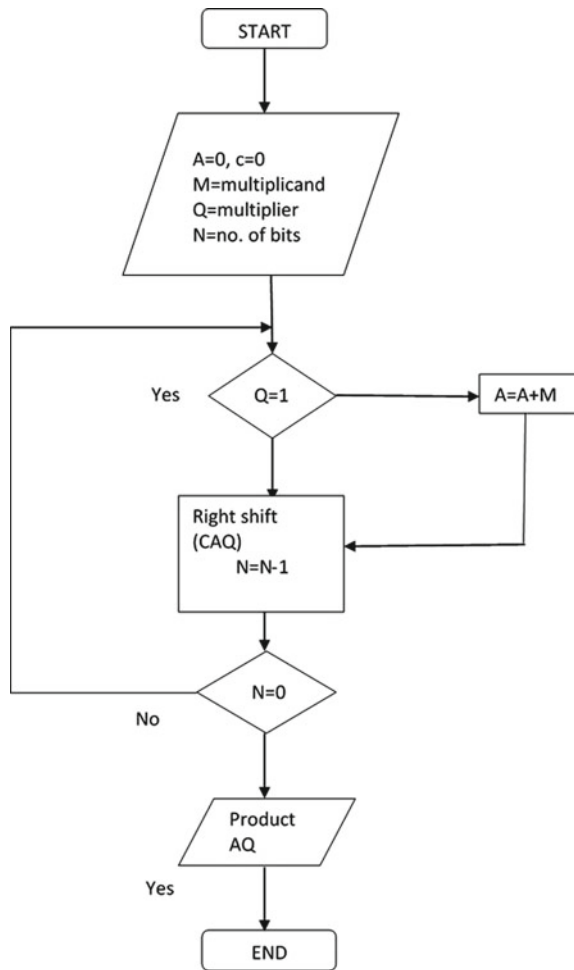


Table 3 Recoded bits

Multiplier bit pair	Multiplier bit on	Recoded pair	Reduced one the right
$i + 1 - i$	$i - 1$		
0 — 0	0	0 0	0
0 — 0	1	+1 -1	+ 1
0 — 1	0	-1 +1	-1
— 1	1	+1 0	+ 2
1 — 0	0	-1 0	-2
1 — 0	1	0 + 1	+ 1
1 — 1	0	0 -1	-1
1 — 1	1	0 0	0

multiplier numbers are clustered in couples, and then every couple is shown by its corresponding single number multiplier. It reduces the whole size of multiplier digits.

For case study based on the above, if we take the recoded pair as + and -1 then it reduces to +1, i.e., the answer which was coming while doing with +1 and -1, the same answer will come with +1 let us see various recoded bits in Table 3.

Let us see one example is it working or not. I will take the multiplicand as.

13— ——— — 1101— M (2 's complement of M is 0011).

If we do this with + 2 then also it gives the same result.

Multiplicand	Recoded pair	Multiplication	Final result
1101	+10	0000 +1101	11010

Now, let us see the actual modified booth multiplier process:

Multiplicand	Recoded bits (reduced)	Multiplication (final result)
1101	+2	11010

Step 1: First we have to take the multiplier and the multiplicand for doing the signed multiplication.

Step 2: After taking the multiplier and multiplicand, do the 2's complement for the multiplicand.

Table 4 Performance comparison of different multipliers

Multipliers	Speed	Time delay	Area	Complexity	Power consumption
Booth multiplier	High	Less	Minimum	Most complex	Less
Array multiplier	Less	Very high	Maximum	Less complex	Most
Wallace tree multiplier	High	High	Moderate	More complex	More
Combinational multiplier	High	High	Maximum	More complex	More
Sequential multiplier	Less	High	Minimum	Complex	More
Logarithm multiplier	High	Less	Minimum area	Most complex	Less power
Modified booth multiplier	Very high	Very less	Minimum	Less complex	Less power

Step 3: After that we have to take the bit pair recoded multiplier by using Table 4. The process is as follows:

- We have to take the multiplier and at the rightmost bit of the multiplier place 0. For example, if we take 011011 as multiplier (0 1 1 0 1 1 0) here rightmost bit is 1, place 0 after 1.
- After placing 0, we have to combine 3 bits as a pair from the right side and assume that as $i - 1, i, i + 1$.
- By using the bit pair recoded table we have to find the recoded values for all the pairs.

Step 4: After finding the recoded values, we have to do the multiplication for the multiplicand and the bit pair recoded values.

Step 5: If we have n bits in the multiplicand, the result will be the $2n$ bits.

Step 6: After doing the multiplication, in the result, the leftmost bits are the signed bit. If it is 0, then result is positive and is 1, result is negative. And we have to do the 2's complement for the remaining bits to get the actual result.

4 Final Result

Herein, we have compared dissimilar types of multipliers in terms of speed, delay, area power consumption, and complexity. Table 4 shows the performance evaluation of dissimilar types of multipliers, and it is observed that the array multiplier have more area and high-power use, while booth multiplier has high speed and less time delay. Wallace tree and combinational multipliers having high speed and more time delay, but differ in their area. Sequential multiplier has some drawbacks like more time delay and power consumption. To get the best possible multiplier, the speed

should be high, the power time delay must be low, and the area must be minimum. All the conditions are satisfied by using a modified booth multiplier.

5 Conclusion

After observing all the multipliers, we concluded that the modified booth multiplier is the best among all the different multipliers up to date based on its characteristics like high speed, low power consumption, less complexity, minimum area occupancy, and less time delay. Thus, it is well-suited for high-speed and low-power applications.

References

1. S. Amanollahi, G. Jaberipur, Fast energy efficient radix-16 sequential multiplier. *IEEE Embed. Syst. Lett.* **9**(3), 73–76 (2017)
2. D. Chen, T. Aoki, N. Homma, T. Higuchi, Pragmatic method for the design of fast constant-coefficient combinational multipliers. *IEE Proc.-Comput. Dig. Techn.* **148**(6), 196–206 (2001)
3. J. Fadavi-Ardekani, M^*n booth encoded multiplier generator using optimized wallace trees. *IEEE Trans. Very Large Scale Integr. (VLSI) Syst.* **1**(2), 120–125 (1993)
4. A.A. Fayed, M.A. Bayoumi, A merged multiplier-accumulator for high speed signal processing applications, in *2002 IEEE International Conference on Acoustics, Speech, and Signal Processing*, vol. 3. (IEEE, 2002), pp. III–3212
5. R. Gnanasekaran, A fast serial-parallel binary multiplier. *IEEE Trans. Comput.* **8**, 741–744 (1985)
6. J.A. Howard, A two's complement array multiplier using true values of the operands. *IEEE Trans. Comput.* **100**(32) (1983)
7. G. Jaberipur, A. Kaivani, Binary-coded decimal digit multipliers. *IET Comput. Dig. Tech.* **1**(4), 377–381 (2007)
8. E. Jagadeeswara Rao, V.K.R. Durgesh Nandan, K. Jayaram Kumar, A systematic review of multipliers: accuracy and performance analysis, pp. 965–969 (2019)
9. S.R. Kuang, J.P. Wang, C.Y. Guo, Modified booth multipliers with a regular partial product array. *IEEE Trans. Circ. Syst. II Expr. Briefs* **56**(5), 404–408 (2009)
10. W. Liu, L. Qian, C. Wang, H. Jiang, J. Han, F. Lombardi, Design of approximate radix-4 booth multipliers for error-tolerant computing. *IEEE Trans. Comput.* **66**(8), 1435–1441 (2017)
11. D.J. Moss, D. Boland, P.H. Leong, A two-speed, radix-4, serial-parallel multiplier. *IEEE Trans. Very Large Scale Integr. (VLSI) Syst.* **27**(4), 769–777 (2018)
12. R. Muralidharan, C.H. Chang, Radix-4 and radix-8 booth encoded multi-modulus multipliers. *IEEE Trans. Circ. Syst. I Regul. Pap.* **60**(11), 2940–2952 (2013)
13. D. Nandan, J. Kanungo, A. Mahajan, An efficient vlsi architecture design for antilogarithmic converter by using the error correction scheme (2016)
14. D. Nandan, J. Kanungo, A. Mahajan, An efficient VLSI architecture design for logarithmic multiplication by using the improved operand decomposition. *Integration* **58**, 134–141 (2017)
15. D. Nandan, J. Kanungo, A. Mahajan, An efficient VLSI architecture for iterative logarithmic multiplier, in *2017 4th International Conference on Signal Processing and Integrated Networks (SPIN)* (IEEE, 2017), pp. 419–423
16. D. Nandan, J. Kanungo, A. Mahajan, 65 years journey of logarithm multiplier. *Int. J. Pure Appl. Math.* **118**, 261–266 (2018)

17. D. Nandan, J. Kanungo, A. Mahajan, An efficient architecture of iterative logarithm multiplier. *Int. J. Eng. Technol.* **7**(2.16), 24–28 (2018)
18. D. Nandan, J. Kanungo, A. Mahajan, An error-efficient gaussian filter for image processing by using the expanded operand decomposition logarithm multiplication. *J. Amb. Intell. Human. Comput.* (2018), pp. 1–8
19. D. Nandan, K. Kumar, J. Kanungo, R.K. Mishra, Compact and errorless 16- region error correction scheme for antilogarithm converter, in *2019 International Conference on Electrical, Electronics and Computer Engineering (UPCON)* (IEEE, 2019), pp. 1–5
20. D. Nandan, A. Mahajan, J. Kanungo, An efficient antilogarithmic converter by using 11- regions error correction scheme, in *2017 4th International Conference on Signal Processing, Computing and Control (ISPCC)* (IEEE, 2017), pp. 118–121
21. N.R. Strader, V.T. Rhyne, A canonical bit-sequential multiplier. *IEEE Trans. Comput.* **100**(8), 791–795 (1982)

Changes in Index Properties of Soil Using Fly Ash



Praful Ranjan

1 Introduction

Thermal power plant generates fly ash as waste, because coal is used as a main fuel. World's most plentiful and widely nonrenewal fossil fuel is coal. Approx 75% of India's total power is thermal, and 90% of coal is used as fuel. Total 82 thermal power plants in India, approx 140 million tons of fly ash are generated in a year. In fly ash as by-product waste production, India has fourth position in the entire world after USSR, USA and China.

In India, the total coal demand in the year 2010–11 was about 730 million tons. It is estimated that it will increase to 2000 million tons in the year 2031–32. More than 600 million tons of fly ash will be generated annually. This amount of fly ash will need about 3, 92,857 acre-ft. of landfill space for its disposal. India has not the best quality of coal reserves, so a massive fly ash generated in thermal power plant. The major issues for power plant operators are to dispose of fly ash. This is major role in environmental hazards. But technological advance in fly ash can utilize in many good applications. It does not mean that whole fly ash can be utilized. In 2010–2011, the total number of mines in all over the world is approx 2628, where 608 mines produce metallic minerals and 574 mines produce with coal and lignite, and remaining mines deal with non-metallic minerals. Presently in India, 90 minerals are active: 4

P. Ranjan (✉)

Department of Electronics and Communication Engineering, THDC Institute of Hydropower Engineering & Technology, Tehri, Uttarakhand, India

e-mail: prf98354@rediffmail.com

© Springer Nature Singapore Pte Ltd. 2021

K. S. Sherpa et al. (eds.), *Advances in Smart Grid and Renewable Energy*,

Lecture Notes in Electrical Engineering 691,

https://doi.org/10.1007/978-981-15-7511-2_32

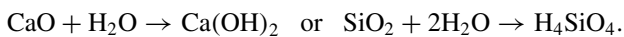
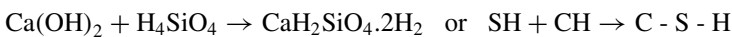
fuel minerals mine, 10 metallic minerals and 56 non-metallic minerals mine. Approx 3 mines are producing atomic minerals, and remaining are minor minerals [1–5].

Thermal power plants which are using coal produce nearly 95 million tons of fly ash annually. Uses of fly ash depend upon several parameters that are the coal sources, plant operation and many factors. Fly ash can be classified in their different characteristics including physical features, chemical composition and chemical properties. Today, generation of power in India depends on coal-based thermal power plant. For high-efficiency power generation, it must be required having high calorific value of coal. 35–38% fly ash generated in through Indian-based coal while coal supply by Australia and other countries coal-generated fly ash only 10–15%. To improve the strength of soil by using fly ash and cement composite [6–8], geotechnical properties of fly ash are to be determined.

2 Compositions and Classification

American society defines two classes of fly ash for testing materials. One is F class fly ash which usually has less than 20% CaO [9–10]. It has pozzolanic properties only, so it needs an activator to produce cementitious compounds, and another one is C class fly ash which has calcium oxide content in surplus of 20%. With pozzolanic properties, it also possesses cementations properties. Chemical composition of fly ash is silica (45–65)%, alumina (20–30)%, ferric oxide (4–20)%, sulfur trioxide (0.2)% and calcium oxide (5–30)% [11–13].

The whole mechanism is based on pozzolanic reaction, which is a combination of pozzolana, calcium hydroxide and water, resulting as a C-S-H complex. As deeper, it is the reaction between calcium hydroxide and silica acid resulting in the formation of calcium silicate hydrate complex which is responsible for the strength [14].



These CaO and SiO₂ present in the pozzolanic material, i.e., fly ash.

3 Experimental Analyses

For experimental purpose graded, Atterberg limit we can check plastic limit, liquid limit and specific gravity test.

Gradation is main property of soil, and it is based on particle size of soil. It indicates such various properties like conductivity of soil, shear strength and compressibility factor. It is also indicating water drainage behavior of soil. In gradation, matter if

soil (poor grained) then its better water drainage. Its value is calculated by analysis of hydrometer [15]. Particle size and finer are shown in Fig. 1 (Table 1).

Coefficient of uniformity (C_u) and curvature (C_c) value depends upon D_{10} , D_{60} and D_{80} , where grain diameter at 60% passing in D_{60} , 30% passing in D_{30} and D_{10} is only 10% passing. As per standard, $C_u > 4$ for well-graded gravel, $C_u > 6$ for well-graded sand and $1 < C_c < 3$ for well-graded soil. As per observation, $D_{10} = 0.705$, $D_{30} = 1.135$, $D_{60} = 1.778$, $C_u = 2.52$ and $C_c = 1.163$. Hence, soil is well-graded soil.

For fine-grained soil, contents of critical water have checked by Atterberg limits like liquid limit, shrinkage limit and plastic limit. When amounts of water increase, it differentiates dry and clayey soil. Behavior changes as per water limit. Water content of the soil may form liquid, plastic, solid or semi-solid. In every state, the behavior and consistency of a soil are dissimilar.

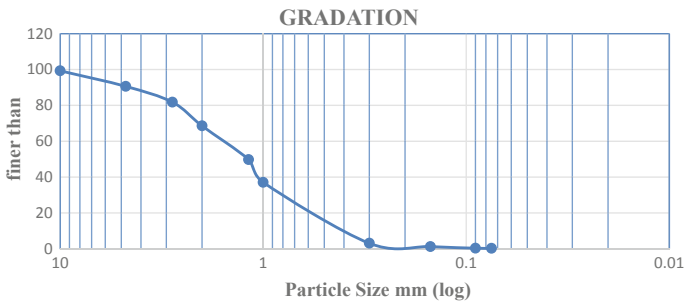


Fig. 1 Graphical representation between particle size and finer

Table 1 Experimental data of gradation

Is sieve	Mass of sieve (mm)	Mass of sieve + soil (mm)	Mass of retained soil (mm)	CUMM. mass (mm)	CUMM. % retained	% finer
10	380.5	387.5	7	7	0.7	99.3
4.75	312.5	399.5	87	94	9.4	90.6
2.8	414	502	88	182	18.2	81.8
2	330.5	463	132.5	314.5	31.45	68.55
1.18	303	491	188	502.5	50.25	49.75
1	375	502	127	629.5	62.95	37.05
0.3	341	681	340	969.5	96.95	3.05
0.15	288.5	307	18.5	988	98.8	1.2
0.09	352	361	9	997	99.7	0.3
0.075	306	307	1	998	99.8	0.2
PAN	286.5	288.5	2	1000	100	0

When behavior of a clayey soil changes from plastic to liquid is called liquid limit (LL). However, change from plastic to liquid behavior is steady and depends upon water contents. Shear strength of the soil is not perfectly zero at the LL. Casagrande which is a technique to measure the liquid limit. We dropped repeatedly 10 mm approx, 120 blows per minute onto a base of hard rubber. Result of impact can be checked continuously and recorded. The liquid limit states that it contents 25 drops of the cup to cause at distance of 13.5 mm. Experimental data to determine LL before fly ash composite is shown in Table 2. Graphical representation is shown in Fig. 2 with number of blows and water content before fly ash composite.

It is observed that liquid limit or water content at 25 no. of blows is 32.7% (after addition of 20% fly ash + 10% cement). It is experiential that with addition of 20% fly ash and 10% cement, the liquid limit or water content at 25 no. of blows is 37.035%. Experimental data after addition with fly ash is shown in Table 3. Figure 3 shows graphical view of blows and water content after fly ash addition. Comparative graph of liquid limit before and after fly ash composite mix is shown in Fig. 4.

The plastic limit (PL) is another property which can be determined on a flat, non-porous surface which can grind soil into fine portion. If it has moisture content, then behavior is plastic. The sample can then be remolded again and again and tested repeatedly. When moisture contents decrease due to disappearance of water content,

Table 2 Experimental data to determine liquid limit (before addition of fly ash composite)

No. of blows	Water content
20	35.2
22	34.8
26	32
30	31.3

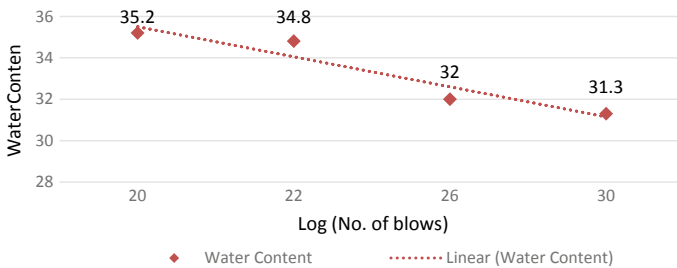


Fig. 2 Graph between number of blows and water content before addition of fly ash composite

Table 3 Experimental data to determine liquid limit (after addition of fly ash composite)

No. of blows	Water content
24	40.74
26	33.33

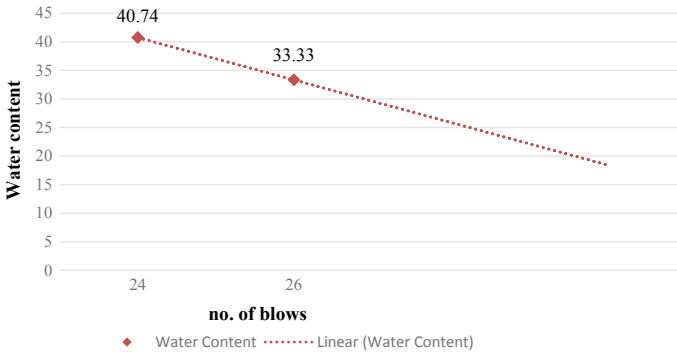


Fig. 3 Graph between number of blows and water content before addition of fly ash composite

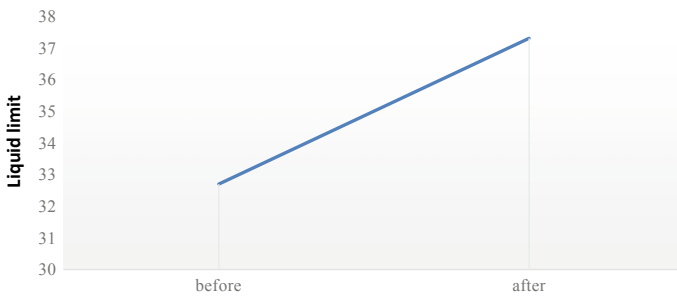


Fig. 4 Comparison of liquid limit before and after addition of fly ash composite

the thread will begin to break apart at 3 mm diameter. It behaves like non-plastic when thread cannot be rolled out below to 3 mm diameter. Before fly ash composite addition, plastic limit is shown in Table 4. Plastic limit is observed 10.783 before addition fly ash. After addition of 20% fly ash + 10% cement, plastic limit is shown in Table 4. Plastic limit is observed 16.537 after fly ash addition in Table 5. Comparison graph of plastic limit before and after fly ash addition is shown in Fig. 5.

Specific gravity test has done by pycnometer for both coarse-grained and fine-grained soils. It can be determined by the given formula where G is equal to 2.61.

$$G = (M_2 - M_1) / ((M_2 - M_1) - (M_3 - M_4))$$

Table 4 Experimental data to determine plastic limit (before addition of fly ash)

Moist soil sample weight	Dry soil sample weight	Plastic limit
0.030	0.027	10.11
0.031	0.028	10.7
0.029	0.026	11.54

Table 5 Experimental data to determine plastic limit (after addition of fly ash)

Moist soil sample weight	Dry soil sample weight	Plastic limit
0.032	0.027	15.625
0.033	0.028	17.857
0.036	0.031	16.857

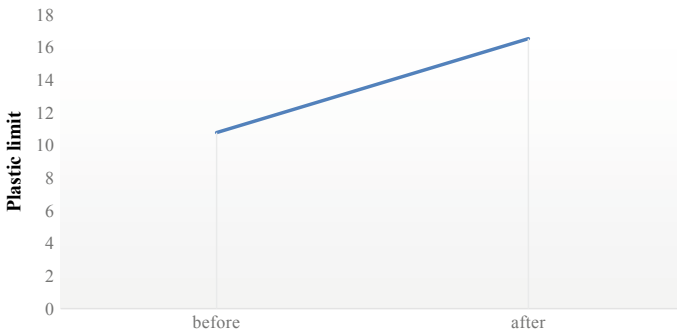


Fig. 5 Comparison of plastic limit before and after fly ash addition

where

M_1 Mass of pycnometer (empty) = 761 g.

M_2 Mass of pycnometer with dry soil = 1160 g.

M_3 Mass of pycnometer with soil + water = 1952 g

M_4 Mass of pycnometer + water = 1705.5 g.

The specific gravity of fly ash is determined using the relation, and G is equal to 1.173 [16], when fly ash composite is mixed where,

M_1 Mass of empty pycnometer = 761 g.

M_2 Mass of pycnometer with dry fly ash = 818.5 g.

M_3 Mass of pycnometer with fly ash + water = 1714 g.

M_4 Mass of pycnometer + water = 1705.5 g.

The specific gravity of soil with (20% fly ash) is determined using the relation, and G is equal to 1.66. Where

M_1 Mass of empty pycnometer = 761 g.

M_2 Mass of pycnometer with dry fly ash = 1040.5 g.

M_3 Mass of pycnometer with fly ash + water = 1817.5 g.

M_4 Mass of pycnometer + water = 1705.5 g.

Table 6 Properties of soil without fly ash and with fly ash

Properties	Before	After
Liquid limit (%)	32.7	37.035
Plastic limit (%)	10.783	16.537
Density	19.11 kN/m ³	

4 Results and Conclusions

Soil was carried out from Dibnu village, Bhagirathipuram, and fly ash from Reeva Enterprises Ltd, Faridabad. The results are obtained by the experiments; the color of soil sample is black. Soil sample is well-graded soil. The specific gravity of

$$\text{Soil} = 2.61$$

$$\text{Fly ash} = 1.173$$

$$\text{Soil} + 20\% \text{ of Fly ash} = 1.66$$

The Atterberg limit of soil sample is tabulated in Table 6.

Soil stabilization technique is useful for reduction in consumption of expensive road construction material. It can be helpful for cost saving and time in project completion. Liquid limit of soil increases by addition of fly ash composite. Plastic limit of soil increases by addition with fly ash composite. It is a need to economies the use of cement.

References

1. G. Ranjan, A.S.R. Rao, *Basic and Applied Soil Mechanics*
2. S. Openshaw, *Utilization of Coal Fly Ash* (University of Florida, Gainesville, 1992)
3. B.C. Punmia, A.K. Jain, J.K. Arun, *Soil Mechanics and Foundation*
4. T. Xiumei, Z. Gengxing, L. Qingbin, Research of soil testing and fertilizer recommendations at county level by GIS. ACSESS no. 7, Sept. 2013
5. S. Diamond, The utilization of fly ash. *Cement Concr. Res.* **14**, 455–462 (1984)
6. T.P. Dolen, Performance of fly ash in roller compacted concrete at upper still water dam, in *Proceedings: Eighth International Ash Utilization Symposium* (1987)
7. M.R.H. Dunstan, Development of high fly ash concrete. *Proc. Inst. Civil Eng.* **74**, 495–513 (1983)
8. R.C. Joshi, R.L. Day, B.W. Langan, M.A. Ward, Strength and durability of concrete with high proportions of fly ash and other mineral admixtures. *Durab. Build. Mater.* **4**, 253–270 (1987)
9. B. Mather, The partial replacement of portland cement in concrete. *Cement Concr.*, 37–73 (1956)
10. P.K. Mehta, Influence of fly ash characteristics on the strength of portland-fly ash mixtures. *Cement Concr. Res.* **15**, 669–674 (1985)
11. P.K. Mukherjee, M.T. Loughborough, V.M. Malhotra, Development of high-strength concrete incorporating a large percentage of fly ash and superplasticizers. *Cement Concr. Aggr.* **4**(2) (1982)

12. T.R. Naik, Setting and hardening of high fly ash content concrete. Paper presented at American Coal Ash 8th International Coal Ash Utilization Symposium (1987)
13. D. Ravina, P.K. Mehta, Properties of fresh concrete containing large amounts of fly ash. *Cement Concr. Res.* **16**, 227–238 (1986)
14. V. Sivasundaram, G.G. Carette, V.M. Malhotra, Long term strength development of high-volume fly selection (1990)
15. M.D.A. Thomas, The effect of curing on the hydration and pore structure of hardened cement paste containing pulverized fuel ash. *Adv. Cement Res.* (1989)
16. R.P. Hardaha, *Use of Fly Ash in Black Cotton Soil for Road Construction*. ISSN 2076-5061, vol-5 (2013)

A Review of Diverse Procedure for Extraction of Fetal ECG



K. M. L. Narasimhulu, N. Murali, M. Girish Kumar, T. Srinivasa Rao, and Durgesh Nandan

1 Introduction

The fetal ECG is used to monitor the health condition of a fetal. This can be done through many techniques. The fetal ECG helped to find out suffering or innating sensitivity defect in the premature stage of pregnancy during the delivery [1]. The fetal ECG helps us to know about the fetal arrhythmias, so we can make a decision to treat it with a pre-schedule or prescription of the delivery [2]. By using this method, it can be saving the fetal. At first, we take the abdominal ECG that contained the mutually maternal and fetal ECG, and next, we can correlate them and get the fetal ECG in which both signals are nonlinear in nature [3]. The main problem of the detection of FEKG is due to its signal-to-noise (SNR) ratio. Because while traveling, the signal encounters different body parts and may get different noises affecting it. The maternal ECG dominates the fetal ECG. In the abdominal f-ECG video recording, the electrical signal generates with the fetal hearts which are calculated by non-invasive electrodes [4]. It is located on the stomach of mother outside in which the fetal ECG is distant small compared to mECG. The fetal heart rate (FHR)

K. M. L. Narasimhulu (✉) · N. Murali · M. Girish Kumar · T. Srinivasa Rao
Department of E.C.E, Aditya Engineering College, Surampalem, Andhra Pradesh, India
e-mail: narasimhulukml1@gmail.com

N. Murali
e-mail: muralinali7@gmail.com

M. Girish Kumar
e-mail: girish.messi666@gmail.com

T. Srinivasa Rao
e-mail: srinivasarao2k2@gmail.com

D. Nandan (✉)
Accendere Knowledge Management Services Pvt. Ltd, CL Educate Ltd, New-Delhi, India
e-mail: durgeshnandano51@gmail.com

is used to help the heart rate monitoring of fetal ECG. The fetal ECG also helps us to identify fetal health conditions [5]. The support vector regression (SVR) is used to know fetal ECG by approximating the both abdominal ECG (taken at abdomen) and thoracic ECG (which is maternal ECG taken at chest) [6]. Despite all these methods, the KPCA analysis helps us to encounter the results to determine fetal ECG as it correlates both maternal and abdominal signals and also analyzes nonlinearity of the both signals [7].

2 Literature Review

The FECG of a fetal can be obtained from different techniques. Here, we have to choose the best technique to find fetal ECG so as to develop the best method to get a better result of fetal ECG. The kernel principal component analysis (KPCA) method uses both co-relation and nonlinearity of the signals which can get better results, but in PCA, we only use correlation and does not consider about the nonlinearity of both maternal and abdominal signals. The KPCA analyzes the abdominal and thoracic signal and gets the required fetal signal [8]. The non-invasive fetal electrocardiogram [NIF-ECG] is obtained from the electrodes positioned on the mother's stomach. In this, the fetal signal is mainly affected by the maternal ECG (MECG). The non-stationary noises like muscular activities affect the signal-to-noise (SNR) of the fetal ECG [9].

The huge developments are using more than the current duration, mostly in case of varying SNR. The current techniques are immobile not capable of producing dependable F-QRS complex [10]. Consequently, the present condition of NIF-ECG explores raise the two applicable issues: The first one, how can the feature of NIF-ECG be quantifying in scenario of varying SNR [11]. The second one combines the data of numerous NIF-ECG channels, after channels and segments contain flawed recognition are present. The primary aim relates to the procedure of gesture excellence index, as formerly addressed by numerous mechanisms on mature ECG monitor [12]. The signal generated in electrical with the fetal spirit is calculated by non-invasive electrode located on the mother stomach exterior part. In the abdominal f-ECG recording, the electrical signal generated by the fetal heart is measured by non-invasive electrodes positioned on the mother stomach outside [6, 13].

This type of measurement is obviously appropriate for long-term surveillance in addition to home monitor throughout all pregnancy [14]. The fetal ECG signal obtained starting stomach of mother is characteristically considered with an incredibly small SNR [15]. Signal traced with this technique are forever a combination of noise produced. For illustration, with fetal's intelligence action, this is explicit signal (equally beginning the fetus and mother). The association maternal and artifact ECG are coming together [16]. Furthermore, the fetal constituent is typically lesser compared to the affectionate one. Since the fetal mind be minor than the mature, in addition this is characteristically attenuated by tissue in the pathway to the measure by the electrodes [17]. Combined the superior gesture meting away non-invasive

and technique to gaining of fetal ECG from side-to-side abdominal electrodes might permit at home permanent observing using WBSN's technologies [18].

Lately, it is intended for mature supervising of physiological gesture throughout daily performance. WBSNs are collected a changing figure of sensor to calculate and condense physiological signal. Signals are characteristically sent to close proximity elegant receiver to allow its communication toward an isolated work station using the Internet [19]. WBSN sensors contain characteristically a lot of constraint, single of the mare small power utilization [20]. Furthermore, as ultra-low-power radio devices, by small statement capability, it is so clear. There are typically warned for transmission; a further restriction is transmitting physiological gesture to be mainly compacted [21]. The other method to find fetal electrocardiogram is by support vector regression (SVR) [8]. The fetal signal can be absorbed by nonlinear mapping of MECG signals from both the abdomen and chest of the mother, and we get the fetal signal. The fetal signal is still affected by the maternal signal. The SVR can be used to find the fetal ECG by mapping the thoracic signal and maternal signal [22].

The multi-dimensional independent constituent analysis (MICA) is better than independent component analysis (ICA) [23]. MICA is a sophisticated gesture dispensation method to use for unscrambling away the fetal ECG from the maternal ECG with the take it easy for the interfering. MICA is a linear inventive reproduction, for example, to worn in ICA [24]. In dissimilarity to ICA, conversely, the mechanisms are not supposed toward everyone equally autonomous. As an alternative, it is supposed to the mechanism be intelligent to be partition keen on group. Mechanism from dissimilar group is statistically autonomous, but mechanism which fits into the similar assemblage might be dependent relative. MICA is additionally suitable than ICA inside the fetal ECG taking out difficulty. The justification after so as to convenient is no confirmation to proposed to the fetal apparatus are autonomous among them self. Although the MICA is usually dependable, experiment that it occasionally fails.

3 Mathematical Equations

Load the multi-leads ECG signals:

$$X_K, \quad K = 1, 2, 3, \dots, N \quad (1)$$

Calculate the dot produce template: $K_{ij} = K(X_i, X_j)$, where K is the kernel function [Gaussian kernels]: used here

$$K(X_i, X_j) = \exp \left[- \left(\frac{X_i}{2\sigma^2} - \frac{X_j}{2\sigma^2} \right)^2 \right] \quad (2)$$

Diagonals ‘ K ’ to attain the eigenvalues in attribute space $V^k, k = 1, 2, \dots, N$, solve

$$N\lambda\alpha = k\alpha, \alpha = (\alpha_1, \alpha_2, \dots, \alpha_N)^T \tag{3}$$

Normalize the eigenvalues with $\lambda_k(\alpha^k\alpha^k) = 1$.

Remove the nonlinear PCs for analysis signal ‘ x ’ in characteristic space by means of the.

First ‘ n ’ PCs:

$$P_n[\varphi(x)] = \sum_{k=1}^n \left(\sum_{i=1}^N \alpha_i^k k(x, x_i) \right) V^k \tag{4}$$

Locate the estimated pre-images ‘ y ’ in the participation gap of the nonlinear PCs in characteristic gap fulfilling $\phi(y) = P_n[\phi(x)]$ that estimate the maternal ECG mechanism [3].

The goal of KF is to approximate the condition of a discrete time prohibited procedure. Reflect on a condition vector x_{k+1} governed by a nonlinear stochastic dissimilarity equation by amount vector y_{k+1} at time instant $k + 1$:

$$x_{k+1} = f(x_k, w_k, k + 1) \tag{5}$$

$$y_{k+1} = h(x_{k+1}, v_{k+1}, k + 1) \tag{6}$$

where the random variables ‘ w_k ’ and ‘ v_k ’ represent the procedure and amount of noises, with associated co-variance matrices [4].

4 Methodologies

4.1 FICA Technique

FICA method is a permanent top iterative algorithm which is used to reduce the share in order to connect the mechanism. When maximum Gaussianity is achieved, we can separate the independent components. There are different types of fast ICA methods like kurtosis and maximum negentropy (MNE). Here, we are using MNE method of fast ICA algorithm which uses maximum negentropy for direction and extracts each independent source signal in turn.

Facing the request of FICA algorithm, we should remove the mean components from the observed signal and should make experiential signal with zero mean. It is observed that signal with zero mean undergoes PCA, so that it can be whitened and its components are uncorrelated. The main reason for the application of FICA

founded on fixed point iterative organization is to make $y = w^T x$ which should have maximum non Gaussianity, where ‘ w ’ is a row of parting matrix ‘ W ’.The objective function is

$$J(y) \approx \{E[G(y)] - E[G(v)]\}^2 \tag{7}$$

Everywhere $E [.]$ is an exponential operative, and ‘ v ’ is Gaussian random coefficients by means of zero unit variance and mean. We should assume that ‘ y ’ also has unit variance and zero mean. $G (.)$ was a non-quadratic utility.

Based on the Kuhn–Tucker state, optimization of $E \{G(w^T x)\}$ can be done by (2) under the condition

$$E\{(w^T x)^2\} = |w|^2 = 1 \tag{8}$$

$$E\{xg(w^T x) - Bw = 0\} \tag{9}$$

4.2 Kernel PCA Method

The PCA is a constructive approach for extraction of prospective linear configuration starting multi-dimensional records. The PCA simply relieves the relationship of the information in addition to not examine its nonlinear difficulty consequently. The essential part of PCA is a simplification that is only appropriate intended to solve the difficulty of nonlinear extraction of feature.

It provides the further characteristics of information and feature of PCA. Because the feature’s quantity offered by the previous is equivalent to the amount of the participation sample. But the amounts of the concluding measurement of the contribution example are shown in Fig. 1. When examining the information through possible nonlinear configuration. The k-PCA map inventive vector to an elevated dimensional break ‘ F ’, and it carried away PCA scheduled ‘ F ’. To carry out the nonlinear plot interested in ‘ F ’, to use a kernel utility in the innovative gap.

The estimation of fetal ECG difficulty to reconstruct the original space in the feature space. It is needed to locate the approximation vectors and pre-images in the features space shown in Figs. 2 and 3.

4.3 Support Vector Regression

At opening, two signals are taken as abdominal and thoracic parts of the pregnant women. Some disturbances like baseline ramble and 50/60 Hz power-line interference can be eliminated during the preprocessing phase. The abdominal ECG

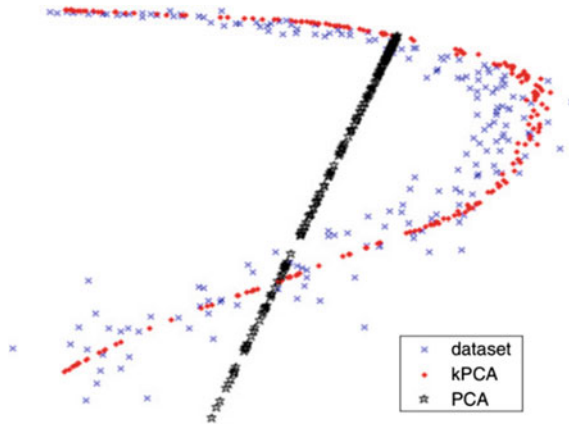


Fig. 1 PCA and k-PCA dataset using Kernel method

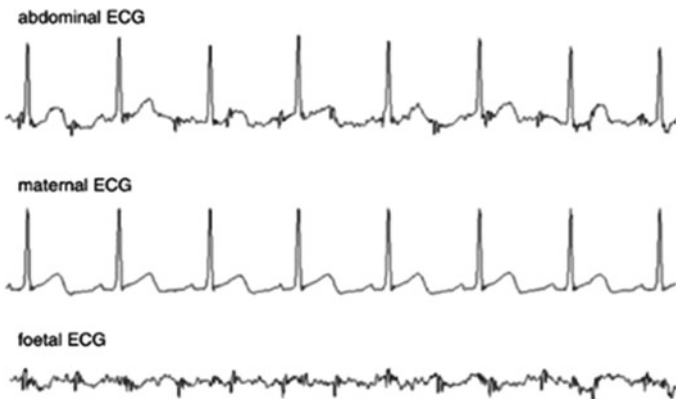


Fig. 2 Estimation of fetal ECG starting actual signal 'ecgca-826' by KPCA

' $a(n)$ ' contains both maternal ECG and fetal ECG ' $f(n)$ ', whereas the maternal ECG is same as the thoracic ECG ' $t(n)$ ' shown in Fig. 4. The operative $t[.]$ points to nonlinear conversions in upper body to stomach. Consequently, the MEEG element in an abdominal gesture can be measured as a nonlinear map thoracic gesture, and the $w(n)$ is the environmental sound shown in Fig. 5.

4.4 Input to MICA as Maternal Abdominal ECG

MICA is frequently applied to MEEG signal occupied by the mother's thoracic section that is approximately liberated starting fetal assistance. This is capable of

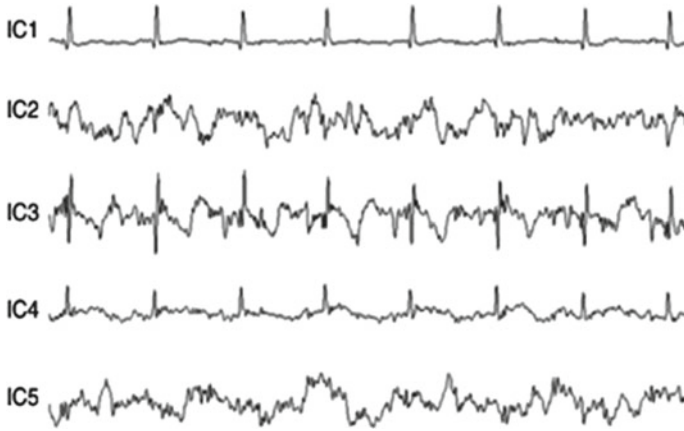


Fig. 3 Estimation of fetal ECG actual signal 'ecga826' by F-ICA

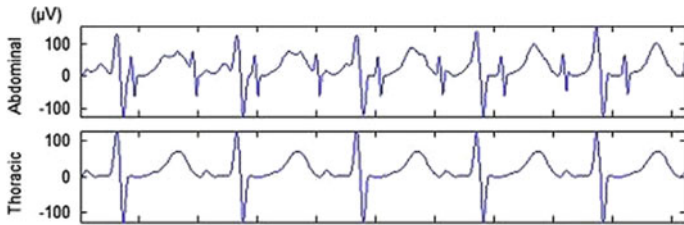


Fig. 4 PCA and k-PCA dataset using kernel method

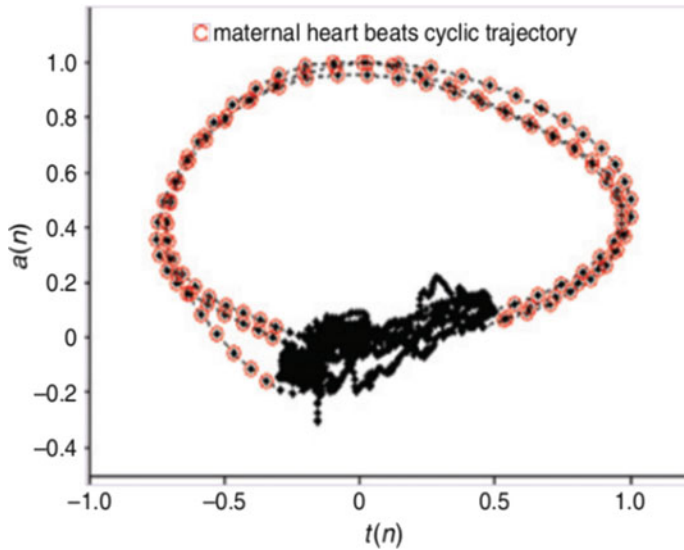


Fig. 5 Maternal heartbeat cyclic trajectory

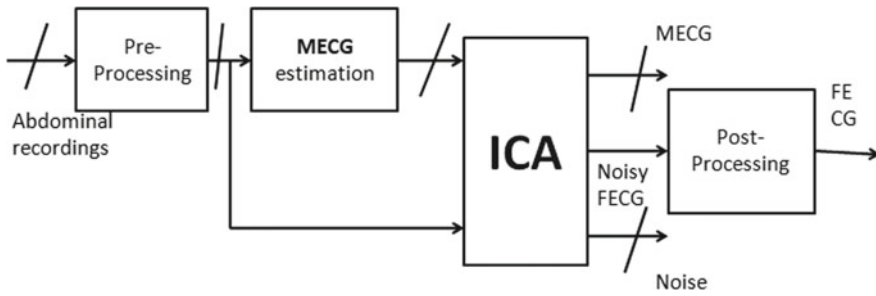


Fig. 6 Block diagram of the proposed system for MICA estimation

be through of as reference and estimated the maternal sources and eliminated the signal recorded the mother abdomen. Based on MICA, the proposed block diagram is shown in Fig. 6.

In Preprocessing: The objective of preprocessing is to eliminate the baseline EMG noise. The power-line noise is interfering with all the signals. Baseline wander noise affects the patient movement, breathing, etc. It could remove the cutoff frequency 1–90 Hz. The power-line noise is discarded by a notch filter.

MECG Estimation: The projected process has been used with achievement as follows: First, filter all the signal that occupied mother stomach by filtering disrupted to execute the linear mapping. The filter outputs lower-dimensional principal component analysis (PCA). This block quality the difficulty getting better gesture is contaminated with noise.

ICA Block: To execute MICA, one method approximates the essential ICA representation after those group components according to their confidence. The ICA inputs are together preprocessor abdominal maternal gesture MECG is estimated. The post-processing block is the final module in the MICA estimation, and it provides the final extracted F-ECG.

5 Conclusion

This paper described different types of f-ECG extraction which is the better method. This method takes a smaller amount of time compared to other fetal ECG extraction methods. So, this algorithm is best powered devices, and their results are more efficient than the other methods. FECG was productively recognized by the expanded ICA algorithm. This was established with the help of ICA method. It had been effectively detached the mechanism enclosed inside each soundtrack. Features identical among every resource gesture and ICA works yield involuntary division involving the recording mechanism. FECG assists in recognizing the generally physical condition of the fetus throughout the pregnancy.

References

1. L. Yuan, Z. Zhou, Y. Yuan, S. Wu, An improved FastICA fetal ECG extraction. *Comput. Math. Methods Med.* **2018**, 1–7 (2018)
2. W. Xueyun, Z. Wei, Application of Kernel PCA for foetal ECG estimation. *Electron. Lett.* **54**(6), 340–342 (2018)
3. Z. Wei, Li. Xiaolong, W. Xueyun, L. Hongxing, Foetal ECG extraction by support vector regression. *Electron. Lett.* **52**(7), 506–507 (2015)
4. M. Niknazar, B. Rivet, C. Jutten, Fetal ECG extraction by extended state Kalman filtering based on single-channel recordings. *IEEE Trans. Biomed. Eng.* **60**(5) 1345–1352 (2012)
5. C. Olivares, J. Luis, M.C. Rubén, H.M. Susana, M.M. Elena, I. Román, The maternal abdominal ECG as input to MICA in the fetal ECG extraction problem. *IEEE Sig. Process. Lett.* **18**(3), 161–164 (2011)
6. E.C. Karvounis, M.G. Tsipouras, D.I. Fotiadis, Detection of fetal heart rate through 3-D phase space analysis from multivariate abdominal recordings. *IEEE Trans. Biomed. Eng.* **56**(5), 1394–1406 (2009)
7. M.C. Ruben, C.O. Jose Luis, H.M. Susana, M. Elena, I. Roman, Fast technique for non invasive fetal ECG extraction. *IEEE Trans. Biomed. Eng.* **58**(2), 227–230 (2010)
8. K. Assaleh, H. Al-Nashash, A novel technique for the extraction of fetal ECG using polynomial networks. *IEEE Trans. Biomed. Eng.* **52**(6), 1148–1152 (2005)
9. E.C. Karvounis, M.G. Tsipouras, D.I. Fotiadis, K.K. Naka, An automated methodology for fetal heart rate extraction from the abdominal electrocardiogram. *IEEE Trans. Inf Technol. Biomed.* **11**(6), 628–638 (2007)
10. M.K. Singh, A.K. Singh, N. Singh, Multimedia analysis for disguised voice and classification efficiency. *Multimedia Tools Appl.*. doi 10. 1007/s11042-018-6718-6
11. P.P. Kanjilal, S. Palit, G. Saha, Fetal ECG extraction from single-channel maternal ECG using singular value decomposition. *IEEE Trans. Biomed. Eng.* **44**(1), 51–59 (1997)
12. M.K. Singh, A.K. Singh, N. Singh, Disguised voice with fast and slow speech and its acoustic analysis. *Int. J. Pure Appl. Math.* **11**(14), 241–246 (2018)
13. A. Khamene, S. Negahdaripour, A new method for the extraction of fetal ECG from the composite abdominal signal. *IEEE Trans. Biomed. Eng.* **47**(4), 507–516 (2000)
14. M. Richter, T. Schreiber, D.T. Kaplan, Fetal ECG extraction with nonlinear state-space projections. *IEEE Trans. Biomed. Eng.* **45**(1), 133–137 (1998)
15. M.K. Singh, A.K. Singh, N. Singh, Multimedia utilization of non-Computerized disguised voice and acoustic similarity measurement. *Multimedia Tools Appl.* <https://doi.org/10.1007/s11042-019-08329-y>
16. M. Sato, Y. Kimura, S. Chida, T. Ito, N. Katayama, K. Okamura, M. Nakao, A novel extraction method of fetal electrocardiogram from the composite abdominal signal. *IEEE Trans. Biomed. Eng.* **54**(1), 49–58 (2006)
17. M.K. Singh, D. Nandan, S. Kumar, Statistical analysis of lower and raised pitch voice signal and its efficiency calculation statistical analysis of lower and raised pitch voice signal and its efficiency calculation. *Traitement du Signal* **36**(5), 455–461 (2019). <https://doi.org/https://doi.org/10.18280/ts.360511>
18. L. He, D. Chen, G. Sun, Detection of fetal ECG R wave from single-lead abdominal ECG using a combination of RR time-series smoothing and template-matching approach. *IEEE Access* (2019)
19. M.K. Singh, N. Singh, A.K. Singh, Speaker’s voice characteristics and similarity measurement using Euclidean distances, in *IEEE Conference (ICSC) 2019* <https://doi.org/10.1109/ICSC45622.2019.8938366>
20. A. Gupta, M.C. Srivastava, V. Khandelwal, A. Gupta, A novel approach to fetal ECG extraction and enhancement using blind source separation (BSS-ICA) and adaptive fetal ECG enhancer (AFE), in *2007 6th International Conference on Information, Communications & Signal Processing* (IEEE, 2007), pp. 1–4

21. Van Hulle, M. Marc Constrained subspace ICA based on mutual information optimization directly. *Neural Comput.* **20**(4), 964–973 (2008)
22. M.K. Singh, A.K. Singh, N. Singh, Acoustic comparison of electronics disguised voice using different semitones. *Int. J. Eng. Technol. (UAE)*. <https://doi.org/10.14419/ijet.v7i2.16.11502>
23. S. Muceli, D. Pani, L. Raffo, Real-time foetal ECG extraction with JADE on floating point DSP. *Electron. Lett.* **43**(18), 963–965 (2007)
24. N.J. Outram, E.C. Ifeachor, P.W.J. Van Eetvelt, S.H. Curnow, Techniques for optimal enhancement and feature extraction of fetal electrocardiogram. *IEE Proc.-Sci. Measure. Technol.* **142**(6), 482–489 (1995)

A Proposed Model for Customer Churn Prediction and Factor Identification Behind Customer Churn in Telecom Industry



Nooria Karimi, Adyasha Dash, Sidharth Swarup Rautaray,
and Manjusha Pandey

1 Introduction

In the present world, telecom organizations at an exceedingly quick rate are producing an enormous volume of data. There is a scope of telecom specialist organizations contending in the market to build their customer base. Customers have numerous alternatives as better and more affordable services. A definitive objective of telecommunication organizations is to boost their benefit and survive in a focused commercial center [1]. A customer attrition happens when a huge level of customers are most certainly not happy with the administrations of any telecom organization, and churn additionally influences the general notoriety and reputation of an organization, which brings about its image misfortune and brand loss. The contender organizations occasionally influence a faithful customer, who produces high income for the organization. Such customers expand the benefit of an organization by alluding it to their companions, relatives, and associates [2].

Telecom organizations consider strategic move when the quantity of customers dips under a specific level, which may bring about an enormous dropping of income [3]. Churn prediction is imperative in the telecommunication division as telecommunication drivers need to hold their important customers and improve their CRM administration [4, 5]. The most testing and challenging activity for CRM is to satisfy

N. Karimi · A. Dash (✉) · S. S. Rautaray (✉) · M. Pandey (✉)
School of Computer Engineering, KIIT Deemed To Be University, Bhubaneswar, India
e-mail: adyasha.dashfcs@kiit.ac.in; siddharthfcs@kiit.ac.in

S. S. Rautaray
e-mail: siddharthfcs@kiit.ac.in

M. Pandey
e-mail: siddharthfcs@kiit.ac.in

N. Karimi
e-mail: Noria.karimi2@gmail.com

and keep remaining customers for long time base [6]. Because of the soaked and aggressive market, consumers have the alternative to change to other specialist organizations.

Telecommunication organizations have created methods to recognize and maintain their customers, as it is more affordable than pulling in the new ones [4]. This is because of the cost engaged with commercials, workforce, and concessions which can scale up to just about five to multiple times then holding and maintaining alive-customers [3]. Little consideration is required for recognizing the churn customers, which can assist in upsetting the circumstance. The necessity of holding customers needs to build up an exact and elite model for recognizing loyal and disloyal customers, who are more likely to leave the company. The proposed model ought to have the capacity to distinguish the customers who are planning to stop using the company's services and afterward discover the explanations behind their churn, to keep away customer defection and give measures to hold them. What's more, it should utilize methods to anticipate when such a circumstance will emerge later on. Because of ongoing headway in the area of big data, there exist numerous data mining and machine learning solutions, which can be utilized to analyze and break down such data. These methods break down the data and distinguish causes for customer turnover; CRM can utilize these systems to augment their benefit [2].

It is difficult to anticipate the reason for churn and its recurrence. Various issues with customer advancement emerge basically in light of the quality component including service quality, network coverage, load errors, billing, costs, technologies, innovations, and so on [2]. These service quality elements enable customers to contrast service quality and benefits and other good service suppliers [4]. The forecast pace of the ordinary customer in the telecommunication division is assessed at 2%, which is the all out yearly drop of roughly 100 billion dollars [7]. Existing examinations uncover that the essential goal is to utilize a huge volume of telecommunication data to distinguish the significant churn customers [2]. Vast amount of data is being produced in the telecommunication arena, and the data holds missing qualities, which produce insignificant consequence of the expectation models. To deal with these matter, data pre-processing techniques are adjusted to expel clamor from data, which is powerful for a model to accurately group the data and enhance the exhibition. Feature selection has been utilized in publication; however, various data feature selection are dismissed while modeling development [8].

In this examination, the proposed model for customer attrition has been created that utilizes different machine learning algorithms. The accuracy of a classifier relies upon the accessible dataset [2]. It is approved by utilizing a telecom dataset, which is publically accessible on Kaggle Web site. The presented churn prediction model is assessed utilizing information retrieval metrics. The accuracy is calculated for churn prediction model utilizing TP rate, FP rate, precision, recall, F-measure and ROC area, and the target of the examination is to research the current procedures in machine learning and data mining to profound a model for customer attrition prediction, as well as recognizing the factors behind customer churn. The gradient boost classifier algorithm created better accuracy and precision, when contrasted with other machine learning algorithms. Remainder of the paper is arranged as follows.

Section 2 gives literature survey. Section 3 defines the problem, Sect. 4 manifests the proposed model for customer churn prediction. Section 5 relates the dataset, Sect. 6 discusses the factors identifying customer churn, and the paper has been shut with the discussion and reference sections.

2 Literature Review

In this chapter, a review of the bibliographic content found is conducted. The focus is the methodologies and strategies applied to customer churn prediction and factors identifying customer churn. Customer churn investigation and customer churn factors expectation in CRM media transmission have been acted in the publications utilizing different methods including machine learning, data mining, and big data analytic. These procedures bolster organizations to investigate customer churn, recognize, anticipate, and maintain churn customers, and help in basic leadership and CRM. Here are a few works that have done in the referenced territory [9].

Three machine learning algorithms utilized [2011] neural networks, support vector machine, and Bayes networks to foresee churn factor. The creator utilized AUC to quantify the exhibition of the calculations. The AUC esteems were 99.10, 99.55, and 99.70% for Bayes networks, neural systems, and bolster vector machine, respectively. The dataset utilized in this investigation is little, and no missing qualities existed. Another element choice strategy is proposed to determine CRM data index with pertinent highlights by joining a productive data mining methods to improve data quality and feature importance [10].

Huang et al. [11] viewed the matter of customer attrition in the large data platform. The aim of the scientists was to reveal that huge data enormously improves the direction toward foresee the churn contingent upon the volume, assortment, and pace of the data [12].

Makhtar et al. [12] proposed a model for churn prediction utilizing rough set theory in telecom. As referenced in this paper, rough set characterization calculation outflanked different calculations like linear regression, decision tree, and voted perception neural network. Different investigation considered the issue of lopsided informational indexes where the stirred client classes are littler than the dynamic client classes, as it is a significant issue in beat expectation issue [13].

Amin et al. [13] looked at six different inspecting strategies for oversampling with respect to telecom churn predicting issue. The outcomes demonstrated that the calculations (MTDF and rules-age dependent on hereditary calculations) outflanked the other analyzed oversampling calculations [14].

Adnan et al. (2018) proposed examination not just exhibited a novel JIT-CCP model for the telecom organization where: (I) an organization is recently settled and do not have recorded data to fabricate a proficient CCP model, (ii) an organization has lost the data because of any uncommon explanation, or (iii) as of late received the cutting edge innovation for keeping up the customer conduct, yet additionally

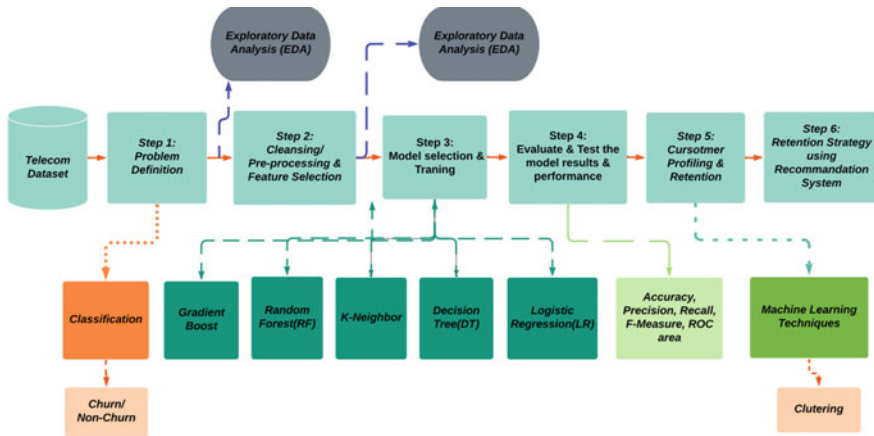


Fig. 1 Proposed model for customer churn prediction

showed the correlation of the impact of with and without data change strategies (e.g., log and rank) for the JIT-CCP [15].

Ahmad et al. [9] in this exploration expected to fabricate a framework that predicts the stir of consumers in Syriatel telecom sector. Four-tree-based calculations were picked on account of their decent variety and relevance in this sort of expectation. These calculations are decision tree, random forest, GBM tree calculation, and XGBOOST algorithm. The strategy for arrangement and choice of highlights and entering the versatile interpersonal organization highlights had the greatest collision on the achievement of this model, as the estimation of AUC in Syriatel arrived at 93.301%. XGBOOST tree model accomplished the best outcomes in all estimations.

In this examination, the feature-engineering stage is mulled over to make our very own features to be utilized in machine learning algorithms. In this examination, we have utilized gradient boost classifier, support vector machine, random forest, N-nearest neighbor, and strategic relapse in which the gradient boost classifier produced the high accuracy and precision which has been utilized for customer churn prediction as well as for identifying factors behind customer churn, and the customer churn prediction model has appeared in Fig. 1.

3 Problem Definition

This paper proposes a model as appeared in Fig. 1. The problem has been identified into following two phases.

Phase 1: Customer churn identification: Customer churn, otherwise called customer defection, in its most fundamental structure, is the point at which a customer decides to quit utilizing your items or services [16]. To begin understanding the customer’s excursion and the encounters they have, there ought to be an important

and all encompassing model to handle this issue. For this, machine learning calculations and data mining methods have been used, and a model has been worked for customer churn prediction, which has been appeared in Fig. 1.

Phase 2: Identifying factors responsible for customer churn The factors of customer attrition are examined in this subsection that is arranged by the attribute selected classier. This technique gives regulation for customer churn prediction as well as gives customer behavior and patterns [2]. These key principles are truly important for the telecom leaders and decision makers to maintain the customers. The attribute selected classier algorithm characters numerous explanation for customer attrition and gives characteristics which rely upon one another. The churn-related principles gave by the attribute selected classier algorithm, which has been shown in Table 3.

4 Proposed Model for Customer Churn Prediction

This chapter exhibits the proposed customer churn prediction model. Figure 1 displays the proposed model and in addition portrays its respected phases. In the initial phase, the problem has been characterized, in the subsequent advance, exploratory data analysis utilized for preparing the data for additional examination, data pre-processing, data filtering for noise removal, removal of imbalanced data, and standardization of data has been done in this progression as well as important features are extracted, and in the third phase, different classification algorithms have been utilized, for grouping the customers into the churn and non-churn consumers. The classification algorithms incorporate gradient boost, random forest (RF), k-neighbor, decision tree (DT), and logistic regression (LR); in the fourth phase, the assessment and testing of the model are performed utilizing confusion matrix, precision and recall, F-measure, and ROC area; in the fifth phase, customer profiling is observed utilizing k-means clustering technique. In the final phase, the model advocates retention master plan for each class of customers. In this investigation, scope of machine learning algorithms is utilized for arranging customer's data utilizing labeled dataset. It is to evaluate which of the algorithm best groups the customers into the churn and non-churn groups. In the first place, the gradient boost algorithm is utilized for classification. Furthermore, random forest, decision tree, k-nearest, and logistic regression are utilized, with tenfold cross-validation. The classification process has been performed by machine learning algorithms, and Weka tool has been utilized for factor identification.

5 Dataset Description

In this investigation, two datasets have been utilized. The initial dataset is utilized for training the model, and the subsequent one is utilized for testing the model,

Table 1 Customer dataset description

#S	Variable	Data type	Description
1	Account length	Integer	How long account has been active
2	Int'l plan	Categorical	International plan activated (Yes, No)
3	Vmail plan	Categorical	Voice mail plan activated (Yes, No)
4	VamilMessage	Integer	No. of voicemail messages
5	DayMins	Integer	Total day minutes
6	DayCalls	Integer	Total day calls made
7	DayCharge	Integer	Total day charge
8	EveMins	Integer	Total evening minutes
9	EveCalls	Integer	Total evening calls
10	EveCharge	Integer	Total evening charges
11	NightMins	Integer	Total night minutes
12	NightCalls	Integer	Total night calls
13	NightCharge	Integer	Total night charges
14	IntlMins	Integer	Total international minutes used
15	IntlCalls	Integer	Total international calls made
16	IntlCharge	Integer	Total international charges
17	CustServCalls	Integer	Number of customer service calls made
18	Churn	Categorical	Customer churn (Yes = churn, No = no-churn)

the dataset has 3333 instances with 21 features, in which exploratory data analysis and feature selection method have been performed, 13 relevant and useful features produced for training and testing the model, as well as feature-engineering has done utilizing machine learning libraries, and it hold labeled data with two classes where 14% of the complete data is named as churn “YES” though 85.5% perception has the value “NO”, non-churn. The dataset variables of customer transactions and their descriptions are introduced in Table 1. The datasets are accessible on Kaggle Web site <https://www.kaggle.com/c/churn-analytics-bda/data> which are in both numerical and categorical structure, the data exploratory analysis has been utilized in the subsection to defeat the issues with the datasets, and for validating the data, the test dataset has been utilized. Table 1 describes the dataset with the related types.

5.1 Data Pre-processing

Data pre-processing is a significant advance on any data mining venture. Real-world data is commonly deficient, conflicting, and even blunders. To create a decent model to an issue, these issues must be addressed. The problems with the dataset have been listed in the subsection below.

1. **Missing data:** In this examination, this issue has been handled by utilizing mean and mode for supplanting the missing values.
2. **Noise removal:** There are many missing values in telecom dataset, wrong qualities like “invalid” and awkwardness characteristics in the dataset. In this dataset, the amount of features is 21. The filtering technique has been done for separating the unnecessary data form relevant data, and the amount of features after applying filtering technique is as shown in Table 2.
3. **Redundant data:** This sort of error is for the most part related to human blunders. The data could have been recorded under various names or in different places. For our situation, fortunately there are no redundant data.
4. **Unbalanced Dataset:** The created dataset was imbalance since it is an uncommon instance of the classification issue where the appropriation of a class is not normally similar to other classes. The predominant class is known as the essential class, and the others are known as the optional class. Dataset is unstable if one of its class is 10% or smaller contrasted with the other one [7]. Dataset was unstable as the level of the optional class that speaks churn customers is about 14.5% of the entire dataset, and the targeted class is 85%. It clearly shows that the data is skewed. Along these lines, if the machine gets trained with this dataset, the machine will produce the outcome as true or churn with accordingly and it will be biased, and we utilize a few strategies for taking care of this issue. There are numerous techniques for taking care of the imbalance data issue, which are under-sampling, over-sampling, smote, and many more; each one is utilized for dealing with imbalance data. In this experiment, we have utilized stratified-k-fold method for solving this problem.
5. **Features Selection:** Feature selection is a critical advance for choosing the important features from a dataset dependent on dominion grasp. Various methods exist in the literature for feature selection [17, 18]. With regard to churn prediction, in this examination, we utilized feature importance method, Feature importance

Table 2 Relevant features

Attributes	Important features ranking
International_Plan	0.25985
No_CS_Calls	0.20875
State	0.01874
Voice_Mail_Plan	0.10215
Total_Intl_Calls	0.05284
Phone_No	0.00573
Total_Night_Calls	0.00614
Account_Length	0.01654
Area_Code	0.00617
Total_Night_Charge	0.0355
Total_Night_Minutes	0.033549
Total_Day_Calls	0.01846

method gives result for each feature of the data, and the higher the result the more important or relevant is the feature towards your output variable [16]. In churn dataset, we chose just the main 13 relevant features out of the complete 21 features, having high-ranking qualities in the result of two techniques. The performance of classification increments in the dataset contains profoundly prescient and important factors [2]. Besides, the dataset with high relationships has been dropped from both datasets. As they do not have any new information, they are only a relationship. The relevant features have shown in Table 2.

5.2 Performance Evaluation Matrix

In this examination, the profound customer churn prediction model is surveyed utilizing accuracy, precision, recall, F-measure, and ROC area. Equation (1) ascertains the accuracy metric. It distinguishes number of occasions accurately characterized.

$$\text{Accuracy} = \frac{\text{True Positive} + \text{True Negative}}{\text{True Positive} + \text{True Negative} + \text{False Positive} + \text{False Negative}} \quad (1)$$

TP rate is generally called sensitivity. It notices the portion of data which is precisely named positive. In addition, it must be high for any classifier. It has dictated by in Eq. (2).

$$\text{TP Rate} = \frac{\text{True Positive}}{\text{Actual Positive}} \quad (2)$$

FP rate uncovers which some part of the data is erroneously assigned positive, and it should be low for any classifier. As it is controlled by utilizing Eq. (3):

$$\text{FP Rate} = \frac{\text{False Positives}}{\text{Actual Negatives}} \quad (3)$$

Accuracy generally called positive predictive value (PPV), and it shows which part of the predicted data is positive. It has controlled by utilizing Equation (4).

$$\text{Precision} = \frac{\text{True Positive}}{\text{True Positive} + \text{False Positive}} \quad (4)$$

The recall is another measure for completeness instances, the likelihood that all the applicable features are picked by the system. It is controlled by utilizing Eq. (5).

$$\text{Recall} = \frac{\text{True Positive}}{\text{True Positive} + \text{False Negative}} \quad (5)$$

The F-measure value is a trade-off between accurately classifying all the data points and guaranteeing that each class contains points of just one class. It is determined by utilizing Eq. (6).

$$F\text{-measure} = 2 \times \frac{\text{Precision} \times \text{Recall}}{\text{Precision} + \text{Recall}} \tag{6}$$

ROC area demonstrates the normal execution against all possible cost proportion between FP and FN in the event that the ROC area value is identical to 1.0, and this is a perfect prediction. In this manner, the values 0.5, 0.6, 0.7, 0.8, and 0.9 speak to irregular expectation, horrendous, moderate, good, and predominant, respectively, and values of ROC area other than these show something is not right [2].

6 Factors Identifying Customer Churn

In light of the examination, network quality, call facilities, Internet facilities, and booster facilities were the high effect factors that give rise to customer turn over in telecommunication industry [19]. The objective of this section is to identify the high effective factors that cause customer attrition. The factors of churn customers are examined in this subsection, by utilizing the attribute selected classifier algorithm with info_Gain_Attribute_Evaluator method in Weka tool, this strategy gives rules for customer churn prediction as well as identifying customer conduct samples, and these key principles are entirely significant for the leaders and decision makers to maintain the customers who are more likely to churn. The attribute selected classifier algorithm recognizes numerous reasons behind customer churn and gives highlights, which rely upon one another [2]. In this experiment, there has been found top five high churn ranking features which cause customer churn and are depicted in Table 3. These five factors are highly dependent features for customer churn, which ought to be considered by decision makers, for retaining them, by taking some vital strategic business planning.

Table 3. Ranked gain information of factors in various categories

S#	Category	Information gain
1	NO_CS_CALLS	0.07072
2	INTERNATIONAL_PLAN	0.03787
3	STATE	0.026616
4	NO_VMAIL_MESSAGES	0.0138
5	TOTAL_INIL_CALLS	0.00467

7 Discussion

Customer churn has always been a major concern for telecommunication industry. Research has shown that acquiring new customer is five to six times costlier than retaining present one. Decision makers and leaders are emphasizing on distinguishing the customers based on their behaviors and maintaining the customers who are more likely to churn for any other service provider; for tackling this issue, there should be a holistic and perfect model to predict customer attrition and the factors behind customers churn.

There are many experiments which has been done to solve customer churn problem; different methodology and technologies have been utilized in this manner, utilizing machine learning algorithms, data mining techniques, and big data analytic to deal with the issue; algorithms like random forest, decision stump, AdaBoost, Naive Bayes, and many more have been utilized; in the current experiment, gradient boost, random forest, k-neighbor, decision tree, and logistic regression have been applied to build the best churn prediction model in which the gradient boost algorithm has been selected as the classifier for customer churn prediction as it had produced high accuracy with high precision; the main objective of this experiment is to build a model which can predict customer attrition as well as identifying factors behind customer attrition.

Due to some restrictions, it was not possible to arrange all the phases in one single paper; therefore, the paper has been separated the phases into two distinct papers. The first paper proposed a model for customer churn prediction as well as identification of customer churn factors. The second paper covers customer profiling and customer retention using recommendation system. The model has portrayed in Fig. 1.

References

1. S. Babu, Dr N.R. Ananthanarayanan, V. Ramesh, A survey on factors impacting churn in telecommunication using data mining techniques. *Int. J. Eng. Res. Technol. (IJERT)* **3**(3) (2014)
2. I. Ullah, et al., A churn prediction model using random forest: analysis of machine learning techniques for churn prediction and factor identification in telecom sector. *IEEE Access* **7**, 60134–60149 (2019)
3. W. Verbeke, et al., Building comprehensible customer churn prediction models with advanced rule induction techniques. *Exp. Syst. Appl.* **38**(3), 2354–2364 (2011)
4. A. Idris, A. Khan, Customer churn prediction for telecommunication: employing various features selection techniques and tree based ensemble classifiers, in *2012 15th International Multitopic Conference (INMIC)* (IEEE, 2012)
5. M. Kaur, K. Singh, N. Sharma, Data mining as a tool to predict the Churn Behaviour among Indian bank customers. *Int. J. Recent Innov. Trends Comput. Commun.* **1**(9), 720–725 (2013)
6. V.L. Miguéis et al., Modeling partial customer churn: On the value of first product-category purchase sequences. *Expert Syst. Appl.* **39**(12), 11250–11256 (2012)
7. M.-M. David, The architecture of a churn prediction system based on stream mining, in *Proceedings of Artificial Intelligence Residue Development 16th International Conference Catalan Association Artificial Intelligence*, vol. 256 (2013)

8. Y. Huang, T. Kechadi, An effective hybrid learning system for telecommunication churn prediction. *Expert Syst. Appl.* **40**(14), 5635–5647 (2013)
9. A.K. Ahmad, A. Jafar, K. Aljoumaa, Customer churn prediction in telecom using machine learning in big data platform. *J. Big Data* **6**(1), 28 (2019)
10. H. Gao, Customer relationship management based on data mining technique—Naive Bayesian classifier, in *2011 International Conference on E-Business and E-Government (ICEE)* (IEEE, 2011)
11. Y. Huang et al, Telco churn prediction with big data, in *Proceedings of the 2015 ACM SIGMOD International Conference on Management of Data* (2015)
12. M. Makhtar et al., Churn classification model for local telecommunication company based on rough set theory. *J. Fund. Appl. Sci.* **9**(6S), 854–868 (2017)
13. A. Adnan et al., Comparing oversampling techniques to handle the class imbalance problem: a customer churn prediction case study. *IEEE Access* **4**, 7940–7957 (2016)
14. A. Adnan et al., Just-in-time customer churn prediction: with and without data transformation, in *2018 IEEE Congress on Evolutionary Computation (CEC)* (IEEE, 2018)
15. H.F. Yu, H.Y. Lo, H.P. Hsieh, J.K. Lou, T.G. McKenzie, K.D.D. cup, ntur.lib.ntu.edu.tw, Feature engineering and classifier ensemble for KDD cup 2010, in *KDD cup* (2010)
16. <https://www.qualtrics.com/experience-management/customer/customer-churn/>
17. L. Zhao et al., K-local maximum margin feature extraction algorithm for churn prediction in telecom. *Cluster Comput.* **20**(2), 1401–1409 (2017)
18. S. Babu, Dr N.R. Ananthanarayanan, V. Ramesh, A survey on factors impacting churn in telecommunication using datamining techniques. *Int. J. Eng. Res. Technol. (IJERT)* **3**(3) (2014)
19. <https://towardsdatascience.com/feature-selection-techniques-n-machine-learning-with-pythhon-f24e7da3f36e>

Fuzzy-Enabled Direct Torque Control for Low Torque Ripple in Induction Motors for EV Applications



Pratyay Maity and A. Vijayakumari

1 Introduction

Zero-emission transportation is envisaged shortly to curtail the predominant pollution components due to road transportations. This ambitious task will not be possible unless the entire transportation is electrified. Today's transportation represents a heterogeneous mix in terms of size, cost, and models, with the major share contributed by the light motor vehicle class. Of late, light motor Electric Vehicles (EV) are proliferating at a much higher rate into the society, especially in populated countries like India. Yet, the cost of today's Electric Cars (EC) are very high which is considered as a barrier for their wide spread diffusion into the market. The major cost component of ECs are the electric motor and their drives. With the recent addition of Permanent magnet and Reluctance machines, the costs of ECs are falling on the higher side. ECs like Mahindra E20, Tesla S and Tata Tigor, prefer Induction motors because of the cost advantages, and ease of control. Control of induction motor with variable frequency and variable voltage has been carried out through different techniques, ranging from simple V/f to the sophisticated vector control techniques. The former exhibits poor dynamic performance while the latter is necessitating high-speed high-cost digital controllers for the execution of rigorous mathematical computations. Direct Torque Control (DTC) is a technique that doesn't involve intense computations thus very simple to implement, simultaneously provides superior dynamic response. As DTC takes control variables like the flux, and torque from the machine, it exhibits an

P. Maity (✉)

Department of Electronics and Communication Engineering, Amrita School of Engineering,
Coimbatore Amrita Vishwa Vidyapeetham, Coimbatore, India
e-mail: pratyay54@gmail.com

A. Vijayakumari

Department of Electrical and Electronics Engineering, Amrita School of Engineering, Coimbatore
Amrita Vishwa Vidyapeetham, Coimbatore, India
e-mail: a_vijayakumari@cb.amrita.edu

© Springer Nature Singapore Pte Ltd. 2021

K. S. Sherpa et al. (eds.), *Advances in Smart Grid and Renewable Energy*,
Lecture Notes in Electrical Engineering 691,
https://doi.org/10.1007/978-981-15-7511-2_35

371

efficient torque control with better dynamics. However, the Conventional DTC has few shortcomings due to the hysteresis comparators, which create high levels of ripple in the torque and flux variables [1, 2]. Such high ripples cause higher acoustic noise and higher harmonics in machine output parameters. AI-based techniques can be amalgamated with DTC, for ripple minimization and performance improvement. Among the AI-based techniques, the Fuzzy logic controller is effective in handling the uncertainty of the DTC switching table [1, 2] especially during transient events. This paper presents a scheme to integrate the Fuzzy logic based techniques into DTC for torque ripple minimization.

2 Conventional Direct Torque Controller

The accuracy and dynamic performance of DTC is based on the accuracy of the torque, stator flux and stator flux position estimation [2]. Such estimations are accomplished from stator variables through the closed-loop mathematical estimator [2, 3]. The overall implementation scheme of the conventional DTC is presented in Fig. 1.

Motor parameters like torque, flux, and speed can be regulated to follow any predefined references by selecting an optimal switching condition of the inverter from the possible switching states [2–4]. The estimated electromagnetic torque and the stator flux are compared with the reference torque and flux to generate the torque and flux magnitude errors E_{T_e} and E_ϕ [3]. The flux error is processed through a two-level hysteresis controller while the torque error is processed through a three-level hysteresis controller to obtain the present status of these quantities [2–4]. The

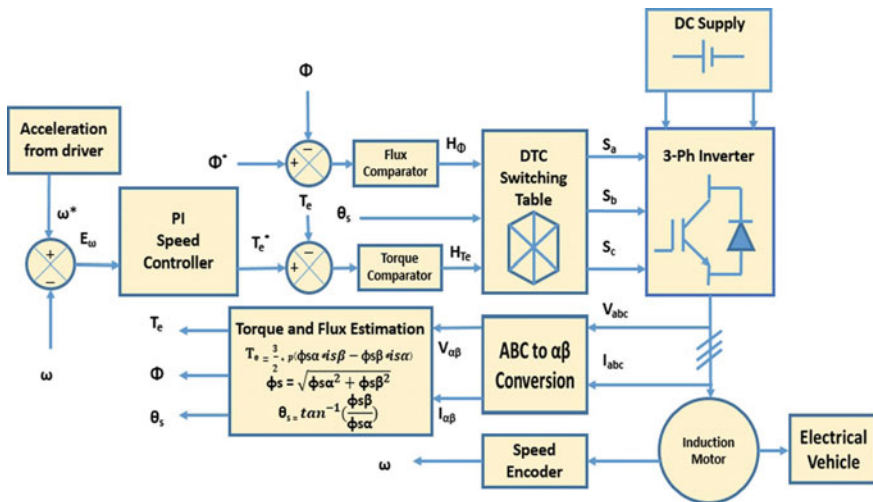


Fig. 1 Schematic diagram of conventional DTC based Induction motor drive

hysteresis comparator outputs together with the angle of the stator flux position decide the control voltage vector from a Look-Up Table (LUT) containing the suggested inverter states. Based on the combination of the two hysteresis controller outputs and the flux position an optimal inverter state will be picked from LUT and applied to the inverter [2–4]. Small hysteresis bands are preferred as they can maintain torque and flux errors within narrow limits [2, 3]. In the conventional DTC, an outer speed loop is provided to obtain the Torque reference for the inner loop [4]. Generally, a PI controller is provided in the outer loop which acts on the speed error as presented in Fig. 1.

2.1 Estimation of Torque and Stator Flux for DTC

The torque and flux estimator utilizes the stator variables of the Induction motor under control. First, these stator variables are converted into two-phase stationary (α, β) reference frame quantities as [1, 3, 4].

$$\begin{bmatrix} X_\alpha \\ X_\beta \end{bmatrix} = \frac{2}{3} \begin{bmatrix} 1 & -\frac{1}{2} & -\frac{1}{2} \\ 0 & \frac{\sqrt{3}}{2} & -\frac{\sqrt{3}}{2} \end{bmatrix} \begin{bmatrix} X_a \\ X_b \\ X_c \end{bmatrix} \tag{1}$$

where, $X = V$ or I

$$\varphi_s(\alpha, \beta) = \int_0^t (V_s(\alpha, \beta) - R_s I_s(\alpha, \beta)) dt \tag{2}$$

$$\begin{cases} \varphi_{s\alpha} = \int_0^t (V_{s\alpha} - R_s I_{s\alpha}) dt \\ \varphi_{s\beta} = \int_0^t (V_{s\beta} - R_s I_{s\beta}) dt \end{cases} \tag{3}$$

$$\varphi_s = \sqrt{\varphi_{s\alpha}^2 + \varphi_{s\beta}^2} \tag{4}$$

$$\theta_s = \tan^{-1} \left(\frac{\varphi_{s\beta}}{\varphi_{s\alpha}} \right) \tag{5}$$

where, R_s is stator resistance and $\varphi_{s\alpha}, \varphi_{s\beta}, V_{s\alpha}, V_{s\beta}, I_{s\alpha}, I_{s\beta}$ are the α and β axis parameters of the stator flux, stator voltage, and stator current [3, 4].

The electromagnetic torque of induction motor, T_e is estimated from the pole pair, p , the stationary reference frame quantities of stator current, I_s and stator flux, φ_s [3, 4] as,

$$T_e = \frac{3}{2} p (\varphi_{s\alpha} I_{s\beta} - \varphi_{s\beta} I_{s\alpha}) \tag{6}$$

2.2 The Hysteresis Controllers in DTC

In Fig. 1, the torque and flux errors [2] are generated through the comparison between estimated torque and flux with the reference values of torque (T_e^*) and flux (φ^*) [2–4]. The two-level hysteresis band shown in Fig. 2(a) is used to regulate the flux error and the three-level hysteresis band shown in Fig. 2(b) is used for the regulation of torque error [2–4].

$$\begin{cases} H_\varphi = +1 & \text{for } E_\varphi > +HB_\varphi \\ H_\varphi = -1 & \text{for } E_\varphi < -HB_\varphi \end{cases} \tag{7}$$

$$\begin{cases} H_{Te} = +1 & \text{for } E_{Te} > +HB_{Te} \\ H_{Te} = 0 & \text{for } -HB_{Te} < E_{Te} < +HB_{Te} \\ H_{Te} = -1 & \text{for } E_{Te} < -HB_{Te} \end{cases} \tag{8}$$

When the inverter is operating in any present sector S (1) to S (6), and if a new flux and torque hysteresis outputs are received, then the next inverter switching state to be applied is obtained from the switching Look-up of Table 1 [2–4]. The selected

Fig. 2 Hysteresis controller for (a) Flux, (b) Torque

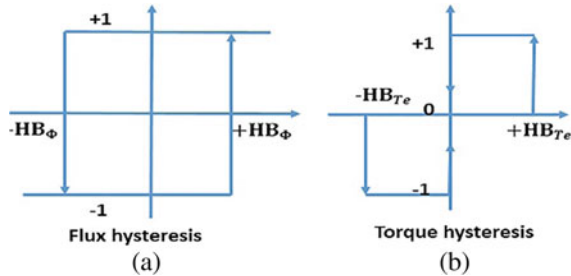


Table 1 Voltage vector selection look-up table for conventional DTC

H_φ	H_{Te}	S (1)	S (2)	S (3)	S (4)	S (5)	S (6)
1	1	110	010	011	001	101	100
	0	111	000	111	000	111	000
	-1	101	100	110	010	011	001
-1	1	010	011	001	101	100	110
	0	000	111	000	111	000	111
	-1	001	101	100	110	010	011

inverter switching state will keep the ripples in flux and torque within the allowed limits [4].

2.3 Fuzzy-Enabled Direct Torque Controller

The major drawback of the conventional DTC is an excessive amount of torque and flux ripple which when transferred to the motor shaft can cause destructive effects. Due to the characteristics of the Fuzzy logic controller in handling the uncertainties, it's become the best choice for motor control applications [1–4]. Motor parameter variations and the associated effects on torque control are inherently taken care while allowing DTC to exhibit better performance.

2.4 Fuzzy Based Speed Controller

In the proposed DTC, the speed control loop and the associated PI controller is replaced by a Fuzzy based speed controller [3]. The error in speed (E) and the rate of change of error in speed (CE) [3–5] are considered as inputs for developing the speed controller rule base. The Fuzzy speed controller accomplishes a reference torque (T_e^*) as its output [3–5]. The applied error in speed and rate change of error in speed are segregated into seven overlapped fuzzy sets and the Output variable of speed controller is segregated into nine overlapped fuzzy sets as presented in Fig. 3 [3]. These $7 \times 7 = 49$ combinations of rules possible for the speed controller are

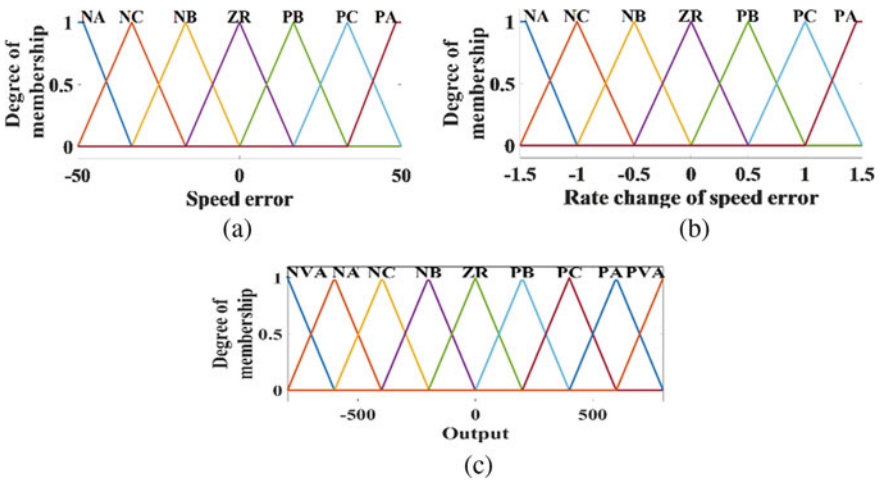


Fig. 3 Fuzzy input and output of speed controller block (a) E , (b) CE , (c) T_e^*

Table 2 Rule table for the fuzzy based speed controller

E/CE	PA	PC	PB	ZR	NB	NC	NA
PA	PVA	PVA	PVA	PA	PC	PB	ZR
PC	PVA	PVA	PA	PC	PB	ZR	NB
PB	PVA	PA	PC	PB	ZR	NB	NC
ZR	PA	PC	PB	ZR	NB	NC	NA
NB	PC	PB	ZR	NB	NC	NA	NVA
NC	PB	ZR	NB	NC	NA	NVA	NVA
NA	ZR	NB	NC	NA	NVA	NVA	NVA

developed and the rule base matrix is presented in Table 2 and is utilized in the proposed DTC [3–5].

2.5 Fuzzy-Enabled Inverter Switching Controller

The fixed value hysteresis comparator in conventional DTC is identified as the main cause for large ripples in flux and torque [2]. On the contrary, the fuzzy enable DTC has been designed with a rule base to allow a varying hysteresis band for the errors by classifying them into different groups based on their values. The error values are clustered based on their ranges and assigned with different degrees of memberships [1–3]. The torque error (E_T), flux error (E_ϕ) and along with the present stator flux position angle, θ_s are applied as the input for the fuzzy logic controller for selecting the optimum voltage vector from the fuzzy rule base [1–3].

• Rule Base Formulation:

For Torque Error: The torque error (E_T) is segregated into five fuzzy sets with trapezoidal membership functions representing the large positive (PL) and large negative (NL) torque errors, while the remaining torque errors viz. negative small (NS), zero error (ZE), and positive small (PS) are assigned with triangular membership functions [1–3]. The graphical representation of the developed rule base for E_T is presented in Fig. 4(a). These divisions are so formulated to confine the torque ripple within small limits [2].

For Flux Error: The flux error (E_ϕ) is segregated into three fuzzy sets with trapezoidal membership functions for large positive (P) and large negative (N) flux error and triangular membership function for the zero (Z) flux error [1–3] as shown in Fig. 4(b). The purpose of such a choice of membership function is to make the flux ripple smaller [2].

For rotor position Angle: The angle of the stator flux is divided into 12 sectors viz. θ_1 to θ_{12} . The input signal range of -180° to 180° has been divided into 12 equally spread triangular membership functions of 60° [2] each with an overlap of 30° to represent the twelve angles θ_1 to θ_{12} . This will allow each fuzzy set to work with

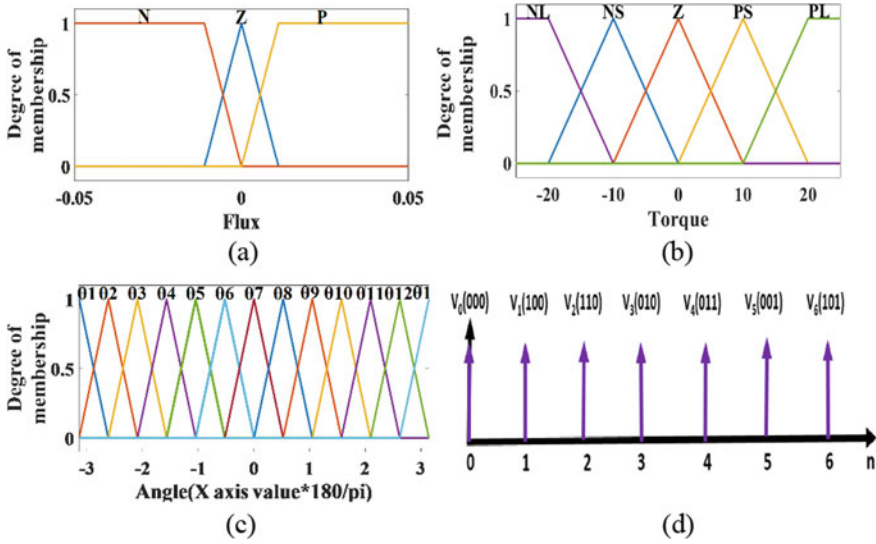


Fig. 4 Fuzzy inputs and output (a) Torque error, (b) Flux error, (c) Angle, (d) Output

an angle of 30° [1–3]. The membership function for the stator angle is presented in Fig. 4(c).

For the Output: The output of the fuzzy logic controller is represented by seven sharp triangular membership functions presented in Fig. 4(d) [2]. Among seven output membership functions, six are for active inverter switching state while the seventh one is for zero inverter switching state [1–3]. Figure 4 shows the membership functions and Table 3 defines the complete rules described to relate E_T , E_ϕ and the inverter switching vectors.

The overall implementation of the proposed fuzzy-enabled DTC is presented in Fig. 5. The speed fuzzy controller defined by the Rule base of Table 2 and the DTC switching rule base of Table 3 is embedded in the scheme of Fig. 5.

3 Mathematical Modeling of EV Dynamics

The motion of the vehicle is based on Newton’s second law of motion and the vehicle has to accelerate against the net force acting on it. In ECs the electric motor provides the tractive power to overcome all resistive forces encountered by the vehicle which are created due to aerodynamic drag, gravity, and weight of the moving vehicle [6]. Thus in the present work, the total tractive power required to maneuver the vehicle is calculated by considering the specifications of Tata Tigor presented in Table 4.

The aerodynamic drag force F_{drag} can be obtained as,

Table 3 Fuzzy logic rule base table for Inverter switching control

E_{Te}	E_{φ}	θ_1	θ_2	θ_3	θ_4	θ_5	θ_6	θ_7	θ_8	θ_9	θ_{10}	θ_{11}	θ_{12}
Positive large (PL)	P	001	101	101	100	100	110	110	010	010	011	011	001
	Z	001	001	101	101	100	100	110	110	010	010	011	011
	N	101	100	100	110	110	010	010	011	011	001	001	101
Positive small (PS)	P	001	101	101	100	100	110	110	010	010	011	011	001
	Z	001	001	101	101	100	100	110	110	010	010	011	011
	N	101	101	100	100	110	110	010	010	011	011	001	001
Zero (ZE)	P	000	000	000	000	000	000	000	000	000	000	000	000
	Z	000	000	000	000	000	000	000	000	000	000	000	000
	N	000	000	000	000	000	000	000	000	000	000	000	000
Negative small (NS)	P	010	011	011	001	001	101	101	100	100	110	110	010
	Z	010	010	011	011	001	001	101	101	100	100	110	110
	N	010	010	011	011	001	001	101	101	100	100	110	110
Negative large (NL)	P	010	011	011	001	001	101	101	100	100	110	110	010
	Z	010	010	011	011	001	001	101	101	100	100	110	110
	N	010	010	011	011	001	001	101	101	100	100	110	110

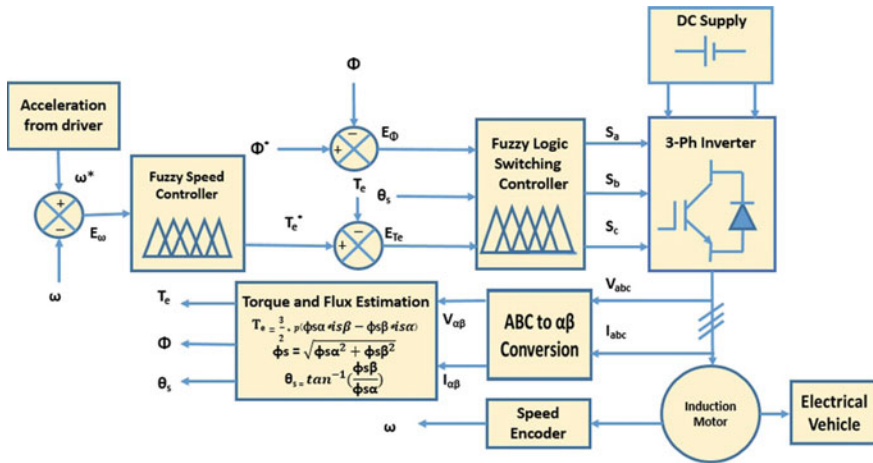


Fig. 5 Diagram of the proposed direct torque controller for torque ripple reduction

$$F_{\text{drag}} = 0.5 \times \rho \times C_d \times A_f \times V^2 \tag{9}$$

Rolling resistance force of the EC, F_{roll} can be calculated as,

$$F_{\text{roll}} = M \times g \times C_o \tag{10}$$

Table 4 Specification of Tata Tigor and parameters of induction motor

Parameters	Value	Parameters	Value
Kerb weight + passenger load (M)	1516 (kg)	Nominal power (P_m)	30 kW
Aerodynamic coefficient (C_d)	0.48	Pole pair (p)	2
Frontal area (A_f)	2.37 (m ²)	Inductance (L_s & L_r)	0.000724 H
Velocity (V)	22.22 (m/s)	Mutual inductance (L_M)	0.02711 H
Density of air (ρ)	1.205 (kg/m ³)	Resistance (R_s & R_r)	0.0823 and 0.0503 Ω
Rolling coefficient (C_o)	0.013	Total viscous friction (F)	0.02791 kg.m ² /s
Gravitational acceleration (g)	9.807 (m/s ²)	Inertia (J)	0.37 kg.m ²

Further, the acceleration resistance F_{acc} is expressed as,

$$F_{acc} = M \times \lambda \times \frac{dV}{dt} \quad (11)$$

Thus, the total tractive force, $F_{tractive}$, can be calculated as,

$$F_{tractive} = F_{drag} + F_{roll} + F_{acc} \quad (12)$$

From Eq. (13), the total tractive power requirement of the EC is obtained as,

$$Tractive_Power = F_{tractive} \times Velocity(V) \quad (13)$$

For the Tigore specifications of Table 4, a tractive power of 29.99 kW is obtained as calculated with Eqs. (9) to (13). An induction motor drive of 30 kW is utilized for the simulation study of the proposed Fuzzy DTC with the Induction motor parameters as presented in Table 4. The simulations are implemented with a sample time of 2 μ s.

4 Analysis of Simulation Results

The entire system of Fig. 5 is tested in MATLAB/Simulink platform with the standard drive cycle obtained from the repository, serving as the driver input. The load torque on the motor is varied and various machine quantities are observed for the drive cycle considered. The study attempts to compare the conventional DTC with the Fuzzy logic based DTC so the simulation is carried out on both the systems.

Fig. 6 Speed response
(a) conventional DTC,
(b) fuzzy-enabled DTC

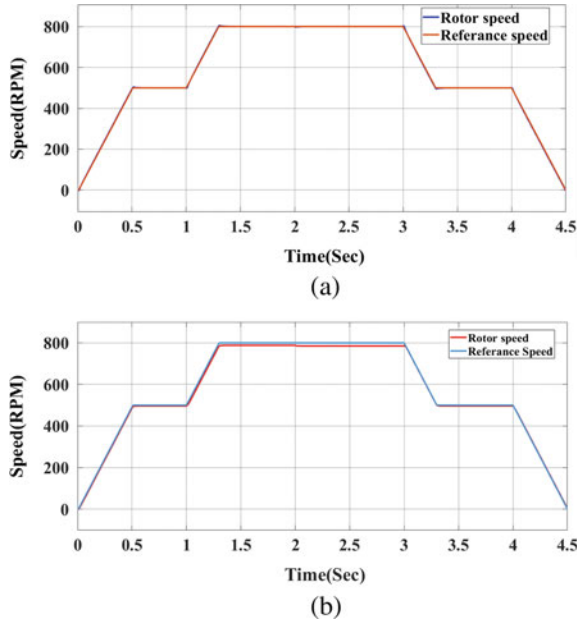


Figure 6(a), (b) presents the motor speed and the reference speed, and it is can be observed that in both the schemes speed response of the motor exhibits superior performance with very minimum fluctuation between each other.

Figure 7(a), (b) presents the electromagnetic torque generated and the reference load torque, a significant reduction in torque ripple is observed in Fuzzy based DTC in comparison to the conventional DTC.

Figure 8(a), (b) present the motor flux and the reference flux, and it can be observed that a significant reduction in flux ripple in Fuzzy based DTC compared to the conventional DTC

Figure 9 presents the stator current waveforms during the operation of the proposed EC system. The stator current is found varying in response to the torque variations. When the load torque increases, the stator current is found increasing to generate higher electromagnetic torque and vice versa. The closer look of the stator currents is shown in the inserts of Fig. 9, wherein the current ripple is observed to be very small due to the proposed Fuzzy DTC.

Tables 5 and 6 Summarizes the percentage improvement in the torque and the flux ripples across the two DTC methods for various reference torques.

From Figs. 7 and 8, it is ascertained that the torque and flux ripples are found to be far below their nominal values with the fuzzy-enabled DTC, simultaneously maintaining a good dynamic torque and speed responses.

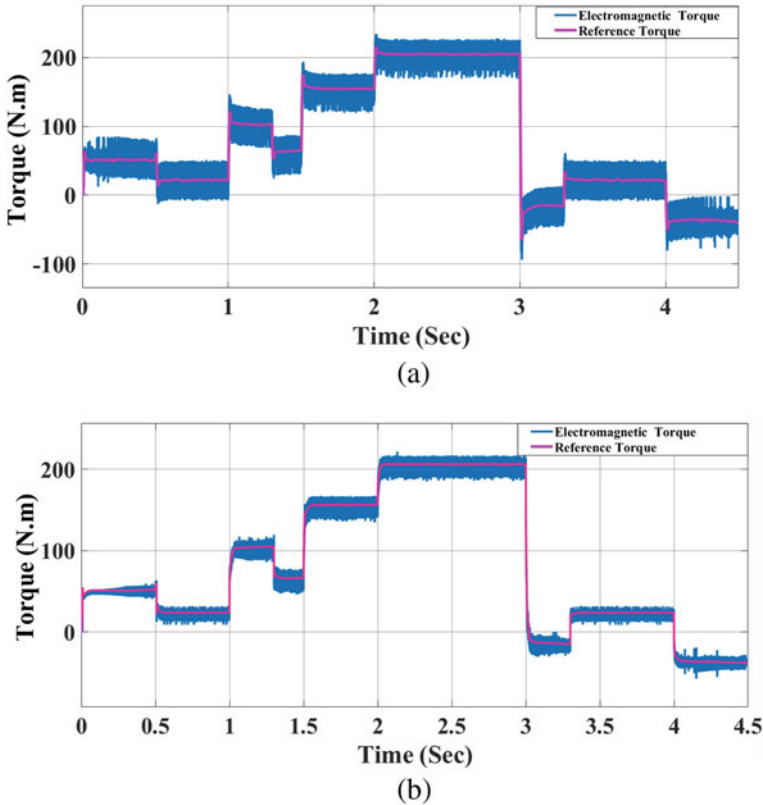
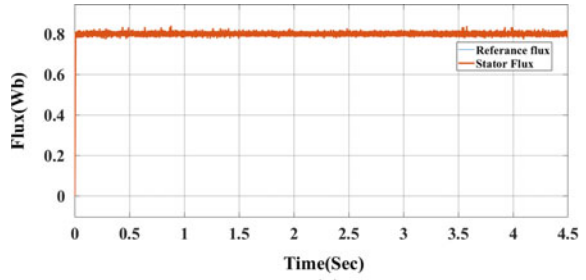


Fig. 7 Torque response (a) conventional DTC, (b) fuzzy-enabled DTC

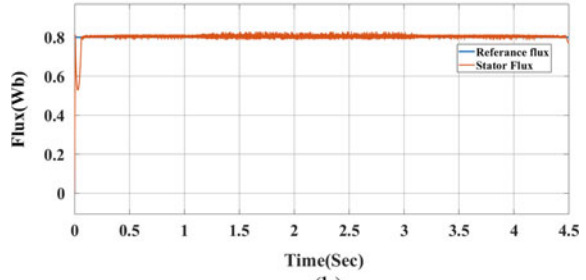
5 Summary

This paper presented a comprehensive Fuzzy logic controlled DTC as applied to induction motor for EV applications. Fuzzy inference system has been developed to improve the dynamic torque and flux response of the induction motor drive. The DTC Look-Up Table (LUT) and fixed band hysteresis comparators has been replaced by a set of flexible Fuzzy rule base. The proposed Fuzzy DTC scheme is observed to minimize the torque and flux ripple and maintained a superior performance under all operating conditions. Besides the torque ripple minimization, a faster dynamic torque response has been achieved by the inclusion of the Fuzzy speed controller in the outer loop. The entire system has been implemented in MATLAB/Simulink with a typical Electric vehicle drive cycle instructing the driver command into the motor drive system. A reasonable amount of torque and flux ripple reduction confirms the success of the suggested scheme.

Fig. 8 Flux response
(a) conventional DTC,
(b) fuzzy-enabled DTC



(a)



(b)

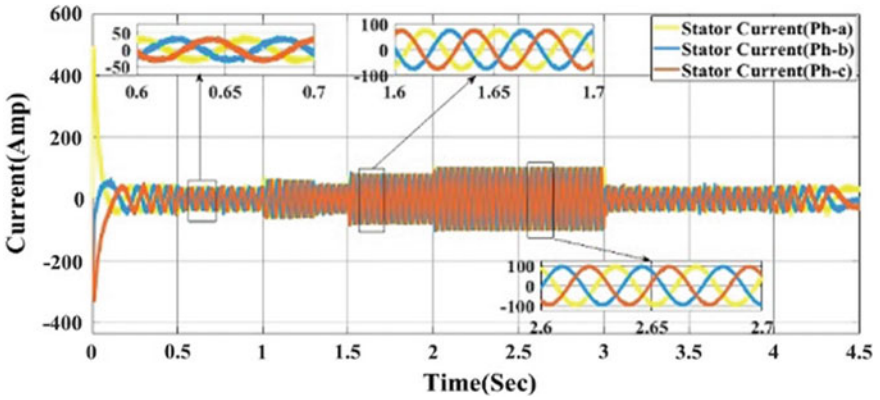


Fig. 9 Stator current waveform for three different phases (ph—a, b, c)

Table 5 Torque ripple comparison of conventional DTC and Fuzzy-enabled DTC

Parameter		Electromagnetic torque generated				
		Conventional DTC		Fuzzy-enabled DTC		Improvement (%)
Reference torque (Nm)	Reference flux (Wb)	Max–Min	Ripple (%)	Max–Min	Ripple (%)	$\frac{(\text{Max}-\text{Min})}{\text{Max}}$
50.00	0.80	54.60	109.2	13.80	27.60	74.72
100.00	0.80	56.60	56.60	26.10	26.10	53.80
150.00	0.80	51.80	34.53	29.00	19.33	44.01
200.00	0.80	51.50	25.75	29.40	14.70	42.91

Table 6 Flux ripple comparison of conventional DTC and Fuzzy-enabled DTC

Parameter		Motor flux generated				
		Conventional DTC		Fuzzy-enabled DTC		Improvement (%)
Reference torque (Nm)	Reference lux (Wb)	Max–Min	Ripple (%)	Max–Min	Ripple (%)	$\frac{(\text{Max}-\text{Min})}{\text{Max}}$
50.00	0.80	0.05	6.25	0.33	4.25	32.00
100.00	0.80	0.05	6.25	0.35	4.37	30.08
150.00	0.80	0.05	6.25	0.39	4.80	23.20
200.00	0.80	0.05	6.25	0.38	4.75	24.00

References

1. K. Bouhoune, K. Yazid, M.S. Boucherit, M. Mena, Fuzzy logic-based direct torque control for induction machine drive, in *2017 25th Mediterranean Conference on Control and Automation (MED)*, pp. 577–582 (IEEE, 2017)
2. S. Gdaim, A. Mtibaa, M.F. Mimouni, Design and experimental implementation of DTC of an induction machine based on fuzzy logic control on FPGA. *IEEE Trans. Fuzzy Syst.* **23**(3), 644–655 (2014)
3. H. Sudheer, S.F. Kodad, B. Sarvesh, Improved fuzzy logic based DTC of Induction machine for wide range of speed control using AI based controllers. *J. Electr. Syst.* **12**(2) (2016)
4. R.K. Bindal, I. Kaur, Torque ripple reduction of induction motor using dynamic fuzzy prediction direct torque control. *ISA Trans.* (2019)
5. N.V.S.K. Avinash, M. Avinash, B. Bharath, B.S. Y. Teja, V. Vidya, Direct torque control of induction motor-a comparison. *Int. J. Control Theor. Appl.* **9**(15) 7547–7556 (2016)
6. F. Mohammadi, G.A. Nazri, M. Saif, Modeling, Simulation, and analysis of hybrid electric vehicle using MATLAB/simulink, in *2019 International Conference on Power Generation Systems and Renewable Energy Technologies (PGSRET)*, pp. 1–5 (IEEE, 2019).

Analysis of UPFC Controller Connected with Multiple Wind Turbines by Using IEEE Bus System



Sunny Vig and Balwinder Singh Surjan

1 Introduction

In sustainable power source assets, wind vitality is the main contender for power generation because of its lower speculation cost and well-created innovation in assembling high-power wind turbines (WTs). An impressive count of huge-scale wind-connected farms is arranged far off from the inland network [1]. The utilization of sustainable power sources which answers moderate the distinction in the middle of force age and request by boosting the supply of electrical force. The FACTS devices are examined as the uttermost adaptable and feasible alternative to circulate the power flow, ongoing in the transmission lines [2, 3]. TCSC being a notable arrangement for FACTS devices and is a periodic system for SSR examinations [4]. To uphold the uniformity of the power system and to control injected power fluctuations to the grid, multi-infeed hybrid HVDC links while various FACTS devices can also be utilized [5]. The thought of the MTDC taking an interest in the frequency control reinforces the combination among AC source and DC source power systems also among asynchronous or induction AC systems [6].

To solve a large number of complications faced by the industries deal with power, the unified power flow controller has been conceived for solving problems related to time along with dynamic allowance of AC transmission-related systems and also giving multifunctional mobility to solve such types of problems. UPFC having the ability to control, selectively or simultaneously, various limitations influencing

S. Vig (✉) · B. S. Surjan

Punjab Engineering College (Deemed To Be University, Chandigarh), Chandigarh, India

e-mail: sunny.ee@cumail.in

B. S. Surjan

e-mail: balwindersingh@pec.ac.in

S. Vig

Punjab Engineering College (Deemed To Be University), Chandigarh, India

© Springer Nature Singapore Pte Ltd. 2021

K. S. Sherpa et al. (eds.), *Advances in Smart Grid and Renewable Energy*,

Lecture Notes in Electrical Engineering 691,

https://doi.org/10.1007/978-981-15-7511-2_36

the circulation of power in transmission lines within the traditional framework of concepts of transmission power [7]. PQ occasions happen because the establishment of a wind turbine with the grid becomes a significant concern. For the protection of sensitive devices at various nonlinear loads, sides from getting damaged and tripped STATCOMs are implemented [8]. Implementation of compensators like SVC and SSC had already been done in many ways. To improve power quality, UPFC being a flexible controller is used with grid-connected WECS [9]. Fuzzy systems and neural networks as mentioned are generally utilized as an identifier or controller in many control methodologies [10]. The utilization of ANFIS is grid-connected supervisory control HRES to decide the power generated must be stored in ESS. UPFC, being the third era of FACTS device has points on interest over different FACTS devices as control of powers, i.e., active and reactive is conceivable. UPFC utilizes a mix of STATCOM and an SSSC coupled employing DC common link which increases the compensation capability of the device concerning different FACTS devices.

2 Literature Review

VSC-HVDC was used to integrate the AC/DC parallel-connected wind farm. HVDC system connected with voltage source converter had benefits to feed passive network, which cannot just rapidly transfer power yet, also besides, can adaptably compensate reactive power to the system which is grid-connected and needs to be stabilized [11] presented an enhanced controlled strategy for offshore arrays of wind farm arrays interconnected employing an HVDC link. A frequency controller was proposed to improve wind turbines and HVDC link fault-ride through capabilities. Capability of various FACTS devices to intensify the implementation of the power system and transmission efficiency was discussed. Uncontrollable cascading effects in a large and heavily loaded interconnected system which may result in large blackouts were also described. A static compensator-based control scheme had been used for improvement in the quality of power within grid-connected wind producing system and with nonlinear load [12].

The advancement in semiconductors with high-voltage high power had effectively helped utilities to accomplish the advantages of the static converter having four-quadrant interlinking two alternate current systems through high-voltage DC transmission with various key-benefits, in particular, autonomous control of active and reactive power, quick dynamic reaction, and probability to associate AC island with no synchronous power generation in the grid [13] developed a new method to investigate the consistency of voltage for AC/DC systems with HVDC connected voltage source converter. Results indicated that voltage source converter with constant control of AC voltage was superior to other modes of control in the stability of voltage. A wind farm has a capacity of 3 MW consisted of ten 300 k-w permanent magnetic AC generators that were simulated to show the dynamic process of the system. A model of a wind farm system having several permanent magnetic generators attached to an individual voltage source converter was presented. To enhance the stability of

transient voltage of asynchronous or induction wind farm two techniques: SVC and TCSC were discussed [14].

Ramesh and Laxmi [15] identified the improved capability of power transmission through a regulated scheme and did a comprehensive investigation for a UPFC based on theoretical facts and computer simulations. Unified power flow controller enhances the system performance within transient as well as under normal operating conditions [16] investigated that a system built with AC/DC suffers few vibrations given low ESCR at the terminals of the inverter. Furthermore, at low ESCR operation of rectifier, reduced the flow of power by the DC link and can further change the working of the system. Incorporated planning and design of UPFC in the AC/DC system with tuned composed parameters may give superior adaptability to network operators which, in turn, bypass swings in power and tripping of area [17] solved the problem of SSR in wind farm integrations by using UPFC. At the linking line of the wind terminal, UPFC was located; thus, the required reactive power of self-excited induction generator was created by the shunt branch of UPFC.

To render sufficient damping characteristics of the network controller, i.e., UPFC was proposed with the damping controller and was designed with modal control theory. A similar investigation of utilizing controllers on the system like UPFC and a STATCOM demonstrated that the UPFC can acquire preferred damping qualities than the system installed with STATCOM regardless of whether the damping controllers like proportionate integral differentiative (PID) for UPFC and STATCOM were planned with utilizing theory of modal control to allocate the predominant system modes on the similar areas of the complex plane [18]. UPFC settings and control modes like optimal control mode were displayed. A power injection model with two sources was utilized for UPFC and the effects of control modes and settings on reliability indices were explored. Another control strategy was suggested for the UPFC. The proposed methodology based on control displayed generally excellent execution in controlling active power oscillations and keeping up the UPFC shunt or parallel bus voltage. It displayed ideal execution when compared with a proportionate integral controller under a few working conditions [19].

Sebastian and Sajith [20] analyzed various limits of unified power flow controller like voltage balance, real and reactive power of the complete system. To verify the effectiveness of the power flow in the transmission line, experimental works had been conducted. Experiments had been performed, both the converters, i.e., shunt and series had been constructed as a three-phase pulse width modulator (PWM) converter with insulated-gate bipolar transistor (IGBT) as the power device.

3 Proposed Control Methodology in IEEE Bus System Using UPFC

Two test bus systems, i.e., IEEE-9 and IEEE-14 are used for analysis in this paper. To simulate the ideal power flow, the IEEE bus systems are shown in Fig. 1. For

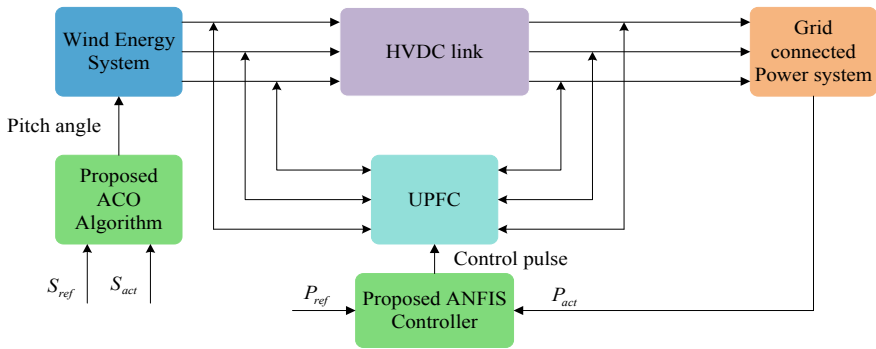


Fig. 1 Structure of optimal power dispatch in WECS

calculating the active and reactive power, voltages, IEEE standard systems are used. To solve problems of power stream in different power systems proposed type of analysis is useful, which can be further helpful for efficient power transmission. The optimal power flow (OPF) is calculated, for a given period, so that all the demands are satisfied in the network and the output power of each generating unit.

The HVDC power transmission system is utilized to transmit bulk electrical energy in the transmission lines. It also helps to connect traditional AC connections and separate power systems that cannot be used. The proposed mechanism for obtaining maximum power from the system is controlled by a pitch angle. The design of the UPFC through a DC condenser consists of connected shunt series branches. Voltage with controllable size and phase angle and a series of inverter connected inverters is inserted into the transmission line, which transforms powers, i.e., active and reactive into the transmission network. The active power in MW is driven by the no. of series branch of the shunt-connected inverter and the losses are independently reactive to the system. ACO is used with the ANFIS controller to further improve the performance of the UPFC. The ANFIS controller is known for the variation in power flow control. Finally, the controlled power is applied to the wind farm system. This mechanism compensates for the difference between actual power and reference power in the power system.

4 Distribution System Investigation with IEEE-9 Test Bus Network

HVDC is the AC-DC power flow solution for two terminals of the IEEE-9 bus network. An HVDC connection is inserted parallel to the extracted AC lines. DC coupling power flow and AC load flow results are presented. An IEEE-9 bus system runs the system simultaneously and loads it. Bus system analysis with load flow studies has been done with the help of iterative method, i.e., Newton–Raphson

method. This design includes the role of the adaptive ACO with the ANFIS framework for controlling the flow of electricity in the event of changes in electrical load, resulting in short-term power oscillations. The proposed system implementation parameters are demonstrated in Table 1 with the IEEE-9 test bus system.

In Table 2, the investigation of IEEE-9 test bus system has been performed with the N-R load flow method.

Here, the IEEE-9 bus test method is taken for analysis. Studies related to operating conditions of the system are restricted to small and gradual changes. Controlling bus voltages to their suggested values is one of the focused areas in this research work. Another important aspect of research work is to make sure that the grid angles between the two buses are not excessively high, and extreme loads of electrical equipment and transmission lines are also examined. A transmission line is associated with UPFC to understand the model of the active power integration controller. Rather than the active power coordination in the middle of series and shunt converters connected control system, but during reactive power transmissions, control of reactive power circulates excessive trips in UPFC bus voltage. The shunt-connected converter

Table 1 Parameters of the proposed system with IEEE-9 test bus network

Parameters	Values
Value of base voltage at 3-phase short circuit level	10 (VA)
Frequency	50 (Hz)
Resistance (magnetizing)	500 Ω
Inductance (magnetizing)	500 H
Capacitance	10 μF

Table 2 Analysis of the IEEE-9 test bus network parameters with the Newton–Raphson (N-R) load flow method

Newton–Raphson (N-R) load flow analysis							
Bus load. No	Voltage (pu)	Injection		Generation		Load	
		MW	MVar	MW	MVar	MW	MVar
1	1.0600	232.593	−15.233	0.000	−15.233	0.000	0.000
2	1.0450	18.300	35.288	40.000	47.928	21.700	12.700
3	1.0100	−94.200	8.758	0.000	27.758	94.200	19.000
4	1.0132	−47.800	3.900	0.000	−0.000	47.800	−3.900
5	1.0166	−7.600	−1.600	0.000	0.000	7.600	1.600
6	1.0700	−11.200	15.526	0.000	23.026	11.200	7.500
7	1.0457	0.000	0.0000	0.000	0.000	0.000	0.000
8	1.0800	0.000	21.030	0.000	21.030	0.000	0.000
9	1.0305	−29.500	−16.600	0.000	−0.000	29.500	16.600
Total		60.5930	51.0090	40.000	104.509	212.000	53.500

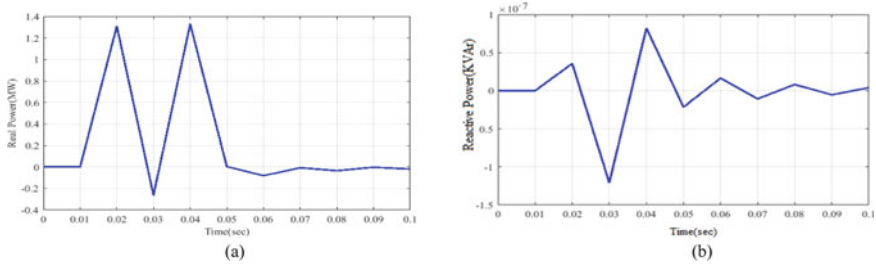


Fig. 2 Analysis of a UPFC real power and b UPFC reactive power at IEEE-9 test bus system

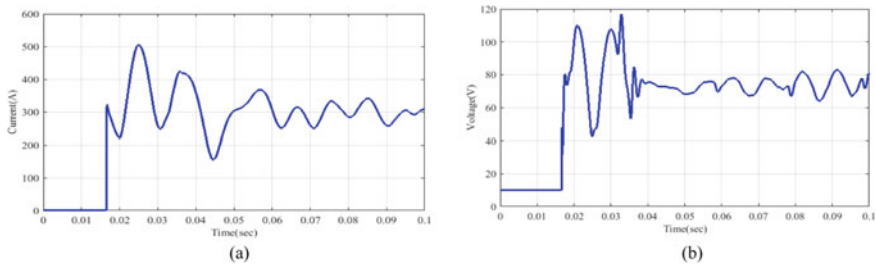


Fig. 3 Performance analysis of a load current and b load voltage in IEEE-9 test bus network

sustains the injected voltage of UPFC and further any changes if required is achieved by changing or setting the magnitude/phase angle of the circulated voltage. The two powers, i.e., active and reactive controlled with UPFC is given in Fig. 2a, b. Values are 1.3 MW and 0.8 MW, respectively. Figure 5.13 shows that the execution analysis of current, voltage and power in the HVDC electric transmission system has been determined. The effectiveness of the HVDC connected transmission system in the unstable state of transferring local loads to the proposed method is investigated. Then, the distributed system transmitted through the HVDC connection is less than the wind turbine force due to stability in the system.

From forecasting methods, data records based on history, a non-generator bus may be derived. In a power system, active power is defined as positive, though the energy exhausted in terms of reactive power is negatively defined. User power is met in this non-generator bus. The analysis of load current and voltage is given in Fig. 3a, b, respectively. The load current is 510 A and the voltage is 118 V.

5 Performance Analysis with IEEE-14 Test Bus Network

The bus network is made up of synchronous generators, capacitors, transmission lines and different loads. Stability analysis of power flow control and distribution system is studied using MATLAB/Simulink. Various wind turbine plant-based voltage, current,

power, i.e., real and reactive of different buses were analyzed. To improve the IEEE-14 bus system through the system’s WECS behavior, various wind turbine generator buses are connected to the HVDC connection-based UPFC controller via a transmission line. Table 3 shows that the operational framework of the suggested system connected with the IEEE-14 test bus system.

In Table 4, the analysis of IEEE-14 test bus network being performed with the Newton–Raphson (N-R) load flow method.

The power system solution is reactivated using load flow techniques. Therefore, it is important to evaluate the initial values as starting points for the solution. The Newton–Raphson e-flow scheme is used to compute the unknown of the system by adding the UPFC. It is important to identify the initial values of this voltage when

Table 3 Parameters of the proposed system with the IEEE-14 test bus network

Parameters	Values
Nominal frequency	50 (Hz)
Active power	0.127 (W)
Snubber resistance	1e ⁵
Nominal phase to phase voltage	1 V
Capacitance	0.01 (F)

Table 4 Analysis of the IEEE-14 test bus network parameters with the Newton–Raphson load process method

Analysis with N-R load process method							
Bus load. No	Voltage in (pu)	Injection		Generation		Load	
		MW	MVAr	MW	MVAr	MW	MVAr
1	1.0600	275.082	−3.370	0.000	−3.3700	0.000	0.000
2	1.0350	−21.700	23.703	275.082	36.603	21.700	12.700
3	1.0100	−94.200	17.537	0.000	36.537	94.200	19.000
4	1.0075	−47.800	3.900	0.000	−0.000	47.800	−3.900
5	1.0103	−7.600	−1.600	0.000	0.000	7.600	1.600
6	1.0600	−11.200	12.669	0.000	20.169	11.200	7.500
7	1.0415	0.000	0.000	0.000	0.000	0.000	0.000
8	1.800	−0.000	23.595	0.000	23.595	0.000	0.000
9	1.0246	−29.500	−16.600	0.000	−0.000	29.500	16.600
10	1.0232	−9.000	−5.800	0.000	0.000	9.000	5.800
11	1.0378	−3.500	−1.800	0.000	0.000	3.500	1.800
12	1.0434	−6.100	−1.600	0.000	−0.000	6.100	1.600
13	1.0371	−13.500	−5.800	0.000	−0.000	13.500	5.800
14	1.0116	−14.900	−5.000	0.000	−0.000	14.900	5.000
Total		16.082	39.834	275.082	113.334	259.000	73.500

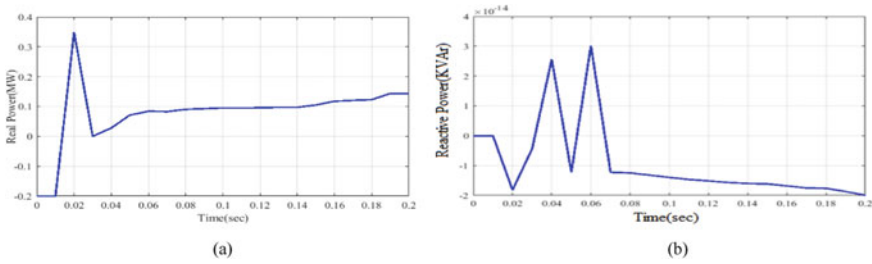


Fig. 4 Analysis of **a** UPFC real power and **b** UPFC reactive power at IEEE-14 test bus system

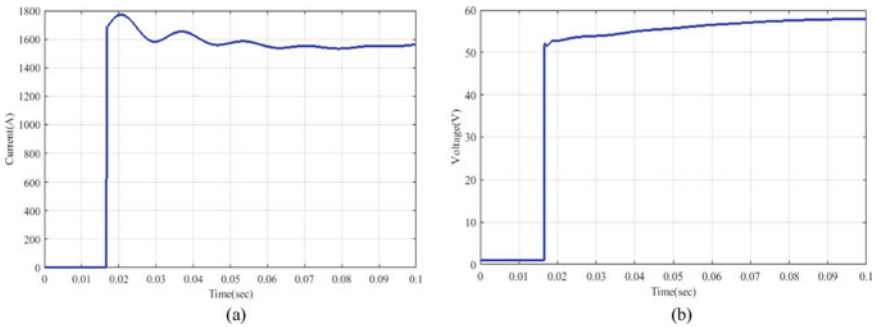


Fig. 5 Performance analysis of **a** load current and **b** load voltage in the IEEE-14 test bus system

determining the magnitude of the serial-injected voltage. The solution stops when the series values and the shunt voltages are outside their set limits. The programs used to incorporate the UPFC model into the Newton-Robson electric flow scheme. A serial converter that is normally run as an SSSC provides the core functionality of the UPFC. It sends active and reactive power to the network utilizing a series voltage at a computer frequency controlled by size and phase. Figure 4a, b demonstrate that the real and reactive power of UPFC is 0.35 MW and 3 MW, respectively.

The load current and voltage are illustrated in Fig. 5a, b with 1780 A and 58 V, respectively.

6 Conclusion

This paper describes the distribution system using the UPFC controller with ACO amplifier, non-controller ACO-ANFIS, and the wind is used as a resource. The control methods here find the optimal power control parameters of the system by minimizing the error between the actual control system and the set-point system response. The optimal power flow control parameters confirm the wind-connected grid power system and distribution system, UPFC controller current, voltage, real and reactive

power. HVDC connection voltage, rotor speed, and wind speed variations. The efficiency of the control systems is analyzed by a distribution system with various wind turbine plants. For each control system, air-connected grid power system, distribution system output performance, stability parameters, and power flow control parameters are analyzed. From that comparative analysis, we can understand that the proposed ACO amplifier with the UPFC controller-based distribution system has real, reactive power, different seasonal rotor, and wind speeds. The proposed system is tested with both IEEE-9 and IEEE-14 test bus networks. The output performance with the advanced method is more efficient.

References

1. Y. Guo, H. Gao, Q. Wu, H. Zhao, J. Østergaard, M. Shahidehpour, Enhanced voltage control of VSC-HVDC-connected offshore wind farms based on model predictive control. *IEEE Trans. Sustain. Energy* **9**, 474–487 (2017)
2. S. Dawn, P. Tiwari, A. Goswami, R. Panda, An approach for system risk assessment and mitigation by optimal process of wind farm & FACTS devices in centralized competitive power market. *IEEE Trans. Sustain. Energy* (2018)
3. D. Sen, P. Acharjee, Optimal line flows based on voltage profile, power loss, cost and conductor temperature using coordinated controlled UPFC. *An Int. J. IETGener. Transm. Distrib.* **13**, 1132–1144 (2019)
4. H. Mohammadpour, M. Islam, E. Santi, Y. Shin, SSR damping in fixed-speed wind farms using series FACTS controllers. *IEEE Trans. Power Deliv.* **31**, 76–86 (2015)
5. L. Wang, C. Lin, H. Wu, A. Prokhorov, Stability analysis of a microgrid system with a hybrid offshore wind and ocean energy farm fed to a power grid through an HVDC link. *IEEE Trans. Indus. Appl.* **54**(3), 2012–2022 (2017)
6. P. Ye, K. An, Low-order response modeling for wind farm-MTDC participating in primary frequency controls. *IEEE Trans. Power Syst.* **34**, 942–952 (2018)
7. A. Mohanty, M. Viswavandya, K. Ray, S. Patra, Stability analysis and reactive power compensation issue in a microgrid with a DFIG based WECS. *Electr. Power Energy Syst.* **62**, 753–762 (2014)
8. K. Rufus, K. Kumar, Power quality improvement on wind energy system by using static compensator. *Int. J. App. Mech. Mater.* **833**, 33–40 (2016)
9. V. Sharmila, K. Keerthivasan, K. Gheetha, B. Anupama, Power quality improvement for a wind farm connected grid incorporating. *Unified Power Flow Controller.* **20** (2016)
10. P. Sarhadi, B. Rezaie, Z. Rahmani, Adaptive predictive control based on adaptive neuro-fuzzy inference system for a class of nonlinear industrial processes. *Int. J. Taiwan Inst. Chem. Eng.* **61**, 132–137 (2016)
11. A. Luque, O. Anaya-Lara, P. Adam, Coordinated control for wind turbine and VSC-HVDC transmission to enhance FRT capability, in *Proceedings of Energy Procedia 10th Deep Sea Offshore Wind R&D Conference*, Trondheim, Norway, pp. 69–80 (2013)
12. M. Hau, M. Shan, M. Wecker, Reactive power control for parallel wind parks comprising Q (U) characteristics, in *Proceedings of European Wind Energy Conference and Exhibition (EWEC)* Copenhagen, vol. 2, pp. 1012–1020 (2012)
13. Y. Wei, Y. Sun, Z. Wei, G. Sun, Voltage stability bifurcation analysis for AC/DC systems with VSC-HVDC. *Hindawi Abstr. Appl. Anal.* **2013**, 1–9 (2013)
14. X. Hou, Y. Sun, H. Hua, A general decentralized control scheme for medium/high voltage cascaded STATCOM. *IEEE Trans. Power Syst.* p. 1 (2018)

15. M. Ramesh, A. Laxmi, Stability of power transmission capability of HVDC system using FACTS controllers, in *Proceedings of IEEE International Conference on Computer Communications and Informatics (ICCCI)*, Coimbatore, India, pp. 1–7 (2012)
16. R.K. Pandey, R. Devarapalli, Performance evaluation of HVDC system with ESCR variation, in *Proceedings of Conference on Engineering and Systems* (2014)
17. S. Golshannavaz, F. Aminifar, D. Nazarpour, Application of UPFC to enhancing oscillatory response of series-compensated wind farm integrations. *IEEE Trans. Smart Grid* **5**(4), 1961–1968 (2014)
18. S. Galvani, M. Sharifian, M. Hagh, Impact of SSSC and STATCOM on power system predictability. *Int. J. Electr. Power Energy Syst.* **56**, 159–167 (2014)
19. R.K. Bindal, A review of benefits of FACTS devices in power system. *Int. J. Eng. Adv. Tech.* **3**(4), 105–108 (2014)
20. L. Sebastian, R. Sajith, Power flow control in a transmission line using UPFC. *Int. J. Mod. Eng. Res. (IJMER)* **4**(8), 36–44 (2014)

Power Loss Reduction Strategies of IEEE-5 Bus System with Neuro-fuzzy UPFC



Ramakanta Jena, Ritesh Dash, and Saratchandra Swain

1 Introduction

Modern power system is highly scattered and interconnected in order to support a number of customer. The demand for electrical energy is increasing day by day which in turn requires a large number of transmission line and a number of electrical power house must be interconnected [1, 2]. Supply of quality power along with its reliability is a major concern from economic and industrial point of view. In order to reduce the transmission cost and the power handling cost, FACTS devices are usually connected in between the transmission lines near the load, where it has to be used. Controlling the facts devices for real and reactive power exchange is not a new technique. It has been found in the literature that some linear controller such as proportional integral controller along with proportional integral development controller had been used in most of the controller. However, this controller shows its inability when it comes for multi-machine analysis [3]. For power transmission economic point of view, it is required to increase the transmission capability of power with the existing transmission facilities rather than creating new transmission lines for the transmission of high end power [4, 5]. This can be achieved by interconnecting suitable facts devices near the receiving load where the power is being utilized. Deregulated electrical power system makes it possible to transmit competitive power at a reasonable cost to its end user requires the use of some robust controller which can increase the reliability and at the same time controlling the power to a predefined path is required. Facts devices

R. Jena (✉) · S. Swain

School of Electrical Engineering, Kalinga Institute of Industrial Technology University,
Bhubaneswar, Odisha 751024, India

e-mail: rjenafel@gmail.com

R. Dash

Department of Electrical Engineering, Christian College of Engineering and Technology, Bhilai,
India

e-mail: rdashee@gmail.com

© Springer Nature Singapore Pte Ltd. 2021

K. S. Sherpa et al. (eds.), *Advances in Smart Grid and Renewable Energy*,

Lecture Notes in Electrical Engineering 691,

https://doi.org/10.1007/978-981-15-7511-2_37

from marketable invention make it possible to use the transmission line at its full capacity by utilizing the line parameters. The main objective of the facts devices used to increase the controlling the capacity of transmission parameters which increases the stability and helps to provide fast control action characteristics to the existing power system.

Power system optimization means that transmitting the electrical power with less cost and thereby maintaining the quality power for the end user [6]. Unified power flow controller is a type of facts devices, which consists of two devices like static synchronous compensator and static synchronous series compensator. Both the device are interconnected by means of a common DC link, which may be a capacitor or a DC storage device. The DC link capacitor is considered in most of the controller by making it fast chargeable during the transient period of operation. Different electrical parameters of the transmission line like voltage, impedance and phase angle of the system can be controlled simultaneously with the unified power controller.

Performance of UPFC can be determined by the control mechanism adopted while designing the controller.

UPFC is a shunt-connected device, which can control both real and reactive power by properly maintaining the bus voltage and shunt reactive power flow in the line. Nonlinear controller such as fuzzy inference system can be used for the control mechanism, which in turn increases the dynamic stability of the power system by controlling the real and reactive power demand off the grid to which it is connected. In this system, Mamdani type of fuzzy logic controller has been used for adaptive fuzzy inference system. A fuzzy proportional controller replaces the classical PID controller and the second controller is a hybrid fuzzy controller. For evaluating the contingency ranking, composite fuzzy criteria have been used for finding out the optimal location. Different time constants have been used to damp out the variations and thereby minimizing the reactive power. With the use of UPFC, controller variation in the real power exchange is not noticed, however, variation in the reactive power at a different bus location depending upon its load value is marked. Out of different control, the method used in fuzzy interval and fuzzy mutual is used in the mechanism of control of UPFC. AI overshoot is found for both real power and bus voltage during a three-phase to ground fault. In this condition, the change in active power is noticed, however, there is no sign of change in reactive power. During the simulation studies, the reactive power is set to zero, as there is no requirement of reactive power in the transmission line during three-phase fault condition.

In the present study, the capability of UPFC in controlling the reactive power and real power has been investigated with different mechanisms like linear control of mechanism and nonlinear control mechanism has been investigated with IEEE-5 bus system.

2 Power Flow Optimization

Optimization method can be classified broadly into two categories like traditional and intelligent method. Out of the different intelligent methods genetic algorithm optimization, ant colony optimization and particle swarm optimization are most popular. Similarly, on the traditional category Newton method, gradient method, quadratic programming and linear programming are some common methods used for optimization of power system. Optimization method includes finding out the different parameters involved in the power system analysis to minimize an objective function defined according to the type of bus and its label. The end solution depends upon the type of model studied and accuracy level can be best described with the method used for optimizing the power system. Before starting the analysis, the objective function needs to be described and the possible solutions must be evaluated with the optimization method. Objective function can be either in the form of power transmission losses or reactive source allocation in the transmission system. However, the main objective is to reduce the cost of generation by scheduling the generating units. Successful scheduling of the power system generating units leads to economic dispatch of a trickle power, and thereby reducing the cost of operation and operational requirements involved in power system network. Optimization problem always involves minimizing certain objectives like power flow equation and equipment scheduling and their operating limits. Some objective functions related to active power can be summarized as economic dispatch consisting of losses, minimum cost of operation and AT&T loss. It also includes scheduling of environmental dispatch and transfer of maximum power that is maximum power transfer capability. On like objective function for real power, reactive power objective function includes powerless minimization, and of course, MVAR are loss minimization. Apart from real and reactive power, some other optimization goals are also used like minimizing the deviation from the target value and minimum control shift. Out of the different objective functions, the most commonly used objective functions are minimizing the cost optimization for active power and active power loss minimization and secondly planning of reactive power to support the cost of reactive power this also includes minimization of reactive power.

2.1 UPFC in Multi-machine System

Two-force commutated voltage source converter is usually used in unified power flow controller connected by a common DC link as described above. Two three-phase controllable bridge converters are used to produce required amount of current that is to be injected to the transmission line using a series transformer. Transformer is used to isolate the power transmission system with that of the controlling system. This enables the control of both active and reactive power in the transmission line. Out of the two converters, one is a shunt-connected converter and other is a series

connected converter. Regulator function of the UPFC can be achieved if the inserted voltage is in phase with the AC voltage off the grid to which it is connected. Phase angle regulator option can also be activated by inserting the voltage in series with the AC voltage with some deviation angle. The performance of UPFC controller can be increased by reducing the interaction of active and reactive power flow in the system. From the literature, it can also be found out that dynamic interaction between the quantity is greatly supported by the nature of series injected voltage which affects the stability enhancement and oscillations damping in the power system. From the characteristic of the UPFC, it is noticed that this facts device is highly nonlinear because of the presence of converter transformer and surge arresters.

2.2 Adaptive Neural Fuzzy Inference System

Single-area and two-area control of a power system can be enhanced by the use of adaptive neuro-fuzzy inference system. The number of research has been carried out in the field of adaptive neural for the inference system and its application to the power system for the enhancement of stability. The basic structure of the fuzzy inference system can be analyzed as a mapping between the input variables to its corresponding membership function. It also maps the input membership functions to its corresponding set of rule at its output characteristics. Finally, it maps the membership function from its output characteristics. The ANFIS considered over here is consists of a fixed member functions and which are chosen randomly based upon the input variables.

ANFIS construct its rules based upon the input variables and the predefined output as desired by the user function. Linear control has been analyzed and its input and output characteristics were recorded for designing of the controller. From the data set, it cannot be suspect that which shapes the membership function is likely to take. In such case, the requirement of ANFIS is much more essential for taking suitable decision file mapping between input to output. The learning method for adaptive neural fuzzy inference system is similar to that of the human brain processing system. The learning technique usually provides a method to the controller to learn the information about the data and its structure how they are related to each other. A neural network similar to that of the human brain is used to interpret output and input variable and its corresponding mapping is used to map any variable to its output. All the parameters, which are associated with the membership functions, can be controlled with respect to the corresponding weight provided to it. Out of the two methods as described above the gradient descent method is most suitable and is widely used because of its ability to discriminate between local and global minima. One the required return vector is measured different optimization method can be applied to find out the error. Here, the error is measured in terms of its squared difference and the desired output.

Layer-1:

In this layer for every node i , square node function becomes $O1, i = \mu A, i(x)$ where $i = 1, 2$

$O1, i = \mu B, i(y)$ where $i = 1, 2$ Layer-4:

This layer referred as adaptive node. Node function for layer-4 can be written as $Oq, i = w_i(p1x + qi y + r_i)$.

From Fig. 1, it can be found out that the network consists of N number of neurons at the input layer and F -number of input membership function for each input. Thus, in the fuzzy layer, $F*N$ neuron are available. This leads to FN number of layer in the defuzzyfication layer and FN rules with FN neurons in the output layer. This can be well described by considering to input x and y and one output as Z (Fig. 2).

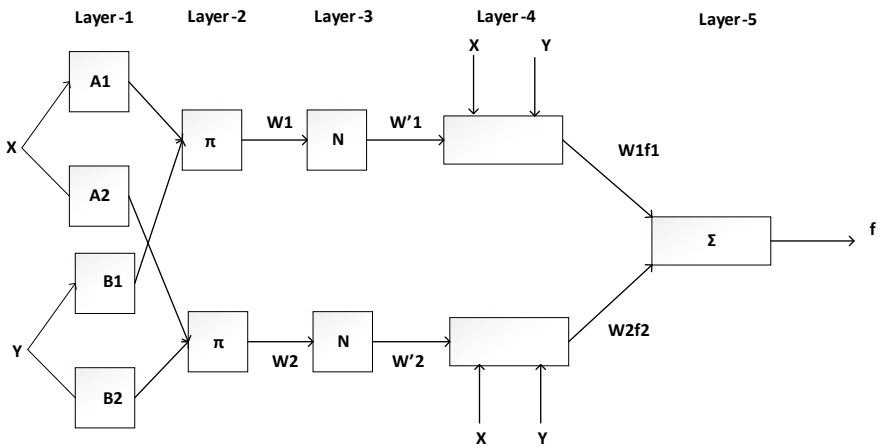


Fig. 1 Basic ANFIS structure

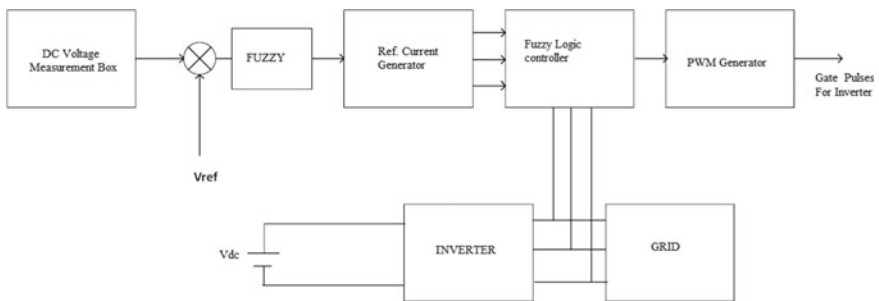


Fig. 2 UPFC internal structure in the form of blocks

3 Simulation and Result Analysis

The simulation model used for the analysis of IEEE-5 bus system is shown in figure above, where general steps were adopted to generate the data that are required for the designing of unified power flow controller. The limit of the input data can be found out from the different buses, which are connected in the power system. Due to unavailability of practical data, simulation model has been used which is exactly the scaled down version of a practical problem. Therefore, that is generated by simulating the model for a period of 5 s. PID controllers input and output data collected in the workspace and the corresponding neuro-fuzzy system was designed with neuro-fuzzy have present in the MATLAB/Simulink software. Input data such as real power and reactive power along with the DC link importers is injected to the P layer and corresponding controlling variable as Z is used for designing of the ANFIS bass's controller. In the present controller, the UPFC is connected to a transmission system where it has to control a voltage level of 500 kV. Loop configuration has been adopted for studying the simulation circuit consisting of five buses. 2-power transformer is connected at different end to support the insertion of facts controller into the transmission system. Two generators of different capacities such as 20 and 40 MW are connected to transmit the required amount of power at a level of 500 kV. Different bus parameters consisting of load and generators as shown in Table 1. From the simulation studies, it can be found that most of the power generated from generator to that is connected to bus-2 is transmitted through the transmission line to its corresponding load. The simulation results as shown in different figures reveal that how the UPFC controller can relieve the power congestion under both heavy load condition and faulted condition. ANFIS-based UPFC is connected at bus number three to support the reactive power as demanded by the system from time to time (Table 2).

Table 1 Performance comparison between the two controllers

Sl. No.	Parameter	PI-controller (under balanced operation condition)	ANFIS-PI-controller (under balanced operation condition)
1	Settling time (s)	0.04	0.027
2	Rise time (s)	0.015	0.005
3	Over shoot (%)	21	11

Table 2 ANFIS optimizer parameters [7, 8]

Sl. No.	Parameters	Measurement
01	Epoch size	9
02	Tolerance level	13.007e-09
03	Initial step size	0.00137
04	Rate of change of step size	0.0035e-05

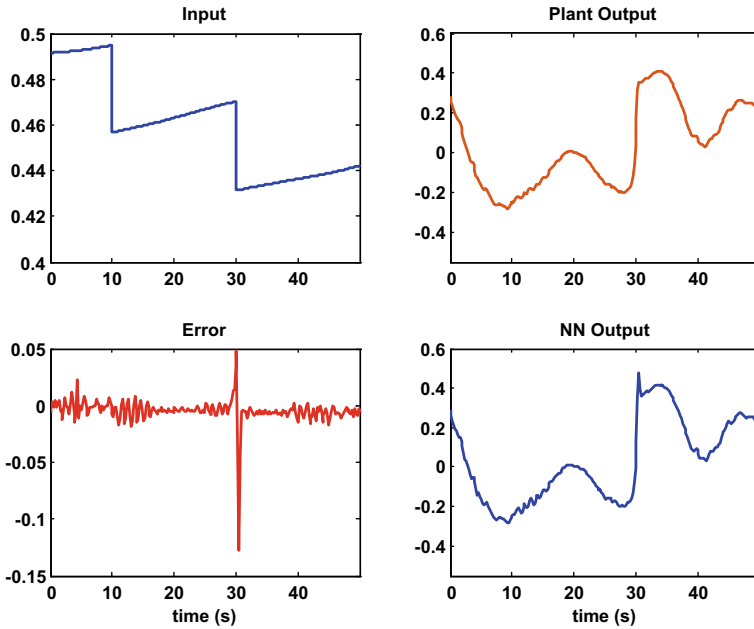


Fig. 3 Validation of neural network

A symmetrical fault is applied at time instant 2.3 s for a period of 8 cycles for a 50 Hz system. The converter in the series arrangement having a rated capacity of 10 MVA with maximum insertion capability of 0.2 p.u., and the shunt converter is having a capacity of 20 MVA is used for the control of real and reactive power demand by the power system. For providing smooth control over real and reactive power, the shunt converter is set to voltage control mode while the series converter is working under power flow control mode.

3.1 Result

See Figs. 3, 4, 5, 6 and 7.

4 Conclusion

In the present work, multi-machine control action is carried out with adaptive fuzzy neuro system. A symmetrical three-phase fault is applied to a multi-machine system for testing the robot of adaptive neuro-fuzzy inference system-based unified power flow controller. The result obtained under different simulation condition shows the

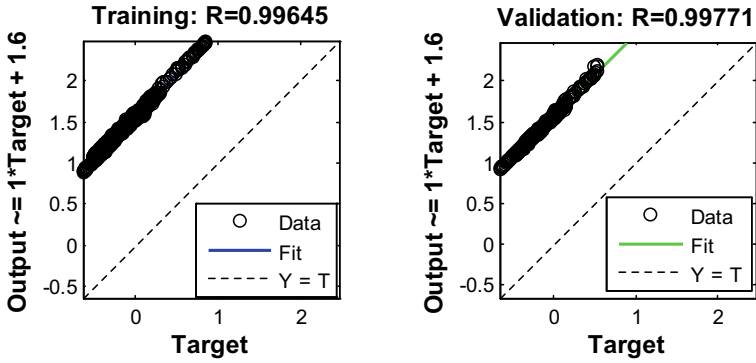


Fig. 4 NN regression analysis

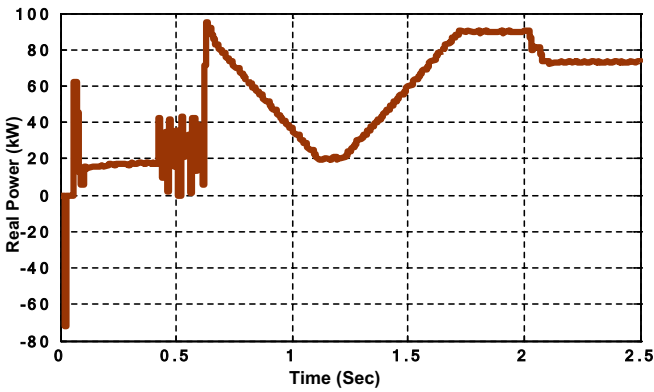


Fig. 5 Real power delivered by the ANFIS controller

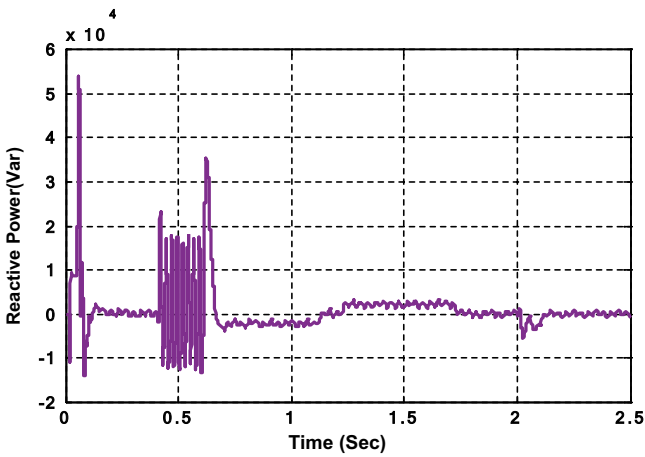


Fig. 6 Reactive power exchanged between renewable source and grid

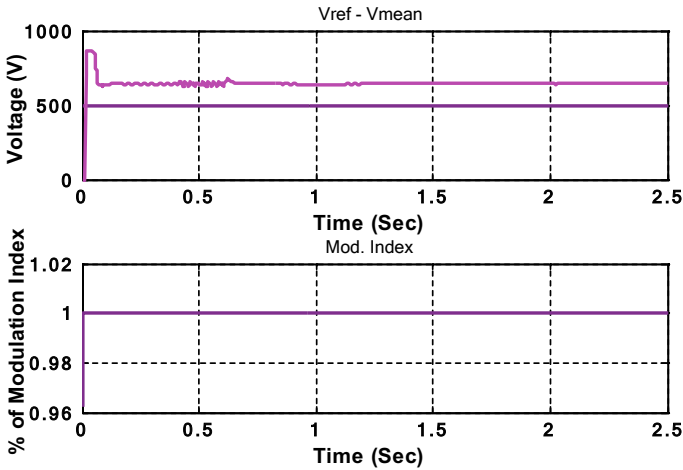


Fig. 7 Reference voltage and modulation index

adaptiveness of neuro-fuzzy controller. The controller has soon a less overshoot during the instant of fault. It is also noticed that neuro controller improves the performance of system in the form of transient stability and dynamic stability under both the light load and heavy load condition.

References

1. R. Syahputra, I. Robandi, M. Ashari, Reconfiguration of distribution network with DER integration using PSO algorithm. *TELKOMNIKA* **13**(3), 759–766 (2015)
2. R. Syahputra, I. Robandi, M. Ashari, Performance analysis of wind turbine as a distributed generation unit in distribution system. *Int. J. Comput. Sci. Inf. Technol. (IJCSIT)* **6**(3), 39–56 (2014)
3. A. Jamal, S. Suropto, R. Syahputra, MultiBand power system stabilizer model for power low optimization in order to improve power system stability. *J. Theoret. Appl. Inf. Technol.* **80**(1), 116–123 (2015)
4. R. Syahputra, I. Soesanti, Performance analysis of a 2 kW wind turbine in the southern each of Bantul. *TELKOMNIKA* **15**(1), 28–35 (2017)
5. R. Syahputra, Fuzzy Multi-Objective Approach for the Improvement of Distribution Network Efficiency by Considering DG. *International Journal of Computer Science & Information Technology (IJCSIT)* **4**(2), 57–68 (2012)
6. I. Soesanti, R. Syahputra, Batik production process optimization using particle swarm optimization method. *J. Theoret. Appl. Inf. Technol. (JATIT)* **86**(2), 272–278 (2016)
7. S. Pattnaik, R. Dash, S.C. Swain, P. Mohapatra, Control of active and reactive power of a three phase grid connected photovoltaic system, in *2016 International Conference on Circuit, Power and Computing Technologies (ICCPCT)*, Nagercoil (2016), pp. 1–6
8. R. Dash, S.C. Swain, Effective power quality improvement using dynamic activate compensation system with renewable grid interfaced sources. *Ain Shams Eng. J.* **9**(4), 2897–2905 (2018)

Compensation of Reactive Power Using STATCOM for Wind Farm



Ganesh Prasad Khuntia, Ritesh Dash, and Saratchandra Swain

1 Introduction

The dynamic behavior of power system is usually determined by the nature of generators connected with the transmission system. Wind turbines usually affect the power system in a different way as compared to the conventional generating units. Therefore, the major power quality issues that have to be addressed are transient stability and voltage stability. From IEEE definition, it is found that voltage stability means maintaining voltage within the operational limit at its different buses. In contradiction, maintaining transient stability after a small and large fluctuation is a great concern in power system stability analysis.

Out of different wind turbine generators, some popular generators which are used are squirrel cage induction generator, variable speed drive generator, doubly fed induction generator, permanent magnet synchronous generator and electrically excited synchronous generator. Operating the wind generator at a particular speed requires squirrel cage induction generator supported by a capacitor bank for self-excited which can achieve maximum efficiency [2]. In contradiction to squirrel cage induction generator, electrically excited synchronous generator required an additional converter for generating excitation system to the router. A large number of

G. P. Khuntia · S. Swain

School of Electrical Engineering, Kalinga Institute of Industrial Technology University,
Bhubaneswar, India

e-mail: ganesh.khuntia@gift.edu.in

S. Swain

e-mail: scs_132@rediffmail.com

R. Dash (✉)

Department of Electrical Engineering, Christian College of Engineering & Technology, Bhilai,
India

e-mail: rdashee@gmail.com

© Springer Nature Singapore Pte Ltd. 2021

K. S. Sherpa et al. (eds.), *Advances in Smart Grid and Renewable Energy*,

Lecture Notes in Electrical Engineering 691,

https://doi.org/10.1007/978-981-15-7511-2_38

poles are required for permanent magnet synchronous generator to generate same amount of power that allows small pole pitch, and it is also worthwhile to mention here that the absence of field winding results in higher efficiency [3].

Generator converter sets consisting of different control strategies are available in the market for meeting the required power demand for a particular wind speed. In this paper step and search algorithm for controlling maximum power and DQ current control system has been used based on hysteresis band controller. The state and search algorithm used in this paper tracks the maximum power from the DC source and its corresponding control logic. The DQ transformation system enables the control of separate real and reactive power as an AC output variable. Hysteresis band control provides control over current major function of current variation and thereby optimizing the switching frequency and total harmonic distortion label that supply the current. The switching frequency can be made variable by changing the band size and the step size.

This paperwork tries to design a variable speed direct drive wind turbine generator with modified controller and investigates the performance of fixed speed squirrel cage induction generator along with capacitor bank and double fed induction generator with standard control scheme. As because more number of wind generators uses fixed speed wind turbine equipped with simple induction generator, therefore, study of voltage stability is a key issue in induction generator system. Induction generator usually consumes reactive power during contingency analysis and thereby deteriorating the local grid voltage stability. Controlling the grid voltage and power factor can be achieved by using doubly fed induction generator because they operate on power electronic converter and thereby generating their own reactive power demand. Because of the use of pulse width modulation, the capability of double field induction generator is limited when controlling the large voltage. Double field induction generator uses a small size of converter however; they disturb the power system largely because their starter winding is directly connected to the electrical grid. In contrast to double fed induction generator, externally excited synchronous generator provides better performance and thereby supplies more amount of reactive power to the power system. Electrically excited synchronous generator is usually silent pole electrical machine, which is excited from the power grid. For providing operation on the low-speed condition, a high pole count synchronous generator is usually recommended on the distorted condition. Over excitation, system for controlling reactive power is possible with electrical excited synchronous generator, thereby enabling the unity power factor operation of the generator.

In order to verify the operation of wind generators, IEEE-14 bus test system has been started with MATLAB Simulink software in this paper [4]. Different power quality issues such as voltage collapse reactive power management and loading margin have been investigated in this paper. Simulation results as obtained under different condition source the superior performance of electrical excited synchronous generator and permanent magnet synchronous generator different loading conditions.

2 Operating Characteristics of Wind Turbine

Almost all the wind turbines share some common features such as startup, cutin and cutout speed of winds. Figure 1 shows a typical output of wind turbine showing the cutin speed and cutout speed. From the figure, it can be found out that the cutting speed is usually 3 m/s of wind speed. From cutting speed to rated output, speed the curve is slightly proportional to each other between power output and wind speed. Startup wind speed is that speed which returns and unloaded rotor from its stand-still position to a rotating position. Similarly, cutin speed is the minimum speed at which the blade rotates and generates usable power. For most of the wind generator, this speed is generally 12 km/h. Betz limit defines the maximum retrievable power from the wind turbine, and for most of the turbine, it is 59%.

2.1 Fixed Speed Wind Turbine

In order to achieve self-excitation system in the squirrel cage induction motor, it is fitted with a capacitor bank. Figure 2 shows the single line diagram in the form of schematic diagram for fixed speed operated squirrel cage type. The basic design constraint is to match the wind turbine and gearbox constraints with that of the wind speed. Unlike other in induction generator, the slip is slightly variable with the amount of real power bank generated and therefore is not constant.

As the variation in the wind, speed is within 1%; therefore, this type of wind turbine is constant speed or fixed speed turbine. Fixed speed wind turbine usually generates power when the turbine shaft rotates faster than the frequency of the electrical grid to which it is connected and thereby creating a negative slip for the system. Due to unavailability of optimal TSR, deficiency cannot be maximized for fixed speed system. Here, the output power can only be controlled by varying the pitch angle.

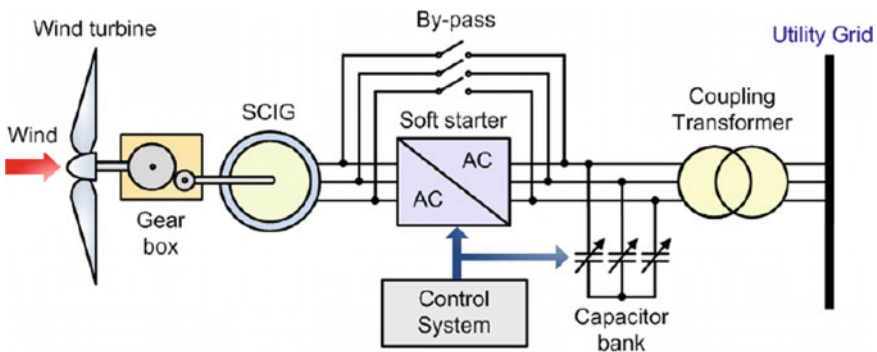


Fig. 1 Fixed speed wind turbine [1]

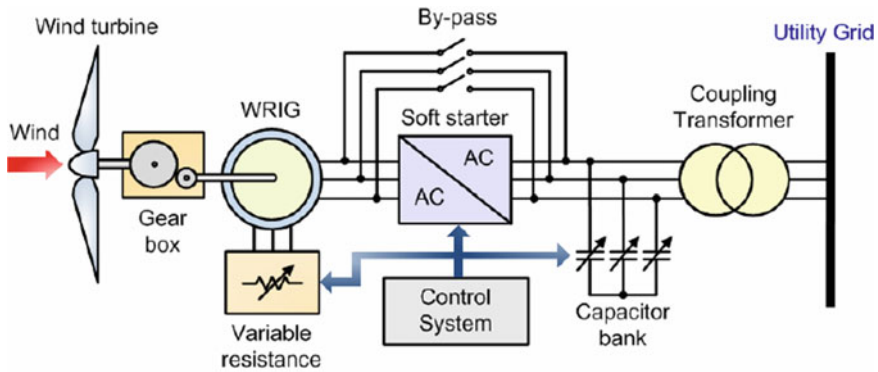


Fig. 2 Variable speed wind turbine [1]

2.2 Variable Speed Wind Turbine

Wind turbine having a gear drive system comes under variable speed wind turbines. Double field induction generator comes under this category where a gearbox is usually located between the rotor shaft and generator shaft. Objective of the gearbox is to increase the speed of the shaft and thereby decreasing the torque; therefore, the small number of poles is enough to generate optimum power output of the generator. Due to use of number of gearbox, the complexity of the system is higher as compared to the direct drive system, thereby making the variable speed wind turbine as less reliable. Due to the use of gearbox, the maintenance and repair cost is higher as compared to fixed speed wind turbine.

In this connection, the rotor is connected to the converter system with suitably calculated reactor and that of the stator winding is connected to the grid to which it has to pump the power. Inner current control loop powered by voltage source inverter is connected to the rotor of the system in back-to-back connection mode. The main purpose of the converter is to compensate against the frequency by coupling the stator with that of the rotor. This is usually achieved by injecting the rotor current in series with that stator current. The entire action of the VSC is shown in Fig. 2.

2.3 Direct Drive Synchronous Generator

Here the gear ratio is typically 1 thereby enabling the windmill to be connected on to the grid? A low-speed multipole windmill with compatible rotational speed converts the energy into its corresponding electricity. Static magnet generator is usually used for direct drive synchronous generator. Unlike variable speed wind, turbine generator, the starter is connected to the grid voltage source converter. Diode rectifier with one

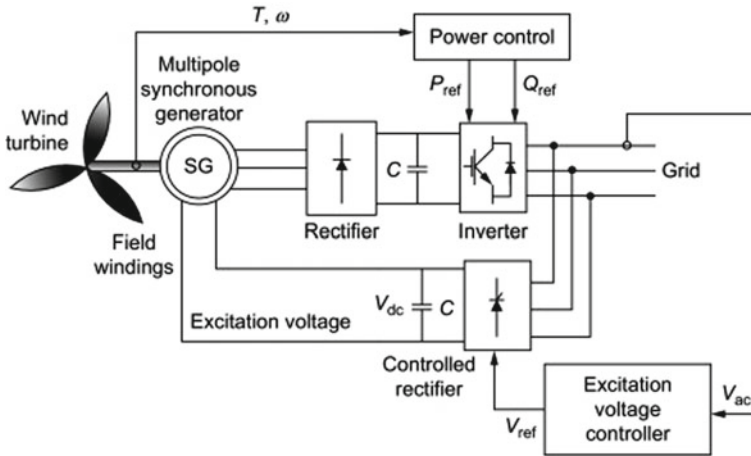


Fig. 3 Direct drive synchronous generator

voltage source converter is typically used to solve this purpose. Figure 3 shows direct drive synchronous generator electrically excited synchronous generator system.

3 Impact of Wind Turbine Generator on Power System

Power system stability and transient behavior need to be at rest while interconnecting a large wind farm to the traditional grid. Power system stability of the concerned grid largely depends upon type of fault, tripping of transmission lines, laws of production and short circuits maybe single line to ground fault or double line to ground faults. Power system on balance and distribution of real and reactive power may lead to drop of voltage level at its boundary value leading to instability of the system. Sometimes, this brownout leads to blackout on the power system if sufficient measures are not taken at the right time. Many power system failures are rectified headed by disconnection of transmission line or by reclosers. During the early stage of development of wind turbine, only a few wind turbines were connected to the grid; on this condition, if any fault occurs in the transmission line which reduces the voltage near wind turbine, then the wind turbine is simply disconnected from the grid and again reconnected after the clearance of the fault. Since every small amount of wind, power was connected to the grid, so disconnection of wind system from the grid does not affect the performance of the system and therefore not affecting the stability problem.

With the rapid increase in the interconnection of renewable energy such as wind energy, the contribution of wind power is significant from the grade point of view. Under the fault condition if the entire power plant is disconnected from the system, then the system will lose its production capacity and leads to blackout. Back out at a particular portion sometimes leads to increase in voltage level at other buses,

which are supported by traditional generator. If the remaining power stations do not have sufficient spinning reserve in order to support the start, present time, then a large amount of frequency and voltage drop may occur and possibly complete loss of power system may occur. This concept leads to design of low ride through capability wind turbine, which can tolerate these small disturbances to avoid total disconnection of power system from the grid. In order to keep the stability of the system, it is necessary to ensure that the wind turbine must gain its normal operation in an appropriate way within the stipulated time. Sometimes, the above statement can be achieved by incorporating the wind turbine with some additional power system protection and quality management devices such as STATCOM and SVC.

4 Result Analysis

An IEEE-14 bus system has been used to analyze the effect of wind turbine on the grid system. Figure 4 sources the three-phase voltage and current at the PCC where both wind and station are connected together. Before the occurrence of power system, fault voltage magnitude was maintained at 22 kv and that of the current is maintained to be 610 A. Simulation period of 0.05 s has been fixed for this particular program.

From the same figure, it can also be noticed that both three-phase voltage and current are in phase with each other. Figure 5 shows three-phase voltage and current at PCC during the grid disturbance. At time, about 2.2 s an induction motor has been turned on which leads to a voltage notch and a current notch in the system. This forces

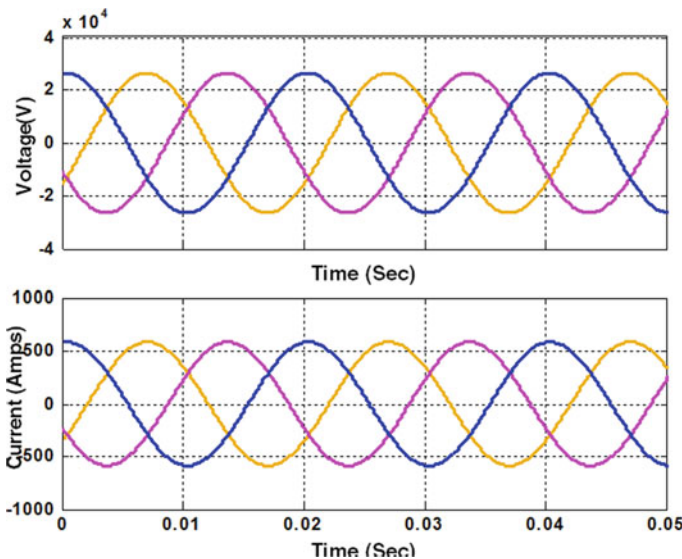


Fig. 4 Three-phase voltage and current at PCC

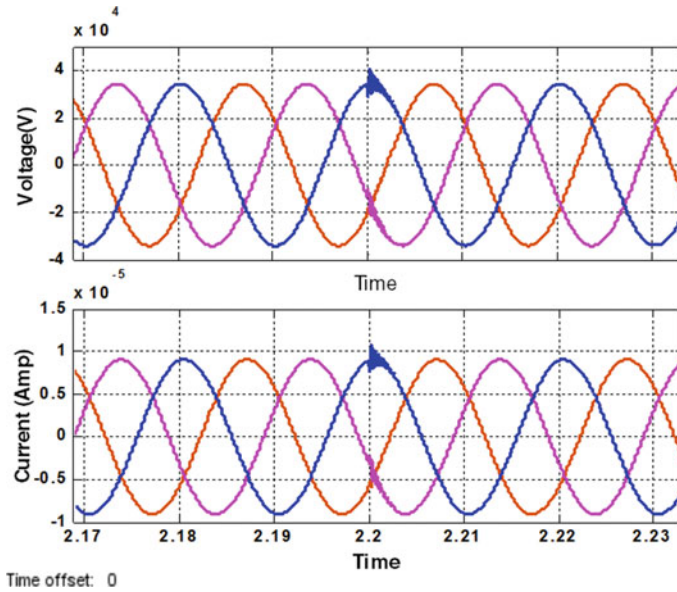


Fig. 5 Three-phase voltage and current at PCC during grid disturbance condition

the STATCOM to compensate against by controlling the voltage at the PCC. Figure 6 shows the reference disallowable and the modulation index that is maintained by the voltage source converter for controlling the voltage. Similarly, Fig. 7 shows VAR controlling action during the grid failure condition. Figures 7 and 8 solve the amount

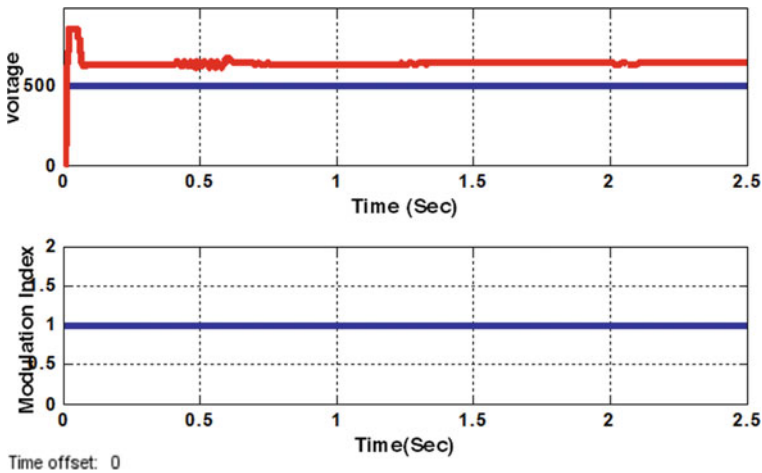


Fig. 6 DC link voltage and modulation index maintained by STATCOM during compensation mode

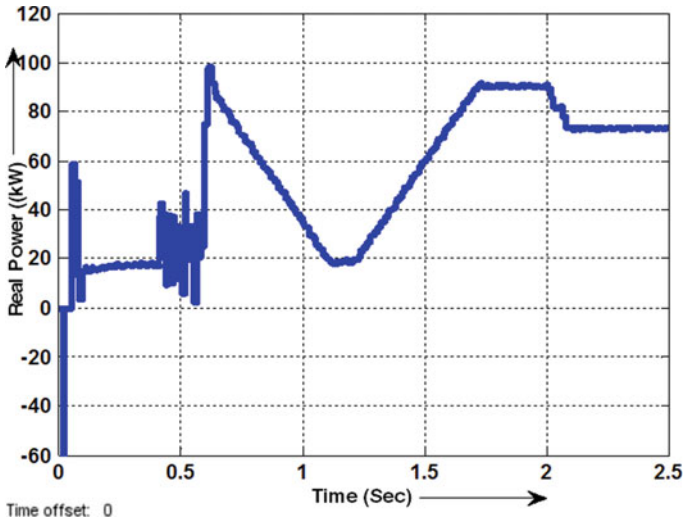


Fig. 7 Real power maintained by STATCOM during VAR compensation mode

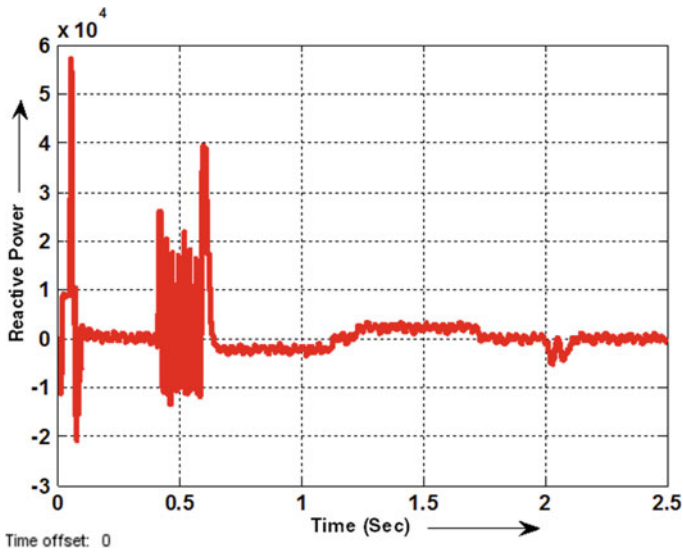


Fig. 8 Real power maintained by STATCOM during

of real and reactive power that is exchanged with the grid. As shown in Fig. 8, the reactive power is maintained at zero level throughout the simulation; however, during the fault condition which begins at 0.22 s STATCOM supports the reactive power and it can be found that the reactive power has increased up to 4 times as required by the system.

5 Conclusion

Detailed load flow analysis has been carried out for IEEE14 bus system. During the occurrence of fault, the generator bus bar voltage decreases to a nominal value, and by the use of STATCOM, it can be again maintained after 2.2 s.

References

1. M. Marcelo, M. Pedro, *Modelling and Control Design of Pitch-Controlled Variable Speed Wind Turbines* (2011). <https://doi.org/10.5772/15880>
2. M.P.S. Gryning, Q. Wu, Ł. Kocewiak, H.H. Niemann, K.P.H. Andersen, M. Blanke, Stability Boundaries for Offshore Wind Park Distributed Voltage Control. *Control Syst. Technol. IEEE Trans.*, **25**(4), 1496–1504 (2017)
3. M.A.H. Rafi, T. Vo, P.H. Nguyen, Effective integration of large-scale wind power using PV-STATCOM. *J. Eng.*, *2019*(18), 5303–5307 (2019).
4. R. Dash, P. Paikray, S.C. Swain, Active power filter for harmonic mitigation in a distributed power generation system, in *2017 Innovations in Power and Advanced Computing Technologies (i-PACT)*, Vellore (2017), pp. 1–6, <https://doi.org/10.1109/IPACT.2017.8245204>.

Grid Interconnection and Challenges Associated to Operation of a Decentralized Solar PV System



Debashish Pattnaik, Ritesh Dash, and Saratchandra Swain

1 Introduction

Solar grid interconnection is a system that allows integration of solar photovoltaic system to the national utility system. Solar photovoltaic system is an important technology because it allows energy optimization for building and thereby balancing and improving the economy of solar photovoltaic grid interconnection. Successful interconnection of solar photovoltaic system can reduce the operational and maintenance cost and thereby providing additional value to the end user [1, 3]. Solar PV interconnection is a common practice adopted by many countries this is because solar PV can be harvested at any part of the country, which is not only economical but also helps in sustainable development.

Interconnecting the solar energy with the grid not only affects the performance of power system but also so being disturbed during fault in transmission line [2]. When a bulk amount of power is disconnected from the main source, its impact can be noticeable at all other buses, which are being supplied from the solar PV system. In order to avoid the solar photovoltaic system from grid disturbances, some modern sophisticated equipments such as anti-islanding technology, solar grid forecasting, grid plant protection and smart grid technology have been used in conjunction with

D. Pattnaik · S. Swain

School of Electrical Engineering, Kalinga Institute of Industrial Technology University,
Bhubaneswar, India

e-mail: devkaran12@gmail.com

S. Swain

e-mail: scs_132@rediffmail.com

R. Dash (✉)

Department of Electrical Engineering, Christian College of Engineering & Technology, Bhilai,
India

e-mail: rdashee@gmail.com

© Springer Nature Singapore Pte Ltd. 2021

K. S. Sherpa et al. (eds.), *Advances in Smart Grid and Renewable Energy*,

Lecture Notes in Electrical Engineering 691,

https://doi.org/10.1007/978-981-15-7511-2_39

the inverter system [5, 6]. Energy directly converted from solar power can be readily used at the point of installation of PV plant and the one used amount of energy can be fed back to the grid, thereby enabling the concept of net metering. This concept leads to the use of anti-islanding inverter, that is, the inverter is capable to detect the fault in the transmission line and thereby sending signal to the inverter to stop the flow of power or injecting power to the grid to which it is connected. In the Present technology DC current generated from solar photovoltaic system can be directly converted into AC system and thereby controlling the voltage and phase angle of the power system to make the system, more stable [4].

Solar PV islanding is a phenomenon where solar PV system continues to power the grid to which it is connected even though there is an electrical fault present in the system. However, IEEE 1547 in Sect. 4 declares that the PV system must be capable to de-energize itself within 2 s from the instant of occurrence of fault in the transmission line and should not be connected up to 60 s after clearance of fault. Reconnection time of solar photovoltaic system after the clearance of fault lies in the range of 1–1.5 min post-fault. Number of active and passive method has been integrated to the inverter for detecting the sliding mode of operation. Generally inverters during its manufacturing time undergoes real-time anti-islanding test to check whether they are capable of connecting and disconnecting the border electricity or not power system forecasting for grade forecasting is the concept where health of the grid is being accessed from time to time in real-time mode and thereby predicting the potential behavior off the grid to adapt dynamic changes in the power system and its parameter when is sudden disturbance occurs in the system that may be due to renewable sources for conventional sources. Smart grid technology is a technology, which can sense the system performance starting from the light load condition to heavy load condition and thereby extracting maximum power from the renewable sources such as solar PV system meet the load demand. In order to extract maximum amount of power, the algorithm must be designed in such a way that it must have the the global data set along with its geographical data in terms of weather condition and solar insolation so that depending upon the geographical location in which it is installed, it can extract maximum amount of power for that location without hampering the power quality. Normally, the renewable energy penetration can be divided into three categories starting from low medium and high [15]. Solar PV injection into the grid greater than 30% is considered high and usually requires smart grid technology that can successfully penetrate the solar generated power into the grid. Again, the maximum amount of solar power that can be inducted into the grid depends upon the substation to which the solar is being supplied. Solar PV must be connected to the highest rating bus bar.

As discussed above, smart grid concept and its technology was coined in order to two successful interconnection of renewable sources surcharge solar PV, wind and biomass with that of the traditional grid. A number of challenges have been noticed while interconnecting the solar PV system with the grid because it is nature dependent and thereby is intermittent [12, 14]. This paper describes the interconnection of solar PV system with traditional grid and gives a comparative analysis of both linear and nonlinear controller and the problems faced by the inverter technology

while reducing the harmonics, thereby converting the input DC source into its corresponding alternating current [9]. The intensity of the impact generally varies with respect to the geographical location of the plant where it is being installed. Different environmental effects and their challenges and benefits have been addressed in this paper with MATLAB Simulink software. A standard model has been developed in the Simulink environment with all the parameters optimized with respect to the original one.

2 Challenges in Solar PV Grid Interconnection

Almost all the electrical system supports unidirectional flow of power; negative power is generated by the generator and flows to the customer with the help of substation. However, solar power required by directional flow of power; therefore, while constructing the solar power, it must be taken care that the power generated by the solar must match with the load [7, 8]. Solar PV systems those which are installed in the remote area a little variation in the power flow and its direction can hamper the transmission parameters and thereby affecting the nearby substations. When demand is less and generation is more, the excessive power can flow back to the substation and thereby affecting the different instruments connected to those particular substations. Potential amount of energy can also damage the system and thereby affecting the other customers, which are connected to the other end of the substation [10, 11]. Again photovoltaic systems are usually installed at a remote location where there is an abandoned amount of solar energy is available there for transmitting the power from that particular source on to the point where it is being utilized; it is required to construct new transmission lines which again involves a lot of cost and thereby increasing the per unit generation cost of solar PV system.

In addition to the above problem, some other problems are also being associated with the solar photovoltaic system that is the stability. Stability in terms of voltage, frequency and overall power quality affects the system performance [13]. Power quality issues also range to harmonics that is being generated by the load mainly because of the power inverter. By the property of the solar photovoltaic system, it usually generates voltage, which is fluctuating in nature thereby requiring an additional storage device in order to support the power grid to which it is connected. Addition of storage device also increases the cost of production and it requires frequent maintenance over the period.

3 Proposed System Description and Result Analysis

The proposed topology based on the above discussion is shown in Fig. 1, for effective interconnection of solar photovoltaic system with the traditional grid.

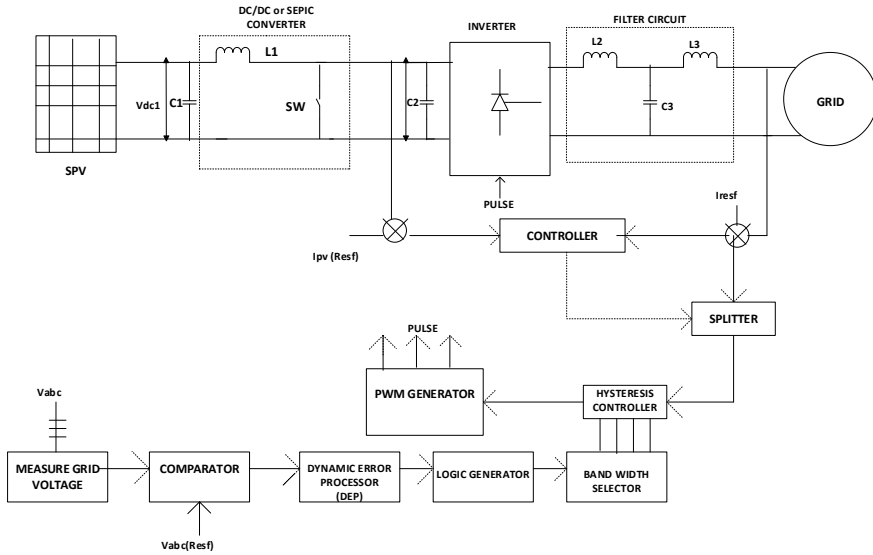


Fig. 1 Proposed circuit diagram of hysteresis controller-based SPV grid interconnection [16]

Here, solar photovoltaic system is used to energize the inverter DC link. The topology used in the figure performs the dual operation that is providing active power during the daytime and compensating against reactive power during nighttime and solar photovoltaic is not there. The two-voltage source converter is provided with a common DC link and energized by four number of series-connected capacitor. Two number of switches such as $S1$ and $S2$ can be used to either generate or consume the power either in the form of STATCOM or SSSC. Dynamic active compensation consisting of both STATCOM AND SSSC provides the real-time solution for different power quality issues occurring in the grid due to solar photovoltaic insertion (Fig. 2).

An inverter prototype for 100 kw solar PV grid-connected system has been designed with MATLAB Simulink. Grid-connected system is designed to inject maximum amount of power strictly to the maximum outgoing feeder connected to that particular system. PWM controller has been used to generate pulses to inject maximum amount of power (Fig. 3).

Figure 4 shows that voltage of solar PV system varies in between 302.4 and 303.8 V. Voltage across the input of inverter is stepped up to 670 V with an allowable ripple content of 5%. This has been limited to 5% through a capacitor, (Figs. 5, 6 and 7).

Performance of both linear controller and nonlinear controller has been studied under different temperature and solar irradiance condition. Based on the comparison, it is found that PI controller has better performance among all the linear controllers with THD level of 5.03%. Similarly, hysteresis controller has a THD level of 8.03%.

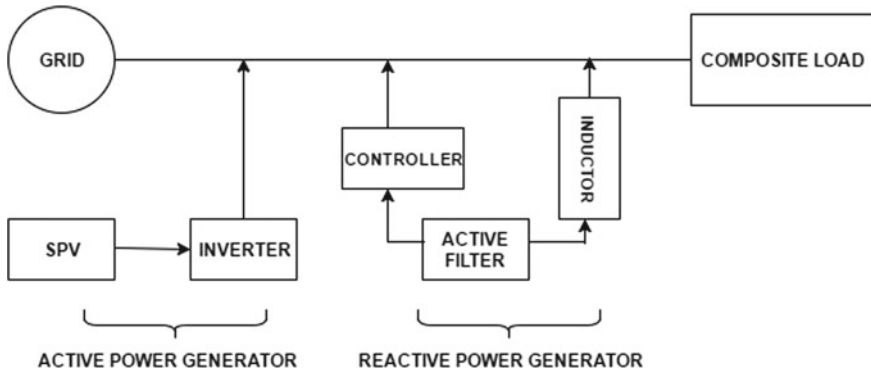


Fig. 2 Block diagram of proposed system

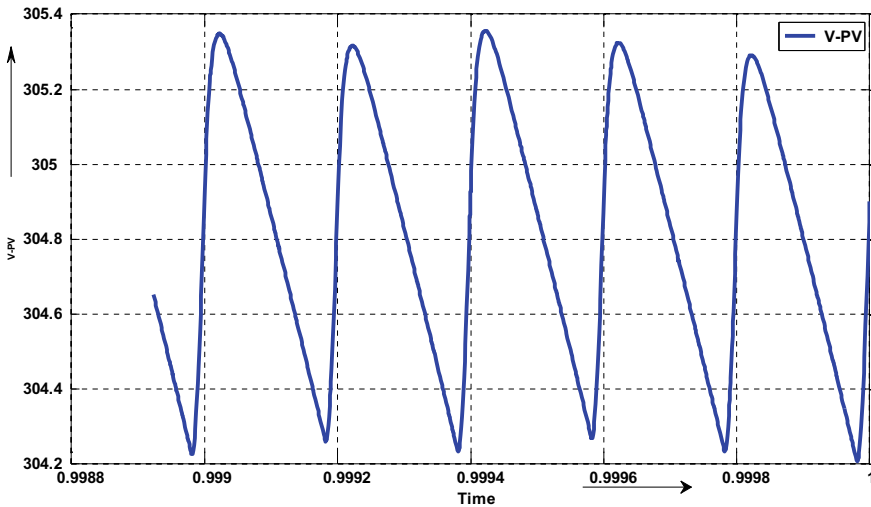


Fig. 3 PV output voltage

4 Conclusion

Evaluation of the linear controller has been carried out under a steady-state condition. Power injected into the grid is maintained at a particular level by fixing the voltage. Current injection quantity has been increased by applying different controller. Stability analysis of the entire discussed controller has been presented with Nyquist plot to check the stability. Best on the result PI controller is found to be best one under non-transient condition.

Fig. 4. d-q controller loop at PV generator side

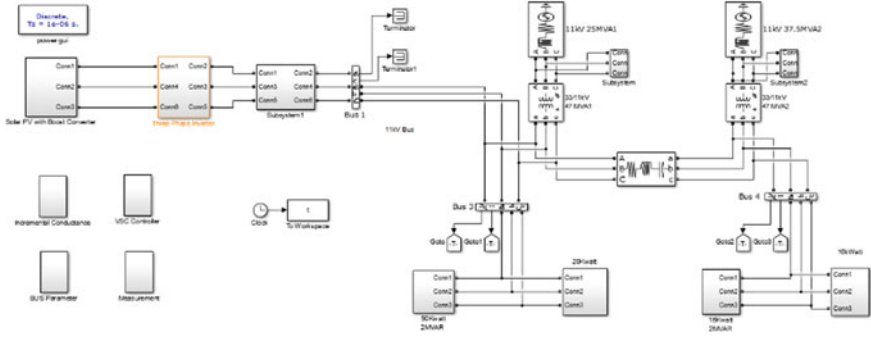
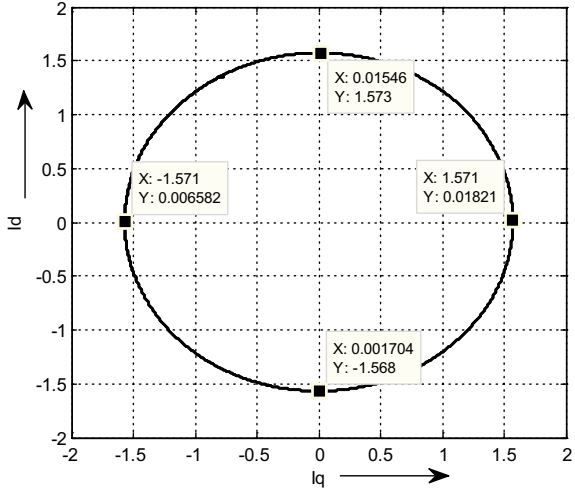


Fig. 5 MATLAB Simulink model of the test system

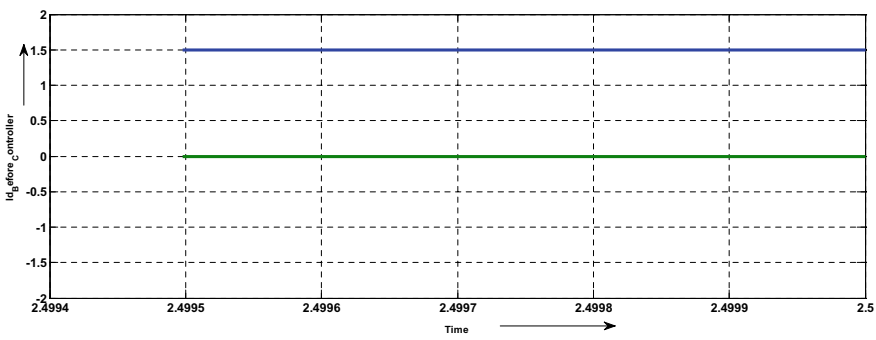


Fig. 6 Input Id, Iq to state feedback controller

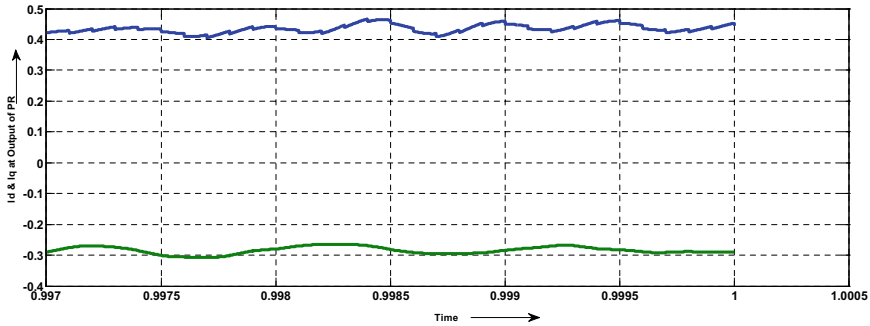


Fig. 7 Input I_d , I_q to PR controller

References

1. D. Graovac, V. Katic, A. Rufer, Power quality problems compensation with universal power quality conditioning system. *IEEE Trans. Power Deliv.* **22**(2), 968–976 (2007)
2. T. Ackermann, G. Andersson, L. Söder, Distributed generation: a definition. *Electr. Power Syst. Res.* **57**(3), 195–204 (2001). ISSN 0378-7796
3. L. Hassaine, E. Olias, J. Quintero, M. Haddadi, Digital power factor control and reactive power regulation for grid-connected photovoltaic inverter. *Renew. Energy* **34**(1), 315–321 (2009). ISSN 0960-1481
4. T. Hoff, D.S. Shugar, The value of grid-support photovoltaics in reducing distribution system losses. *IEEE Trans. Energy Convers.* **10**(3), 569–576 (1995)
5. S. Krauter, R. Rüter, Considerations for the calculation of greenhouse gas reduction by photovoltaic solar energy. *Renew. Energy* **29**(3), 345–355 (2004). ISSN 0960-1481
6. S.K. Salman, I.M. Rida, Investigating the impact of embedded generation on relay settings of utilities electrical feeders. *IEEE Trans. Power Deliv.* **16**(2), 246–251 (2001)
7. H. Yu, J. Pan, A. Xiang, A multi-function grid-connected PV system with reactive power compensation for the grid. *Solar Energy* **79**(1), 101–106 (2005). ISSN 0038-092X
8. J.H.R. Enslin, P.J.M. Heskes, Harmonic interaction between a large number of distributed power inverters and the distribution network, in *Power Electronics Specialist Conference, 2003. PESC '03. 2003 IEEE 34th Annual*, vol. 4 (2003), pp. 1742–1747
9. U. Borup, F. Blaabjerg, P.N. Enjeti, Sharing of nonlinear load in parallel-connected three-phase converters. *IEEE Trans. Ind. Appl.* **37**(6), 1817–1823 (2001)
10. A. Moreno-Munoz, J.J.G. de-la-Rosa, M.A. Lopez-Rodriguez, J.M. Flores-Arias, F.J. Bellido-Outerino, M. Ruiz-de-Adana, Improvement of power quality using distributed generation. *Int. J. Electr. Power Energy Syst.* **32**(10), 1069–1076 (2010). ISSN 0142-0615
11. H. Jintakosonwit, H. Fujita, Akagi, S. Ogasawara, Implementation and performance of cooperative control of shunt active filters for harmonic damping throughout a power distribution system, in *37th IAS Annual Meeting. Conference Record of the Industry Applications Conference, 2002*, vol. 1 (Pittsburgh, PA, USA, 2002), pp. 51–58
12. B. Rahmani, W. Li, G. Liu, An advanced universal power quality conditioning system and MPPT method for grid integration of photovoltaic systems. *Int. J. Electr. Power Energy Syst.*, **69**, 76–84 (2015). ISSN 0142-0615
13. L.K. Goel, S.K. Kottayil, V. Renukadevi, B. Jayanand, Smart grid technologies harmonic and reactive power compensation of grid connected photovoltaic system. *Proc. Technol.* **21**, 438–442 (2015). ISSN 2212-0173
14. J.S.R. Jang, ANFIS: adaptive-network-based fuzzy inference system. *IEEE Trans. Syst. Man Cybernet.* **23**(3), 665–685 (1993)

15. S. Pattnaik, R. Dash, S.C. Swain, P. Mohapatra, Control of active and reactive power of a three phase grid connected photovoltaic system, in *2016 International Conference on Circuit, Power and Computing Technologies (ICCPCT)* (Nagercoil, 2016), pp. 1–6
16. R. Dash, S.C. Swain, Effective power quality improvement using dynamic activate compensation system with renewable grid interfaced sources. *Ain Shams Eng. J.* **9**(4), 2897–2905 (2018)

A Comprehensive Study on Load Balancing Algorithms in Cloud



Mohona Bandyopadhyay, Manoj Kumar Mishra,
Bhabani Shankar Prasad Mishra, and Samaresh Mishra

1 Introduction

Cloud computing has become essential technology in industrial and research use. IaaS, SaaS, and PaaS are the three main services which are delivered by cloud computing [1]. But the entire services are being provided with the help of virtualization over the Internet. Cloud computing becomes more popular for the users as well as for industries and continues to expand its arms [2]. The main challenging area in cloud computing is security issue, data center energy consumption, scheduling of resources, performance monitoring, efficient load balancing, and deadlock for resources availability. Load balancing is one of these problems, which plays a vital role in cloud computing. Load balance is a process for improving the throughput and the performance by assigning and reassigning the load among the available resources.

“On-demand services concept” in cloud is a concept of paid services in which the user has to pay a bill amount to service provider for accessing on-demand services. Hence, reducing execution time of tasks in a cloud is a problem of interest. In cloud computing environment, virtual machine is known as processing unit, and all VMs can concurrently execute various tasks. Therefore, there is a need of proper scheduling strategy to schedule tasks into available VMs in such a manner that all the resources

M. Bandyopadhyay · M. K. Mishra (✉) · B. S. P. Mishra (✉) · S. Mishra (✉)
School of Computer Engineering, KIIT Deemed to be University, Bhubaneswar, Odisha 751024,
India

e-mail: manojku.mishra05@gmail.com

B. S. P. Mishra

e-mail: mishra.bsp@gmail.com

S. Mishra

e-mail: smishrafcs@kiit.ac.in

M. Bandyopadhyay

e-mail: mohonaacst15@gmail.com

can be utilized effectively. That will help us to minimize the makespan in all VMs [2]. However, this scenario calls for proper load balancing across VMs such that no VM becomes overloaded or ideal [1]. The foremost goal of load balancing algorithm is to optimize resource utilization, achieving maximum throughput, etc.

The rest of the paper is organized as follows. Section 2 describes the literature on load balancing. Metrics for load balancing is discussed in Sect. 3. Section 4 describes dynamic load balancing policies. Challenges of load balancing in cloud computing for task scheduling are given in Sect. 5. Section 6 provides virtual machine level load balancing. Section 7 is about different cloud models. Classification of load balancing algorithms is introduced in Sect. 8. Virtual machine placement algorithms are discussed in Sect. 9. Distributed dynamic load balancer for virtual machine is presented in Sect. 10. Last section is about conclusion and future work.

2 Literature on Load Balancing

Load balancing is broadly categorized into two kinds: task level and virtual level load balancing (Fig. 1).

2.1 Tasks Level Load Balancing Model

Load balancing algorithm is designed to distribute the tasks submitted by the user into the virtual machines. Here decision should be made by the load balancer that which virtual machine is allocated for the next request. Load balancer applies load balancing algorithm to assign tasks into suitable VM after receiving the task from the user. User never compromises with QoS. VM monitor is used for establishing and maintaining of the VMs. VMM consists of four operations highly essential for load balancing, and they are multiplexing, storage, and resume and life migration [3] (Fig. 2).

Again task level load balancing splits up into two categories: static algorithm and another one is dynamic algorithm.

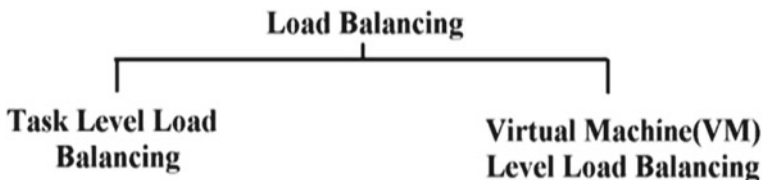
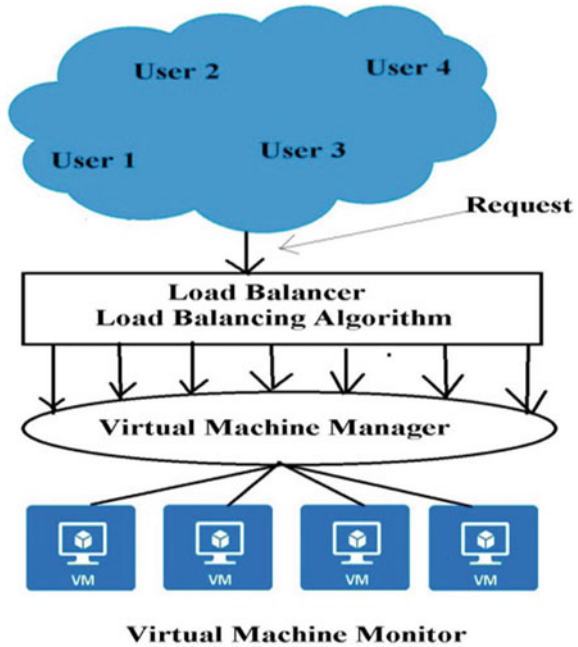


Fig. 1 Classification of load balancing

Fig. 2 Architecture model of task load balancing



2.2 Static Algorithm

This kind of algorithm is applicable to those systems which are related to low adaption to load distribution. It uses the system-related application knowledge and static information in advance [1]. Once the task is submitted, they can be easily assigned into the processor otherwise not, and during its execution, static task cannot be moved from one machine to another for maintaining load balance which is the major disadvantage of static algorithms [2].

2.3 Dynamic Algorithm

This type of algorithm first identifies the underloaded or ideal server of the entire network, and then it will place the load into the appropriate server. In this century, traffic is increasing day by day due to extreme communication over the network. The present situation of a system plays a major role to organize the load [2]. Dynamic load balancing algorithm falls under three strategies [4], viz. distributed, semi-distributed, and centralized.

2.4 Process Initiated

Load balancing decision process is initiated from the sender or by the receiver side.

2.4.1 Sender Initiated

Here overloaded node tries to transfer their work into lightweight node. For average system, load performance sender initiate is always better than receiver initiate because generally it is easy for finding lightly loaded node as compared to finding heavy-loaded node.

2.4.2 Receiver Initiated

Here lightweighted nodes constantly look into overloaded node for receiving the task from that node. For heavy system, load receiver initiate is working better than sender initiate because of finding heavy-loaded node rather than lightly loaded node is faster.

2.4.3 Symmetric

It is the mash-up of sender and receiver initiated approach (Fig. 3).

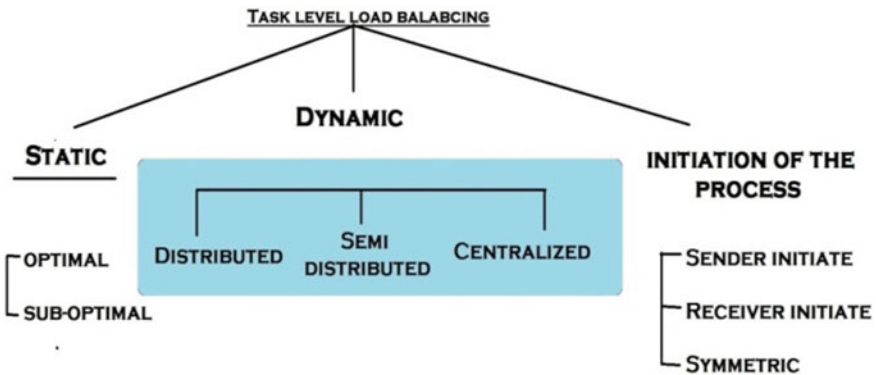


Fig. 3 Task level load balancing

3 Metrics for Load Balancing

Load balancing algorithms can be measured by using several metrics, which are enumerated as below [3, 5].

Performance: After applying load balancing algorithm, it is used to calculate system efficiency. It involves the calculation of response time of a task.

Response time: It is used to calculate total time of the system for executing the arrived task.

Throughput: The number of successful operations performed within a given time period, e.g., the quantity of data successfully moved on a given time period from one node to another node.

Fault tolerant: With the help of this parameter, we came to know whether the algorithm is able to tolerate any kind of fault or not. If some kind of fault occurs, the algorithm is capable to operate continuously.

Migration time: It is the time required to migrate task from one node to other node, e.g., from heavy-loaded node to light-loaded node.

Makespan: It is about the maximum completion time.

Scalability: It refers to a scenario where the performance of an algorithm never degrades while increase the number of nodes in the system.

Energy Consumption: It is used to calculate the quantity of energy needed by all nodes. Mostly, overheating is avoided by load balancing.

4 Dynamic Load Balancing Policies

Transfer policy: This policy determines at what circumstances task should migrate from one node to another node. For instance, overloaded nodes try to transfer their task.

Selection policy: Here the selection of a task is performed for transferring from one node to another node. On the basis of some constraints, task selection is performed such as amount of overhead needed for transfer and task execution time.

Location policy: This policy finds lightly or underloaded machines so that load can be balanced by transfer tasks from heavily loaded machine to lightly loaded machine.

Information policy: Information is collected from all systems which helps in decision-making procedure. While collecting the information, the time stamp of is also recorded.

5 Challenges of Load Balancing in Cloud Computing for Task Scheduling

This section mentions the important parameters required in scheduling tasks in a cloud computing environment.

Virtual machine migration: The important characteristic of cloud computing is resource allocation which is only provided when there is a valid request. Sometimes VM is required to transfer from one server to another server. But when the location is too far, they create some challenges for the designer of load balance algorithm to manage two issues—one is migration time and another is performance.

Distribution of nodes in a cloud: Primarily nodes are distributed in a wide area network. Hence, while designing a load balancing algorithm the parameters like bandwidth of network, transmission speed, and node distance have to be taken into consideration.

Single point of failure: When any network is controlled by a single node, there is chance of failure of the network due to the malfunction of that single node.

Complexity of algorithm: Generally, algorithm should be simple for execution and maintainance. Complex algorithm is responsible for degrading the performance of the whole system.

Adaption of small data center: Small data center became more efficient than large data center as terms of cost and energy. But the main challenge for the designer is to maintain response time.

6 Virtual Machine Level Load Balancing

Cloud data server is highly dynamic and arbitrary due to the following salient points:

- Resource consumption is highly asymmetrical.
- Irregularity in rise and fall of resources requirements in VM.
- Unordered rate of entry and exit of data center consumers.
- Performance fluctuate happens due to varying level of load on host (Fig. 4).

Load balancing is the process of distributing of excess dynamic workload into ideal nodes. This process should apply for achieving better user fulfillment and enhanced resources utilization, and it also ensures that no single node becomes ideal. The main aim of VM scheduling with load balancing is for assigning virtual machine to the appropriate host and properly balancing the resources among all host. Many applications are installed in a VM, and all applications are executed on a VM. Every host is assigned with multiple VMs. Resources are provided by the host such as storage or memory. Server virtualization platform creates physical resources and manages virtualization. Load balancing is applied on both virtual machine level and application level. There are many challenges in the placement of VMs, like overhead, system efficiency resource utilization, scalability, response time, and fault tolerance.

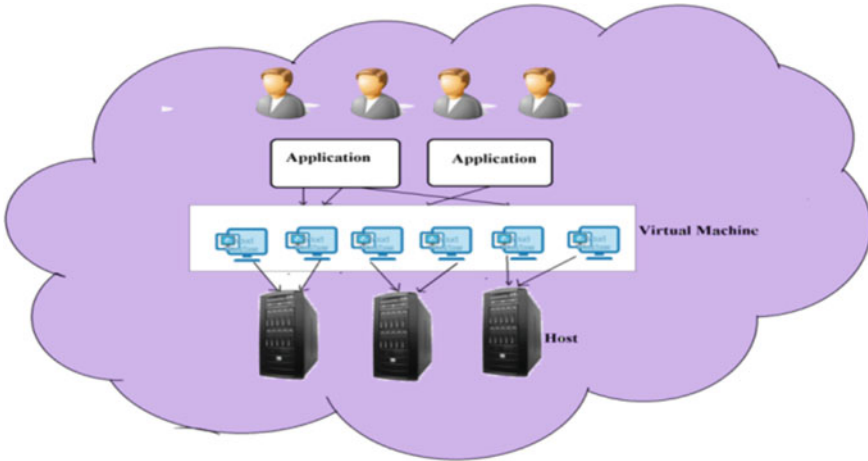


Fig. 4 Virtual machine level load balancing

7 Scenario of Different Cloud Model

Cloud models can be classified under three categories: public, private, and hybrid.

Public Cloud Services which provided by third party over the Internet. The major advantage of public cloud is that the capital investment is very less. But due to large size of network, there is lack of control over data, security, management, and network, which makes it difficult to achieve effectiveness in many business scenarios.

Private Cloud Private cloud is well known as Internet cloud or corporate cloud as its service is generally offered over organization or any private Internet network. In many institutional experiments, small-sized private clouds are implemented for estimating the performance of load balancing in VMs.

Hybrid Cloud The mixtures of public and private cloud that are bound with the limitation of each model. In hybrid cloud infrastructure, some part is running in public cloud and some part in private cloud. Flexibility in hybrid cloud is higher as compared to public and private cloud.

8 Classification of Load Balancing Algorithms

Load balancing algorithms can be classified based on the nature of the algorithm adopted for balancing purpose [3]. It is depicted in Fig. 5.

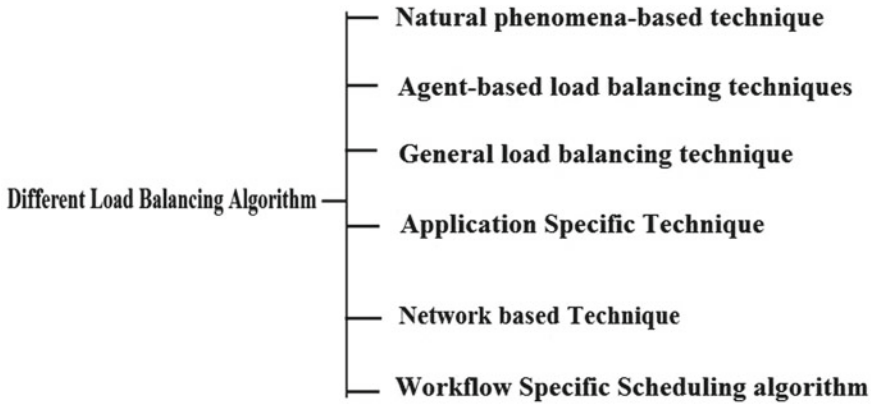


Fig. 5 Different load balancing algorithms

8.1 Natural Phenomena-Based Technique

Lagawal et al. [6] have proposed a noble approach for managing load balancing in the cloud by using genetic algorithm. In this technique, VM is arranged according to processing power and length of the cloudlets. For allocation of the tasks, all the VMs and cloudlets are slender to the broker. The broker identifies resources with the help of genetic algorithm.

Tawfeek et al. [7] have proposed an approach for task scheduling based on the ant colony optimization algorithm, and different algorithms are compared with this technique like round robin and FCFS. The aim of the algorithm is to reduce the makespan of the particular task.

Dhinesh Babu et al.[3] proposed a honey bee behavior inspired load balancing (HBB-LB) algorithm. In this proposed model, authors have taken care of two objectives like throughput and prioritization of tasks, on the machine to minimize the waiting time of the task.

8.2 Agent-Based Load Balancing Techniques

Singh et al. [3] have proposed an autonomous agent-based load balancing for the cloud platform with the support of three different agents: migration, load, and channel agent. Generally, static agent is regarded as channel and load agents and ant as migration agent. After assigning the jobs into a virtual machine, measuring the VMs load and information policy is in the control of load agent. All the detail of VMs such as load, the status of VMs, Id, memory is maintained by fitness table in the data center. Selection, transfer, and location policy are under the control of channel agent. Lastly, the migration agent is initiated by the channel agent.

Gutierrez-Garcia et al. [3] author proposed an agent-based load balancing (AB-LB) technique for cloud data center. By the help of VMs live migration, the author uses agent-based problem-solving method to make load balancing across commodity and heterogeneous server.

Keshvadi and Faghieh [3] have proposed a new technique in IaaS environment which is based on multi-agent. This model supports both sender and receiver-initiated approach for balancing the load to reduce the waiting time of the task and also provides assured service level agreement. The author claims that this algorithm is more efficient in terms of load balancing, makespan, and response time.

Tasquier et al. [3] have proposed the algorithm for multi-cloud environments and are an application-aware load balancing technique on mobile agent paradigms. This architecture consists of three different agents: an executor, a provisioned, and monitor agent. An executor agent represents the application running in the multi-cloud environment. The management of cloud infrastructure such as removing or adding of resources is done by provisioned agent. The monitor agent is responsible to manage overload and underloaded conditions. The proposed algorithm claims to overcome the provider lock-in challenge in the cloud and is flexible enough to utilize the extreme elasticity.

8.3 General Load Balancing Technique

Kamaraswami and Muthuswami [3] proposed a dynamic load balancing approach in the cloud scenario with effective bin packing and VM reconfiguration (DLBPR). DLBPR schedules the jobs into a VM considering processing capability and processing power requirements of a job. The aim is to execute the job within their deadline and balancing load when required. This approach enhances the throughput and resource utilization.

Domanal and Reddy [3] the authors design a hybrid scheduling algorithm for achieving efficient load balancing in a distributed environment. Two well-known techniques, throttled and divided and conquer have been used for designing the algorithm. This method exploits the VMs more efficiently and decreases overall time for executing the jobs.

Chien et al. [3] provide an algorithm for load balancing using end-of-service time. This technique considers the immediate processing speed of a virtual machine and job size. The load balancing algorithm claims to improve the processing time and response time.

Kulkarni and BA [3] proposed a load balancing algorithm that assures a uniform allocation of requests to VM during essential hours for giving a quick response to the user. All information regarding VM reservation should be maintained by reservation table, based on the suggestion of the load balancer to the data center controller. The allocation table is updated until any acknowledgment comes from the allocation phase. The result of this algorithm shows allocation request to VM in the essential hour.

8.4 *Application Specific Technique*

Wei et al. [3] proposed an application scheduling algorithm based on max–min for mobile computing. It provides a detailed structure of application scheduling with local cloud model of mobile. The paper mentions an enhancement in the performance of the mobile cloud.

Wei et al. [3] presented a hybrid local mobile cloud model, which contains a mobile device and cloudlet. Here, the cloudlet acts as the central broker with neighboring mobile device and cloudlet acts as the service provider. The scheduling aims to maximize profit with an increase in the lifetime of this model. For solving the scheduling problem, the author uses hybrid ant colony based on an application scheduling algorithm. The algorithm never considers the overhead while measuring the advantage ratio of mobile devices. Under such assumptions, the method shows maximum profit with minimum energy consumption.

Deye et al. [3] provided an approach for dynamic load balancing to have better control of QoS parameters of multi-instance application in cloud. The shortcoming of the approach is the limited number of the request through a load balancer. The approach observes improvement in system performance.

8.5 *Network-Based Technique*

Shen et al. [3] proposed a probabilities network-aware task placing for MapReduce scheduling which helps to reduce the cost of data transmission and delay. The author found that every task has to face three challenges. Firstly, the servers available for executing task are dynamically changing and secondly, size and location of intermediate data. Finally, the link load on the routing path has also an impact on the data access latency. The strategy shows the great improvement in completion time of jobs and proper resources utilization.

Scharf et al. [3], the authors provide the enhancement of the open stack scheduler which enables network-aware placement of instances by taking into account bandwidth constraints of two or more nodes. The solution always tracks localhost network for resources allocation.

Shen et al. [3] designed a job scheduler for cloud with bandwidth reservation, in which each occupant required specific job deadline and bandwidth reservation by jobs that are elastically determined by use of the maximum elastic feature for the maximum the total job rewards. Finally, scheduler tries to minimize the processing time of every job. The result has shown the effectiveness and efficiency of the algorithm.

8.6 Workflow-Specific Scheduling Algorithm

Ghosh and Banerjee [3] presented a modified algorithm which is applied in the cloud environment with some additional features, like every service has its priority. The request is assigned to VMs before priority is assigned to the request. For holding the request, they proposed the switching queue to manage whenever any higher priority request joins. Authors measure its performance with respect to round robin and throttled load balancing algorithm.

Jaikar et al. [3] have proposed the architecture for load balance in scientific federation cloud and VM allocation algorithm. They tested this approach in the scientific federated cloud. Finally, the result shows that not only minimizes the energy consumption but also increases the resource utilization.

Cai et al. [3] provided a dynamic scheduling algorithm that is based on delay dynamic scheduling algorithm. It is a resource provisioning of dynamic cloud and scheduling algorithm which help for reducing the renting cost of resources. The dynamic VM is rented by DDS on the basis of practical running state and calculates the running time of task to fulfill the workflow deadline. For reducing the total renting cost, bag structure is considered by both bag-based delay scheduling and bag based deadline. The authors claim that it reduces the renting cost.

Zhang and Li [3] have proposed improved adaptive heuristic algorithm (IAHA) where the priorities of the tasks are presented in the complex graph, and based on the graph topology, they consider their impact each other. Application compilation time is gradually decreased and controlled with the help of adaptive mutation and crossover rate which leads it to give the optimal solution. The result of this algorithm shows improvements in the makespan and response time (Table 1).

9 Virtual Machine Placement Algorithm

Song et al. [8] proposed an algorithm for VM load balancing in high-level application is called migration management agent. The communication and computation load vary dynamically in large-scale military HLA system. This algorithm allows virtual machine to switch from one federation to other for performing load balance but communication cost is suffered. So the main target of algorithm is minimizing the load on the overloaded host so that the communication cost can be reduced.

Tordsson et al. [8] proposed an algorithm for VM placement and are a multi-objective scheduling that includes cost of load balancing and performances. Due to multi-cloud environment, various cloud providers are there who support different types of infrastructure and offer various types of VMs. The algorithm is a cloud broker and responsible for managing various virtual resources and optimizing VM placement. Integer programming formulation-based metaheuristic algorithm is explored by the author.

Table 1 Achieved matrices on load balancing

	Performance	Response time	Throughput	Fault tolerant	Migration time	Makespan	Scalability	Energy
Lagawal et al.	Yes	No	No	No	No	No	No	No
Tawfee et al.	Yes	No	No	No	No	No	No	No
Dasguptha et al.	Yes	No	No	No	No	Yes	No	No
Dhimesh Babu et al	No	No	Yes	No	No	No	No	No
Singh et al.	Yes	Yes	No	No	No	No	No	No
Gutierrez-Garcia et al.	Yes	No	No	No	No	No	No	No
Kesavadi and Faghieh	Yes	No	No	No	Yes	No	No	No
Tasquier et al.	No	No	No	No	No	No	No	Yes
Kamaraswami et al.	Yes	No	Yes	No	No	No	No	No
Domanal and Reddy	Yes	No	Yes	No	No	Yes	No	No
Chein et al.	Yes	Yes	No	No	No	No	No	No
Kulkami and BA	No	No	No	No	No	No	Yes	No
Wei et al.	Yes	No	No	No	No	No	No	Yes
Wei et al.	No	Yes	No	No	No	No	No	Yes
Deye et al.	No	Yes	No	No	No	No	Yes	No
Shen et al.	No	No	No	No	No	Yes	No	No
Scarf et al.	Yes	No	Yes	No	No	No	No	No
Shen et al.	No	No	No	No	No	No	Yes	No
Ghosh and Banerjee	Yes	Yes	No	No	No	No	No	No
Jaikar et al.	Yes	No	No	No	No	Yes	No	No
Cai et al.	Yes	No	No	No	No	No	No	No
Zhang and Li	No	Yes	No	Yes	No	Yes	No	No

A balance and comparison-based distributed load balancing procedure is presented by Zhao et al. [8]. For balancing load in the intra-cloud, the main target is that every host has equal access to the processor and I/O usage. Cost function is modeled for considering the I/O and CPU usage, and every host can measure the functional value itself. At the time of live migration, the approach tries to reduce the downtime of the host to increase the stability of system.

CLBVM “Central Load Balancing Policy for VM” Bhadani et al [8] performs load balancing in cloud environment with an aim for higher throughput and lesser response time. Different characteristics are used for achieving this goal: (1) algorithm generates low overhead, (2) load information is collected and updated from time to time, and (3) minimum downtime due to live migration, which helps to improve the throughput.

10 Distributed Dynamic Load Balancer for Virtual Machine

Rouzaud and Carnabas [8] presented distributed dynamic load balancing for VM based on the P2P framework, whose main aim is to decrease the load of particular host by moving load (VM) to new host with more resources. Due to the non-deterministic and complex nature, it is difficult to predict VM behavior for dynamic scheduling. The aim of this approach is to achieve better scalability.

For balancing VM, dynamic and integrated resource scheduling algorithm is proposed by Tian et al. [8]. For cloud environment, the proposed algorithm considers network bandwidth, memory, and CPU as integrated resources. The proposed algorithm executes the VM request as happens in a pipeline. Thus, the management of VM is converted into the management of queue. Every time interval algorithm updates the load information, and if the host is overloaded, then VMs are allowed to have delayed allocation.

For optimizing and scheduling of VMs, the author Thiruvankadam et al. [8] proposed a hybrid genetic algorithm. The main aim of approach is to reduce the number of migrations at the time of balancing load of VMs. The author focused on dynamically allocation of VMs and the host with variable load. For achieving the goal, it uses two techniques: (1) VM packing is done by comparing the host load and user requirement, (2) optimizing the VM placement by applying genetic algorithm.

Hu et al. [8] presented metaheuristic based genetic algorithm. The heuristic aims to search appropriate mapping solutions for reaching the best load balancing effort and thus reducing migration time. The approach takes into consideration of both the historical data and current data for computing the probabilities, thereby capturing the influence in advance.

The two well-known load balancing algorithms such as ant colony optimization and particle swarm optimization are combined by Cho et al. [8] for handling VM load

balancing in cloud computing with an aim to load balance and resource utilization. Here both the memory and CPU resources are considered for scheduling.

11 Conclusion and Future Work

In this paper, we have classified the load balancing algorithm by considering several parameters. This gives a clear idea on the algorithm efficiency. We have also introduced taxonomy by categorizing the load balancing algorithms in cloud. Future work includes the development an algorithm for load balancing and to evaluate it in real-world environment along with an analysis on all the discussed techniques.

References

1. [https://en.wikipedia.org/wiki/Load_balancing_\(computing\)](https://en.wikipedia.org/wiki/Load_balancing_(computing))
2. Gupta et al., Honey bee behavior based load balancing of tasks in cloud computing. *Int. J. Sci. Res.* **3** (6) (2014)
3. Ghomi et al., Load-balancing algorithms in cloud computing: a survey. *J. Netw. Comput. Appl.* **88**, 5071 (2017)
4. N. Haryani, D. Jagli, Dynamic method for load balancing in cloud computing. *IOSR J. Comput. Eng. (IOSR-JCE)* **16**(4), 23–28. e-ISSN: 2278-0661,p-ISSN: 2278-8727 (2014)
5. S. Rajoriya, Load balancing techniques in cloud computing: an overview. *Int. J. Sci. Res. (IJSR)* **3**(7) (2014)
6. M. Lagwal, N. Bhardwaj, Load balancing in cloud computing using genetic algorithm, in *International Conference on Intelligent Computing and Control Systems (ICICCS)* (2017)
7. M.A. Tawfeek, A. El-Sisi, A.E. Keshk, F.A. Torkey, Cloud task scheduling based on ant colony optimization, in *2013 8th International Conference on Computer Engineering & Systems (ICCES)* (2013). <https://doi.org/10.1109/ICCES.2013.6707172>
8. Xu et al., A survey on load balancing algorithms for virtual machines placement in cloud computing, in *Concurrency and Computation: Practice and Experience* (2017)

Implementation of an Efficient SVPWM Technique to a Cascaded Multilevel Inverter-Based SAF



Ashish Ranjan Dash, Ranjeeta Patel, Mrutyunjaya Mangaraj,
and Anup Kumar Panda

1 Introduction

Nowadays, active power filters (APF) emerged to be a key solution for harmonic compensation under highly nonlinear loading. These APFs are designed in order to mitigate the harmonics and reactive compensation under highly nonlinear conditions. The APF based on classical two-level inverter suffers from high switching loss and incapable in handling high power [1]. In comparison with two-level inverters, the multilevel inverter (MLI)-based SAF are capable for significant harmonic reduction and operates at lesser switching frequency at a same output level [2]. In literature, different carrier-based and a space vector modulation technique is discussed elaborately, and the performance is discussed when the inverter is not coupled with the grid. However, when the proposed inverter operates as a SAF, it should be able to generate harmonic current with an extended bandwidth compared to its open loop operation. So the conventional SVM approach requires higher memory for the storage of switching states, and the computation time also increases exponentially with added complexity. In [3], a SVM-based algorithm is applied to multilevel inverters. This algorithm can be implemented to different multilevel inverter structures, can be applied to any no. of phase and has less computational cost and also suitable for

A. R. Dash (✉)

Centurion University of Technology and Management, Paralakhemundi, Odisha, India
e-mail: ashishdashnitrkl@gmail.com

R. Patel

KIIT University, Rourkela, India

M. Mangaraj

Lendi Institute of Engineering & Technology, Vizianagaram, India

A. K. Panda

National Institute of Technology, Rourkela, Odisha, India
e-mail: akpanda.ee@gmail.com

© Springer Nature Singapore Pte Ltd. 2021

K. S. Sherpa et al. (eds.), *Advances in Smart Grid and Renewable Energy*,
Lecture Notes in Electrical Engineering 691,
https://doi.org/10.1007/978-981-15-7511-2_41

hardware implementation. Inspired by the SVM approach presented in [4], a novel space vector modulation technique is adopted considering the requirement of the proposed SAF.

The paper describes the logical approach and implementation of the suggested SVPWM algorithm. A comparison is made with two different, multilevel PWM techniques for switching of the proposed SAF. Finally, the effectiveness of the SVPWM algorithm is confirmed over simulation and experimental results.

2 SVPWM Algorithm Formulation

In power converters, the switching states are normally found in discrete states, in each modulation period, the voltage vector reference U_r can be approximated by the space vectors $S_l = \{U_{s1}, U_{s2}, \dots U_{sl}\}$. The reference vector is synthesized by applying each switching vector U_{sj} during an interval T_j . In the proposed system, the output voltage of each phase U_s is the product of an integer with DC side reference U_{dc} . Thus, the switching vectors and switching times are normalized by DC side voltage U_{dc} and modulation period T . The above vectors are represented as follows:

$$u_r = [u_r^1, u_r^2, \dots u_r^N]^T \tag{1}$$

$$u_{sj} = [u_{sj}^1, u_{sj}^2, \dots, u_{sj}^N]^T \tag{2}$$

Then, Eqs. (1) and (2) can be written in matrix format as

$$\begin{bmatrix} 1 \\ u_r^1 \\ u_r^2 \\ \vdots \\ u_r^N \end{bmatrix} = \begin{bmatrix} 1 & 1 & \dots & 1 \\ u_{s1}^1 & u_{s2}^1 & \dots & u_{sl}^1 \\ u_{s1}^2 & u_{s2}^2 & \dots & u_{sl}^2 \\ \vdots & \vdots & \vdots & \vdots \\ u_{s1}^N & u_{s2}^N & \dots & u_{sl}^N \end{bmatrix} \begin{bmatrix} t_1 \\ t_2 \\ \vdots \\ t_l \end{bmatrix} \tag{3}$$

The new modulation law formed by the linear equations need be solved by the proposed SVM algorithm. This main steps involved in the SVM algorithm are:

1. An integer set is found using coefficient matrix.
2. Switching time is calculated by solving the model equations.
3. The sequence of the switching vectors is extracted from the coefficient matrix.

The proposed SVM algorithm can be simplified by decomposing into the two-level SVM algorithm with a displacement. So the reference voltage can be represented by the sum of integral and fractional parts.

$$u_r = u_i + u_f \tag{4}$$

The switching vectors are displaced by u_i to find a new set of switching vector.

$$u_{dj} = u_{sj} - u_i \tag{5}$$

So (5) becomes

$$\begin{bmatrix} 1 \\ u_r^1 \\ u_r^2 \\ \vdots \\ u_r^N \end{bmatrix} = \begin{bmatrix} 0 \\ u_i^1 \\ u_i^2 \\ \vdots \\ u_i^N \end{bmatrix} + \begin{bmatrix} 1 & 1 & \dots & 1 \\ u_{d1}^1 & u_{d2}^1 & \dots & u_{dl}^1 \\ u_{d1}^2 & u_{d2}^2 & \dots & u_{dl}^2 \\ \vdots & \vdots & \vdots & \vdots \\ u_{d1}^N & u_{d2}^N & \dots & u_{dl}^N \end{bmatrix} \begin{bmatrix} t_1 \\ t_2 \\ \vdots \\ t_l \end{bmatrix} \tag{6}$$

Also (6) can be presented in matrix form as

$$\begin{bmatrix} 1 \\ u_r^1 \\ u_r^2 \\ \vdots \\ u_r^N \end{bmatrix} = \begin{bmatrix} 0 \\ u_i^1 \\ u_i^2 \\ \vdots \\ u_i^N \end{bmatrix} + \begin{bmatrix} 1 \\ u_f^1 \\ u_f^2 \\ \vdots \\ u_f^N \end{bmatrix} \tag{7}$$

By comparing (6) and (7), the displaced switching vectors and the reference voltage are represented as:

$$\begin{bmatrix} 1 \\ u_f^1 \\ u_f^2 \\ \vdots \\ u_f^N \end{bmatrix} = \begin{bmatrix} 1 & 1 & \dots & 1 \\ u_{d1}^1 & u_{d2}^1 & \dots & u_{dl}^1 \\ u_{d1}^2 & u_{d2}^2 & \dots & u_{dl}^2 \\ \vdots & \vdots & \vdots & \vdots \\ u_{d1}^N & u_{d2}^N & \dots & u_{dl}^N \end{bmatrix} \begin{bmatrix} t_1 \\ t_2 \\ \vdots \\ t_l \end{bmatrix} \tag{8}$$

The obtained linear equation follows the general modulation law presented in (8). As the fractional reference U_f is bounded, the reference approximation can be achieved through U_{dj} with binary components. The vector U_f and the displaced vector U_{dj} represent modulation for two-level inverter. The switching times are equal for both multilevel and two-level modulations. The algorithm for two-level modulation is solved by filling the coefficient matrix of Eq. (8) with zero and one, so that the switching vector sequence can be found out. Additionally, the coefficients are chosen in such a way where the switching time should remain positive always.

So, (8) can be presented as

$$\begin{bmatrix} 1 \\ u_f \end{bmatrix} = Dt \tag{9}$$

For putting the reference voltage u_f in descending order a permutation matrix **P** can be found as:

$$P \begin{bmatrix} 1 \\ u_f \end{bmatrix} = \begin{bmatrix} 1 \\ \hat{u}_f \end{bmatrix} \tag{10}$$

Multiplying (3) by a permutation matrix P

$$\begin{bmatrix} 1 \\ \hat{u}_f \end{bmatrix} = \hat{D}t \tag{11}$$

where

$$\hat{D} = PD \tag{12}$$

where \hat{D} is the upper triangular matrix and D is the coefficient matrix. Since P matrix is orthogonal, the coefficient matrix **Din** (12) can be written as:

$$D = P^T \hat{D} \tag{13}$$

The column vector u_f is transformed by a permutation matrix P through elementary row switching transformations. Similarly, the matrix \hat{D} is transformed by the matrix P^T through inverse row switching transformations. Since zeros and ones in every column remain same after transformation with same adjacent consecutive vectors, it minimizes the switching number. The switching time **can be calculated either from** (10) or (11). If the switching time is calculated by (11), then the solution is trivial as shown below, which seems as best option for the presented algorithm.

$$t_j = \begin{cases} 1 - \hat{u}_f^1 & \text{if } j = 1 \\ \hat{u}_f^{j-1} - \hat{u}_f^j, & \text{if } 2 \leq j \leq 3 \\ \hat{u}_f^3 & \text{if } j = 3 + 1 \end{cases} \tag{14}$$

The matrix **Dis solved by the** classical modulation law with minimized switching number and positive switching times. The coefficient matrix enables the switching sequence of the proposed system. The proposed multilevel SVM technique uses two-level modulators for carrying out multilevel modulation.

3 Proposed Cascaded MLI-Based SAF System Structure

The SAF employed in this work is a cascaded MLI with single DC excitation. In the proposed work, three modules are used in each phase and each module is connected

to a toroidal core transformer. The cascaded arrangement of the secondary of transformers enables single DC source operation [5, 6]. The proposed system structure is depicted in Fig. 1. A seven-level phase voltage can be generated using three similar H-bridge modules. As the proposed inverter operates as a SAF, the inverter injects the required compensation current at PCC via filter impedance. For introducing harmonics in the present system, a nonlinear load is employed. For simulation and

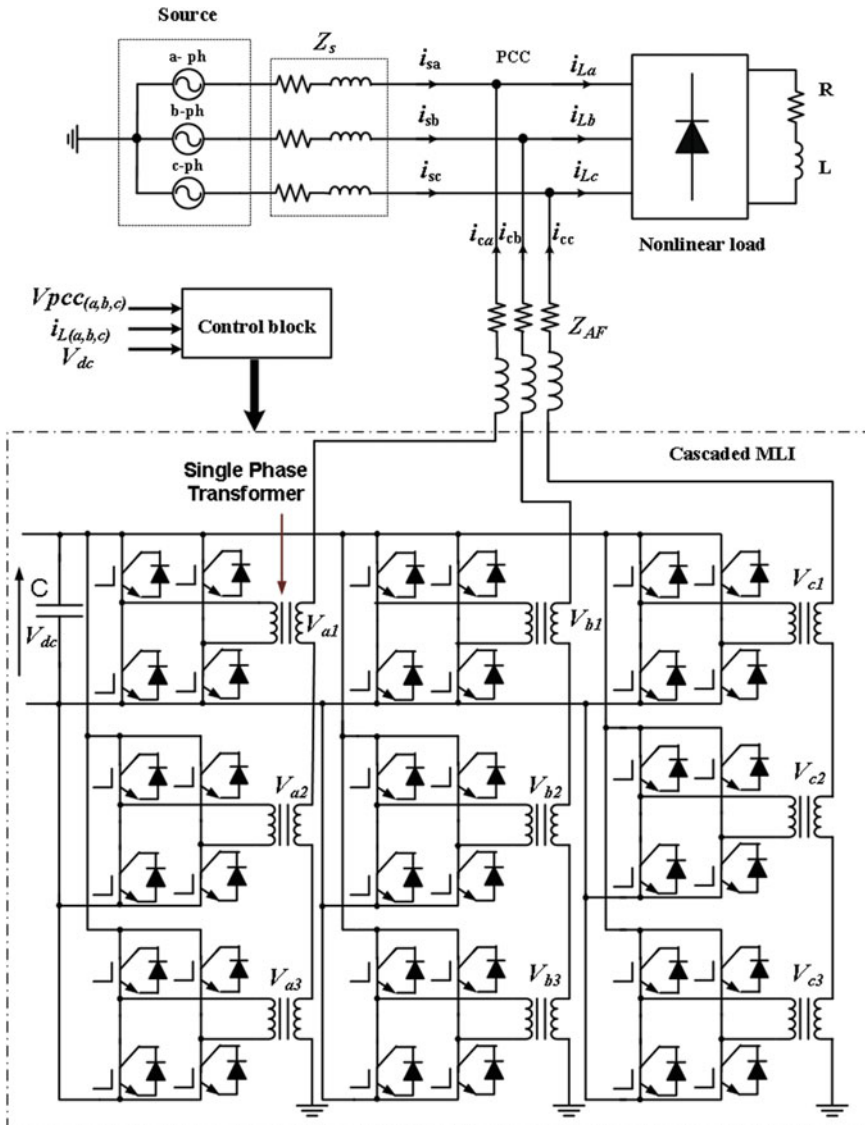


Fig. 1 Proposed SAF structure

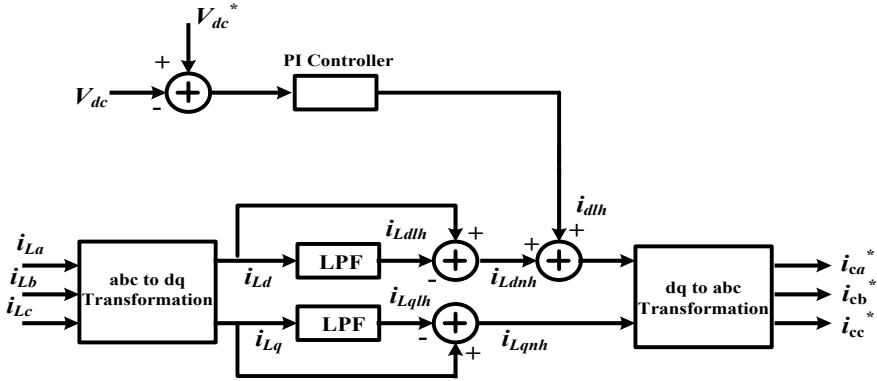


Fig. 2 Control technique for SAF

experimentation, the nonlinear load used is a diode bridge rectifier with RL load. The control algorithm employed in the proposed system has a vital role to track the harmonics present in source current, and then, the required compensating current is fed by the SAF which cancels the harmonics produced due to nonlinear load. The grid system is three-phase three-wire system at 50 Hz system frequency. The advantages associated in the proposed configuration are its improved harmonic performance with less loss. Another aspect of this configuration is its lesser control requirement due to single DC-link capacitor. The leakage reactance effect of cascaded transformers also helps improving system power quality.

3.1 Control Structure

The control block drawing presented in Fig. 2 demonstrates the extraction of compensation current. The harmonics created by the load is measured by sensing the current at each phase load terminal i_{La} , i_{Lb} and i_{Lc} . The respective load current at each phase is converted to d - q frame using abc-dq transformation through the transformation matrix.

The obtained d - q frame currents is to be passed through low-pass filter (LPF) to filter out the fundamental and oscillating component of the load current. The fundamental components of load current are i_{Ld1h} and i_{Lq1h} which is the output of the LPF. The harmonic components i_{Ldnh} and i_{Lqnh} are found by deducting i_{Ld1h} and i_{Lq1h} from i_{Ld} and i_{Lq} . The DC-link voltage V_{dc} is measured, and the sensed DC voltage is passed through a comparator and equated with the DC-link reference. The obtained signal after the comparator is passed through a PI controller to determine i_{d1h} , which decides the magnitude of compensation requirement. Then, these compensation currents in d - q frame are converted to abc frame using inverse transformation, and the obtained compensation currents are i_{ca}^* , i_{cb}^* , i_{cc}^* . The compensation current generated at each

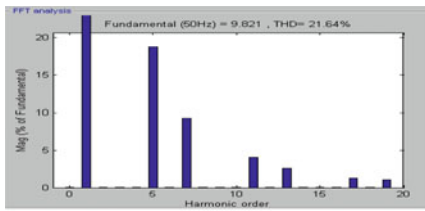
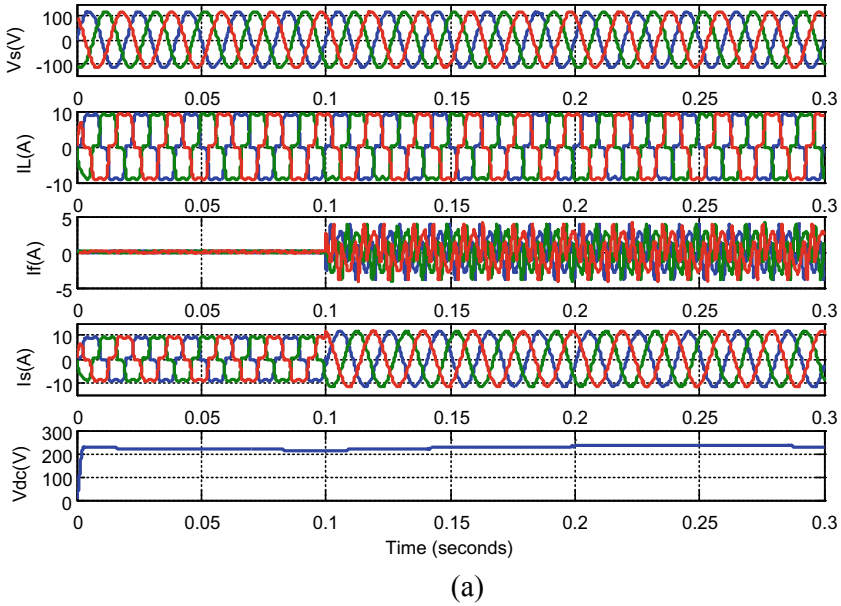
phase is passed through the filter inductor and fed at PCC to neutralize the harmonics generated due to nonlinear load.

4 Results and Discussion

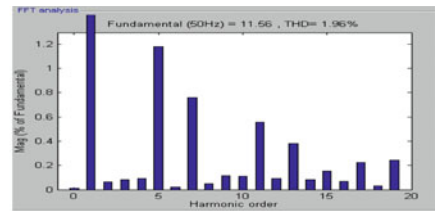
The presented cascaded MLI-based SAF is analyzed using MATLAB/SIMULINK software tool. The nonlinear load chosen for Simulation is balanced in nature, and the test is carried out considering the grid voltage to be balanced. For harmonic current extraction ($i_d - i_q$), control is adopted for all the considered modulation strategy. A comparison among the modulation technique is carried out using phase-shifted in-phase disposition (IPD) and SVM. The nonlinear load used in simulation is a three-phase bridge rectifier with $R = 20 \Omega$ and $L = 20\text{mH}$. The frequency of the presented model is retained at 50 Hz. Figure 3 shows the performance of the SAF using the proposed SVM modulation before and after the actuation of the SAF. In the above result, the SAF is ON at 0.1 s of the simulation period. In Fig. 3a V_s is the source voltage, i_L , i_s and i_f are the load current, source current and filter current, whereas V_{dc} indicates the voltage of DC side capacitor. The THD of the grid current with and without compensation is depicted in Fig. 3b, c.

A comparative evaluation of all the presented modulation technique with ($i_d - i_q$) control technique is carried out and is shown in Fig. 4. It is evident from the obtained results that the compensation capability of the proposed configuration is significant with ($i_d - i_q$) controller under balanced grid voltage state. After compensation, the source current THD falls to 2.3% for PSPWM, 2.55% for IPDPWM and 1.96% for SVPWM. So among the different modulation approaches, SVPWM has comparatively better harmonic compensation ability. A hardware archetype of the presented model is configured and investigated under ideal grid voltage conditions. Different current sensors are employed in the setup for sensing load and source current of each phase. Each phase voltage and the DC-link voltage are also sensed using voltage sensors. The sensed signals of the setup are taken to the Spartan FPGA, where it is first processed and converted to digital signal using ADC. Then, the obtained signal is processed as per the control logic for generating the compensating current. Then, the obtained compensation current from spartan-6 FPGA board is fed to the PCC after passing over filter impedance [7]. The rating of the DC capacitor [8–11] employed in the hardware setup is 2200 μF . The filter inductor is 2.5 mH in each phase, and 1:1 toroidal core transformer of 1 KVA rating is chosen for hardware implementation.

The grid phase voltage during hardware experimentation is kept at 120 V, and the DC-link reference is kept at 250 V. The act of the SAF is shown both in steady state and transient circumstances to show the effectiveness of the hardware prototype. The steady-state result of the proposed system is shown in Fig. 5, where the upper channel of the power analyzer shows the steady V_{dc} voltage and V_s voltage and I_s current with filter ON condition. The middle channel displays the filter current and the lower channel displays the load current.



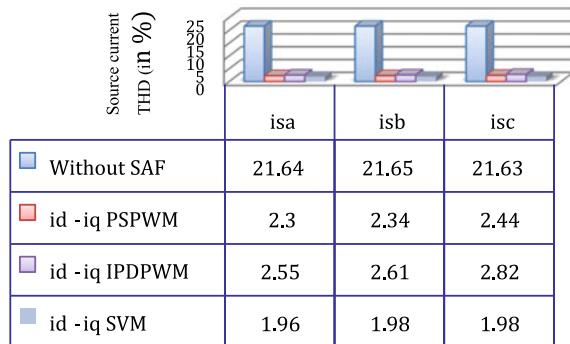
(b)



(c)

Fig. 3 a Proposed SAF performance using $i_d - i_q$ control and SVM modulation, FFT analysis of phase-a current. b Without filter, c with filter

Fig. 4 Comparative analysis of the source current THD with different modulation approach



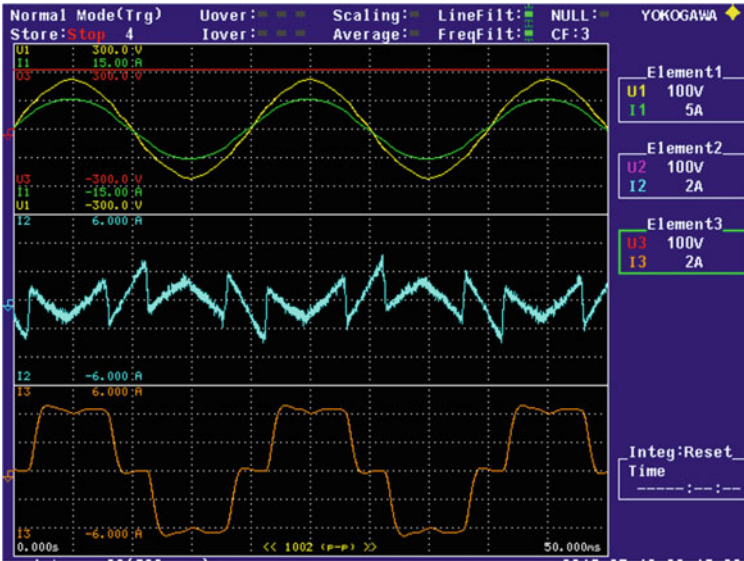


Fig. 5 Performance of the proposed SAF under steady-state conditions

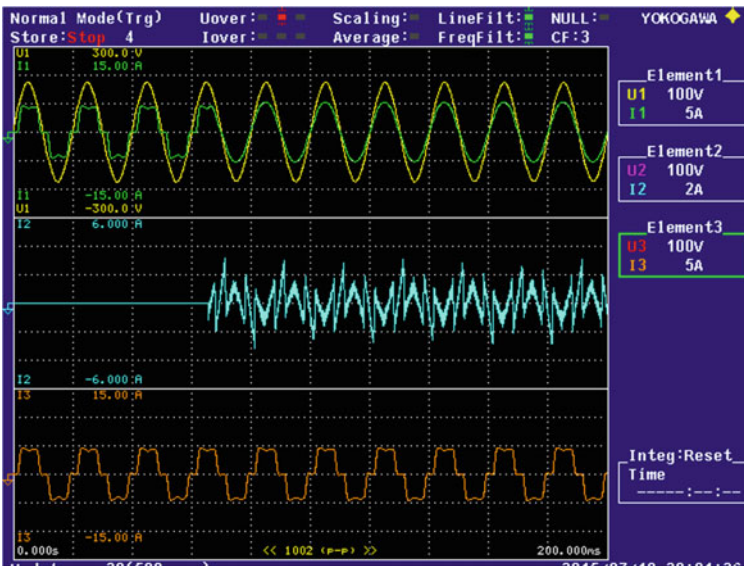


Fig. 6 Performance of the proposed SAF under transient conditions

Figure 6 depicts the transient performance of the hardware prototype where the response of source current is recorded before and after initiation of the filter. The

upper channel of the power analyzer displays the grid voltage and grid current, and the other two channels show compensation current and load current correspondingly.

5 Conclusion

A modified SVM technique based on generic algorithm is configured as per the SAF system structure. The proposed SVM technique is superior compared to the conventional SVM technique and carrier-based PWM due its faster response, less computational time and less memory requirement. The harmonic mitigation standard using the SVM approach is significant under ideal grid voltage. The switching state at any point can be easily determined from the SVM algorithm which enables effective real-time experimentation with lesser computational problem. The enactment of the SAF is investigated using $i_d - i_q$ control technique and a comparative evaluation is carried out by applying carrier-based PWM and SVM technique.

References

1. H. Akagi, Trends in active power line conditioners. *IEEE Trans. Power Electron.* **9**(3), 263–268 (1994)
2. Ó Lopez et al., Comparison of the FPGA implementation of two multilevel space vector PWM algorithms. *IEEE Trans. Industr. Electron.* **55**(4), 1537–1547 (2008)
3. I. Colak, E. Kabalci, R. Bayindir, Review of multilevel voltage source inverter topologies and control schemes. *Energy Convers. Manage.* **52**(2), 1114–1128 (2011)
4. H.K. Al-Hadidi, A.M. Gole, D.A. Jacobson, A Novel configuration for a cascade inverter-based dynamic voltage restorer with reduced energy storage requirements. *IEEE Trans. Power Deliv.* **23**(2), 881–888 (2008)
5. A.R. Dash, A.K. Panda, Experimental validation of a shunt active filter based on cascaded multilevel inverter with single excited DC source, in *Proceedings of IEEE International Conference on Power, Instrumentation, Control and Computing (PICC)*, pp. 1–6 (2018)
6. A.R. Dash, A.K. Panda, R. Patel et al., Design and implementation of a cascaded transformer coupled multilevel inverter-based shunt active filter under different grid voltage conditions. *Int. Trans. Electr. Energy Syst.* **29**(2), 2728 (2019)
7. A.K. Panda, Y. Suresh, Research on cascade multilevel inverter with single DC source by using three-phase transformers. *Int. J. Electr. Power Energy Syst.* (2012)
8. H. Wang, F. Blaabjerg, Reliability of capacitors for dc-link applications in power electronic converters—An overview. *IEEE Tran. Ind. Appl.* **50**(5), 3569–3578 (2014)
9. X.S. Pu, T.H. Nguyen, D.C. Lee, K.B. Lee, J.M. Kim, Fault diagnosis of DC-link capacitors in three-phase AC/DC PWM converters by online estimation of equivalent series resistance. *IEEE Trans. Ind. Electron.* **60**(9), 4118–4127 (2013)
10. G.A. de Almeida Carlos, C.B. Jacobina, J.P.R.A. Mélio, E.C.D. Santos, Shunt active power filter based on cascaded transformers coupled with three-phase bridge converters. *IEEE Tran. Ind. Appl.* **53**(5), 4673–4681 (2017)
11. Ó. López, J. Álvarez, J. Doval-Gandoy, F.D. Freijedo, Multilevel multiphase space vector PWM algorithm with switching state redundancy. *IEEE Trans. Ind. Electron.* **56**(3), 792–804 (2009)

Synthesis of Reconfigurable Unequally Spaced Linear Arrays Through Time Modulation



S. Patra , S. K. Mandal , G. K. Mahanti, and N. Pathak

1 Introduction

Shanks in 1959 [1], first introduced the ‘time-modulation’ method to synthesize power pattern in linear arrays by controlling ON–OFF sequence of the radiating elements using high-speed RF switches. In this method, ‘time’ is additionally used to control the array pattern and the corresponding antenna array is termed as ‘Four dimensional (4D)’ antenna array. Later, this 4D antenna array is known as time-modulated array (TMA). In last two decades, the time-modulation principle is proved to be effective to provide low/ultra-low sidelobe power pattern with uniform or comparatively lower dynamic range ratio (DRR) of time-independent excitation amplitude for different communication system [2–4]. The technique is employed in many antenna array synthesis problems to realize different power patterns. To mention, few of them are synthesis of flat-top patterns [2], sum and difference pattern in linear arrays [3], and rectangular arrays [4]. Since, the power pattern in TMAs is controlled by set of switch on-time sequence of the radiating elements. Further, in

S. Patra (✉)

Department of Electronics and Communication Engineering, SMIT-TIG, Guptipara, Hooghly, West Bengal, India

e-mail: somnath.tech@gmail.com

S. Patra · S. K. Mandal · G. K. Mahanti

Department of Electronics and Communication Engineering, National Institute of Technology Durgapur, Durgapur, West Bengal, India

e-mail: skmandal2006@gmail.com

G. K. Mahanti

e-mail: gautammahanti@yahoo.com

N. Pathak

Department of Electronics and Communication Engineering, Dr. B.C. Roy Engineering College, Durgapur, West Bengal, India

© Springer Nature Singapore Pte Ltd. 2021

K. S. Sherpa et al. (eds.), *Advances in Smart Grid and Renewable Energy*,

Lecture Notes in Electrical Engineering 691,

https://doi.org/10.1007/978-981-15-7511-2_42

contrast to the traditional method, the switching sequence can be accurately maintained instantly at a fast rate with the help of software. As a result, the strategy is useful in designing reconfigurable antenna array applications. In this paper, the effectiveness of time-modulation strategy is introduced in synthesizing sum and difference pattern in unequally spaced linear arrays for the first time. For a uniformly excited antenna array, two patterns with low SLLs are obtained only by changing the switching on-time sequence of the radiating elements while the element position for the patterns remain unaltered. Differential evolution (DE) [5]-based stochastic search technique is employed to obtain the optimum set of common element position for the two target patterns and different set of switching sequences for the respective patterns.

2 Theoretical Analysis

Let, an unequally spaced linear array made with $2N$ isotropic elements is aligned along the z -axis with ‘ N ’ being a natural number representing half of the array elements. Let, each antenna radiator is fed through RF switches that are controlled by periodic signal (voltage/current) pulses of frequency $f = 1/T$ with T being the time period of the pulses. If $t_{i,n}$ and $\tau_n \in (0, T) \forall n \in [1, N]$ be the on-time instants (OTIs) and on-time durations (OTDs) of the switches, the corresponding expression for the array factor at p th harmonic with uniform excitation of the array can be obtained from [3] and is given as

$$AF_p(\theta, t) = e^{j(\omega_0 t \pm p\omega t)} \sum_{\substack{n=-N \\ n \neq 0}}^N \zeta_n \left[\frac{\sin(p\pi \zeta_n)}{p\pi \zeta_n} \right] e^{jp\pi(2\partial_n + \zeta_n)} e^{j\beta z_n \cos\theta} \quad (1)$$

where, ω_0 is the operating carrier frequency; $p = 0, \pm 1, \pm 2, \dots$ represent the harmonic indices of the angular modulation frequency $\omega = 2\pi f = 2\pi/T$; $\partial_n = t_{i,n}/T$ and $\zeta_n = \tau_n/T$; $\forall n \in (1, N)$ are, respectively, the normalized ‘ON’-time instants (OTIs) and ‘ON’-time durations (OTDs) of the RF switch connected to the n th element; β is the propagation constant, z_n is the n th element position and θ is the elevation angle of the conventional spherical coordinate system. When $p = 0$, (1) refers to the main beam pattern at center frequency as

$$AF_p(\theta, t)|_{p=0} = e^{j\omega_0 t} \sum_{\substack{n=-N \\ n \neq 0}}^N \zeta_n e^{j\beta z_n \cos\theta} \quad (2)$$

From (2), the sum pattern is obtained with $\zeta_n = \zeta_{-n}$ and $z_n = z_{-n}$, whereas the difference pattern is obtained with $\zeta_n = -\zeta_{-n}$ and with same z_n . The proposed cost function for synthesizing the targeted patterns is expressed as,

$$\psi = \sum_{b=S,D} \left\{ \sum_{a=1}^3 W_a^b \delta_a^b H_a(\delta_a^b) \right\} \tag{3}$$

where $b = S, D$ represent the specified beam as sum and difference patterns. δ_a^b with $a = 1, 2,$ and 3 represent the difference between targeted and calculated values of proper design specifications of the respective beam and is given as $\delta_1^b = |SLL_d^b - SLL_{\max}^b|$; $\delta_2^b = |SBL_d^b - SBL_{\max}^b|$ and $\delta_3^b = |FNBW_d^b - FNBW^b|$. Where SLL_{\max} and SBL_{\max} represent the maximum values of sidelobe and sideband level; $FNBW$ is the obtained beam-width between first null of the main beam; SLL_d, SBL_d and $FNBW_d$ are the respective targeted values of the design parameters; W_a is the weighting factors of the related design parameters and H_a is Heaviside step function.

3 Numerical Results

To demonstrate the usefulness of the work, a 20 element linear array is considered. It is further assumed that the array is placed symmetrical about the origin of the coordinate axis. The pulse shifting strategy [6] for time modulation is used to synthesize the desired patterns. In order to find out the optimum set of possible solution, DE is applied to minimize the cost function as defined in (3). Thus, individual element position, OTD, and OTI are chosen as the optimization parameter vectors for the DE. As mentioned previously, the element position is taken as the common optimization parameter vector for both the patterns while different sets of OTIs and OTDs are used to realize the desired sum and difference patterns. The DE parameter values are chosen as follows: population size 90, crossover rate (CR) = 0.85, and mutation constant (F) = 0.5. Objective is to find out same element positions for both the patterns, but different set of OTD and OTI for the respective sum and difference pattern. The search spaces for the optimization parameter vectors are taken as follows: element positions (0.5, 1), OTD (0.1, 1), and OTI = {0, (1-OTD)}. For both the patterns, the desired values of SLL, SBL and FNBW are set as -25 dB, -25 dB, and 20°, respectively. DE runs for 700 iterations and the best possible result as obtained are shown in Fig. 1 and 2. For sum pattern, the obtained values of SLL, SBL, and FNBW are -24.8 dB, -23.7 dB, and 18° and for the difference pattern, these are observed as -24.7 dB, -19 dB, and 15.7°, respectively. The possible solutions for the common element position and different set of on-time duration and on-time instants are presented in Table 1. As compared to [7], approximately 5 dB improvement in SLL is realized. In [8], almost the same pattern is obtained in conventional antenna arrays by using static excitation amplitude with dynamic range ratio of 5. However, in the proposed method, two power patterns are obtained with uniform static excitation amplitudes. Therefore, the feed network becomes simpler with electronically controlled switching system.

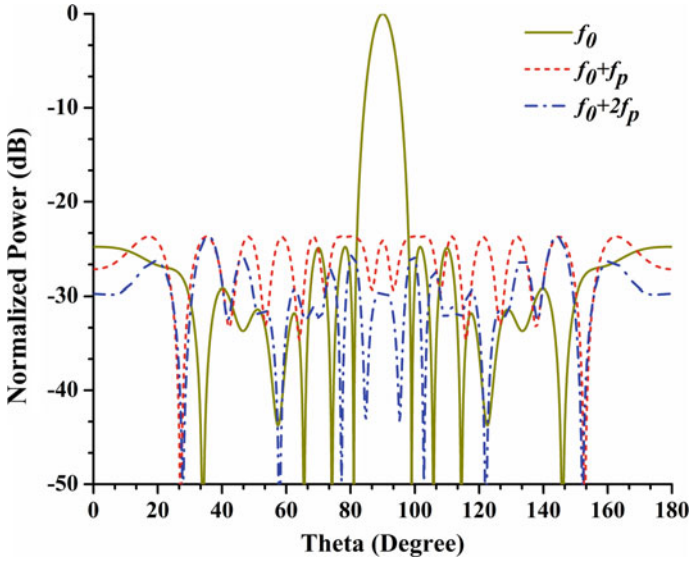


Fig. 1 Normalized sum pattern for 20 element linear array

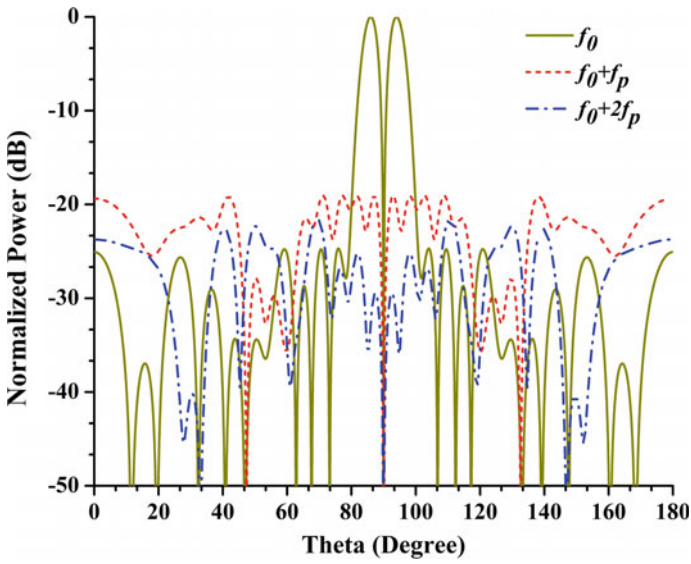


Fig. 2 Normalized difference pattern for 20 element linear array

Table 1 Element-wise optimization parameter values obtained using DEA

Element Number, $\pm N$	Normalized element position, $\pm Z_n$	Normalized sum pattern		Normalized difference pattern	
		OTDs	OTIs	OTDs	OTIs
± 1	± 5.70	0.10	0.000022	0.37	0.62
± 2	± 4.92	0.10	0.89	0.65	0.33
± 3	± 4.19	0.21	0.62	0.66	0.22
± 4	± 3.62	0.39	0.60	0.69	0.00012
± 5	± 3.07	0.72	0.04	1	0
± 6	± 2.46	0.87	0.12	0.99	0.000054
± 7	± 1.88	0.99	0.00027	1	0
± 8	± 1.25	0.99	0.0016	0.88	0.10
± 9	± 0.75	0.99	0.000034	0.26	0
± 10	± 0.25	0.99	0.000023	0.21	0.59

4 Conclusions

In conventional antenna arrays, complex feed network for time-independent excitation amplitude and phase is required to realize low SLL reconfigurable power patterns. In this work, along with the additional degree of freedom, ‘time’, the element position is also used to synthesize the targeted sum and difference pattern in unequally spaced time-modulated linear arrays with uniform excitation amplitude and phase. The sum and difference patterns are obtained with relatively low sidelobe level as compared with the conventional array synthesis method. Moreover, the primary advantage of the proposed technique is the possibilities of applying simple RF switches with differ in on-time sequence in the feed network to reduce the complication in the array feed network. The synthesized power pattern has practical application for direction finding in radar technology.

References

1. H.E. Shanks, R.W. Bickmore, Four-dimentional electromagnetic radiators. . *Canad J. Phys.* **37**, 263–275 (1959)
2. S. Yang, Y.B. Gan, P.K. Tan, A new technique for power pattern synthesis in time modulated linear arrays. *IEEE Antennas Wirel. Propagat. Lett.* **2**(1), 285–287 (2003)
3. J. Fondevila, J.C. Brégains, F. Ares, E. Moreno, Application of time modulation in the synthesis of sum and difference patterns by using linear arrays. *Microw. Opt. Technol. Lett.* **48**(5), 829–832 (2006)
4. R.S. Elliott, Synthesis of rectangular planar arrays for sum patterns with ring side lobes of arbitrary topography. *Radio Sci.* **12**(5), 653–657 (1977)
5. R. Storn, K. Price, Differential evolution—a simple and efficient adaptive scheme for global optimization over continuous spaces. *J. Global Optim.* **11**, 341–359 (1995)

6. L. Poli, P. Rocca, L. Manica, A. Massa, Pattern synthesis in time-modulated linear arrays through pulse shifting. *IET Microwaves Antennas Propag.* **4**(9), 1157–1164 (2010)
7. S. Yang, Y. Chen, Z. Nie, Multiple patterns from time-modulated linear antenna arrays. *Electromagnetics* **28**, 562–571 (2008)
8. J.R. Mohammed, Synthesizing sum and difference patterns with low complexity feeding network by sharing element excitations. *Int. J. Antennas Propagat.* **2017**, 1–7. Article ID 2563901 (2017)

Development of Microcontroller-Based Economic Real-Time Temperature Measurement System



G. Raja Kullyappa, C. Mani Kumar, P. Srilakshmi, and Shahid Ali

1 Introduction

Temperature monitoring is very essential in day-to-day life. Regular monitoring of temperature is helpful in weather forecasting. Human body temperature is a predominant parameter in healthcare. The need of a cost-effective temperature monitoring system is inevitable. The proposed system is an economical system with good accuracy. The usage of microcontroller has helped in a great deal in making it a faster system. The temperature sensor is interfaced with microcontroller by using an analog-to-digital convertor. The measurement of temperature with respect to time is worthwhile. The real-time clock is interfaced to microcontroller. The I2C protocol is used for interfacing the RTC. The software was developed using Keil Compiler. The simulation was performed using Proteus software to make sure that the designed hardware and software are working well in tandem.

G. Raja Kullyappa · C. Mani Kumar (✉) · P. Srilakshmi · S. Ali
Department of Electronics and Physics GIS, Gandhi Institute of Technology and Management
(Deemed to Be University), Visakhapatnam, Andhra Pradesh, India
e-mail: mani.k.ele@gmail.com

G. Raja Kullyappa
e-mail: rajaseworld@gmail.com

P. Srilakshmi
e-mail: p.srilakshmi.ele@gmail.com

S. Ali
e-mail: ckp786shahid@gmail.com

2 Hardware

The major hardware blocks employed in the implementation of the system are as depicted in Fig. 1. The AT89C51 is a single-chip microcontroller, and it has 4 K bytes of flash memory [1]. The memory has the endurance of one thousand write/read cycles. The 128 bytes of inbuilt RAM enriches its speed. The availability of 32 programmable I/O pins attracts the embedded engineers to the microcontroller as they can connect more number of devices. The controller supports low-power idle mode and power-down mode for making it energy efficient.

The temperature sensor LM35 is used to detect the temperature. The sensor is directly calibrated in centigrade. The sensor has linearity in the output with respect to the temperature. It produces an output of 10 mV for every 1 °C of temperature. Its self-heating is as low as 0.1 °C. This is a very low-cost sensor because of the wafer-level trimming. The range of the temperature sensor LM35 is -55 to 155 °C [2]. It can be configured in different modes such as basic centigrade mode, full-range mode with dual supply, and full-range mode with single supply. In the designed circuit, the basic centigrade mode is used because of simplicity and the ability to work with a single power supply. This is interfaced with the microcontroller with the help of the ADC 0808. The IC0808 is an 8 bit analog-to-digital convertor with total adjustable error of $\pm\frac{1}{2}$ LSB. It requires only +5 V of single power supply which can also be used as the reference voltage of the ADC. It has a very low power dissipation of 15 mW, and the speed of conversion is very high as it takes only 100 μ s for each conversion. It has an eight-channel multiplexer with address logic which ensures that only one ADC is enough to connect as many as eight different analog inputs [3].

The DS1307 real-time clock is interfaced with microcontroller using I2C protocol. This is a full BCD clock/calendar [4]. The clock can be used in 24 h mode as well as 12 h mode. The calendar is very much helpful with adjustability for the months less than 31 days and leap year. It requires only two pins of the microcontroller. The pins are named as Serial Data (SDA) pin and Serial Clock (SCL) pin used for transfer of data, address, and clock signals. These two pins are connected to the +VCC using pull-up resistors. It requires an external clock of 32.768 kHz and is connected by using simple quartz crystal. It can also be connected with an external backup battery

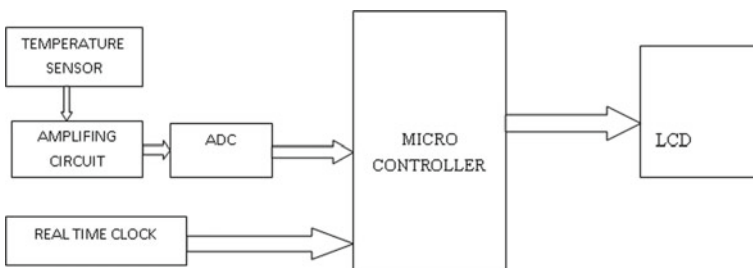


Fig. 1 Block diagram

to keep the clock running even if the power is switched off. It can also generate square wave output of different frequencies. The frequency of 32 kHz is connected to ADC 0808 as it requires an input clock.

A 20×4 LCD is used for displaying the output of the system. This display can be configured in both 8 bit mode as well as 4 bit mode. In this system, the 8 bit mode is used as there are many pins available in the microcontroller, and this mode is relatively simple when compared to the 4 bit mode. The display consists of 16 pins, 8 of them are data pins $D0-D7$. It has three control pins RS, Read/Write, and Enable [5]. It also consists of anode and cathode pins to light the LED to make it visible even in the dark. Apart from VCC and ground pins, it has contrast pin which can be connected to a potentiometer to adjust the contrast of the display.

3 Simulation and Hardware Development

The circuit is simulated by using Proteus simulation software. The Proteus simulation software supports simulation of components ranging from basic components like resistor, capacitors to the advanced microprocessors. It gives us a provision for constructing the circuit and to foresee the result. The simulation is performed for measuring the temperature values below and above 0°C using full-range single supply mode. The I2C signals are observed with the help of the I2C debugger of the Proteus simulation software. The construction of the circuit begins from the selection of microcontroller AT89C51 employed in the designed schematic. This IC belongs to 8051 family of microcontrollers.

The temperature sensor LM35 is selected and is interfaced with microcontroller using an interfacing circuitry consisting an amplifier, an inverter, a comparator, and an ADC. The amplifier amplifies the voltage received from the temperature sensor, and the comparator compares whether the temperature is above or below 0°C , whereas the comparator inverts the voltage values of the amplifier. The outputs of inverter circuit and the amplifier circuit are given to different channels of 8 bit ADC. The output of comparator is used to select the channel based on the value of temperature. If the value is positive, the comparator produces an output a logic high output and selects channel 1 where the amplifier output is connected, otherwise channel 2 where the output of inverting amplifier is connected. The output of the comparator is given to a NOT logic gate which generates the sign bit for the temperature records which is connected to an IO pin of the AT89C51. Then, the real-time clock is interfaced with the microcontroller. Finally, the 16×2 LCD is interfaced to microcontroller to display the output. The simulated output can be observed in Fig. 2.

The hardware implementation is further simplified as the system is tested in the Visakhapatnam where there is hardly any possibility of the temperatures ranging below 2°C . The temperature sensor is interfaced in basic centigrade mode using an amplifier and an ADC. The amplifier integrated circuit is used to amplify the sensor input before it is given to the ADC as the sensor gives only 10 mV for centigrade, but the ADC has the resolution 19.5 mV with respect to the reference voltage of

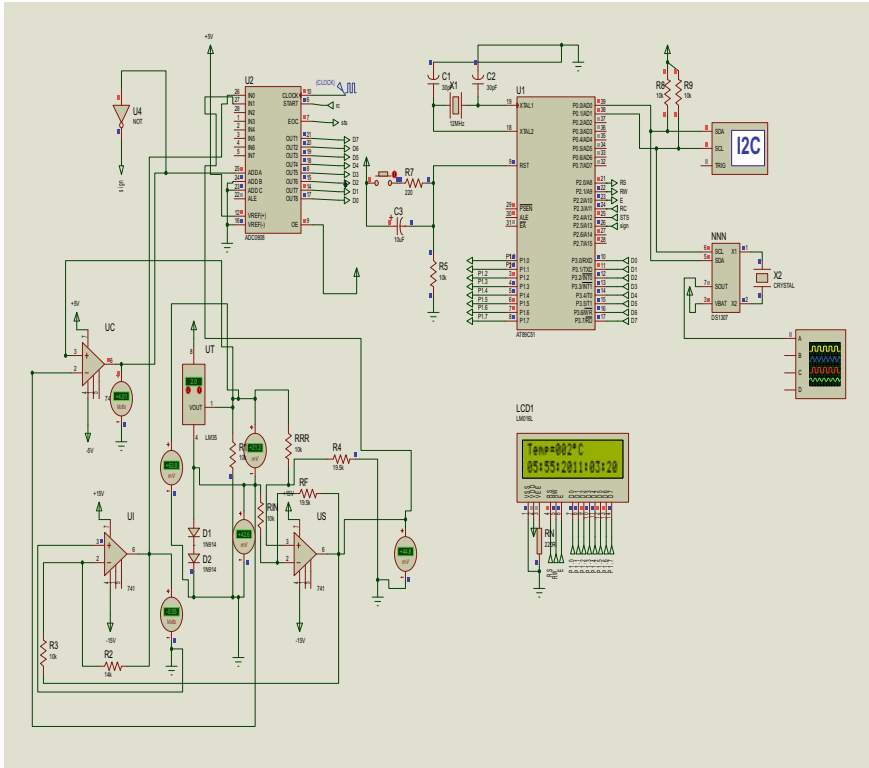


Fig. 2 Simulation of the system using Proteus

5 V. The amplifying circuit is constructed by using an op-amp 741 in non-inverting configuration. The RTC IC is interfaced with the microcontroller using a couple of 4.7 kΩ one-watt pull-up resistors. A 20 × 4 LCD is interfaced to display the results such as day, date, and time and the temperature as depicted in Fig. 3.

4 Software Implementation

The Keil Compiler is used for writing the program to the designed circuit. The program is written in embedded C. There are different functional blocks of the program for doing different tasks such as reading the clock and temperature and displaying them in the LCD. The microcontroller reads the temperature through ADC. The real-time clock is implemented using I2C using the functions such as i2cstart, i2cread, i2cwrite, and i2cstop. The RTC is used in slave transmit and slave receive modes. Both ACK and NACK were used during the transmission of data between the microcontroller and the RTC. In the write operation, there are some

Fig. 3 Real-time temperature measurement system prototype



steps involved. First the start condition is initiated from the microcontroller, then the slave (RTC) address is written on SDL line. Then, the timekeeper addresses were written. Further, the data such as seconds, minutes, hours, date, month, and year was sent to appropriate registers of RTC. Finally, the stop bit is sent. The data is read by using read operation. After completion of the program, the embedded C program must be converted into a .hex file. The .hex file is dumped in to the microcontroller using Xeltek programmer. The flow of software implementation is represented in Fig. 4.

5 Results and Discussion

The microcontroller-based real-time temperature measurement system is developed using I2C protocol. The system working is compared against the values of Andhra Pradesh Pollution Control board (APPCB), Visakhapatnam. The prototype is tested under different areas such as a highly populated area, a port area, and a heavy traffic area in Visakhapatnam city. The records are plotted as shown in Figs. 5, 6, and 7, respectively.

The results were in good agreement with the standard records provided by the APPCB. The system works continuously while the power is switched on. If the power

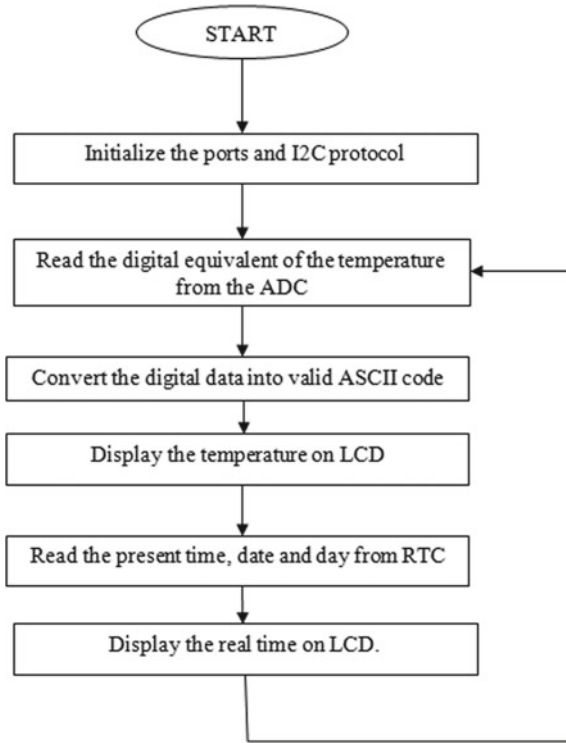


Fig. 4 Flowchart of the designed system

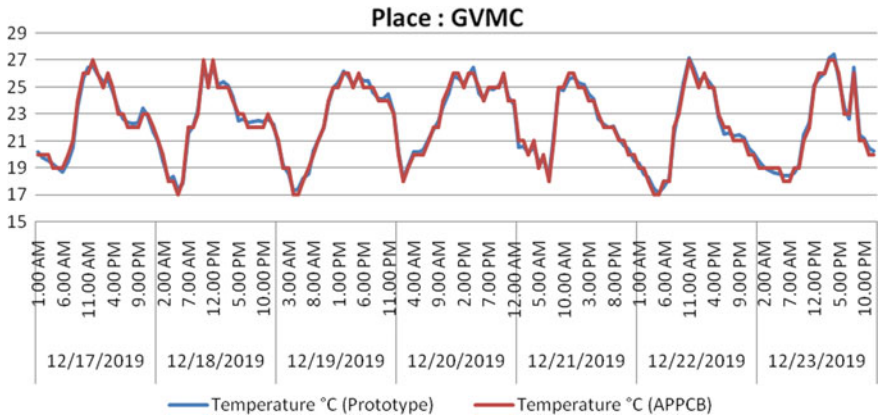


Fig. 5 Values recorded at GVMC

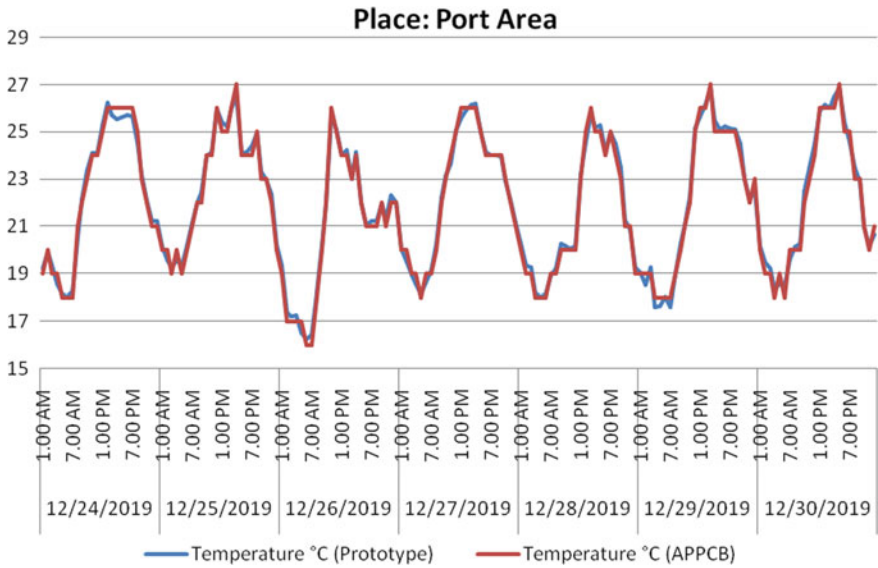


Fig. 6 Values recorded at port area

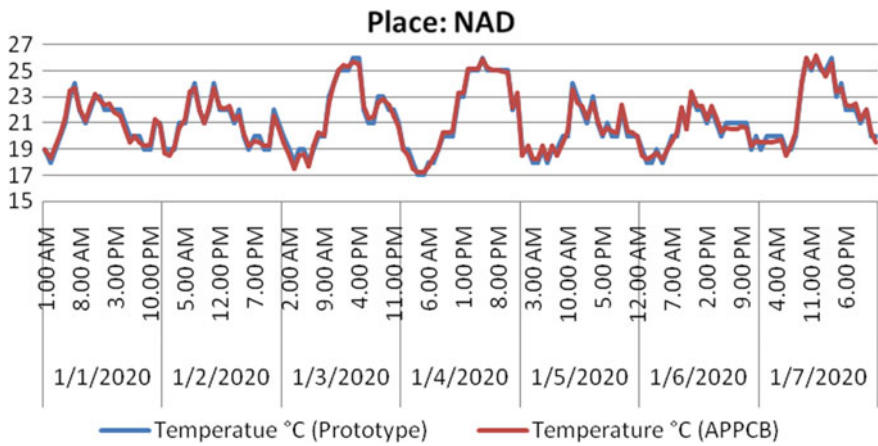


Fig. 7 Values recorded at NAD

is switched off, the real-time clock do not stop as it is connected to an external backup battery. This system is a low-cost and reliable system with diligent performance. The system is useful in domestic and industrial applications.

Reference

1. C.-F. Wen-YuanTsai, T.-L. Liao, New implementation of high-precision and instant-response air thermometer by ultrasonic sensors. *Sens. Actuators A Phy.* **5**(1), 88–94 (2005)
2. C. Liu, W. Ren, B. Zhang, C. Lv, The application of soil temperature measurement by LM35 temperature sensors, in *Proceedings of 2011 International Conference on Electronic & Mechanical Engineering and Information Technology*, pp. 1825–1828. Harbin, Heilongjiang, China (2011)
3. J.T. Devaraju, P.H. Suresha, Ramani, M.C. Radhakrishna, Development of microcontroller based thermogravimetric analyzer. *Measurement* **44**, 2096–2103 (2011)
4. C. Mani Kumar, M. Vishnu Chittan, D. Sailaja, Embedded based ethernet measurement system for the for the studies of studies of di-electric electric electric constant of binary liquids binary liquids binary liquids. *IJREAT Int. J. Res. Eng. Adv. Technol.* **2**(6), 7–15 (2015)
5. P. SriLakshmi, N. Lakshmana Das, C. Mani Kumar, Low-cost wireless instrumentation for monitoring humidity, wind speed, and direction. *J. Instrum. Sci. Technol.* **45**(5), 479–485 (2017)

Temperature Impact on SiC Waveguide for Investigation of Sensing



C. S. Mishra, K. P. Swain, M. R. Nayak, and G. Palai

1 Introduction

Silicon carbide (SiC) is a very popular material in different applications, for example, the band gap [1, 2] of 6H-SiC is around 3 eV, which is around multiple times more prominent in comparison with silicon band gap. Furthermore, in this approach, silicon carbide gadgets can encourage higher breakdown field, 3–5 MVcm⁻¹. Its high softening temperature (around 3100 K) and also incredibly low inherent transporter fixation permit it to work at raised temperatures. Sensors are the utmost elementary components in monitoring the activity of most building framework precisely. They perform a significant job in the advancement of people to come innovation (e.g., ignition and gas turbine frameworks for power age), information procurement and governing frameworks. The performances of sensor in high temperature are often questionable, off base and exorbitant. Sensor disappointment can prompt costly framework upkeep and fix costs. Customary sensors dependent on silicon are constrained to working temperatures underneath 3500 °C, because of their thin band hole and poor warm stability. SiC is a hard and stable compound which can continue its mechanical properties above 10,000 °C. Size of hardness comes behind precious stone. Individuals appeared enthusiasm for SiC to supplant precious stone in cutting and grating modern devices. The first electroluminescence has been accounted for in 1907 when SiC light-emitting diode was made. This revelation prompted consideration toward electronic and electrical properties of SiC. Though, Si and C inside

C. S. Mishra · K. P. Swain · G. Palai (✉)

Department of Electronics and Communication Engineering, GITA, Bhubaneswar, Odisha, India

e-mail: gpalai28@gmail.com

C. S. Mishra

Biju Patnaik University and Technology Odhisha, Rourkela, India

M. R. Nayak

Department of EE, Biju Patnaik University of Technology, Rourkela, Odisha, India

© Springer Nature Singapore Pte Ltd. 2021

K. S. Sherpa et al. (eds.), *Advances in Smart Grid and Renewable Energy*,

Lecture Notes in Electrical Engineering 691,

https://doi.org/10.1007/978-981-15-7511-2_44

the SiC precious stone cross section have diverse plan, each SiC poly-type shows a particular type of optical and electrical properties. An examination of the absolute most significant semiconductor electrical properties of the 3C, 4H, and 6H silicon carbide poly-types with different semiconductors are prearranged. The natural bearer centralization of SiC is low, and band hole is very more extensive in correlation with Silicon. These properties permit SiC to keep up semiconductor conduct what is more, gadget execution at a lot higher temperatures than silicon. Regularly Si band semiconductor gadgets work in the temperature extend where inherent bearers are irrelevant and conductivity is constrained by dopant-polluting influences which are presented purposefully. Keeping the significance of SiC for the diverse application, this original reproduction is considered with SiC waveguide at frequency 1550 nm for assessment of temperature. The comparative sort of work is acted in the reference [3–7].

2 Structure Analysis of SiC Waveguide

Here, we analyze temperature sensor utilizing SiC waveguide. SiC air grating structure is appeared in Fig. 1.

Figure 1 shows SiC grating structure having thickness 490 nm, with the end goal that SiC is set in the first, third, fifth, and seventh isolated via air at the second, fourth, and sixth layer. The width of SiC and air are in use as 70 nm each one. The frequency of 1550 nm light encroaches SiC grating structure, at that point transmission and reflection happened between SiC and air face. T_r is transmittance from such constitution which is created with the assistance of PWE procedure. Accounting reflection and absorption loss, the transmitted energy is calculated by concerning transmittance and absorption coefficient utilizing reference [8].

The mathematical formula will be

$$I_T = I_o T_{ra} e^{-\beta(t_1+t_2+t_3+t_4+t_5+t_6+t_7)} \tag{1}$$

where

I_T = The impinged energy relating frequency 1550 nm.

T_{ra} = Transmittance.

β = Absorption coefficient.

$t_1, t_2, t_3, t_4, t_5, t_6, t_7$ are the thickness of different structure.

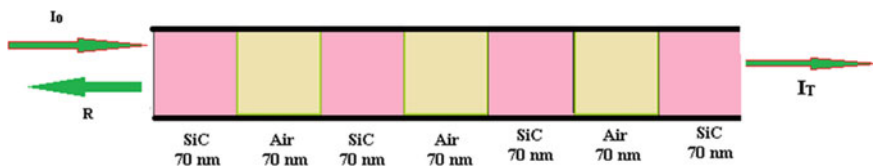


Fig. 1 SiC air grating structure

3 Result and Discussion

Considering the above grating structure, the light having frequency 1550 nm is arranged to fall on seven-layer waveguide configurations. Then, it is revealed that some amount of light is transmitted through the structure and rest amount of light is absorbed by the structure. The transmitted light energy which is passed through SiC grating structure can be calculated by Eq. 1 by considering the value represented in Table 1 (the values of refractive index at 1550 nm are considered from reference [9]). It is seen that transmitted energy relies on absorption coefficient, the width of layers, and transmittance.

The PWE simulations are performed for calculation of transmittance by considering the various temperature values of SiC. The simulation outcomes for 100 °C is represented in Fig. 2 where the value of transmittance is found 0.7051. Likewise, the simulations are made for other temperature (200, 300, 400, 500, 600, 700) which are not indicated here.

In Fig. 2, it is seen that frequency (1550 nm) is appeared in *x*-axis, whereas transmittance (Arbi unit) is appeared in vertical axis. From Fig. 1b, the transmittance is found 0.7051 for the temperature of 100 °C at 1550 nm. Likewise, transmittance for other temperatures are simulated. It is seen that transmittance decrements from 0.7051 (Arbi) to 0.674 with respect to the increasing values of temperature from 200 to 700 °C.

Table 1 Information of refractive indicis of SiC with respect to the temperature

Temperature (<i>T</i>) in C	100	200	300	400	500	600	700
Refractive index	2.42	2.43	2.44	2.45	2.455	2.46	2.47

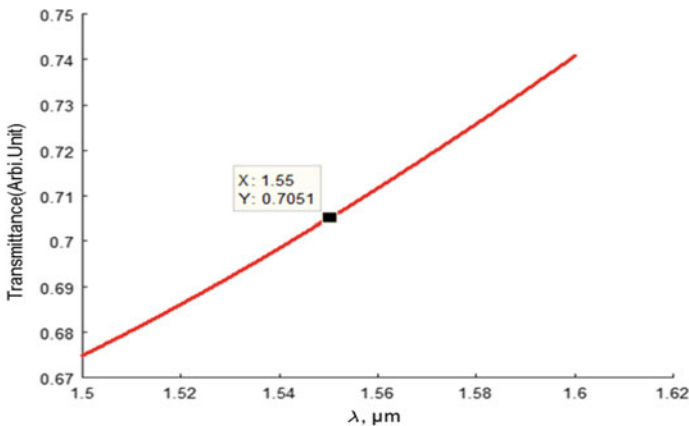


Fig. 2 Deviation of reflectance as for temperature at 100 °C

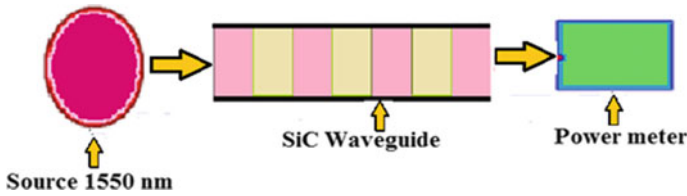


Fig. 3 Proposed configuration to ascertain transmitted energy all through SiC waveguide

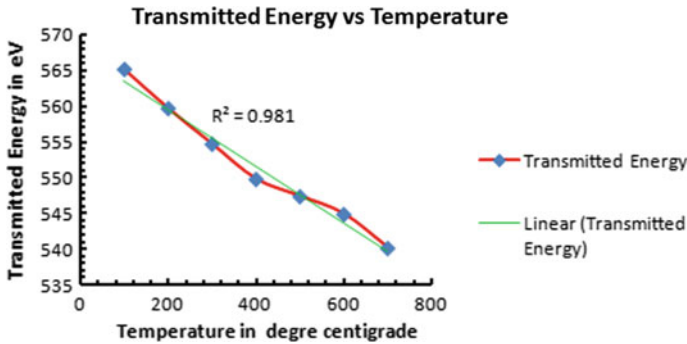


Fig. 4 Deviation of transmitted energy with temperature SiC waveguide

Figure 3 represents an experimental proposal for the above discussion where a light source of 1550 nm is taken as input source which is made to fall on the silicon grating waveguide. As discussed earlier, the power of the transmitted light is caught by a power meter for different temperature variations of temperature.

Fig. 4 represents the graph between the transmitted energy (eV) (in y-axis) and the temperature (in x-axis). It is seen that transmitted energy diminishes directly from 565.1604 to 540.2328 eV concerning the temperature. The linear pattern line $R^2 (=0.981)$ indicates the precise estimation of temperature which prompts the great result.

4 Conclusion

The temperature sensor using SiC waveguide is examined lucidly using the input source of light wavelength 1550 nm. The transmitted energy is computed using PWE simulation by including both transmittance and absorption. It is revealed that light energy which is transmitted through the waveguide is linearly ($R^2 = 0.981$) varied with the temperature of silicon carbide.

References

1. A. Sukhoivanov, V. Guryev, *Physics and Practical Modeling: Photonic Crystals*, 1st edn. (Springer, Heidelberg, 2009)
2. F. Poli, A. Cucinotta, S. Selleri, *Photonic Crystal Fibers: Properties and Applications* (Springer, Netherlands, 2007)
3. S.K. Sahu, S. Sahu, C.S. Mishra, G. Palai, Analysis of reflected frequency band of meta material grating at THz frequency: a future application of filter. *Optik* **127**, 4547–4550 (2016)
4. C.S. Mishra, G. Palai, Temperature and pressure effect on GaN waveguide at 428.71 terahertz frequency for sensing application. *Optik* **126**, 4685–4687 (2015)
5. C.S. Mishra, K.K. Sethi, G. Palai, Bandgap analysis of quasi bandgap semiconductor using FDTD technique. *J. Microelectr. Solid State Dev.* **2**, 1–4 (2015)
6. C.S. Mishra, G. Palai, Manipulating light with porous silicon for investigation of porosity using finite difference time domain method. *Optik* **127**, 1195–1197 (2016)
7. C.S. Mishra, G. Palai, Simulation studies for reflected light of polymer waveguide for realization of temperature. *Optik* **126**, 3656–3658 (2015)
8. M. Vijaya, G. Rangarajan, *Materials Science* (Tata McGraw-Hill Education, New Delhi, 2003)
9. S. Dakshinamurthy, N.R. Quick, A. Kar, Temperature-dependent optical properties of silicon carbide for wireless temperature sensors. *J. Phys. D: Appl. Phys.* **40**, 353–360 (2007)

Practical Implementation of Flexible Antenna for Hiper LAN Application



Janabeg Loni, Jaideep Dewangan, Vinod Kumar Singh,
and Anand Kumar Tripathi

1 Introduction

Antenna is such type of a transducer device which transmits or receives electromagnetic waves. It is used for communication purpose. Also there are variety of medium in communication that it can be wired or wireless. Now we concern most preferably on which substrate antenna is designed. So today we are using textile material for this that is flexible but some problems are also facing with it that it behaves a resistive component and provide losses in transmission between body and antenna [1–3]. But in many cases, it provides great transmission between antennas. Also wearable textile antenna has many applications especially in body related communications in which antenna can be fitted with clothes or body etc. These type of antennas provide enhanced form of communication and improved living quality of human life [4–10].

There will be three main types of wearable antenna which can be put under these three categories. First, these type of systems can be worn directly on the body; secondly the type of systems which can be directly integrated with clothing and

J. Loni · A. K. Tripathi

Department of Electronics and Communication Engineering, P.K. University Shivpuri, Thanara,
Madhya Pradesh, India

e-mail: jloni100774@gmail.com

A. K. Tripathi

e-mail: dr.aktipathi@gmail.com

J. Dewangan

Department of Electronics and Communication Engineering, Bhilai Institute of Technology,
Kendri, New Raipur, Chhattisgarh, India

e-mail: jaideepdewangan11@bitraipur.ac.in

V. K. Singh (✉)

Department of Electrical Engineering, SR Group of Institutions, Jhansi, Uttar Pradesh, India

e-mail: singhvinod34@gmail.com

© Springer Nature Singapore Pte Ltd. 2021

K. S. Sherpa et al. (eds.), *Advances in Smart Grid and Renewable Energy*,

Lecture Notes in Electrical Engineering 691,

https://doi.org/10.1007/978-981-15-7511-2_45

thirdly which can be used as accessories. These smart clothing and devices are most popular among the defense services. Huge and heavy devices may create hindrance in mobility of soldiers and that can easily be targeted by the enemies. Hence, the small and invisible, lightweight and integrated wearable electronics will be utilized more to secure soldiers. E-textiles and smart clothing's can have multiple scope in various application like sports, health monitoring, astronauts, military, emergency workers like bomb diffusing squad or fire fighters and in entertainment industry. It will be simply accomplished by embracing and integrating required electronic parts in the clothing. As compared to hand held devices these wearable devices are on upper edge as they provide free hands and people can perform their tasks freely [11–16].

2 Wearable Antenna Design

Here antenna is designed by using CST software. The proposed antenna is designed on a substrate that is textile in nature. The anticipated antenna is designed using slotting technique. The final design for required output is proposed by executing many iteration steps. The substrate or dielectric material plays a vital role in designing process that affects outcomes. The proposed antenna design can be divided mainly into three parts; antenna, matching network and rectifier circuit. Every antenna use metal material for conduction or transmission. Here copper tape is used for that purpose but its shape depends on antenna design. The design is fabricated on the substrate material with partial ground structure. A microstrip feed line is also used for giving input power. Figure 1 shows the geometry of anticipated antenna and dimensions of parameters of are given in Table 1.

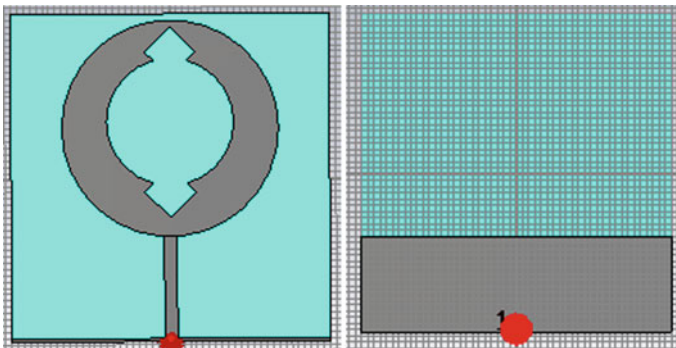


Fig. 1 Geometry of front view and back view of anticipated antenna

Table 1 Dimension of parameters of anticipated antenna

Design parameters	Value
Width of ground plane (W_g)	15.5 mm
Length of ground plane (L_g)	50 mm
Width of substrate (W_s)	50 mm
Length of substrate (L_s)	50 mm
Substrate height (h)	1.0 mm
Outer circle radius	17 mm
Inner circle radius	10 mm
Line feed	2×16

3 Result and Discussion

The resonant frequencies 3.2 GHz and 4.8 GHz are shown in Fig. 2, which have large bandwidth. The magnitude of reflection coefficients is shown in Fig. 2. The bandwidth can be calculated by Eq. (1) and finally the received bandwidth of given slotted antenna is 106.30%. Far field radiation pattern with $\phi = 90^\circ$ at 3.2 GHz and far field pattern with $\phi = 90^\circ$ at 4.8 GHz of anticipated antenna is shown in Fig. 3 and the directivity is 3.609 dBi at 3.2 GHz and 4.519 dBi at 4.8 GHz is shown in Fig. 4. The photograph of hardware is shown in Fig. 5. Figure 6 depicted the comparison of reflection coefficient versus frequency of the measured and simulated outcomes of the designed antenna. The Simulated and measured outcome of proposed textile antenna is given in Table 2 and Performance comparison of existing and anticipated antennas are shown in Table 3.

$$\text{Bandwidth} = \frac{f_2 - f_1}{\left(f_1 + f_2/2\right)} \times 100 \tag{1}$$

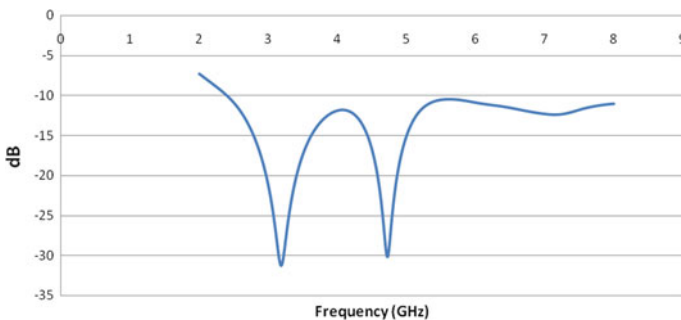


Fig. 2 Reflection coefficient of anticipated antenna

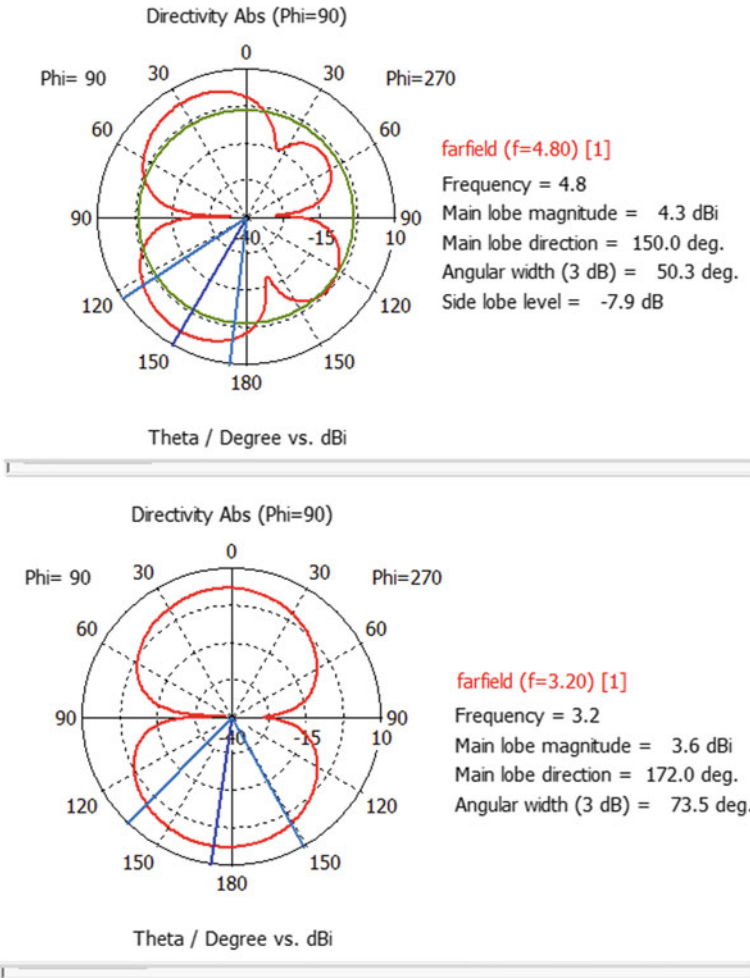


Fig. 3 2D radiation pattern of anticipated antenna

4 Conclusion

The proposed antenna is designed using Jeans substrate that is easily available and flexible in nature. The anticipated antenna is simulated to get improved bandwidth of 106.30%, and directivity is 3.609 dBi at 3.2 GHz and 4.519 dBi at 4.8 GHz. The proposed antenna design is quite simple, light weighted and cost effective as less copper will be needed to fabricate the patch and ground. As it is proposed from the satisfied result, it has many such as in telecom industry, aircraft surveillance and different wireless communication systems.

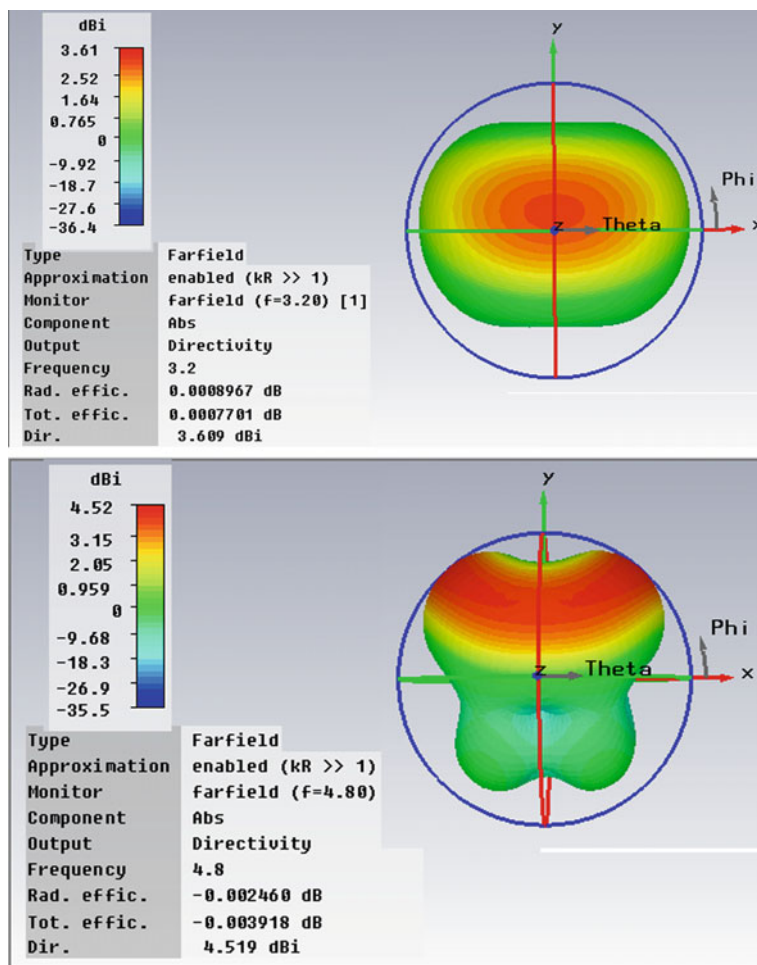


Fig. 4 Far field pattern with directivity

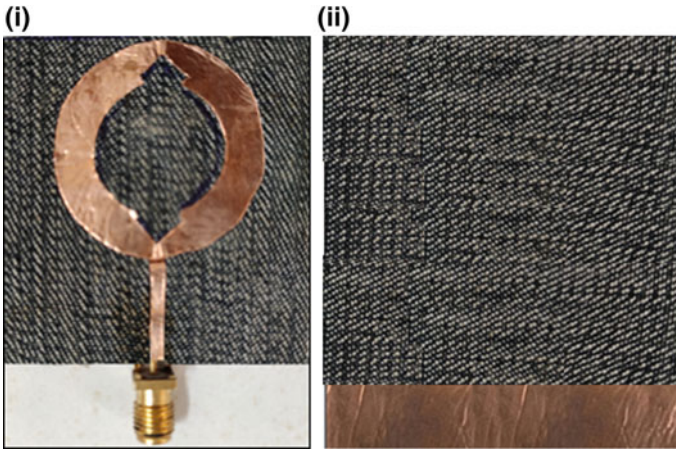


Fig. 5 Fabricated antenna using jeans substrate **i** front view **ii** back view

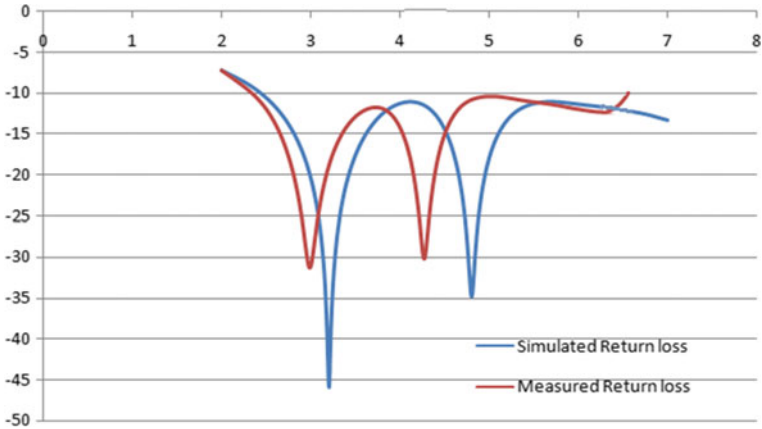


Fig. 6 Comparison of reflection coefficients of fabricated antenna

Table 2 Simulated and measured outcome of proposed textile antenna

Antenna designs	Simulated bandwidth		Measured bandwidth	
	Frequency range (GHz)	Bandwidth (%)	Frequency range (GHz)	Bandwidth (%)
Proposed antenna	2.445–8.0	106.30	2.33–6.49	94.33

Table 3 Performance comparison of existing and anticipated antenna

References	Substrate	Frequency range (GHz)	Size (mm)	Band width (%)	Peak gain (dB)
L. Xu [17]	Felt $\epsilon_r = 2.4$	2.4–2.5	$70 \times 40 \times 3$	2.40	2.7
		5.725–5.875		6.40	
Marcus Grilo [18]	Denim $\epsilon_r = 1.77$	2.45	$43.3 \times 38 \times 1.4$	15.0	0.78
Rawat and Sharma [13]	FR-4 $\epsilon_r = 4.4$	4.04–7.28	$30 \times 30 \times 1.59$	60.30	3.0
Proposed antenna	Jes $\epsilon_r = 1.7$	2.445–8.0	$50 \times 50 \times 1.0$	106.30	4.519

References

1. C.A. Balanis, *Antenna Theory: Analysis and Design* (Wiley, New York, 2004)
2. A. Yadav, V.K. Singh, Design of U-shape with DGS circularly polarized wearable antenna on fabric substrate for WLAN and C-band applications. *J. Comput. Electron.* (Springer). ISSN 1569-8025
3. V.K. Singh, S. Dhupkariya, N. Bangari, Wearable ultra wide dual band flexible textile antenna for WiMax/WLAN application. *Int. J. Wirel. Pers. Commun.* **95**(2), 1075–1086 (2017) (Springer) ISSN 0929-6212
4. V.K. Singh, Z. Ali, S. Ayub, A.K. Singh, A wide band compact microstrip antenna for GPS/DCS/PCS/WLAN applications, in *Intelligent Computing, Networking, and Informatics*, vol. 243 (Springer, 2014), pp. 1107–1113. ISBN: 978-81-322-1664-3
5. N. Singh, A.K. Singh, V.K. Singh, Design and performance of wearable ultra wide band textile antenna for medical applications. *Microw. Opt. Technol. Lett.* **57**(7), 1553–1557 (2015) (Wiley Publications, USA, 2015). ISSN: 0895-2477
6. S. Srivastava, V.K. Singh, Z. Ali, A.K. Singh, Duo triangle shaped microstrip patch antenna analysis for WiMAX lower band application, in *International Conference on Computational Intelligence: Modeling Techniques and Applications (CIMTA-2013)*, vol. 10. Department of Computer Science and Engineering, University of Kalyani, Procedia Technology (Elsevier, 2013), pp. 554–563
7. N.K. Singh, V.K. Singh, B. Naresh, Textile antenna for microwave wireless power transmission, in *International Conference on Computational Modeling and Security (CMS 2016)*. Procedia Computer Science (Science Direct, 2016).
8. J. Loni, S. Ayub, V.K. Singh, Performance analysis of microstrip patch antenna by varying slot size for UMTS application, in *Communication Systems and Network Technologies (CSNT-2014)*. IEEE Publication, NITTR, Bhopal, India, 7–9 Apr 2014, pp. 01–05. Print ISBN: 978-1-4799-3070-8/14
9. R. Srivastava, S. Ayub, V.K. Singh, Dual band rectangular and circular slot loaded microstrip antenna for WLAN/GPS/WiMax applications, in *Communication Systems and Network Technologies (CSNT-2014)*. IEEE Publication, India, Apr 2014, pp 45–48. Print ISBN: 978-1-4799-3070-8/14
10. S. Dhupkariya, V.K. Singh, Textile antenna for C-band satellite communication application. *J. Telecommun. Switch. Syst. Netw.* **2**(2), 20–25 (2015). ISSN: 2394-1987
11. V.K. Singh, N.K. Singh, Compact circular slotted microstrip antenna for wireless communication systems. *J. Microw. Eng. Technol.* **1**(1), 07–14 (2015). ISSN: 2349-9001
12. J. Loni, V.K. Singh, Development of bandwidth enhanced microstrip patch antenna for UMTS application. *J. Microw. Eng. Technol.* **2**(1), 01–07 (2015). ISSN: 2349-9001

13. S. Rawat, K.K. Sharma, A compact broadband microstrip patch antenna with defected ground structure for C-band applications. *Cent. Eur. J. Eng.* **4**(3), 287–292 (2014)
14. V.K. Singh, B. Naresh, Multi resonant microstrip antenna with partial ground for radar application. *J. Telecommun. Switch. Syst. Netw.* **2**(1), 01–05 (2015). ISSN: 2349-9001
15. M. Singh, V.K. Singh, B. Naresh, Rectangular slot loaded circular patch antenna for WLAN application. *J. Telecommun. Switch. Syst. Netw.* **2**(1), 07–10 (2015). ISSN: 2349-9001
16. R. Srivastava, V.K. Singh, S. Ayub, Comparative analysis and bandwidth enhancement with direct coupled C slotted microstrip antenna for dual wide band applications, in *Frontiers of Intelligent Computing: Theory and Applications*, vol. 328 (Springer, 2015), pp. 449–455. ISBN: 978-3-319-12011-9
17. L. Xu, J.L. Li, A dualband microstrip antenna for wearable application, ISAPE2012, Xian (2012), pp. 109–112 <https://doi.org/10.1109/ISAPE.2012.6408720>.
18. M. Grilo, F.S. Correra. Rectangular patch antenna on textile substrate fed by proximity coupling. *J. Microwaves Optoelectron. Electromagnet. Appl. (JMoe)*, **14**, SI-103, 2015.

Wearable Textile Antenna for C-Band Application



Zakir Ali, Abhinab Shukla, Anurag Saxena, and Vinod Kumar Singh

1 Introduction

Nowadays, for wireless applications, wearable antennas have become first choice for researchers. These types of antennas are generally mounted on the substrate. The upper and lower part of the substrate are generally made by conducting material like copper adhesive material whose conductivity is generally very high that is very advantageous for radiation purpose. For making the antenna wearable, we use substrate material such as jeans, cotton and polyester [1–4]. The near field and far field propagation play a vital role in antenna designing and simulation. The near field characterizes the power at different points. By the results, it can be understood its communication. The far field also characterizes an important role in applications between sensors and bigger units such as laptops, mobile phones and in applications with long distance [4–8].

There are different types of antenna available in the industry prior that were simple in design or complex. But the sizes and cost of antenna structure were also increasing with respect to its applications. To overcome these drawbacks, the microstrip patch antenna was introduced in the industry, these antennas are

Z. Ali

Department of ECE, IET, Bundelkhand University, Jhansi, India

e-mail: zakirali008@gmail.com

A. Shukla

Department of EEE, Bhilai Institute of Technology, Kendri, New Raipur, Chhattisgarh, India

e-mail: Abhinab.shukla@gmail.com

A. Saxena · V. K. Singh (✉)

Department of Electrical Engineering, SR Group of Institutions, Jhansi, Uttar Pradesh, India

e-mail: singhvinod34@gmail.com

A. Saxena

e-mail: anurag.saxena.anurag@gmail.com

© Springer Nature Singapore Pte Ltd. 2021

K. S. Sherpa et al. (eds.), *Advances in Smart Grid and Renewable Energy*,

Lecture Notes in Electrical Engineering 691,

https://doi.org/10.1007/978-981-15-7511-2_46

small in size, lightweight, cost effective and also wearable in nature [9–13, 14]. The microstrip antennas are designed in different shapes. There are various applications of antennas in each and every field such as medical applications, satellite communications, geographic navigation, telecom industry and in remote areas [14–16].

There will be three main types of wearable antenna which can be put under these three categories. First, these type of systems can be worn directly on the body; secondly the type of systems which can be directly integrated with clothing and thirdly which can be used as accessories. These smart clothing and devices are most popular among the defense services. Huge and heavy devices may create hindrance in mobility of soldiers and that can easily be targeted by the enemies. Hence, the small and invisible, lightweight and integrated wearable electronics will be utilized more to secure soldiers. E-textiles and smart clothing can have multiple scope in various application like sports, health monitoring, astronauts, military, emergency workers like bomb diffusing squad or fire fighters and in entertainment industry. It will be simply accomplished by embracing and integrating required electronic parts in the clothing. As compared to hand-held devices, these wearable devices are on upper edge as they provide free hands, and people can perform their tasks freely.

2 Proposed Antenna Design

The proposed antenna design was designed with many iteration steps using CST software. Here, only the final design has shown that fulfill the desired objectives. The geometry of the design is shown in Fig. 1a, b with the help of its front and back view. The dimension of the parameters of design is also represented by Table 1. The

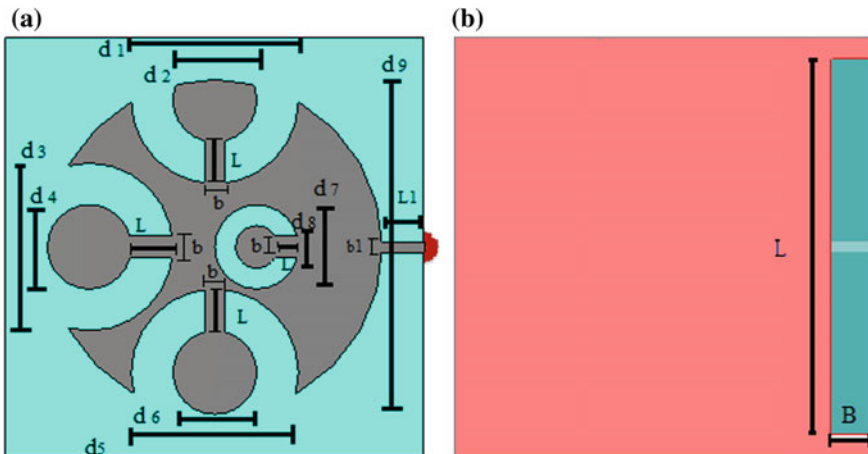


Fig. 1 Geometry of antenna design **a** Front view and **b** back view

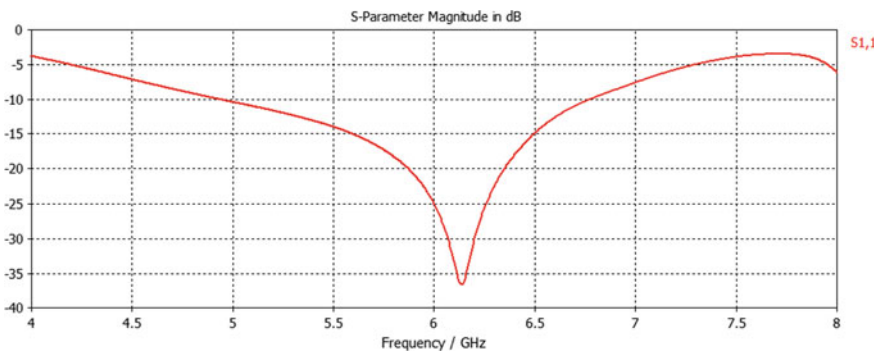
Table 1 Dimension of geometry of antenna

S. No.	Antenna parameter	Values
1.	Ground length (L)	18 mm
2.	Ground breadth (B)	2 mm
3.	Substrate dimension	20 mm \times 20 mm
4.	Substrate height	1 mm
5.	Large circle diameter of patch (d_9)	16 mm
6.	Smaller inner circle diameter of patch (d_2, d_4, d_6)	4 mm
7.	Smaller outer circle diameter of patch (d_1, d_3, d_5)	8 mm
8.	Middle inner circle diameter	2 mm
9.	Middle outer circle diameter	4 mm
10.	Dimension of line feed	3 mm \times 1 mm

design is prepared using substrate material of jeans which has dielectric constant 1.7 and thickness 1 mm. For patch and ground plane, copper tape as a conducting material is used. A microstrip feed line is also connected for feeding the input to antenna design.

3 Result Analysis

After designing the antenna, the next step is its simulation. Here, for simulation purpose, CST software is used. After simulation, the various graphs are obtained such as return loss versus frequency, radiation pattern, field energy per dB and lastly the comparison result for return loss between simulated result versus measured result in Figs. 2, 3, 4 and 6, respectively.

**Fig. 2** Graph representing return loss (dB) versus frequency (GHz) of anticipated antenna

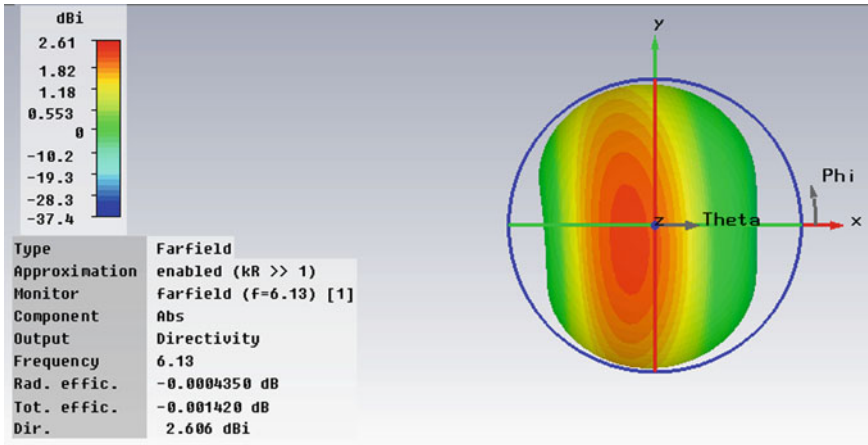


Fig. 3 Radiation pattern of anticipated antenna at 6.13 GHz

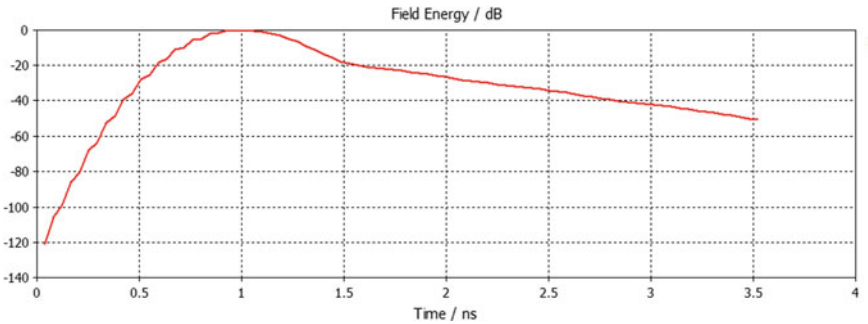


Fig. 4 Field energy per dB of anticipated antenna

Firstly, in Fig. 2, the return loss graph represents the proposed antenna design that has single band with a good bandwidth at resonant frequency 6.13 GHz. Then, in next Fig. 3, the three-dimensional radiation pattern has shown that represents the radiation efficiency approximately -0.0004350 dB and directivity of 2.606 dBi. Other parameter field energy per dB is analyzed by using CST simulation of proposed antenna in Fig. 4 at resonant frequency. The hardware implementation of design is also done for the justification of results that are shown in Fig. 5, and lastly, the comparison is done between simulation and measured results for satisfaction of results with respect to return loss (Fig. 6).

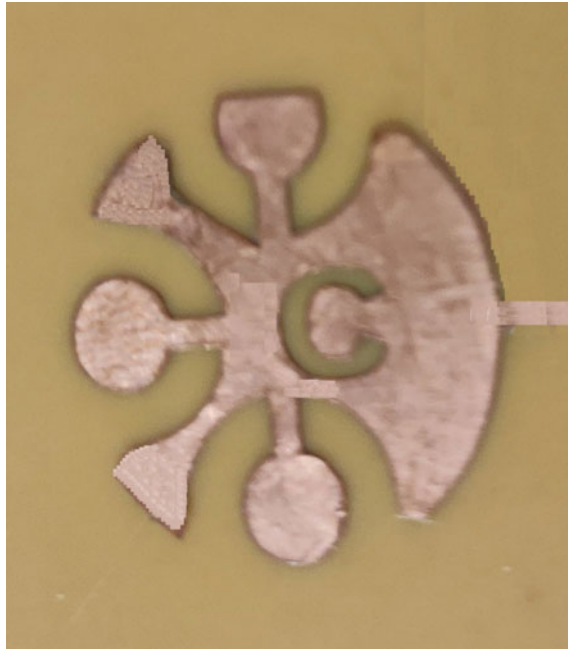


Fig. 5 Front view of hardware implementation of anticipated antenna

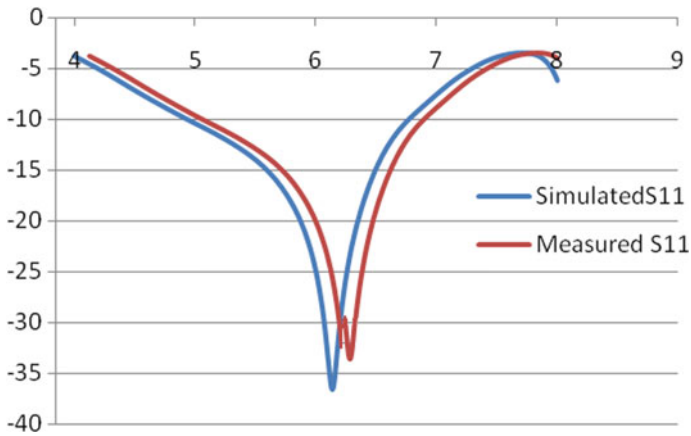


Fig. 6 Comparison result between simulated and measured return loss (S_{11}) of anticipated antenna

4 Conclusion

The anticipated antenna is simulated using CST software. For designing, the substrate material jeans are used for making it wearable. The directivity of the designed antenna

is 2.606 dBi at resonant frequency 6.13 GHz. The presented proposed shaped antenna has designed by using a textile material jeans with a thickness of 1 mm. The frequency range of the designed antenna is 4.92–6.75 GHz for C-band applications. A great compatibility between measured and simulated reflection coefficients is shown and justified.

References

1. A. Yadav, V.K. Singh, P. Yadav, A.K. Belya, A.K. Bhoi, P. Barsocchi, Design of Circularly Polarized Triple-Band Wearable Textile Antenna with Safe Low SAR for Human Health. *Electron.* **9**, 1366, (2020)
2. V.K. Singh, B. Naresh, Multi resonant microstrip antenna with partial ground for radar application. *J. Telecommun. Switch. Syst. Netw.* **2**(1), 01–05 (2015). ISSN: 2349-9001
3. M. Singh, V.K. Singh, B. Naresh, Rectangular slot loaded circular patch antenna for WLAN application. *J. Telecommun. Switch. Syst. Netw.* **2**(1), 07–10 (2015). ISSN: 2349-9001
4. V.K. Singh, S. Dhupkariya, N. Bangari, Wearable Ultra Wide Dual Band Flexible Textile Antenna for WiMax/WLAN Application. *Int. J. Wirel. Pers. Commun.* **2**(2), 1075–1086 (2017)
5. V.K. Singh, R. Tiwari, V. Dubey, Design and Optimization of Sensors and Antennas for Wearable Devices (ISBN: 9781522596837), IGI Global Publication USA, September (2019).
6. V.K. Singh, A. Saxena, B.B. Khare, V. Shayka, G.-S. Chae, A. Sharma, A.K. Bhoi, Power harvesting through flexible Rectenna at dual resonant frequency for low power devices. *Int. J. Eng. Technol.* **7**(2.33), 647–649 (2018)
7. N. Singh, A.K. Singh, V.K. Singh, Design & Performance of Wearable Ultra Wide Band Textile Antenna for Medical Applications. *Microwave Opt. Technol. Lett.* **57**(7), 1553–1557 (2015), Wiley Publications, USA
8. B. Naresh, V.K. Singh, V. Bhargavi, Low power circularly polarized wearable Rectenna for RF energy harvesting, in *Advances in Power Systems and Energy Management*, ed. by A. Garg, A. Bhoi, Lecture notes in electrical engineering, vol. 436. (Springer, Singapore, 2018)
9. V.K. Singh, N.K. Singh, Compact circular slotted microstrip antenna for wireless communication systems. *J. Microw. Eng. Technol.* **1**(1), 07–14 (2015). ISSN: 2349-9001
10. J. Loni, V.K. Singh, Development of bandwidth enhanced microstrip patch antenna for UMTS application. *J. Microw. Eng. Technol.* **2**(1), 01–07 (2015). ISSN: 2349-9001
11. V.K. Singh, S. Khan, Ultra Wide Band Wearable Textile Antenna for Multi Band Applications. Lambert Academic Publishing, (2016)
12. M. Grilo, F.S. Correr, Rectangular patch antenna on textile substrate fed by proximity coupling. *J. Microw. Optoelectron. Electromagn. Appl.* **14**, 103–112 (2015)
13. S. Rawat, K.K. Sharma, A compact broadband microstrip patch antenna with defected ground structure for C-band applications. *Cent. Eur. J. Eng.* **4**(3), 287–292 (2014)
14. A. Yadav, V.K. Singh, A.K. Bhoi, G. Marques, B. Garcia-Zapirain, I. de la Torre Díez, Wireless Body Area Networks: UWB Wearable Textile Antenna for Telemedicine and Mobile Health Systems. *Micromach.* **11**(6), 558 (2020)
15. V.K. Singh, R. Tiwari, V. Dubey, Design and Optimization of Sensors and Antennas for Wearable Devices” (ISBN: 9781522596837), IGI Global Publication USA, (2019)
16. R. Singh, V.K. Singh, P. Khanna, A Compact CPW-Fed Defected Ground Microstrip Antenna for Ku Band Application. *Adv. Electron. Commun. Comput. Lecture Notes in Electrical Eng.* **443**, 231–237 (2018)

Mechanoluminescence Induced in Rare Earth Activated Cementitious Materials



R. K. Mishra, A. K. Beliya, Vikas Dubey, and Neha Dubey

1 Introduction

As we know that mechanoluminescence is a type of luminescence in which solid samples are mechanically deformed. In our study, when phosphor is impulsively deformed, fracture occurs in phosphor. It is called fracto ML (FML). In the FML induced by impulsive deformation, a moving piston makes an impact on to a crystal and the ML is produced during fracture of the crystal [1–6].

The present manuscript gives information about mechanoluminescence behaviour of concrete crystal which is prepared by conventional method using different cements and different replacements of sand. The manuscript gives information regarding formation of crack centres and responsible centre for luminescence mechanism. Also, the variation of impact velocity with respect to intensity of ML increases linearly. Effects of mass on the ML pattern and time dependence ML phenomenon explain in details. In this study, we have found several applications such as formation of cracks and durability of the prepared material in building blocks.

R. K. Mishra

Department of Civil Engineering, Bhilai Institute of Technology, Kendri, New Raipur, Chhattisgarh, India

e-mail: rkmishra4776@gmail.com

A. K. Beliya

Department of Physics, Chandra Vijay College, Dindori, Madhya Pradesh, India

V. Dubey (✉)

Department of Physics, Bhilai Institute of Technology, Kendri, New Raipur, Chhattisgarh, India

e-mail: jsvikasdubey@gmail.com

N. Dubey

Department of Physics, Government Vishwanath Yadav Tamaskar Post Graduate Autonomous College, Durg, Chhattisgarh 491001, India

© Springer Nature Singapore Pte Ltd. 2021

K. S. Sherpa et al. (eds.), *Advances in Smart Grid and Renewable Energy*,

Lecture Notes in Electrical Engineering 691,

https://doi.org/10.1007/978-981-15-7511-2_47

Table 1 Mix proportions (with 50% slag and pond ash replacements)

Mix	Type of cement	Cement (in KG)	Water	Sand (in KG)	GBFS (in KG)	Pond ash (in KG)	Coarse aggregate (in KG)	W/C ratio
M_1	OPC	380	208	757			1028	0.55
M_2	OPC	365	208	355	355		1026	0.55
M_3	OPC	420	233	289		289	1035	0.55

2 Material Characterization

The cement used in this study was ordinary Portland cement (OPC), and specific gravity of OPC cement was found 3.15. Initial setting time was found 2 h 48 min.

Fillers are natural river sand with specific gravity 2.56, which is replaced 50% through granulated blast furnace slag (GBFS), and pond ash (PA) having specific gravity 2.39 and 1.98, respectively.

Crushed lime stone with specific gravity of 2.73 was used as coarse aggregate. The available coarse aggregate were used directly as required in the mix design. All the aggregates were tested as per the provisions of IS: 383-1970 [7], IS: 2386 (Part I-VII)-1963 and satisfying its requirement [8, 9].

3 Concrete Mix

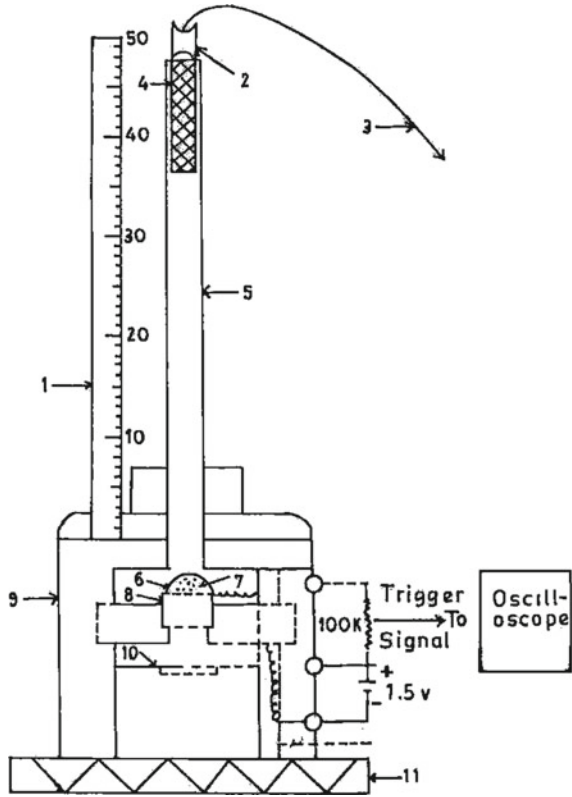
Design mix concrete was prepared with w/c ratio 0.55 taking mix M_1 as reference mix in standard manner as directed in IS 516: 1959 with material quantity taken as given in Table 1. And verifying the slump as directed in IS: 1199-1959 [10]. The concrete specimen is prepared in cube form for sufficient in number to give various exposer. 50% samples are kept in carbonation chamber to check the variation in properties of concrete before testing in its surfacial material up to 5 mm depth to observe ML pattern [10].

In this study, we used the sample M_1 and sample M_2 for the variation of ML pattern with respect to time.

4 Experimental

Figure 1 shows the schematic diagram of experimental setup used for deforming the sample and measuring the ML. When the 450 g load were dropped from 55 cm height on sample, there was impulsive deformation of crystal occurs. Mechanoluminescent intensity is sensed by photomultiplier tube and ML pattern traced by storage oscilloscope, which is connected by photomultiplier tube.

Fig. 1 Experimental arrangements of ML measuring device [1, 3]



5 Results and Discussion

See Figs. 2 and 3.

Mechanoluminescence characteristics of concrete crystal induced by the impact of a moving piston of weight 500 g onto the crystal were measured (Fig. 4).

It is shown in Fig. 5 that initially ML intensity is increases with impact velocity then attain a maximum value, then decreases with further increases in impact velocity. In Fig. 6, peak ML intensity is increases linearly for different impact velocity.

Figure 6 shows that ML intensity increases linearly with $t - t_m$. In Fig. 7, it is shown that peak time t_m decreases with increasing impact velocity because deformation occurs earlier at higher impact velocity. Linear response is shown in $\ln 1000/V_0$ versus t_m plot (Fig. 8).

It is shown in Fig. 9 that peak ML intensity increases linearly with the mass of crystals, because as the mass of crystal increases, rate of generation and rate of recombination of electron-hole pair is increases.

Using OPC cement as a fine aggregate, the ML pattern as shown in Figs. 10 and 11 for fixed impact velocity and parameters are calculated for the same. It has found that

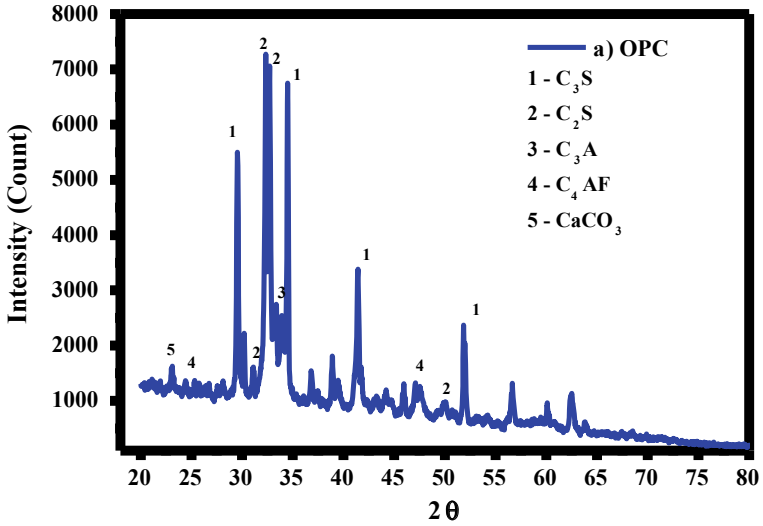


Fig. 2 XRD pattern of OPC

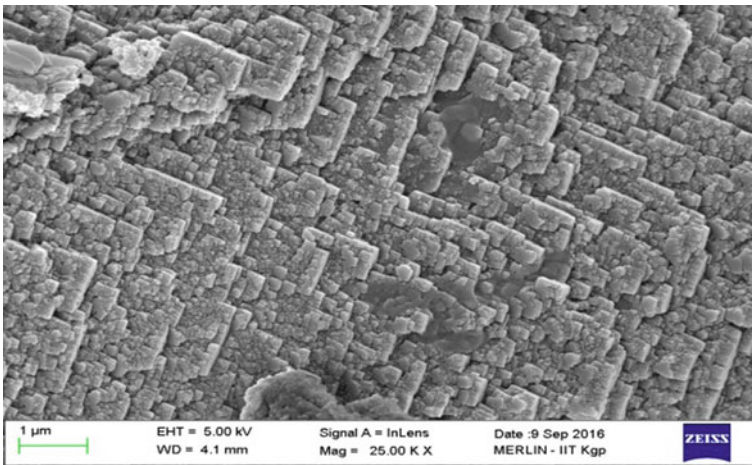


Fig. 3 The adhesion of aggregate to gel produced in OPC SA concrete is somewhat less than the OPC PA Mix where less gap between interface of aggregate and paste

there are two different peaks in lower time and shoulder peak in higher time present over here means that two luminescence centre formed for that. All ML parameters are supported theory is reported for only intense peak which is found here for lower time.

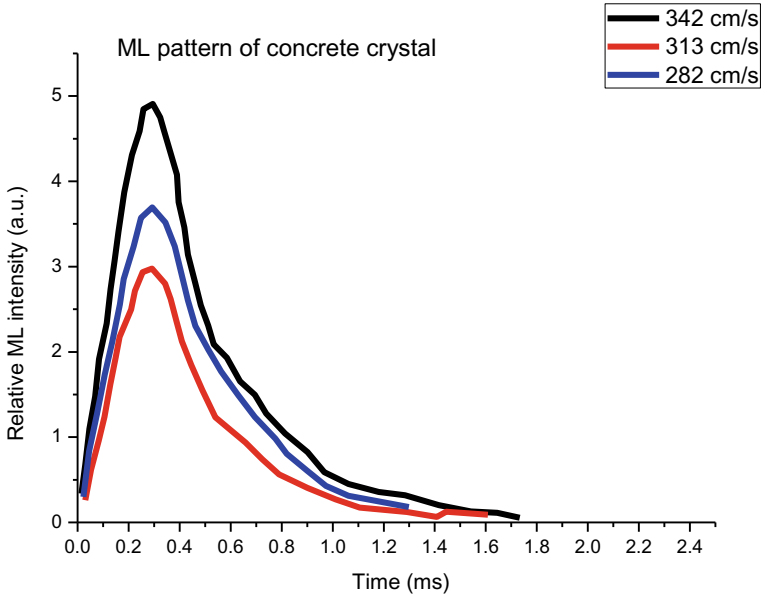


Fig. 4 ML pattern of concrete crystal with different impact velocity

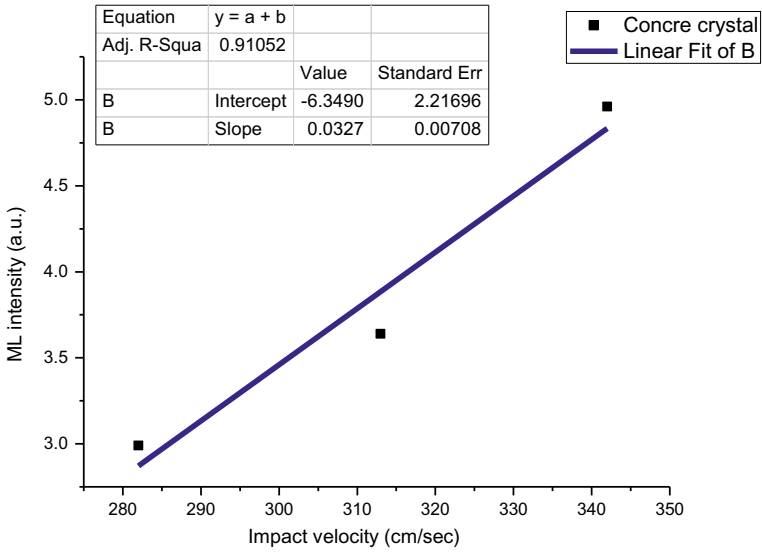


Fig. 5 Impact velocities versus intensity plot

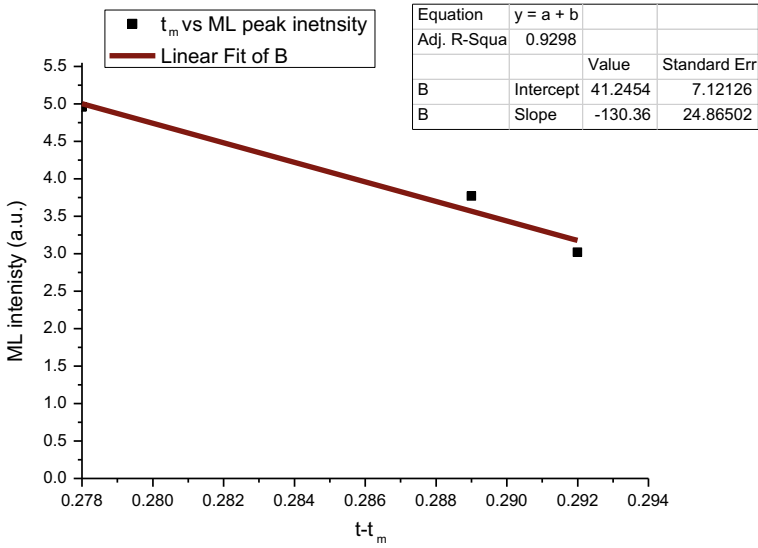


Fig. 6 ($t - t_m$) versus ML intensity

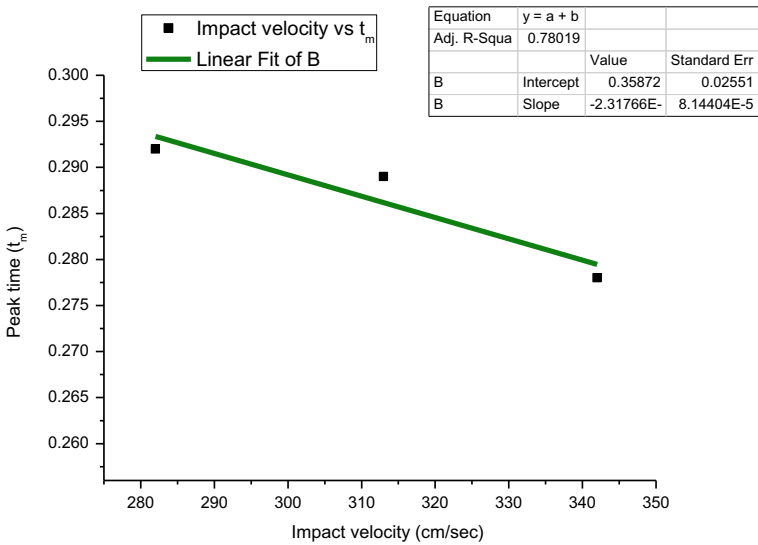


Fig. 7 ML peak time (t_m) versus impact velocity

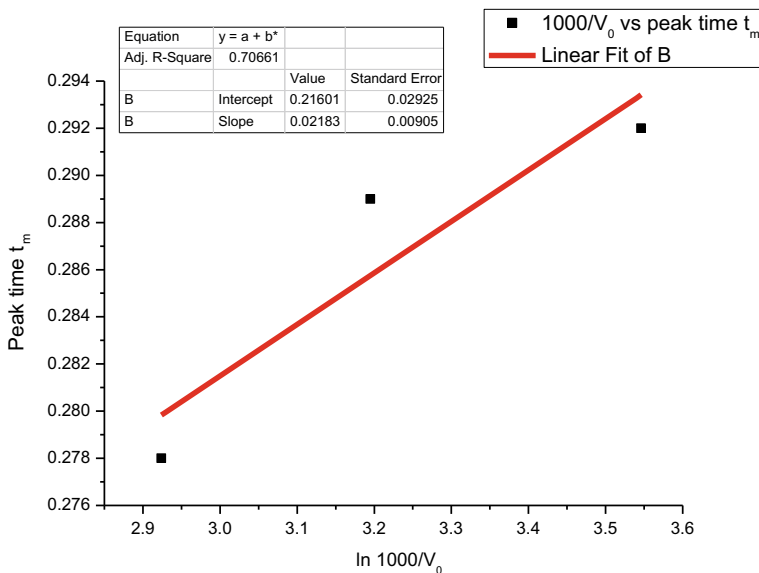


Fig. 8 $\ln 1000/V_0$ versus peak time t_m

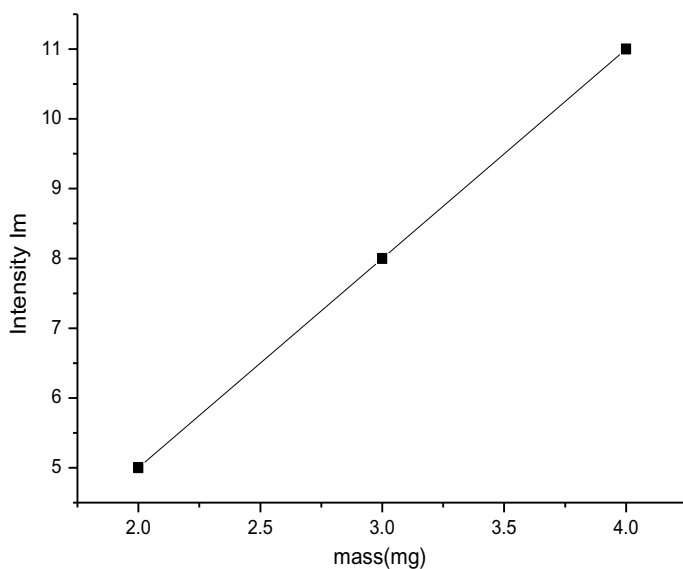


Fig. 9 Dependence of peak ML intensity on the mass of crystals

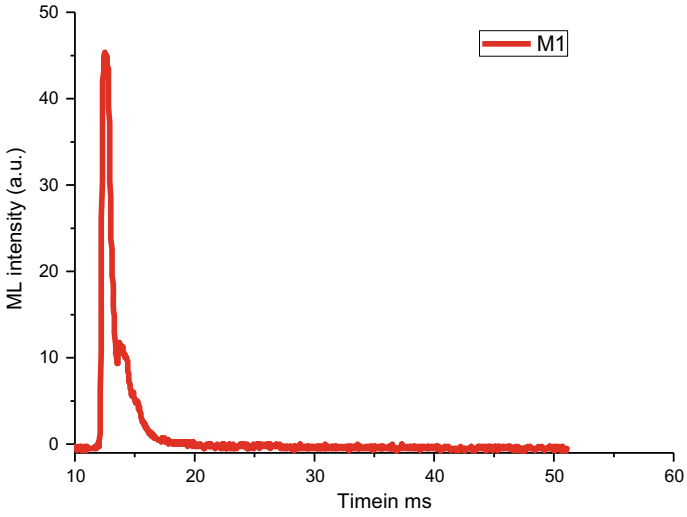


Fig. 10 ML pattern of M_1 sample using OPC with constant impact velocity

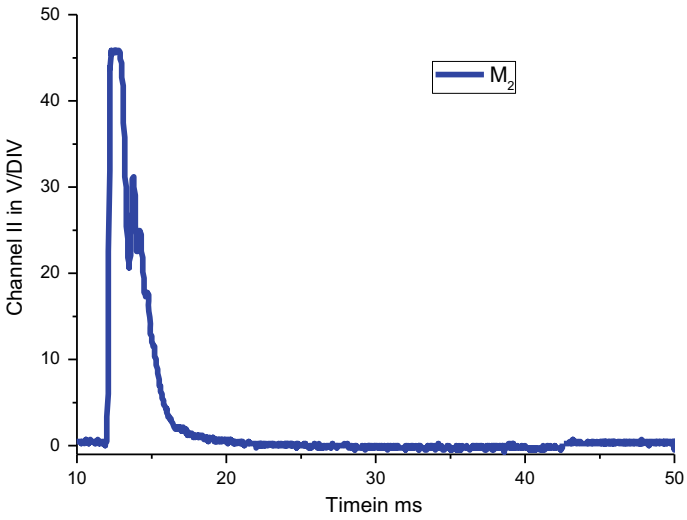


Fig. 11 ML pattern of M_1 sample using OPC with constant impact velocity

6 Theory Supported for ML Pattern in the Present Manuscript

6.1 Theory of Mechanoluminescence Induced by Impulsive Deformation

As we know that mechanoluminescence is a type of luminescence in which solid samples are mechanically deformed. In our study, when phosphor is impulsively deformed, fracture occurs in phosphor. It is called fracto ML (FML). In the FML induced by impulsive deformation, a moving piston makes an impact on to a crystal and the ML is produced during fracture of the crystal. Let dN be the number of cracks produced during the change of strain from ε to $(\varepsilon + d\varepsilon)$, then dN may be written as

$$dN = M d\varepsilon \quad (1)$$

where M is the correlation factor between the number of cracks and the strain of the crystals [11–29].

7 Conclusion

From the present study, we have concluded that when concrete crystal is deformed impulsively, deformation occurs. Single peak is observed in ML pattern of concrete crystal. ML intensity increases with impact velocity attain a maximum value then decreases with the further increase of impact velocity. peak time t_m decreases with increasing impact velocity because deformation occurs earlier with increasing impact velocity. There is a linear relation found between $\ln 1000/V_0$ and peak time t_m . Peak ML intensity increases linearly with the mass of crystals. ML study of concrete crystal may be helpful for the study of crack propagation of in the crystals and provide important information about mine failure and earthquake determination.

Acknowledgements Authors are very thankful to TEQIP-III CSVTU Bhilai for funding through collaborative research project. Also very thankful to Govt. V.Y.T.PG. Auto. College Durg for providing facilities of research laboratory.

References

1. J. Kaur, V. Dubey, N.S. Suryanarayana, Comparative study of ML and PL spectra of different impurity-doped (Zn, Cd)S mixed phosphors. *Res. Chem. Intermed.* **39**(9), 4337–4349 (2013)
2. R. Tiwari, V. Dubey, B.P. Chandra, Exact model for the elastico mechanoluminescence of II–VI phosphors. *Mater. Phys. Mech.* **19**, 25–38 (2014)

3. J. Kaur, N.S. Suryanarayana, V. Dubey, Effect of temperature on the ML of Au doped (Zn, Cd)S mixed phosphors. *Chinese Chem. Lett.* **22**(6), 709–712 (2011)
4. V. Dubey, N.S. Suryanarayana, J. Kaur, J. Min. Mater. Character. Eng. **9**(12), 1101 (2010)
5. J. Kaur, N.S. Suryanarayana, V. Dubey, ML spectra of gold doped (Zn, Cd) S mixed phosphors. *Chalcogenide Lett.* **7**(5), 329–334 (2010)
6. B.P. Chandra, in *Luminescence of Solids*. ed. by D.R. Vij (Plenum Press, New York, 1998), p. 361
7. IS: 383-1970, *Specification for Coarse and Fine Aggregate from Natural Sources of Concrete* (Bureau of Indian Standards, New Delhi, 2002)
8. IS: 2386 (Part III) *Methods of Test for Aggregates for Concrete Part III Specific Gravity, Density, Voids, Absorption and Bulking* (Bureau of Indian Standards, New Delhi, 1963)
9. IS 516, *Methods of Tests for Strength of Concrete* (Bureau of Indian Standards, New Delhi, 1959)
10. IS: 1199-1959, *Methods of Sampling and Analysis of Concrete. Slump Test Clause 5.1* (Bureau of Indian Standards, New Delhi, 2004), pp. 6–10
11. B.P. Chandra, Mechanoluminescent smart materials and their applications, in *Electronic and Catalytic Properties of Advanced Materials*. ed. by A. Stashans, S. Gonzalez, H.P. Pinto (Transworld Research Network, Trivandrum, Kerala, India, 2011), pp. 1–37
12. B.P. Chandra, J.I. Zink, *Phys. Rev. B* **21**, 816 (1980)
13. B.P. Chandra, S.K. Mahobia, P. Jha, R.K. Kurariya, S.R. Kurariya, R.N. Baghel, S. Thakre, J. Lumin. **128**, 2038 (2008)
14. I. Sage, R. Badcock, L. Humberstone, N. Geddes, M. Kemp, G. Bourhill, *Smart Mater. Struct.* **8**, 504 (1999)
15. I. Sage, L. Humberstone, I. Oswald, P. Lloyd, G. Bourhill, *Smart Mater. Struct.* **9**, 1 (2000)
16. N. Takada, J.I. Sugiyama, R. Katoh, N. Minami, S. Hieda, *Synth. Metals* **91**, 351 (1997)
17. I. Sage, R. Badcock, L. Humberstone, S.N. Gedde, M. Kemp, S. Bishop, G. Bourhill, in *SPIE Conference on Smart Structures and Materials Technologies*
18. B.T. Brady, G.A. Rowell, *Nature* **321**, 488 (1986)
19. J.S. Derr, *Bull. Seis. Soc. Am.* **63**, 2177 (1973)
20. F. Freund, *J. Scientific, Exploration* **17**, 37 (2003)
21. R. Zito, *Icarus* **82**, 419 (1989) (Newport Beach, CA, USA, 1999, p. 169)
22. C.N. Xu, *AIST Today* **10**, 18 (2010)
23. C.M. Glass, J.G. Dante, *USA Report* (Secretary of Army, USA, 1977)
24. J.G. Dante, *Reports* (The Secretary of Army, USA, 1983)
25. J.T. Dickinson, J.T. Jensen, L.C. Jensen, S.C. Langford, P.E. Rosenberg, D.L. Blanchard, *Phys. Chem. Miner.* **18**, 320 (1991)
26. G.O. Cress, B.T. Brady, G.A. Rowell, *Geophys. Res. Lett.* **14**, 331 (1987)
27. G.A. Baird, P.S. Kennan, *Tectonophysics* **111**, 147 (1985)
28. J.W. Warwick, C. Stoker, T.R. Meyer, *J. Geophys. Res.* **87**, 2851 (1982)
29. L. Slifkin, *Tectonophysics* **224**, 149 (1993)

Customer Stress Prediction in Telecom Industries Using Machine Learning



K. N. R. Srinivas, K. S. S. Manikanta, T. Prem Jacob, G. Nagarajan, and A. Pravin

1 Introduction

In the current era, the average person spends over four hours a day on their devices. Most of the people spend a full quarter of their waking hours on their available gadgets [1, 2]. It shows that humans depend more on current technology. To acquire knowledge, we have books and newspapers, but they are not using professionally to gain information. In human life, communication played a prominent role from the ancient to the current period. Initially, people depended on the letters to communicate with each other [3–5].

Running a telecom industry is not an easy matter. The telecom industries depend on information and communication services, which provides in different ways like phone services, Internet services, Television, etc. [6, 7]. By providing all services to thousands of customers will cause stress among the services. The stress may be caused by industry or some other changes in climate and so on [8]. The stress will lose a customer by moving to another industry.

K. N. R. Srinivas (✉) · K. S. S. Manikanta · T. Prem Jacob · G. Nagarajan · A. Pravin
Department of Computer Science and Engineering, Sathyabama Institute of Science and
Technology, Chennai, India
e-mail: srinivasjustsree7777@gmail.com

K. S. S. Manikanta
e-mail: kalepumanikanta07@gmail.com

T. Prem Jacob
e-mail: premjac@yahoo.com

G. Nagarajan
e-mail: nagarajanme@yahoo.co.in

A. Pravin
e-mail: pravin_ane@rediffmail.com

The customer stress will lead to falling of the market and causes significant loss. For this cause, the telecom industry must and should retain the existing customers because the cost of acquiring a new customer is higher than retaining existing customers [9, 10]. The machine learning algorithms will help to predict customer stress and accurate percentage value [11]. At first, we must collaborate with customers and collect data into an open dataset and start the process [12–14].

2 Related Work

In these days, many corporations are collaborating with customers and collecting the information where the customer was stressed and launching the services with an updated version to the last version, which was provided by the old telecom industry and attracting customers by their advertisement, which leads to significant loss to other telecom industries [15, 16]. By observing this problem, Reichheld and Sasser in 1990 started customer relationship management, which can impact stress rates overall telecom industry [17, 18]. Numerous studies fix several unusual types of predictors to develop a customer stress model. This model can take demographic characteristics, environmental changes, and other factors into account.

In the beginning, the customer stress prediction process started by Abbas Keramati in 2014 featuring demographics, usage patterns, customer service using binomial logistic and regression models [19].

Ismail Mohammad in 2016 predicted customer stress by featuring demographic billing data, usage patterns, and customer relationships and using neural network and regression models [20].

Chih Fong Tsai and Yu Hsin Lu in 2019 predicted customer stress by using hybrid neural networks. In this paper, we mainly discuss the following.

3 Existing System

Earlier, the authors used hybrid neural networks which lead to back-propagation, the accuracy value of the models was not much accuracy, the confusion matrix will lead to error I and error II, and the clustering process was the main problem to missing of data, so the accuracy was less.

4 Proposed System

In this paper, the customer stress was predicted by supervised machine learning algorithms mainly using linear discriminant analysis (LDA) and support vector machine

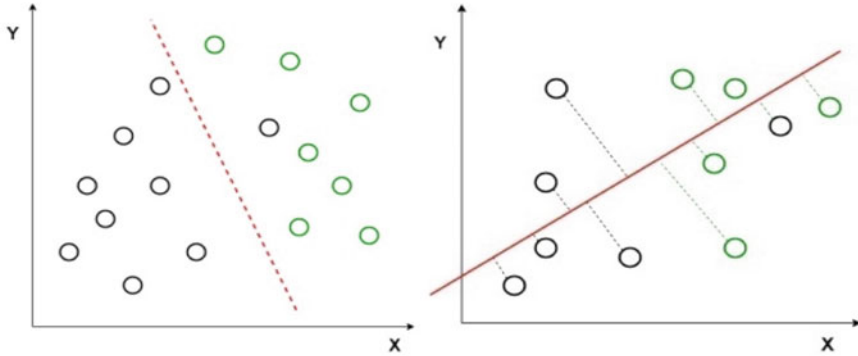


Fig. 1 LDA process

(SVM), and the accuracy value will take by comparing the best of each accuracy values.

Linear Discriminant Analysis (LDA)

This algorithm mainly considers dimensionality reduction used for supervised classification problem. It will convert from higher into lower dimension space (Fig. 1).

Support Vector Machine (SVM)

In this algorithm, it will construct a hyperplane to classify the data and regression analysis and leads to an optimal hyperplane in a nonlinear manner.

Random Forest

This algorithm is used for classification, regression, and decision trees at the training period and gives the mean prediction of the individual trees. It picks an accurate solution through voting (Fig. 2).

5 System Architecture

See Fig. 3.

6 Results and Discussion

See Figs. 4, 5, 6, 7, and 8.

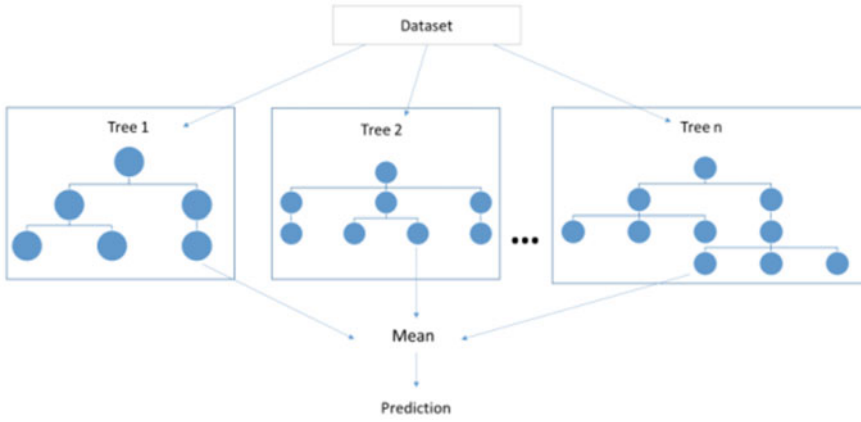


Fig. 2 Random forest process

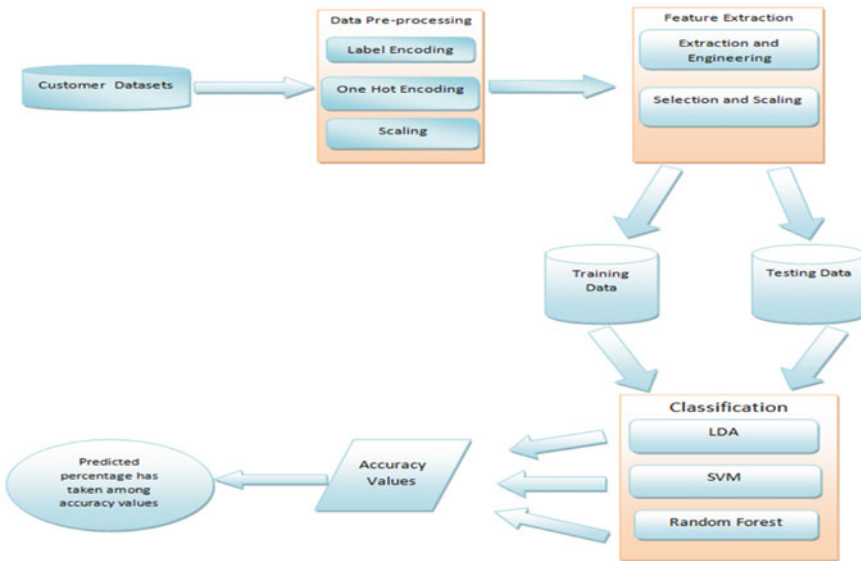


Fig. 3 Overall system design

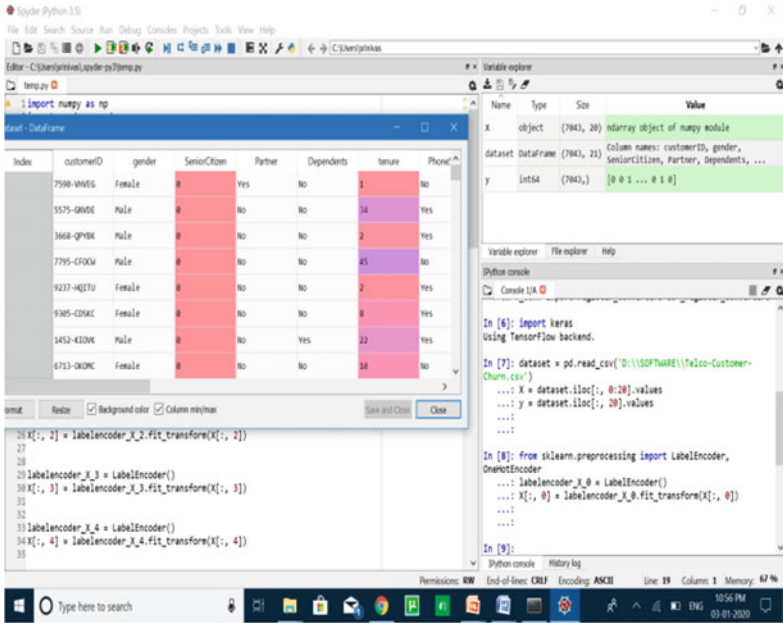


Fig. 4 Data collected from the customers

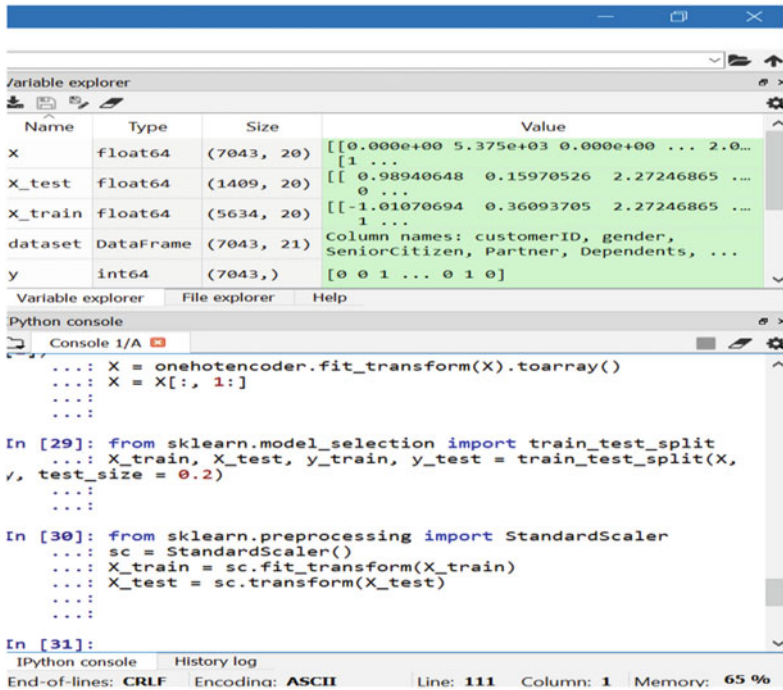


Fig. 5 In the above image, the data are split into training and testing

```
Console 1/A
Epoch 89/100
5634/5634 [=====] - 1s 95us/step -
loss: 0.4043 - acc: 0.8069
Epoch 90/100
5634/5634 [=====] - 1s 97us/step -
loss: 0.4041 - acc: 0.8064
Epoch 91/100
5634/5634 [=====] - 1s 96us/step -
loss: 0.4040 - acc: 0.8090
Epoch 92/100
5634/5634 [=====] - 1s 97us/step -
loss: 0.4040 - acc: 0.8078
Epoch 93/100
5634/5634 [=====] - 1s 98us/step -
loss: 0.4044 - acc: 0.8085
Epoch 94/100
5634/5634 [=====] - 1s 92us/step -
loss: 0.4040 - acc: 0.8088

IPython console History log
End-of-lines: CRLF Encoding: ASCII Line: 9 Column: 1 Memory: 58 %
```

Fig. 6 In the above image, the datasets are trained and tested up to 100%

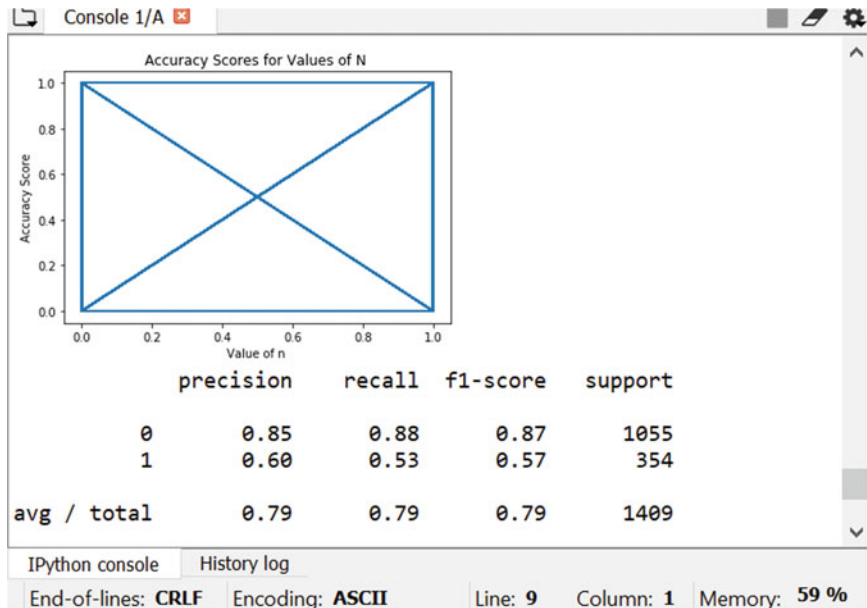


Fig. 7 Above image is the graphical representation of the accuracy scores

```

1      0.60      0.53      0.57      354
avg / total      0.79      0.79      0.79      1409

[[989 79]
 [209 132]]
Accuracy LDA = 0.7955997161107168
[[942 126]
 [153 188]]
Accuracy svm = 0.8019872249822569
[[989 79]
 [209 132]]
Accuracy RF = 0.7955997161107168

In [12]:
    
```

IPython console History log

End-of-lines: CRLF Encoding: ASCII Line: 9 Column: 1 Memory: 60 %

Fig. 8 Above image shows the accuracy values of the three algorithms

7 Conclusion

In the paper, we considered the best of the three algorithms, namely support vector machine, random forest, and linear discriminant analysis, according to the accuracy values given by these algorithms.

The highest percentile among the three algorithms shows the maximum customers affecting their respective services, in which they were in the long-lasting relationship to the industry. Finally, the telecom industry must satisfy old customers without interrupting the services using stress prediction.

References

1. J.T. Tou, R.C. Gonzalez, *Pattern Recognition Principles* (Addison-Wesley, 1974)
2. D. Van den Poel, B. Larivière, Customer attrition analysis for financial services using proportional hazard models. *Eur. J. Oper. Res.* **157**, 196–217 (2004)
3. C.P. Wei, I.T. Chiu, Turning telecommunications call details to churn prediction: a data mining approach. *Exp. Syst. Appl.* **23**, 103–112 (2002)
4. G.V.K. Sai, P.S. Kumar, A.V.A. Mary, Incremental frequent mining human activity patterns for health care applications. *IOP Conf. Ser. Mater. Sci. Eng.* **590**(1), 012050 (IOP Publishing)
5. B. Bharathi, P. Vijayalakshmi, T. Nagarajan, Speaker identification using utterances correspond to speaker-specific-text, in *IEEE Technology Students' Symposium*. IEEE, Jan 2011, pp. 171–174

6. B.K. Wong, T.A. Bodnovich, Y. Selvi, Neural network applications in business: a review and analysis of the literature (1988–1995). *Decis. Supp. Syst.* **19**, 301–320 (1997)
7. S.M. Vaniya, B. Bharathi, Exploring object segmentation methods in visual surveillance for human activity recognition, in *2016 International Conference on Global Trends in Signal Processing, Information Computing and Communication (ICGTSPICC)*. IEEE, Dec 2016, pp. 520–525
8. X. Zhang, J. Edwards, J. Harding, Personalized online sales using web usage data mining. *Comput. Ind.* **58**, 772–782 (2007)
9. M.J.A. Berry, G.S. Linoff, *Data Mining Techniques: For Promotion Sales and Customer Support* (Wiley, 2003)
10. J. Sujolincy, M.D. Kamalesh, An authenticated smart card service using cross-cloud and big data, in *2016 International Conference on Control, Instrumentation, Communication and Computational Technologies (ICCICCT)*. IEEE, Dec 2016, pp. 634–638
11. G. Zhan, B.E. Patuwo, M.Y. Hu, Forecasting with artificial neural network: the state of the art. *Int. J. Forecast.* **14**, 35–62 (1998)
12. R.S.B. Krishna, M. Aramudhan, Unsupervised spectral sparse regression feature selection using social media datasets, in *Proceedings of the International Conference on Informatics and Analytics*, Aug 2016, pp. 1–5
13. N. Srinivasan, C. Lakshmi, A novel prediction based tree structured data using machine learning techniques. *Res. J. Pharm. Biol. Chem. Sci.* **7**(5), 527–531 (2016)
14. M.V. Ishwarya, D. Deepa, S. Hemalatha, A. Venkata Sai Nynesh, A. Prudhvi Tej, Gridlock surveillance and management system. *J. Comput. Theoret. Nanosci.* **16**(8), 3281–3284 (2019)
15. W. Buckinx, D. Van den Poel, Customer base studies partial defection of loyal behavioural clients in a non-contractual FMCG trade setting. *Eur. Mag. Oper. Res.* **164**(1), 252–268 (2005)
16. S.P. Shyry, Novel enhanced encryption algorithm for shared key generation, in *Proceedings of the 2014 International Conference on Interdisciplinary Advances in Applied Computing*, Oct 2014, pp. 1–7
17. J. Burez, D. Van den Poel, CRM at a pay-TV company: using systematic models to decrease customer grinding down by targeted marketing for subscription services. *Exp. Syst. Appl.* **32**, 277–288 (2007)
18. R. Aishwarya, R. Yogitha, V. Kiruthiga, Smart road surface monitoring with privacy preserved scheme for vehicle crowd sensing. *J. Comput. Theor. Nanosci.* **16**(8), 3204–3210 (2019)
19. D.A. Chiang, Y.F. Wang, S.L. Lee, C.J. Lin, A goal-oriented sequential pattern for network banking churn analysis. *Exp. Syst. Appl.* **25**, 293–302 (2003)
20. K. Coussement, D. Van den Poel, Churn prediction in subscription services: an application of support vector machines while comparing two parameter-selection techniques. *Exp. Syst. Appl.* **34**, 313–327. H. Cyben, Approximation by superpositions of sigmoidal (1998)

Intelligent Traffic Management in Emergency Situations



J. Rajesh, I. Naveen, A. Pravin, T. Prem Jacob, and G. Nagarajan

1 Introduction

Survey taken during past decade has unveiled a tragic up rise of increasing moral rate due to poor traffic management that acts as hindrance for rescue vehicle and delaying them from reaching their respective destinations on time. Rescue vans have a strict and important responsibility for maintaining a punctuality for arriving on time for rescue. There are various factors that affect current discussed issue. One of those factors is due to poor traffic management and insufficient personal that control or assist during emergency situation. Figure 1 shows the traffic situation. India is a developing country and contains many developing communities and administrative personal. This increase in economic value of an individuals' drives them to purchase valuable cars. This increasing number of automobiles makes it difficult manage. Recent reports suggest that there is decent reduce in administrative personal that could provide better advice thus increase the efficiency. And also by making the public come to know the present scenario, how the general problems the government facing to control.

J. Rajesh (✉) · I. Naveen · A. Pravin · T. Prem Jacob · G. Nagarajan
Department of Computer Science and Engineering, Sathyabama Institute of Science and Technology, Chennai, India
e-mail: jajjara12rajesh@gmail.com

I. Naveen
e-mail: naveen.inaganti248@gmail.com

A. Pravin
e-mail: pravin_ane@rediffmail.com

T. Prem Jacob
e-mail: premjac@yahoo.com

G. Nagarajan
e-mail: nagarajanme@yahoo.co.in

Fig. 1 Traffic issues as hindrance to rescue vehicles



To reduce this issue, many have introduced various devices that could provide better advices and thereby increasing efficiency. In our proposed system, we are going to add additional functionality that could help to clear traffic in other public areas. For providing better passage through traffic, we are going to implement a cloud-based application integrated to Arduino device that is connected to traffic management cloud database. For this, we can make use of Google-based maps. Due to improving technological parameters and demands, there are various inventions emerging in the society. We can take advantage of artificial intelligence provided by various map management applications to provide path that is chronologically better. By using Arduino electronic component as main computing device that process the information gathered. First, the input of dedicated path is fed into the driver's device providing most efficient path possible. The traffic management device present in the path will be alerted about the emergency and respective security measures are added to evade the risk situation. The main component will begin to execute the emergency protocol whenever the vehicle comes into the effective range. To provide a short-range communication between sender and receiver, we are going to use Bluetooth-oriented component like ZigBee. Using high aspect ratio camera, we can track the vehicle in high traffic zones. Additional functionality is also added into this device that would also alert other public areas like toll gates and hospitals to provide immediate aid to the patient. Further modifications can be done to the current system like integrating the system to a mobile device that would reduce device maintenance.

2 Related Works

The system for facing the traffic issues is proposed in a brilliant way [1]. Where the way he invented is making all the signals to be turned red, whenever the emergency vans went through the traffic area, then automatically the signals will be getting turned to green. When the van enters the corresponding zone by all the way, when the van is assigned a way in which makes all the traffic signals turns to green. So by this way, we can even make the way to emergency vehicles like ambulance, fire engines, and police vehicles, all belongs to emergency purpose vehicles [2–4]. There

are many ways for the emergency vehicles to make the changes. We invited this system to make the people know the problem, how hard to face the situation in the hard times. So to make the things happen and make the situation to be favor to the priority vehicles. Here, we invented the system not to change the system but can make at least a small change to the environment by helping them. This is one of the finest way to clear the problem and the system invented to help them to even reduce the small problem by this way. Even though we that there are ways to define many ways to, but making the way finest in single one is not such easy we should consider every single to be in and make the things to righteous way. The consideration is important here, making the lights change to green is the change we invented for vehicles.

A system called auto-controlling mechanism is proposed [5]. The main purpose in this mechanism is to make the things happen automatically without waiting for the commands or condition from some one. Here, main objective is to make things to be in a command-wise execution where it does not sit and wait for the command from some one. It automatically take the decisions based on the situation. Where it has some set conditions; when the condition's met by that system, it automatically takes the decision. It does not need any approvals and it checks for situations. Command of situations are listed to make it crystal clear [6, 7]. The main objective is only to make it user friendly and to help the environment. So this even helps in many ways by which using this technique, we can achieve many problems possible, where the mankind is not able to solve the problem or cannot enter the situations. There are many situations where humans cannot solve the issues or humans are enough to maintain the situations, so to make the things all happen even in the situations the humans cannot solve them can also be cleared and solved by taking the automatic decisions by it self is the best way to by setting the some sort of conditions to it [8, 9]. So that it can solve all of them.

A system on traffic management on which it works for managing the traffic [10]. Here, the objective of this system is to make some vehicles, van, cars, and some other which belong to the family of emergency auto mobiles. Here, we used a sensor called IR (Infra red) for this defining of vehicles. Which does senses the automobiles based on their priority defined in the system [11]. Whenever it detects, it automatically changes the light accordingly based on the situation present all over the surrounding; if the traffic is very high, then it automatically changes them to green based on the situation. For example, if we have a ambulance(or) fire engine in the way passing by, then whenever it enters to zone or surrounding of that sensor, then it automatically detects and changes the light to green. By making the light changing to green, there is no way for problem to that type of situations met. So by this, we can except some what change to those important automobiles. Another advantage is to the important vehicles such as government vehicles [5, 12]. For example, if any important government vehicles are passing by, we can manage the situation in an ample time and we can even reduce the man power with out wasting the time of humans. We can control the situation from a single standing position based on the situation and the admin can react immediately by accessing the device from a single place.

Proposed system M2M-based service coverage management [13, 14]. The importance of this system to make the signals and information and data from the devices or

notifications is received and replied automatically. The meaning of M2M is machine to machine, in which it works for sending the data from one end to another end based on the importance. Here, the device is to decide and give the signal to end user, who are sending the notifications then this device automatically gets connected to it and starts sending the information based on the query they requested for sends the related query which and where they are related for. It also have the quality of high frequency communication with one another in a single communication channel. Here, it establishes a separate channel secure the connect and makes the connection to stronger and send the reply frequently until the situation get resolved and it has also the option of checking the issue or incident is resolved or not. Proposed a system a RFID technology [6, 15]. The technology works on the part of traffic in which it was designed by keeping the standard methods, which are being normally faced by the environment outside every where. The ongoing activity gives the verdict of traffic police officer to be obliged. This device works for even multiple type of problems which are generally faced by the public outside. The process of this to main the key objective to be achieved. This system is invented for automatically things to happen. RFID is to fix in the vehicles when they met the situation. The technology was invented and developed by considering the general problems faced by, so to overcome that issues we invented this to overcome situations [16–18]. Here, the activity is to define and evaluate the particular thing has undergone in a excepted method or not, if any automobile consisting this device or technology automatically identified easily and getting the details of the particular vehicles does have all the information about. Nowadays, this system is automatically predefined or affixed during the manufacturing of product. This device also being already used by many motives presently in order to reduce the compatibility for present scenario outside.

3 Proposed System

Emergency reaction vehicles, for example, ambulances and fire engines, cannot wait idly while looking out for signals. These types of vehicles need a separate secure way to cross the signals immediately. That is why we are inventing this technology to be in lime light to overcome the situations commonly faced at signals by important vehicles. The device follows a technique to overcome the situations by checking the following condition; they are: vehicles passing on the way the after route splitting on three different ways the choosing the best way to be consider by calculation all the considerations to be taken under it, for example time taken, distance, route specifications, etc. And owner registers their primary secondary details on application which is connected to server which is a cloud-based technology and this is connected to pc server and the toll gate contains of ZigBee with LED and the automatic amount deduction from account.

The flowchart Fig. 2 consists of over all overview of this invented technology. The proposed idea utilizes IR as sensor interface. Versatile application is utilized for distinguishing proof of best course. Our proposed work is to actualize a similar idea

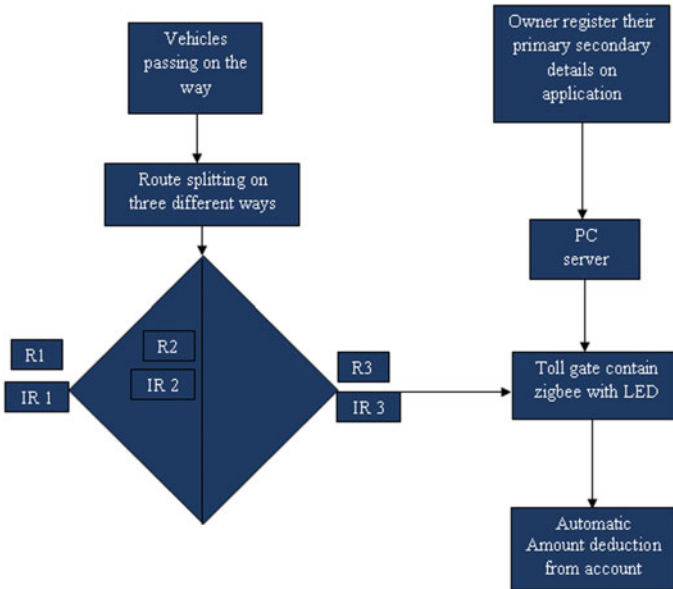


Fig. 2 Overview of the proposed system

to maintain a strategic distance from time squandering in the signs for emergency vehicle, however, utilizing ZigBee as the idea. The fundamental preferred position of utilizing ZigBee in the long scope of correspondence. Sings can be moved to green mode even the vehicle comes in the long range. IR is utilized for controlling the signals. Aside from this work, we likewise send ZigBee-based cost door installment robotization framework right now. Installment is taken naturally from the vehicle proprietors record even the vehicle originates from the long range from the cost door. Vehicle proprietor needs to give 2 records, sum would be consider, on the off chance that there is no adequate equalization, and at that point, the sum would be taken from the second record consequently. We likewise send android application for best course just as for cost installment framework.

4 Device Components

Arduino

It is a single-board microcontroller device used for building digital devices. Here, Fig. 3 explains the device. It takes its input from various sensors. Arduino will settle on choices dependent on information given in the sensor. Arduino is a small-scale controller to which sensors are associated. It tends to be bought either on the Web or in any store. Arduino appears as though a Mastercard estimated board. There are numerous forms of Arduino. They are available in various forms. For now, we

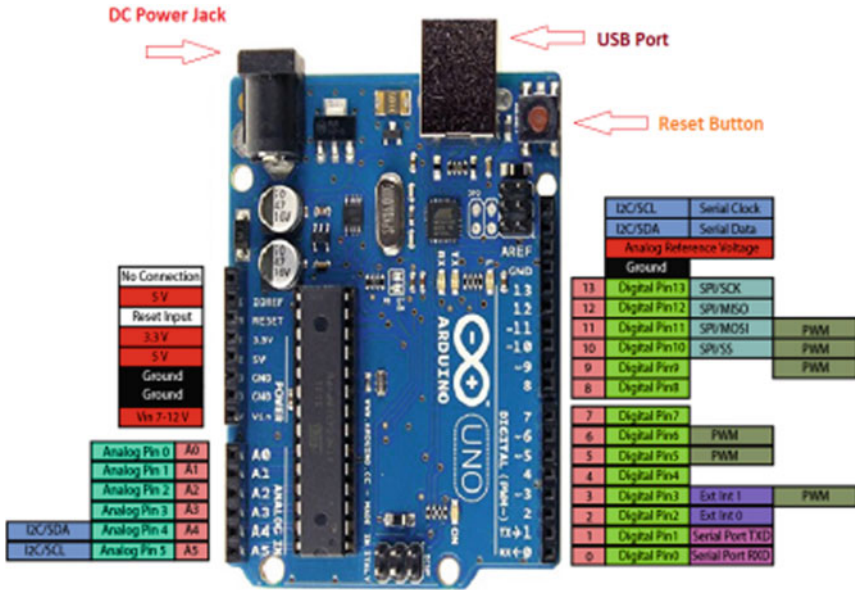


Fig. 3 Arduino UNO

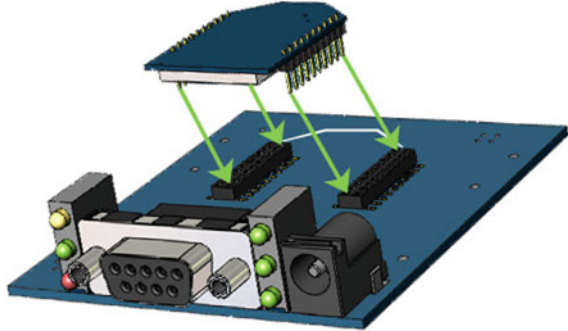
are going to use Uno master board. This circuit component acts as main computing component in the proposed architecture.

It is a single-board microcontroller device used for building digital devices. Here, Fig. 3 explains the device. It takes its input from various sensors. Arduino will settle on choices dependent on information given in the sensor. Arduino is a small-scale controller to which sensors are associated. It tends to be bought either on the Web or in any store. Arduino appears as though a Mastercard estimated board. There are numerous forms of Arduino. They are available in various forms. For now, we are going to use Uno master board. This circuit component acts as main computing component in the proposed architecture.

ZigBee

ZigBee is a Bluetooth-style-oriented device that provides short-range communication. Figure 4 component or device provides low data rate transfer suitable for small-scale projects. They are used to create a personalized area network and device maintenance. It is also called IEEE 802.15.4. In current project, we are going to use ZigBee interface to provide a short-range communication between vehicle and traffic checkpoint. This allows betterment in traffic flow in emergency situations. These ZigBee components are less expensive than other communication modules. Applications of ZigBee are basic home automations, data collection device for medical devices, and many others.

Fig. 4 ZigBee component



5 Results and Discussion

- Better traffic management during emergency situations.
- Replaces the issue of insufficient administrative personal.
- Reduction of mortality rate.
- Increase in efficiency of various emergency service provider by removing the traffic hindrance.
- Existing arrangements consideration of individuals by which they can facilitate and move according to the situations and help the important vehicles like ambulance or fire engines.
- Emergency vehicles to be pass by easily during the traffic blockages is by making the traffic clear by the way in which the important or emergency vehicles are going on before it arrives to the exact traffics point.
- We can clear the way and automatically changing the traffic light to green and remaining to red making the way to emergency automotive.
- Device components can be access and is open for cyber-attack; thus, decreases the liability of the proposed architecture.
- Initially, the device maintenance is difficult. To resolve this issue, we can implement this system protocol through mobile devices thereby increasing accessibility.

6 Conclusion

Thus, we have implemented the proposed system using various individual electronic components like Arduino, Zigbee, and sensors. Future work can be done to improve the functionality of the current device by integrating it into various available platforms. This version of system can be minimized to be implemented on any various other situation. We can add urgency value to report the priority value of the situation in other events and report it to respective department.

References

1. R. Saravanan, P.V. Paul, M. Nivedha, B. Nirosha, Optimal path planning and traffic signal control system for emergency vehicle—a survey, in *2017 International Conference on Computation of Power, Energy Information and Communication (ICCPR)* (Melmaruvathur, 2017), pp. 283–289
2. A.K. Mittal, D. Bhandari, A novel approach to implement green wave system and detection of stolen vehicles, in *2013 3rd IEEE International Advance Computing Conference (IACC)* (Ghaziabad, 2013), pp. 1055–1059. <https://doi.org/10.1109/IAdCC.2013.6514372>
3. Y. Moroi, K. Takami, A method of securing priority-use routes for emergency vehicles using inter-vehicle and vehicle-road communication, in *2015 7th International Conference on New Technologies, Mobility and Security (NTMS)*, Paris, in the year of conference paper published 2015, pp. 1–5. <https://doi.org/10.1109/NTMS.2015.7266466>
4. N. Srinivasan, C. Lakshmi, A novel prediction based tree structured data using machine learning techniques. *Res. J. Pharm. Biolog. Chem. Sci.* **7**(5), 527–531 (2016)
5. R. Anand, et al. Middle where: a middleware for location awareness in ubiquitous computing applications, in *ACM/IFIP/USENIX International Conference on Distributed Systems Platforms and Open Distributed Processing* (Springer, Berlin, Heidelberg, 2004)
6. N. Shlayan, K. Challapali, D. Cavalcanti, T. Oliveira, Y. Yang, A novel illuminance control strategy for roadway lighting based on greenshields macroscopic traffic model. *IEEE Photon. J.* **10**(1), 1–11 (2018) (Where it is the Only Method to Automate). Art no. 8200211. <https://doi.org/10.1109/JPHOT.2017.2782801>
7. S. Shuo, H. Tian, Y. Zhai, Design of intelligent traffic light controller based on VHDL, in *2009 Second International Workshop on Knowledge Discovery and Data Mining* (Moscow, 2009), pp. 272–275. <https://doi.org/10.1109/WKDD.2009.19>
8. Q. Ye, J. Song, Z. Yang, L. Wang, Emergency vehicle location model and algorithm under uncertainty, in *2011 2nd IEEE International Conference on Emergency Management and Management Sciences*, Beijing, by the way here the paper discusses as to regulate the vision in year 2011, pp. 1–4. <https://doi.org/10.1109/ICEMMS.2011.6015604>
9. N. Wang, Y. Qiao, W. Wang, S. Tang, J. Shen, Visible light communication based intelligent traffic light system: designing and implementation, in *2018 Asia Communications and Photonics Conference (ACP)*. Hangzhou, Designed to Make Ways Simpler Way to Communicate and Contact Each Other 2018, pp. 1–3. <https://doi.org/10.1109/ACP.2018.8595791>
10. N. Díaz, J. Guerra, J. Nicola, Smart traffic light control system, in *2018 IEEE Third Ecuador Technical Chapters Meeting (ETCM), and Cuenca, has Published Paper in the Year 2018 were Having Extent*, pp. 1–4. <https://doi.org/10.1109/ETCM.2018.8580282>.
11. B. Pratama, J. Christanto, M.T. Hadyantama, A. Muis, Adaptive traffic lights through traffic density calculation on road pattern, in *2018 International Conference on Applied Science and Technology (iCAST)*. Manado, Indonesia, and Some Other International Journals Had Discussed About the Traffic Management in the Year 2018, Hence Most of the Paper Released on the Settle Down the Issues of Traffic, pp. 82–86. <https://doi.org/10.1109/iCAST1.2018.8751540>
12. R.S.B. Krishna, M. Aramudhan, Feature selection based on information theory for pattern classification, in *2014 International Conference on Control, Instrumentation, Communication and Computational Technologies (ICCICCT)*. IEEE, July 2014, pp. 1233–1236
13. H. Zhao, J. Leng, G. Ma, Research on highway emergency vehicle dispatching model, in *2009 International Conference on Measuring Technology and Mechatronics Automation, Zhangjiajie, Hunan, 2009, to Automate the High Management and Maintenance in the Proper Method Explanation*, pp. 296–299. <https://doi.org/10.1109/ICMTMA.2009.216>
14. M.L. Suarez, et al., Dynamic allocation of traffic light plans as a traffic reduction strategy, in *MOVICI-MOYCOT 2018: Joint Conference for Urban Mobility in the Smart City* (Medellin, 2018), pp. 1–7. <https://doi.org/10.1049/ic.2018.0012>

15. S.C. Mana, A feature based comparison study of big data scheduling algorithms, in *2018 International Conference on Computer, Communication, and Signal Processing (ICCCSP)* (Chennai, 2018), pp. 1–3
16. T. Anandhi, K.V. Kishore, G.S. Maha, R.M. Gomathi, A sustainable vehicle parking using IoT, in *2019 3rd International Conference on Trends in Electronics and Informatics (ICOEI)*. IEEE, Apr 2019, pp. 950–952
17. K.E. Gnanesh, T. Dheeraj Bhavan Narayana, M.D. Kamalesh, Retrieval of encrypted data using trapdoor method in cloud computing. *J. Comput. Theoret. Nanosci.* **16**(8), 3237–3241 (2019)
18. S.P. Shyry, Efficient identification of bots by *K*-means clustering, in *Proceedings of the International Conference on Soft Computing Systems* (Springer, New Delhi, 2016), pp. 307–318

Dengue Prediction Using Machine Learning Techniques



O. Shireesha, P. Hema Sri, T. Prem Jacob, G. Nagarajan, and A. Pravin

1 Introduction

Dengue is a mosquito-borne affliction achieved by the dengue contamination spread by the *Aedes* mosquito, and the disease is progressively fundamental in tropical regions.

Simply female mosquitoes spread the disease, and it eats both outside and inside homes during daytime. Dengue is, in any case, called the ‘breakbone fever’ as the earnestness of the distress achieved by this devastating affliction resembles the torment realized by breaking of a bone.

Protecting yourself from getting snacked by mosquitoes is the best well-being measure you could take to save yourself from dengue. You can moreover prevent the raising of the mosquitoes by discarding old oil drums, window boxes, and tires and compartments.

Data mining is a computer science term. It is also sometimes used called knowledge discovery in databases. Data mining consists of finding new ones in many, and

O. Shireesha (✉) · P. H. Sri · T. Prem Jacob · G. Nagarajan · A. Pravin
Department of Computer Science and Engineering, Sathyabama Institute of Science and
Technology, Chennai, India
e-mail: reddyshireesha.23@gmail.com

P. H. Sri
e-mail: srihemaparvathaneni@gmail.com

T. Prem Jacob
e-mail: premjac@yahoo.com

G. Nagarajan
e-mail: nagarajanme@yahoo.co.in

A. Pravin
e-mail: pravin_ane@rediffmail.com

the information obtained from data mining is expected to be new and useful. In many cases, the data is archived so that it can be used later. The data is saved with a target.

A shop wants to save what has been purchased. They want to do it to know how much they should buy, to have enough to sell later. Saving this information generates a lot of data. For data, there are many different types of data mining to get new information. Only female mosquitoes transmit the disease and tidbits both inside and outside homes during the day.

Dengue is also known as ‘fracture fever’ since the severity of the torment caused by this disease of disability is like the torment caused by the bone fracture. To avoid dengue, you can also prevent mosquito breeding by removing old bins, pots, tires, and holders. The spread of dengue can eventually be controlled by improving cleanliness, and the disease is transmitted when a mosquito bites the contaminated individual and similar mosquito chews on a healthy person.

2 Related Work

Sathya et al. [1] dengue is an alarming illness realized by youngster mosquitoes. It is regularly found in vast hot regions. From a long haul of time, experts are endeavoring to find some of the characteristics of dengue malady with the objective that they can properly arrange patients considering the way that different patients require different sorts of treatment. Pakistan has been a focal point of dengue infection from the latest couple of years. Dengue fever is used in gathering frameworks to evaluate their exhibition. The dataset was aggregated from lotus and 24 thought crisis centers [2, 3]. For suitably organizing our dataset, distinctive grouping strategies are used. Assess the show of the significant number of procedures singular subject to tables and diagrams depending on the dataset.

Kamran Shaukat et al. [4, 5] represent the extraction of dengue infection data using the decision tree in which each dataset is composed. To carry out the information disclosure task, we consider using the options tree as an information extraction device. We offer many important qualities of transitional information. Our tests are divided into four sections. The two initial test results demonstrate the valuable information to characterize dengue disease from two separate datasets. Another goal of this exploration is to recognize the day of fever defervescence, which is called day 0. Toward the end, we acquire extremely low accuracy on day 4 when we discover that the tree is too fit. The test results showed that the tree of choice approach is sometimes not up to this task in this way, we believe we should choose another grouping approach later in the work.

Subitha et al. [6] represent the grouping procedures to decide the number of inhabitants in cases contaminated by dengue fever in the city of Jhelum and the territories they cover topographically. In this way, we can think of running distinctive array systems. The goal of this survey also includes the correlation of numerous grouping calculations with the help of graphs, given our dataset. We have updated all the strategies using the weka device, and the whole execution system is inside

it. Toward the end, after examining our dataset with each method, they eventually resemble us. The moment we did the exam between each of them, we deduce that Bayes' innocent technique is most remarkable among all the others.

Mufli Muzakki et al. [7] In this article, they proposed the DHF conjecture in Bandung Regency using K -means clustering as a method of preprocessing and estimation of the support vector machine (SVM). The data used in the evaluation of the Meteorological, Climate and Geophysical Agency in the Bandung Regency. Atmosphere data can be used to predict DHF disease because there is an association between the ownership of the atmosphere and DHF disease [8–11]. The technique of the K -means clustering brand shows an accuracy of more than 86%.

3 Existing System

The machine can anticipate maladies however cannot foresee the subtypes of the infections brought about by the event of one sickness. It neglects to foresee every single imaginable state of the individuals. The current framework handles just organized information [12, 13]. The forecasting framework is wide and uncertain. In the momentum past, endless sickness gauge characterizations have been progressed in the method. The standing associations mastermind a mix of machine learning which is reasonably definite in visualizing illnesses [14, 15]. Be that as it may, the restriction with the overall frameworks is dotted. To begin with, the predominant frameworks are dearer just rich individuals could pay for to such figuring frameworks. Furthermore, concerning people, it turns out to be much higher [16, 17]. Second, the supposition frameworks are vague and inconclusive up until now. Along these lines, a machine can visualize a positive infection however cannot expect the subtypes of the illnesses and maladies brought about by the presence of one bug. For the event, if a gathering of individuals is predicted with diabetes, without a doubt some of them may have an intricate hazard for heart infections because of the reality of diabetes [18, 19]. The rest of the plans neglect to predict all conceivable environmental factors of the tolerant.

4 Proposed System

In the proposed work, Naïve Bayes machine learning algorithm predicts the dengue disease. It is implemented to increase operational efficiency. It reduces query retrieval time. Accuracy is improved using a data mining algorithm. The proposed system begins with the thought that was not executed by the ancestors. Therefore, this research aimed to develop an accurate model that could better detect early signs and symptoms of dengue fever and a practical system for self-notification of the disease.

User Module: This is the primary movement that opens the site. The client needs to give the right contact number and a secret key, which the client enters while enrolling, to log in to the application. On the off chance that the data furnished by the client matches with the information in the database table, then the client effectively log in into the application else message of login fizzled is shown and the client needs to return the right data. A connection to the enlisted movement has additionally accommodated the enrollment of new clients.

In this paper, the customer stress was predicted by supervised machine learning algorithms mainly using linear discriminant analysis (LDA), support vector machine (SVM), and the accuracy value will take by comparing the best of each accuracy values.

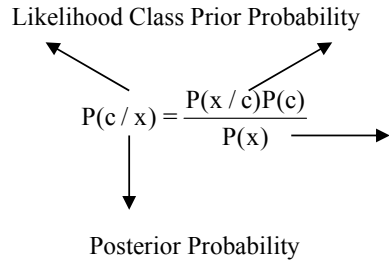
Registration Module: Another client who needs to get to the site needs to enroll first before login. By tapping on the register button in the login movement, the enlisted action gets open. Another client enlists by entering the complete name, secret word, and contact number. A client needs to enter the secret word again in affirm secret phrase textbox for affirmation. At the point when the client enters the data in all content boxes, on the snap of the register button, the information is moved to the database, and the client is coordinated to log in action once more. The enrolled client then needs to log in to get to the application. Approvals are applied to all the textboxes for the correct working of the application. As the data in each textbox is must that is each textbox, possibly it is of name, contact, secret key or affirms secret key, will not be vacant while enlisting. On the off chance that any such textbox is the void application will give a message of data is should in each textbox. Additionally, information in the secret phrase and affirm secret word fields must counterpart for fruitful enrollment. Another approval is contact number must be a legitimate one that is of ten digits. If any such approval is damaged, at that point, enrollment will be ineffective, and afterward, the client needs to enlist once more patient should login into the app with some information when he miss the some fields it will show that one of the field is vacant. On the off chance that all such data is the right client will be coordinated to login action for login into the application.

Admin Module: In this module, the admin can add and view new doctor details, disease details, and drug details. And then admin can view feedback provided by various users.

5 Naïve Bayes Algorithm

It is a classification technique based on Bayes' theorem with an assumption of independence among predictors. In simple terms, a Naïve Bayes classifier assumes that the presence of a particular feature in a class is unrelated to the presence of any other feature. For example, a fruit may be considered to be an apple if it is red, round, and about 3 in. in diameter. Even if these features depend on each other or upon the existence of the other features, all of these properties independently contribute to the probability that this fruit is an apple and that is why it is known as 'Naïve'.

Fig. 1 Posterior probability



Naïve Bayes model is easy to build and particularly useful for very large datasets. Along with simplicity, Naïve Bayes is known to outperform even highly sophisticated classification methods. Bayes’ theorem provides a way of calculating posterior probability $P(c|x)$ from $P(c)$, $P(x)$ and $P(x|c)$. Look at the equation shown in Fig. 1:

- $P(c|x)$ is the posterior probability of class (c , target) given predictor (x , attributes).
- $P(c)$ is the prior probability of class.
- $P(x|c)$ is the likelihood which is the probability of predictor given class.
- $P(x)$ is the prior probability of predictor.

6 System Architecture

The datasets collected from customers by using different attributes along with customer stress. The datasets will split into test and train data. 80% of datasets will split to train, and 20% of datasets will split to test. First we have to train the data and we have to test the machine after that we have to go for preprocessing that means we have to remove the unwanted data. The data should be classified based on the conditions. After the classification, the data is transferring to Naïve Bayes algorithms. The algorithm will check different accuracy values. By comparing the accuracy value of the algorithm, we come to know the patient results (Fig. 2).

7 Results and Discussion

See Figs. 3, 4, 5, 6 and 7.

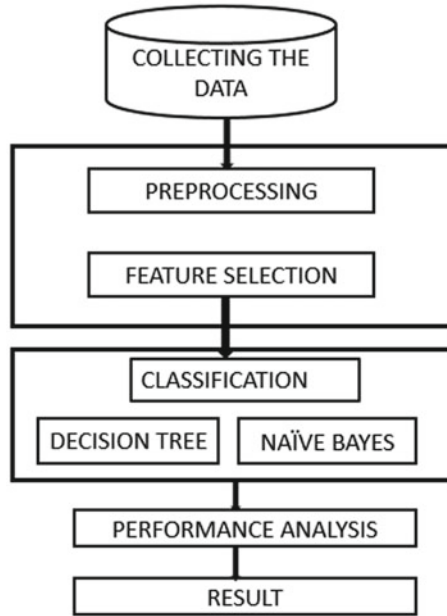


Fig. 2 Architecture

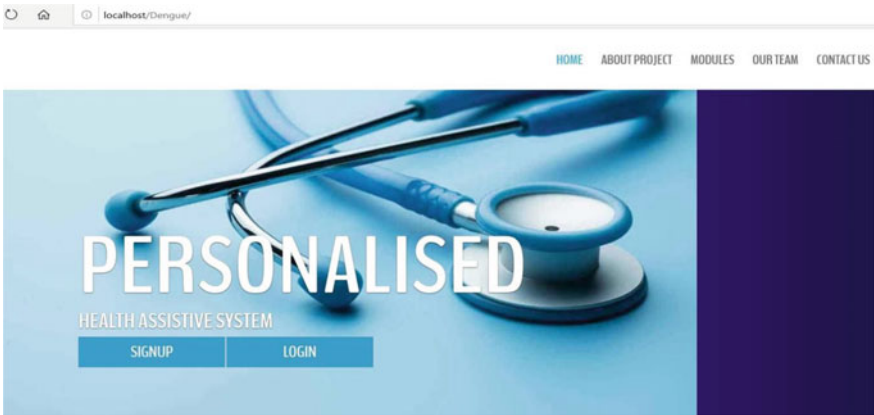


Fig. 3 Home page of the dengue prediction

8 Conclusion

The dataset is a collection of data or a single statistical data in which each data attribute represents a variable and each instance has its description. For the prediction of dengue disease, the dengue dataset is used for predicting and classifying

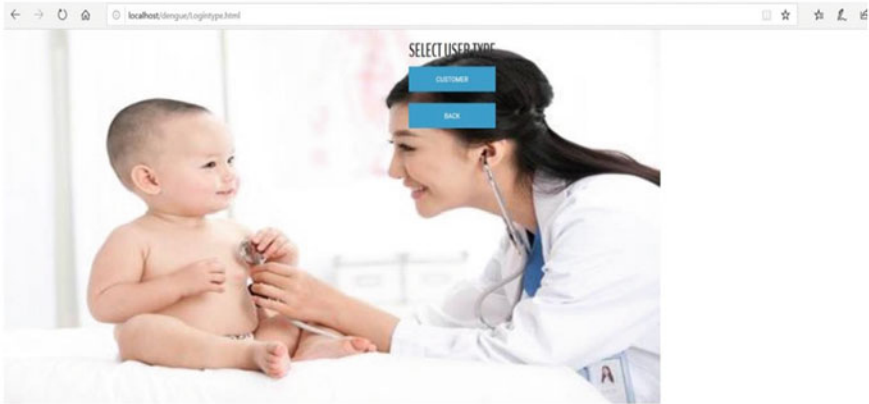


Fig. 4 Screenshot describes the selection of customer

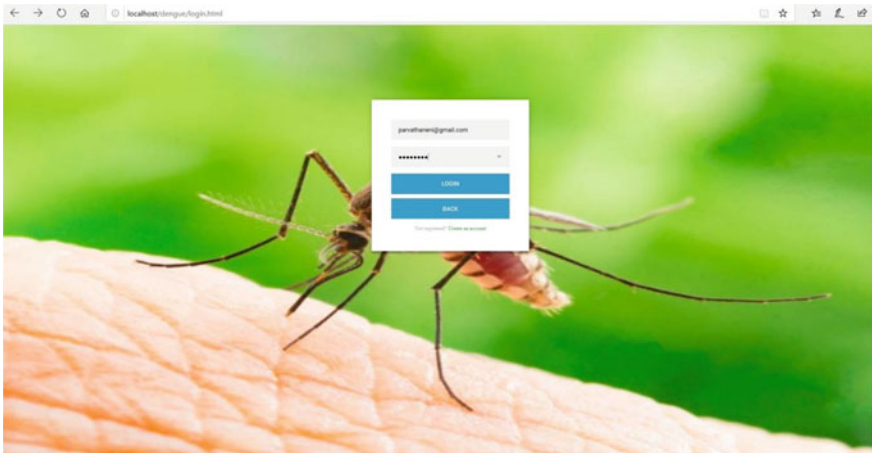


Fig. 5 Screenshot illustrates that the person can provide his/her information

algorithms to compare its accuracy using the data mining technique. The dengue fever dataset contains the classification and accuracy of dengue disease. Apply classification algorithms using a data mining tool for analysis purposes. In this document, we propose an approach to answer questions about medications to support prescription drugs. Our focus is on how to obtain and classify responses based on incomplete information and provide personalization. To handle incomplete and noisy data, we allow exact and close matches when answering questions. We also present an intuitive approach to show responses to users, the goal of which is to help users understand classified and possibly results refine your questions.



Fig. 6 In this page, we can select symptoms regarding a patient’s condition

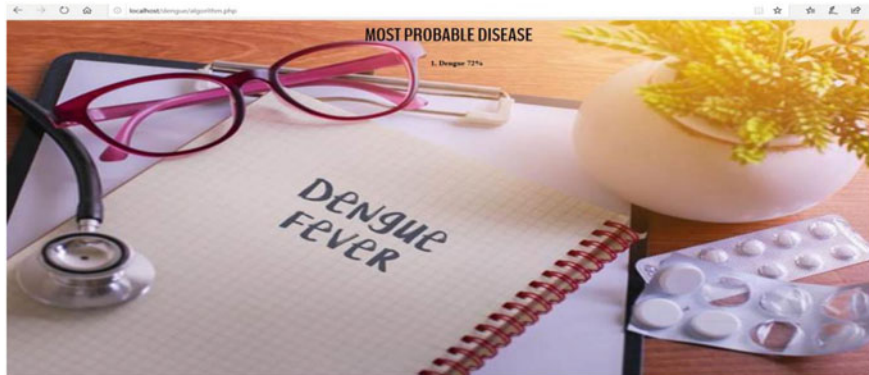


Fig. 7 Image shows the accuracy values of dengue fever

References

1. P. Manivannan, P. Isakki, Dengue fever prediction using K-means clustering algorithm, in *IEEE International Conference on Intelligent Techniques in Control, Optimization and Signal Processing*, 978-1-5090-4778-9/17/©2017
2. I.I. Wiratmadja, S.Y. Salamah, R. Govindaraju, *J. Eng. Technol. Sci.* **50**(1), 110–126 (2018)
3. M.A. Chowdary, M. Kundan, D.A.V.A. Mary, Effective credit card forgery prevention using multilevel authentication. *IOP Conf. Ser. Mater. Sci. Eng.* **590**(1), 012021 (2019) (IOP Publishing)
4. P. Mekha, K. Osathanunkul, et al., in *Gene Classification of Dengue Virus Type Based on Codon Usage*, 978-1-5090-4420-7/16/ ©2016 IEEE
5. T. Anandhi, K.V. Kishore, G.S. Maha, R.M. Gomathi, A sustainable vehicle parking using IoT, in *2019 3rd International Conference on Trends in Electronics and Informatics (ICOEI)*. IEEE, Apr 2019, pp. 950–952

6. A.M. Najar, M.I. Irawan, et al., Extreme learning machine method for dengue hemorrhagic fever outbreak risk level prediction, in *IEEE International Conference on Smart Computing and Electronic Enterprise (ICSCEE2018)* ©2018
7. M. Muflī Muzakki, F. Nhita, The spreading prediction of dengue hemorrhagic fever (DHF), in Bandung regency using *K*-means clustering and support vector machine algorithm, in *6th International Conference on Information and Communication Technology* (2018)
8. K.E. Gnanesh, T. Dheeraj Bhavan Narayana, M.D. Kamalesh, Retrieval of encrypted data using trapdoor method in cloud computing. *J. Comput. Theoret. Nanosci.* **16**(8), 3237–3241 (2019)
9. S.P. Shyry, Biometric-based three-tier microservice architecture for mitigating the fraudulent behaviour, in *Proceedings of the 2nd International Conference on Communication, Devices and Computing* (Springer, Singapore, 2020), pp. 399–404
10. R.S.B. Krishna, M. Aramudhan, Feature selection based on information theory for pattern classification, in *2014 International Conference on Control, Instrumentation, Communication and Computational Technologies (ICCICCT)*. IEEE, July 2014, pp. 1233–1236
11. N. Srinivasan, C. Lakshmi, Stock price prediction using rule based genetic algorithm approach. *Res. J. Pharm. Technol.* **10**(1), 87–90 (2017)
12. P.S. Songkok, H.A. Wibawa, et al., Performance comparison of artificial neural network models for dengue fever disease detection, in *1st International Conference on Informatics and Computational Sciences (ICICoS)* (2017)
13. S.C. Mana, A feature based comparison study of big data scheduling algorithms, in *2018 International Conference on Computer, Communication, and Signal Processing (ICCCSP)* (Chennai, 2018), pp. 1–3
14. B. Omkar, D. Preet, et al., *Int. Res. J. Eng. Technol. (IRJET)* 04(10) (2017)
15. R. Yogitha, G. Mathivanan, Performance analysis of transfer functions in an artificial neural network, in *2018 International Conference on Communication and Signal Processing (ICCSP)*. IEEE, Apr 2018, pp. 0393–0397
16. N.M. Zainee, K. Chellappan, A preliminary dengue fever prediction model based on vital signs and blood profile, in *IEEE EMBS Conference on Biomedical Engineering and Sciences (IECBES)* (2016)
17. K. Sangeetha, P. Vishnuraja, D. Deepa, Stable clustered topology and secured routing using mobile agents in mobile ad hoc networks. *Asian J. Inf. Technol.* **15**(23), 4806–4811 (2016)
18. N. Mathur, V.S. Asirvadam, Visualization of dengue incidences using expectation-maximization (EM) algorithm. *IEEE 978-1-5090-0845-2/16/© 2016*
19. T. Marimuthu, V. Balamurugan, A novel bio-computational model for mining the dengue gene sequences. *Int. J. Comput. Eng. Technol. (IJCET)* **6**(10), 17–33 (2015). Article ID: IJCET_06_10_003

Twitter Data Analysis for Live Streaming by Using Flume Technology



Vissamsetti Mohan Manoj, Yalamandala Prasanth, T. Prem Jacob, G. Nagarajan, and A. Pravin

1 Introduction

Twitter is among the largest social media sites, tweets in millions on different platforms every day. Social media is quite popular as well as an exciting platform to express your viewpoints as well as different kinds of ideas globally just by sitting at one place [1, 2]. Being a passive application, we can follow the tweets of a person and will reach us through a notification [3, 4]. Twitter will generate nearly 1 TB of text data in the form of tweets [5]. There is an option on Twitter to follow the tweets of persons that you admire [6]. It is being essential for business purposes while clients, as well as customers, are recurrent Twitter users as well as expected to follow the feeds [7–10]. Twitter is been one of the trending social media, and their updates will be instantly posted to the Twitter feed [11, 12]. The facility to tweet using mobile phones also permits to continue this real-time linking does not matter where you are present [13]. The requirement is to have an account in a device that has Internet connectivity [14]. All this process will be under the extraction module. In the transformation module, the data which we extracted will be transformed into

V. Mohan Manoj (✉) · Y. Prasanth · T. Prem Jacob · G. Nagarajan · A. Pravin
Department of Computer Science and Engineering, Sathyabama Institute of Science and Technology, Chennai, India
e-mail: vmohanmanoj.avg.9@gmail.com

Y. Prasanth
e-mail: prasanthyalamandala99@gmail.com

T. Prem Jacob
e-mail: premjac@yahoo.com

G. Nagarajan
e-mail: nagarajanme@yahoo.co.in

A. Pravin
e-mail: pravin_ane@rediffmail.com

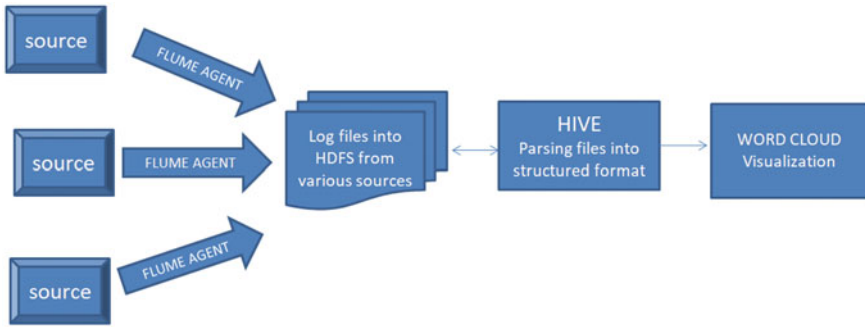


Fig. 1 System architecture

the normal text using hive which is constructed on the top of Hadoop [15, 16]. Based on the analyzed data, it will be visualized using a Word Cloud based on repeated words [17–19] (Fig. 1).

The most repeated word will be displayed in higher font size, and based on the total number of times, the word is repeated in the analyzed data. Several times the word recurs in tweets will have a higher font size. Least times the word has recurred in tweets will have the lower font size. The most repeated words will be displayed in the central position of the Word Cloud.

2 Related Work

Any process that has to be done continuously for the analysis of data has been produced continuously. The process is to focus on how data generated from Twitter can be mined and utilized by different companies to make targeted, real-time and informed decisions about their product that can increase their market share or find out the views of people on a specific topic of interest.

Barskar and Phulre [1]: Opinion mining of Twitter data using Hadoop and apache pig: It is mainly used for knowing the opinions for a particular situation.

This method composed of an HDFS system based on Hadoop echo system and MapReduce functions for sentimental analysis.

Pooja et al. [7]: Sentiment analysis on Twitter Data Using Apache Flume and Hive: The data which we extracted from Twitter will be stored in the Hadoop distributed file system in the format of JSON. The data which we extracted from Twitter will be stored in the Hadoop distributed file system. By using the user-defined functions, we are going to convert the other format to a structured format, and analysis also was done using that function.

Kavitha et al. [11]: Discovery Public Opinion by Execution of Sentimental Analysis on Real-Time Twitter Data: In this paper, they are visualizing the data through a bar chart using Hadoop framework and corresponding its tools.

3 Overview of Hadoop Framework

Hadoop gives the agenda for handling the large clusters of data, and it is also termed as the ecosystem for all the open-source projects. The large data sets also processed by the assistance of the Hadoop in distributed computing. Hadoop contains Hadoop distributed file system (HDFS) as well as connected to handling huge data. MapReduce as well as (HDFS) are the primary components of Hadoop. To handle more amount of data, different computers connected as a single system. Such computer clusters meant for Hadoop are known as Hadoop clusters. These clusters will execute in low-cost commodity computers. The Hadoop architecture is composed of the huge Hadoop clusters that are organized in various racks. In each record, there will be master machines and slave machines. Job trackers are referred to as masters as well as some machines work as name node. They are favoring with more RAM and CPU and less storage. Task trackers and data node are mentioned as slaves, and these slaves have huge storage at the local disk as well as modest totals of CPU along with RAM. Job trackers will be under the map to reduce components. Secondary name, as well as name node, will be under the HDFS component. The client neither plays the role of a slave nor a master for loading the data within the cluster, acquiesce, MapReduce jobs, retrieve the data to observe the response afterward the job is done. The master is made up of three main parts name and secondary name node, job tracker. Name node holds the metadata for HDFS like which part of the file is stored in which portion of the cluster, block information and user permissions. When in use all this information is stored in ram, but this information also stored in disk for persistence storage (Fig. 2).

Hive is the infrastructure instrument of data warehouse for processing the organized data in Hadoop. It stores its data in his system. Hive stores its meta store in one RDBMS database. It exists at the top of Hadoop to recapitulate the big data, as well as generates queries as well as analyzes it effortlessly. In a database, the schema is stored by the Hive as well as it also processes the data in HDFS. An SQL query language is provided by Hive and is called as HQLor HIVEQL. It owns data in the Hive table means it is called a Hive internal table.

It does not own the data. This means it is a part of Hive, HDFS only owns the external Hive tables. To create the external table, it is required to use an external keyword. An external table is a way to protect data against accidentally drop commands. It provides a bucketing concept, another technique for decomposing table sets into manageable parts. Joins can also be performed using it.

Apache Flume is a tool to collect, aggregate as well as transport the huge quantities of streaming data like events, log files from different sources to the centralized data storage unit. It is a system utilized for transmitting huge amounts of streaming data within the HDFS. Accumulating log data existing in the log files from the Web servers as well as combining it in HDFS for its analysis is the main usage of this system. There are few Flume components lists event, client, agent, source, channel and sink.

An event is a fundamental unit of data transported like single log entry or a tweet by a Flume from its originating points to the destination. The client produces data

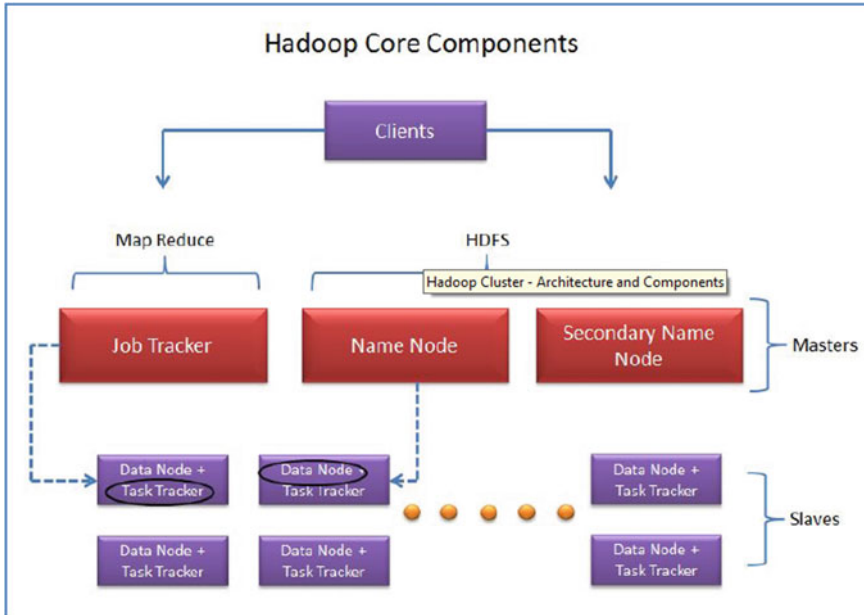


Fig. 2 Hadoop core component

in the form of events. The agent is referred to as a self-governing JVM process that can host components of Flume like sinks, channels as well as sources.

Therefore, provided with the capability of collecting, storing as well as forwarding events from one place to another. The source is an active component that receives the event and places it in the channel. Channel is a passive component that buffers the event and sends it to the sink. The method Flume agents use to transfer events from their sources to destination. Sink removes the event from a channel as well as move them to the upcoming agent to the event's final destination or in the flow Flume pushes data to the sink because of which writes to sink can overwhelm data read from sinks.

Javascript Object Notation is a lightweight and data-interchange notation. It is primarily utilized for transmitting data between the server as well as the web application. JSON is used for storing as well as organizing the content generated with the help of CMS at the site. It is a self-governing data format and is the best substitute for XML.

Word Cloud is a visualization tool to act easily. The more exact a word seems in the source of text, the bolder and bigger it looks in the cloud of words. It is the group or cluster of the words shown in unique sizes. If the word appears in a bigger size as well as bolder, the more frequently it is declared in the text provided. These are the ideal methods to highlight the relevant portions of the data in the textual form from blogs to databases. Significant textual data points can be highlighted using a Word Cloud (Fig. 3).

Fig. 3 Visualization of the Word Cloud



Twitter Application Creation, extract the tweets, we have to make a Twitter application. The creation of the Twitter application is as follows.

Step 1: Initially, we have to sign in to the Twitter account as well as do little work with the Twitter application window in which we can manage, delete and create Twitter apps by navigating to the following link <https://apps.twitter.com>.

Step 2: From the above link, click on the button written with create New App. Then, you will be going to a window and has to fill your detail information to get an application.

Step 3: A new app will be created which is used to create Consumer and Consumer secret key, Access token and Access token secret used to edit in a Flume. conf. file. To fetch Twitter data which is lively tweeting in the account, these above-mentioned keys are used.

Step 4: In the details of the app, we can find the keys under keys and tokens. Out of which, consumer keys will be shown, and access tokens will be generated for every instance.

Step 5: Consumer Key, Consumer Secret, Access tokens are used to configure the Flume agent (Fig. 4).

4 Proposed Analyzation Incentive in Twitter

The proposed framework we have seen in the earlier papers the analysis of Twitter data has done to the log files. To overcome the drawbacks, we are using Hadoop as well as its ecosystems. For getting raw data from Twitter, we are using Apache Flume. We have utilized the standard platform as Hadoop on a single node Ubuntu machine for solving the problems related to the big data by the MapReduce framework. The Flume has been utilized to fetch the real-time data on Twitter as well as store it in HDFS. The condition for Flume as well as Hive is that Hadoop must be installed before its use. The format used to transfer the data between server and Web application is JSON. Hive is used to transform the data into text.

The workflow of the project is shown above, the data which is stored in sources will be extracted using the Flume agent and will be stored in a Hadoop environment. The extracted data will be in the format of JSON, as many tools have been developed

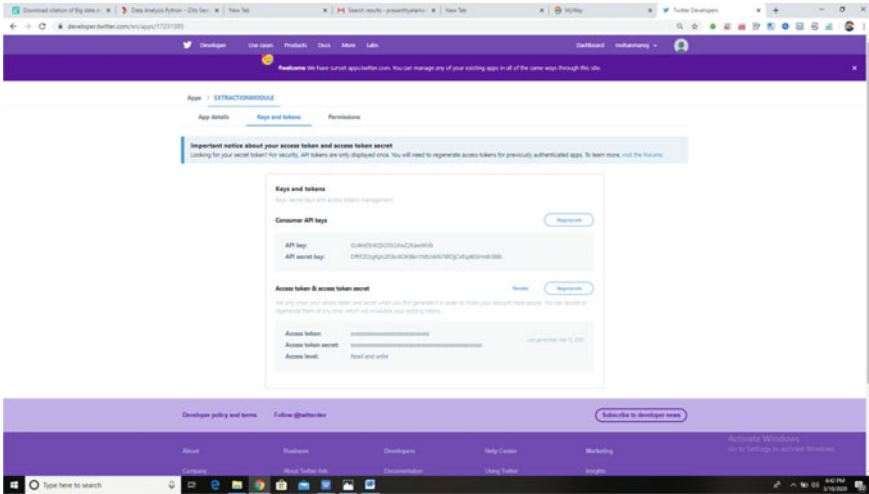


Fig. 4 Twitter keys and tokens

over the Hadoop to manage the data. Using the tools of Hadoop, we can manage the data to transform from semi-structured format to structured format. Each technology used in the above process is explained below.

The following procedure is used to achieve the purpose of the proposed system. The steps that include are

1. Initially, we have to create a Twitter app that includes the Twitter tokens which will be used for fetching real-time data.
2. The data will be extracted from Twitter using Flume technology, and it will be stored in local HDFS. The Twitter data comes from the site will be in an unstructured format known as JSON.
3. The analysis part will be done after storing Twitter data into HDFS, and the analysis part will be done using Hive. We can transform into a structured format using Hive.
4. The structured data will be in the form of text and will be visualized through Word Cloud using Python.

5 Results and Discussion

These are the commands required to extract Twitter data from the server of live streaming. The data extracted from Twitter will be in the format of JSON as shown in Figs. 5 and 6.

The Twitter data will be stored in the browsed directory (UNIX) as shown in Fig. 7.

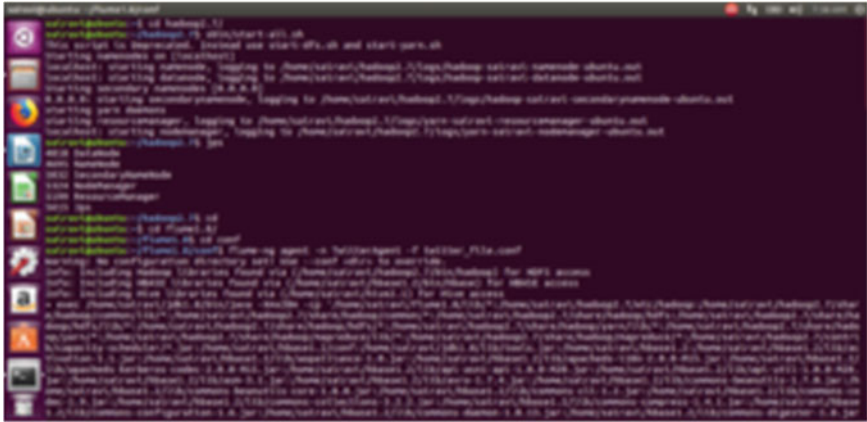


Fig. 5 Commands to extract Twitter data



Fig. 6 Twitter data in the format of JSON

6 Conclusion

Previously, the data of Twitter in which we analyzing was a log file. To achieve this, we have to perform a code of lines coding to achieve this. To perform sentimental analysis on stored data we have to perform complex operations. Here we can extract Twitter data of live streaming by using Flume. The extracted Twitter data file has to be transformed from JSON format to text format using Hive. From this approach, we can perform a task in less time. Visualization can be done using a Word Cloud.

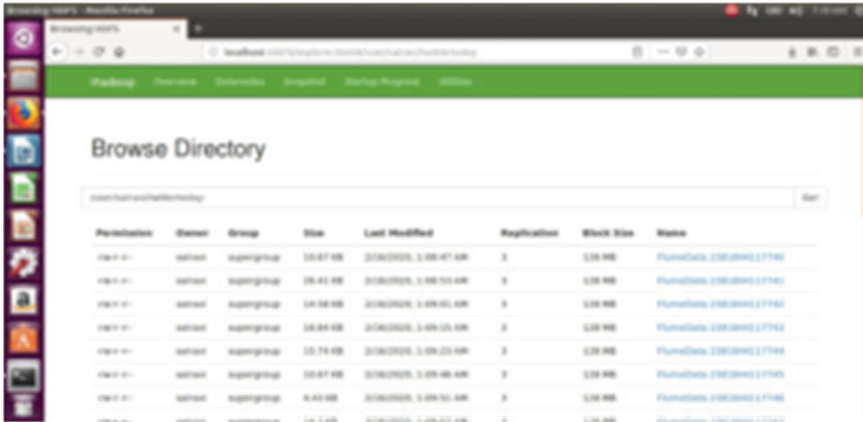


Fig. 7 Data fetched from Twitter and sank into HDFS

References

1. A. Baskar, A. Phurle, Opinion mining of twitter data using Hadoop and apache pig. *Int. J. Comput. Appl. (IJCA)* 158(9) (2017)
2. S.P. Shyry, Biometric-based three-tier microservice architecture for mitigating the fraudulent behaviour, in *Proceedings of the 2nd International Conference on Communication, Devices and Computing* (Springer, Singapore, 2020), pp. 399–404
3. A.S. Nagdive, R.M. Tugnayat, G.B. Regulwar, D. Petkar, Web server log analysis for unstructured data using apache flume and pig. *Int. J. Comput. Sci. Eng. (JCSE)* 7(3) (2019). e-ISSN:2347-2693
4. T. Anandhi, K.V. Kishore, G.S. Maha, R.M. Gomathi, A sustainable vehicle parking using IoT, in *2019 3rd International Conference on Trends in Electronics and Informatics (ICOEI)*. IEEE, Apr 2019, pp. 950–952
5. S. Sharma, S. Kumar, Sentimental analysis on twitter posts using Hadoop. *Int. Res. J. Eng. Technol. (IRJET)* 06(04) (2019). e-ISSN:2395-0056, p-ISSN:2395-0072
6. M. Wankhede, V. Trivei, V. Richhariya, Location based analysis of twitter data using apache hive. *Int. J. Comput. Appl. (IJCA)* 153(10) (2016)
7. P.S. Patil, P.B. Sable, R.J. Fasale, P.A. Chougule, Sentimental analysis on twitter data using apache flume and hive. *Int. Res. J. Eng. Technol. (IRJET)* 03(02) (2016). e-ISSN:2395-0056, p-ISSN:2395-0072
8. K.E. Gnanesh, T. Dheeraj Bhavan Narayana, M.D. Kamalesh, Retrieval of encrypted data using trapdoor method in cloud computing. *J. Comput. Theoret. Nanosci.* 16(8), 3237–3241 (2019)
9. S. Nadagoud, D. Kotresh Naik, Market sentimental analysis for popularity of Flipkart. *Int. J. Adv. Res. Comput. Eng. Technol. (IJARCET)* 04(05) (2015)
10. G.V.K. Sai, P.S. Kumar, A.V.A. Mary, Incremental frequent mining human activity patterns for health care applications. *IOP Conf. Ser. Mater. Sci. Eng.* 590(1), 012050 (2019) (IOP Publishing)
11. G. Kavitha, B. Saveen, N. Imtiaz, Discovery public opinion by performing sentimental analysis on real time twitter data, in *International Conference on Circuits and Systems in Digital Enterprise Technology (ICCSDET)* (IEEE, 2018)
12. S.C. Mana, T. Sasiprabha, A study on various semantic metadata standards to improve data usability, in *2019 International Conference on Computational Intelligence in Data Science (ICCIDS)* (Chennai, India, 2019), pp. 1–4

13. A.B. Patel, M. Birla, U. Nair, in *Addressing Big Data Problem Using Hadoop and Map Reduce*, Dec 2012, pp 6–8
14. V.A. Kharde, S.S. Sonawane, Sentiment analysis of twitter data: a survey of techniques. *Int. J. Comput. Appl.* **139**(11), 5–15 (2016)
15. S. Sharma, S. Chakraverty, A. Sharma, A context-based algorithm for sentiment analysis. *Int. J. Comput. Vis. Robot.* **7**(5) (2017) (NetajiSubhas Institute of Technology, Dwarka, New Delhi, India, 2017)
16. P.V. Raja, K. Sangeetha, D. Deepa, Extractive text summarization system using fuzzy clustering algorithm for mobile devices. *Asian J. Inf. Technol.* **15**(5), 933–939 (2016)
17. R.S.B. Krishna, M. Aramudhan, Feature selection based on information theory for pattern classification, in *2014 International Conference on Control, Instrumentation, Communication and Computational Technologies (ICCICCT)*. IEEE, July 2014, pp. 1233–1236
18. N. Srinivasan, C. Lakshmi, A novel prediction based tree structured data using machine learning techniques. *Res. J. Pharm. Biolog. Chem. Sci.* **7**(5), 527–531 (2016)
19. R. Yogitha, G. Mathivanan, Performance analysis of transfer functions in an artificial neural network, in *2018 International Conference on Communication and Signal Processing (ICCSP)*. IEEE, Apr 2018, pp. 0393–0397

Blockchain Integration in House Voting System



Hemanth Chebrolu, Saikumar Buragadda, A. Viji Amutha Mary, and Jancy

1 Introduction

Electronic democratic frameworks are an outcome of the existing research subject, within a time limit length as a goal, point of limiting the cost of running a political decision with assuring the honor of political race by agreeing to the necessities of safety, defense, and compliance. By replacing the old paper-based and pen-based plot with other appointive frameworks can improve in modifying the democratic procedure more recognizable and undeniable. Will of the individuals is a very much regarded wonder for the portrayal of sentiment in the arrangement of constituent bodies. These discretionary bodies differ from the school associations to the parliaments. Throughout the years, 'vote' has risen as an apparatus for speaking to the desire of the individuals for their determination settlement among the accessible decisions. The democratic [1, 2] instrument needs to bring faith over individuals for the choice of their vote of lion's share. This undoubtedly has become useful for democratizing the democratic procedure and the benefit of casting a ballot framework to choose the parliaments and governments. In 2018, there are 167 areas out of minimal more than 200 who have a popular government: full, defective, or half breed and so forth [3]. From then, the faith of individuals is expanding in majority rule governments

H. Chebrolu · S. Buragadda · A. Viji Amutha Mary (✉) · Jancy
Department of Computer Science and Engineering, Sathyabama Institute of Science and Technology, Chennai, India
e-mail: vijiamumar@gmail.com

H. Chebrolu
e-mail: hemanth.chebrolu100@gmail.com

S. Buragadda
e-mail: sai.bsdlvs@gmail.com

Jancy
e-mail: jancy.cse@sathyabama.ac.in

and has become clear that while casting a ballot framework they will have faith over it. By the righteousness of the developing trust on the vote-based foundations, the democratic framework rose as a stage to help individuals to choose their delegates, who therefore structure the legislatures [4–7]. The intensity of the portrayal enables the individuals with a trust that the legislature will deal with the national security, national issues like well-being and instruction approaches universal relations, and tax collection to serve the individuals. To make the democratic procedure increasingly successful, the establishments like ‘Political decision Commission’ appeared in changed parliamentary majority rule governments. The organizations, alongside setting up the procedure and enactment for leading the races, framed the democratic areas, discretionary procedure, voting democratic frameworks for providing direction of straightforward, free, and reasonable rates. The idea of mystery casting a ballot was presented since the start of the democratic framework. Since the trust in law-based frameworks is expanding maintain that the trust in casting a ballot ought not to diminish. In the ongoing past, there have been a few models where it was noticed that the democratic procedure was not clean and confronted a few issues including straightforwardness and decency, and the desire of individuals was not seen to be adequately evaluated and interpreted as far as the development of the legislatures.

Electronic democratic frameworks are the outcome of the dynamic research subject, within a time limit length as a goal, point of limiting the cost of running a political decision with assuring the honor of political race by agreeing to the necessities of safety, defense, and compliance [1]. By replacing the old paper-based and pen-based plot with other appointive frameworks can diminish extortion while detectability and confirmation of the democratic procedure. Blockchain is an open record dispersed, perpetual, incontrovertible. Modern innovation consists of 3 primary attributes: (I) Immutability: For any ‘new square’ in stored record is to allude to its past adaptation of that record. The resultant is the unchanging chain named blockchain takes its name and keeps it from changing the trustworthiness of the past passages. (II) Verification: The record is decentralized, repeated, and conveyed over different destinations. This guarantees more accuracy (by wiping out unnecessary points) and confirms outsiders, are kept as records of agreement form in all hubs. Disseminated Consensus: an accord convention conveyed to find out who will have the option to add new data over to record for exchange [8, 9]. System hubs of the greater part must agree before the new proposed section square turns into a lasting piece of the book.

2 Related Work

Li et al. [1] hardware and programming framework structure utilizing RFID innovation. It is a secure strategy for electronic democratic in a survey and region setting. Contrasted with ‘polling form’ on direct account gear (DRE) and optical checking, the e-voting form can be utilized for tallying. Voter check quick describes

open bulletins and security issues are examined together with an endeavor to plan equipment programming for secure remote PC casting a ballot at home.

Pan et al. [3] E-casting a ballot framework, known as enhanced NOTE (E-NOTE), is enhanced by another convention structure and guard dog equipment to guarantee privacy and casting a ballot precision. The Ballot Distribution Center (BDC) is introduced to disseminate polling forms in our improved framework other than Election Committee (EC) and Vote Counting Committee (VCC). BDC is an unbiased outsider. At the point when the voters cast their votes, the votes and the names of the competitors are isolated into two sections and they cast their votes when the voters.

Thomas [4] the procedure to make and oversee casting a ballot and political decision subtleties, as all clients must log in by client name and secret key and snap on their ideal contender to enlist casting a ballot. All the client needs to do is login and snap on his contender to enlist his vote.

Olaniyi et al. [5] the creator has built up a strong cryptological model for secure electronic democratic. The presentation examination was done as per the degree to which the model meets the general and practical necessities of the protected e-casting a ballot framework: confirmation, trustworthiness, classification, and check to utilize exploratory factor investigation, different relationships, and nonparametric inferential test measurements.

Woller [6] Reflecting looking into it of the Indonesian e-casting a ballot activity to analyze the intentions behind e-government appropriation by the neighborhood government. Subjective information was gathered from five government pioneers at civil and town levels in a district that recently held e-casting ballot decisions in the town.

van der Meer [7] votes are as yet being completed at casting ballot stalls truly. This procedure does not ensure security, and control cases have been watched. The creator utilized blockchain for security to take care of this issue. Blockchain utilizes encryption and hashing to shield each cast a ballot. One vote is viewed as an exchange right now. A distributed system is made to make a private blockchain which imparts this disseminated book to a democratic exchange.

Schmid [10] the versatile democratic framework will empower the balloter to enlist for web-based democratic by utilizing the Internet from anyplace and make his/her choice and view the outcomes. This SRS covers the portable democratic framework with both programming and equipment prerequisites just as the framework's essential highlights.

3 Existing System

Casting a ballot, regardless of whether the conventional expressive dance-based or electronic democratic (e-casting a ballot) is the thing that the cutting edge majority rule governments are expanding upon [11–13]. As of late, voter lack of concern is expanding particularly among the more youthful PC/technically knowledgeable age. E-voting is pushed forward as a potential answer for the draw in youthful voters

[14, 15]. For a hearty e-casting a ballot plot, various functional and security prerequisites are determined including straightforwardness, exactness, suitability, framework and information honesty, mystery/protection, accessibility, and conveyance of power. The current framework depends on blockchain usage [16–18]. The current framework works in a protected electronic democratic framework, which assures the safety and decency of existing democratic, without compromising in straightforwardness, and flexibility [19, 20]. This has only been a trial for current frameworks. The current framework utilization of blockchain as assistance is to execute circulated electronic democratic frameworks [21, 22]. From the customary democratic framework, deceitful is going on consistently. There is some security executing; however, in an equal manner fake is expanding [23, 24]. The biometric validated vote throwing utilizing blockchain.

4 Proposed System

The proposed system is a blockchain-dependent e-casting ballot framework. This electronic democratic framework is improved from the existing framework by using blockchain structures. The portions of impediments are used to assess the enhancement made from the existing system. In modifying that part of the undertaking, we coordinate aadhar card connected versatile number for OTP age; at exactly that point the voter can make the choice, and this framework forestalls throwing and re-throwing of intermediaries. Powerful hashing strategies are executed to guarantee the security of the information. The idea of square creation and square fixing is presented right now. The presentation of a square fixing idea resolves the issue of addressing the surveying procedure by improving the blockchain movement more flexible. Voters can make their own choice from their home itself (Fig. 1).

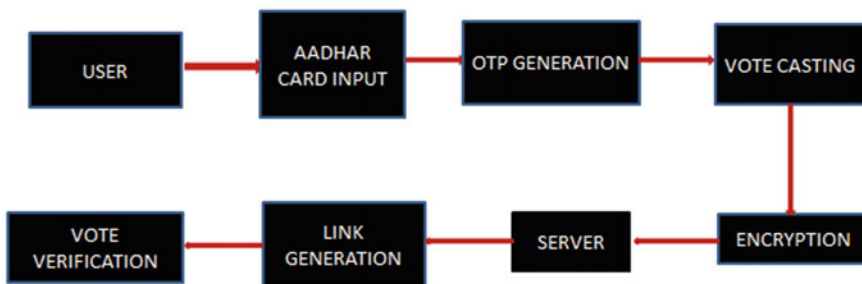


Fig. 1 Overview of the proposed system

5 Module Description

5.1 User Registration

The enlistment eliminates will be conveyed by the appointive chairmen. At the point when a political decision is made, the user needs to register themselves into the application by creating a record for their own, and then they can log in into application to access their record. In light of the client's solicitation, the server will react to the client. All the client subtleties are uploaded over to the server and stored in a database. Clients and competitors need to enlist their subtleties alongside aadhar number.

5.2 Candidate Registration

Right now the competitor will enroll and register by utilizing their aadhar number. Applicant enrollment will be made utilizing aadhar number and voting public of that competitor. On the off chance that client competitor gives inappropriate data framework that will dispose of that enlistment procedure.

5.3 Voting Server

The complete voter's data and other information will be stored in the database at the main server. The server can verify the voter with the previously uploaded data. The applicant's data, which is stored over the database, can be retrieved to confirm whenever necessary. The server will refresh each new voter's refreshing in its database. The server will validate every voter by aadhar before they get to the application. So the client can get to the application.

5.4 Blockchain Formation

A block is a structural container for a lot of information. The memory mostly consumed by block with data is up to 1 MB at maximum by all means. Every block will be made up with client information, and a Hash code will be generated for providing security to that block with information. Here each casting a ballot data will be put away on the square chain. On the off chance that we store the data on the blockchain, it is more verified and each square is made dependent on body electorate.

5.5 Verification

Right now get OTP after they surveyed the vote. OTP is the reason for the affirmation of vote. At the point when the client survey the vote OTP will be sent to the client check; after that affirmation of OTP, system will refresh the vote on the database (Figs. 2, 3, 4, 5, and 6).

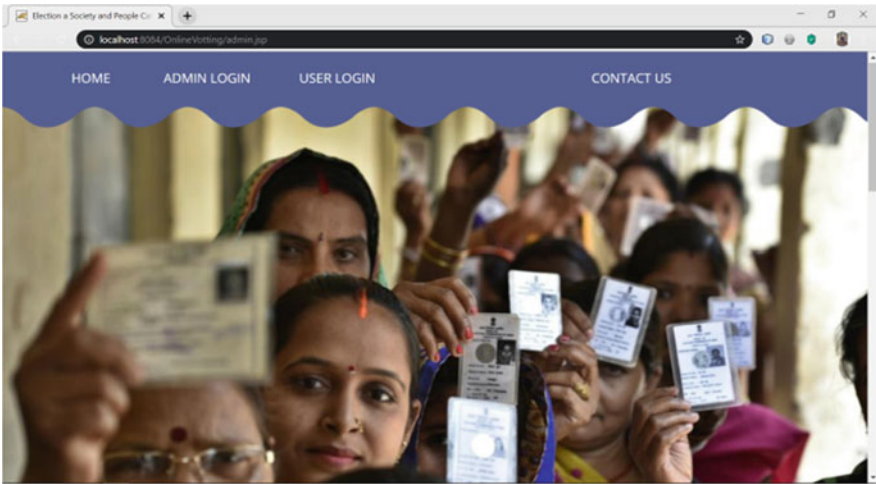


Fig. 2 Home page

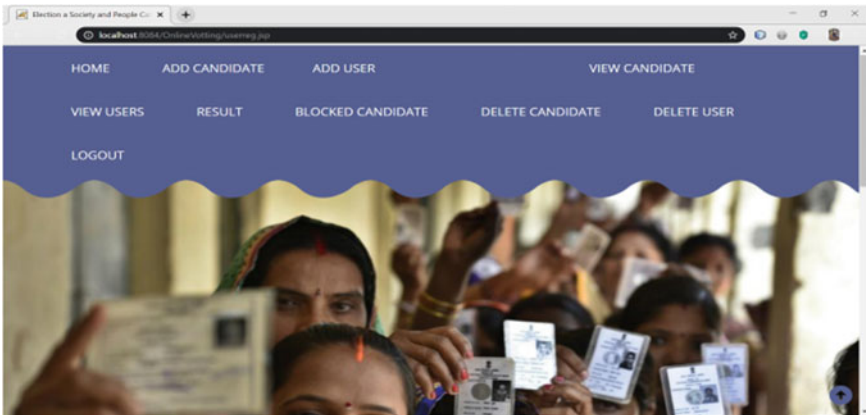


Fig. 3 Admin page

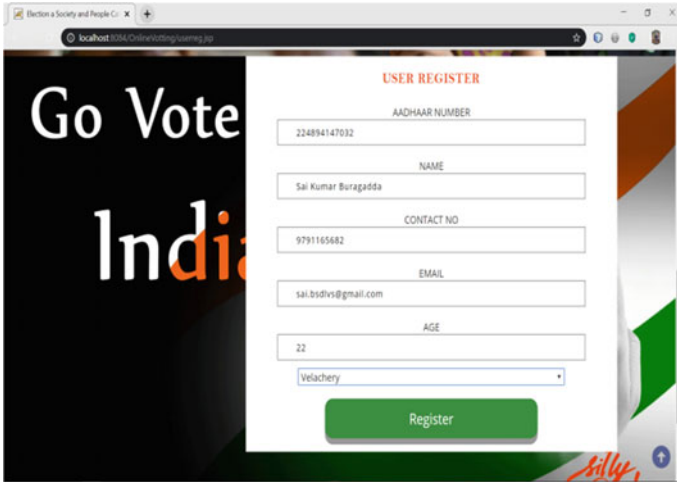


Fig. 4 Candidate registration



Fig. 5 OTP verification

6 Conclusion

Right now, it presented a blockchain-based electronic democratic framework that utilizes clever agreements to verify and financially savvy races while ensuring the protection of voters. We have indicated that blockchain innovation offers another chance to conquer the imperatives and hindrances to the appropriation of electronic democratic frameworks that ensure the security and trustworthiness of decisions and



Fig. 6 Casting window

establish the framework for straightforwardness. In this way, the task construes that each individual can survey their vote through a portable application. Verifying the vote of the voter. The voter can make their choice from home.

References

1. X. Li, et al., in *What are Intelligent Contracts? A Guide for Intelligent Contracts for Beginners* (Blockgeeks, 2016). At: <https://blockgeeks.com/guides/intelligentcontracts/>
2. T.P. Jacob, T. Ravi, Optimal regression test case prioritization using genetic algorithm. *Life Sci. J.* **10**(3), 1021–1033 (2013)
3. H. Pan et al., A multi-part ballot based E-voting system with clash attack protection (2015)
4. A. Barnes, B. Christopher, P. Thomas, Digital voting using Blockchain technology (2016). <https://www.Economist.com/sites/default/files/plymouth.pdf>
5. O.M. Olaniyi, et al., Secure vote today (2016). Available at: <https://www.lawfareblog.com/secure-vote-today>
6. T. Kunioka, G.M. Woller, In (a) democracy we trust: social and economic determinants of support for democratic procedures in Central and Eastern Europe'. *J. Soc. Econ.* **28**(5), 577–596 (1999)
7. T. van der Meer, 'In what we trust? A multi-level study into trust in parliament as an evaluation of state characteristics.' *Int. Rev. Administr. Sci.* **76**(3), 517–536 (2010)
8. G. Nagarajan, R.I. Minu, B. Muthukumar, V. Vedanarayanan, S.D. Sundarsingh, Hybrid genetic algorithm for medical image feature extraction and selection. *Proc. Comput. Sci.* **85**, 455–462 (2016)
9. J. Andrews, Evaluation of various compiler optimization techniques related to mibench benchmark applications (2013)

10. D. Basin, H. Gersbach, A. Mamagishvili, L. Schmid, O. Tejada, Election security and economics: it's all about eve, in *Proceedings of the International Joint Conference on Electronic Voting* (2017), pp. 1–28
11. P. Bevelander, R. Pendakur, Electoral participation as a measure of social inclusion for natives, immigrants, and descendants in Sweden. Technical report (2008), p. 33
12. S. Wolchok et al., Security analysis of India's electronic voting machines, in *Proceedings of the 17th ACM Conference on Computer and Communications Security* (2010), pp. 1–14
13. A. Viji Amutha Mary, S. Justin Samuel, Automated trinity based web data extraction for simultaneous comparison. *Contemp. Eng. Sci.* **8**(11), 491–497 (2015) (HIKARI Ltd., Scopus)
14. J. Stern, Vote—voting for a mobile world. Accessed: 31 July 2018 [Online]. Available: <https://votem.com/>
15. M. Pilkington, 11 Blockchain technology: principles and applications, in *Research Handbook on Digital Transformations* (2016), p. 225
16. G. Gabison, Policy considerations for the blockchain technology public and private applications. *SMU Sci. Tech. Rev.* **19**, 327 (2016)
17. M. Feldhofer, S. Dominikus, J. Wolkerstorfer, Strong authentication for RFID systems using the AES algorithm, in *Cryptographic Hardware and Embedded Systems* (2004), pp. 357–370
18. Y. Stein, H. Primo, Programmable data encryption engine for advanced encryption standard algorithm. U.S. Patent 7 508 937 B2 (2009). Accessed: 1 Aug 2018 [Online]. Available: <https://patents.google.com/patent/US7508937B2/en>
19. B. Shehzad, K.M. Awan, M.I.-U. Lali, W. Aslam, Identification of patterns in the failure of software projects. *J. Inf. Sci. Eng.* **33**(6), 1465–1480 (2017)
20. A.M. Abdullatif, B. Shahzad, A. Hussain, Evolution of social media in scientific research: a case of technology and healthcare professionals in Saudi Universities. *J. Med. Imag. Health Inform.* **7**(6), 1461–1468 (2017)
21. B. Shahzad, Identification of risk factors in large scale software projects: a quantitative study. *Int. J. Knowl. Soc. Res.* **5**(1), 1–11 (2014)
22. A.B. Shahzad, A. Said, Application of quantitative research methods in identifying software project factors. *Int. J. Inf. Technol. Elect. Eng.* **1**(1), 30–33 (2012)
23. A. Viji Amutha Mary, M. Paul Selvan, Christy, Public auditing for secure cloud storage using MD5 algorithm. *Int. J. Recent Technol. Eng. (IJRTE)* **8**(3) (2019). ISSN: 2277-3878
24. M.A. Chowdary, M. Kundan, D.A.V.A. Mary, Effective credit card forgery prevention using multilevel authentication. *IOP Conf. Ser. Mater. Sci. Eng.* **590**(1), 012021 (2019) (IOP Publishing)



Karri Yaswanth Teja Reddy, Karnati Madhava Sai Kumar, A. Pravin,
T. Prem Jacob, and G. Nagarajan

1 Introduction

(i) **Digital Art:**

Digital art is a moved UI that engages creating etymological characters in every practical sense in three-dimensional open space through hand development signals. Customers could create message as if on a whimsical board. Such interfaces are useful choices as opposed to the traditional instrument of forming on the reassure or creating on the track pad/contact screen.

(ii) **OpenCV:**

Open Source Computer Vision Library (OpenCV) is an open source computer and machine learning library. OpenCV was built to provide a common infrastructure for computer vision applications and to accelerate the use of machine vision in commercial products. Being a BSD licensed product, OpenCV makes it easy for businesses to use and modify the code for various purposes. The library has over 2500 structured algorithms, including a comprehensive set of computer and state-of-the-art computer and machine learning algorithms. These

K. Yaswanth Teja Reddy (✉) · K. M. Sai Kumar · A. Pravin · T. Prem Jacob · G. Nagarajan
Department of Computer Science and Engineering, Sathyabama Institute of Science and
Technology, Chennai, India
e-mail: karriyaswanthtejareddy@gmail.com

K. M. Sai Kumar
e-mail: madhavrockzz007@gmail.com

A. Pravin
e-mail: pravin_ane@rediffmail.com

T. Prem Jacob
e-mail: premjac@yahoo.com

G. Nagarajan
e-mail: nagarajanme@yahoo.co.in

algorithms can be used to find and recognize faces, to view objects, to segment human actions in videos. It is highly beneficial to track camera movements of objects as well as to extract 3D object models and generate 3D point clouds from stereo cameras. It cluster all the images to produce high resolution picture of the whole event, find similar pictures in the photo database, get the red eyes out of the photos taken with flash, follow the eye movements, recognize the beauty of the place and set up a marker to pinch undesirable facts, etc.

2 Related Works

Our work is the part to suggest in every way that really matters making semantic characters with hand gestures in graphical space with few degrees of opportunity. At the present time, customary camcorder subordinate convolutional neural framework-based air-making structure has been proposed [1, 2]. Signs are performed using a object of determined concealing before a customary camcorder next by concealing-based division to mark the marker and track the header of the marker tip. The pre-arranged network is then used to organize the identity. Confirmation accuracy is also enhanced by the use of late data moving. Close to the end we guided a test to affirm that Brisk making capacity moves to the support mode. In the earlier model (support mode), the segmentation of data rate has been calculated according to the time limit which was not sufficient. Anyhow by giving end to those problems, we created a scribble. Then, the stylus mode was not at high speed, anyway we found Brisk creating sensible for multi-contraption purpose. Scribble has continued proceeding as a strategy for correspondence and recording information in regular daily existence even with the introduction of new advances. Given its inescapability in human trades, machine affirmation of scribble has down to earth significance, as in examining physically composed notes in a PDA, in postal areas on envelopes, in entireties in bank checks, in translated fields in structures, etc. Both the online case (which identifies with the openness of course data during making) and the separated case (which identifies with checked pictures) are considered. Computations for preprocessing, character and word affirmation and execution with down to earth systems are illustrated [3]. Various fields of utilization, like mark affirmation, writer authentication and scribble learning gadgets are moreover considered. An activity-based full system was proposed, and it gains a better visibility [4, 5]. The planning and 6D was proposed, and it really helps in developing movements [6]. The work focuses on processing using the pen and extracts a better outcome [7]. The proposed work provides a better writting experience, and it will be easy for the user to handle and perform the corresponding task [8, 9]. The procedure based on the content was devised, and it will inturn decrease the time [10]. The process is performed by using a controller for game, and it will show an better performance [11, 12]. The new proposed model can be extended for various purposes in future by adding varieties of features to it especially for children [13]. Techniques are proposed for cursive

handwriting, and it will affirmation online [12, 14]. Provides information about the hop development and swipe [15, 16].

Existing System

We have many handwriting recognition techniques which have been existing for years. These techniques require excessive devices for giving various gestures an input require. In the past, the development of depth sensors such as Leap Motion and Microsoft Connect provided the opportunity to develop frameworks for collaboration and systems. The devices are capable of 3D point cloud computing and have been used successfully in many human-computer-interaction programs, including 3D handwriting recognition and character recognition. Leap Motion Device is designed to track finger and hand movements in 3D space with the help of 3D LED infrared and two infrared sensors. This method for signal matching is built with 3D histogram oriental optical flow (HOOF) and histogram oriental trajectories (HOT).

Disadvantage

- It is time consuming, because of which needs hand-held devices.
- Cost is very high
- It is very difficult to handle the device.

3 Proposed System

The issue of digital art acknowledgment could be drawn nearer dynamically. Detached air-composing conveys the suspicion hand movement of issuing a letter is generally restricted. Movement distance can be planted using a tracker, which can be turned active or not properly to indicate the start and end of a continuous process. One level up, a development letter is surrounded by partner development characters with multicolor digital art developments in the digital art. When there is no touchpad or display device analysis, the standard left-to-right creating design is hard to keep up without spread or shape mutilation. In our key examination, we found that customers will all in all clinician and spread the last relatively few characters. If the data which are exhibited are scattered or having gaps, then the customers will immediately go demand to display a data with no spaces or gaps. Right now, demand that the customer makes each character out of a characters in a layer-by-layer way, covering all characters of the characters in the equal visualization, a making style we term “secured multi color digital art,” which replaces the average related forming design and has every one of the reserves of being logically proper for air-creating.

Advantage

- Easy to adopt in all environment.
- It is easy to handle.
- Easy to integrate with design.

3.1 Module Description

Module 1: Sensing

Distinguishing hand signal affirmation structure is to make a trademark interaction among human and PC which could restrict the apparent movements or passing the significant information between the user and the interface. It came about hand signs to be specified in a clear way and very much deciphered with the personal computer regarded as the issue for the movement association like PC of human correspondence furthermore changed as man-machine collaboration (MMC).

Module 2: Spotting of Scribble

The visual platform is used to play two exposures of the data stream to locations that contain certain inbound components. The so-called parts of writing development are given a kind acknowledgment. The purpose of the visit phase is to separate these parts from the list work. To allow consistent usage and mobility in trusted data streams, we use a smoother Windows system. Separate cover windows are requested, and the merger results of all cover windows are compiled and promptly provided for approval type.

Module 3: Scribble Storing and Displaying

Content composed perceptible all around is portrayed with the help of the air bearing. Enhancement in hand is the circumstance for two-dimensional multicolored-based scribble. By then, the made substance could be saved as picture similarly as pdf gathering with more efficient features.

System Implementation

In the initial implementation, we have to capture video through the webcam using a hand-held recognition system to create a natural connection between the human computer and the touch-sensitive device to control or transfer sensitive information. The effect of hand gestures to be understood and interpreted correctly by the computer has been considered to be a problem of body communication. Second, it recognizes the handwriting of the data. The virtual platform is used to perform binary partitioning of the data stream into potentially compositional and inbound categories. Parts classified as a handwriting step are referred to the recognition phase.

The purpose of the visualization phase is to detect the discrimination of these parts of the background function. To allow real-time use and functionality in continuous data streams, we use the Windows operating system. The overlapping windows are separated by the split results of all overlapping windows and then transferred to the recognition phase immediately. Finally, at the end of this phase, the storage and display are done. The text in the air is defined by the patent trajectory of the movement of the hand as it is by the handwriting method based on the two letters. Subsequently, the text can also be saved as an image and in a pdf format.

4 Algorithm

- Step 1:** In the first step, we set in the environment for running the project.
- Step 2:** Now after running, we get two windows on screen, one for sensing the gestures and the other for spotting and displaying pattern.
- Step 3:** We give in some movements so that our camera could detect the gestures and display the pattern.
- Step 4:** We can also specify some background and add colors through our gestures.
- Step 5:** We can save and modify the colored images in various formats.

5 System Architecture

The system architecture is given in Fig. 1 depends up on the input that is given by the user the next set of process such as detect and tracking of the hand. The next process is it will segment the input, and then finally, the features are extracted. Depends upon the features extracted, there will be both static and the dynamic gesture. In static, it will normalize and classify the instance, and the classification process is performed. The other process will be in terms of dynamic labeling, translation and classification is performed. The models are loaded based on the request that is given.

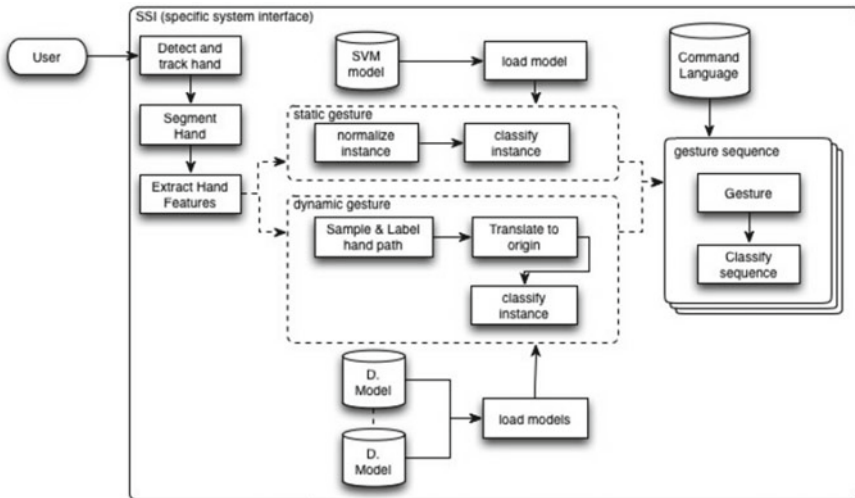


Fig. 1 Architecture diagram

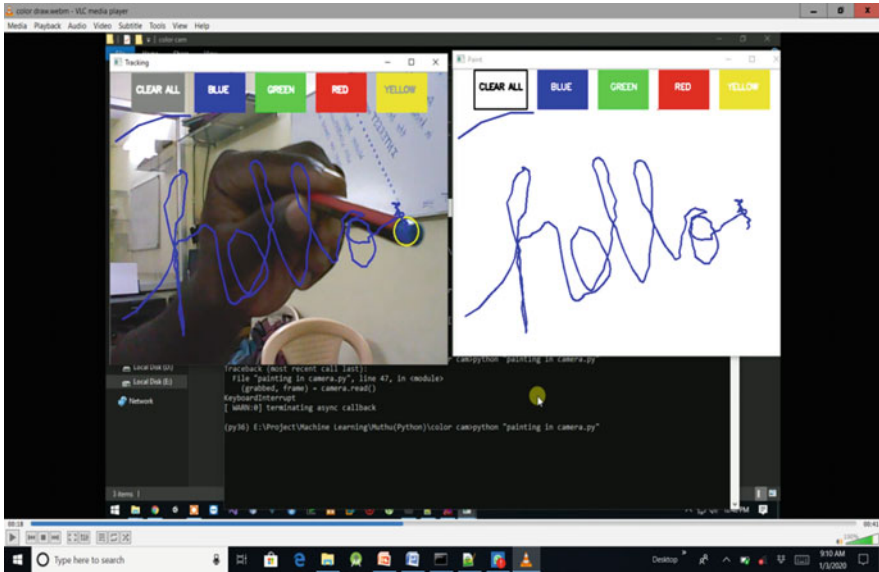


Fig. 2 Recognizing of the pattern

6 Results and Discussions

The patterns are recognized, and the process is explained in Fig. 2. The recognition process is based on the selection process. The next step is to fill the color for the design and is described in Fig. 3. The color filling is tested by us, and it gives more accurate and correct form.

7 Conclusion

Digital art of digital art with multicolor strokes is produced. Depending upon the signals which we have made through sensors, there is a chance of recognizing all those characters which have been spotted and predicted. The proposed structure can complete as a data port for wearable PCs, allowing for object commitments in a humane way and without the need to work with multiple devices. The results could be moved to various territories of sign affirmation tasks where unequivocal movements are worked from a smaller course of action of locals. None of the used techniques is altered to the issue of scribble affirmation. The proposed plan and systems license the execution of a structure working continuously on diligent data.

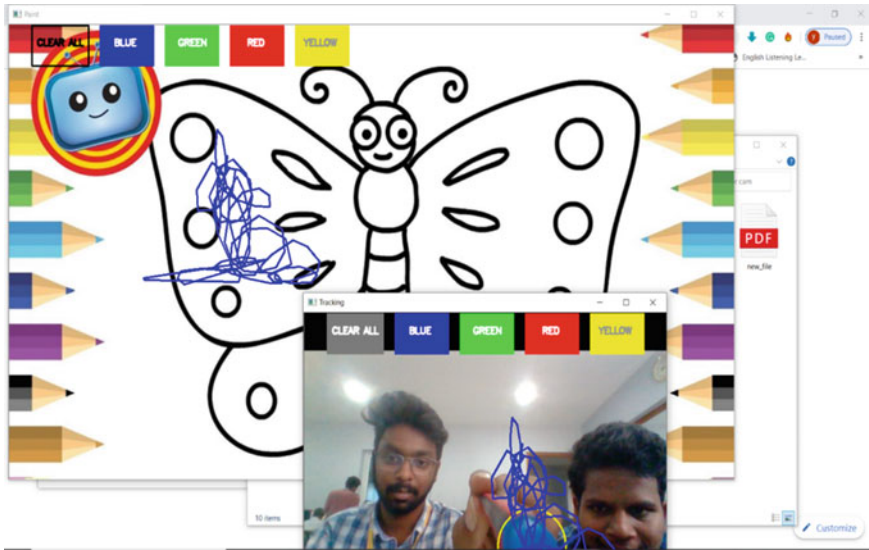


Fig. 3 Filling the colors for design

References

1. B. Bharathi, P. Vijayalakshmi, T. Nagarajan, Speaker identification using utterances correspond to speaker-specific-text, in *IEEE Technology Students' Symposium*. IEEE, Jan 2011, pp. 171–174
2. J., Sujolincy, M.D. Kamalesh, An authenticated smart card service using cross-cloud and big data, in *2016 International Conference on Control, Instrumentation, Communication and Computational Technologies (ICCICCT)*. IEEE, Dec 2016, pp. 634–638
3. P.V. Raja, K. Sangeetha, D. Deepa, Extractive text summarization system using fuzzy clustering algorithm for mobile devices. *Asian J. Inf. Technol.* **15**(5), 933–939 (2016)
4. M. Chen, G. AlRegib, B.-H. Juang, Air-making affirmation—part II: identification and affirmation of making activity in consistent stream of development data. *IEEE Trans. Hum. Mach. Syst.* to be disseminated
5. S.P. Shyry, Novel enhanced encryption algorithm for shared key generation, in *Proceedings of the 2014 International Conference on Interdisciplinary Advances in Applied Computing*, Oct 2014, pp. 1–7
6. M. Chen, G. AlRegib, B.-H. Juang, Feature planning and showing for 6d development movement affirmation. *IEEE Trans. Blend. Med.* **15**(3), 561–571 (2013)
7. C.H. Blickenstorfer, Graffiti: Amazing! *Pen Process. Mag.* **1**, 30–31 (1995)
8. K. Perlin, Quikwriting: constant stylus-based substance section, in *Proceedings of the Eleventh Annual ACM Symposium on UI Software and Technology* (1998), pp. 215–216.
9. R.S.B. Krishna, M. Aramudhan, Unsupervised spectral sparse regression feature selection using social media datasets, in *Proceedings of the International Conference on Informatics and Analytics*, Aug 2016, pp. 1–5
10. P. Isokoski, R. Raisamo, Quikwriting as a multi-contraption content area procedure, in *Proceedings of the Third Nordic Conference on Human-PC Connection* (2004), pp. 105–108
11. T. Költringer, P. Isokoski, T. Grechenig, Twostick: composing with a game controller. *Proc. Graph. Interface*, 103–110 (2007)

12. N. Srinivasan, C. Lakshmi, A novel prediction based tree structured data using machine learning techniques. *Res. J. Pharm. Biol. Chem. Sci.* **7**(5), 527–531 (2016)
13. R. Plamondon, S. Srihari, On the web and disengaged scribble affirmation: an extensive diagram. *IEEE Trans. Model Butt-Driven. Mach. Intell.* **22**(1), 63–84 (2000)
14. J. Makhoul, T. Starner, R. Schwartz, G. Chou, On-line cursive hand-making affirmation using hid markov models and quantifiable gram-mutilates. *Proc*
15. Hop development (2015) [Online]. Available: <https://www.leapmotion.com>
16. Swype—type brisk, swype speedier (2013) [Online]. Available: <https://www.swype.com/>

Twitter Topic Analysis Using Multi-tweet Sequential Summarization for Sentimental Data



B. Melanshiya, P. Mirium Swarna, and Ramya G. Franklin

1 Introduction

From a couple of years, online networking is quickly growing up now heaps of administrations existing, for example, Facebook, Twitter, and so on. Today billions of individuals utilize Facebook and Twitter; thus, the colossal information is created [1, 2]. These information comprise the images, videos, text messages, and events. On consistently, number of occasions made and shared over the world through Facebook and Twitter. Identifying and observing the occasions are one of the most testing errands [3, 4]. Twitter is one of the most generally utilized administrations in only 780 days, and it crosses the 10 million clients [5, 6]. As indicated by this thousand of occasions made and shared over the world in only minutes [7]. With the goal that distinguishing an occasion isn't simple for the conventional technique in light of the fact that these methods depend on human intercession and the exactness is likewise less [8]. As indicated by Statista in India, Twitter has in excess of 30 million dynamic clients until December 2018. In the field of information investigation, occasion location assumes a significant job in checking the top hot occasions [9]. Because of the more established techniques, web watch official cannot follow the hot occasions in an auspicious way [10]. To address this issue, we use a three-advance model based on Hypertext-induced [11], theme scan, and latent Dirichlet allocation. We propose a HITS-based subject choice strategy [12]. This methodology makes a littler top-notch

B. Melanshiya · P. M. Swarna · R. G. Franklin (✉)
Department of Computer Science and Engineering, Sathyabama Institute of Science and
Technology, Chennai, India
e-mail: ramyagfranklin.cse@sathyabama.ac.in

B. Melanshiya
e-mail: melanshiyabazil@gmail.com

P. M. Swarna
e-mail: miriumswarna333@gmail.com

preparing dataset by choosing excellent posts and compelling clients from among an assortment of clients and posts, which to a great extent diminishes the effect of superfluous posts and normal clients, and improves the productivity and exactness of occasion location contrasted [13, 14]. Therefore, the proposed methodology would automatically identify the quantity of points and discern main occasion related posts from a huge number of posts, further improving the efficacy and precision of the position of the opportunity and beating existing methods [15]. We propose a LDA-based three-advance model that recognizes basic occasions dependent on the quantity of subjects and distinguishes powerful spreaders engaged with sharing these basic occasions [16, 17]. The test results on a Twitter dataset demonstrate the knowledge and accuracy of our models during related work occasional exploration and the detection of strong spreaders.

2 Related Work

Lately, occasion location has been the focal point of a wide scope of research, particularly from the web-based life viewpoint, because of its receptiveness and information accessibility [18]. Existing web-based life recognition models are ordered either as highlight pivot or as pivot report models. A recognized occasions by gathering bursty words [2, 19]. Be that as it may, this technique does not have a vigorous probabilistic establishment and concentrates just on occasion discovery; it neglects to distinguish key occasion related posts or the powerful spreaders engaged with these basic occurrences [20]. Micro-blogs is furthermore called get-togethers; get-togethers may hold essential materials that depict the conditions during a crisis [21]. Recognizing a target occasion in social frameworks reliant on a single source needs to analyze the composite occasions contributed by different social clients [22]. Up until this point, the issue of fusing unclear viewpoints from different clients isn't all around investigated [23]. To address this issue, we propose a novel framework to recognize composite get-togethers over streams, which totally abuses the information of social data over different estimations [24]. Micro-blogs, for instance, Twitter reflect the general populace's reactions to genuine occasions. Bursty subjects from micro-blogs reveal what occasions have pulled in the most online thought. In spite of the way that bursty occasion identification from content streams has been considered beforehand, past work may not be proper for micro-blogs considering the way that differentiated and other substance streams, for instance, reports and intelligent disseminations, micro-blog posts are particularly various and uproarious. To find points that have bursty plans on micro-blogs, we propose a subject model that at the same time gets two observations: posts circulated around a comparable time will undoubtedly have a comparable theme, and posts conveyed by a comparable customer will undoubtedly have a comparable subject. Wavelet [25] analysis was applied to the recurrence-based crude signs of words in constructing signals for singular terms, and channels trifling words by looking at their auto-relationships in comparing signals. This strategy distinguishes occasions utilizing a seclusion based

chart parceling system. Notwithstanding, it likewise concentrates just on occasion location and does not consider key posts or compelling spreaders, which expands the complexities engaged with instantly following and controlling occasions. Archive rotate models distinguish occasions by bunching records as per the semantic separations between them. The use of LDA point models for viewing the subjects in content streams. The creators additionally utilized a development lattice to record the assortments of themes, which accomplished great execution. A proposed subject model for the bursty event detection (BEE) which, by demonstrating these opportunities, distinguishes new bursty occasions. Anyway all of these periodic exploration techniques expose flaws in the programmed recognition of the number of trends and the recognizable evidence of related key posts and convincing spreaders associated with these specific occasions. TDT frameworks give general layouts and basics with respect to occasion identification. Be that as it may, boisterous posts and the extraordinary quantities of common clients make these strategies inadmissible for either basic occasion recognition or the recognizable proof of persuasive spreaders for enormous amounts of online networking information. In outline, the above models do not will in general perform well in occasion location in the accompanying regards: First, the attributes of micro-blogging, for example, the connections among clients and their posts, cannot successfully address the impact of clients and the significance of posts. These methods are centered uniquely around occasion discovery by the gathering of words. Second, existing methods think about just occasion identification and are not worried about the revelation of key posts.

3 Methodology

We also suggest a three-step model based on the latent Dirichlet allocation, which can identify the most persuasive hot occasional spreaders depending on both post and client data. Using a Twitter dataset for our investigation, our test results show the adequacy of our proposed techniques for both the recognition of occasions and the distinctive evidence of persuasive spreaders. The proposed framework through foreground dynamic topic modeling. This empowers an end client to totally investigate a slanting theme to a more prominent degree of detail. Pre-preparing stage the proposed framework additionally handles non-English tweet interpretation that is fundamental to forestall disposing of general feeling about the inclining subject. It is called as stream-based methodology and semantic-based methodology. Repetition check is performed to expel copies from the chose tweets followed by an edge check to guarantee reasonable blend of client's assessments. Trending topic collection inclining subjects will be removed utilizing the locale's "WOEID" which particularly recognizes any district on the planet. Twitter API will empower the extraction of area astute patterns. Extricated pattern will be dissected to affirm to the necessity that the theme includes a few sub-points covered up in it. Inclining subjects will be put away in the database. While putting away the slanting themes into the database, they will be labeled with the month run during which it drifted.

This will empower client to pick a theme to examine dependent on the month run. Tweets ordinarily include numerous loud substances and not well-framed words on the grounds that the clients are permitted to tweet just inside restricted characters. In this way, cleaning and setting up the significant information is basic for any sort of examination to be performed on the information. Tweet pre-preparing includes the accompanying errand: URL Removal-URL and connections will be expelled from the tweet content. Slang Word Replacement: Slang words like LOL and OMG will be supplanted its proper English words, for example, Roar with laughter, Oh My God, and so on. Non-English word channel through tweets could be separated utilizing explicit language, some loud terms and words degenerate the objective information. Non-English words will be separated with the assistance of a lexicon. Stemmer and Stop word evacuation English words will be stemmed and just the root words will be held. Stop words in the tweet substance will be evacuated. Highlight extraction associated with this framework makes a critical effect in the presentation of the supposition characterization task. Tweets have an uncommon nature not at all like typical English sentences like @ image used to allude to a client, emojis communicated in the tweets, and so forth. Consolidating such highlights while performing highlight extraction improves the general procedure. Content highlights are a blend of common sentiment words and theme assumption words which will be utilized to prepare the classifier. With POS labeling for tweets on a subject and evacuating the basic assessment words, the proposed system chooses the continuous descriptors, action words, things, and qualifiers as applicants of theme versatile. On-content highlights incorporate the @-organize highlights, client supposition highlights, and emojis. These highlights catch the exceptional idea of tweets as highlights. In twitter, @ image in a tweet is utilized to allude to a client whom an individual would tweet to, for example, @abc implies that the tweet is alluding the client abc. In conventional framework, outlines may content clashing substance that decreases the comprehensibility and the general effect of synopses produced. Mostly like, this framework plans to perform estimation order and afterward utilizing subject savvy supposition named information continues to the rundown module. Assumption order is a delicate subject errand, i.e., a classifier prepared from one topic would perform more unfortunate on another. In comparison with the item survey, Twitter also requires details naming and a rating system to receive conclusion points. Incredibly meager tweet content even cuts off a supposition classifier display. Propose a flexible estimation order model for the semi-regulated subject right now, beginning with a classifier focused on usual highlights and blended marked details from different themes (Fig. 1).

4 Experimental Results

Social media is an integral part of the world and will only continue to build its impact in the future. This humongous dataset could be analyzed to boost other networks and industries. We used one method of analysis called an analysis of sentiments. Many innovative compressor and filter algorithms can play an important role in bridging

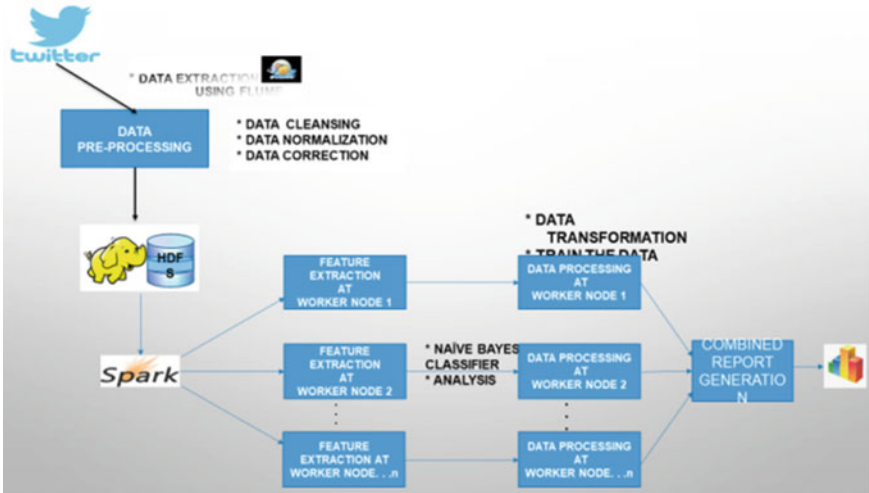


Fig. 1 System architecture

the language barrier and coping with noisy material and unformed words. Twitter’s sentiment analysis using big data has helped us to analyze large amounts of data sets. We concentrate on a study of general sentiment. In the field of sentiment analysis, there is scope for research with a partly defined background (Figs. 2 and 3).

5 Conclusion

In this proposed model, by hash labels, we can give a basic mechanized strategy to what individuals think. Subsequently, gathering data from systems and dissecting it utilizing big data methods has behind the conventional database approach. Slant examination of Twitter utilizing huge information helped us to investigate immense measure of datasets. We can additionally think about the different suppliers and judge which one is the best. So as to quantify the presentation with the current framework we at first actualize with Map lessen design. In the following stage, we will actualize with Spark outline with and the exhibition will be analyzed. Our exploratory outcomes the adequacy of our suggested approaches in occasion identification, key post discovery, and identifiable proof of convincing spreaders for a Twitter dataset is demonstrated. We intend to additionally examine the practices of persuasive spreaders and build up a powerful network location model that can advance after some time.

```
jpasolutions@ubuntu: ~
Time taken: 0.258 seconds, Fetched: 1447 row(s)
hive> select SUM(IF(rating>0, 1, 0))/COUNT(*)*100 FROM result as positive;
Query ID = jpasolutions_20181114000452_7fdb662b-8fa4-496b-b71d-439c890aee7
Total jobs = 1
Launching Job 1 out of 1

Status: Running (Executing on YARN cluster with App id application_1542180896310_

-----
VERTICES    MODE           STATUS  TOTAL  COMPLETED  RUNNING  PENDING  FAI
-----
Map 1 ..... container  SUCCEEDED  1      1          0          0
Reducer 2 ..... container  SUCCEEDED  1      1          0          0
-----
VERTICES: 02/02 [=====] 100% ELAPSED TIME: 8.59 s
-----
OK
46.5100207325501
Time taken: 9.77 seconds, Fetched: 1 row(s)
hive>
> select SUM(IF(rating<0, 1, 0))/COUNT(*)*100 FROM result as negative;
Query ID = jpasolutions_20181114000502_6889ded0-3d7a-4284-a6e5-94c0646c4db8
Total jobs = 1
Launching Job 1 out of 1

Status: Running (Executing on YARN cluster with App id application_1542180896310_

-----
VERTICES    MODE           STATUS  TOTAL  COMPLETED  RUNNING  PENDING  FAI
-----
```

Fig. 2 Negative analysis

```
jpasolutions@ubuntu: ~
Map 1 ..... container  SUCCEEDED  1      1          0          0
Reducer 2 ..... container  SUCCEEDED  1      1          0          0
-----
VERTICES: 02/02 [=====] 100% ELAPSED TIME: 1.30 s
-----
OK
49.68901174844506
Time taken: 2.236 seconds, Fetched: 1 row(s)
hive>
> select SUM(IF(rating=0, 1, 0))/COUNT(*)*100 FROM result as neutral;
Query ID = jpasolutions_20181114000504_40e8fbc4-57b4-499a-97ec-02cb138580b2
Total jobs = 1
Launching Job 1 out of 1

Status: Running (Executing on YARN cluster with App id application_1542180896310_

-----
VERTICES    MODE           STATUS  TOTAL  COMPLETED  RUNNING  PENDING  FAI
-----
Map 1 ..... container  SUCCEEDED  1      1          0          0
Reducer 2 ..... container  SUCCEEDED  1      1          0          0
-----
VERTICES: 02/02 [=====] 100% ELAPSED TIME: 0.86 s
-----
OK
3.8009675190048373
Time taken: 1.786 seconds, Fetched: 1 row(s)
hive>
>
```

Fig. 3 Positive and neutral analysis

References

1. X.M. Zhou, L. Chen, Event detection over twitter social media streams. *VLDB J.* **23**(3), 381–400 (2014)
2. G. Nagarajan, R.I. Minu, Fuzzy ontology based multi-modal semantic information retrieval. *Proc. Comput. Sci.* **48**, 101–106 (2015)
3. A. Aldhaheri, J. Lee, Event detection on large social media using temporal analysis, in *Proceedings of the 7th Annual Computing and Communication Workshop and Conference* (Las Vegas, NV, USA, 2017), pp. 1–6
4. A. Pravin, T. Prem Jacob, P. Asha, Enhancement of plant monitoring using IoT. *Int. J. Eng. Technol. (UAE)* **7**(3), 53–55 (2018)
5. P. Yan, MapReduce and semantics enabled event detection using social media. *J. Artif. Intell. Soft Comput. Res.* **7**(3), 201–213 (2017)
6. J. Andrews, Evaluation of various compiler optimization techniques related to mibench benchmark applications (2013)
7. Y.D. Zhou, H. Xu, L. Lei, Event detection based on interactive communication streams in social network, in *Proceedings of the 9th EAI International Conference on Mobile Multimedia Communications* (Xi'an, China, 2016), pp. 54–57
8. T. Hofmann, Probabilistic latent semantic indexing, in *Proceedings of the 22nd Annual International ACM SIGIR Conference on Research and Development in Information Retrieval* (Berkeley, CA, USA, 1999), pp. 50–57
9. D.M. Blei, A.Y. Ng, M.I. Jordan, Latent Dirichlet allocation. *J. Mach. Learn. Res.* **3**, 993–1022 (2003)
10. Q.M. Diao, J. Jiang, F.D. Zhu, E.P. Lim, Finding bursty topics from microblogs, in *Proceedings of the 50th Annual Meeting of the Association for Computational Linguistics: Long Papers*, vol. 1 (Jeju Island, Korea, 2012), pp. 536–544
11. X.H. Wang, C.X. Zhai, X. Hu, R. Sproat, Mining correlated bursty topic patterns from coordinated text streams, in *Proceedings of the 13th ACM SIGKDD International Conference on Knowledge Discovery and Data Mining* (San Jose, CA, USA, 2007), pp. 784–793
12. L. AlSumait, D. Barbara, C. Domeniconi, On-line LDA: adaptive topic models for mining text streams with applications to topic detection and tracking, in *Proceedings of the 8th IEEE International Conference on Data Mining* (Pisa, Italy, 2008), pp. 3–12
13. J.X. Li, Z.Y. Tai, R.C. Zhang, W.R. Yu, L. Liu, Online bursty event detection from microblog, in *Proceedings of the 7th IEEE/ACM International Conference on Utility and Cloud Computing* (London, UK, 2014), pp. 865–870
14. T.P. Jacob, T. Ravi, Optimal regression test case prioritization using genetic algorithm. *Life Sci. J.* **10**(3), 1021–1033 (2013)
15. S. Chakrabarti, B. Dom, P. Raghavan, S. Rajagopalan, D. Gibson, J. Kleinberg, Automatic resource compilation by analyzing hyperlink structure and associated text. *Comput. Netw. ISDN Syst.* **30**(1–7), 65–74 (1998)
16. J. Bao, Y. Zheng, M.F. Mokbel, Location-based and preference-aware recommendation using sparse geo-social networking data, in *Proceedings of the 20th International Conference on Advances in Geographic Information Systems* (Redondo Beach, CA, USA, 2012), pp. 199–208
17. G. Nagarajan, K.K. Thyagarajan, Rule-based semantic content extraction in image using fuzzy ontology. *Int. Rev. Comput. Softw.* **9**(2), 266–277 (2014)
18. J. Kleinberg, Bursty and hierarchical structure in streams, in *Proc. 8th ACM SIGKDD Int. Conf. Knowledge Discovery and Data Mining (KDD'02)*, Edmonton, Canada, 2002, pp. 91–101.
19. Y.M. Yang, T. Pierce, J. Carbonell, A study of retrospective and on-line event detection, in *Proceedings of the 21st Annual International ACM SIGIR Conference on Research and Development in Information Retrieval (SIGIR'98)* (Melbourne, Australia, 1998), pp. 28–36
20. M. Mathioudakis, N. Koudas, Twittermonitor: trend detection over the twitter stream, in *Proceedings of the 2010 ACM SIGMOD International Conference on Management of Data* (Indianapolis, IN, USA, 2010), pp. 1155–1158

21. J. Allan, V. Lavrenko, D. Malin, R. Swan, Detections, bounds, and timelines: UMass and TDT-3, in *Proceedings of the Topic Detection and Tracking Workshop, TDT-3* (Vienna, Austria, 2000), pp. 167–174
22. F. Atefeh, W. Khreich, A survey of techniques for event detection in twitter. *Comput. Intell.* **31**(1), 132–164 (2015)
23. Twitter, REST API v1.1 resources (2017). <https://dev.twitter.com/docs/api/1.1/>
24. A. Balamurugan, R. Jeberson Retna Raj, Effective analysis of social networks for emergency alert and disaster management using Android. *ARPN J. Eng. Appl. Sci.* **11**(17) (2016). ISSN 1819-6608 (Scopus Indexed)
25. G. Nagarajan, R.I. Minu, A. Jayanthiladevi, Brain computer interface for smart hardware device. *Int. J. RF Technol.* **10**(3–4), 131–139 (2019)

Content-Based Image Retrieval in Cloud Image Repositories



Vishnu Vardhan Kathika, K. S. G. Jagadeesh Babu, A. Pravin,
T. Prem Jacob, and G. Nagarajan

1 Introduction

BOEW is one of the highest rising area of research work in the cloud computing field as the chances of getting it are drastically increased when compared to recent years. Image retrieval is considered that has seen a drastic growth in the era of digitization and has also been an initiative for several new applications and techniques that are used globally by numerous people [1, 2], which is also considered as one of the most significant areas of research that used various techniques. Content-based image could be stated as a type of learning that is done without using any human intervention. The performance of any task by making use of this technique is improved by continuous learning. When it comes to learning, it is of two areas [3, 4]. The first area is content-based where the features of the dataset are given and are used for training purposes. The second area is image based where the encryption takes place without having any feature set [5–8]. Most commonly, images are used for extracting the features from the dataset and then using them for further classification purposes [9, 10]. We have projected a model that makes use of various schemes for classification and AES and RSA algorithm for retrieval that particularly for content-based image areas. The rest of the paper consists of some related works proposed by various researchers, the methodologies and algorithms used in the proposed technique, and the results and discussions [11].

V. V. Kathika (✉) · K. S. G. Jagadeesh Babu · A. Pravin · T. Prem Jacob · G. Nagarajan
Department of Computer Science and Engineering, Sathyabama Institute of Science and
Technology, Chennai, India

e-mail: vishnuvardhan.kathika@gmail.com

K. S. G. Jagadeesh Babu

e-mail: sgjbabu2000@gmail.com

A. Pravin

e-mail: pravin_ane@rediffmail.com

2 Related Works

Many scientist for segmenting or classifying a specific object or a certain area from an image [12, 13]. A semi-automatic retrieval method is proposed for cloud computing [14]. In [15, 16], most of the system will have unique identifications on getting the image and more classification will not have accurate value as we expected. In that cases, we have to use segmentation and machine learning schemes for detecting the perfect area inside the image.[17, 18], this paper have proposed the unique system for retrieval inside the database in image based and vision based. In [19], by integrating the content with the Bayesian model. Weighted aggregation algorithm was used for the detection of image. The performance evaluation was done on a larger dataset where stochastic models were used to extract the features [20]. The model could be enhanced by providing an accurate boundary of the images. Simultaneous image and bias correction were performed by some researchers [21, 22], where minimization of energy was performed by an efficient encryption approach. The technique stated that the experimental results were performed on a real dataset of images and produced an accurate intensity of homogeneity [23, 24] classified lung cancer images from random scans using the BOEW technique yielding a good accuracy of 96.67%. Encryption approach used in [25] described the retrieval technique producing an accuracy of 92%.

3 Proposed System Approach

Numerous methods and classification techniques are enhanced and efficient model designed in the current paper first retrieves the sequence of content from the scanner database. The images are then preprocessed where all the features of the images are extracted using various techniques.

The retrieval scheme is initially done by random image analysis where all the images are processed in such a way that it generates new content-based images. The validation of the dataset is done step by step for a particular time period. As the proposed model is an iterative process, the model tends to produce a more accurate result when compared with other existing techniques.

Advantage

- Provides high accuracy results.
- It is fast and easy to handle.
- Easy to integrate with design.

3.1 Module Description

Create Repository and Upload Images

Repository is storage space of collection of data. Each repository is created by single user. He is the owner of that repository. Then, he generates a key for that repository by using RSA algorithm and shared with the users who are all have an account to access it. Now, repository can be accessed by multiple users with the permission of an owner. Then, owner uploads huge amount of image datasets as zip file into the cloud.

Codebook and Index Generation

The admin of cloud has responsibility to create documents based on images which are useful for searching of images by users. So, he extracts zip file and applies CBIR encryption technique. It encrypts images based on color values and texture features and shuffling the pixels in column-wise as well as row-wise. Then, he creates codebook, index, and image key for those encrypted images. These files are used to improve the searching efficiency of cloud and manage the time properly while retrieving answer.

Add Image/Query to Cloud

Now, users can access the cloud to add their own images into the repository. So, if that cloud has ' n ' number of users, then repository has chance to increase rapidly. Now, the repository has collection of ' n ' number of images in different domains. All the images are stored in encrypted format for security. Then, user must ask query to cloud. Its take query in the format of encrypted image using CBIR encryption technique.

Content-Based Searching and Retrieval

After receiving encrypted image query, the cloud extracts the features of an original image. Now applying content-based searching on the codebook and image index by using that extracted features. Obviously, now searching results will be an encrypted image. This resulted answer will be send to that corresponding user. Now, user can apply CBIR decryption technique to decrypt the retrieved images. So, the answer will be very fine and delicious due to huge dataset.

System Implementation

In the system implementation, the repository is storage space of collection of data. Each repository is created by single user. He is the owner of that repository. Then, he generates a key for that repository by using RSA algorithm and shared with the users who are all have an account to access it. Now, repository can be accessed by multiple users with the permission of an owner. Then, owner uploads huge amount of image datasets as zip file into the cloud. The admin of cloud has responsibility to create documents based on images which is useful for searching of images by users. So, he extracts zip file and applies CBIR encryption technique. It encrypts images based on color values and texture features and shuffling the pixels in column-wise as well

as row-wise. Then, he creates codebook, index, and image key for those encrypted images. These files are used to improve the searching efficiency of cloud and manage the time properly while retrieving answer. Now, users can access the cloud to add their own images into the repository. So, if that cloud has 'n' number of users, then repository has chance to increase rapidly. Now, the repository has collection of 'n' number of images in different domains. All the images are stored in encrypted format for security. Then, user must ask query to cloud. Its take query is in the format of encrypted image using CBIR encryption technique. After receiving encrypted image query, the cloud extracts the features of an original image. Now applying content-based searching on the codebook and image index by using that extracted features. Obviously, now searching results will be an encrypted image. This resulted answer will send to that corresponding user. Now, user can apply CBIR decryption technique to decrypt the retrieved images. So, the answer will be very fine and delicious due to huge dataset.

4 Algorithm

Step 1: Initially, to set the environment.

Step 2: Now, after running, we have to create a registration for admin, owner, and user. The owner adds all the images into the repository.

Step 3: The admin maintains all the data inside the repository by maintaining the codebook.

Step 4: Similarly, an account creation should be made based on the same user data so that the bank account is directly linked to the Web site and to access or purchase of items.

Step 5: The user logins into the Web site and when given an image as a query the image through object detection technique shows all the related images as product and the can directly purchase them.

5 System Architecture

The architecture is given in Fig. 1. Where the owner is going to share the key with the users who are connected. The role of the owner is to upload the image and create the repository. The owner will also provide the key which will be in turn used by the users. The user will add image and the query will be in the form of encrypted image. The final image will be passed to the user from the cloud.

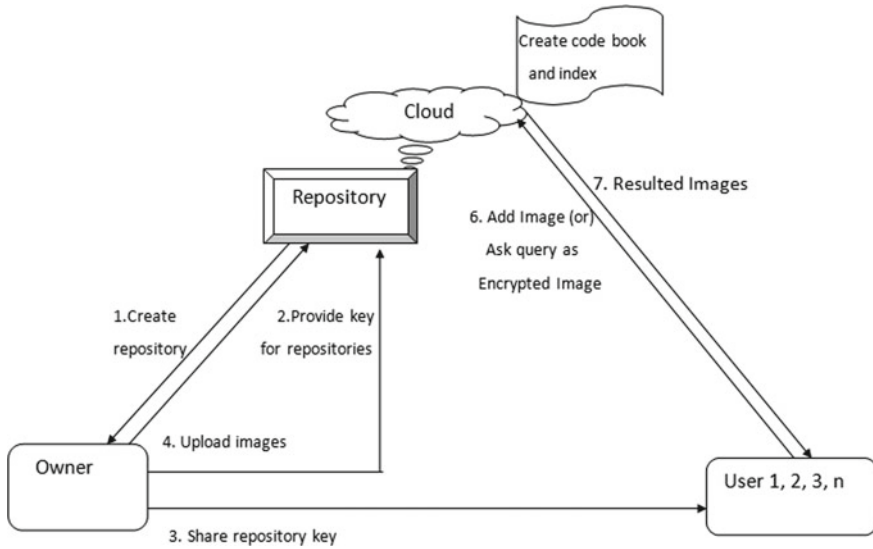


Fig. 1 Architecture diagram

6 Results and Discussions

Figure 2 is a page where the admin maintains the repository. He can do various operations like create repository, create repository key, share repository key, and upload the zip file. Here, the admin shares the key to all its registered users so that the registered users can access the data. The admin also uploads the zip which contains the various images to encrypted data and store in the form of code book. Figure 3 depicts how to generate the codebook and index from the given zip file.

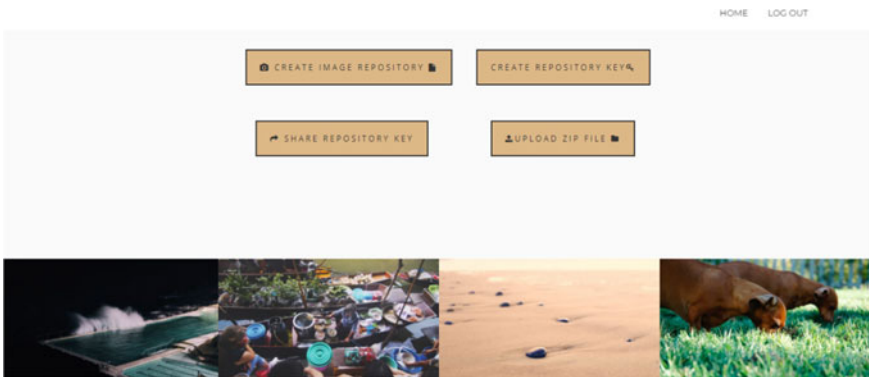


Fig. 2 Content-based image retrieval

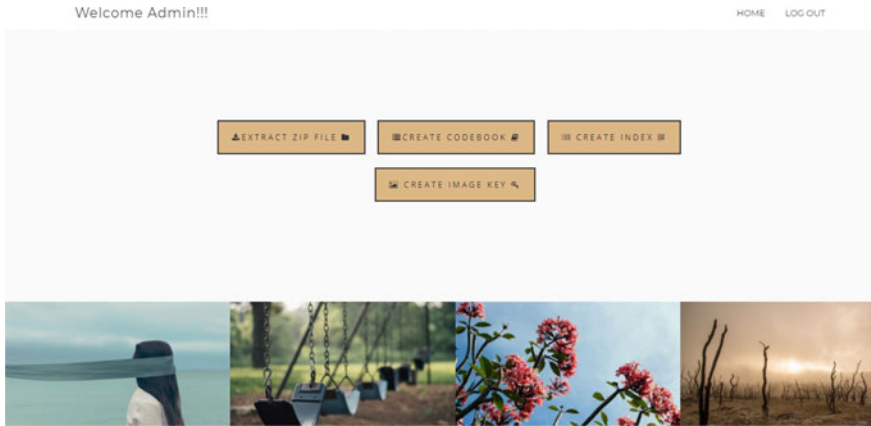


Fig. 3 Generation of codebook and index

7 Conclusion

We have proposed an efficient method of producing an image using content-based retrieval scheme, and these give more comfort to the cloud users as well as backend management team. These areas come under data analytics. The images obtained from random scanners are used for fusion in such a way that they generate high image quality. Classification of the images is done using BOEW. These images are then used for further classification. Process is done using the RSA and AES algorithm. The techniques can be extensively used for detecting images using content and has obtained an accuracy level of about 99.69%.

References

1. G. Nithya, S.L. Shabu, A novel framework in reusing the ontological health record. *Res. J. Pharm. Biol. Chem. Sci.* 7(3), 215–220 (2016)
2. R.S.B. Krishna, M. Aramudhan, Feature selection based on information theory for pattern classification, in *2014 International Conference on Control, Instrumentation, Communication and Computational Technologies (ICCICCT)*. IEEE, July 2014, pp. 1233–1236
3. P.S. Maran, P.M. Velumurugan, B.P.D. Batvari, Wind characteristics and Weibull parameter analysis to predict wind power potential along the South-East Coastline of Tamil Nadu, in *International Conference on Intelligent Information Technologies* (Springer, Singapore, 2018), pp. 190–199
4. A. Karthik, M.D. Kamalesh, Rat trap: inviting, detection & identification of attacker using honey words in purchase portal, in *2017 Third International Conference on Science Technology Engineering & Management (ICONSTEM)*. IEEE, Mar 2017, pp. 130–132
5. S.C. Mana, B.K. Samhitha, J. Jose, M.V. Swaroop, P.C.K. Reddy, Traffic violation detection using principal component analysis and viola jones algorithms. *Int. J. Rec. Technol. Eng. (IJRTE)* 8(3) (2019). ISSN: 2277-3878

6. M.V. Ishwarya, D. Deepa, S. Hemalatha, A.V.S. Nynesh, A. Prudhvi Tej, Gridlock surveillance and management system. *J. Comput. Theor. Nanosci.* **16**(8), 3281–3284 (2019)
7. A. Ponraj, Optimistic virtual machine placement in cloud data centers using queuing approach. *Future Gener. Comput. Syst.* **93**, 338–344 (2019)
8. R. Yogitha, G. Mathivanan, Performance analysis of transfer functions in an artificial neural network, in *2018 International Conference on Communication and Signal Processing (ICCSP)*. IEEE, Apr 2018, pp. 0393–0397
9. M. Selvi, P.M. Joe Prathap, Analysis & classification of secure data aggregation in wireless sensor networks. *Int. J. Eng. Adv. Technol.* **8**(4), 1404–1407 (2019)
10. N. Srinivasan, C. Lakshmi, Forecasting stock price using soft computing techniques, in *2017 Third International Conference on Science Technology Engineering & Management (ICONSTEM)*. IEEE, Mar 2017, pp. 158–161
11. V.V. Kaveri, V. Maheswari, A model based resource recommender system on social tagging data. *Indian J. Sci. Technol.* **9**, 25 (2016)
12. R. Neha, J.Y. Bevis, A survey on security challenges and malicious vehicle detection in vehicular ad hoc networks. *Contemp. Eng. Sci.* **8**(5), 235–240 (2015)
13. S. Ancy, R. Kumar, R. Asokan, R. Subhashini, Prediction of onset of south west monsoon using multiple regression, in *Proceedings of IEEE International Conference on Computer Communication and Systems (ICCCS14)*. IEEE, Feb 2014, pp. 170–175
14. M. Meeker, Internet trends 2015, in *Proceedings of the Code Conference* (2015), pp. 1–196
15. Global Web Index, Instagram tops the list of social network growth, 2013 [Online]. Available: <https://tinyurl.com/hnwvlzm>
16. N. Srinivasan, C. Lakshmi, Stock prediction and analysis using intermittent training data with artificial neural networks, in *2017 International Conference on Innovations in Information, Embedded and Communication Systems (ICIIECS)*. IEEE Mar 2017, pp. 1–4
17. C.D. Manning, P. Raghavan, H. Schütze, *An Introduction to Information Retrieval*, vol. 1 (Cambridge University Press, Cambridge, UK, 2009)
18. S.P. Shyry, Efficient identification of bots by *K*-means clustering, in *Proceedings of the International Conference on Soft Computing Systems* (Springer, New Delhi, 2016), pp. 307–318
19. R. Chow, et al., Controlling data in the cloud: outsourcing computation without outsourcing control, in *Proceedings of the ACM Workshop Cloud Computing Security* (2009), pp. 85–90
20. A. Chen, GCreep: google engineer stalked teens, spied on chats (2010) [Online]. Available: <https://gawker.com/5637234>
21. D. Rushe, Google: don't expect privacy when sending to Gmail, 2013 [Online]. Available: <https://tinyurl.com/kjga34x>
22. G. Greenwald, E. MacAskill, NSA prism program taps into user data of Apple, Google and others (2013) [Online]. Available: <https://tinyurl.com/oea3g8t>
23. J. Halderman, S. Schoen, Lest we remember: cold-boot attacks on encryption keys. *Commun. ACM* **52**(5), 91–98 (2009)
24. National vulnerability database, in *CVE Statistics* (2014) [Online]. Available: <https://web.nvd.nist.gov/view/vuln/statistics>. Statistics (2014) [Online]. Available: <https://web.nvd.nist.gov/view/vuln/statistics>
25. D. Lewis, *iCloud Data Breach: Hacking and Celebrity Photos* (2014) [Online]. Available: <https://tinyurl.com/nohznmr>

Feature Selection Using Multiple Kernel Learning Methods



K. Siva Sandeep Reddy, K. Gunavardhan Reddy, A. Pravin, G. Nagarajan,
and T. Prem Jacob

1 Introduction

Kernel-based clustering calculations, for example, k -mean part, can catch the characteristic nonlinear structure in numerous genuine world datasets and consequently by and large perform preferred in bunch execution over direct parcel techniques [1]. In genuine applications, we can assemble a few centers and apply a few principle capacities. Be that as it may gathering execution to a great extent relies upon the decision of grains [2]. Sadly, it is as yet a test to decide a reasonable among a wide scope of potential centers for information gave and undertakings ahead of time. It is increasingly troublesome, particularly in solo learning exercises, for example, gathering, because of the nonattendance of labels. To conquer this trouble, numerous solo different portion learning strategies are accessible proposed [2, 3], which plan to become familiar with a center of agreement of a gathering of client characterized centers. Customary multi-center learning strategies without supervision gain proficiency with an accord center by directly joining a set of applicant beans. For instance, [4] gave a strategy for otherworldly gathering of numerous perspectives in a direct manner joined phantom embeddings to get the last bunching. The technique proposed a restricted various parts k -implies strategy for malignant growth

K. Siva Sandeep Reddy (✉) · K. Gunavardhan Reddy · A. Pravin · G. Nagarajan · T. Prem Jacob
Department of Computer Science and Engineering, Sathyabama Institute of Science and
Technology, Chennai, India
e-mail: Kssr143.143@gmail.com

K. Gunavardhan Reddy
e-mail: gunavardhan8285@gmail.com

A. Pravin
e-mail: Pravin_ane@rediffmail.com

G. Nagarajan
e-mail: nagarajanme@yahoo.co.in

science applications [5]. A different piece learning technique is learning the ideal neighborhood for the bunching [3].

The above strategies focus on consolidating all up-and-comer bits, while overlook the vigor of the techniques. In any case, in certifiable applications, the bits are regularly tainted by clamors. For instance, since the first information may contain clamors and exceptions, the piece built with these information will likewise be defiled. What is more, despite the fact that the information is spotless, ill-advised piece capacities may likewise present clamors.

2 Related Works

To ease the exertion of commotions, as of late, some strong different piece learning strategies [6, 7] are proposed. These techniques center around the commotions brought about by the defiled occurrences, though cannot catch the commotions initiated by piece works well. Note that, some different part learning techniques dole out bigger load on the more suitable parts can catch the commotion incited by bit capacities to a few degree. Be that as it may, in these techniques, the weight is forced on all components of the piece lattice, and it is a piece excessively harsh. For model, some wrong pieces may have a low weight in these techniques, which implies all components including the helpful parts in the piece lattice will have a similar low weight and won't be useful to the kernel-based learning. To deal with commotions all the more extensively, right now, we propose a novel local and global de-noising multiple bit learning technique. We see that the piece grid may contain two sorts of clamors: one is brought about by debased occurrences, and the other is brought about by unseemly portion capacities. Primary proposed by Yohai (1988), MM-estimators have become increasingly popular and perhaps now in the most commonly employed robust regression technique. They combine a heavy breakdown point (50%) with good efficiency (approximately 95%). The "MM" in the name refers to the fact that more than one M -estimation procedure is used to calculate the final estimates. It has both the high breakdown property and a higher statistical efficiency than S estimation.

3 Proposed Work

Multiple portion learning has been effectively examined [3, 5, 8]. In view of the accessibility of class marks, different piece learning can be classified into two classes: directed calculations and unaided strategies. In supervised learning, names of occasions are accessible, which can be useful to take in an agreement portion from different parts. For instance, Liu et al. coordinated range data into numerous part learning to improve the bit learning execution; stretched out extraordinary learning machine to various portion picking up prompting a numerous bit outrageous learning

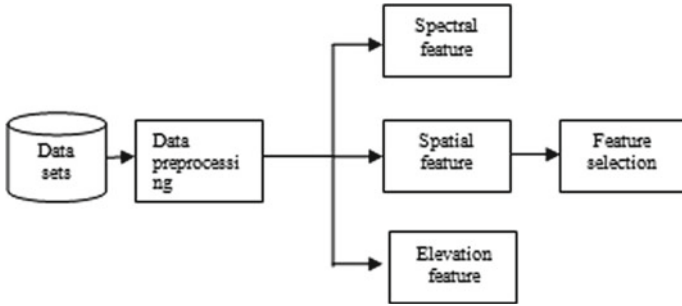


Fig. 1 Architectural view

machine. Albeit administered various portion learning has been broadly contemplated, solo calculation is all the more testing because of the nonappearance of class names. In unaided learning, a few techniques broaden single piece-based bunching strategy into various bit setting. For instance, proposed a different part fluffy grouping techniques by presenting a network initiated regularization and gave a self-weighted different part learning calculation and applied it to a diagram-based bunching technique. Since part k -implies is a well-known bunching strategy, numerous unaided different piece learning techniques have P. Zhou et al.: Unsupervised robust multiple kernel Learning by means of extracting local and global noises been created in its system. They likewise proposed two co-regularization-based methodologies for multi-see ghostly grouping by upholding the bunching theories on various perspectives to concur with one another collected pieces with various loads into a brought together one for ghastrly grouping. By falling back on the otherworldly technique, additionally proposed to unravel a different part k -implies related with two-layer loads [5]. Like [5, 6] first introduced a various bit k -implies strategy which considered the portion connections, and afterward relying upon the outcomes in [1], they move the part k -intends to phantom strategies furthermore, get the grouping results from eigenvalue decay.

Figure 1 gives the architectural view of the system. The datasets that are collected are grouped, and it will be given for the next stage. The next process will be the data preprocessing. The output will be the extraction of the special feature and the elevation feature, and finally, the feature selection is performed.

4 Results and Discussion

We provide in the reference color scene in Fig. 2 and after the computation we get noisy low-resolution depth map and after that we get reconstructed high-resolution depth map.

We provide the black and white image in Fig. 3 containing some noise and specify the user required colors and after the execution we obtain the desired outcome.

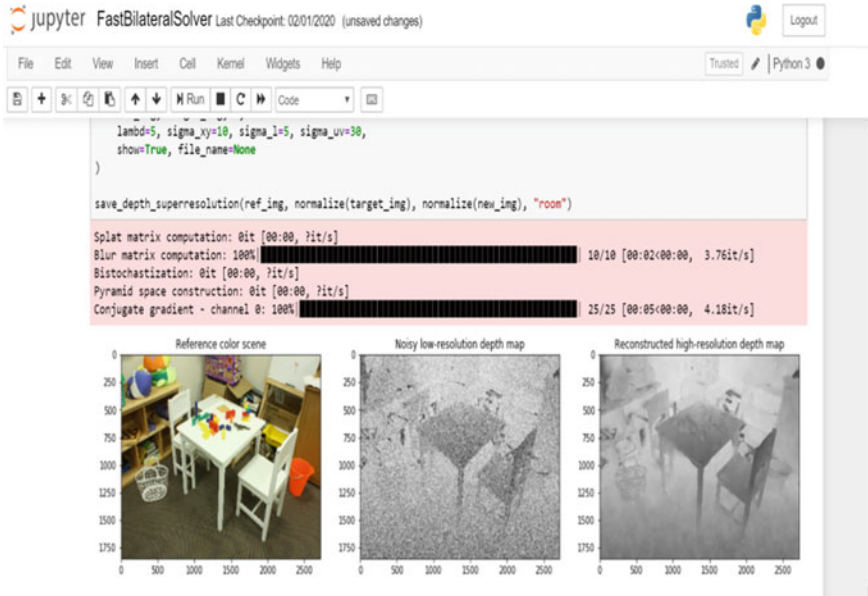


Fig. 2 Reference color scene

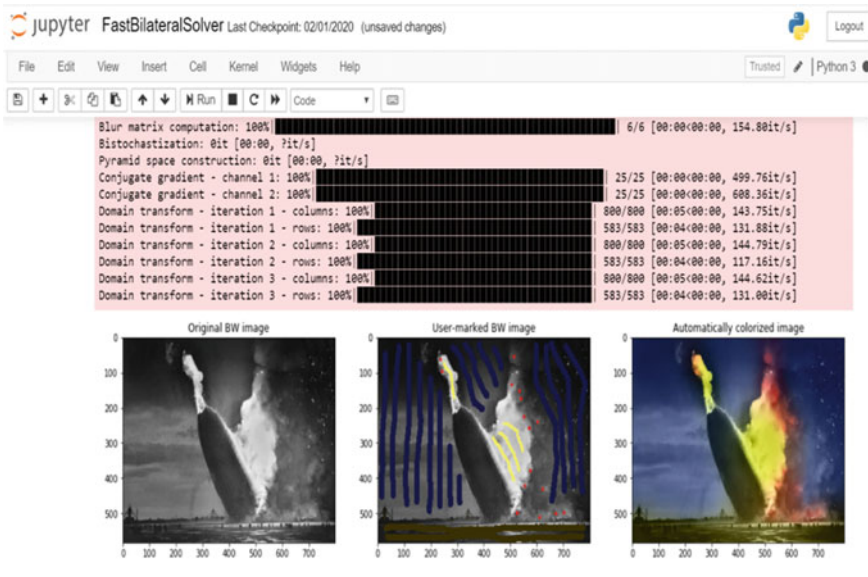


Fig. 3 Original BW image to automatically image

5 Conclusion

Contrasted and the isotropic dispersion model and the absolute variety model, the new model inferred right now dependent on PDEs. It conquers the staircase impact, which is inalienable in the idea of the picture denoising by the isotropic dissemination in the level area, while secures the limit highlights; it defeats the square impact, which is innate in the idea of the picture denoising by the all-out variety model, while holds the neighborhood subtleties and qualities. From the presentation of the reenactments, the new model has more denoise capacity regarding PSNR contrasted with the isotropic dispersion model and the absolute variety model. Note that numerical estimations do not consider other proficient counts and progressively appropriate weight capacities. On the off chance that different techniques for comprehending the halfway differential conditions are applied to the new model, the intermingling rate might be improved. Furthermore, because of the absence of the earlier information on the picture and the investigation of the general structure of the picture, the exhibition of denoising of the new model should be improved, and these are inspired us for future research.

References

1. K. Dabov, A. Foi, V. Katkovnik, Image denoising by sparse 3-D transform-domain collaborative filtering. *IEEE Trans. Image Process.* **16**(8), 2080–2095 (2007)
2. Y.J. Li, J. Zhang, J. Wang, Improved BM3D denoising method. *IET Image Process.* **11**(12), 1197–1204 (2017)
3. L. Du et al., Robust multiple kernel k -means using 2,1-norm, in *Proceedings of the 4th International Joint Conference on Artificial Intelligence*, Jun 2015, pp. 3476–3482
4. X. Liu, Y. Dou, J. Yin, L. Wang, E. Zhu, Multiple kernel k -means clustering with matrix-induced regularization, in *Proceedings of the 30th AAAI Conference on Artificial Intelligence*, Feb 2016, pp. 1888–1894
5. X. Liu, M. Li, L. Wang, Y. Dou, J. Yin, E. Zhu, Multiple kernel k -means with incomplete kernels, in *Proceedings of the 31st AAAI Conference on Artificial Intelligence*, Feb. 2017, pp. 2259–2265
6. M. Gönen, A.A. Margolin, Localized data fusion for kernel k -means clustering with application to cancer biology. *Proc. NIPS* **2**, 1305–1313 (2014)
7. V.R. Sarma Dhulipala, P. Devadas, P.H.S. Tejo Murthy, Mobile phone sensing mechanism for stress relaxation using sensor networks: a survey. *Wirel. Pers. Commun.* **86**, 1013–1022 (2016). <https://doi.org/10.1007/s11277-015-2969-y>
8. X.J. Mao, C. Shen, Y.B. Yang, Image restoration using very deep convolutional encoder-decoder networks with symmetric skip connections (2016). arXiv preprint arXiv:1603.09056
9. J. Xie, L. Xu, E. Chen, Image denoising and inpainting with deep neural networks, in *Advances in Neural Information Processing Systems* (Nevada, USA, 2012), pp. 341–349
10. F. Zhang, N. Cai, J. Wu, G. Cen, H. Wang, X. Chen, Image denoising method based on a deep convolution neural network. *IET Image Processing.* **12**(4), 485–493 (2018)

Detection of Ransomware Based on Recurrent Neural Network (RNN)



Saketh Kanumuri, Vinay Teja Kantipudi, A. Viji Amutha Mary, and Mercy Paul Selvan

1 Introduction

With the expanded utilization of PC frameworks and the development of the Internet, cybercrime has additionally expanded [1]. In the created world, processing and Web use is imbued in the public eye, the economy and foundation. This perplexing blend has made a rewarding situation of potential unfortunate casualties, which can be gone after by cybercriminals [2]. Digital assaults are expanding day by day, regularly powered by advancing innovation [3, 4]. Ransomware has developed as a significant danger to people and organizations the same. Given the pervasive idea of figuring, ransomware is regularly profoundly computerized, consequently empowering lawbreakers to focus on a wide scope of exploited people like ventures, administrative organizations and people [5].

Ransomware is getting progressively hazardous, causing critical harm around the world. Ransomware—a compound expression of payoff and programming—is utilized to encode and incapacitate a client's important information, expecting instalment to recuperate it. The high identification exactness of grouping learning models is for the most part fuelled by the capacity of repetitive neural systems, for example, a Long Short-Term Memory (LSTM) [6], to tie between relatedness

S. Kanumuri · V. T. Kantipudi · A. V. A. Mary (✉) · M. P. Selvan
Department of Computer Science and Engineering, Sathyabama Institute of Science and Technology, Chennai, India
e-mail: vijiamumar@gmail.com

S. Kanumuri
e-mail: saketh.kanumuri@gmail.com

V. T. Kantipudi
e-mail: vinaytejakantipudi@gmail.com

M. P. Selvan
e-mail: mercupaulselvan.cse@sathyabama.ac.in

between occasions happening in a specific consecutive request. While such request can be caught correspondingly in ransomware successions, we accept that these arrangements display certain extra properties.

The ransomware scrambles the documents surprisingly fast once it begins activity making the records out of reach [7, 8]. A strategy that investigations the executables even before they start is to be created [9]. The proposed work does an itemized investigation of API calls as it tends to be utilized to perform malignant exercises. Since API calls are the essential square of a program, its examination can be utilized for seeing how a record acts. The work done right now is as follows:

- Dealing with class awkwardness as the quantity of ransomware tests are a lot higher than kind examples
- Applying different AI classifiers to distinguish the best model for identifying ransomware
- Analysis of a colossal corpus of ransomware and generous documents to recognize the most distinctive API calls among ransomware and amiable records.

2 Relatedwork

The present assemblage of writing contains some work concentrating on the investigation and discovery of ransomware assaults dependent on arrange traffic. Cabaj et al. [10] dissected Crypto ransomware powerfully in a devoted domain utilizing a honeypot and programmed run-time malware systematic framework. They recognized a portion of the system exercises of Crypto and introduced functional outcomes, i.e. distinguishing some intermediary servers, the conventions utilized and the hard-coded addresses of certain servers. It does not remove any nonexclusive social component that can be applied to the recognition of different sorts of Crypto ransomware. Ahmadian et al. [11] proposed the Connection Monitor and Connection Breaker (CM&CB) system to recognize 'high survivable ransomwares' which utilize Domain Generation Algorithm (DGA). The proposed strategy examines the mentioned area names against a recently prepared English language Markov chain model. This work is assembled exclusively upon a solitary system highlight. Further, the viability of utilizing a Markov chain model against short messages, i.e. an area name, is faulty and may cause high bogus positive rates. This technique requires the structure and support of Markov chain models for some non-English dialects, which would be a costly procedure. Ramya et al. proposed a technique for restricting mischievous users in anonymous networks [12].

Kharraz et al. [13] examined ransomware having a place with different classifications like work area locking and those utilizing encryption procedures for locking the client documents. They arrived at the determination that there are various ransomware which show comparative examples and they can be separated from ordinary amiable processes. They recommended procedures dependent on observing of record framework exercises; however, these techniques were not assessed by the creators Kharraz et al. has recommended strategies which check for the similitude

of screen captures that are taken before executing a ransomware and subsequent to executing a ransomware which has a place with the storage family. Their techniques do not proactively recognize ransomware when it enters the framework and starts its activity. An elective reinforcement office is likewise excluded from their investigation.

2.1 Network Traffic Analysis

$$\begin{aligned} R_t &= \text{MATRIX}(S_t) \\ M_t &= \text{DENSE}(W_d * R_t) \end{aligned} \quad (1)$$

$$\begin{aligned} \alpha_t &= \text{SoftMax}(\omega T M_t) \\ r_t &= R_t \alpha T_t. \end{aligned} \quad (2)$$

3 Proposed system

The approach for the investigation and arrangement of the different kinds of record in our work is talked about underneath. When an executable is gotten by the framework, our model ought to have the option to mark it as (a) Ransomware, i.e. malevolent programming that scrambles the client records. Benign applications are not pernicious. The fundamental plan to accomplish this objective is by a static investigation of the executable and utilizing API calls utilized as the most separating highlight to recognize ransomware and amiable documents. The various advances done to land at this are (1) Feature extraction and investigation: We remove out the API calls utilized in the different kinds of executables, and a point by point examination is done to recognize the most separating sets of highlights to be utilized for arrangement. (2) Dealing with class unevenness: Class awkwardness happens when there are extensively a larger number of instances of one objective class than another. We have an imbalanced dataset as the ransomware class is the dominant part. This is a significant issue looked by numerous malware location frameworks [13, 14]. Class lop-sidedness may influence the working of the classifier, and there is an inclination towards the greater part class. We have managed this issue by applying Smote method by chawla et al. [3]. (3) Classification: The information removed from the component extractor is sent to an essential classifier like choice tree or troupe of classifiers like an irregular woodland for preparing. At the point when another st of test information is given, the classifier yields the forecast whether the given record is ransomware or not. The proposed model is appeared in Fig. 1. The executable document which might be a ransomware or an amiable record initially experiences a

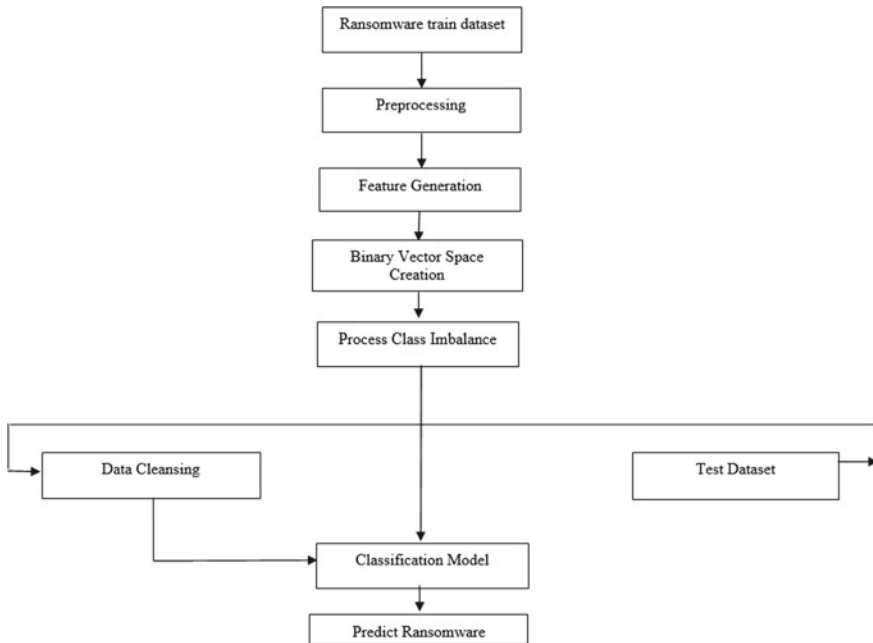
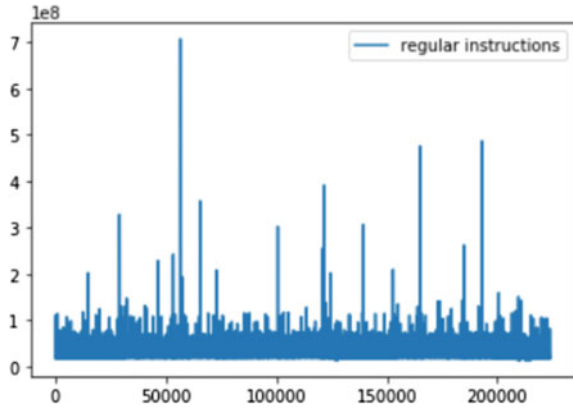


Fig. 1 Architecture

pre-processing stage where the static code of the executable is broken down to extricate all the API calls that are habitually found. Programming interface calls that are huge are recognized, and its essence in the executable is meant as a parallel vector. The quantity of ordinary/kind-hearted documents that are accessible is far less in number than the quantity of ransomware accessible through different sources. This prompts the issue of class lop-sidedness which may influence the presentation of the order model. This issue is managed, and the decent preparing information is nourished to the characterization model which can foresee whether the an inconspicuous document is a ransomware ornot.

We can decide if a record might be pernicious by its API calls, some of which are regular for particular kinds for ransomware. Programming interface capacities and framework calls are connected with administrations given by working frameworks. Programming interface capacities and framework calls bolster different key activities given by working frameworks, for example, arrange, security, framework administrations, document the board, etc. Moreover, they incorporate different capacities for using framework assets, for example, memory, document framework, system, or illustrations. The examples of API work calls can give key data that can be utilized to identify the development of programming and to speak to practices of the product. Examination on API capacities and framework is considered an import job in conducting investigation of ransomware. In an investigation done by Kharazz et al., the significant level I/O of ransomware is illustrated in Fig. 2. In the different

Fig. 2 Graphical representation of instructions



cases appeared in the figure, the Attacker overwrites the clients document with an encoded form or the assailant peruses, scrambles and erases records without cleaning them from capacity. On the off chance the aggressor peruses, makes another encoded variant, and safely erases the first records by overwriting the content. On examination, it is seen that the API calls comparing to these exercises are utilized vigorously in ransomware documents as opposed to in kind-hearted documents. On dismantling the different ransomware and generous records, it is seen that there are sure API calls that are available just in ransomware [15] documents. This incorporates certain based APIs calls and a few API calls that are Crypto calls. On analysing the different API calls all the more intently, we found that specific API calls are available in both ransomware and kind records; however, how they are utilized and the recurrence of their utilization fluctuated among ransomware and favourable. These API calls are available in a bigger number of ransomware records.

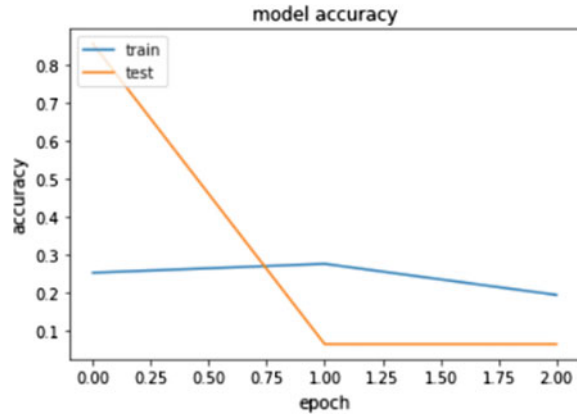
4 Architecture

See Fig. 1.

5 Result Analysis

See Figs. 2 and 3.

Fig. 3 Graph depicts prediction of ransomware



6 Conclusion

Right now, identification of ransomware has been finished by extricating the API calls utilized by the ransomware and benevolent documents. Methods to keep away from that destroyed was applied on the preparation set and the presentation has essentially improved. It is seen that arbitrary backwoods applied on the fair preparing set subsequent to applying destroyed gives the best execution. Ransomware is a malware that catches the clients' PC, encodes the information, keeps the getting to of the documents from the PC and requests cash to get to those information and ordinary working of the framework. The paper began with clarifying session ransomware, assaults of ransomware and the impact of this on India. Ransomware examination and CryptoLocker are likewise clarified. This paper additionally clarifies the ransomware procedure and associations between various strides right now. The hazard from ransomware is genuine, and the hazard is enormous. Obviously, ransomware is a major risk and powerful measure, and method must be produced for counteraction.

References

1. W. Mattias, F. Jan, S. Andreas, J. Eric, A novel method for recovery from crypto ransomware infection, in *2nd IEEE International Conference on Computer and Communications*, (2016), pp. 1354–1358
2. K.E. Gnanesh, T. Dheeraj Bhavan Narayana, M.D. Kamalesh, Retrieval of encrypted data using trapdoor method in cloud computing. *J. Comput. Theor. Nanosci.* **16**(8), 3237–3241 (2019)
3. M. Reeta, Strategies: to defeat ransomware attacks. *Int. J. Eng. Res. General Sci.* **5**, 112–116 (2017)
4. M.A. Chowdary, M. Kundan, D.A.V.A. Mary, Effective credit card forgery prevention using multilevel authentication, in *IOP Conference Series: Materials Science and Engineering*, vol.

- 590, issue no. 1, (IOP Publishing, 2019), p. 012021. <https://doi.org/10.1088/1757-899X/590/1/012021>
5. T.P. Jacob, T. Ravi, Optimal regression test case prioritization using genetic algorithm. *Life Sci. J.* **10**(3), 1021–1033 (2013)
 6. Bleeping Computer, Locky Ransomware Information, Help Guide and FAQ, May, 2016, Last Accessed Oct 2017
 7. Korea Internet and Security Agency, 16 Ransomware Trends and 17 Outlook, 2017
 8. T. Anandhi, K.V. Kishore, G.S. Maha, R.M. Gomathi, A sustainable vehicle parking using IoT, in *2019 3rd International Conference on Trends in Electronics and Informatics (ICOEI)* (IEEE, 2019), pp. 950–952
 9. M. Anand, T. Sasikala, Efficient energy optimization in mobile ad hoc network (MANET) using better-quality AODV protocol. *Cluster Comput.* **22**(5), 12681–12687 (2019)
 10. A. Kapratwar, F. Di Troia, M. Stamp, Static and dynamic analysis of android malware, *Hindawi Security and Communication Networks*, 2018
 11. M.K. Alzaylaee, S.Y. Yerima, S. Sezer, Improving dynamic analysis of android apps using hybrid test input generation, in *IEEE International Conference On Cyber Security And Protection Of Digital Services (Cyber Security 2017)*, (2017)
 12. G. Ramya, A.V.A. Mary, Restricting mischievous users in anonymizing networks. *IJETT* **9**(2) (2014)
 13. Kharraz, A., et al., Cutting the Gordian knot: a look under the hood of ransomware attacks, in eds by F. Maggi, M. Almgren, V. Gulisano, *12th International Conference on Detection of Intrusions and Malware, and Vulnerability Assessment, DIMVA 2015*. (Springer, Heidelberg, 2015), pp. 3–24
 14. L. Li, T.F. Bissyandé, M. Papadakis, S. Rasthofer, A. Bartel, D. Ocateau, J. Klein, L. Traon, Static analysis of android apps: a systematic literature review, *Inf. Softw. Technol.* **88** (2017)
 15. Nirmalraj, S., Nagarajan, G. (2019). An adaptive fusion of infrared and visible image based on learning of sparse fuzzy cognitive maps on compressive sensing. *Journal of Ambient Intelligence and Humanized Computing*, 1–11.
 16. X. Luo, Q. Liao, Awareness education as the key to ransomware prevention. *Inf. Syst. Secur.* **16**(4), 195–202 (2007)
 17. B.A.S. Al-rimy, M.A. Maarof, S.Z.M. Shaid, A 0-day aware crypto ransomware early behavioral detection framework. *Recent Trends Inf. Commun. Technol.*
 18. A. Bhardwaj, G.V.B. Subrahmanyam, V. Avasthi, H. Sastry, Ransomware: a rising threat of new age digital extortion. in arXiv preprint [arXiv:1512.01980](https://arxiv.org/abs/1512.01980), 2015. V. Weafer, McAfee Labs Threats RepOlt, McAfee, March 2016
 19. M. Kanwal, S. Thakur, R. Lashkari, An app based on static analysis for Android ransomware, in *2017 8th International Conference on Computing, Communication and Automation* (2017)
 20. J. Chen, C. Wang, Z. Zhao, K. Chen, R. Du, G.J. Ahn, Uncovering the face of android ransomware characterization and real-time detection. *IEEE Trans. Inf. Forensics Secur.* (2017)
 21. D.Y. Kim, G.Y. Choi, J.H. Lee, White list-based ransomware real-time detection and prevention for user device protection, in *2018 IEEE International Conference on Consumer Electronics* (2018)
 22. McAfee, Part of Intel Security, What's on the Horizon for 2016, Mobile Threat Report of Intel Security, 2016
 23. Selvan, M.P., Gupta, A. and Mukherjee, A. Give attention to overlapping network detection in network for multimedia. *J. Comput. Theor. Nanosci.* **16**(8) (2019)

A Unique Adaptive Framework for Predicting Lane Changing Intention Based on CNN



K. Pavan, M. Dhanaveera Teja, A. Pravin, T. Prem Jacob, and G. Nagarajan

1 Introduction

Driver wellbeing has consistently been a territory important to car examine. With the progression of semiconductor plan, ground- breaking electronic gadgets with little impressions are beginning to show up in numerous vehicles. These gadgets are fit for performing different assignments to help the driver of a car preparing for Driver Assistance frameworks. One sort of Driver Assistance framework is Lane Departure Warning which helps the driver in lane changes. LDW depends on lane recognition which can be portrayed as an issue of distinguishing painted white or yellow markings out and about surface with practically no earlier information out and about geometry. Vision based lane discovery is performed with the assistance of a camera that mounted is under the back view mirror and takes a gander at the street ahead. Utilizing highlight extraction calculations, pictures caught by the camera framework are deciphered to extricate important data like lane marker positions and limits [1, 2]. Traffic lane detection is one of the theoretically simplest applications in automatic driving technologies: however, given the need for a very robust solution to ensure

K. Pavan (✉) · M. D. Teja · A. Pravin · T. P. Jacob · G. Nagarajan
Department of Computer Science and Engineering, Sathyabama Institute of Science and Technology, Chennai, India
e-mail: pavansunny12143@gmail.com

M. D. Teja
e-mail: dhanaveeratejamallireddy@gmail.com

A. Pravin
e-mail: pravin_ane@rediffmail.com

T. P. Jacob
e-mail: premjac@yahoo.com

G. Nagarajan
e-mail: nagarajanme@yahoo.co.in

the safety of travelers under any route, weather and light conditions, even a simple application poses challenges that need to be addressed [3, 4]. In the demo below, we see an example of a lane detection system that recognizes concrete boundaries and uses them to determine when the car moves from its location in a lane to one of the lines that delimit it [5]. Lane lines are clearly identified and the machine knows with completed certainty when the car approaches one of them, when it passes it and when it drives on a different lane than the one from which it originates.; finally, detect the position of a line even when another vehicle or any other obstacles prevent the camera from seeing it, in full or impetrate system desires to be flawlessly calibrated in order in no way to loose touch with the ideal directly strains delimitating each sides of the lane, no matter climate or visitors conditions. There is not any need for multiple camera, if you want to make this digicam calibration gadget robust sufficient. The set of rules takes into account the perspective given by means of the incoming photographs and exploits the properties of vanishing factors, computed through identifying the 2 parallel lines [6]. Knowing at every unmarried moment the width of the lane leaves the developer with a extraordinarily simple geometric problem to resolve. As a result, the system is aware of whilst the auto (both driving force or driverless) is deviating from its lane, voluntarily or not: this system mastering based totally answer may be very sturdy, as obviously required through protection standards. RSIP Vision works on several ADAS-associated projects, generally more complex than visitors lanes detection Modern technology allows the vehicle to have internet connection [7, 8].This helps the vehicle to know heavy traffic areas ahead of time and also decrease the time complexity. Some companies include a voice assist to help user to navigate or alert him incoming object behind the vehicle [9, 10].

2 Related Works

So J. H. Jung, Y. Shin and Y. Kwon, “Extension of Convolutional Neural Network with General Image Processing Kernels,” in 2018. This paper introduced increased efficiency of Lane management system through by adding CNN(Convolutional Neural Network) which refines the video inputs though repeated frame max pool and thereby increasing clarity of the image which can be used to detect faint edges of smaller object [11, 12].

Lucas Has introduced “Optical character recognition with Hough transform based neural networks” which was published on 1993 introduced various computer vision based of the proposed system [13–16].

S. Changand Chen-Ju Chou, “Rear-end collision warning system with a rear-end surveillance camera” published in 2009 introduced safety mechanism to alert driver of incoming obstacle from rear of the vehicle. This module Increases the safety of the driver and also increases the awareness of the driver [17, 18]. This Module is integrated into proposed system to 360 degree view awareness to the vehicle.

2.1 Core Concepts

2.1.1 Edge Detection

Edges are important changes in intensity in a picture at the local level. Edges typically occur in a picture at the border between two distinct regions [14, 15]. The noticeable edge in the photo is the vertical line between the white paper and the black paper. There is a relatively sudden change between the black pixels and the white pixels to our eyes. But the transformation is really that sudden on a pixel-by-pixel basis [19].

2.1.2 Prediction

A family of algorithms where they all share a common definition, i.e. each pair of characteristics to be classified is independent of each other [16, 20]. The Naive Bayes classifiers are a group of classification algorithms based on Bayes' Theorem. Bayes' formula gives relation to $P(A)$ and $P(B)$.

3 Proposed Work

Keep Examine Most of the lanes are planned to be relatively straightforward not only to promote orderliness but also to make steering vehicles with consistent speed easier for human drivers. Our natural arrangement may hence be to initially recognize conspicuous straight lines in the camera that feed through edge recognition and extraction systems. We are going to be utilizing OpenCV, an open source library of pc vision calculations for usage.

We will feed in our sample video for lane detection as a series of continuous frames (images) by intervals of 10 ms. We can quit the program anytime by pressing the 'q' key.

The Canny Detector is a multi-stage algorithm optimized for fast real-time edge detection. The fundamental goal of the algorithm is to detect sharp changes in luminosity (large gradients), such as a shift from white to black, and defines them as edges, given a set of thresholds. The Canny algorithm has four main stages: As with all algorithms for edge detection, noise is a crucial issue which often leads to false detection. To convert (smooth) the signal, a 5×5 Gaussian filter is applied to lower the sensitivity of the detector to noise. This is achieved by using a kernel of normally distributed numbers (in this case a 5×5 kernel) to run through the entire image, setting each pixel value.

Initial Module used for lane detection was derived from paper published on 2018. In this paper they make use of monocular camera to get the image as grey scale and use Canny edge detection along with Hough Transform to find lane and also help System to align the vehicle along the centre of the lane. This paper also Introduced

Example	Description
<code>cv::FileNode fn</code>	File node object default constructor
<code>cv::FileNode fn1(fn0)</code>	File node object copy constructor; creates a node <code>fn1</code> from a node <code>fn0</code>
<code>cv::FileNode fn1(fs, node)</code>	File node constructor; creates a C++ style <code>cv::FileNode</code> object from a C-style <code>CvFileStorage*</code> pointer <code>fs</code> and a C-style <code>CvFileNode*</code> pointer <code>node</code>
<code>fn[(string)key]</code> <code>fn[(const char*)key]</code>	STL string or C-string accessor for named child (of mapping node); converts key to the appropriate child node
<code>fn[(int)id]</code>	Accessor for numbered child (of sequence node); converts ID to the appropriate child node
<code>fn.type()</code>	Returns node type enum
<code>fn.empty()</code>	Determines if node is empty
<code>fn.isNone()</code>	Determines if node has value None
<code>fn.isSeq()</code>	Determines if node is a sequence
<code>fn.isMap()</code>	Determines if node is a mapping
<code>fn.isInt()</code> <code>fn.isReal()</code> <code>fn.isString()</code>	Determines if node is an integer, a floating-point number, or a string (respectively)
<code>fn.name()</code>	Returns nodes name if node is a child of a mapping
<code>size_t sz=fn.size()</code>	Returns a number of elements in a sequence or mapping
<code>(int)fn</code> <code>(float)fn</code> <code>(double)fn</code> <code>(string)fn</code>	Extracts the value from a node containing an integer, 32-bit float, 64-bit float, or string (respectively)

Fig. 1 Function descriptions

various Formulas to detect the curvature of their the end map of edges after non-maximum suppression. Weak curved lane and manoeuvring accordingly. Using two predefined `minVal` and `maxVal` threshold values, we set that any pixels with gradient intensity higher than `maxVal` are edges and any pixels with gradient intensity lower than `minVal` are not edges and discarded. Pixels with an intensity gradient between `minVal`, and `maxVal` are called edges only when related to a pixel above `maxVal`, with an intensity gradient (Fig. 1).

3.1 Architecture

After the examination, lane change information were extricated physically, in view of controlling wheel point and vehicle’s sidelong position information. As appeared in Fig. 3, during an ordinary lane change, driver modified directing wheel edge as an

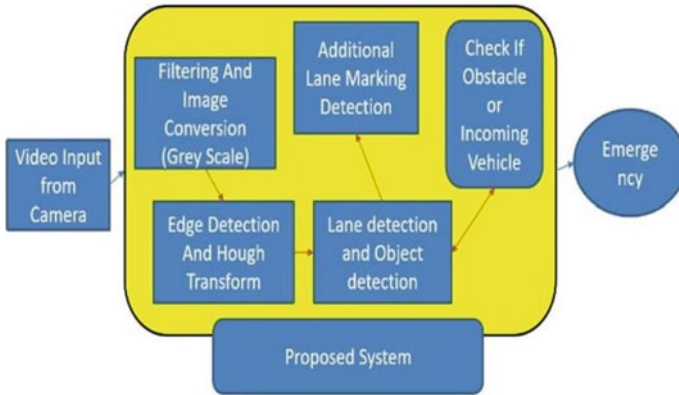


Fig. 2 System architecture

estimated sine bend. Consequently, in the present examination, the beginning of lane change t_0 was characterized toward the start of controlling wheel edge sine bend. The directing wheel speed was determined as the pace of changes in controlling wheel edges. Hypothetically, controlling wheel speed goes before directing wheel edge in a quarter stage (LA stage in Fig. 3). Subsequently, three stages: LK (t_0 up to 13 s earlier), LA, and ALC (t_0 to the primary pinnacle of controlling wheel point t_1) were broke down in the accompanying areas. Inside subject structure was applied in the present investigation. Examination of change and combined examples t-test strategy were utilized to investigation the information, with p esteem under 0.05 as factual importance.

Since we can show a picture to a client, we may likewise need to permit the client to collaborate with the picture we have made. Since we are working in a window situation and since we previously figured out how to catch single keystrokes with `cv::wait Key()`, the following legitimate interesting point is the manner by which to “tune in to” and react to mouse occasions. In contrast to console occasions, mouse occasions are dealt with by an increasingly customary callback system. This implies, to empower reaction to mouse clicks, we should initially compose a callback schedule that OpenCV can call at whatever point a mouse occasion happens. When we have done that, we should enroll the callback with OpenCV, accordingly advising OpenCV this is the right capacity to utilize at whatever point the client accomplishes something with the mouse over a specific window (Fig. 2).

3.2 Advantages

- Prediction for the future
- Useful for taking business decision

- Deeper understanding of employee requirements which, in turn, builds better business relationships.

3.3 Results

See Figs. 3 and 4.



Fig. 3 Lane detection I



Fig. 4 Lane detection II

4 Conclusion

The Perception paper contains a summarized, version of various aspects involved in Autonomous Vehicle. This Proposed architecture of the program is used to evaluate lane management concepts using computer vision. We make use of Canny edge detection along with Hough Transform. The proposed was initially introduced to autonomous vehicle where a system is used to drive the vehicle, but this can also be used as semi autonomous, which can help driver to be aware of incoming vehicles from side and rear better than normal mirrors. In order to further increase awareness in the system we can add various lane detection constraints like detection of traffic signals and incoming object detections. For future works we can include connection to the internet so that the proposed system can take the latest updates of traffic and suggest various alternatives for the destination. This Models can be used in various Vehicle management system and also advanced robotics for development of a better AI.

References

1. Integrals of Lipschitz-Hankel type involving products of Bessel functions. *Phil. Trans. Roy. Soc. Lond.* **A247**, 529–551 (1955) (references)
2. J. Clerk Maxwell, *A Treatise on Electricity and Magnetism*, 3rd ed., vol
3. Y. Yorozu, M. Hirano, K. Oka, Y. Tagawa, Electron spectroscopy studies on magneto-optical media and plastic substrate interface. *IEEE Transl. J. Magn. Jpn.* **2**, 740–741 (1987) (Digests 9th Annual Conf. Magnetism Japan, p. 301, 1982).
4. M. Young, *The Technical Writer's Handbook* (University Science, Mill Valley, CA) 19 M. Bahram, A. Lohrer, M. Aeberhard, Generatives Prädiktionsmodell zur frühzeitigen Spurwechselerkennung, in *9. Workshop Fahrerassistenzsysteme* (2014)
5. H.M. Salvucci, M.D.D. Using support vector machines for lane-change detection, in *Proceedings of the Human Factors and Ergonomics Society Annual Meeting, Los Angeles, CA, USA, 26–30 October 2015*, vol. 49, pp. 1965–1969
6. S. Jacobs, C.P. Bean, Fine particles, thin films and exchange anisotropy, in *Magnetism*, vol. III, ed. by G.T. Rado, H. Suhl (Academic, New York, 1963), pp. 271–350
7. A. Khosroshahi, E. Ohn-Bar, M.M. Trivedi, Surround vehicles trajectory analysis with recurrent neural networks, in *IEEE International Conference on Intelligent Transportation Systems* (2016)
8. M. Kuderer, S. Gulati, W. Burgard, Learning driving styles for autonomous vehicles from demonstration (2015)
9. K. Elissa, “Title of paper if known” unpublished
10. R. Nicole, “Title of paper with only first word capitalized,” *J. Name Stand. Abbrev.* (in press)
11. A. Velmurugan, T. Ravi, Allergy information ontology for enlightening people, in *2016 International Conference on Computing Technologies and Intelligent Data Engineering (ICCTIDE'16)*. (IEEE, 2016), pp. 1–7
12. N. Srinivasan, C. Lakshmi, Stock price prediction using fuzzy time-series population based gravity search algorithm. *Int. J. Softw. Innov. (IJSI)* **7**(2), 50–64 (2019)
13. R.S.B. Krishna, M. Aramudhan, Feature selection based on information theory for pattern classification, in *2014 International Conference on Control, Instrumentation, Communication and Computational Technologies (ICCICCT)* (IEEE, 2014), pp. 1233–1236

14. K.A. Kumar, C.C. Sekar, Data management and heterogeneous data integration in grid computing environments, in *2010 International Conference on Communication and Computational Intelligence (INCOCCI)* (2010)
15. R. Subhashini, B. Keerthi Samhitha, S.C. Mana, J. Jose, Data analytics to study the impact of firework emission on air quality: a case study, in *AIP Conference Proceedings* (2019)
16. D.S.R. Vignesh, R. Revathy, A Distinctive model to classify tumor using random forest classifier, in *2019 Third International Conference on Inventive Systems and Control (ICISC), Coimbatore, India, 2019*, pp. 44–47
17. K. Sangeetha, P. Vishnuraja, D. Deepa, Stable Clustered Topology and secured routing using mobile agents in mobile ad hoc networks. *Asian J. Inf. Technol.* **15**(23), 4806–4811 (2016)
18. A. Ponraj, Optimistic virtual machine placement in cloud data centers using queuing approach. *Future Gener. Comput. Syst.* **93**, 338–344 (2019)
19. S.C. Mana, T. Sasiprabha, A study on various semantic metadata standards to improve data usability, in *2019 International Conference on Computational Intelligence in Data Science (ICCIDS), Chennai, India, 2019*, pp. 1–4.
20. K.K. Thyagarajan, G. Kalaiarasi, Pulse coupled neural network based near-duplicate detection of images (PCNN–NDD). *Adv. Electr. Comput. Eng.* **18**(3), 87–97 (2018)

A Novel Biometric Inspired Robust Security Framework for Medical Images



D. Vishnu Vardhan, D. Gopeeswar, and A. Viji Amutha Mary

1 Introduction

In the quick advancement of computerized information trade, security of any data gets imperative in information stockpiling and transmission [1]. Because of the expanding utilization of pictures in different fields, it is important to secretly protect against unapproved images. Remedial imaging was one of the amazing picture-ready technology areas [2]. Various security methods like cryptographing, watermarking, steganographics, etc., are essential to guarantee the secrecy of restorative photographs sent over remote networks. In restorative picture encryption, the first picture is changed over into figure picture by changing the pixel esteems so that the first picture becomes evidently good for nothing with the end goal that it ought not uncover the significant data contained in the first medicinal picture. In any case, an approved individual can replicate the first picture utilizing the decoding procedure for various purposes. As of late, different encryption methods have been proposed in the writing. In any case, these systems are missing the mark to cook the necessities having helplessness to various pernicious assaults and give a lower level of security. To build the security, therapeutic picture encryption strategies have been introduced dependent on the tumult hypothesis in [3–5]. In any case, these methods are not totally verified because of poor key administration system [6, 7]. By and large, the security of an encryption procedure is essentially relying upon the related keys with the end goal that on the off chance that these keys are replicated or taken, at that point unapproved substance can get to the information. Then again, in the event that

D. V. Vardhan (✉) · D. Gopeeswar · A. V. A. Mary
Department of Computer Science and Engineering, Sathyabama Institute of Science and Technology, Chennai, India
e-mail: vishnudumpa03@gmail.com

A. V. A. Mary
e-mail: vijiamumar@gmail.com

these keys are devastated or ruined, at that point getting to the information would not be conceivable and subsequently the key administration related with security system must be secure and untraceable [8, 9]. These issues can be tended to by utilizing an ideal key administration framework which is basic, remarkable, untraceable and non-revocation. One approach to accomplish this is to utilize the biometrics of the patients/proprietors. Biometrics alludes to organic or conduct attributes that exceptionally distinguishes a people. A portion of the well-known attributes is facial structure, unique mark, irises, palm prints, voice, and step. Be that as it may, social attributes cannot be utilized for the recognizable proof purposes as they can be imitated. In this way, the natural attributes acquired in the biometrics can be utilized in the key administration to reinforce the security of the encryption strategy.

Unique finger impression has magnificent factual properties among all biometrics. The unique mark basically speak to the example comprising of dull lines of edges and valley alongside white lines over the finger. Because of variety in edges design, it is one of a kind of everybody and there are no fingers having same edge design throughout the entire existence of fingerprinting. Indeed, even hereditarily indistinguishable people do not have a similar edge designs nor are it is shared by two fingers of a similar individual. • Each unique finger impression can be perceived utilizing a lot of exceptional point generally called particulars, which basically portrays the unmistakable component as area and bearing. • Fingerprints are thought to be ever-enduring. The edges are made before birth and stays considerably after death, until the skin rots. The edges designs are hearty and are not influenced by maladies. Maladies may just change skin shading and surface however edges are strikingly steady and invulnerable. The general nature of edges stays unaltered for the duration of the existence makes fingerprints an honorable biometric. • The collectivity and quantifiability of biometric have essentially significant job in a few applications. The unique mark is effectively quantifiable biometric when contrasted with different biometrics and along these lines is perfect for a few application. By the by, different biometrics, for example, palm-print, iris, face, marks can likewise be utilized in the proposed picture encryption strategy. The center thought is to catch the unique mark of the patient and utilized it to create a key age, the executives framework, which basically give the keys to be utilized. These keys are the parameter associated with PR-APBST and the underlying incentive for the disorganized guide. The biometric picture is first changed into PR-APBST coefficients followed by solitary worth disintegration and QR decay to scramble the restorative picture. The medicinal picture is then scrambled utilizing PR-APBST, QR and solitary worth deterioration and is prepared for secure transmission or a security examination. Finally, a strong unraveling process is used to reproduce the main helpful picture from the mixed picture. The authenticity and reasonableness of the proposed framework have been shown using a wide examination on various remedial. The principle point of this undertaking is to secure the touchy and private restorative information, which contains the significant data of the patients. The proposed strategy uses the biometrics of the patient/proprietor to create a key administration framework to acquire the parameters engaged with the proposed method.

2 Related Work

Ojha et al. [10, 11] recommended a confirmed remediation over a crowded platform utilizing codebase encryption. McEliece key cryptography has been used for encryption for safe communication. Sequitter pressure was then used to make use of the moving limit of data like the river and the canal [12–14]. The receiver viewed the picture on the hand. This system has been used to easily encrypt and uncheck. Nevertheless, the sizes of the keys were that, rendering it a clumsy process [15, 16]. The online progressive learning calculation for one protected layer feeding forward frames (SLPFs), including secret centerpoints, has been drawn up by Guang-Container Huang et al. [17]. Here, the preparation period has reduced with high precision performance. Its equation can be easily used with a minimal database and data can be combined if appropriate. The responsibility of knowledge and the preferences was arbitrary and the yield loads were picked regularly. Over time, other control parameters needed OSELM to be adjusted mostly required the number of center points protected. Ismail et al. [13] proposed that the pixels be combined with iterative analysis based on the figure module and data-based reference frames for the late encoding of existing encryption parameters. The riddle key was changed after each pixel of the image was encrypted to render the figure increasingly spectacular against any embossment. If the hidden key was changed, the primary picture as sent was difficult to unscrew. A Face Acquiring, Gender and Age Arrangement (FEBFRGAC) calculation suggested in Ramesha et al. [18, 19]. Presently, the procedure has been conducted with respect to the morphology of human faces and the variety of dull stages, head, nose and mouth, and organized through the operation of the Manager of Vigilant's tip. The sexual advice was arranged based on the likelihood of post-grade and the age was obtained using the shape and surface details of the falsified neural system. The list had a smile the company scale is 100%, the number of sexual participants 95%, and the age of 90%. In the case of the Multi-Righthead Fragment Analysis (MPCA) and Field Shielding projection (LPP), Shermina [20] indicated the face-report framework. Presently, preprocessing of the facial picture is carried out using MPCA and decreased dimensionality. The characteristics were isolated by LPP in low-dimensional space which provided a neighboring search. Affirmation was performed by calculation of the L2 similarity section, described between the image of a collection and the request image. Both the MPCA and the LPP were merged to achieve a high acceptance score Shermina [21]. The Discrete Cosine (DCT) and the PCA Face Affirmation System were proposed by b. Small recurrent DCT components are used now in the illuminated picture standardization. 64 lighting elements are listed. This paper had 94.2% accuracy and assumed that DCT mix with some other recognition strategies provided a remarkable explanation of invariant recognition accuracy.

Thamizharasi [22] suggested a research paper on the confirmation of face by mixing multi-scale structures with the Fluffy-k nearest neighbor-classifier homomorphic interface. The two multi-scale techniques used are currently and independent

wavelet transition (DWT). For institutionalizing illumination, homomorphic channels were used. K shows that the cluster count is used to build up the pixels in the pre-processed image based on the gray side. In order to represent the image in the test database, the Euclidean partition processed was used in the train database with the closest neighbor-classifier Cushionk. DCT given an acknowledgement rate of 89.5% when DWT gave the Homorphic Web, K Infers Selection and Fuzzy K closest neighbor classification rate to 90%, respectively. The system was technically unstable in view of the fact that there was no more approaches and more processing resources.

Khriji et al. [23] addressed updated AES camera encryption estimates. This form is still used as a private key encryption system. AES has been combined with a main stream generator to improve the functionality introduction. The W7 key stream generator was used to provide a prevalent protection for the safety requirements of quantifiable test ambushes [24].

3 Existing System

In the current framework, different systems have been created to ensure the clinical pictures, for example, encryption, hashing, stenography, and watermarking. Among these, encryption is the most appropriate system to ensure the uprightness of the information. As standard, for instance, propelled Encryption Standard (AES), Information Encryption Standard (DES), the common methods for encryption and Universal Information Encryption Standard (IDES) [25] are not appropriate for the encryption of clinical pictures because of the essential highlights of the clinical pictures, for example, high relationship between's neighboring pixels and excess. Medical images may be exposed to the serious threats like illegal manipulation, privacy leakage and data integrity [26]. The main problem arises during the storage and communication of these images for various purposes. The security of clinical pictures is a urgent issue and should be tended to.

4 Proposed System

In the proposed framework, a high efficiency and strong encryption system to secure clinical pictures is proposed. The patient will enroll and login and gets a token with which they have to visit emergency clinic. The doctor will register and login to see the patient details. Then, the doctor will check the patient and gives the report and asks them to visit the laboratory for test. The medical images taken in the laboratory will get encrypted using the fingerprint biometrics of the particular patient. The status of test results will be sent to patient through mail and they will decrypt the images by using the fingerprint by visiting the hospital. By using this technique, the medical images will be secured with robust security (Fig. 1).

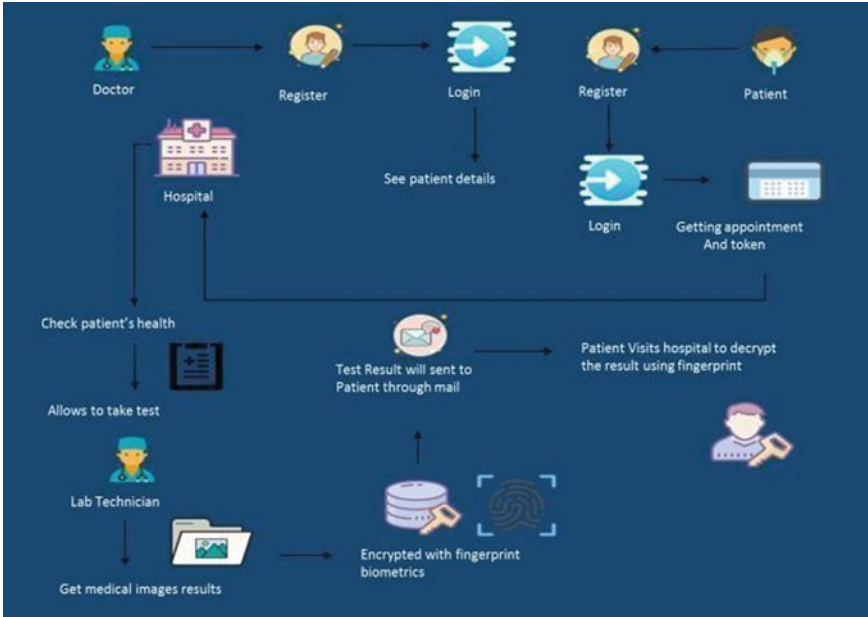


Fig. 1 Overview of the proposed system

5 Module Description

5.1 Patient Registration

When the patient makes a record, they are permitted to login into their record to get to the application. In view of the patient’s solicitation, the server will react to the patient. All the client subtleties will be put away in the database of the server. Patient can apply for appointment of the specialist and separate token will be produced.

5.2 Doctor Registration

In this module, doctor will register using their mail ID. The doctor also adds his specialization with experience. After the registration, doctor login into the application by using their credentials.

5.3 Report Module

In this module, after the appointment has accepted by the doctor, the doctor will add the reports to respective patient. The patient will check their reports and goes to laboratory for the further testing. The test results will be sent to the patient mail.

5.4 Verification

In this module, the medical images taken in the laboratory will get encrypted using the finger print biometric of particular patient. Using the fingerprint, the patient can access their reports. By using this technique, the medical images will be secured with robust security.

6 Conclusion

Right now, high-proficiency and vigorous encryption system to secure clinical pictures are proposed. It is furnished with a proficient key administration framework consolidating the biometrics of the patient. The biometrics improve the security of clinical information because of its one of a kind and characteristic highlights. It basically gives another instrument of entering the mystery key in the framework. Another finding in the meaning of all stage symmetrical change in particular parameterized all stage symmetrical change has been made where the change is parameterized utilizing higher request revolution lattice. PR-APBST is then combined with QR and particular worth decay to proposed a rich encryption system. A point-by-part check review, perceptual health, key space inspection, key affectability, edge twisting, and empirical analysis were carried out for the approval of the system proposed to show high heartbeat and protection of clinical picture details.

7 Result

See Figs. 2, 3 and 4.

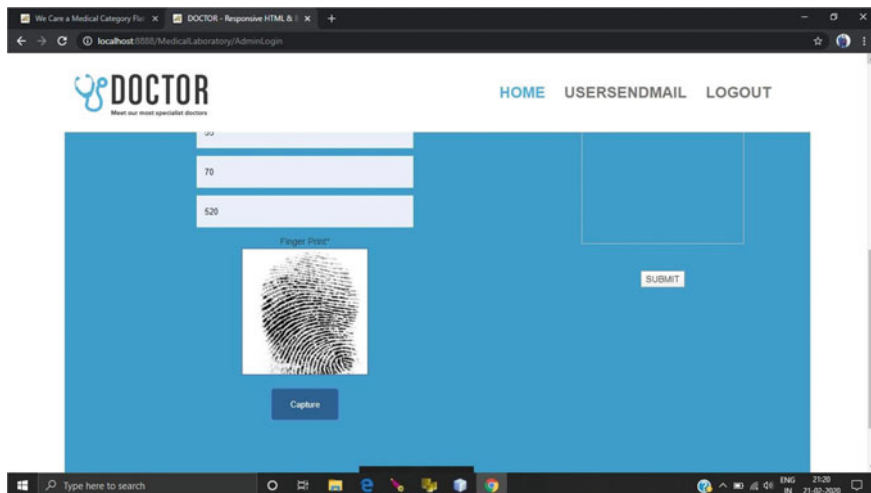


Fig. 2 Finger print encrypt

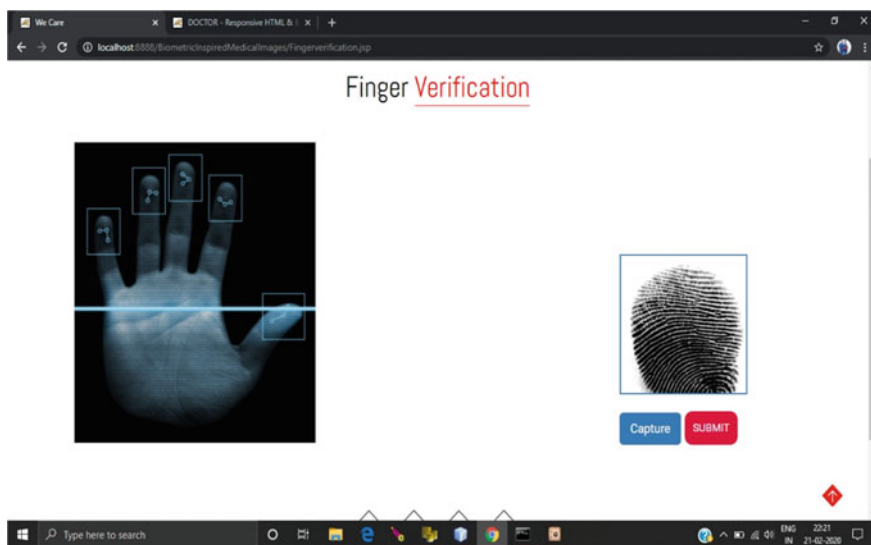


Fig. 3 Finger verification



Fig. 4 Medical image

References

1. K. Pradeep, T.P. Jacob, A hybrid approach for task scheduling using the cuckoo and harmony search in cloud computing environment. *Wirel. Pers. Commun.* **101**(4), 2287–2311 (2018)
2. M. Anand, T. Sasikala, Efficient energy optimization in mobile ad hoc network (MANET) using better-quality AODV protocol. *Cluster Comput.* **22**(5), 12681–12687 (2019)
3. Face images databases from www.cs.cmu.edu/~cil/v-images/html and www.face-reg.org/databases/html. and Medical images from brain images: mr-tip.com, radiologyinfo.ca and breastimaging.cancer.gov
4. L.-B. Zhang, Z.-L. Zhu, B.-Q. Yang, W.-Y. Liu, H.-F. Zhu, M.-Y. Zou, Medical image encryption and compression scheme using compressive sensing and pixel swapping based permutation approach. *Math. Probl. Eng.* **1** (2015)
5. H.-I. Hsiao, J. Lee, Fingerprint image cryptography based on multiple chaotic systems. *Signal Process.* **113**, 169–181 (2015)
6. A.K. Jain, A. Ross, S. Pankanti, Biometrics: a tool for information security. *IEEE Trans. Inf. Forensics Secur.* **1**(2), 125–143 (2006)
7. U. Uludag, S. Pankanti, S. Prabhakar, A.K. Jain, Biometric cryptosystems: issues and challenges. *Proc. IEEE* **92**(6), 948–960 (2004)
8. P. Sharmila, A. Viji Amutha Mary, Secure and data hiding mechanism using biometrics based on face and finger print. *GJPAM* **13**(7), (2017)
9. A. Viji Amutha Mary, A random projection approach to strengthen the privacy level of medical images. *J. of Comput. Theor. Nanosci.* **16**(8), 3219–3221 (2019)
10. A. Assadi, A. Behrad, A new method for human face recognition using texture and depth information. *IEEE Trans. Neural Netw. Appl. Electr. Eng. (NEUREL)* 201–205 (2010)
11. D. Brat Ojha et al., An Authenticated two tier security on transmission of medical image using codebase cryptosystem over teeming channel. *Int. J. Comput. Appl.* **12**(9), 22–26 (2011)
12. I.A. Ismail, M. Amin, H. Diab, A digital image encryption algorithm based a composition of two chaotic logistic maps. *Int. J. Netw. Secur.* **11**(1), 1–10 (2010)
13. L. Krikor et al., Image encryption using DCT and stream cipher. *Eur. J. Sci. Res.* **32**(1), 47–57 (2009)
14. M. Philip, A. Das, Survey: image encryption using chaotic cryptography schemes. *IJCA Special Issue on “Computational Science—New Dimensions & Perspectives” NCCSE* (2011)
15. M. A. Bani Younes, A. Jantan, Image encryption using Block based transformation algorithm. *IAENG Int. J. Comput. Sci.* (2008)
16. N.-Y. Liang, G.-B. Huang, P. Saratchandran, N. Sundararajan, A fast and accurate online sequential learning algorithm for feed forward networks. *IEEE Trans. Neural Netw.* **17**(6) (2006)

17. H.T. Panduranga, S.K. Naveen Kumar, Hybrid approach for Image encryption using SCAN patterns and carrier images. *Int. J. Comput. Sci. Eng.* **02**(02), 297–300 (2010)
18. K. Ramesha et al., Feature extraction based face recognition, gender and age classification. *Int. J. Comput. Sci. Eng. (IJCSE)* **02**(01S), 14–23 (2010)
19. J. Shermina, Face recognition system using multilinear principal component analysis and locality preservation projection, in *IEEE GCC conference and exhibition Dubai, United Arab Emirates* (2011)
20. J. Shermina, Illumination invariant face recognition system based on Discrete Cosine Transform and Principal Component Analysis, in *International Conference on Emerging Trends in Electrical and Computer Technology (ICETECT)*, pp. 826–830 (2011)
21. A. Thamizharasi, Performance analysis on face recognition by combining multi scale techniques and homomorphic filter using Fuzzy k nearest neighbor classifier, in *IEEE International Conference on Communication Control and Computing Technologies (ICCCCT)*, pp. 643–650 (2010)
22. M. Turk, Pentland, Face recognition using Eigen faces, in *IEEE International Conference on Computer Vision and Pattern Recognition* (1991)
23. M. Zeghid, M. Machhout, L. Khriji, A. Baganne, R. Tourki, A modified AES based algorithm for image encryption. *Int. J. Comput. Sci. Eng.* 1(1)
24. Z. Xiong, K. Ramchandran, M.T. Orchard, Y.-Q. Zhang, A comparative study of DCT- and Wavelet-based image coding. *IEEE Trans. Circ. Syst. Video Technol.* **9**(1) (1999)
25. G. Nagarajan, R.I. Minu, B. Muthukumar, V. Vedanarayanan, S.D. Sundarsingh, Hybrid genetic algorithm for medical image feature extraction and selection. *Procedia Comput. Sci.* **85**, 455–462 (2016)
26. M.D.V. Ajay, N. Adithya, A. Mary Posonia, TECHNICAL ERA: An Online Web Application. in *IOP Conference Series: Materials Science and Engineering* (IOP Publishing, 2019), vol. 590, no. 1, p. 012002

Agricultural Analysis Using Machine Learning Techniques



S. Dhanush Sai, S. Satyanand, A. Pravin, G. Nagarajan, and T. Prem Jacob

1 Introduction

The three fundamental needs of a man are nourishment, fabric, and safe house. Out of these, nourishment remains the preeminent [1, 2]. This is so on the grounds that nourishment frames some portion of the qualities of any living thing. The trick states the need for nourishment creation [3, 4]. Since everybody around the world needs to amplify the advantage collecting from the cutting-edge technology, this paper attempts to take a gander at how information and communication technology (ICT) assists with improving nourishment creation in Nigeria as well as the world on the loose. As indicated by a well-known Malthusian hypothesis on the pattern of nourishment, creation against the populace development cautioned that exertion ought to be multiplied if man needs to continue nourishment security. The hypothesis expressed that while nourishment creation is developing numerically, the populace propels geometrically [5, 6]. Despite the fact that the perception was right as at that

S. D. Sai (✉) · S. Satyanand · A. Pravin · G. Nagarajan · T. Prem Jacob
Department of Computer Science and Engineering, Sathyabama Institute of Science and
Technology, Chennai, India
e-mail: dhanushsai.dhanush@gmail.com

S. Satyanand
e-mail: satyanandnaidu284@gmail.com

A. Pravin
e-mail: pravin_ane@rediffmail.com

G. Nagarajan
e-mail: nagarajanme@yahoo.co.in

T. Prem Jacob
e-mail: premjac@yahoo.com

point, particularly with the pace of populace development, the instance of nourishment creation has accepted an alternate example and the same number of elements have impacted the creation rate. One of such factors is the progression in technology.

Computer-based intelligence is a champion among the most propelling advances close by gigantic data developments and snappy figuring devices. They are creating in each part to make new opportunities to understand the diverse data structures related to the biological limits. Computer-based intelligence can be portrayed as coherent technique that will empower the machines to see each issue and to disentangle it without the help of programming contraptions. The enthusiasm for sharp advances, for instance, big data, cloud-based organizations, and GPS, and the machine learning is getting pace in the agribusiness business [7, 8]. All of these progressions can enable the cultivation to part to help the things by getting together the data from the field which will improve high precision crop examination, motorized developing techniques, right now and Japan, wide-scale utilization of cell phones, and web of things (IOT) frameworks have prompted increment in the development of accuracy farming arrangements. The fundamental assortments of a few nations have additionally comprehended the requirement for smart frameworks, and the benefits of these technologies, and accordingly, their drives to advance brilliant cultivating methods are to drive the development of the market further. Sharp farming applications do not will by and large objective simply broad, customary developing, anyway could in like manner to update other ordinary or creating designs in provincial territories, for instance, family developing normal developing [9, 10].

Splendid farming can moreover give unimaginable results with respect to characteristic stress, for example, min water use, or give contamination free reaps. Sharp developing systems furnished with dataset exactness agribusiness will engage farmers to diminish crop costs similarly as enhanced crop age and advantages. For preliminary explanation, the quantifiable data or datasets related to agriculture are accumulated. Various estimations, for instance, SVM and random boondocks count can be used. Reinforce vector machine (SVM) is a kind of helper danger minimization computations. As a pervasive AI algorithm, SVM has been commonly used in various fields for information gathering. Self-assertive, a mind boggling result is a general rule. Sporadic timberland chooses decision trees that outlines various yields and combines them to shape an exact and stable estimate.

2 Related Works

Atmosphere smart agribusiness framework is a strategy to check the climate of the zone and to develop fundamental items as the atmosphere of that region. This will assist ranchers with growing right measure of harvests in the necessary land and to know the precipitation max temp and min temp of that area. The forecast of the most beneficial yield can be developed in the horticultural land utilizing AI strategies [1, 11]. This paper incorporates the utilization of an android framework that will give the continuous yield investigation utilizing different climate station reports and soil

quality. In this way, ranchers can develop the most productive harvest in the best appropriate months. Sensor networking is an advancement which is new to India where it will, in general, be used in agricultural field in India for extending crop yield by giving conjecture of plant diseases and bug [5, 12]. This should be conceivable by venturing through assessment data with reasonable AI figurings for this data to get foreseen yield. It gives us the chance for the correct examination using WSN frameworks and to keep from the irritations and to use pesticides that would not hurt the yields well-being.

Proposed an item instrument named ‘Gather Advisor Tool’ has been used as a site page for foreseeing the principal climatic parameters on the yields [13]. C4.5 computation is used, i.e., made by Ross quinoa to find the fundamental climatic characteristics on the yields consequences of picked crops in picked areas of MP. These items offer us the hint of various climate changes that can affect the crop improvement in a territory.

Internet of Things (IoT), one of the new time of calculation, is utilized to propel the need of agribusiness division [14, 15]. Using the IOT highlights shrewd cultivating can be chronicle in these paper, and we are utilizing a Bluetooth gadget and a wide region system to get the subtleties of the encompassing, for example, soil water level, pesticide location, and so forth. These will give ranchers computerization in the field of cultivating as all the subtleties will be associated with a gadget use by the ranchers. Every subtleties of the homestead can be refreshed in the application utilizing the IOT modules [16, 17]. Information about the agriculture product and food is described [18, 19]. List of tools which can be used and their importance is given [20]. The mobile and other categories of agriculture ideas are proposed [21, 22]. Data giving information about certain infections are collected and processed [23, 24].

3 Proposed System

The proposed framework likewise causes the ranchers to locate the present interest of yield developed in their own property, which bring about mindfulness about the harvest revolution and rancher’s development. Application permits to rapidly observing what is going on in the ranch and what necessities to occur straightaway. Figure 1 describes the view of system. Here the point of the venture is to give ranchers a powerful and dependable device or data for overseeing farming and permits clients to design exercises, sort out staff, screen agribusiness inputs and rural apparatuses use, attempt monetary and money-related investigation of exercises pesticide, and time to do specific cultivating activities. In light of planting date of harvest, rancher will get updates about utilization of manure according to plan and conditional development plan which is structured by crop master.

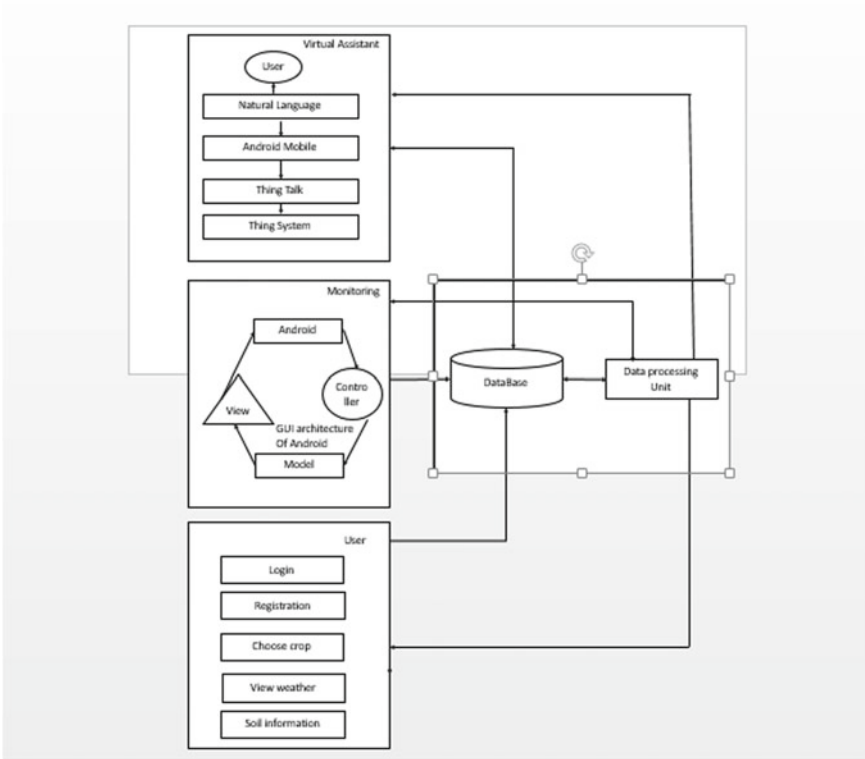


Fig. 1 Proposed system

3.1 Advantages of Proposed System

- Cost insightful low.
- Complexity is less.
- Automatically controlled.
- Minimize work cost

One of the reason is that it logically performs better.

4 Module Explanation

4.1 Admin Module

4.1.1 Login

The main opens when client introduces the application. Clients need to give a contact numerical and a secret word format, in which client enters during registration time, so as to signing into the application. There was a chance that data provided by client relate the information in the table and then client enters into application else message of sign in fizzled as shown and client needs to merge correspondent data. This is connected to the register action likewise given to enlistment of new clients.

4.1.2 Add Crops Data

In this module, administrator can check the harvests and afterward include a few yields data about horticulture for utilizing rancher. Harvest included will be given at regular intervals all through the developing season.

4.1.3 Update Crops Data

In this module, administrator can check the harvests and update a few yields data about horticulture for utilization of rancher. Yield updates will be given at regular intervals all through the developing season.

4.1.4 View Criticism

In this module, administrator can see the criticism about agribusiness application from client.

4.2 User Module

4.2.1 Registration

Client who needs to get the application needs to enlist first before login. By tapping on register button in login movement, the register action gets open. Enlisted client then needs to login in order to interact with the application. Approval is done through the 10 digit contact number. On the off chance that any such approval is disregarded, at that point enrolment will be fruitless and afterward client needs to enlist once more.

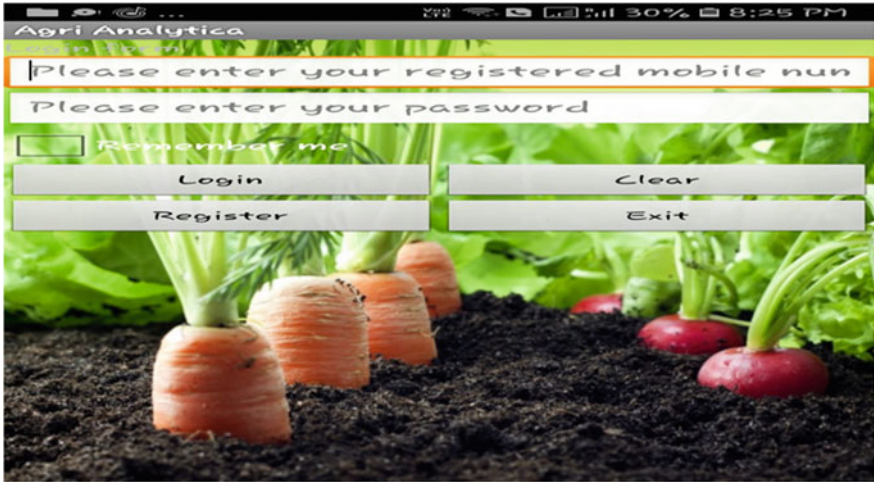


Fig. 2 Login credentials

Message is that application will show when one of the fields is vacant. There is the chance on off that all such data in client will be coordinated by signing movement for signing into personal instance.

4.2.2 Login

This is a movement which opens client introduces the application. The detail is explained in Fig. 2. Client need to provide their contact number and a secret code in order to interact with the application. The off chance is that data furnished by the client matches with the data in the database table, and then signing into the application or messaging of login fizzled is shown and clients need to reappear data. The connect to register targeting is additionally given to enrolment of clients data or information. Affirmation structure is to make a trademark interaction between human and PC where the apparent movements could be used for controlling or passing information. It came about hand signs to be understood and very much deciphered by the PC considered as the issue of movement association like human PC correspondence (HCI) furthermore named man-machine collaboration (MMI).

4.2.3 View Yields

In this module, client can see the refreshed yield data about horticulture.

4.2.4 Feedback

In this module, client can view and refresh the criticism about horticulture application.

4.3 Monitoring

4.3.1 Weather

Climatic conditions play a major role in horticultural. Climatic changes affect crop yield and also damage the water resources which is the major component of agriculture. Due to this, the productivity of a crop in that particular season decreases. These climatic changes not only affect the present growth but also affect the future crop by decreasing the fertility of soil. Based upon the weather, we need to cultivate the crops which helps to give more profits. Proper weather conditions help in good yield.

4.3.2 Soil Testing

Soil testing is to be done in agricultural lands in order to know the pH level, how much amount of nitrogen, etc., is present in the soil. This helps us to know which kind of crop should be cultivated in that particular land to give more yield. Soil testing is done by the local laboratories who are familiar with the soil. Soil testing also helps to find the nutrient deficiencies in the soil. Testing the soil often checks for nutrients such as phosphorus, sulphur, calcium, iron, copper, and zinc.

4.3.3 Fertilizer

A compost is a characteristic or engineered, synthetic-based substance that is utilized to upgrade plant development and fruitfulness. Composts may likewise upgrade water maintenance and channel any abundance fluid, thus improving soil viability. Manures normally enhance the fertility of the soil. There are various sorts of composts that can be utilized on explicit plants to advance their development. For instance, espresso beans are ordinarily utilized for plants that flourish with acidic substances, for example, azaleas, blueberries, roses, and tomatoes. When working with espresso beans, it is critical to water the dirt subsequently to advance assimilation. Since they have a high level of calcium, eggshells are likewise utilized as preparing specialists for produce like peppers and tomatoes. The calcium can help forestall decay while boosting the plant's development. Matured excrement and manure are by a long shot the most well-known composts utilized with pretty much any sort of plant. Contingent upon your plant and weeds can likewise be utilized as compost. Chickweed, horsetail,

burdock, yellow dock, comfrey, and weeds are regularly utilized on account of their high nitrogen content.

4.3.4 Pesticides

Pesticides are concoction substances that are intended to slaughter bugs. It represents a natural specialist such as virus, bacterium, pests, and antimicrobials. This utilization of pesticides is normal to the point. It is usually used to dispense with or control an assortment of agrarian vermin that can harm harvests and animals and diminish ranch profitability. The most ordinarily applied pesticides are bug sprays to slaughter bugs, herbicides to murder weeds, rodenticides to execute rodents, and fungicides to control parasites, form, and build-up.

4.4 Virtual Assistant

Nowadays, we are seeing most of the people using voice assistants instead of typing the information they require. Virtual assistant is that kind of thing commonly known as ‘Chatbot’ helps the farmer to ask the doubts they have and real-time solutions for the problem. The virtual helping agent is given in Fig. 3. This reduces the work of farmer.

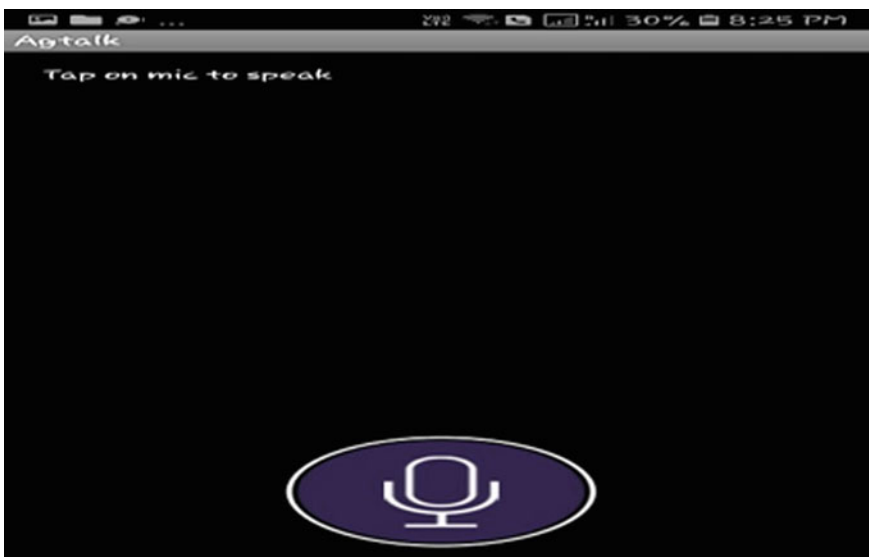


Fig. 3 Virtual helping agent

5 Conclusion

- Data and communication technology in agriculture otherwise called e-horticulture is creating and applying the imaginative.
- Approaches to utilize ICT in the provincial area.
- Existing systems are of high complexity, and they involve in high-cost maintenance.
- To overcome this, we are proposing one framework which helps us to break down the dirt parameters with the help of sensors and information mining methods.
- The soil test is done to all the agricultural lands, and data are stores in the database so that it will be used by all. Existing system is a static use system which is useful in single way only.
- Virtual assistant is that kind of thing commonly known as ‘Chatbot’ helps the farmer to ask the doubts they have and real-time solutions for the problem.
- Matured excrement and manure are by a long shot the most well-known composts utilized with pretty much any sort of plant

References

1. K. Daine, *Our Needs as Human Beings*. <https://blogs.Kareldonk.com/our-basic-needs-as-human-beings>. Retrieved 21st May 2019 (2013)
2. A. Karthik, M.D. Kamalesh, Rat trap: inviting, detection & identification of attacker using honey words in purchase portal, in *2017 Third International Conference on Science Technology Engineering & Management (ICONSTEM)* (IEEE, 2017), pp. 130–132
3. B.K. Samhitha, S.C. Mana, J. Jose, M. Mohith, L. Siva Chandhrahasa Reddy, An efficient implementation of a method to detect sybil attacks in vehicular ad hoc networks using received signal strength indicator. *Int. J. Innov. Technol. Explor. Eng. (IJITEE)*, **9**(1) (2010)
4. D.S.R. Vignesh, R. Revathy, A distinctive model to classify tumor using random forest classifier, in *2019 Third International Conference on Inventive Systems and Control (ICISC), Coimbatore, India* (2019), pp. 44–47
5. A. Deger, *Malthusian Theory of Population*. Retrieved on 21st May 2019 (2019)
6. K.A. Kumar, C.C. Sekar, Data management and heterogeneous data integration in Grid computing environments, in *2010 International Conference on Communication and Computational Intelligence (INCOCCI)* (2010)
7. V.V. Kaveri, V. Maheswari, Cluster based anonymization for privacy preservation in social network data community, *J. Theor. Appl. Inf. Technol.* **73**(2), 269–274 (2015)
8. G. Dhanisha, J.M. Seles, E. Brumancia, Android interface based GCM home security system using object motion detection, in *2015 International Conference on Communications and Signal Processing (ICCSPP)* (IEEE, 2015), pp. 1928–1931
9. S.P. Shyry, Efficient identification of bots by K-means clustering, in *Proceedings of the International Conference on Soft Computing Systems* (Springer, New Delhi, 2016), pp. 307–318
10. G. Nithya, S.L. Shabu, A novel framework in reusing the ontological health record. *Res. J. Pharmaceut. Biol. Chem. Sci.* **7**(3), 215–220 (2016)
11. K.K. Thyagarajan, G. Kalaiarasi, A review on near-duplicate detection of images using computer vision techniques. *Arch. Computat. Methods Eng.* 1–20 (2020)
12. N. Srinivasan, C. Lakshmi, Stock price prediction using rule based genetic algorithm approach. *Res. J. Pharmacy Technol.* **10**(1), 87–90 (2017)

13. U.S.D.A., Definition of Food Security. Assistance/food-security-in-the-us/definitions of food security. Retrieved 21st May 2019 (2018)
14. R. Gal, ICT (Inf. Commun. Technol.). Retrieved 2 Aug 2013, from TechTarget (2005)
15. S.C. Mana, A feature based comparison study of big data scheduling algorithms, in *2018 International Conference on Computer, Communication, and Signal Processing (ICCCSP), Chennai* (2018), pp. 1–3
16. RAPPEV, *Technology Advantages & Types of Technology*. Retrieved 21st May 2019 (2018).
17. An authentication method for secure web services access with preventing tautology type SQL injection
18. Varma C, What is the definition of an agricultural product? Online what is an agricultural product-2533211. Retrieved 21st May 2019 (2019)
19. FAO, *The State of Food and Agriculture*. www.fao.org/3/a-2050e.pdf. Retrieved 21st May 2019 (2011)
20. L. Dooley, H. Hammond, *The Use of Farm Tools by Rural Professionals and Farmers*. Retrieved 2 Aug 2013, from One Farm (2012)
21. Waruru, *ICTs Could Fill Agricultural Extension Gap*. Retrieved 17 Aug 2013, from SciDev (2011)
22. M. Hopkins, *10 Best Mobile Agriculture Apps for 2012*. <https://www.croplife.com>. Retrieved 9 July 2013, from CropLife (2013)
23. T. Dinh; K. Wahid, An IoT data collection system for fungal detection in crop fields, in *2017 IEEE 30th Canadian Conference on Electrical and Computer Engineering (CCECE)*
24. P.S. Maran, P.M. Velumurugan, B.P.D. Batvari, Wind characteristics and Weibull parameter analysis to predict wind power potential along the south-east coastline of Tamil Nadu, in *International Conference on Intelligent Information Technologies* (Springer, Singapore, 2018), pp. 190–199

Multi-strategy Sentiment Analysis of Banking Reviews Based on Semantic Fuzziness



R. Rahul, K. Mohana Prasad, and J. Refonaa

1 Introduction

The Internet is as of now a significant wellspring of data, yet in addition a foundation of communicating perspectives and sharing encounters. Right now, can without much of a stretch gather audits about items or administrations. Assessment examination is helpful in business insight application condition and recommender frameworks [1, 2] on the grounds that it is an advantageous channel for the two parts of the bargains to impart. In the conclusion investigation, numerous methodologies and strategies were utilized, for example, AI [3], extremity vocabularies [4, 5], regular language preparing, and psychometric scales, which decide various sorts of estimation examination, for example, presumptions made, strategy uncovers, and approval datasets[6, 7]. At present, feeling examination is made at three levels: word, sentence, and report, of which the sentence and the record are generally utilized in most current investigations[8, 9]. The word level, the crucial, and thus the more critical and additionally testing level, be that as it may, is only from time to time examined. Sentiment examination has increased a lot of consideration as of late. Feeling grouping is utilized to analyze the item remarks to extricate the survey from it. Feeling investigation is a sort of content grouping AI approach dependent on sentimental orientation (SO) of

R. Rahul · K. M. Prasad (✉) · J. Refonaa (✉)
Department of Computer Science and Engineering, Sathyabama Institute of Science and
Technology, Chennai, India
e-mail: mohanaprasad1983@gmail.com

J. Refonaa
e-mail: refonaa@gmail.com

R. Rahul
e-mail: rahul7ramesh@gmail.com

assessment they contain. For the investigation of conclusion and surveys, assumption examination in which the machines assess and classify the human supposition, feeling, and so forth.

The item surveys are communicated by utilizing literary structure, star rating, and emoticon. With the notion investigation method, it is conceivable to assess the colossal measure of accessible information and acquire a supposition from them that can help the specialist organizations and item maker to accomplish their objective [10]. As the interest of Web expands, the client survey is additionally developing at an incredible rate, for example, some client audit in single word, for example, “astonishing,” “great,” or “awful” though others talk about the issues happen when they utilize the items. A few people referenced the issues about the conveyance, awful bundling, showed up after the expected time or trade the item, and so forth, which is actually not identified with the item quality. Be that as it may, a few people clarified the item quality precisely by giving component shrewd subtleties of the items. In this way, we ought to distinguish the sentiment and highlights exclusively and register the extremity score of each element [11, 12].

2 Related Work

They originally decided the slant propensity of words or expresses and evaluated them as a proportion of genuine qualities, Rain et al. [13], which can be additionally used to decide the supposition inclination of sentences and passages. They examined the estimation propensity of content through AI techniques or strategies dependent on extremity dictionary. Past work indicated that conventional slant investigation approaches can be very viable. To computerize the investigation of assessment materials, various methodologies were utilized for the forecast for the slants of words, articulations, and furthermore documents, Trupthi et al. [14], which incorporate natural language processing (NLP) and example-based Nasukawa et al. [15], AI calculations, for instance NB, ME, SVM [16], and solo learning He et al. [17]. Ku in [18] first contemplated the characters about the feeling phrases in the NTUSD extremity word bank to get their polarities and qualities dependent on their characters. Cambria in [19] embraced human-PC association, data recovery, and multi-modular sign handling advancements to extricate individuals’ opinions among the ever-developing on the Web social database. Since every one of the above investigations had restricted inclusion and inadequacies in expectation, we should think about semantic fluffiness when building feeling vocabulary. This paper proposed another methodology, for example, multi-strategy notion investigation dependent on semantic fluffiness, which is a blend of AI and assumption dictionaries-based methodology.

Xing Fang and Zhan et al. [2] contemplated the emotional substance that handled a central issue of estimation extremity order dependent on sentence level and review level. The trial results for the two degrees of classifications are uncovered promising results. In an examination article, Hussein et al. [3] portrayed the past work, the

objective is to locate the greatest considerable. Find how to acquire great exact outcomes that are pertinent to the pre-owned techniques and challenges in opinion investigation. In the article, Khairnar et al. [4] proposed a framework utilizing support vector machine (SVM). The SVM, an administered AI strategy has been utilized for feeling mining. In Rajeev et al. [20], a framework has been created to remove the client surveys by utilizing AI systems with Python instruments and the information were broke down dependent on that item recommended. In [13], another strategy was proposed to acquire the extremity of surveys by utilizing the natural language processing (NLP) procedure and AdaBoost classifier is utilized for improved execution and handling audits structure from various E-commerce destinations.

In Trupthi et al. [14], an intelligent programmed framework has been proposed by utilizing Hadoop strategy which predicts opinion extremity that assists with improving showcasing strategies and furthermore manage the difficulties that happen during the time spent anticipating assessment extremity and perform constant notion examination and convey time sensitive investigation to the client. The writing reasoned that E-business applications or deals proprietors are a lot of inquisitive about the surveys of their items from clients and needs to improve it as much as they can. Conclusion analysis or opinion mining is a rising exploration field of study that looks at individuals' mentalities, notions, or feelings toward specific substances, we acquired audits from the Amazon.com about excellence items and instruments for our underlying slant investigation testing utilizing the AI strategy SVM. We proposed the constant conclusion investigation framework for E-commerce applications that help clients to spare time to break down items from surveys and for specialist organizations too [21–24].

3 Existing System

Internet business surveys uncover the clients' perspectives on the items, which are useful for clients to know others' assessments on intrigued items. In the meantime, makers can become familiar with the open opinion on their items being sold in E-trade stages. For the most part, E-trade surveys include numerous parts of items, e.g., appearance, quality, value, coordination, etc., in this way, assumption investigation on E-business audits needs to adapt to those various perspectives. The issue with open closeout is that the interest of the overall population is constrained.

4 Disadvantages of the Existing System

- Digital bullying
- Higher risk of fraud and wholesale fraud
- Protection issues.

5 Proposed System

Recommender system (RS): Special sort of data sifting framework that gives a forecast that helps the client in assessing things from a huge assortment that the client is probably going to discover fascinating or valuable. Announcement (micro-post): Short message, partook in an online social stage, communicating an action, perspective, or feeling. Folksonomy: Whole arrangement of labels that comprises an unstructured community-oriented information characterization conspire in a social labeling framework. This progression includes distinguishing and extricating those particular item includes and the sentiments on them. The point of the venture is to mingle the closeout so individuals from far and wide and even over the mainland can partake in it.

6 Advantages of the Proposed System

- Communitarian filtering
- Content-based filtering
- Bunching
- Arrangement.

7 Modules Description

7.1 *Collection of User's Reviews*

Audits are important for doing the sentiment analysis task. For the collection of audits, there are various methods which are utilized right now. The audits can be an organized, semi-organized, and unstructured sort. Assessment analysis explore, there are open-source system where specialist can get their information for the exploration reason. R is one of the programming languages and programming conditions for factual processing and designs upheld by the R foundation for statistical computing. By introducing the required bundles and validation procedure of social site, to creep the surveys from that site is simple undertaking. When we have our content information with us, then we can utilize that information for pre-handling reason.

7.2 *Pre-Processing*

In pre-handling following are a few assignments: Removing URLs, special characters, numbers, punctuations, and so forth. Removing stop words, removal of retweets (if there should arise an occurrence of Twitter dataset), stemming, and tokenization.

7.3 *Feature Extraction*

Highlight determination from preprepared content is the troublesome undertaking in estimation investigation. The principle objective of the element determination is to diminish the dimensionality of the component space and hence computational expense. Highlight determination will decrease the over fitting of the learning plan to the preparation information. In various AI, calculations were dissected on a news survey dataset with various element determination strategies highlights are typically unigrams, bigrams, and grams. POS labeling is utilized in include choice procedures.

7.4 *Sentiment Word Identification*

Feeling word recognizable proof is a central work in various uses of assessment investigation and conclusion mining, for example, survey mining, supposition holder finding, and audit arrangement. Opinion words can be arranged into positive, negative, and nonpartisan words.

7.5 *Sentiment Polarity Identification*

The fundamental undertaking in SA is characterizing the extremity of a given book at the record, sentence, or highlight. The extremity is in three classes, for example, positive, negative, and neutral. Extremity recognizable proof is finished by utilizing various vocabularies which help to compute opinion score, supposition quality, and so on.

7.6 *Sentiment Classification*

Slant order of news survey dataset and item audit dataset is finished utilizing regulated AI approaches like guileless Bayes, SVM, maximum entropy, and so on. Precision is relying upon which dataset is utilized for which characterization strategies. On

account of supervised AI approaches, the training dataset is utilized to prepare the characterization model which at that point help to group the test information.

7.7 Analysis of Reviews

At long last analysis of result is critical to settle on choice to individual and industry. If there should arise an occurrence of news surveys on the off chance that more outcome is certain, at that point client can choose to go that news occasion. Examination is utilized in business insight.

8 Result and Discussion

1. The final output shows which bank is the based on customer reviews.
2. It also displays the rating in a graph format.
3. Users can also give their reviews in the Web site.
4. Only admin can add and remove banks.
5. So, the results are based on real-time customer reviews (Figs. 1, 2 and 3).

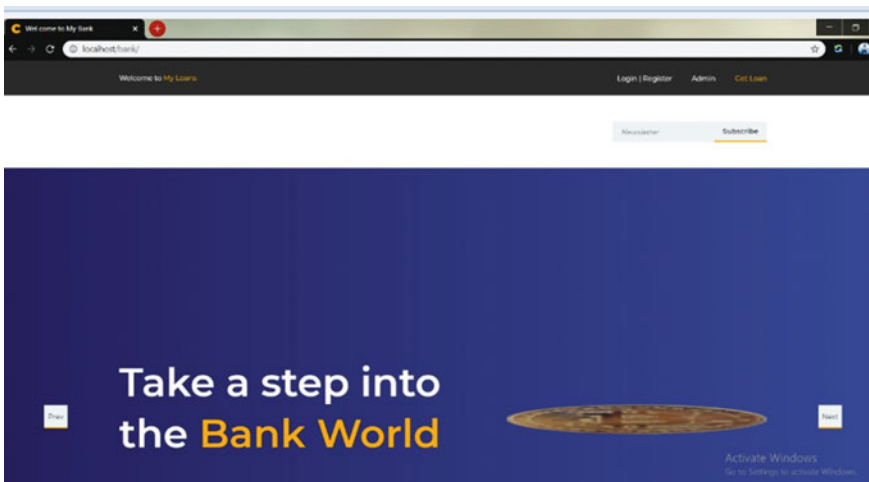


Fig. 1 Home page

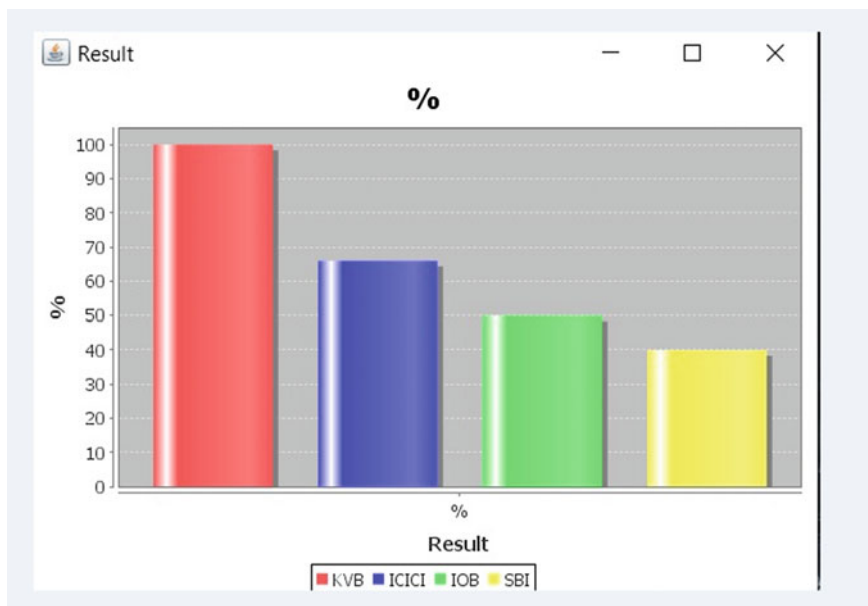


Fig. 2 Rating graph



Fig. 3 Analysis process

9 Conclusion

Right now, we utilized Twitter API utilizing R device which is open source. Tweets from Twitter have been gathered and provide for pre-preparing task in that apparatus. R open-source device is utilized in content mining and furthermore to slither gushing information from online networking like Twitter, Facebook, and so on. Film surveys information likewise preprepared in R apparatus for estimation examination and sentiment mining. There are diverse directed and solo methodologies and various vocabularies, word references, and corpus-based strategies which are exceptionally useful in sentiment analysis. Diverse dataset is accessible for film audit, item survey, opinions dataset, and so forth. Right now, the score has been determined and tallied number of positive, negative, and impartial tweets for given Hash tag and can anticipate the general assessment of specific occasion. According to above investigation of various #Hash tags tweets for supposition examination, individual and industry can locate the popular assessment behind that occasion.

References

1. P.D. Turney, Thumbs up or thumbs down?: semantic orientation applied to unsupervised classification of reviews, in *Proceedings of the 40th Annual Meeting of the Association for Computational Linguistics* (2002), pp. 417–424. <https://arxiv.org/abs/cs/0212032>
2. X. Fang, J. Zhan, Sentiment analysis using product review data. *J. Big Data* **2**, 5 (2015). <https://doi.org/https://doi.org/10.1186/s40537-015-0015-2>
3. D.M.E.-D.M. Hussein, A survey on sentiment analysis challenges. *J. King Saud Univ. Eng. Sci.* **30**, 330–338 (2018). <https://doi.org/10.1016/j.jksues.2016.04.002>
4. J. Khairnar, M. Kinikar, Machine learning algorithms for opinion mining and sentiment classification. *Int. J. Sci. Res. Publ.* **3**, 1–6 (2013). doi: 10.1.1.414.8110
5. A. Pravin, T. Prem Jacob, P. Asha, Enhancement of plant monitoring using IoT. *Int. J. Eng. Technol. (UAE)* **7**(3), 53–55 (2018)
6. K. Pradeep, T.P. Jacob, A hybrid approach for task scheduling using the cuckoo and harmony search in cloud computing environment. *Wireless Pers. Commun.* **101**(4), 2287–2311 (2018)
7. G. Nagarajan, R.I. Minu, Fuzzy ontology based multi-modal semantic information retrieval. *Procedia Comput. Sci.* **48**, 101–106 (2015)
8. S.P. Shyry, Efficient identification of bots by K-means clustering, in *Proceedings of the International Conference on Soft Computing Systems* (Springer, New Delhi, 2016), pp. 307–318
9. S.C. Mana, M. Saipriya, S.K. Sangeetha, Identification of land document duplication and black money transaction using big data analytics, in *2019 5th International Conference on Science Technology Engineering and Mathematics (ICONSTEM), Chennai, India* (2019), pp. 114–118
10. S.C. Mana, T. Sasiprabha, A study on various semantic metadata standards to improve data usability, in *2019 International Conference on Computational Intelligence in Data Science (ICCIDS), Chennai, India* (2019), pp. 1–4
11. P.S. Maran, P.M. Velumurugan, B.P.D. Batvari, Wind characteristics and Weibull parameter analysis to predict wind power potential along the south-east coastline of Tamil Nadu, in *International Conference on Intelligent Information Technologies* (Springer, Singapore, 2018), pp. 190–199
12. A. Karthik, M.D. Kamalesh, Rat trap: inviting, detection & identification of attacker using honey words in purchase portal, in *2017 3rd International Conference on Science Technology Engineering and Management (ICONSTEM)* (IEEE, 2017), pp. 130–132

13. C. Rain, *Sentiment Analysis in Amazon Reviews Using Probabilistic Machine Learning*. (Swarthmore College, 2013)
14. M. Trupthi, S. Pabboju, G. Narasimha, Sentiment analysis on twitter using streaming API, in *2017 IEEE 7th International Advance Computing Conference (IACC)* (2017), pp. 915–919. doi: <https://doi.org/10.1109/IACC.2017.0186>
15. T. Nasukawa, J. Yi, Sentiment analysis: capturing favorability using natural language processing. In *Proceedings of the 2nd International Conference on Knowledge Capture*. (ACM, 2003), pp. 70–77
16. R. He, J. McAuley, Ups and downs: modeling the visual evolution of fashion trends with one-class collaborative filtering, in *Proceedings of the 25th International Conference on World Wide Web, International World Wide Web Conferences Steering Committee* (2016). doi: <https://doi.org/10.1145/2872427.2883037>
17. Amazon review data Julian McAuley, UCSD, (2019). (Online). Available: <http://jmcauley.ucsd.edu/data/amazon/>
18. M. Tavakolifard, K.C. Almeroth, Social computing: an intersection of recommender systems, trust/reputation systems, and social networks. *IEEE Netw.* **26**(4), 53–58 (2012)
19. B. Amini et al., A reference ontology for profiling scholar's background knowledge in recommender systems. *Expert Syst. Appl.* **42**(2), 913–928 (2015)
20. P.V. Rajeev, V.S. Rekha, Recommending products to customers using opinion mining of online product reviews and features, in *2015 International Conference on Circuits, Power and Computing Technologies (ICCPCT-2015)* (2015), pp. 1–5. doi: <https://doi.org/10.1109/ICCPCT.2015.7159433>.
21. M. Anand, T. Sasikala, Efficient energy optimization in mobile ad hoc network (MANET) using better-quality AODV protocol. *Cluster Comput.* **22**(5), 12681–12687 (2019)
22. N.N. Priyanka, N. Geetha, A.V.A. Mary, Cross-Platform Recognition of Unknown Identical Users in Multiple Social Media Networks (2006)
23. G. Nagarajan, R.I. Minu, A.J. Devi, Optimal nonparametric bayesian model-based multimodal BoVW creation using multilayer pLSA. *Circ. Syst. Sign. Process* **39**(2), 1123–1132 (2020)
24. S. Nirmalraj, G. Nagarajan, An adaptive fusion of infrared and visible image based on learning of sparse fuzzy cognitive maps on compressive sensing. *J. Ambient Intell. Humanized Comput.* 1–11 (2019)
25. J. Yi, T. Nasukawa, R. Bunescu et al., Sentiment analyzer: extracting sentiments about a given topic using natural language processing techniques. In *Data Mining, 2003. ICDM 2003. Third IEEE International Conference*. (IEEE, 2003), pp. 427–434
26. K. Hiroshi, N. Tetsuya, W. Hideo, Deeper sentiment analysis using machine translation technology, in *Proceedings of the 20th international conference on Computational Linguistics. Association for Computational Linguistics* (2004), p. 494
27. R. Dheepa, D.U. Nandini, Privacy protection using sensitive data protection algorithm in frequent itemset mining of medical datasets. *Res. J. Pharm. Biol. Chem. Sci.* **7**(4), 308–316 (2016)

Effective Gene Mapping System with Disease Prediction and Corrective Measures



Sathi Lakshmi Samhitha, Sanku Shravani, and T. Sasikala

1 Introduction

Atomic controllers and their objective qualities have complex associations in cells, bringing about quality administrative systems [1]. Quality administrative systems are not static, yet frequently experience changes between various obsessive states [2]. Along these lines, investigating the reworking example of quality administrative systems from quality articulation information is vital in computational science.

Gaussian graphical models (GGMs) are broadly used to display quality systems [3–5]. By accepting that the quality articulation estimations pursue a multivariate Gaussian dispersion, the restrictive relationships between qualities can be resolved straightforwardly by the comparing exactness framework (or opposite covariance grid) [6]. Two qualities are restrictively free given different qualities if and just if the comparing component of the exactness grid is zero. The differential system between two state-explicit quality systems can be displayed as the contrast between these two by comparing state-explicit exactness frameworks [7].

In light of GGMs, there are two principle sorts of techniques to evaluate the differential system. The clear sort of strategies is to initially assess the state-explicit exactness frameworks and afterward process their distinction (called roundabout estimation techniques) [2, 8–12]. The second sort of techniques is to legitimately gauge the distinction between state-specific accuracy networks without evaluating the individual exactness grids (called direct estimation strategies) [7, 13–17]. Since the quantity of parameters which should be evaluated in aberrant estimation strategies is

S. L. Samhitha (✉) · S. Shravani · T. Sasikala
Department of Computer Science and Engineering, Sathyabama Institute of Science and Technology, Chennai, India
e-mail: samhithasathi1999@gmail.com

T. Sasikala
e-mail: dean.computing@sathyabama.ac.in

twice of that in heading estimation techniques, the immediate estimation techniques regularly outflank the circuitous estimation techniques as far as the precision of coming about differential systems [14]. Subsequently, we focus on direct estimation techniques in this work [14] proposed another misfortune work in their model to legitimately assess the differential system. In light of the D-follow misfortune work which was created to appraise the exactness grid [13, 18] built up a comparable misfortune work (called D-follow). In spite of the fact that the above techniques have effectively applied to address some significant organic issues, they have constrained execution since they just use quality articulation information (Fig. 1). With the improvement of high-throughput advancements and computational science techniques, countless static quality administrative connections have been given in open databases (e.g., Transcriptional Regulatory Relationships Unraveled by Sentence-based Text-mining (TRRUST) database [19]). These static quality administrative systems can give valuable data to recognize quality system revamping. It is settled that a differential edge can be molded just if there is in any event one edge in the two state-explicit quality systems. New computational strategies that can utilize the constructive outcome and decrease the negative impact of static quality system through joining static quality system information with quality articulation information are required.

In the proposed work, another differential system induction model recognizes quality system overhauling by joining quality articulation and quality transformation information. Similitudes and contrasts between various information types are found out by means of a gathering span punishment work. In the modification procedure, venture is to prescribe diet design and regular medications which can be prescribed to those individuals who may get into the ailment in a course of time by confirming the transformed genes. What is more, our work going to remove the patient's quality

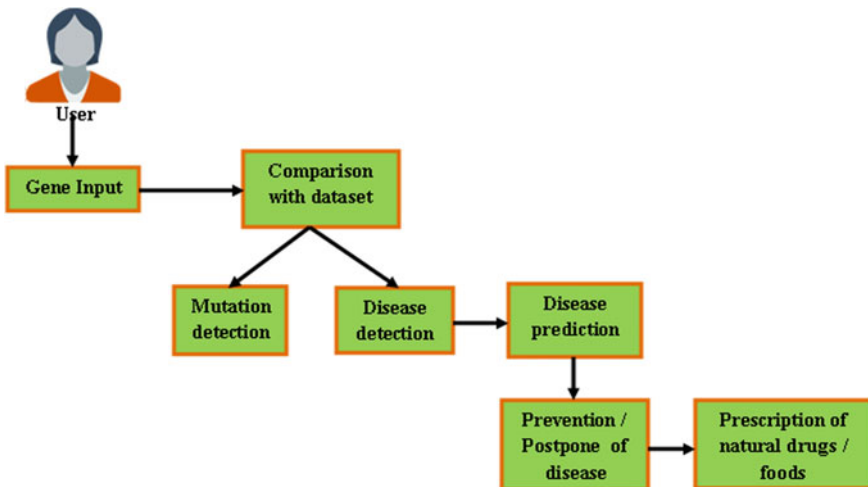


Fig. 1 Architecture of the proposed system

arrangement coding (exons) from the given dataset and contrast and the institutionalized amino corrosive succession. Quality sequence contains rehashed of four nucleotides to be specific adenine (A), thymine (T), guanine (G), and cytosine (C). This shaped protein is contrasted and derived as the anticipated protein. In an event that both are same, at that point it is proclaimed as should be expected, if the protein frame changed, at that point sickness is analyzed.

2 Related Work

In paper [1, 20], the authors presented a two-dimensional joint graphical rope (TDJGL) model which can obtain quality crosswise over various patient gatherings and information stages to improve the exactness of assessed systems. Reproduction contemplates exhibit that TDJGL gives increasingly precise evaluations of quality systems and differential systems than past contending approaches. Ou-Yang et al. [2] developed a hub-based multi-see differential system examination model to all the while gauge various quality administrative systems and their disparities from multi-stage quality articulation information. In [3], authors described about graphical models that have been utilized to appraise GRN. Most existing strategies gauge GRN for a particular cell or tissue type or in a tissue-innocent way, or do not explicitly concentrate on arrange overhauling between various tissues. Here, we portray another strategy called latent differential graphical model (LDGM). Zhang et al. and Maran et al. [4, 21] determined how these systems change crosswise over two conditions, a significant undertaking in genomics and build up a hub-based differential system investigation (N-DNA) model to legitimately evaluate the differential system that is driven by certain center point hubs. Differential systems can likewise be surmised from quality change information utilizing Ising models [5, 22]. By accepting that the quality change estimations pursue a Bernoulli circulation, the contingent conditions among qualities can be perused from the communication parameters related with the structure of the Markov arrange. Gaussian Markov systems [6] gathering differential system utilizing Ising models can be diminished to learn the contrast between the two state-explicit cooperation parameters. The techniques can be isolated into backhanded estimation strategies and direct estimation strategies also [7, 23]. The immediate estimation strategies are famous since they do not force specific suspicion on the state-explicit collaboration parameters using Markov networks [8]. The authors [9, 24] said that the inspiration of their technique is to appraise the differential system between two tissue types, for cancer genome which resulted in obtaining the expression for cancer. Authors [10–15] developed a strategy that involves the combination of gene expression with gene mutation. This may yield results for the prediction of disease in a very accurate manner [25, 26].

We inferred from the above study that many authors approached various techniques for observing the gene mutations, and they have done only for cancer [16]. Some of the techniques discussed above are only to find the mutation [17]. Majority of them have predicted for ovarian cancer which is very limited [18, 19]. Some

have explained the detailed variation in genes. None of them have done for other genetic diseases or some precautions. Thus, we propose a gene mapping system which predicts the disease by observing gene patterns from the understanding of above studies and provides precautions of food and drugs for some number of genetic diseases.

3 Proposed System

The distinguishing proof of illness qualities is a fundamental issue to unravel the systems of complex sicknesses. In any case, the greater part of past strategies just spot light on quality articulation information. Consequently, how to consolidate static quality administrative and quality articulation information to recognize quality system reworking is an intriguing issue. In this paper, we propose another strategy to address this issue. The aggressive presentation of our technique is exhibited utilizing both reproduction and genuine information. The usage of the task is to remove the patient's quality grouping coding (exons) from the given dataset and contrast and the institutionalized amino corrosive succession. The quality succession is chiefly arranged into two orders to be specific introns and exons. Introns are the non-coding grouping which is trailed by exons.

Quality sequence contains rehashed of four nucleotides to be specific adenine (A), thymine (T), guanine (G), and cytosine (C). Aminoacids will frame a protein as yield. On the off chance that both are same, at that point it is proclaimed as expected, in the event that the protein framed is transformed, at that point illness is analyzed. The undertaking is to prescribe diet design or whatever other normal medications which can be prescribed to those individuals who is relied upon to get into the malady in a course of time by checking the transformed genes. This paper gathers that distinguishing ailment is dependent on quality utilizing SVM calculation. Through this framework separated from malady distinguishing proof, we additionally propose the medication dependent on the problem occurred for the individual.

3.1 Procedure

In the system which we are designing, the procedure is given as follows:

- User can login through a login page.
- Details of the patient are filled accordingly.
- Patient id will be generated and data will be stored in database table.
- Through this id, processing is done in the database.
- The gene pattern of particular patient is compared with the dataset which is fed to the program already.

- The changes will be observed and the disease would be predicted with respect to the change observed as in the dataset.
- Prediction is done using SVM algorithm.
- Food and drug details for corresponding disease are stored in another table and retrieved as output and the flow of this process is shown below (Fig. 2).

SVM, a machine learning algorithm, develops a hyperplane which is used in classification and prediction process of the disease [18]. It has been applied vigorously in biological and molecular sciences. The classification performed on proteins is very

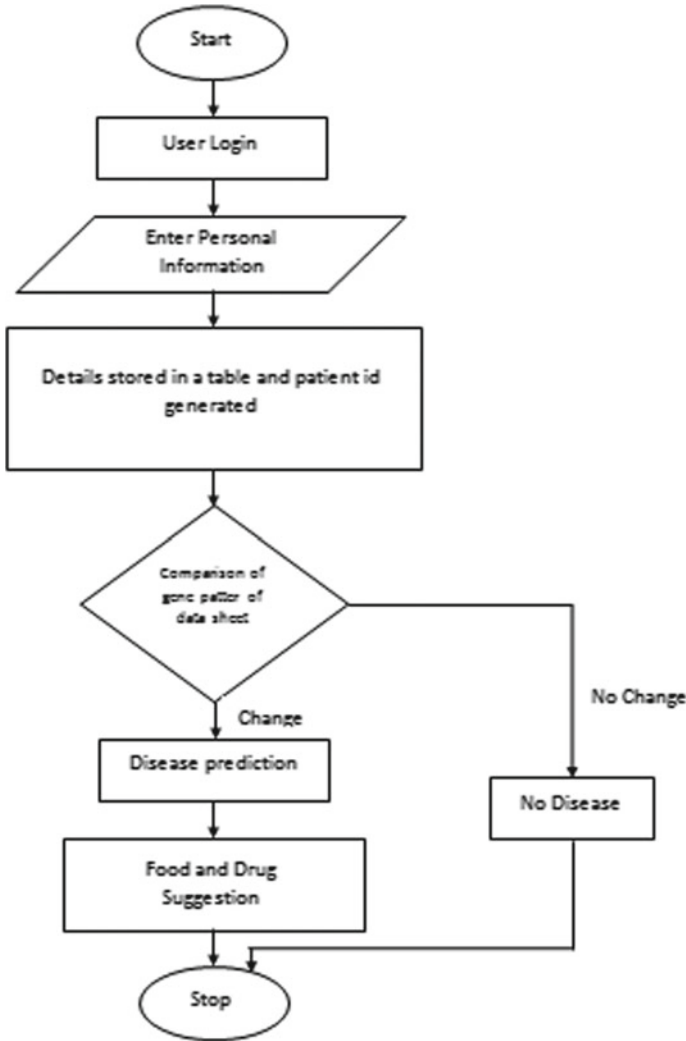


Fig. 2 Flow of the proposed system

accurate than by any other methods present. Therefore, we have opted for SVM algorithm. The classification and prediction process in the system are where the algorithm comes into use.

3.2 Advantages of the Proposed System

- Identifying the disease
- Suggest food and drugs to prolong the occurrence of the disease.

4 Modules Description

4.1 User Interface Design

UI plan is the appearance of the system. To build up our project, we use netbeans as an IDE and MSQl as a back end. The way it looks which includes login page, user details would be designed in this module programmed in Java.

4.2 Dataset Maintenance

There is a quality grouping of a in A, G, C, T positions for various ailments. It will contain close by 2000 quality succession as unique. There is a need to maintain the dataset safe for comparison which is a major part of the process.

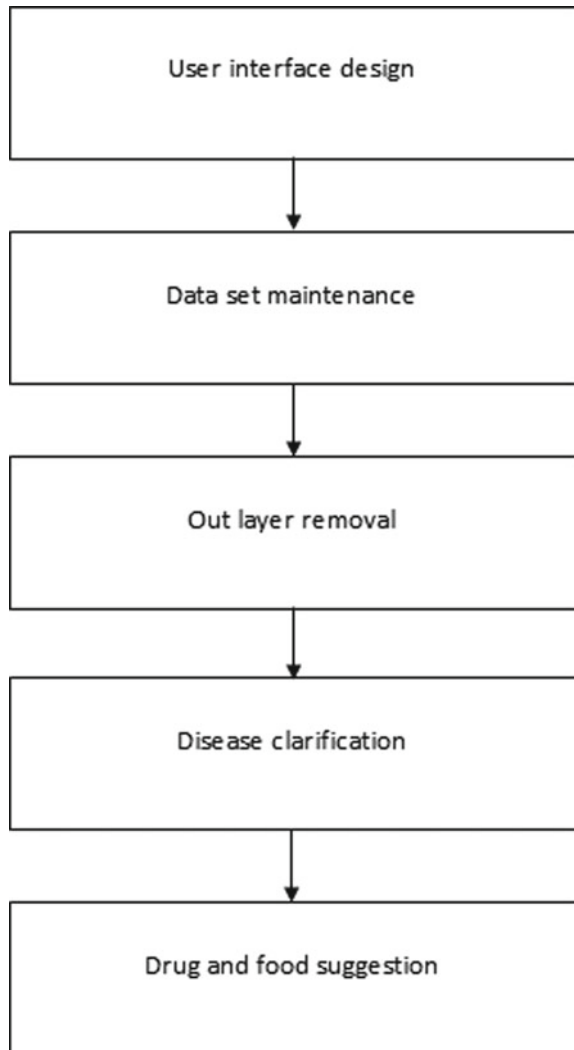
4.3 Outlayer Removal

A quality transformation is a perpetual adjustment in the DNA arrangement that makes up a quality, with the end goal that the succession contrasts based on what is found in the vast majority. Changes go in size; they can influence anyplace from a solitary DNA building square (base pair) to a huge fragment of a chromosome that incorporates numerous qualities. The transformed quality is considered as equivalent to typical quality and it will be expelled from the datasets. The quality change will made here as thyracine into uracil. All quality grouping will separate into formats like UUU, UUG, UGU, and so on, and this is the transformation of AGCT to AGCU.

4.4 Disease Classification

An illness is a specific unusual condition that contrarily influences the structure or capacity of part or the entirety of a creature [1,2]. Diseases are understood as ailments that are related with explicit manifestations and signs [1]. For instance, interior dysfunctions of the resistant framework can deliver a wide range of sicknesses, including different types of immune deficiency, extreme touchiness, sensitivities, and immune system issue. In our module, we characterize ailment by parent quality ailment and ordinary-based quality illness (Fig. 3) depicts the modules of the system.

Fig. 3 Modules of the proposed system



4.5 Disease Prediction

In this module, we distinguish the malady by actualizing SVM calculation. We will distinguish the sickness type that implies, the quality which will be given as an information, that will be sent to the dataset for examination and to recognize the ailment type whether it is quality-based ailment or contamination-based malady. The disease would be predicted based on the changes on the gene pattern, and framework will foresee ailment name.

4.6 Drug Suggestion

In this module, after illness discovery, framework will inform the potential outcomes and propose the medication to that tainted individual. The disease predicted would be checked for the respective drugs. The data would contain the general drugs and food to be taken as preventive measures. This will help in ailment occurrence to be prolonged.

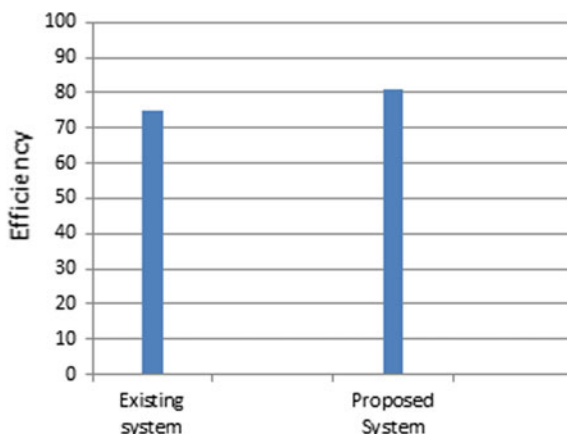
5 Result and Discussion

As of existing system, it does the gene mapping and finds the mutation in the genes which is abnormal. If the base work is considered, it deals with a single disease cancer. When proposed system is observed, it understands the base work, the concept of finding the mutation is extracted from the existing system and developed to predict more than one genetic disease with food and drug suggestion to prevent or prolong its occurrence. So, the comparison of efficiency is quite difficult because of the variation in the existing system and proposed system. But the features are high in proposed than existing one as it predicts more diseases, which is taken into consideration and proposed system resulted as a little more efficient than existing system (Fig. 4).

6 Conclusion

Open storehouses of quality administrative system information keep on developing. The static quality administrative information can give significant earlier data to gather differential systems between two unique states. In any case, a large portion of past techniques just spotlight on quality articulation information. In this way, how to consolidate static quality administrative and quality articulation information to distinguish quality system reworking is a fascinating issue. In this paper, we propose another strategy to address this issue. The focused exhibition of our strategy

Fig. 4 Comparison graph with existing system



is shown utilizing both reenactment and genuine information. This paper construes that recognizing malady dependent on quality utilizing SVM calculation. Through this framework separated from illness recognizable proof, we additionally propose the medication dependent on the infection.

Acknowledgements We are very thankful to our guide Dr. T. Sasikala M.E., Ph.D., Dean, School of Computing, for her valuable guidance, suggestions and encouragement throughout this work. We convey our thanks to Dr. S. Vigneshwari M.E., Ph.D., and Dr. L. Lakshmanan M.E., Ph.D., Heads of the Department, Computer Science and Engineering, for providing full support during the reviews. We also thank all the teaching and non-teaching staff for their support in many ways.

References

1. X.F. Zhang, L. Ou-Yang, X.M. Zhao, H. Yan, Differential network analysis from cross-platform gene expression data. *Sci. Rep.* **6** (2016)
2. L. Ou-Yang, X.F. Zhang, M. Wu, X.L. Li, Node-based learning of differential networks from multi-platform gene expression data. *Methods* (2017)
3. D. Tian, Q. Gu, J. Ma, Identifying gene regulatory network rewiring using latent differential graphical models. *Nucleic Acids Res.* **44**(17), e140 (2016)
4. X.F. Zhang, L. Ou-Yang, H. Yan, Node-based differential network analysis in genomics. *Comput. Biol. Chem.* (2017)
5. S. Liu, J.A. Quinn, M.U. Gutmann, M. Sugiyama, Direct learning of sparse changes in Markov networks by density ratio estimation, in *Joint European Conference on Machine Learning and Knowledge Discovery in Databases* (Springer, 2013), pp. 596–611
6. S. Liu, J.A. Quinn, M.U. Gutmann, T. Suzuki, M. Sugiyama, Direct learning of sparse changes in Markov networks by density ratio estimation. *Neural Comput.* **26**(6), 1169–1197 (2014)
7. F. Fazayeli, A. Banerjee, Generalized direct change estimation in ising model structure, in *International Conference on Machine Learning* (2016), pp. 2281–2290
8. S. Liu, T. Suzuki, R. Relator, J. Sese, M. Sugiyama, K. Fukumizu et al., Support consistency of direct sparse-change learning in Markov networks. *Ann. Stat.* **45**(3), 959–990 (2017)

9. J.N. Weinstein, E.A. Collisson, G.B. Mills, K.R.M. Shaw, B.A. Ozenberger, K. Ellrott, I. Shmulevich, C. Sander, J.M. Stuart, C.G.A.R. Network, The cancer genome atlas pan-cancer analysis project. *Nat. Genet.* **45**(10), 1113–1120 (2013)
10. M. Gerstung, A. Pellagatti, L. Malcovati, A. Giagounidis, M.G. Porta, M. Jdersten, H. Dolatshad, A. Verma, N.C. Cross, P. Vyas, Combining gene mutation with gene expression data improves outcome prediction in myelodysplastic syndromes. *Nat. Commun.* **6**(23), 5901 (2015)
11. J.L. Fleck, A.B. Pavel, C.G. Cassandras, Integrating mutation and gene expression cross-sectional data to infer cancer progression. *BMC Syst. Biol.* **10**(1), 1–12 (2016)
12. J. Huang, S. Ma, H. Xie, C.H. Zhang, A group bridge approach for variable selection. *Biometrika* **96**(2), 339–355 (2009)
13. J. Guo, E. Levina, G. Michailidis, J. Zhu, Joint estimation of multiple graphical models. *Biometrika* **98**(1), 1–15 (2011)
14. J. Friedman, T. Hastie, R. Tibshirani, A note on the group lasso and a sparse group lasso (2010). arXiv preprint [arXiv:1001.0736](https://arxiv.org/abs/1001.0736)
15. H. Zou, R. Li, One-step sparse estimates in nonconcave penalized likelihood models. *Ann. Stat.* **36**(4), 1509 (2008)
16. N. Parikh, S. Boyd, Proximal algorithms. *Found. Trends Optim.* **1**(3), 127–239 (2014)
17. H. Liu, K. Roeder, L. Wasserman, Stability approach to regularization selection (stars) for high dimensional graphical models, in *Advances in Neural Information Processing Systems* (2010), pp. 1432–1440
18. S. Prince Mary, B. Bharathi, S. Vigneshwari, R. Sathyabama, Neural computation based general disease prediction model. *Int. J. Recent Technol. Eng. (IJRTE)* **8**(2), 5646–5449 (2019). ISSN: 2277-3878
19. S. Vigneshwari, B. Bharathi, T. Sasikala, S. Mukkamala, A study on the application of machine learning algorithms using R. *J. Comput. Theoret. Nanosci.* **16**(8), 3466–3472 (2019)
20. A. Pravin, T. Prem Jacob, P. Asha, Enhancement of plant monitoring using IoT. *Int. J. Eng. Technol. (UAE)* **7**(3), 53–55 (2018)
21. P.S. Maran, P.M. Velumurugan, B.P.D. Batvari, Wind characteristics and Weibull parameter analysis to predict wind power potential along the south-east coastline of Tamil Nadu, in *International Conference on Intelligent Information Technologies* (Springer, Singapore, 2018), pp. 190–199
22. K. Pradeep, T.P. Jacob, A hybrid approach for task scheduling using the cuckoo and harmony search in cloud computing environment. *Wirel. Pers. Commun.* **101**(4), 2287–2311 (2018)
23. G. Nagarajan, R.I. Minu, Fuzzy ontology based multi-modal semantic information retrieval. *Procedia Comput. Sci.* **48**, 101–106 (2015)
24. A. Karthik, M.D. Kamalesh, Rat trap: inviting, detection & identification of attacker using honey words in purchase portal, in *2017 Third International Conference on Science Technology Engineering & Management (ICONSTEM)* (IEEE, 2017), pp. 130–132
25. K.S. Kumar, T. Sasikala, A technique for web security using mutual authentication and clicking-cropping based image captcha technology. *Int. Rev. Comput. Softw.* **9**(1), 110–118 (2014)
26. M.A. Chowdary, M. Kundan, D.A.V.A. Mary, Effective credit card forgery prevention using multilevel authentication. *IOP Conf. Ser. Mater. Sci. Eng.* **590**(1), 012021 (2019)

Face Recognition Based Attendance System and Emotion Classification



Vallu Sri Satya Kala, Vanka Bhavyasri, and S. Vigneshwari

1 Introduction

Currently, the automation, numerous logical progressions, and new inventions have transpired to Lagniappe method, in order to augment the correctness and to amplify the lives. Maintaining attendance in all institutions is compulsory and important for knowing the performance of students. Attendance is crucial for students because they get their final grade by the end of their semester on the basis of their attendance. So considering these, students attend their classes without fail [1, 2]. And attendance should be marked accurately. Mechanized attendance systems mainly consist of biometric-based, acute card-based, and network-based system. These configuration schemes are broadly deployed in miscellaneous alliance. The innovation points in bestowing gigantic information arranged specialized advancements nowadays [3, 4].

Profound learning is one among the fascinating area that empowers the machine to prepare itself by giving some datasets as info and gives a proper yield during testing by applying distinctive learning algorithms. As a consequence, the computer distinguishes the participation execution of the understudies with the advance of the profound learning invention and keeps a record of those gathered information [5]. This computerized attendance-based system is done without lecturer intervention or the employee. Participation is the prime significance for both the educator and understudy of an instructive association [6, 7]. The issue emerges when we consider

V. S. S. Kala (✉) · V. Bhavyasri · S. Vigneshwari
Department of Computer Science and Engineering, Sathyabama Institute of Science and Technology, Chennai, India
e-mail: satyakalavallu1905@gmail.com

V. Bhavyasri
e-mail: vankabhavyasri@gmail.com

S. Vigneshwari
e-mail: vigneshwari.cse@sathyabama.ac.in

the customary procedure of gauging participation in the study hall [8, 9]. Calling name or number of the understudy for participation sits around idle, yet in addition it requires vitality. So, an establishment of a programmed participation framework will look after these issues [10–12]. There are some programmed participation taking frameworks which are at present being utilized by different establishments. Case of one such framework is the utilization of biometric procedure. Even though the reality that it is programmed and a stage in front of the customary technique, it neglects to converge the time imperative. The understudy needs to sit tight in line for giving participation, which is time taking. This undertaking presents an automatic participation checking framework, without any sort of obstruction with the typical instructing strategy. This framework can likewise be executed during test sessions or in other instructing exercises where participation is profoundly basic. This framework disposes of old style understudy recognizable proof, which can meddle with the continuous training process as well as be unpleasant for understudies during assessment sessions. A programmed participation framework by facial recognition utilizing AI is a shrewd and sorted out route for any association which requests the normal upkeep of the participation of the representatives, specialist or understudies. This methodology will set aside the cash of association, spare time and extra you with the dissatisfaction of the manual contribution of participation, which is being followed since ages. The programmed approach of participation will expand proficiency, by the usage of the electronic, coordinated time, and participation framework bringing about benefit in each angle [13, 14].

2 Related Work

Mohamed and Raghu [15] have proposed a versatile unique finger impression gadget. This framework ensures an idiot proof technique for denoting the participation. The issue with this methodology is that going of the gadget during the talk time may occupy the consideration of the understudies.

Lim et al. [16] proposed RFID based framework where RFID is placed per user's ID card to record their participation. This framework may offer ascent to the issue of deceitful access. An unapproved individual may utilize approved ID card and go into the association.

Kadry and Smaili [17] have proposed Daugman's algorithm-based iris recognition system. This framework uses the iris recognition framework for executives that captures the picture of iris recognition, extraction, putting away, and coordination. As a result, the trouble lays the transmission rays in the spots where the geology is appalling.

Shehu and Dika [18] presented a continuous PC vision algorithm in programmed participation, the executives framework. This framework additionally utilized AI algorithm which is normally utilized in PC vision. Additionally, Haar classifiers are used to prepare the pictures from the camera catching.

Nithya et al. [19] have proposed the planetary mapping that enables high determination images with few megapixels.

Vijai et al. [20] have put forwarded the system that catches the red-handed intruders in real time. With the help of Raspberry Pi chipset, the surveillance camera is made precisely constructed.

Sankari and Vigneshwari [21] used deeper CNN architectures for brain tumor segmentation performance that can be ameliorate.

Singh et al. [22] have presented the crime face recognition for fraud detection using pattern recognition, neural networks, and content-based video processing.

Barnouti et al. [23] have proposed face recognition using mobile device or webcam by PCA, BPNN, and RBF. The system is evaluated to achieve high recognition values. Research on Machine Learning for prediction and pattern recognition have been carried out [24, 25]

3 Materials and Methods

3.1 Problem Description

Automated attendance system by utilizing face recognition suggests that the framework depends on face detection and recognition algorithms, which is utilized consequently to distinguish the understudy face. When he/she enters the class, the framework is able to mark the participation by detecting and matching the person with the database pictures. And we proposed emotion recognition framework by utilizing various strategies. Commonly a mechanized face appearance recognition framework is used that cooperates with camera for catching the facial picture. This is pre-prepared in such a way that it limits the ecological and different varieties in the picture. This incorporates the activities of picture scaling and splendor alteration. After detection of face, mouth, and eye locale, Viola–Jones algorithm has been utilized for extracting the facial features and classifying emotions.

The recognition of emotions depends on the count of separations between different highlights. Right now separations between testing picture and nonpartisan picture are done and furthermore it chooses the most ideal match of testing picture from trained envelope. It additionally arranges or perceives the emotions on the premise from different separations determined. What is more, the conclusive outcomes are shown. In conclusive outcomes, best match from preparing pictures is additionally appeared and a book record Result.txt is shown in MATLAB window that contains the information of people present (time and date).

Proposed framework

Figure 1 depicts the overview of the proposed system.

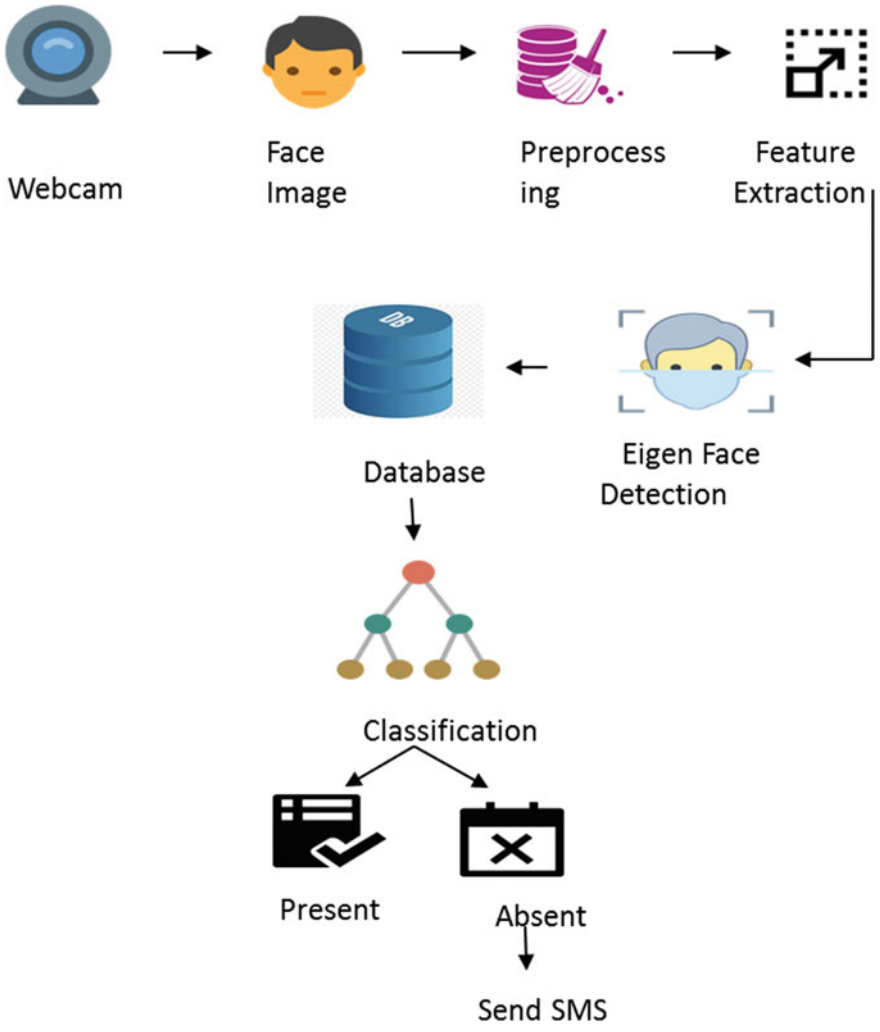


Fig. 1 Overview of the proposed system

4 Algorithms

4.1 Viola–Jones Detection

The classification of emotions is done by using Viola–Jones algorithm. This involves five stages preprocessing, edge detection, feature extraction, face detection, and emotion classification. After the emotion is classified, it gives the data in the excel sheet whether they are interested or uninterested.

4.2 Eigenface Algorithm

Eigenface algorithm is utilized for face recognition. Eigenface algorithm requires different attributes of the face pictures all together for productive recognition such as mean, normal, and eigenfaces. We figure the covariance network from which we get the eigenworth and eigenvector.

4.3 Classification

The identified countenances are contrasted, and the parameters are prepared from database. At the point when face of an understudy matches with dataset, it denotes the understudy as present and afterward at long last it will send the SMS to the portable which understudies is missing through hardware. In emotion recognition, after classifying, it loads the data in excel sheet.

5 Hardware

5.1 Arduino UNO

The Arduino UNO is a board based on the ATmega1280 (datasheet) microcontroller. It has 54 digital input/output pins (of which 14 can be used as PWM outputs), 16 analog inputs, 4 UARTs (serial hardware ports), a 16 MHz crystal oscillator, a USB connection, a power jack, an ICSP header, and a reset key. It contains everything necessary to support the microcontroller; simply connect it to a computer with a USB cable, or power it to get started with an AC-to-DC adapter or battery. The Uno is compatible with most Arduino Duemilanove or Diecimila designed shields. In this project, by using Arduino and GSM model SMS is sent (Fig. 2).

Fig. 2 Arduino UNO



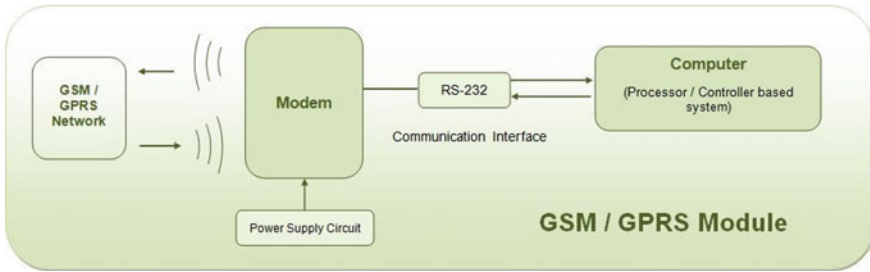


Fig. 3 GSM/GPRS module

5.2 GSM/GPRS Module

A GSM/GPRS module manufactures a GSM/GPRS modem with reliable connectivity to work effectively with a device or microprocessor interfacing and a microcontroller-based system. Also, the power supply circuit is built into the module, which can be activated using an appropriate adaptor. A sim card slot is made available in order to place a sim card that sends sms to the parents of absentees (Fig. 3).

6 Results and Discussions

When the project is made to run, a login page is opened, then an admin should enter the password to launch the system. First input images should be added to the database with appropriate names. The dataset should be trained. Finally, start matching by opening the live webcam. It detects the face in the live cam and checks for the matching in the database. If matched it displays both input and output images with a message “hello, xxx your attendance is marked” or else “you are an invalid person.” The log of present people is maintained and stored in a file with their name, date and time. At last, hardware part is made to run, to send SMS to the parent of absentees (Figs. 4 and 5).

Emotions are classified by passing through various stages. First it detects the image and trains the image with normalized training dataset and extracts features. It calculates the mean value, eigenvector, and PCA values and classifies whether interesting or not interesting. It gives the information of no. of students interesting and uninteresting in the excel sheet (Figs. 6 and 7).

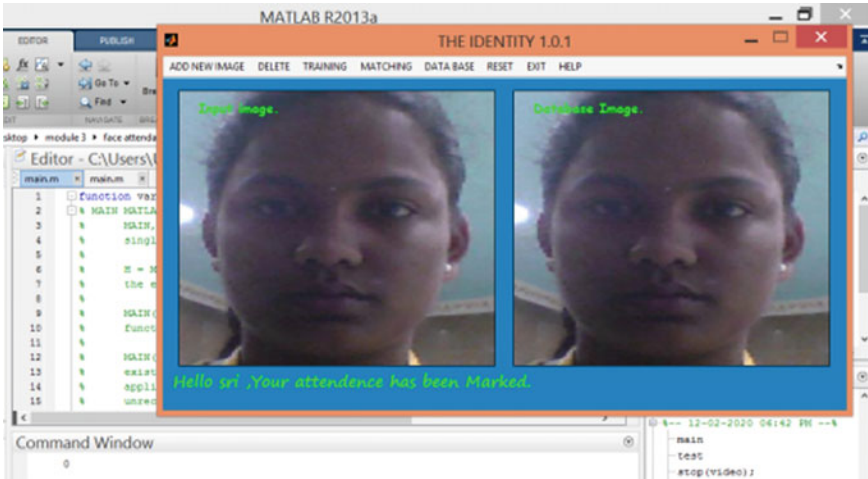


Fig. 4 Detecting and classifying

Name	Date	Time	Attendance
bavyasree	17-Feb-2020	1:9:44	Present
bavyasree	17-Feb-2020	2:2:43	Present
satyakala	17-Feb-2020	2:6:40	Present
bavyasree	19-Feb-2020	9:32:28	Present
sri	19-Feb-2020	9:37:6	Present

Fig. 5 Log details

7 Conclusion

It spares time and effort of undertaking, specifically on the fluke that means it is a talk with vast quantity of understudies. Mechanized attendance system has been imagined to decrease the downsides in the conventional framework. This participation framework shows the utilization of picture preparing systems. This framework can just assist the participation framework, yet in addition improve the generosity of an organization. The recognition of emotions depends on the computation of separations between different highlights focuses.

The significant commitment of this paper is that the proposed technique can recognize edges of the pictures and from that edges separation between different highlights is determined by utilizing Euclidean separation formulae. This separation

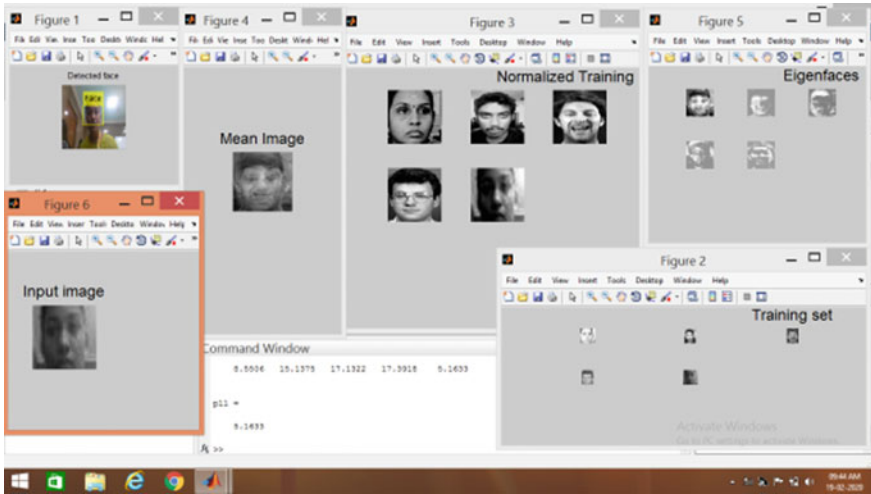


Fig. 6 Feature extraction and selection

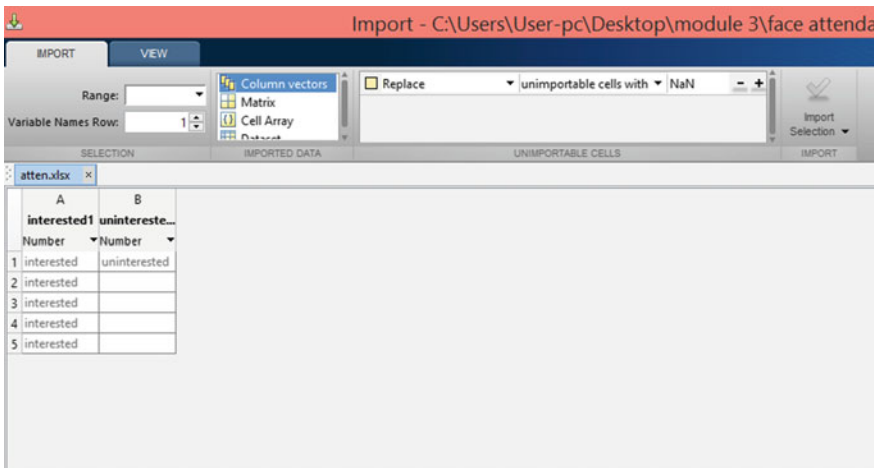


Fig. 7 Emotion status

is distinctive for each picture presenting various emotions. Based on this separation, emotions are characterized. Viola–Jones algorithm has been utilized for face identification which identifies human face utilizing course classifier and PCA algorithm for highlight choice and afterward at long last it will send the SMS to the versatile which understudies are missing. At the point where it is contrasted with customary participation denoting this framework spares time and also helps to have an accurate check of the understudies in addition.

References

1. S.K. Bhattacharyya, K. Rahul, Face recognition by linear discriminant analysis. *Int. J. Commun. Netw. Secur.* **2**(2), 2231–1882 (2013)
2. S. Marlin, S.S. Jebaseelan, B. Padmanabhan, G. Nagarajan, Power quality improvement for thirty bus system using UPFC and TCSC. *Indian J. Sci. Technol.* **7**(9), 1316–1320 (2014)
3. U.A. Kamerikar, M.S. Chavan, Experimental assessment of LDA and KLDA for face recognition. *Int. J. Adv. Res. Comput. Sci. Manag. Stud.* **2**(2), 137–146
4. A. Pravin, T. Prem Jacob, P. Asha, Enhancement of plant monitoring using Iot. *Int. J. Eng. Technol. (UAE)* **7**(3), 53–55 (2018)
5. M.P. Gawande, D.G. Agrawal, Face recognition using PCA and different distance classifiers. *IOSR J. Electron. Commun. Eng.* **9**(1), 1–5
6. K.S. Kumar, T. Sasikala, A Technique for web security using mutual authentication and clicking-cropping based image Captcha technology. *Int. Rev. Comput. Softw.* **9**(1), 110–118 (2014)
7. N.N. Priyanka, N. Geetha, A.V.A. Mary, Cross-platform recognition of unknown identical users in multiple social media networks (2006)
8. N.H. Barnouti, Improve face recognition rate using different image pre-processing techniques, *Am J Eng Re (AJER)* **5**(4), 46–53 (2016)
9. K. Pradeep, T.P. Jacob, A hybrid approach for task scheduling using the cuckoo and harmony search in cloud computing environment. *Wirel. Pers. Commun.* **101**(4), 2287–2311 (2018)
10. R. Dheepa, D.U. Nandini, Privacy protection using sensitive data protection algorithm in frequent itemset mining of medical datasets. *Res. J. Pharm. Biol. Chem. Sci.* **7**(4), 308–316 (2016)
11. G. Nithya, S.L. Shabu, A novel framework in reusing the ontological health record. *Res. J. Pharm. Biol. Chem. Sci.* **7**(3), 215–220 (2016)
12. G. Nagarajan, R.I. Minu, A.J. Devi, Optimal nonparametric bayesian model-based multimodal BoVW creation using multilayer pLSA. *Circuits Syst. Signal Process.* **39**(2), 1123–1132 (2020)
13. P.S. Maran, P.M. Velumurugan, B.P.D. Batvari, Wind characteristics and weibull parameter analysis to predict wind power potential along the South-east coastline of Tamil Nadu, in *International Conference On Intelligent Information Technologies* (Springer, Singapore, 2018), pp. 190–199
14. M. Divya, M.D. Kamalesh, Recovery of watermarked image from geometrics attacks using effective histogram shape based index. *Indian J. Sci. Technol.* **9**(44), 1–6 (2016)
15. Mohamed, B.K., Raghu, C., Fingerprint attendance system for classroom needs, in *India Conference (Indicon), 2012 Annual IEEE*. IEEE (2012), pp. 433–438
16. T. Lim, S. Sim, M. Mansor, RFID based attendance system, in *IEEE Symposium on Industrial Electronics & Applications*, 2009. ISIEA 2009, vol. 2. IEEE (2009), pp. 778–782
17. S. Kadry, K. Smaili, A design and implementation of a wireless iris recognition attendance management system, *Information Technology and Control*, vol. 36, No. 3 (2007), pp. 323–329
18. V. Shehu, A. Dika, Using real time computer vision algorithms in automatic attendance management systems, *Information Technology Interfaces (ITI)*, 2010 32nd International Conference (2010), pp. 397–402
19. R. Nithya, K. Muthu Priya, S. Vigneshwari, Stitching large images by enhancing surf and Ransac algorithm, in *2017 Second IEEE International Conference On Electrical, Computer And Communication Technologies*, 22–24 Febr 2017, SVS Engineering College, Coimbatore. Scopus. <https://doi.org/10.1109/Iceect.2017.8117868>
20. R. Vijai Chandra Prasad, M. Yashwanth Sai, P.R. Niveditha, T. Sasipraba, S. Vigneswari, S. Gowri, Low cost automated facial recognition system, in *2017 Second IEEE International Conference On Electrical, Computer and Communication Technologies*, 22–24 Febr 2017, SVS Engineering College, Coimbatore. 10.1109/Iceect.2017.8117829, Scopus
21. A. Sankari, S. Vigneshwari, Automatic tumour segmentation using CNN, in *Third IEEE International Conference On Science Technology, Engineering Management-ICONSTEM 2017*, 23–24 Mar 2017, Chennai. Scopus (2017)

22. A. Singh, S.K. Singh, S. Tiwari, Comparison of face recognition algorithms on dummy faces. *Int. J. Multimed. Its Appl.* **4**(4), 121–135 (2012)
23. N.H. Barnouti, Face recognition using Eigen-face implemented on DSP processor. *Int. J. Eng. Res. General Sci.* **4**(2), 107–113
24. A. Mary Psonia, S. Vigneshwari, J. Albert Mayan, D. Jamunarani, Service direct: platform that incorporates service providers and consumers directly. *Int. J. Eng. Adv. Technol.* **8**(6), 3301–3304 (2019)
25. S. Prince Mary, B. Bharathi, S. Vigneshwari, R. Sathyabama, Neural computation based general disease prediction model. *Int. J. Recent Technol. Eng. (IJRTE)* **8**(2), 5646–5449 (2019). ISSN: 2277–3878

Classification and Prediction of Text Data by Using a Natural Language Processing Algorithm



Kakarlapudi Lavadhan Varma, Kaipa Subhash Reddy, S. Jancy, and Mercy Paul Selvan

1 Introduction

Machine studying is one present-day innovation that has helped man decorate not first-rate many commercial and expert processes; [1–3] however, it additionally advances healthy living. But what is device mastering? It is a subset of AI, which makes a specialty of using statistical techniques to create intelligent laptop structures so you can find out from databases available to it [4–6]. Currently, machine studying has it is completing in multiple fields and industries [24], for example, diagnosis, photo processing, prediction, classification, [7, 8] studying association, regression, etc. The intelligent systems constructed on gadget mastering algorithms can discover from experience or historical data [21, 22, 26]. Machine reading applications provide results on the concept of preceding revel [23, 25]. In this article, we'll speak ten real-existence samples of how devices getting to know permits in creating a better era to strengthen today's ideas. Neural networks are machine learning mechanism which includes itself similar to intellect of human brain [15, 16]. An artificial neural network can be created by adopted the information in computer system. A computer with neural network is to do job using training of datasets [17, 18].

K. L. Varma (✉) · K. S. Reddy · S. Jancy · M. P. Selvan
Department of Computer Science and Engineering, Sathyabama Institute of Science and Technology, Chennai, India
e-mail: lavadhan98@gmail.com

K. S. Reddy
e-mail: kaipasubash222@gmail.com

S. Jancy
e-mail: jancymtech11@gmail.com

2 Existing System

Given current limit on proposal of the existing system, which has become a reality in all areas of outsourcing work is increasingly clear that it is necessary to get the students to computer science and skills development to cope with global IT outsourcing [9, 10]. This article describes the learning of English for its shortage in terms of global outsourcing of PC software environments [11, 13].

And according to these three aspects for they be persuaded, this requires investigation report of outsourcing conference on IT and combining the characteristics of the education of a new computer system consists of English courses and the other half ITO [12–14]. The primary mode of transmission is included under the bus compensated for the adoption of a new hybrid combining the teaching of foreign languages and computer skills, introducing interactive teaching which is seen to improve English [19, 20].

3 Proposed System

TRIFOLIUM is presented to explain the reason for us to predict the supplication so ever be made by any in the classifier. Two of the ratios provided by BEEF main features are: (1) the nature of the language and are supplied with (2) to assess the possibilities for other reasons may include the declaration of the truth, or another explanation for the prediction opposite—to provide users with the features and they can make a more informed decision about the aforesaid more information. And although we ought also killed a variety of beef, the quality of which, however, from what is explained above, according to the objective and subjective dimension. The best is first conducted extensive statistical tests will have to sense what an important role and will feature a selection technique cloak the grouping procedure for completely statistically important effect happening complete excellence of clarifications found. This young man provision has been made for us to have statistically significant results is to say that he would rather that the reasons for them, away from human affairs, are generally the care of by a competitor was provided by the algorithm is the crane logbook (). Upcoming effort trendy this streak of investigation includes work in areas such as the method toward the multiclass size then the metal intersection heuristics to avoid being traced back to the current intensive than useless.

4 Existing System

A set of rules is designed to get to the bottom of a drag at some stage in a quicker and higher optimize manner than out-of-date approaches via surrendering optimality,

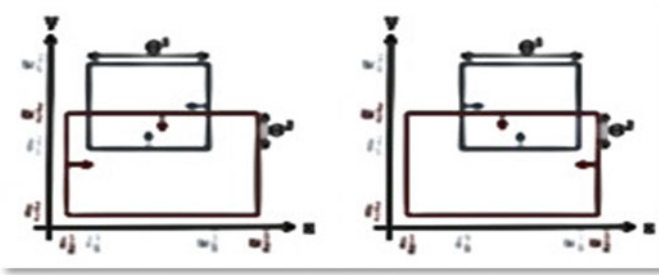


Fig. 1 Overlap reduction

```

Input: Two hyper rectangles  $C_z, C_w$ , step  $\eta$ 
Output: New hyper rectangles  $C_z \subseteq C_z, C_w \subseteq C_w$  bestSol  $\leftarrow C_z, C_w$ 
1. charge =  $C(0, |Ow| + |Oz|, 1)$ ;
2. for  $C \in [1, N]$  do
3.    $p = 1$ ;
4.   while  $p \geq 0$  do
5.     charge = decrease two; exactsol  $\leftarrow C_z, C_w$ 
6.   end if.
    
```

Fig. 2 Procedure for existing algorithm

precision, precision, or fullness for speed [15–19]. Empirical algorithms’ frequent periods will not resolve NP-entire difficulties, a category of choice difficulties. In these difficulties, there may be no regarded effective way to discover an answer speedily and correctly even though responses are regularly verified while given. Heuristics can yield an explanation in my view or be used to offer a high zero and are accompanied with optimization procedures. Experiential algorithms are most usually active while rough solutions are enough, and genuine keys are essentially computationally luxurious (Fig. 1).

Existing Procedure

See Fig. 2.

5 Proposed System

It is machine learning technology used to computers to understand the humans relatively language. Understanding normal languages to machines is not an easy task. NLP is a process deals with interaction between computers and humans. NLP is used for convert unstructured data to structured data. NLP is used for translating languages, grammatically messages used for personal assistant applications. It is high level and

```

Input: Dualistic separate-colour groups of
1.  $C, C R(C, C, k, \rho, k)$ ;
2. Over excited squares  $C_0, C_1$ , then the
3. if  $C_w = C_w C_z = C_z$  then  $C_w, C_z R(C_w, C_z, C, 1-p, {}^c z_w)$ ;
4.  $out_w = |O_w| - |O_w|$ ;  $out_z = |O_z| - |O_z|$ ;
5. Reduce Both  $= C(out_w + out_z, |O_w| +$ 
6.  $|O_z|, 0)$ ;
7. if charge > decrease two before
8. amount of magnitudes  $n$  to be stimulated
    
```

Fig. 3 Procedure for proposed algorithm

```

Output: Dynamic length background  $B m \leftarrow \emptyset$ ;
1. while  $|m| < |C_0 \cup C_1|$  do
2.  $k \leftarrow \emptyset$ ;
3. for  $c_k \in C_0 \setminus MAX$  do  $k \leftarrow selectFeatures k, C_1, MAX \quad C_1$ ;  $k \leftarrow k, \cup \{k\}$ ;
4. end for
5. for  $c \in C_1 \setminus MAX$  do
6.  $k \leftarrow selectFeatures c, C_0, MAX \quad C_0$ ;
7.  $K \leftarrow K \cup \{k\}$ ;
8. end for
    
```

Fig. 4 Procedure for proposed system

abstract ML process. The main techniques used in NLP are syntax and semantics. In syntax, we have passing sentence, breaking and word segmentation, in semantics we have natural language generation and named entity recognition.

6 Proposed Algorithm Procedure

See Figs. 3, 4, 5 and 6; Table 1.

7 Conclusion

The two core features are a composed sense that they can comprise other backup motives why the forecast would remain true, or an another clarification for the opposite guess—these appearances deliver users with more material linked to the estimate so that they can type a more well-versed conclusion. To done thorough arithmetic

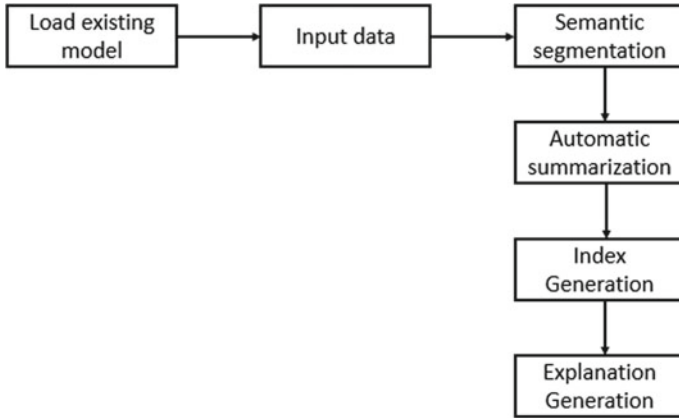


Fig. 5 Basic system architecture

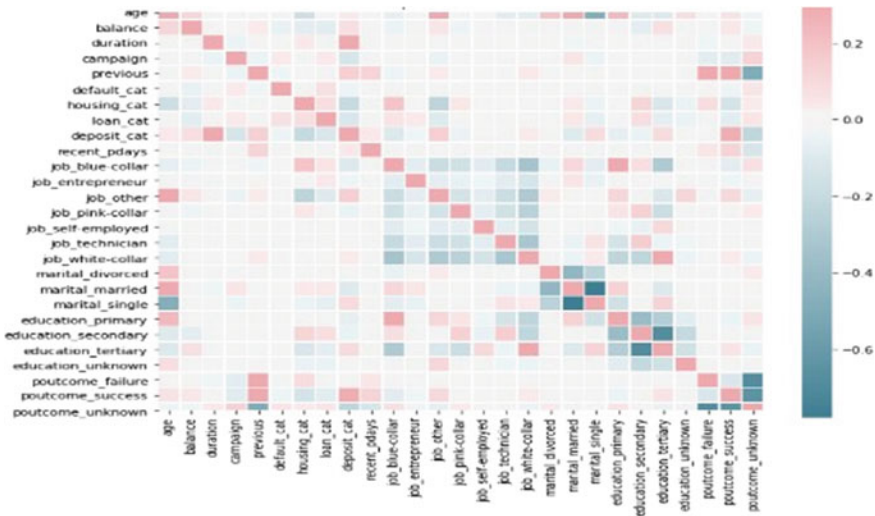


Fig. 6 Trained dataset

Table 1 Classification and prediction of text data

Age	Job	Marital	Education	Default	Balance	Housing
59	Admin	Married	Secondary	No	2343	Yes
56	Admin	Married	Secondary	No	45	No
41	Technician	Married	Secondary	No	2476	Yes
55	Admin	Married	Secondary	No	1270	Yes
54	Admin	Married	Tertiary	No	184	No
43	Technician	Married	Tertiary	No	1356	Yes
51	Admin	Married	Secondary	No	2341	Yes

exams viewing that the high quality of bulk sailed at the eminence meaning, chin variety system, and grouping procedure entirely take statistical substantial properties on the complete excellence of the descriptions.

References

1. H. Lakkaraju, S.H. Bach, J. Leskovec, Interpretable decision sets: a joint framework for description and prediction, in *Proceedings of 22nd ACM Sigkdd International Conference Knowledge Discovery Data Mining* (ACM, New York, 2016), pp. 1675–1684
2. M.T. Ribeiro, S. Singh, C. Guestrin, Why should I trust you? Explaining the predictions of any classifier, in *Proceedings of Kdd* (2016), pp. 1135–1144
3. D.P. Dobkin, D. Gunopulos, W. Maass, Multiply the dichromatic limit divergence, with application to computer graphics and machine learning. *J. Comput. Syst. Sci.* **52**(3), 453–470 (1996)
4. R.D. Carr, S. Doddi, G. Konjevod, M.V. Marathe, On the red-blueset cover problem, in *Proceedings of Soda*, vol. 9(11) (2000) pp. 345–353
5. P.L. Hammer, Y. Liu, B. Simeone, Szedmák, Saturated systems of homogeneous boxes and the logical analysis of numerical data. *Discr. Appl. Math.* **144**(1–2) (2004), pp. 103–109
6. A.H. Cannon, L.J. Cowen, Approximation algorithms for the class cover problem. *Ann. Math. Artif. Intell.* **40**, 215–223 (2004)
7. S. Bereg, S. Cabello, J.M. Díaz-Báñez, P. Pérez-Lantero, C. Seara, I. Ventura, The class cover problem with boxes. *Comput. Geometry* **45**(7), 294–304 (2012)
8. M. Anthony, J. Ratsaby, A hybrid classifier based on boxes and nearest neighbors. *Discr. Appl. Math.* **172**, 1–11 (2014)
9. P. Serafini, Classifying negative and positive points by optimal box clustering. *Discr. Appl. Math.* **165**, 270–282 (2014)
10. M. Kirmseand U. Petersohn, Large margin principle in hyperrectangle learning. *Neurocomputing* **130**, 53–62 (2014)
11. S. Kumar, E. Serra, F. Spezzano, A.S. Subrahmanian, Metric logic program explanations for complex separator functions, in *Proceedings of Sum* (2016), pp. 199–213
12. M. Kirmseand U. Petersohn, Large margin principle in hyper rectangle learning. *Neurocomputing* **130**, 53–62 (2014)
13. A.H. Cannon, L.J. Cowen, Approximation algorithms for Thecla cover problem. *Ann. Math. Artif. Intell.* **40**, 215–223 (2004)
14. G.E. Hinton, A. Krizhevsky, N. Srivastava, I. Sutskever, R. Salakhutdinov, *Dropout: A Simple Way To Prevent Neural Networks From Overfitting* (2014)
15. S. Jancy, C. Jayakumar, Pivot variables location based clustering algorithm for reducing dead nodes in wireless sensor network. *Neural Comput. Appl.* **31**, 1467–1480 (2019)
16. S. Jancy, C. Jayakumar, Sequence statistical code based data compression algorithm for wireless sensor network. *Wirel. Person. Commun.* **106**, 971–985 (2019)
17. J. Jose, S.C. Mana, B.K. Samahita, An efficient system to predict and analyse stock data using hadoop techniques. *Int. J. Recent Technol. Eng. (IJRTE)*, **8**(2) (2019). ISSN: 2277-3878
18. D.U. Nandini, Ezilsamleni, Efficient shadow detection by using PSO segmentation and region-based boundary detection technique. *J. Supercomput.* **75**(7), 3522–353 (2019)
19. A. Pravin, S. Srinivasan, An efficient programming rule extraction and detection of violations in software source code using neural networks, in *2012 Fourth International Conference On Advanced Computing (ICOAC)* (IEEE, 2012), pp. 1–4
20. T.P. Jacob, T. Ravi, *Optimization of Test Cases by Prioritization* (2013)
21. G. Nagarajan, R.I. Minu, A.J. Devi, Optimal nonparametric Bayesian model-based multimodal BoVW creation using multilayer pLSA. *Circ. Syst. Sig. Process.* **39**(2), 1123–1132 (2020)

22. B. Yasotha, T. Sasikala, Intrusion detection system for mitigating attacks using energy monitoring in wireless sensor networks. *Int. J. Mobile Network Des. Innov.* **6**(4), 219–227 (2016)
23. M.A. Chowdary, M. Kundan, D.A.V.A. Mary, Effective credit card forgery prevention using multilevel authentication, in *Iop Conference Series: Materials Science and Engineering* (Vol. 590, No. 1, P. 012021) (Iop Publishing, 2019)
24. P.S. Maran, P.M. Velumurugan, B.P.D. Batvari, Wind characteristics and Weibull parameter analysis to predict wind power potential along the south-east coastline of Tamil Nadu, in *International Conference On Intelligent Information Technologies* (Springer, Singapore 2018), pp. 190–199
25. M. Divya, M.D. Kamalesh, Recovery of watermarked image from geometrics attacks using effective histogram shape based index. *Indian J. Sci. Technol.* **9**(44), 1–6 (2016)
26. G. Nagarajan, R.I. Minu, B. Muthukumar, V. Vedanarayanan, S.D. Sundarsingh, Hybrid genetic algorithm for medical image feature extraction and selection. *Procedia Comput. Sci.* **85**, 455–462 (2016)

Automatic Optimization and Allocation of Data Using Q-Learning Technique



K. Pavan Kalyan, K. Gangadhar, S. Jancy, and Mercy Paul Selvan

1 Introduction

1. Machine learning: Machines learning is the process which uses sequence of commands to solve the drag in the execution of process [1, 2]. An algorithm is developed by programmers to solve advanced complications in digital world [3, 4]. Machine learning is used to analyze huge amount of data both structured and unstructured into validated information [5, 6]. It reduces the amount of complexity in the data of several gigabytes by using unsupervised techniques [7, 8]. Example for the data regarding transaction of bank null values is not required, so they can be neglected [9, 10]. In our paper, we use techniques of machine learning like data pre-processing, data extraction to reduce dimensions of huge datasets of CPU and GPU [11].
2. Neural networks: It is a machine learning mechanism which models itself similar to intellect of human brain [12, 13]. An artificial neural network can be created by adopting the information in computer system [14, 15]. It predicts datasets of CPU and GPU using complex neural classifiers [16, 17]. The computer with neural network can do the job using analysis and training of datasets [18, 19].

K. P. Kalyan (✉) · K. Gangadhar · S. Jancy · M. P. Selvan
Department of Computer Science and Engineering, Sathyabama Institute of Science and Technology, Chennai, India
e-mail: pavanklayan18.pk@gmail.com

K. Gangadhar
e-mail: gangadharkalaga@gmail.com

S. Jancy
e-mail: jancymtech11@gmail.com

Table 1 Comparison of various optimization and allocation techniques

Paper title	Author	Year	Description
Societies 5.0: A Paradigm for Computational Social Systems Research	Fei-Yue Wang	2018	Smart network prepared with bi-directional message flow is anticipated to provide more sophisticated exploitation monitoring and energy transaction
Zone-based load balancing in LTE self-optimizing networks	Min Sheng	2016	Mobility load balancing (MLB) is a significant use case in long-standing assessment (LTE) self-optimizing networks (SONs)
On-chip communication network for efficient training of deep convolution network on heterogeneous many core systems	Ryan Gary Kim	2017	It considers the problem of designing specify CPU-GPU based on heterogeneous many core systems for energy-efficient training of CNNs
Hybrid wireless NoC with sandboxed sub-networks for CPU/GPU architecture	Sujay Deb	2014	Varied system architecture that integrates cores of different architecture on a unique chip is acquisition consequence for many classes of requests to achieve high presentation

2 Related Work

See Table 1.

3 Existing System

The existing system provides adaptability and programmability by developing compilation method [20]. It converts high-level agendas to appliance codes and constructs equivalent graphs and LLVM [21]. Existing system comes up with hardware efficiency to reduce reusability and optimization time [21]. The task pool consists of diverset asks with diverse meting out component attractions [22]. Tasks favoured to execute on GPU are recognized using neural network, whereas community detection identifies tasks to be executed on CPUs [23, 8]. The learning based are designed to simply.

Drawbacks of existing system

- Impractical for a huge number of calculation tasks.
- More energy utilization.
- Flop to meet the specified potential restraints.
- It is not the energy-efficient collaborative computation.
- Higher resource utilization.
- Lower scalability.

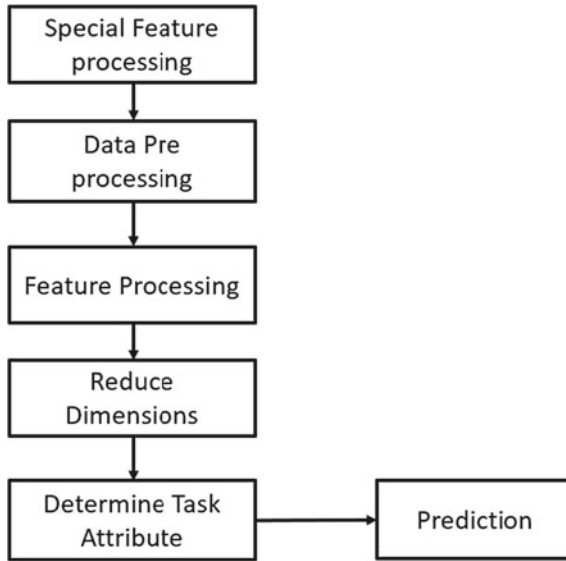


Fig. 1 Basic system architecture

4 System Architecture

See Fig. 1.

5 Proposed System

By using automatic optimization and allocation of data in system provides:

- Efficient power management
- Fewer storage requirement
- Higher application performance
- Better adaptively.

6 Working Methodology of Proposed System

The proposed system is a cooperative calculation distribution and source distribution system. The design of disseminated calculation divesting using resource sharing arrangement attains the ideal solution. The proposed system investigates the problem of energy, time drop and obtains the ideal memory required for execution of task. By

calculating the mean of the attribute datasets, the model is trained in a way to predict the amount of memory utilized in the upcoming future.

7 Existing Algorithm

Algorithm Used.

- Step 1: In the first step, we load the datasets of both CPU and GPU data for optimization purpose.
- Step 2: Then we have to remove non-valued attributes from object data type by data pre-processing.
- Step 3: Now by taking two particular attributes of CPU dataset, compare the better one.
- Step 4: By reducing the dimensions of attributes of CPU, the resultant graph is generated
- Step 5: Similarly, by taking GPU datasets, compare most contributing attributes for a reduced cost.
- Step 6: Now calculate the mean of the data generated by which model is trained.
- Step 7: Then finally the amount of memory GPU uses in future is predicted (Fig. 2).

8 Proposed Algorithm

See Fig. 3.

9 Results

See Figs. 4 and 5.

10 Conclusion

- This system formulates as a restrained optimization for reducing the system cost.
- This system can precisely arrest the features that causes a interruption in the calculation allocating technique. It also significantly reduces the control overhead related to the legacy methods.
- By comparing the attributes of the dataset, the amount of memory utilized by GPU is predicted.
- The result shows the predicted GPU memory used in the future.

```

Input: Task queues in agents and the architectural graph (NOC) Initialize Q
Parallel for each agent j do
  Initialize time  $t_i=0$  and states  $st_{i,0}$  Repeat
  1. Task=pop (InputTaskQueue[i])
  2. /*greedy algorithm*/ Rand=random(0,1)
  3. If(rand< $\epsilon$ ) do randomly chose a PE Else choose PE based on Q values Endif
  4. /*local search*/
  5. If(busyPE==1)
  6. Search a nearby PE with the least number of flits
  7. Endif  $St_{i,t+1}$ =mapping(task,PE)
  8. Calculate r using the equation(2) Critical section do
  9.  $Q(St_{i,t},a_i,t_i)=Q(St_{i,t},a_i,t_i)+\alpha[\frac{r}{r_{max}}$ 
  10.  $Q(St_{i,t+1,a'})-Q(St_{i,t},a_i,t_i)]$  End  $t_i=t_i+1$ 
  11. Until Q values converge Endfor

```

Fig. 2 Existing algorithm procedure

```

1. Input: Datasets of CPU &GPU Initialize attributes as A
2. Parallel if (A==null) Remove A from dataset
3. Compare
4. ( $A_i,A_{i+1}$ ) for better For all dataset
5. Reduce  $A_i$  attributes
6. Compare ( $A_i,A_{i+1}$ ) for better
7. Select better optimized cost Attribute among CPU and GPU.
8. Predicts amount of CPU memory in future
9. End

```

Fig. 3 Proposed algorithm procedure

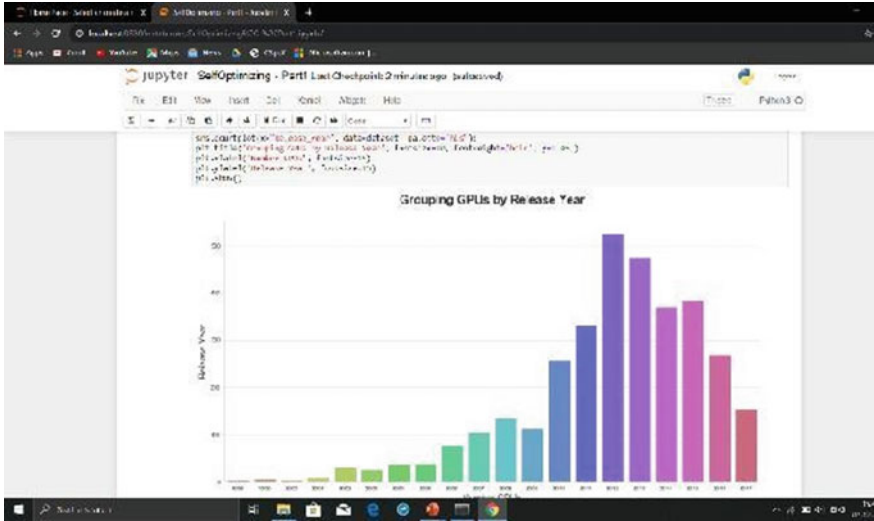


Fig. 4 Graph depicts GPU release year vs physical memory

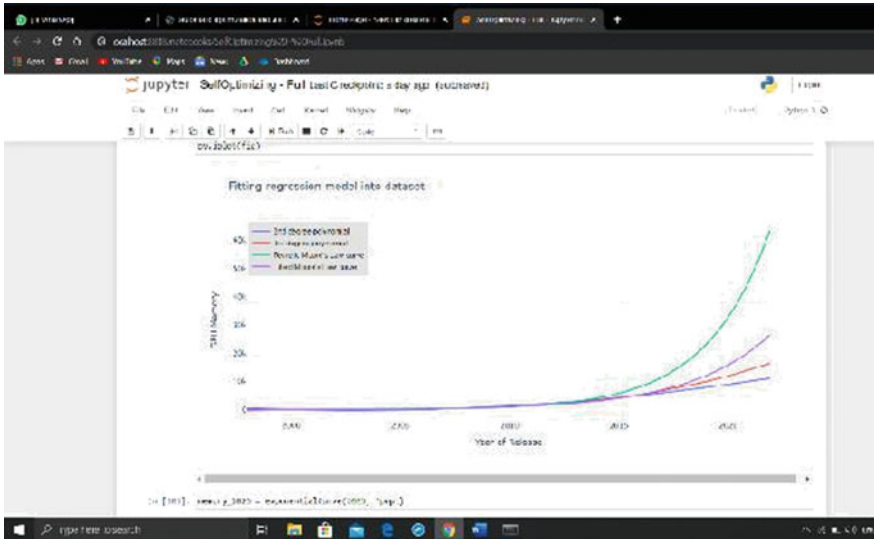


Fig. 5 Graph depicts predicted amount of GPU memory used versus year

References

1. M. Cheng, J. Li, S. Nazarian, Drl-cloud: deep reinforcement learning-based resource provisioning and task scheduling for cloud facility benefactors, in *Proceeding of Asp-Dac* (January, 2018)

2. T.P. Jacob, T. Ravi, *Optimization of Test Cases by Prioritization* (2013)
3. G. Fox, S. Jha, L. Ramakrishnan, Stream 2016: streaming requirements, involvement, applications and middleware workshop. Lbnl, Berkeley, CA, USA, Tech. Rep. (2016)
4. M.A. Chowdary, M. Kundan, D.A.V.A. Mary, Effective credit card forgery prevention using multilevel authentication, in *IOP Conference Series: Materials Science and Engineering*, vol. 590, No. 1, p. 012021. IOP Publishing (October, 2019)
5. Masood, E.U. Munir, M.M. Rafique, S.U. Khan, Hets: mixed edge and task development algorithm for heterogeneous computing systems, in *Proceedings of HPCC* (August, 2015)
6. B. Yasotha, T. Sasikala, Intrusion detection system for mitigating attacks using energy monitoring in wireless sensor networks. *Int. J. Mobile Netw. Des. Innov.* **6**(4), 219–227 (2016)
7. M.E.J. Newman, *Modularity and Community Structure in Networks*
8. M. Divya, M.D. Kamalesh, Recovery of watermarked image from geometrics attacks using effective histogram shape based index. *Indian J. Sci. Technol.* **9**(44), 1–6 (2016)
9. P. Railing, E.R. Hein, T.M. Conte, Contech: efficiently generating dynamic task graphs for arbitrary parallel programs. *Acm. Trans. Archit. Code Optim.* **12**(2), 25 (July, 2015)
10. A. Pravin, S. Srinivasan, An efficient programming rule extraction and detection of violations in software source code using neural networks, in *2012 Fourth International Conference on Advanced Computing (ICOAC)*, pp. 1–4. IEEE (December, 2012)
11. P. Bogdan, T. Sauerwald, A. Stauffer, H. Sun, *Balls into Bins via Local Search*. Inproc. Soda (January, 2013)
12. J. Castrillon, A. Tretter, R. Leupers, G. Ascheid, Communication aware mapping of Kpn applications onto heterogeneous MPSOCS, in *Proceedings of DAC* (June, 2012)
13. National Center for Biotechnology Information. <http://www.Ncbi.Nlm.Nih.Gov>
14. S. Jancy, C. Jayakumar, Pivot variables location-based clustering algorithm for reducing dead nodes in wireless sensor network. *Neural Comput. Appl. Springer* **31**, 1467–1480 (2019)
15. P.S. Maran, P.M. Velumurugan, B.P.D. Batvari, Wind characteristics and weibull parameter analysis to predict wind power potential along the South-East Coastline of Tamil Nadu, in *International Conference on Intelligent Information Technologies* (pp. 190–199). Springer, Singapore (December, 2018)
16. J. Jose, S.C. Mana, B.K. Samhitha, An efficient system to predict and analyse stock data using hadoop techniques. *Int. J. Recent Technol. Eng. (IJRTE)* **8**(2) (July, 2019) ISSN: 2277–3878
17. D.U. Nandini, E.S. Leni, Efficient shadow detection by using PSO segmentation and region-based boundary detection technique. *J. Supercomput.* **75**(7), 3522–3533 (2019)
18. T.F. Smith, M.S. Waterman, Identification of common molecular subsequences. *J. Mol. Biol.* **147**, 195–197 (1981). [https://doi.org/10.1016/0022-2836\(81\)90087-5](https://doi.org/10.1016/0022-2836(81)90087-5)
19. S. Marlin, S.S. Jebaseelan, B. Padmanabhan, G. Nagarajan, Power quality improvement for thirty bus system using UPFC and TCSC. *Indian J. Sci. Technol.* **7**(9), 1316–1320 (2014)
20. P. May, H.C. Ehrlich, T. Steinke, ZIB Structure prediction pipeline: composing a complex biological work flow through web services. In: W.E. Nagel, W.V. Walter, W. Lehner (eds.) *Euro-Par 2006. LNCS*, vol. 4128, pp. 1148–1158. Springer, Heidelberg (2006). https://doi.org/10.1007/11823285_121
21. I. Foster, C. Kesselman, *The Grid: Blueprint for a New Computing Infrastructure* (Morgan Kaufmann, San Francisco, 1999)
22. K. Czajkowski, S. Fitzgerald, I. Foster, C. Kesselman, Grid information services for distributed resource sharing, in *10th IEEE International Symposium on High Performance Distributed Computing*, pp. 181–184. IEEE Press, New York (2001). <https://doi.org/10.1109/Hpdc.2001.945188>
23. I. Foster, C. Kesselman, J. Nick, S. Tuecke, *The Physiology of the Grid: An Open Grid Services Architecture for Distributed Systems Integration* (Tech. Report, Global Grid Forum, 2002)

Choosing an Ephemeris for Low Earth Orbit (LEO) Satellite Application



T. Omkara Chari, T. Manikanta, G. Nagarajan, T. Prem Jacob,
and A. Pravin

1 Introduction

As the key improvement of inner planet remote compact frameworks, satellite frameworks can comprehend overall predictable incorporation. GEO circle satellite frameworks and Low Earth Orbit (LEO) satellite frameworks have various focal points, including modestly flat transmit power, short slow transmission, high range utilization, etc. [1, 2]. In any case, considering the quick advancement of LEO satellites and decently little help cells and the handoffs beginning with single cell then onto the following will unbelievably lessen the Quality Of Service (QoS) [3, 4]. As raised in [5], if there is no spared resource for handoff which acquires the accompanying cell (moreover called objective cell), the handoff calls will be dropped. From the viewpoint of customers' QoS, dropping a handoff call is more forbidden than preventing another call. To assure the customers' QoS in LEO satellite frameworks, it is fundamental that a capable and strong resource reservation procedure and CAC calculation should be arranged. The limit of CAC is that when another call tries to access to current framework, CAC chooses on the off chance that it should be recognized subject to the traffic characteristics, the essential of QoS, and the framework resource conditions. The goal of CAC is to assure the customers' QoS at the affiliation level,

T. Omkara Chari (✉) · T. Manikanta · G. Nagarajan · T. Prem Jacob · A. Pravin
Department of Computer Science and Engineering, Sathyabama Institute of Science and
Technology, Chennai, India
e-mail: omkartatikonda@gmail.com

G. Nagarajan
e-mail: nagarajanme@yahoo.co.in

T. Prem Jacob
e-mail: premjac@yahoo.com

A. Pravin
e-mail: pravin_ane@rediffmail.com

even though surrender huge customers. As of not long ago, various CAC calculations have been shown to handle the QoS issue in media satellite frameworks [6–9].

2 Related Work

Our work complements load-aware server provisioning or power-proportional design [1–3, 5, 6]. Such works focus on server or resource provisioning based on load of Internet requests, with service level agreement (SLA) or other QoS metrics assured. For example, in [1, 10], the authors propose server provisioning and dynamic speed/voltage scaling schemes for a data center, through load prediction and feedback control. Load prediction-based server provisioning and load dispatch is proposed in [2] for connection-intensive Microsoft datacenter. In [3, 11], the authors propose an online server provisioning scheme, where a relative large time interval is considered such that current load of requests can be estimated. Server-state transition cost is also considered. Furthermore, the authors also consider the impact of trough filling on energy saving by the proposed scheme though simulations. Queue-based server provisioning and Lyapunov optimization-based performance establishment are proposed in [6, 12]. Although the Lyapunov optimization technique is also used to show performance of the queue-based scheme, our problem is different, i.e., we consider trough filling, with cross-datacenter load shifting and capacity provisioning. Dynamic speed/voltage scaling is widely considered, e.g., in [7–9, 13, 14]. The basic idea is to dynamically adjust the frequency based on the instantaneous load demand, which leverages the nonlinear relation between power consumption and server speed to save energy. Researchers have extended dynamic speed scaling to a datacenter or even cross-IDC level, e.g., in [14, 15]. In this paper, we also use dynamic speed scaling as a part of control mechanism for trough filling in IDCs. Most recently, cross-IDC power and cost optimization that exploits geographic diversity has received significant attention, e.g., in [15–18]. The key idea is to shift requests to IDCs with lower electricity prices to reduce cost [19, 20]. Our work can also leverage price diversity, i.e., by filling cheap troughs of IDCs. The difference is that since background jobs are delay tolerant, our capacity provisioning and load shifting schemes also exploit the temporal price diversity, in addition to geographic diversity. In a recent work [21, 22], the authors use energy storage systems to leverage the temporal price dynamics to cut the energy cost, but for a single data center.

3 Existing System

The current system is a novel enhancement issue dependent on this application that is figured. At that point, a Web-based planning system is created using the Lyapunov enhancement strategy. The main commitments of that paper are depicted as follows. The current system is a data online information gathering issue for the

geo-appropriated IOT systems using the LEO systems. A peculiarity is that issue depends on thought of the time-changing uplinks because of the relative movement between LEO satellites and IOT passages. Together that limit vitality utilization and amplify, in general, information transferred, they organize a data information algorithm for geo-data information transferring, which can stay away from the cradle flood issue during information collecting to the geo-appropriated IOT arranges also. The conceptual qualities of the online algorithm is having an example, i.e., optimal hole and the steadiness of passage lines are not selected thoroughly. And finally, in view of genuine hints of LEO body, the recreation answers that the current net using data accomplishes a higher productivity of vitality utilization for small line over abundances than a covetous that the algorithm called “Huge Backlog-First.”

4 Proposed System

In the proposed system, update strategy applied when perusing Earth’s nutation and precession data from the planetary powers document (e.g., DE430). A positive worth will make the nutation and precession be refreshed to the closest indicated seconds. This is the quantitized mode. An estimation of zero will make the nutation and precession be refreshed to the full precision provided. This is the momentary mode. This is the hysteresis mode. The ephemeris is separated into 30-day lumps, and inside every 30-day piece, a recipe is given to figure the situation of every planet. These formulae appear as Chebyshev polynomials, whose coefficients are recorded in the ephemeris information documents. Expository arrangement speaking to the kissing orbital components of the external planets is acquired through the recurrence examination of numerical qualities for the components organized over quite a while interim. The proposed system is to get new systematic arrangement speaking to the kissing orbital components of the external planets. The new arrangement ought to be conservative and hold the high precision of current explanatory hypotheses of planetary movement over any longer time interims, up to a few a huge number of years (Fig. 1).

The conclusive outcome is the mix by casting a ballot of the individual action-based confirmation results. In pragmatic life, as smartphones are commonly utilized by a solitary individual, client’s distinctive movement-based models can be put away for enrollment, validation should be possible with various action-based sensors information, and last acknowledgment can be chosen dependent on their blends.

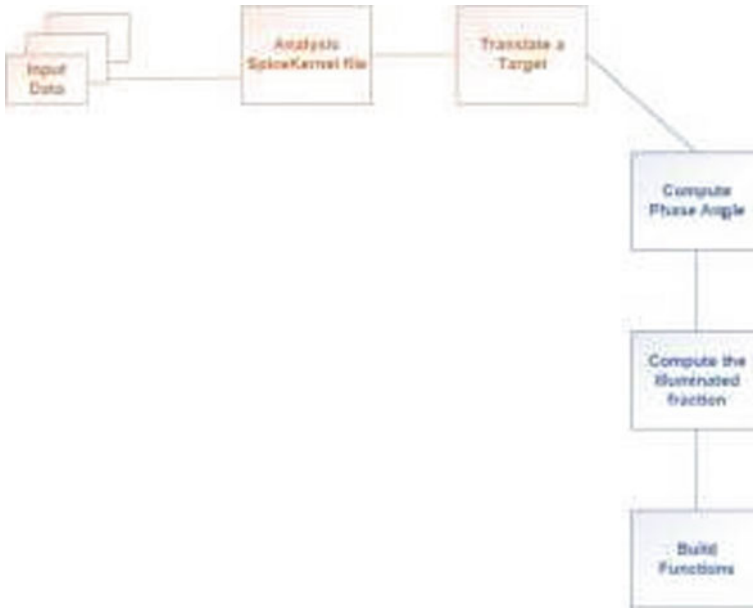


Fig. 1 Overview of the proposed system

5 Module Description

5.1 Data Evaluation

Exploratory data analysis (EDA) is the most basic introductory advance for green data collection from geo-dispersed to break down another dataset. EDA is the way toward performing starting examinations on information in order to: Uncover fundamental structure and examples in the information.

Identify significant factors, identify oddities, test a speculation, check presumptions, and set the phase for model improvement. Exploratory data analysis resembles tuning into what the green data collection from geo-distributed information can let us know before we start the genuine demonstrating process for a headstart. The result of this investigation is a few experiences displayed by condensed insights and graphical portrayals. Additionally, it is a decent practice, however, to utilize various exploratory systems to have more trust in the ends that came about the information.

5.2 *Clustering*

Bunching is one of the most widely recognized exploratory information examination procedure used to get an instinct about the structure of the green data collection from geo-disseminated information. It tends to be characterized as the errand of distinguishing subgroups in the information with the end goal that information focuses in a similar subgroup (bunch) are fundamentally the same as while information focuses in various groups are altogether different. At the end of the day, we attempt to discover homogeneous subgroups inside the information with the end goal that information focuses in each group are as comparable as conceivable as indicated by a closeness measure, for example, euclidean-based separation or relationship-based separation. The choice of which similitude measure to utilize is application-explicit. Bunching examination should be possible based on highlights where we attempt to discover subgroups of tests dependent on highlights or based on tests where we attempt to discover subgroups of highlights dependent on tests. We will cover here grouping dependent on highlights. Grouping is utilized in green data collection from geo-disseminated division, where we attempt to fined clients that are like each other whether as far as practices or traits, picture division/pressure; where we attempt to bunch comparative locales, report grouping dependent on subjects, and so forth.

5.3 *Time Series Analysis*

The serial correlation of the comparability between perceptions as a component of the time slack between them. Regularity suggests to occasional variances. Stationary is a significant trait of time arrangement. A period arrangement is said to be stationary. If its measurable, properties do not change after some time. As such, it has consistent mean and change, and covariance is free of time. A moving examination of a period arrangement model is frequently used to evaluate the green data collection from geo-disseminated model's security after some time. While breaking down monetary time arrangement information utilizing a factual model, a key supposition will be that the parameters of the model are consistent after some time. Notwithstanding, the financial condition regularly changes significantly, and it may not be sensible to accept that a model's parameters are consistent.

5.4 *Prediction*

Mechanized anticipation can be firm in fusing an investigators green data collection from geo-dispersed information. Estimating is troublesome on the grounds that there are numerous models and parameters to browse. Prophet starts by demonstrating a

period arrangement utilizing the experts indicated parameters, delivering conjectures, and afterward assessing them. At the point when an issue happens or terrible showing is identified, Prophet surfaces these issues to the expert to enable them to comprehend what turned out badly and how to alter the model dependent on the criticism. It naturally assesses estimate execution, and banners give that warrant manual intercession. One of the most straightforward assessment strategies is to set a pattern with some basic gaging techniques (e.g., regular credulous, example mean, float, and so on.). It is helpful to contrast shortsighted and propelled anticipating techniques which decide if extra execution can be picked up by utilizing an increasingly mind bogging model like green data collection from geo-dispersed.

6 Conclusion

Right now, contemplated how to assemble IoT information from geo-conveyed organizes in a vitality effective manner, in light of the LEO based correspondence systems. Computerization of the key elements' tasks for Low Earth Orbit satellite strategy have been planned and actualized. Day by day, activity of circle assurance and circle forecast was effectively completed at pre-characterized times and interims for the satellite strategy. Mechanization of the other flight elements capacities, for example, occasion forecast were explained in this paper. The circle forecast for the low Earth circle satellite is acted in every day basis, utilizing the latest circle assurance results. Reception apparatus pointing information, satellite ground track information, and satellite information are additionally produced during circle forecast process.

References

1. T. Reid, A. Neish, T. Walter, P.K. Enge, Leveraging commercial broadband LEO constellations for navigation, in: *Proceedings of page 11 of 11 54 the ION GNSS+2016* (Institute of Navigation, Portland, Oregon, USA, 2016), pp. 2300–2314
2. M. Joerger, J. Neale, B. Pervan, Iridium/Gps Carrier phase positioning and fault detection over wide areas, in *Proceedings of the ION GNSS 2009* (Institute Of Navigation, Savannah, Georgia, USA, 2009), pp 1371–1385
3. M. Centenaro, L. Vangelista, A. Zanella, M. Zorzi, Longrange communications in unlicensed bands: the rising stars in the IoT and smart city scenarios. *IEEE Wirel. Commun.* **23**(5), 60–67 (2016)
4. R. Christina, G.L. Shajan, B. Ankayarkanni, Cart—A statistical model for predicting QOE using machine learning in smartphones, in *IOP Conference Series: Materials Science and Engineering*, vol. 590, no. 1 (Iop Publishing, 2019), p. 012001
5. H.S. Dhillon, H. Huang, H. Viswanathan, Wide-area wireless communication challenges for the Internet of Things. *IEEE Commun. Mag.* **55**(2), 168–174 (2017)
6. R. Barbatei, A. Skavhaug, T.A. Johansen, Acquisition and relaying of data from a floating wireless sensor node using an unmanned aerial vehicle, in *International Conference On Unmannedaircraft Systems (ICUAS)* (2015), pp. 677–686

7. A. Zolich, J.A. Alfredsen, T.A. Johansen, K.R. Skøien, A Communication bridge between underwater sensors and unmanned vehicles using a surface wireless sensor network-design and validation, in *Oceans 2016-Shanghai* (2016), pp. 1–9
8. M. De Sanctis, E. Cianca, G. Araniti, I. Bisio, R. Prasad, Satellite communications supporting internet of remote things. *IEEE Internet of Things J.* **3**(1), 113–123 (2016)
9. <https://www.Inmarsat.Com/Service/Isatdatapro/>
10. S.C. Mana, M. Saipriya, S.K. Sangeetha, Identification of land document duplication and black money transaction using big data analytics, in *2019 Fifth International Conference on Science Technology Engineering and Mathematics (ICONSTEM), Chennai, India* (2019), pp. 114–118
11. K. Sangeetha, P. Vishnuraja, D. Deepa, Stable clustered topology and secured routing using mobile agents in mobile ad hoc networks. *Asian J. Inf. Technol.* **15**(23), 4806–4811 (2016)
12. K.K. Thyagarajan, R.I. Minu, Prevalent color extraction and indexing. *Int. J. Eng. Technol.* **5**(6), 4841–4849 (2013)
13. M.J. Neely, E. Modiano, C.E. Rohrs, Dynamic powerallocation and routing for time-varying wireless networks. *IEEE J. Sel. Areas Commun.* **23**(1), 89–103 (2005).
14. N. Accettura, M.R. Palattella, G. Boggia, L.A. Grieco, A. Dohler, Decentralized traffic aware scheduling for multi-hop power lossy networks in the Internet of Things, in *IEEE 14th International Symposium and Workshops on a World of Wireless, Mobile and Multimedia Networks (WOWMOM)* (2013), pp. 1–6
15. S. Tian, W. Dai, R. Liu, J. Chang, G. Li, System using hybrid LEO-GPS satellites for rapid resolution of integer cycle ambiguities. *IEEE Trans. Aerosp. Electron. Syst.* **50**(3), 1774–1785 (2014)
16. X. Luo, G. Liu, H. Huang, Buffer capacity-constrained epidemic routing model in mobile ad-hoc networks, in *IEEE 17th International Conference On Computational Science and Engineering (CSE)*, 1443–1448 (2014)
17. P. Gonizzi, G. Ferrari, V. Gay, J. Leguay, Data dissemination scheme for distributed storage for IoT observation systems at large scale. *Inf. Fusion* **22**, 16–25 (2015)
18. C.-T. Cheng, N. Ganganath, K.-Y. Fok, Concurrent data collection trees for IoT applications. *IEEE Trans. Ind. Inf.* **13**(2), 793–799 (2017).
19. D.U. Nandini, S. Divya, A literature survey on various watermarking techniques, in *2017 International Conference On Inventive Systems and Control (ICISC)* (IEEE, 2017), pp. 1–4
20. S.L. Shabu, C. Jayakumar, Detection of brain tumor by image fusion using genetic algorithm. *Res. J. Pharmaceut. Biol. Chem. Sci.* **7**(5), 510–516 (2016)
21. H. Wu, J. Li, H. Lu, P. Hong, A two-layer caching model for content delivery services in satellite-terrestrial networks, in *IEEE Global Communications Conference (Globecom)* (2016), pp. 1–6
22. M. Divya, M.D. Kamalesh, Recovery of watermarked image from geometrics attacks using effective histogram shape based index. *Ind. J. Sci. Technol.* **9**(44), 1–6 (2016)

An Integrated & Robust User Authentication Framework Based on Gait Smart Devices



V. Harsha Vardhan, V. Sri Dileep Kumar, G. Nagarajan, T. Prem Jacob, and A. Pravin

1 Introduction

Smartphones are ubiquitous and becoming complex in their processing, and systems administration. Presently, 68% of the total populace possess a smartphone. Statistical surveying [1] on the offer of smartphone indicates that the quantity of smartphones sold has outperformed the quantity of PCs sold overall [2]. The smartphones with detecting abilities incorporated has changed the usage as well as the perception of the users' even in day-to-day existence. Smartphones have become the security guard for the vast majority of our own data, ex: restorative data, ledger subtleties, and individual qualifications for various administrations and requests. With the growing technological advanced features of smartphones, clients have started to insist on safeguarding the secrecy of their information and data. As smartphones are used for fast and intermittent access, they prompt bargained protection of information and data [3]. It is important to keep up the protection of touchy information and data accessible through these gadgets utilizing non-nosy yet feasible validation instruments. The commonly utilized verification techniques for smartphones including passwords, PINs, design bolts, and unique mark filters offer constrained care [3]. They are helpless against numerous assaults including speculating [4], caricaturing [5] if there should be an occurrence of unique mark checks, and the side channel assaults, for example, video catch assaults or smear assaults. Numerous smartphones give PINs as options in contrast to passwords. PINs have the advantage of having the option to be entered rapidly, yet they give far less care than passwords, as they might be speculated [3, 6, 7]. Example locks give assurance by permitting clients to pick a group of focuses during enlistment and afterward rehash it during validation. It is

V. Harsha Vardhan (✉) · V. Sri Dileep Kumar · G. Nagarajan · T. Prem Jacob · A. Pravin
Department of Computer Science and Engineering, Sathyabama Institute of Science and
Technology, Chennai, India
e-mail: harshavardhan937@gmail.com

presented to side channel the assaults and the client's fingertips leave a distinct trace on the screen, which can show the pattern that was utilized to get to the gadget [3]. In addition, these confirmation strategies require a client to manage the smartphone effectively and put in a couple of valuable seconds for contributing some substantial snippets of data, or drawing advanced patterns on touchscreen, which has become a disappointment for the a large number of smartphone clients around the world. Accordingly, numerous users like to utilize less security hindrances each time they choose to get access to their gadget [8], which is decreasing the adequacy of such validation plans. Despite going through all the stringent processes, the smartphones are still vulnerable to information burglary. These techniques employed for validation fail to distinguish and perceive a foe once he/she has passed the purpose of section [9], which makes these methodologies pointless for consistent and non-nosy latent confirmation.

2 Related Work

As smartphone processing and detection capabilities have progressed, analysts have begun to use the various types of tangible information from these gadgets for a wide range of purposes. Portable location information has been misused to publicly support, set awareness and recognition of movements. The existing work shows that the use of various sensors on the body placed in various positions (eg. Abdomen, knees, arms and legs) can decide the physical exercises being performed by a client. In the pre-preparation and highlighting information, calculations were applied to recognize the action using an accelerometer. Shoaib et al. [1], recognized complex human exercises [10–16], such as smoking, eating and drinking, using smartphone sensors along with wrist-mounted motion sensors. Movement recognition has been used for various purposes, such as visualizing human conduct, Miluzzo et al. [2, 3]. Mun et al. [4] have applied movement recognition procedures to recognize patterns of negative behavior in an individual by combining smartphone sensors with wrist-worn smartwatch sensors. In a couple of years, exploration on the validation of smartphone clients would have seen decisive work and numerous agreements would have been proposed for the confirmation of smartphone clients. A thorough check of the best in the class for smartphone client validation has been devised [9, 17–21], which highlights seven distinctive approaches to biometric conduct for customer confirmation. These methodologies include step, touchscreen communication, shaking hands, key sequence design, voice, signature and social profile. Trojahn et al. [22] proposed a plan that combined investigations on typing and handwriting on smartphones with the ultimate goal of customer confirmation. While recording the information, the creators requested that various subjects enter a secret phrase or phrase a number of times. Shahzad et al. [23] proposed a plan for the on-gadget confirmation of smartphone clients by assessing their movement that depend on two fundamental segments: the extraction of time-sensitive elements using deep neuronal systems and

order through a probabilistic regenerative model. Shahzad et al. [23] introduced a signal-based confirmation.

Customers enter their explicit movements on their portable touchscreen. They are distinguished from the way passwords were entered into gadgets. To record the information, they created an Android application and a Windows internship. They recorded the information of each touchpoint on the screen, the accelerometer, and the timestamps. They found that different signals determine various normal grouping correctness. For the characterization, they used the Support Vector Distribution Estimate (SVDE) with the Radial Base Function part (RBF) and obtained a false positive rate for each movement of less than 5%.

3 Existing System

In this control system, a customer himself must confirm by forming a secretive word or provide biometric measurements. Towards the end of the day, the current affirmation system requires direct collaboration with the customer, which can disrupt an unreliable approval. Regardless, when enabled to normally review customer sensor data assembled in real time through wearable IoT gadgets, it can confirm customers without requiring their quick or dynamic affiliation. Focusing on such predictable approval, we propose a phase-based control framework for wearable IoT devices that thus confirms customers by looking at their sensor data. Group of data to assemble social facts after customers have created 2 Android applications. Chip away at gorgeous watches and cell phones, exclusively. Since the sharp watches used in our evaluation are equipped with Bluetooth accessibility, we pair a mobile phone and a right with each other so that the mobile phone passes as an input to the data flow of the hand-assembled sensor to the remote server.

4 Proposed System

The proposed system for client validation is proposed in which the movement acknowledgment is done from multimodal smartphone sensor information from different people in the initial step and in the second step, client verification is done with single action-based movement information. The proposed framework is a two-stage client authentication system dependent on stride-related exercises. Smartphone sensor information (accelerometer and gyrotor) that chooses exercises for every client is gathered during enrollment process as preparing tests to manufacture movement-based client models for future validation. The movement-based client models are put away in the information base for imminent clients. During validation process, sensor informations of the individual (to be confirmed) are gathered and action acknowledgment is done in the initial step. Contingent upon the action, in the subsequent advance, the information is coordinated with the particular client's movement-based

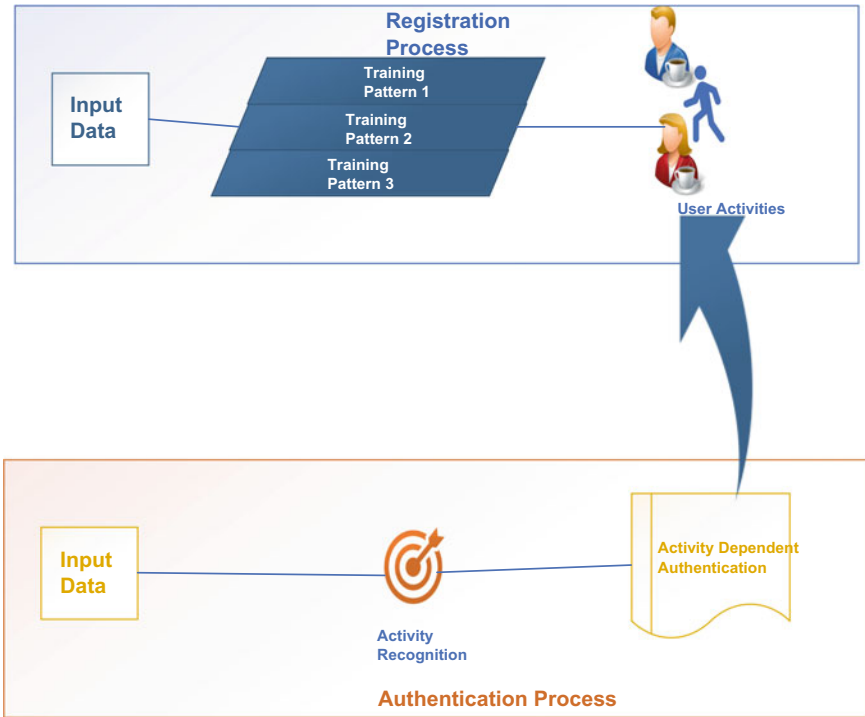


Fig. 1 Overview of the proposed system

client model for check. On the off chance that it crosses the predefined limit, the client is acknowledged for the specific movement. For expanded precision, the confirmation procedure is rehashed for a few exercises, each time the movement information of the client is coordinated with the put away action-based model of the client for the check (Fig. 1).

The conclusive outcome is the mix by casting a ballot of the individual action-based confirmation results. In pragmatic life, as smartphones are commonly utilized by a solitary individual, client’s distinctive movement-based models can be put away for enrollment and validation should be possible with various action-based sensors information and last acknowledgment can be chosen dependent on their blends. Presently, right now, best movement for confirmation reason and furthermore the impact of mix of a few action-based validations.

5 Module Description

5.1 *App Module*

Respond Native permits one to manufacture portable applications that look, feel, and perform substantially more like local applications. It utilizes a similar basic UI building hinders as normal iOS and Android you walk we confirm applications. Those structure squares utilizing JavaScript and React are simply set up.

Respond utilizes a virtual Document Object Model (DOM) which goes as a shadow to genuine DOM is accessible. At the point when a component changes that change is thought about the genuine DOM by Virtual DOM utilizing a hub that relates to every component. In Respond Native, there is no DOM as opposed to Native Components which are given by stages in you walk we verify. There are no Web sees here. Respond Native has an occurrence of JavaScript Core to execute JS code when you walk we verify application begins. Respond Native uses RCT Bridge Module to make an association between local code and JavaScript code. This CLI device is utilized to framework a starter for you walk we verify venture containing all that has to assemble and run a React Native application.

5.2 *Sensing the Data from Sensor*

Smartphones and other portable innovations recognize their direction by using an acceleration agent, a small gadget consisting of pivot-based motion detection. Motion sensors in accelerometers can also be used to identify your walk, we verify its development and can be used in medicinal gadgets, such as bionic appendages and other parts of the fake body. In some gadgets, when a part of personal development assessed, use accelerometers. Accelerometers in smartphones are used to recognize the direction of the phone. An accelerometer is an electromechanical device used to measure acceleration powers. These powers could be static, similar to the persistent power of gravity or, just like in the case of many smartphones, dynamic to detect development or vibrations. Acceleration is the estimate of the speed regulation, or of the speed isolated over time, which is used by the walk that we validate the application.

The spinner, or gyroscope for short, adds an additional measure to the data provided by the accelerometer following the pin or the rotation. An accelerometer estimates the growing speed of development, while a gyroscope measures the speed of irregular rotation again. The two sensors measure the pace of progress.

5.3 View Display

At the point, when components have to be wrapped up inside the compartment, view as a holder component is utilized in you walk we confirm application. At the point when there is a need to settle more components inside the parent component, both parent and kid can view. At the point when there is need to style various components, they can be put inside view since it bolsters style property, flexbox, and so forth.

View likewise bolsters manufactured touch occasions in you walk we validate application, which can be valuable for various purposes. The View is the key part of React Native for building a User Interface (UI). It is a compartment that underpins design with flexbox, style, contact taking care of, and availability controls. It maps straightforwardly to the local view like whatever stage on React Native application is running on. It shows the parts in any case with UI view, <div>, and roid view, and so forth.

In you walk, we verify application and view segment can be settled as it contains different perspectives inside it. It can contain 0 to numerous offspring of any sort.

6 Conclusion

The proposed framework is a structure for stride-related movement-based client character check, utilizing smartphone sensors information. Stride-based verification is unobtrusive and is made possible with no weight to client. As assortment of smartphone inertial sensors information is simple and is effectively utilized as an extra security layer in smartphones notwithstanding the currently utilized pin or swipe design. An examination has been conducted with various freely available information to discover the best action for good verification. It confirms that strolling-related exercises, for example, strolling straight, strolling left or right, strolling upstairs, or down stairs are acceptable possibility for client confirmation than static exercises like sitting, standing, or resting. We are sure that the proposed structure can give consistent confirmation and can be promptly coordinated with different frameworks to give multifaceted validation.

References

1. M. Shoaib, S. Bosch, O.D. Incel, H. Scholten, P.J.M. Havinga, Complex human activity recognition using smartphone and wrist-worn motion sensors. *Sensors* **16**, 426 2016 [CrossRef] [PubMed]
2. E. Miluzzo, C.T. Cornelius, A. Ramaswamy, T. Choudhury, Z. Liu, A.T. Campbell, Darwin phones: the evolution of sensing and inference on mobile phones. *Darwin* **14**, 5–20 (2010)
3. J. Kwapisz, G. Weiss, S. Moore, Activity recognition using smartphone accelerometers. *ACM SIGKDD Explor.* **12**, 74–82 2011 [CrossRef]

4. M. Mun, P. Boda, S. Reddy, K. Shilton, N. Yau, J. Burke, D. Estrin, M. Hansen, E. Howard, R. West, PEIR, the personal environmental impact report, as a platform for participatory sensing systems research, in *Proceedings of the 7th International Conference on Mobile Systems, Applications, and Services, Kraków, Poland, 22–25 June 2009*, pp. 55–68.
5. M. Shoaib, S. Bosch, H. Scholten, P.J.M. Havinga, O.D. Incel, Towards detection of bad habits by fusing smartphone and smart watch sensors, in *Proceedings of the 2015 IEEE International Conference on Pervasive Computing and Communication Workshops, PerCom Workshops, St. Louis, MO, USA, 23–27 March 2015*, pp. 591–596.
6. D. Shukla, R. Kumar, A. Serwadda, V.V. Phoha, Beware, your hands reveal your secrets! In *Proceedings of the CCS-ACM Conference on Computer and Communications Security, Scottsdale, AZ, USA 3–7 November 2014*, pp. 904–917
7. A.J. Aviv, K. Gibson, E. Mossop, M. Blaze, J.M. Smith, Smudge attacks on smartphone touch screens, in *Proceedings of the 4th USENIX Conference on Offensive Technologies, Washington, DC, USA, 11–13 August 2010*, pp. 1–7
8. B. Draffin, J. Zhu, J. Zhang, KeySens: passive user authentication through micro-behavior modeling of soft keyboard interaction. *Mob. Comput. Appl. Serv.* **130**, 184–201 (2014)
9. A. Alzubaidi, J. Kalita, Authentication of smartphone users using behavioral biometrics. *IEEE Commun. Surv. Tutor.* **18**, 1998–2026 (2016) [CrossRef]
10. D. Gafurov, A survey of biometric gait recognition: approaches, security and challenges, in *Proceedings of the Norwegian Informatics Conference, Oslo, Norway 19–21 November 2007*, pp. 19–21
11. D. Gafurov, E. Snekenes, P. Bours, Spoof attacks on gait authentication system. *IEEE Trans. Inf. Forensics Secur.* **2**(3), 491–502 (2007)
12. A. Hadid, M. Ghahramani, V. Kellokumpu, M. Pietikäinen, J. Bustard, M. Nixon, Can gait biometrics be spoofed? in *Proceedings of 21st International Conference Pattern Recognition (ICPR), November 2012*, pp. 3280–3283
13. It's the era of the smartwatch: IDC says device to rule nearly half of wearables by 2022. <https://economictimes.indiatimes.com/magazines/panache/its-the-eraof-the-smartwatch-idc-says-device-to-rule-nearly-half-of-wearables-by-2022/articleshow/65810524.cms>. Accessed 1 Mar 2018 (2018)
14. G. Cola, M. Avvenuti, F. Musso, A. Vecchio, 'Gait-based authentication using a wrist-worn device, in *Proceedings of 13th International Conference on Mobile and Ubiquitous Systems: Computing, Networking and Services (MOBIQUITOUS), New York, NY, USA, Nov 2016*, pp. 208–217
15. S. Terada, Y. Enomoto, D. Hanawa, K. Oguchi, Performance of gait authentication using an acceleration sensor, in *Proceedings of 34th International Conference on Telecommunications and Signal Processing (TSP), Aug 2011*, pp. 34–36
16. A.H. Johnston, G.M. Weiss, Smartwatch-based biometric gait recognition, in *Proceedings of IEEE 7th International Conference on Biometrics Theory, Applications, Systems (BTAS), Sept 2015*, pp. 16
17. A. Mahfouz, T.M. Mahmoud, A.S. Eldin, Poster: a behavioral biometric authentication framework on smartphones, in *Proceedings of ACM Asia Conference Computers and Communications Security (ASIA CCS), New York, NY, USA, Apr 2017*, pp. 923–925. <https://doi.acm.org.proxy.library.stonybrook.edu/10.1145/3052973.3055160>
18. R. Christina, G.L. Shajan, B. Ankayarkanni, CART—A statistical model for predicting QoE using machine learning in smartphones, in *IOP Conference Series: Materials Science and Engineering*, vol. 590, no. 1 (IOP Publishing 2019), p. 012001.
19. T. Rajalakshmi, R. I. Minu, Improving relevance feedback for content based medical image retrieval, in *International Conference on Information Communication and Embedded Systems (ICICES2014)* (IEEE, 2014), pp. 1–5
20. A.M. Psonia, V.L. Jyothi, XML document retrieval by developing an effective indexing technique, in *2014 Sixth International Conference on Advanced Computing (ICoAC)* (IEEE, 2014), pp. 120–123

21. R.I. Minu, K.K. Thyagarajan, Scrutinizing the video and video retrieval concept. *Int. J. Soft Comput. Eng.* **1**(5), 270–275 (2011)
22. M. Muaaz, R. Mayrhofer, Smartphone-based gait recognition: from authentication to imitation. *IEEE Trans. Mobile Comput.* **16**(11), 3209–3221 (2017)
23. M. Shahzad, A.X. Liu, A. Samuel, Secure unlocking of mobile touch screen devices by simple gestures: You can see it but you can not do it, in *Proceedings of 19th Annual International Conference on Mobile Computing Network (MobiCom), New York, NY, USA, 2013*, pp. 3950. <https://doi.acm.org.proxy.library.stonybrook.edu/10.1145/2500423.2500434>

Predicting Bike Rental Based on Environment and Seasons



Nettem Gopi, Nare Thoshan Kumar Reddy, and T. Sasikala

1 Introduction

Predicting bike rental may be a real-life application project which is used to train the machine to understand the data that are available from the previous records, and it has to predict the count of the requirement that is going to register in the future work or the input that has given to predict [1, 2]. Here we use some regression algorithms and make the machine to understand those data [3]. The data which we provide to the machine is the cleaned data, the cleaned is the thing which we processed the given raw by using some processing methods which include missing value analysis, duplicate values, etc. The reason why we are providing only the cleaned data is just because the machine cannot understand the human readable format, so to understand that we converted the data to machine understandable or machine readable [4].

So after the machine has been trained, then it has to be tested with different inputs with the same number of columns that are provided in the train dataset. So this will provide the result in the form of a graphical representation which is one among the regression algorithm [5]. Also we consider score which is nothing but the accuracy of the prediction percentage that has been predicted. We need to provide the input in such a way that it should have all the columns that are provided in the train data and that has been included in an array form just because to make sure that it should provide an accurate prediction values or the outcome, the accuracy score will tell that at what level of percentage it has been predicting [6, 7].

(1) In odd times, the need of consumers will vary from their fulfilling. (2) While sometimes there will be a very less count that customers are going to register, this leads to loss of the time, and they have invested on it. (3) Or else in times there will

N. Gopi (✉) · N. T. K. Reddy · T. Sasikala
Department of Computer Science and Engineering, Sathyabama Institute of Science and
Technology, Chennai, India
e-mail: gopinathnettem@gmail.com

be a huge number who is going to register but the count of resources are very less, all this is happened just because we do not have any idea how and when the requirement of resources are high and when it will be low [8]. So to overcome this issue, we came up with this real-life application. So the data which we collected from the previous records is the raw data which we need to clean them and make sure that it should not contain any unwanted data in them [9]. So to achieve this, we need to perform certain techniques to clean the raw data and they are called preprocessing steps [10].

2 Related Work

The related work is defined as the thing that it briefly explains the construction of the project along with the modules that are required to implement those techniques; this is an extension of that has been discussed in the introduction part [11, 12]. As discussed above that data from different resources which includes the data from geographical locations, based on environment and seasons, casual and the registered ones and some other columns that are required to perform as a part of the project, all this data has been merged or grouped into one component; then the content available is the raw data which nothing but the data that contains missing values, duplicate values, and various other kinds of data that are not required as a part of this, so to overcome this, we need to implement some data cleaning method or the data processing techniques which will completely change the unwanted data, and if there are multiple records contain the same data, then that duplication of data has been removed, also the boundary missing values which is nothing but some of the records contain empty values and that have been filled up with some random data values that are related to it, and finally the categorical variables and this contains two more divisions: firstly the label encoding and secondly the one-hot encoder [13, 14].

The prediction module or method involves two divisions: One is the unsupervised learning algorithms and the other one is the regressions. Similarly, the classification methods also contain the supervised learning algorithms and the classifiers [15, 16].

3 Proposed System

This paper helps the way to solve the important problem behind the prediction technique and uses the machine learning algorithms which unravel the real-life application (Fig. 1).

This bike rental prediction system will present us a general diagram which is shown in the below figure that will be the system architecture of the bike rental predicting model; this architecture shows us that we have used different types of agents which are used to the collect different types of data. The agents collect the data from different resources they are: registered resources, weather and environment, geographical data, data processor, data workflow. The data workflow will be the

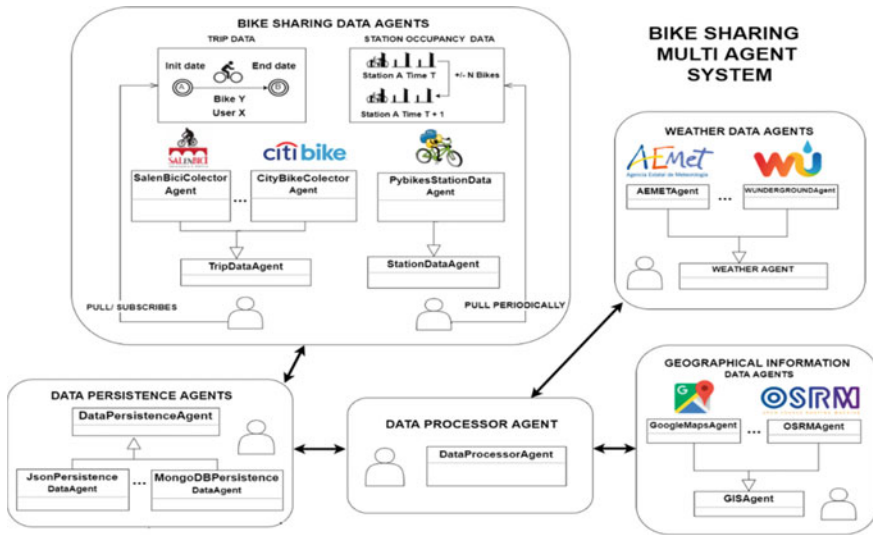


Fig. 1 General proposed multiagent system architecture

subpart in the data processor; these are the four different types of data that we collect the information from and five regression techniques that have been used in this model. This is implemented in machine learning techniques (Anaconda Spyder) and executed in it.

3.1 Registered Resources

The registered resources are the thing which tell us that how many users are going to use that product or the units that are available there. This registered resource or registered data is broadly classified into two categories: One is the casual that is the frequently visited or used customers and secondly is the registered ones who visited after registering, and these are briefly explained in the below way.

Casual: The term casual indicates that the customers are visited just randomly to use their product without any registration or simply we can say that they are casually visited ones just like that. They use the product based on the availability of their time and some other issues.

Registered: In this, the term registered itself indicates that the customer has registered their visit and use of the product previously itself and the product is reserved for them; they are the ones who regularly comes and uses their product. Sometimes the casual count will be high, and in general, sometimes the registered count will be high, but the only advantage of the registered count is that their visit will continuously increase without any fail. And the drawback of the casual ones is that their count will vary from time to time and person to person.

3.2 Weather and Environment

Weather and environment data consists of the weather data of different dates and months. we can get the data of a particular date and time from this weather report; then we will merge the weather data with the trip data to get the prediction. This data will be collected by an agent. The weather data collected from them will be the wind speed, temperature, maximum and minimum speeds of the wind, and the rain forecast will also be present in that the minimum and maximum pressures in which direction the wind is moving, and also the humidity of the environment at a particular location. This collected data set may contain some duplicate values which have been taken care during the preprocessing techniques.

3.3 Geographic Information Data

The geographical information will have the geographical data from different locations and places what is the altitude at a particular place whether it is a mountain region or a plain surface. It will contain the maps of roads, and it will be updating as day to day the roads are increasing in the real life; with this we can analyze the map data and the location data; these data are also merged with the environment data and the trip data to get the results and the accurate score.

3.4 Data Processor

The data processing is the thing which processes all the data that has been collected from various resources like the data from the geographical location, weather conditions, and also based on the seasons. Then, the collected data has been merged as a group and needs to clean those raw data by implementing or apply some techniques which include the missing value analysis the purpose of this is to fill those missing data with some random data; then, the duplicate data is required to make sure that none of the data record is available in multiple times, those records has been eliminated, then the boundary value analysis and the handling categorical variables and the final dataset has been applied to the machine to train it. So this is how the data processing has been done that is mandatory for the application to perform its operations and calculate the accurate result.

3.5 Data Workflow

This is a subpart in the data processor; in this data work flow, we will describe how the data will be flowing and merged from one direction to another direction the trip data, geographical data, weather data all this is collected and merged, and this will be in one direction flow the above diagram the work flow of the data processor in a step by step manner. The data processor will request the weather report and it will eliminate the duplicate and the null data the whole record of the data will be analyzed and then a new future of data set will be added. These datasets consist of different days; these days may be split into years, months, weeks, weekdays, and weekends. These all will be arranged in a workflow; first we will take the data from the agents, and then, the trip data will be taken; then the data will be cleaned and merged with weather report; then the calendar information will be added after that data will be split into different locations, and we need the data at only one location that we are going to predict; then we will get the information of that particular location; we will train the machine with that previous data which we have, and then we can get a score of the registered users we have now we can predict the accurate score.

4 Results and Discussion

The results of the ratio of actual and predicted values of the bike rental data are taken, and the raw data is collected from the previous records; this raw data is cleaned and we applied five different regression algorithms to get the accurate score, and in this model, we performed all the those techniques, so that we will get the score of each regression and compared with other results, and we consider the regression technique that is predicting more accurately (Fig. 2).

The x -axis represents the predicting data, and the y -axis represents the data points, as the data size increases the more accurately we will get the predicted score if we have smaller amount of data, we will get the predicting score but that will not be much accurate if we have more data then we can perform all the regression models or techniques that we have and then we will get the best one that means which will show more prediction value then that will be our accurate score (Fig. 3).

The above is the input conditions that have been assigned to the model to test the data, till then the regression algorithms have been used to train the model, and now it's the thing to test, so input the conditions based on how the geographical data, based in seasons, based on weekday or weekend, temp, wind speed, etc., all those conditions have been applied and it is going to predict how many users are going to register or how many count of requirements has to be needed, it is going to predict in either +ve values or – negative values in the prediction values dataset (Fig. 4).

The above is the prediction values that have been evaluated based on the input conditions that have been assigned for the model to analyse and predict the output count with an accuracy score; all this has been generated by following all the above

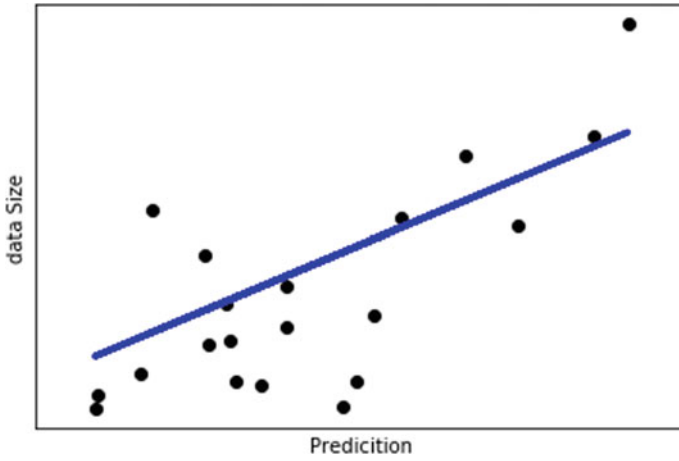


Fig. 2 Graph showing data size with respect to prediction line

	0	1	2	3	4	5	6	7	8	9	10
0	2	1	6	0	0	1	1	0.6025	0.525892	0.467917	0.160446
1	2	1	6	0	0	1	1	0.6025	0.525892	0.696087	0.248539
2	2	1	6	0	6	0	1	0.583333	0.566288	0.549167	0.186562
3	2	1	6	0	0	0	1	0.6025	0.575133	0.493333	0.184087
4	2	1	6	0	0	1	1	0.6025	0.525892	0.467917	0.15735
5	2	1	6	0	2	1	2	0.540833	0.525892	0.613333	0.289575
6	2	1	6	0	4	1	1	0.6025	0.569442	0.567083	0.15735
7	2	1	6	0	5	1	1	0.649167	0.597862	0.467917	0.175383
8	2	1	6	0	0	1	1	0.6025	0.525892	0.57375	0.182842

Fig. 3 Input data conditions assigned to model

Fig. 4 Prediction values based on input conditions

0
933.774
856.872
1560.42
1509.21
935.31
630.252
950.97
1059.59
987.267

conditions and the steps that have been assigned to it either to train the model or to test the model with the unique set of data conditions available for it. So thus all the prediction values of registered count have been predicted.

5 Conclusion and Future Work

In this, we will conclude that the accurate score of the users is going to be registered, taking the raw data and the regression techniques made the work easier to get the prediction of the bike rental system. Moreover, the data which has been collected from the previous records has allowed us to clean the data easily; by using this knowledge, we can train the machine in well manner so that will give us more accurate results. By this, we can conclude how many bikes we need for the upcoming days and we can keep the required amount of bikes the unwanted bikes can be shifted to any other docking stations. In the future works, we will analyze and say how many number of users are going to be registered.

Acknowledgements I am pleased to acknowledge our sincere thanks to Board of management of **SATHYABAMA** for their kind encouragement in doing this project and for completing it successfully. I am grateful to them.

I would like to express our sincere and deep sense of gratitude to our project guide **Dr. T. Sasikala M.E., Ph.D.**, for her valuable guidance, suggestions, and constant encouragement paved way for the successful completion of my project work.

References

1. T. Mátrai, J. Tóth, Comparative assessment of public bike sharing systems. *Transp. Res. Procedia*, **14**, 2344–2351 (2016) (CrossRef)
2. S. Prince Mary, B. Bharathi, Vigneshwari. S, Sathyabama R, Neural computation based general disease prediction model. *Int J Recent Technol Eng (IJRTE)* **8**(2), 5646–5449. ISSN 2277-3878. <https://www.ijrte.org/wp-content/uploads/papers/v8i2/B2329078219.pdf>.
3. D.U. Nandini, S. Divya, S, A literature survey on various watermarking techniques, in *2017 International Conference on Inventive Systems and Control (ICISC)*. (IEEE, 2017), pp. 1–4
4. European Commission—PRESS RELEASES—Press Release—Energy Union and Climate Action, Driving Europe’s transition to a low-carbon economy. https://europa.eu/rapid/press-release_IP-16-2545_en.htm. Accessed 28 June 2017
5. P. Midgley, Bicycle-sharing schemes: Enhancing sustainable mobility in urban areas. *Commun. Sustain. Dev.* **18**, 1–12 (2011)
6. Station-Free Bike Sharing. <https://www.ofo.com/us/en>. Accessed on 29 Dec 2017.
7. A. Pravin, S. Srinivasan, An efficient programming rule extraction and detection of violations in software source code using neural networks, in *2012 Fourth International Conference on Advanced Computing (ICoAC)* (IEEE, 2012), pp. 1–4
8. The World’s First & Largest Smart Bike Share. Mobike. <https://mobike.com/global/>. Accessed on 29 Dec 2017
9. L. Di Gaspero, A. Rendl, T. Uri, Balancing bikes haring systems with constraint programming. *Constraints* **21** 318–348 (2016) (CrossRef)

10. A.M. Psonia, V.L. Jyothi, XML document retrieval by developing an effective indexing technique. in *2014 Sixth International Conference on Advanced Computing (ICoAC)* (IEEE, 2014), pp. 120–123
11. R. Giot, R. Cherrier, Predicting bike share system usage up to one day ahead, in *IEEE Symposium Series on Computational Intelligence* (2014), pp. 1–8 (CrossRef)
12. S. Marlin, S.S. Jebaseelan, B. Padmanabhan, G. Nagarajan, Power quality improvement for thirty bus system using UPFC and TCSC. *Ind. J. Sci. Technol.* **7**(9), 1316–1320 (2014)
13. S. Vigneshwari, B. Bharathi, T. Sasikala, S. Mukkamala, A study on the application of machine learning algorithms using R, *Journal of Computational and Theoretical Nanoscience. J. Comput. Theor. Nanosci.* **16**(8), 3466–3472 (2019)
14. B. Yasotha, T. Sasikala, Intrusion detection system for mitigating attacks using energy monitoring in wireless sensor networks. *Int. J. Mobile Network Des. Innov.* **6**(4), 219–227 (2016)
15. M.A. Chowdary, M. Kundan, M., D.A.V.A. Mary, Effective credit card forgery prevention using multilevel authentication, in *IOP Conference Series: Materials Science and Engineering*, vol. 590, no. 1 (IOP Publishing, 2019), p. 012021.
16. M. Ps, B. Ab, Wind energy location prediction between meteorological stations using ANN (2014)

Automatic Recognition of Medicinal Plants



P. Krishna Vinesha, P. Lakshmi Priyanka, and L. Lakshmanan

1 Introduction

Plant ID has a significant job in current logical issues, for example, biodiversity, environment and pharmacology among others. In biology, plant distinguishing proof includes breaking down numerous organs, for example, blossoms, seeds, leaves and woody parts [1, 2]. This methodology renders the errand troublesome as blossoms and seeds, which are occasional and subject to the plant's age and condition, are difficult to discover. In exceptional circumstances, for example, discovering fossils or uncommon plants, the material accessible to distinguish a plant is only the leaves [3]. To comprehend these circumstances, a leaf morphological scientific categorization method is proposed, which considers just the leaves to play out the distinguishing proof errands [4]. This methodology joins different highlights of leaves, for example, shape, vein structure, surface and some histological data. Recognizing plants is a troublesome and complex undertaking because of the idea of the leaves. Although the leaves present some major highlights, they additionally present a wide example of the variety. This variety may happen in various leaves from a similar plant, where attributes, for example, development and presentation to the sun produce varieties in the size, shading, surface and state of the leaves [5]. These varieties are additionally present in leaves from similar species, however, from various plants. Right now, it

P. Krishna Vinesha (✉) · P. Lakshmi Priyanka · L. Lakshmanan
Department of Computer Science and Engineering, Sathyabama Institute of Science and
Technology, Chennai, India
e-mail: pabbithivineesha@gmail.com

P. Lakshmi Priyanka
e-mail: Lakshmi.priyanka565@gmail.com

L. Lakshmanan
e-mail: lakshmanan.cse@sathyabama.acin

is an outcome of soil impact, atmosphere or even condition when the leaf is being shaped.

The frames have grown so far using programmed order procedures; however, the procedures are very comparative. These means include the configuration of the collected leaves, the realization of some previous management to distinguish their particular characteristics, the arrangement of the leaves, the compilation of the database, the preparation for the recognition and evaluation of the results [6–10]. The world has a more number of plant species, a significant amount of which have remedial qualities, close to elimination and others are destructive to humans. The recognition of dark plants depends very much on the intrinsic information of a specialized botanist. The best technique for distinguishing plants effectively and effectively is a manual processing strategy based on morphological qualities. In this way, a large number of procedures relating to the organization of these plant species “depend on the accumulation of information and the skills of individuals” [11]. Be that as it may, this procedure of manual acknowledgment is regularly relentless and time-consuming [12, 13]. Henceforth, numerous scientists have directed examinations to help the programmed grouping of plants dependent on their physical qualities.

The frames have grown so far using programmed order procedures, however, the procedures are very comparative. These means include the configuration of the collected leaves, the realization of some previous management to distinguish their particular characteristics, the arrangement of the leaves, the compilation of the database, the preparation for the recognition and evaluation of the results. A computerized plant distinguishing proof framework can be utilized by non-botanical specialists to rapidly recognize plant species easily [14].

Normally, the customary individuals are doled out with the activity of gathering the plants from the timberlands. Once in a while, they could not perceive the uncommon and significant plants due to human blunder. These uncommon sorts of plants are critical to spare the life of a patient. Additionally, here and there these individuals could get off base species which might be hurtful plants. In such cases, it is important to utilize the programmed plant acknowledgment framework. This framework helps a conventional people or any layman to perceive the diverse plant species. These sorts of frameworks are likewise extremely accommodating for the trekking individuals if they are intrigued to gather the plant species while trekking the mountains [15].

2 Related Work

Some tests have been performed to create tools for distinctive tests on plants in the past 10 years. Wu et al. they completed the most definitive works in the plant field disposal [16]. From five fundamental graphic aspects, twelve structural aspects are deduced and, therefore, the analysis of the main components (PCA) is used to reduce the measurement in order to send fewer sources of information to a feasibility neural system (PNN). They achieved normal accuracy of 90.3% with the Flavia set of data, which is its creation. Using an alternative data set but a similar algorithm,

Hossain et al. [17] have achieved a degree of accuracy comparable to the comparative highlights [18].

The image was in the size of $256 * 256$ pixels. Du et al. [19] proposed a methodology that depends on the measurement of the fractal highlighted on the basis of the shape of the leaf and the designs of the veins for the recognition and order of the leaves of the plant [19]. By using a closer k-classifier with 20 highlights, they achieved the high identification rate of 85.1%. Using a form of volumetric fractal measurement to try to create a surface mark by a sheet and calculating the linear discriminant analysis (LDA), Backes et al. [20] had the opportunity to overcome the conventional methodologies that depended on the Gabor channels and the Fourier test achieved 87.3% accuracy in a data set of 640 leaves from 32 distinctive plant species [21]. They used to model and combine data as it were. Sixteen sources of information (6 geometric aspects, 8 surfaces and 2 morphological highlights) were sent to a counterfeit neuronal system (ANN) with 60 centers in the covered layer and a learning frequency of over 0.100 pages. Using the equivalent data set, Chaki et al. [22] obtained an accuracy of 97.6% using a neuro-fuzzy (NFC) algorithm with a 44-component surface vector and a 3-component shape vector [23]. Use of the module only includes the Flavia and Pattern Net data set (a type of neural system). His neuronal advancement system consists of two-hidden layers with twenty-six neurons each and was prepared for more than 100 pages.

Fascinating work has been done. They performed the calculation of the scale curvature histogram (HCoS) to extract the shape data and the modification of the almost corresponding example (LBPV) to eliminate the surface data. In the best case, the clean data set exceeded the 7.3% data set. This recommends that legitimately acquired images using a mobile phone can create good levels of proven accuracy and images that are physically prepared in a laboratory and then grouped together. Previously, Amin et al. [1] used an appropriate neuronal level diagram (DHGN) to acquire fold data using 64 element vectors and the closest k-classifier with Canberra separation to acquire 71.5% accuracy [24].

3 System Architecture

The initial step is to delete the RGB channel data from the information image to distinguish the implant data from the anterior area. To do this, data is extracted from the excess green (ExG) and excess red (Exp) channels. Then, the red overabundance data is removed from the abundance of green data to progressively contain the green channel data in Fig. 1. When the double limit is applied in the improved vegetative archive, the ExGExR data, a double intrigue district is divided into plants. The next advance is to use the first double image shadow pixel as a cover that separates the leaves as secondary images. The division of the test sheet images into the data set using the vegetative record mentioned above. The important component in the representation of an image is shading. The shading minutes are obtained through the highlighted facts, for example, the average and the standard deviation evaluated

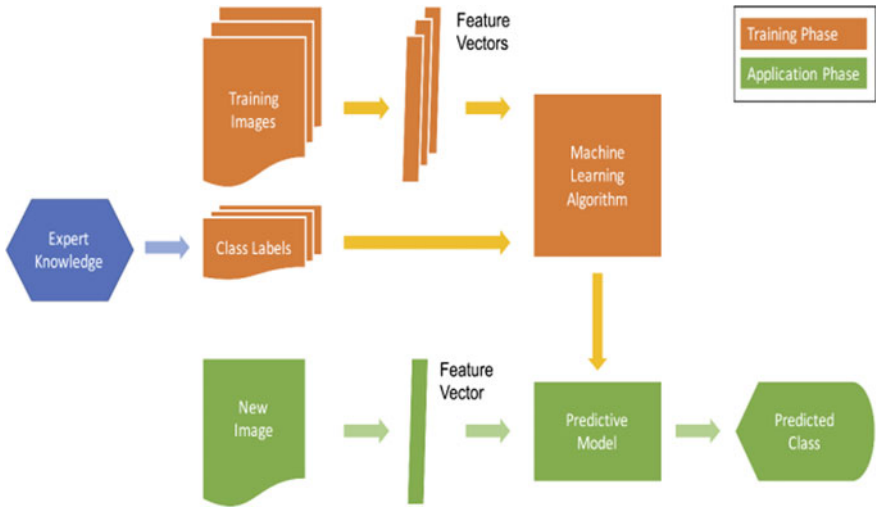


Fig. 1 Overall system design

in the three RGB channels (red, green, blue). The main measures for requesting an image are acquired from the standard deviation and the average.

The surface of the image can be estimated using the concurrency pane, the different shading elements or the gray scale estimates of the image. The highlights that are created using this strategy are known as Haralick highlights. A calculated regression classifier is used to distinguish the restoration plan. Since our proposed strategy consists of the characterization of numerous classes, the relapse model calculated in parallel has been extended to the calculated multinomial relapse. Through a combination of relapses calculated in pairs, the multinomial log it thinks of different encounters. This allows you to compare each brand class with a reference classification in the data set.

4 Algorithm Used

A convolutional neural network (CNN) is a deep friendly neural network designed from biologically controlled modules. They are applied most frequently used for image processing. CNN’s work differently in that they treat data as spatial. Instead of being connected to all the neurons in the previous layer, the neurons are connected only to neighboring neurons and all have the same weight. This simplification in connections means that the network maintains the spatial aspect of the data set. The word convolution refers to the filtering process that occurs in this type of network. If an image is complex, the convolutional neural network simplifies it, so it can be better elaborated and understood. Like a normal neural network, CNN is also composed

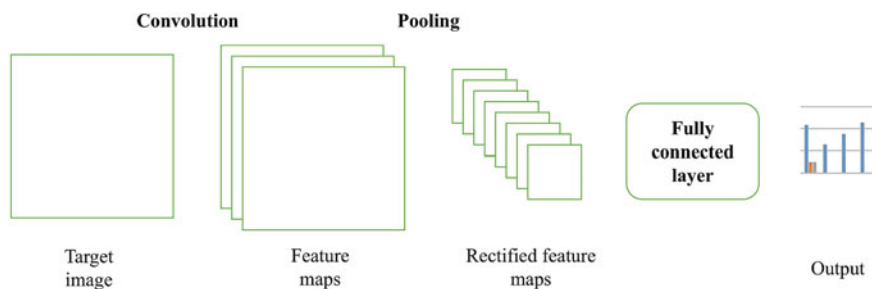


Fig. 2 Steps in CNN

of several levels. There are a couple of levels that make the convolutional level and the grouping level unique. However, like other neural networks, it will also have a rectified linear unit layer and a fully connected layer as shown in Fig. 2. The ReLU level acts as an activation function, ensuring nonlinearity as the data moves through each level of the network.

Without it, the data entered in each level would lose the dimensionality that we want to maintain. Meanwhile, the fully connected layer allows you to classify the data set.

5 Results and Discussion

The obtained results of training accuracy and validation accuracy values are shown in Fig. 3. Where there has less number of epochs (up to 13), we can know that validation accuracy is same as the training accuracy. In case if we need more number of epochs the training accuracy and validation accuracy values are almost comparable (Figs. 4, 5, 6 and 7).

6 Conclusion

Another set of data on therapeutic plants in Mauritius has been made openly accessible at the entrance of the AI store. At this time, vision strategies have been used to extract some reflexes based on the shape of the leaves of the therapeutic plants. AI calculations were used to group the leaves of 25 distinctive plant types into their suitable classifications. The most remarkable precision of 98.3% was obtained by the irregular forest classifier. Normally, the conventional individuals are doled out with the activity of gathering the plants from the timberlands. Once in a while, they could not perceive the uncommon and significant plants in light of human blunder. These uncommon sorts of plants are essential to spare the life of a patient. Likewise,

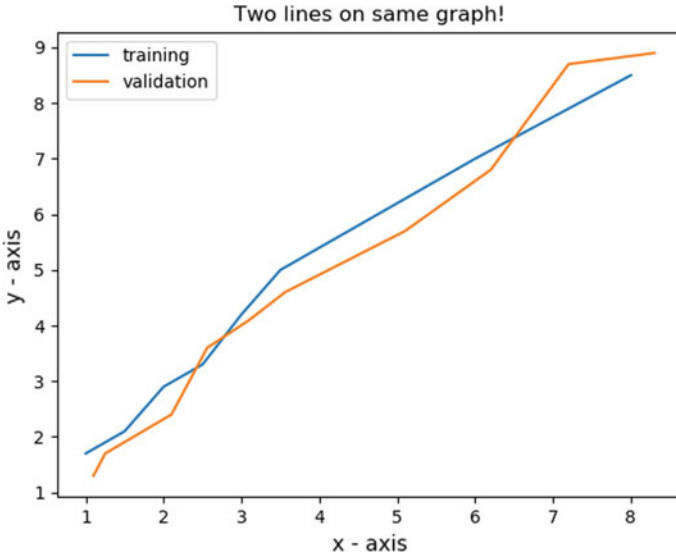


Fig. 3 Training accuracy versus validation accuracy graph

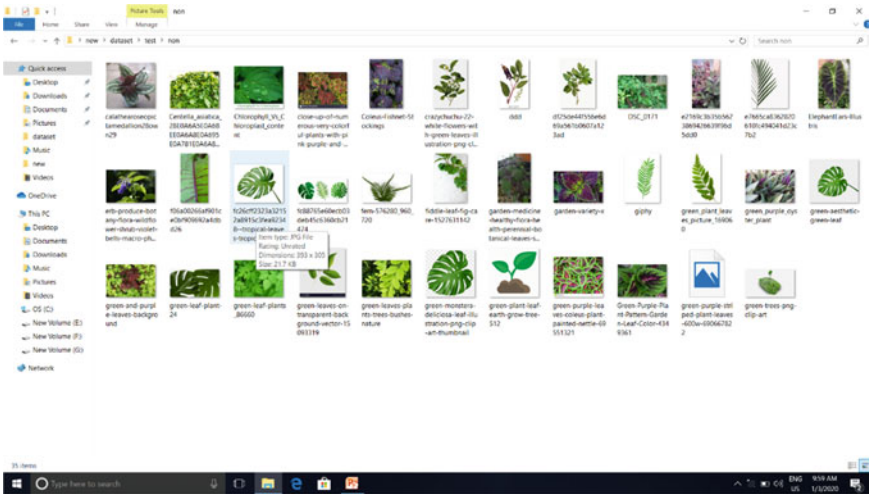


Fig. 4 Images before conversion into gray scale

here and these individuals could get erroneous species which might be hurtful plants. In such cases, it is important to utilize the programmed plant acknowledgment framework. These sorts of frameworks are likewise helpful for the trekking individuals.

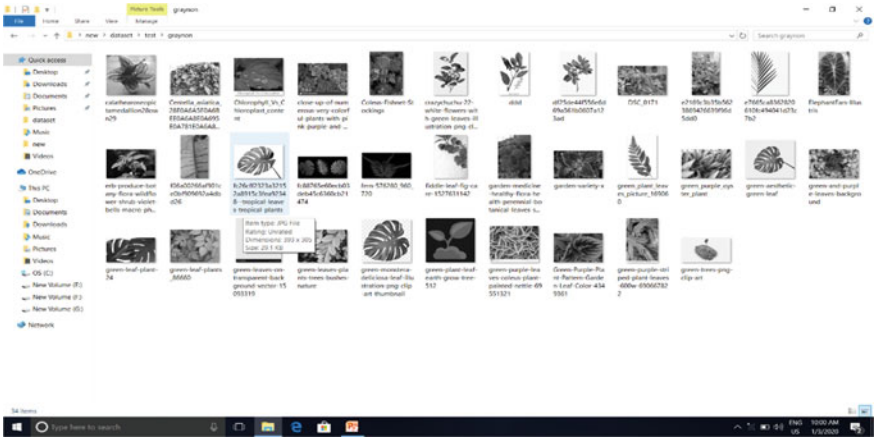


Fig. 5 Images after gray scale conversion

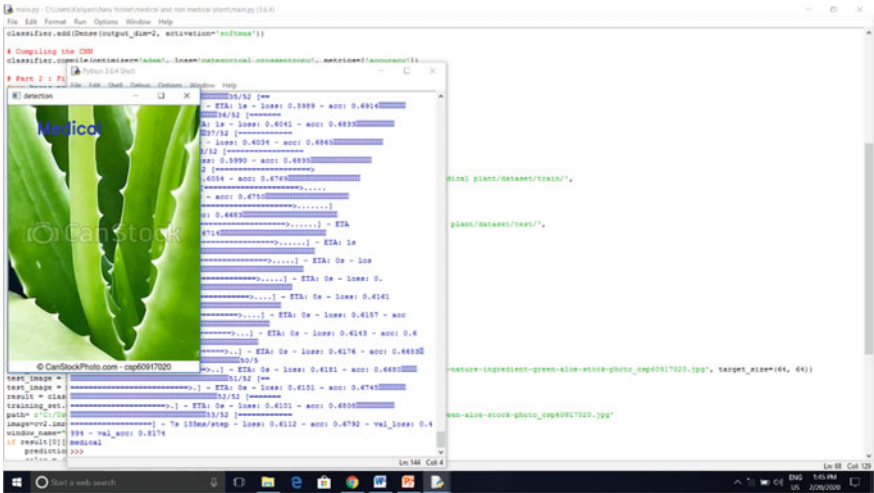


Fig. 6 Recognition of medicinal plants

7 Future Work

It is necessary to study about medicinal plants that find place in folklore. As a result, such plants should be investigated to understand their physical and chemical properties as well as safety and efficacy. The medicinal plants find applications in many industries. The use of medicinal plants for curing diseases has been increased. In order to identify the medicinal or non-medicinal, it will take more time. So that we can create an application by using this project. Then, it will be easy to identify the medicinal plants. It is easy to use and also takes less time.

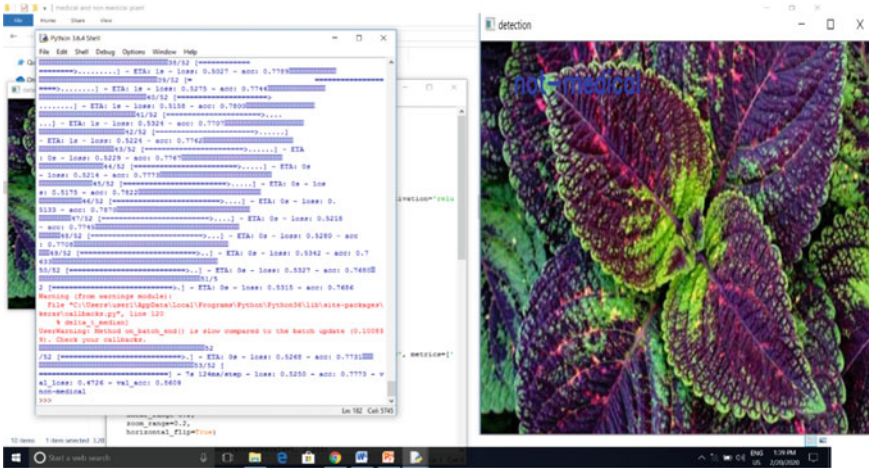


Fig. 7 Recognition of non-medical plants

References

1. A.C.Q. Siravenha, S.R. Carvalho, Exploring the use of leaf shape frequencies for plant classification, in *28th SIBGRAPI Conference on Graphics, Patterns, and Images, Salvador, Brazil* (2015), pp. 297–304
2. X. Zhang, Y. Liu, H. Lin, Y. Liu, Research on SVM plant leaf identification method based on CSA, in ed. by W. Che, et al. *Social Computing, ICYCSEE 2016. Communications in Computer and Information Science*, vol. 624 (Springer, Singapore, 2016)
3. A. Pravin, S. Srinivasan, An efficient programming rule extraction and detection of violations in software source code using neural networks. In *2012 Fourth International Conference on Advanced Computing (ICoAC)* (IEEE, 2012), pp. 1–4
4. T.L. Le, D.T. Tran, V.N. Hoang, Fully Automatic leaf-based plant identification, application for Vietnamese medicinal plant search, in *Fifth Symposium on Information and Communication Technology Hanoi, Vietnam* (2014), pp. 146–154
5. T.P. Jacob, T. Ravi, Optimization of test cases by prioritization (2013)
6. J. Chaki, R. Parekh, S. Bhattacharya, Plant leaf recognition using texture and shape features with neural classifiers. *Pattern Recogn. Lett.* **58**, 61–68 (2015)
7. J.X. Du, X.F. Wang, G.J. Zhang, Leaf shape based plant species recognition. *Appl. Math. Comput.* **185**, 883–893 (2007)
8. J.X. Du, C.M. Zhai, Q.P. Wang, Recognition of plant leaf image based on fractal dimension features. *Neurocomputing* **116**, 150–156 (2013)
9. M. Du, S. Zhang, H. Wang, Supervised isomap for plant leaf image classification, in *5th International Conference on Emerging Intelligent Computing Technology and Applications, Ulsan, South Korea*, (2009), pp. 627–634
10. W. Gao, W. Lin, Frontal parietal control network regulates the anti-correlated default and dorsal attention networks. *Hum. Brain Mapp.* **33**(1), 192–202 (2012)
11. A.H.M. Amin, A.I. Khan, One-shot classification of 2-D leaf shapes using distributed hierarchical graph neuron (DHGN) scheme with a k-NN classifier. *Procedia Comput. Sci.* **24**, 84–96 (2013)
12. J. Carranza-Rojas, E. Mata-Montero, Combining leaf shape and texture for costa rican plant species identification. *CLEI Electron. J.* **19**(1), 7 (2016)

13. G. Nagarajan, R.I. Minu, Wireless soil monitoring sensor for sprinkler irrigation automation system. *Wireless Pers. Commun.* **98**(2), 1835–1851 (2018)
14. B. Yasotha, T. Sasikala, Intrusion detection system for mitigating attacks using energy monitoring in wireless sensor networks. *Int. J. Mobile Network Des. Innov.* **6**(4), 219–227 (2016)
15. S. Kalpana, S. Vigneshwari, Selecting multiview point similarity from different methods of similarity measure to perform document comparison. *Ind. J. Sci. Technol.* **9**(10), 1–6 (2016)
16. K. Arai, I.N. Abdullah, H. Okumura, Identification of ornamental plant functioned as medicinal plant-based on redundant discrete wavelet transformation. *Int. J. Adv. Res. Artif. Intel.* **2**(3), 60–64 (2013)
17. A. Babatunde, L. Armstrong, D. Diepeveen, J. Leng, A survey of computer- based vision systems for automatic identification of plant species. *J. Agric. Inf.* **6**(1), 61–71 (2015)
18. A.R. Backes, D. Casanova, O.M. Bruno, Plant leaf identification based on volumetric fractal dimension. *Int. J. Pattern Recognit Artif Intell.* **23**(6), 145–1160 (2009)
19. Y. Herdiyeni, N.K.S. Wahyuni, Mobile application for indonesian medicinal plants identification using fuzzy local binary pattern and fuzzy color histogram, in *International Conference on Advanced Computer Science and Information Systems (ICACSIS), West Java, Indonesia* (2012), pp. 301–306
20. A. Hernandez-Serna, L.F. Jimenez-Segura, Automatic identification of species with neural networks. *Peer J.* **2**, e563 (2014). <https://doi.org/10.7717/peerj.563>
21. J. Hossain, M.A. Amin, Leaf shape identification based plant biometrics, in *13th International Conference on Computer and Information Technology, Dhaka, Bangladesh* (2010), pp. 458–463
22. E. Mata-Montero, J. Carranza-Rojas, Automated plant species identification: challenges and opportunities. *IFIP Adv. Inf. Commun. Technol.* **481**, 26–36 (2016)
23. T. Munisami, M. Ramsurn, S. Krishnan, S. Pudaruth, Plant leaf recognition using shape features and color histogram with k-nearest neighbor classifiers. *Procedia Comput. Sci.* **58**, 740–747 (2015)
24. S.G. Wu, F.S. Bao, E.Y. Xu, Y.X. Wang, Y.F. Chang, Q.L. Xiang, A leaf recognition algorithm for plant classification using probabilistic neural network, in *7th IEEE International Symposium on Signal Processing and Information Technology, Giza, Egypt* (2007), pp. 11–16

Number Plate Detection Using Support Vector Machine



Bodla Sai, B. Rama Brahmam, and T. Sasikala

1 Introduction

Intelligent transport is growing sector in India, traffic management, traffic crime detection, toll collection and management, automatic parking solutions, road and accident monitoring are real-world applications, where license plate detection and recognition is needed [1]. This is under research area in recent decades, many researchers are providing with various solutions, still is considered to be highly researchable area to focus and bring a best solutions [2].

Artificial intelligence, machine learning, and deep learning are emerging technologies, which is widely used license plate recognition [3]. Nowadays, living standards among people in urban cities are developing, due to which number of vehicles also increasing leads to traffic problem becomes more prominent [4]. The increased vehicles due to improvement in technology has paved the way for finding efficient solution for license plate detection [5]. Existing vehicle or traffic management is not effective due to high labor, less technology use, and increase in number of vehicles [6, 7]. The recent evolvement in technology has given better solution for this, which reduces time in taking entry in toll gates in National Highways in India [8].

License plate detection finds the exact location of the plate in the whole image. The plate is detected and segmented using image processing to get the characters [9, 10]. The accurate detection of number directly depends on positioning of the

B. Sai (✉) · B. R. Brahmam · T. Sasikala
Department of Computer Science and Engineering, Sathyabama Institute of Science and Technology, Chennai, India
e-mail: bodlasai924@gmail.com

B. R. Brahmam
e-mail: ramabrahmambotla@gmail.com

T. Sasikala
e-mail: dean.computing@sathyabama.ac.in

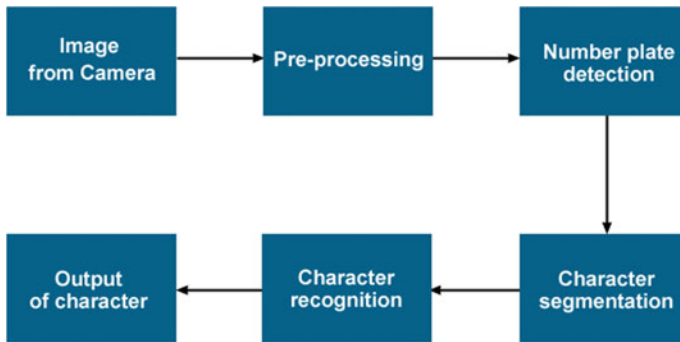


Fig. 1 Overview of number plate detection

plate. License plate detection can be done effectively when the input image clarity is high [11, 12]. This paper studies the license plate detection through connected component analysis, after identifying the plate, the numbers are segmented. Through SVM, learning numbers and alphabets in the segmented image are identified [13]. The further chapters describe the existing systems, proposed solution, algorithm details, and results and discussion [14, 15]. The overall architecture of number plate recognition is shown in Fig. 1, this handles image input from high resolution camera is given pre-processing steps. Generally, pre-processing may evolve with one or more steps including gray scale conversion, edge detection, and re-size the image, etc. Once character segmentation is done, the characters are matched with trained pickle from SVM algorithm, which classifies the best matching character and bring the output [16].

2 Related Work

Many existing techniques have been studied by the researchers on license plate recognition and related applications and similarly attendance monitoring system, few of them are discussed below.

In [1], the author studied vehicle plate detection using AdaBoost algorithm. They trained the algorithm with adaptive threshold for identifying plate, they used 10,000 samples of dataset in which 2000 positive and 8000 negative samples. The author's aim is to eventually detect the plate with or without cover in plate. This study helps for identifying fraud taxi and take necessary action.

The authors in paper [3] defined the work on multiple licenses plate detection from images. The author used Spanish and Indian number plates for detection. The images are taken from infrared camera, they went some of the pre-processing techniques like gray scale conversion and Sobel filter is applied. For character recognition, they used SVM algorithm. However, through they used high resolution images from infrared camera, the accuracy is less.

The author in [6] proposed plate recognition based on multilayer perceptron from convolutional neural network (CNN) algorithm. The author discussed the region of interest (ROI) extraction from still images and pre-processing with binary iteration process for removing excessive noise around and character like elements from the segmented image. In this paper, the author achieved around 90% accuracy.

In [11], the author discussed license plate recognition with optical character recognition techniques. They extracted the license plate and did verifications such as overlapping of characters, angle to the fit line and center of segment, deviation of line from fit, and total number of symbols. These verification processes make the identification of number plate more accurate. However, this work not represented the character verification from the number plate.

In [14], the author discussed license plate detection for Chinese plates, they used backpropagation neural network (BPNN) for character recognition. The author specifically designed the Chinese plate detection with specific length and width parameter. For identifying characters, they used BPNN, which is trained with 50 epoch. However, their model is good, but applicable only to Chinese number plates.

3 Proposed System

This paper studies the license plate recognition using connected component analysis and character recognition using SVM algorithm. There were number of pre-processing handled to make effective for identification. Connected component is used for structure and shape analysis, which detects the license plate area from the input image. SVM training model is important in character recognition.

The work is handled in two phases, one is license plate detection and character recognition. Both of these phases are studied detail in the following.

- License plate detection—connected component analysis (CCA)
- Character recognition—support Vector machine (SVM).

Connected Component Analysis

CCA analysis is done for plate detection where the input given to this model is minimum and maximum height and width parameters. The region in the image is labeled using this property. Then, we define a threshold to identify the matching property, for this, we used 50 as threshold. If the area region is less than 50, then it is considered to be license plate. The region which satisfies the condition is extracted and identified as number plate (Fig. 2).

Support Vector Machine

Support vector machine is one of most common used supervised learning techniques, which is commonly used for both classification and regression problems. The algorithm works in such a way that each data is plotted as point in n -dimensional space with the feature values represents the values of each co-ordinate, SVM used for

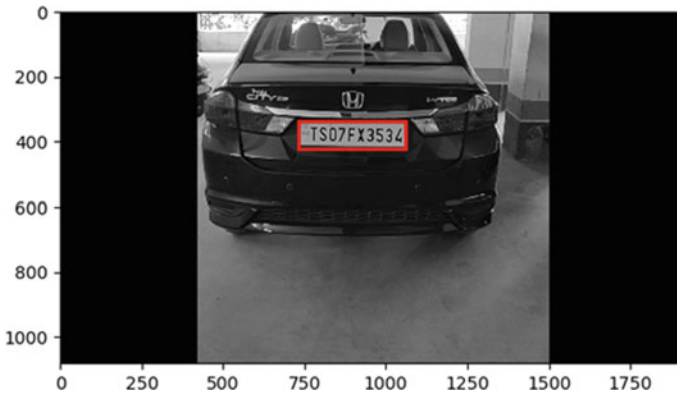


Fig. 2 License plate extraction

character recognition, which works in such a way that it constructs n -dimensional hyperplane. It is assumed that there are set of points on the plane and every points belong to the class value.

4 Implementation Procedure

The architecture of proposed system is shown in Fig. 3. The implementation is done in two phases, the first phase is plate detection and second phase is plate number recognition. In the plate detection phase, connected component analysis is used, from which we give input of height and width parameters.

The architecture of proposed system is shown in Fig. 3. The implementation is done in two phase, the first phase is plate detection and second phase is plate number recognition.

In this paper, we proposed to improve the detection of number plate accurately using CCA analysis. Existing studies mostly perform through feature and texture classification and RGB color-based models. These are static techniques, which cannot be adopted for most of scenarios, whereas our proposed approach can be made dynamic by changing the plate parameters for detection.

Figure 4 shows the pre-processed input video. The input video is taken and is converted/split to many frames, the output frames are stored in folder for further processing. This is given for the next module input, where image pre-processing is done.

The below figure shows the pre-processed input image. The input image is taken and gray scale conversion is done, and the image is converted to gray scale image as shows below. This is given for the next module input, where plate detection is done.

$$\text{Plate_dimension} = (0.03 * \text{width}, 0.08 * \text{width}, 0.15 * \text{height}, 0.3 * \text{height})$$

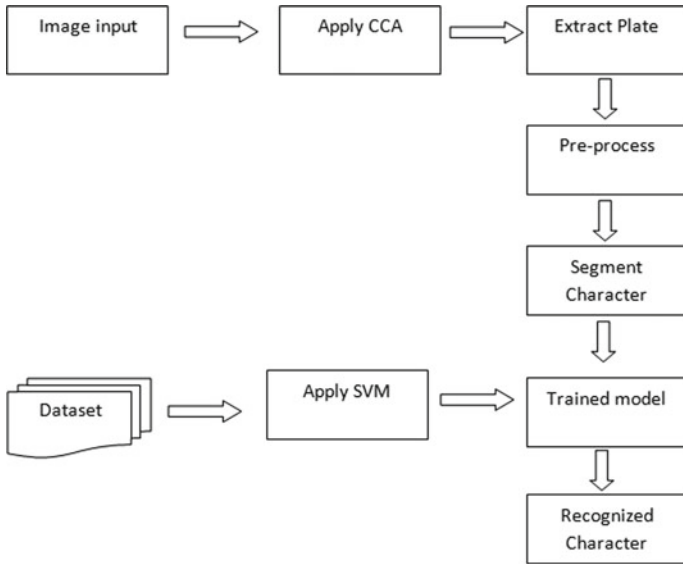


Fig. 3 System architecture

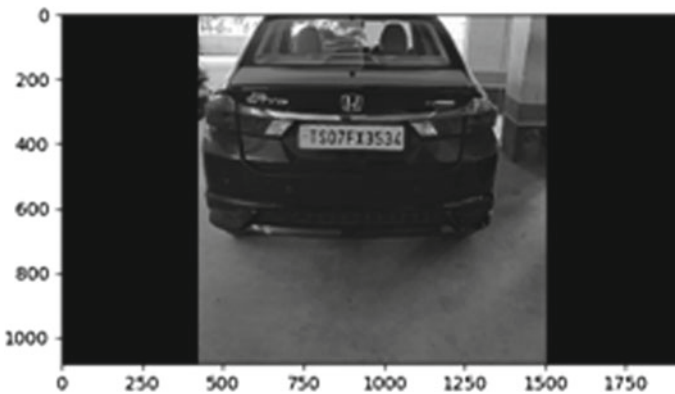


Fig. 4 Converting video to image frames

If the region property is satisfied the threshold, then bounding boxes is drawn on the detected area as license plate as shown in Fig. 5.

Then, it shows plate detection in gray scale image. The bounding box is drawn using CCA technique and this ensures highly accurate detection of license plate on car image. Then, we follow the procedure of segmentation technique. The CCA property is also applied in segmenting character. The region property is extracted

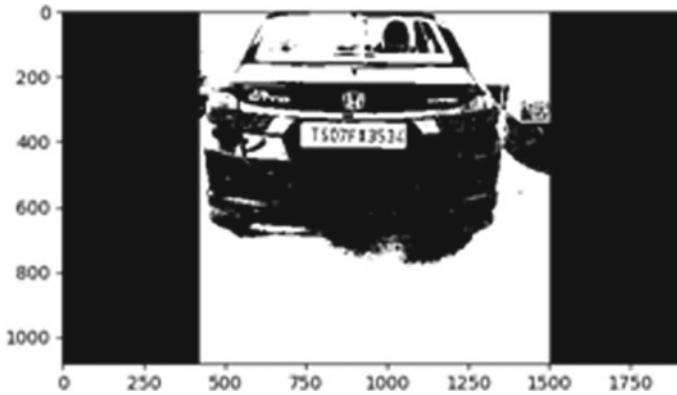


Fig. 5 Pre-processed input image

from image and character like image is drawn a red colored bounding boxes. The each segmented characters are resized to 20*20 size for the next process.

Number Recognition

The license plate number is recognized by using support vector machine (SVM) algorithm. The input dataset is total 36 classes and each of 10 samples is taken. Total 360 images of 36 different classes are taken as input. We ensure that image input shape should be 20×20 .

The execution is carried out with the following steps.

- a. Pre-processing dataset
- b. Splitting dataset into train and test
- c. Learning model using decision tree and linear regression
- d. Give fourfold set cross validate
- e. Plot the prediction values.

The dataset considered is split into train set and test set. We have considered 70% of data as training input for our machine learning algorithm model to train the model. The remaining 30% of data is considered as test for result prediction.

We exploited SVM algorithm to predict the character dataset. We performed fourfold validation of dataset and we achieved 88% accuracy on validation. The trained SVM model generates an output of statistical file in.sav format. This file is loaded for character prediction and classifies the character.

5 Result and Discussion

The implementation is done using Python 3 with a graphical user interface (GUI) designed in TKINTER. In the user interface, we designed to train the SVM algorithm.

It is also designed to load the image and video input and perform prediction. MySQL database is created for storing the number and detection time in table. This is used for tracking vehicles in tolls and other surveillance systems. The proposed system is more suitable for plate recognition as we detect plate with more accuracy. The CCA technique works in such a way that every pixel and its adjacent pixel are checked and grouped together to create the detection area.

Figure 6, shows the character training output. We considered letter from A to Z and numbers 0–9 in a 20×20 input shape and fourfold validation is done. The results are plotted as above, it clearly depicts that the accuracy of learning increase with number of folds. The last fold has achieved more than 96% accuracy on cross validation.

Figure 7 shows the output of segmentation. Connected component is extracted from image, which is identified by the pixel value and adjacent pixel value, we draw

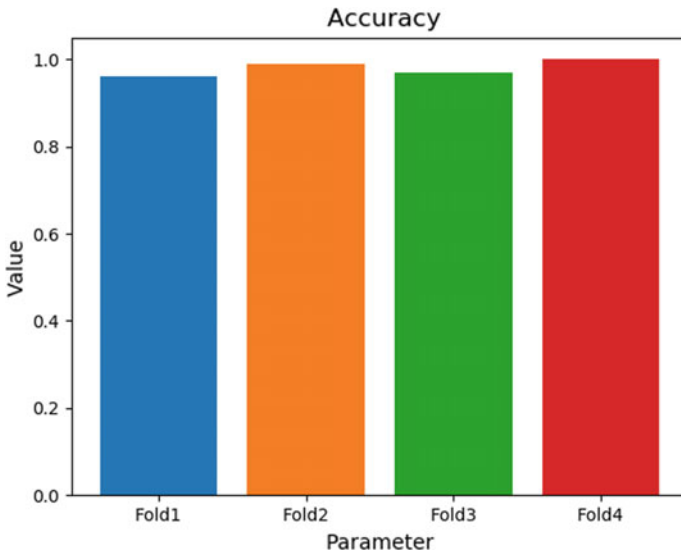


Fig. 6 Validation accuracy for fourfold using SVM



Fig. 7 Report of student

the bounding boxes when the image property, which is the pixel values are same. Each red colored box shows the segmented characters.

6 Conclusion

Traffic management and surveillance are growing demand in highly populated countries like India. As the number of vehicles increase, the traffic maintenance is a problem. Thus, to manage and provide effective solutions, many researchers are working in this filed. In this paper, we tried to provide an efficient solution for license plate detection and character recognition. For this, the implementation is done in two phases, first phase we conducted the plate detection problem using CCA and segmentation is done. In the second phase, we used SVM algorithm and four-fold cross validation to achieve high accuracy on learning to recognize the character. The experimental evolution is done. In the future, we are interested to develop the object detection model for plate detection and deep learning approach on character recognition.

Acknowledgements We are very thankful to our guide Dr. T. Sasikala M.E., Ph.D., Dean school of Computing for her valuable guidance and convey our thanks to Dr. vigneshwari M.E., Ph.D and Dr. L. Lakshmanam M.E., Ph.D., Heads of Department Computer Science and Engineering for providing full support during the reviews, and I also thank all the teaching and nonteaching staff of the department for their support.

References

1. S. Prince Mary, B. Bharathi, S. Vigneshwari, R. Sathyabama, Neural computation based general disease prediction model. *I. J. Recent Technol. Eng. (IJRTE)* **8**(2), 5646–5449 (2019). ISSN: 2277-3878
2. A. Pravin, S. Srinivasan, An efficient programming rule extraction and detection of violations in software source code using neural networks, In *2012 4th International Conference on Advanced Computing (ICOAC)* (IEEE, 2012), pp. 1–4
3. S. Vigneshwari, B. Bharathi, T. Sasikala, S. Mukkamala, A Study on the application of machine learning algorithms using R. *J. Comput. Theor. Nanosci. J. Comput. Theor. Nanosci.* **16**(8), 3466–3472 (2019)
4. T.P. Jacob, T. Ravi, *Optimization of Test Cases by Prioritization* (2013)
5. A.M. Posaonia, V.L. Jyothi, Xml document retrieval by developing an effective indexing technique, in *2014 6th International Conference on Advanced Computing (ICOAC)* (IEEE, 2014), pp. 120–123
6. W. Nie, P. Liu, K. Jia, H. Liao, X. Huang, Taxi license plate block detection based on complex environment, in *2018 IEEE 3rd International Conference on Image, Vision and Computing (ICIVC), Chongqing* (2018), pp. 81–85
7. A.M. Posaonia, D.V. Jyothi, Improving data access performance by reverse indexing. *Int. J. Eng. Technol. (IJET)* **7**(3) (2015)
8. G. Nagarajan, R.I. Minu, Wireless soil monitoring sensor for sprinkler irrigation automation system. *Wirel. Pers. Commun.* **98**(2), 1835–1851 (2018)

9. S.L. Shabu, C. Jayakumar, Detection of brain tumour by image fusion using genetic algorithm. *Res. J. Pharm. Biol. Chem. Sci.* **7**(5), 510–516 (2016)
10. S.P. Maniraj, P.S. Maran, Skin cancer-computer aided diagnosis by feature analysis and machine learning: a survey. *Indian J. Pub. Health Res. Dev.* **9**(6), 544–549 (2018)
11. H. Blickenstorfer, A. Menon, B. Omman, Detection and recognition of multiple license plate from still images, in *2018 International Conference on Circuits and Systems in Digital Enterprise Technology (ICCSDET), Kottayam, India* (2018)
12. S. Kalpana, S. Vigneshwari, Selecting Multiview point similarity from different methods of similarity measure to perform document comparison. *Indian J. Sci. Technol.* **9**(10), 1–6 (2016)
13. D.U. Nandini, S. Divya, A literature survey on various watermarking techniques, in *2017 International Conference on Inventive Systems and Control (ICISC)* (IEEE, 2017), pp. 1–4
14. K.C.M. Wang, J.-H. Liu, License plate recognition system, in *2015 12th International Conference on Fuzzy Systems and Knowledge Discovery (FSKD), Zhangjiajie* (2015), pp. 1708–1710
15. S. Jancy, C. Jayakumar, Pivot variable location-based clustering algorithm for reducing dead nodes in wireless sensor networks. *Neural Comput. Appl.* **31**(5), 1467–1480 (2019)
16. P.S., Maran, A.B., Bing, *Wind Energy Location Prediction between Meteorological Stations Using ANN* (2014)

A Weighted Frequent Itemsets Mining Algorithm for Intelligent Decision in Smart Systems



P. Gopinath Reddy, P. Avinash, and A. Velmurugan

1 Introduction

The key innovation is the keen buyer counsel Mining frameworks in data innovation plays an undeniably a significant job in the activities and dynamic [1, 2]. The weight judgment descending conclusion property for weighted successive items and the presence belongings of weighted regular subgroups are presented and illustrate first. In light of these two properties, the WD-FIM (Weight judgment Downward conclusion property-based Frequent Items Mining) measure is suggested to limit the glance through space of weighted incessant datasets and enhance the time productivity [3, 4]. Information mining is a rising procedure that tends to the issue of rebuilding the information into the helpful data [5]. The age skills are used in the area of instruction mining to declare the connectivity between different things [6, 7]. The Association Rule Mining is more utilized for creating information designs that uncovers the mix of occasions happening all the while dependent on the relationship among an enormous arrangement of information things [8, 9]. The Apriori calculation [3] is a well-known calculation for separating high regular itemsets from a database utilizing the predefined limit estimates, for example, least help and least confidence [10, 11]. In this paper, based on the weight judgment descending conclusion property, the E-FWARM (Enhanced Fuzzy-Based Weighted Association Rule Mining Algorithm)

P. G. Reddy · P. Avinash · A. Velmurugan (✉)
Department of Computer Science and Engineering, Sathyabama Institute of Science and Technology, Chennai, India
e-mail: velmurugan.cse@sathyabama.ac.in

P. G. Reddy
e-mail: gopidvbnd@gmail.com

P. Avinash
e-mail: avipotpally@gmail.com

algorithm is proposed to yields greatest continuous things, affiliation rules, exactness and least execution time[12–14].

The primary commitments of this paper are recorded as follows.

1. The weight discernment descending conclusion property and the presence belongings of weighted continuous subsets for unsure databases are presented and illustrated. The weight judgment descending conclusion property can be utilized to limit the glance through space of weighted continuous datasets. The presence property of weighted continuous subsets can guarantee all the weighted regular datasets be found.
2. The E-FWARM calculation is proposed to yield most extreme regular things, affiliation rules, exactness and least execution time.
3. A lot of investigations are led on both reality and manufactured datasets to assess the exhibition of the proposed E-FWARM calculation regarding runtime, number of examples and memory utilization.

2 Literature Survey

2.1 Introduction

When these things are completed, at that point of similar stage is to design out which working design and language can be used for building up the instrument [15, 16]. When the software engineers begin constructing the instrument, the inaugurator wants part of outer help [11, 17]. Some help can be taken from seniors [18]. The sort of working designing the undertaking has required, and what are on the whole the essential programming are expected to continue with the following stage, for example, building up the instruments, and the related tasks.

Title 1: IWFP: Interested Weighted Frequent Pattern Mining with Multiple Supports.

Creator: Xuyang Wei^{*}, Zhongliang Li¹, Tengfei Zhou¹, Haoran Zhang¹, Guocai Yang¹.

Affiliation rules mining has been under incredible consideration and considered as one of ground-breaking territory in information mining. Old-style affiliation rules mining approaches make verifiable presumption that items importance is the equivalent and set a solitary help for all things. This paper introduces an effective methodology for mining clients advantage weighted successive examples from a value-based database. Our worldview is to dole out proper least help (mins up) and weight for everything, which diminishes the quantity of superfluous examples. Besides, we additionally expand the help certainty system and characterize an intrigue measure to the digging calculation for exhuming clients' intrigued designs adequately. At last, it investigates both manufactured and genuine world datasets which show that the proposed calculation can create progressively intrigued designs.

Title 2: Discovery of Infrequent Weighted Itemset with High Utility.

Creator: Kalyani Tukaram Bhandwalkar¹, Mansi Bhonsle².

Information disclosure has been a fascinating region of research because of its different applications. Generally, visit design mining assumes a significant job. By and large, inconsistent things inside the dataset are disregarded. Rare dataset mining is a different continuous dataset mining where infrequently happening designs are found. Additionally, high-utility datasets are found spending growth calculation. Proposed framework considers the recurrence of the itemsets as well as considers the utility related with the itemsets.

Title 3: An Unreliability-locate address: Repeated Itemset Mining from Unreliability Data with dissimilar Item Importance.

Creator: Gangin Lee, Unil Yun¹ and HeungmoRyang.

Since itemset mining was proposed, different methodologies have been concocted, extending from handling simple item-based databases to managing progressively complex databases including arrangement, utility, or chart data. Particularly, as opposed to the mining approaches that procedure such databases containing careful nearness or nonattendance data of things, unsure example mining finds important examples from dubious databases with things' existential likelihood data. Nonetheless, customary questionable mining strategies have an issue in that it cannot make a difference significance of everything acquired from this present reality into the mining procedure. Right now, take care of such an issue and perform dubious itemset mining activities all the more proficiently, and we propose another unsure itemset mining calculation moreover considering significance of things, for example, weight imperatives. In our calculation, the two things' existential probabilities and weight factors are considered; thus, we can specifically acquire progressively significant itemsets with high significance and existential probabilities. Likewise, the calculation can work all the more rapidly with less memory by proficiently decreasing the quantity of estimations causing pointless itemset ages. Trial brings about this paper which shows that the proposed calculation is more proficient and adaptable than best-in-class strategies.

Title 4: Valency Based Weighted Association Rule Mining.

Creator: Yun Sing Koh, Russel Pears, and Wai Yeap.

Affiliation rule mining is a significant information mining task that finds connections among things in an exchange database. Most ways to deal with affiliation decide mining accept that all things inside a dataset have a uniform dissemination as for help. In this manner, weighted affiliation rule mining (WARM) was acquainted with give a thought of significance to singular things. Past ways to deal with the weighted affiliation rule mining issue expect clients to allot loads to things. This is infeasible when a large number of things are available in a dataset. Right now proposed a technique that depends on a novel valency model that consequently induces thing loads dependent on collaborations between things. Our experimentation shows that

the weighting plan brings about guidelines that better catch the regular variety that happens in a dataset when contrasted with an excavator that does not utilize such a weighting plan.

Title 5: Mining Weighted Frequent Itemsets without Candidate Generation in Uncertain Databases.

Creator: Jerry Chun-Wei Lin, Wensheng Gan, Philippe Fournier-Viger, Tzung-Pei Hong and Han-Chieh Chao.

Visit dataset mining is a key arrangement of procedures used to find helpful and important connections between things in exchange databases. In late decades, expansions of FIM, for example, weighted regular dataset mining.

3 System Architecture

3.1 Introduction

Arrangement is a different stage that represents around details design programming engineering, procedure details, measuring and so on... and an area between modules. The plan follow supplementary makes an expounding of the necessities; best investigation and fringe understanding move along. Programming configuration is at relatively inception time in its upset. In this way, programming plan strategy comes up short on the profundity, adaptability and quantitative nature that are regularly affix with progressively traditional building regulation. Anyway strategies for programming structures do leave, strategy to make element are adoptable and structure declaration can be applied.

4 Architecture Diagram

See Fig. 1.

5 Existing System

A hyperlinked structure-based calculation called UH-mine to mine successive examples from dubious information.

A tree-based mining calculation called UF-development which additionally builds a tree structure to store the substance of the questionable datasets, similar to its partner—the FP-development calculation for mining exact information.

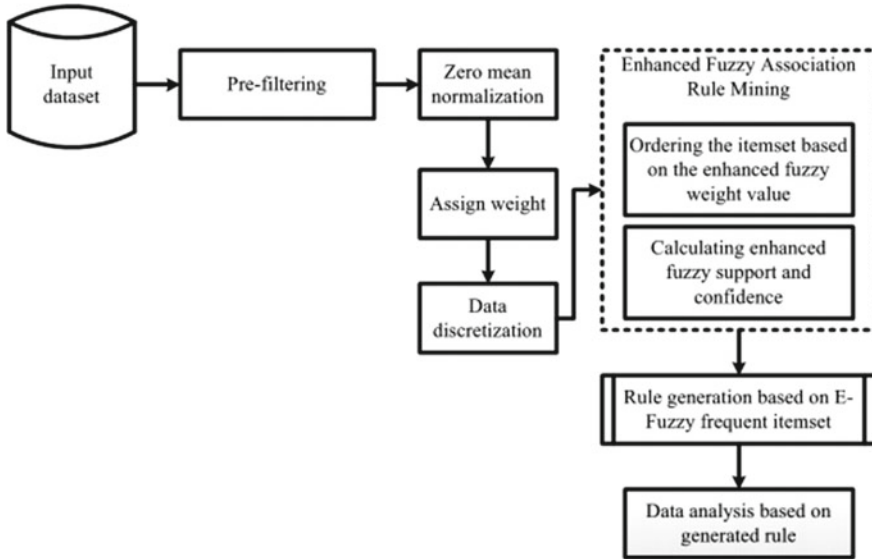


Fig. 1 Flow off the E-FWARM algorithm

AT-Mine is another tree-based productive methodology proposed to conquer the deadly issues of CUFP-Mine tree.

5.1 Disadvantages of Existing System

In the WDFIM strategy to utilizing to get low measure of mining itemsets.

- Low mining effectiveness and inclusion

5.2 Proposed System

We present an Enhanced Fuzzy-based Weighted Association Rule Mining (E-FWARM) calculation for effective mining of the successive itemsets. The prefiltering technique is applied to the info dataset to evacuate the thing having low difference.

Data discretization is performed, and E-FWARM is applied for mining the successive itemsets.

The proposed E-FWARM calculation yields greatest incessant things, affiliation rules, precision and least execution time than the current calculations.

5.3 *Advantages of Proposed System*

- Prediction accuracy is improved by using the association rules.
- Effective generation of the frequent itemsets and association rules is ensured by maintaining the feasibility of the neural network.

6 **Module Description**

6.1 *Project Modules*

- Registration module
- Sign-in module
- User module
- Admin module
- Frequent dataset module.

Register Module

This module is utilized for the client to enroll their login id by giving the negligible data. So they can login to the site.

Sign-in Module

Right now, login to the site by enrolled login id and a substantial secret key. Just the verified client can login and utilize the site.

Client module

Right now, separates itemsets which are every now and again united with a general rating better than expected.

Administrator Module

Right now, checks the thing list, include the things and evacuate the undesirable things.

Visit Dataset Module

We present an Enhanced Fuzzy-based Weighted Association Rule Mining (E-FWARM) calculation for effective mining of the incessant itemsets. The prefiltering technique is applied to the information dataset to evacuate the thing having low fluctuation.

7 Conclusion

So as to acknowledge keen dynamic in brilliant frameworks, a weight judgment descending conclusion property-based continuous itemset mining calculation is proposed right now tight the glance by space of weighted recurrent itemsets and enhance the time efficiency. The weight judgment descending conclusion property for weighted successive itemsets and illustrated first. In view of these two belongings, the WD-FIM calculation is portrayed in detail. Besides, the fulfillment and time.

References

1. Agarwal, A. Nanavati, N. Association rule mining using hybrid Ga-psofor multi-objective optimisation, *IEEE International Conference on Computational Intelligence and Computing Research (ICIC)*, (IEEE, 2016)
2. Vigneshwari, S. (2015). SEFOS: semantic enriched fuzzy based ontological integration of web data tables, in *2015 International Conference on Circuits, Power and Computing Technologies [ICCPCT-2015]*, (IEEE, 2015), pp. 1–4
3. R. Agrawal, R. Srikant, Fast algorithms for mining association rules, in *Proceedings of Proceedings of the 20th International Conference on Very Large Data Bases*, (Vldb, 1994), pp. 487–499
4. S. Jancy, C. Jayakumar, Packet level data compression techniques for wireless sensor networks. *J. Theor. Appl. Inf. Technol.* **75**(1) (2015)
5. A. Pravin, S. Srinivasan, An efficient programming rule extraction and detection of violations in software source code using neural networks, in *2012 4th International Conference on Advanced Computing (ICOAC)* (IEEE, 2012), pp. 1–4
6. S. Altuntas, T. Dereli, H. Selim, Fuzzy Weighted association rule based solution approaches to facility layout problem in cellular manufacturing system. *Int. J. Ind. Syst. Eng.* **15**, 253–271 (2013)
7. PS, Maran, AB, Bing, *Wind Energy Location Prediction Between Meteorological Stations Using ANN* (2014)
8. A.H. Azadnia, S. Taheri, P. Ghadimi, M.Z. Mat Saman, K.Y. Wong, order batching in warehouses by minimizing total tardiness: a hybrid approach of weighted association rule mining and genetic algorithms. *Sci. World J.* (2013)
9. A.M. Psonia, V.L. Jyothi, XML document retrieval by developing an effective indexing technique, in *2014 6th International Conference on Advanced Computing (ICOAC)* (Pp. 120–123) (IEEE, 2014)
10. S. Bandyopadhyay, S. Mallik, A. Mukhopadhyay, A survey and comparative study of statistical tests for identifying differential expression from microarray data. *IEEE/ACM Trans. Comput. Biol. Bioinf.* **11**, 95–115 (2014)
11. M. Bansal, D. Grover, D. Sharma, Sensitivity association rule mining using weight based fuzzy logic. *Global J. Enterp. Inf. Syst.* **9**, 1–9 (2017)
12. S.L. Janyshabu, C. Jayakumar, Multimodal image fusion using an evolutionary based algorithm for brain tumour detection (2018)
13. G. Nagarajan, K.K. Thyagarajan, A machine learning technique for semantic search engine. *Procedia Eng.* **38**, 2164–2171 (2012)
14. G. Nagarajan, R.I. Minu, V. Vedanarayanan, S.S. Jebaseelan, K. Vasanth, CIMTEL-mining algorithm for big data in telecommunication. *Int. J. Eng. Technol. (IJET)* **7**(5), 1709–1715 (2015)
15. Jacob, T. P., & Ravi, T. (2013). Optimization Of Test Cases By Prioritization.

16. D.U. Nandini, S. Divya, A literature survey on various watermarking techniques, in *2017 International Conference On Inventive Systems And Control (ICISC)* (IEEE, 2017), pp. 1–4
17. C.C. Aggarwal, P.S. Yu, A survey of uncertain data algorithms and applications, *IEEE Trans. Knowl. Dataeng.* **21**(5), 609–623 (2009)
18. G. Nagarajan, R.I. Minu, Wireless soil monitoring sensor for sprinkler irrigation automation system. *Wirel. Pers. Commun.* **98**(2), 1835–1851 (2018)

Activity-Based Attribute Selection for Effective Advertising Using Pattern Mining



R. B. Sarooraj and S. Prayla Shyry

1 Introduction

Advertisements are part of everyone's everyday life. Starting from ads in televisions to the ones in social websites, each one of the ads try and convince the user to start or continue using the product they are trying to sell [1, 2]. The products are of almost all varieties and price ranges [3, 4]. They try to attract all sections of society into using them. Technological growth in terms of Internet, computer sciences etc. has been vast over the past decade [5]. These evolutions have played a major role in almost all the industries [6]. It's no different in the advertising industry. With the growing use of Internet, the advertising industry had its breakthrough with the "sticky ads" [7]. With its help marketers could advertise their products not only in print media but also in websites that are frequently visited by customers [8, 9]. With customer viewability being a major question, the eye tracking technology helped in another breakthrough. The eye tracking technology uses infrared light source to predict the direction of gaze [10]. The centre of the eye, pupil centre, is tracked on relation to the corneal reflection [11]. The relative distance between the two areas allows the calculation of the direction of the gaze. With its speed accuracy and effectiveness, digital ads could now be classified as viewable and non-viewable ads [12]. Of all the digital ads, 50% are viewable. Of the 50%, many ads are not seen by people at all [13]. For an ad to be considered "viewed", at least half the creative of the ad must be viewed for "one second" as constituted by the Internet Advertising Bureau [14].

R. B. Sarooraj (✉) · S. P. Shyry
Department of Computer Science and Engineering, Sathyabama Institute of Science and
Technology, Chennai, India
e-mail: sarooraj@gmail.com

S. P. Shyry
e-mail: praylashyry.cse@sathyabama.ac.in

The amount of effort to be put in combined with the viewability of ads, make the success of an advertisement imperative and its failure could be the loss of millions of dollars [15]. To ensure the success of an advertisement, all the attributes of any ad like, “Seen Rate”, “Ad Brand”, “Tenure”, “Position”, “Usability”, must be taken into comparison and the most influential attributes must be filtered out [16]. These attributes then can be referred to while creating an ad to ensure high probability for the success of an ad, thus making the marketing of a product successful [17]. In this paper, we have used Data Analysis and its various types like Exploratory, Predictive and Linear Regression analysis to filter out the most influential attributes of an ad to make the ad a success. We have done Linear Regression on a Sticky Ad Data Set and we compared and evaluated various ads using them.

2 Related Work

Nowadays many marketers are trying to improve the efficiency of the advertisements they are creating. Thus, a lot of research has been done in the past few years on improving the sticky ads and their success rate. The financial aspect has also attracted potential research institutions to develop an efficient method in forecasting the behaviour of an advertisement based on its attributes and its values [18].

Earlier systems used standard excel sheet and its functions to represent a pictorial form of any data set in the form of pie chart, bar graphs etc. But this and any similar software are not intuitive enough to what the user wants to understand and don't provide an accurate reading of the data set. Moreover, software like excel sheet, could not possibly perform analyses by learning from its previous work, learning continuously, or in other words by applying machine learning algorithms [19]. Various time-series analyses have also been done in the past and various other fields like stock market prediction, energy saving systems have benefited from the same [20]. But they are quite complicated to reproduce and understand for any layman with limited knowledge about Data Science. Time-series analyses also uses extrapolation of data unlike regression which has interpolation of data. Time-series refers to an ordered series of data. Time-series models usually forecast what comes next in the series. But Regression can also be applied to non-ordered series where a target variable is dependent on values taken by other variables. These other variables are called as Features. When making a prediction, new values of Features are provided and Regression provides an answer for the Target variable. Thus, essentially, we can say that, Regression is a kind of interpolation technique [21]. Many predictive analyses like fraud analysis, client behaviour analysis also have been done in the past and in present on data sets of wide range and provided with results of extreme accuracy. One of the major challenges that is faced in predictive analysis is the multicollinearity. Multicollinearity is the inter-relation between any two or more attributes. Multicollinearity results in inaccuracy of the values which lead to wrong analyses results. There are various treatments that can be done to reduce the multicollinearity in any data set [22].

This may involve removing the data with any null attribute or using some method like Laplace smoothing. With more and more advertisements to be created in the coming years, more emphasis will be given to making the ads successful. This brings the analysed ads into more value since these ads provide the template to a perfect ad barring external physical condition. The eye tracking technology used by Sticky allows for collection of the perfect data set with emotions being recorded when the eyes see any and every part of various ads displayed on the screen. The related work exclusively on Sticky Ads is quite less though [23, 24].

3 Contribution

This paper provides an efficient method to predict the success of any Sticky Ad by using the data set collected from sticky.ai. With over 500 ads and 25 + attributes for each ad, the data set is quite vast and provides a deep insight to anyone interested on what makes a Sticky Ad success or a failure. With such Big Dataset, understanding them for any non-professional data scientist is very difficult. The paper provides a method to analyse such data sets and arrive at 4 or 5 of the most influential attributes of any advertisement. These attributes can then be taken care of while making a sticky ad by the client.

All the different types of analyses have sort of limitations and assumptions made for them to work. Linear Regression has few of them as well. They include homoscedascity, multicollinearity, goodness of fit, normality of dataset, etc.

There are certain plots or graphs available that tell the programmer about the goodness of fit and normality of dataset. They are scatter plot pp plot qq plot or histogram over normal curve. RStudio is used for most of the analysis done. Lot of libraries are available in RStudio for the specific purpose of analysing data. The output results can then be viewed in a R shiny application, which is an inbuilt code in RStudio. The R shiny application helps anybody to view the analysis done on the data set and come to conclusions they like.

The problem of multicollinearity is also easily solved by using the RStudio. Beta-coefficients, r -square and adjusted r -squared values are found between the variables themselves and the multicollinearity is checked between the variables. If its value is below 3, there is no need to do data cleaning.

R Shiny Application is an interactive tool provided by the RStudio. It helps the users to easily describe any analysis to clients and for their better understanding. Sticky Ad analysis is a very important task as it involves repercussions in the advertisement industry and thus has deep roots in the country's development. Software used for analysis in this paper is RStudio and for the interface an application, called R Shiny Application (Fig. 1).

RStudio:

See Fig. 2.

RStudio is a free open source software used for data modelling, graphical representation and data analysis. It has many libraries like cars, ggplot2 etc. In this paper

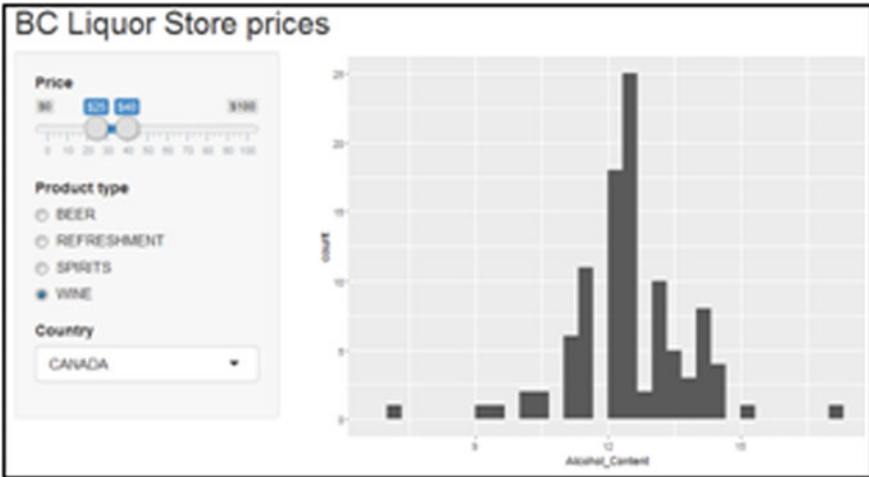


Fig. 1 R Shiny application

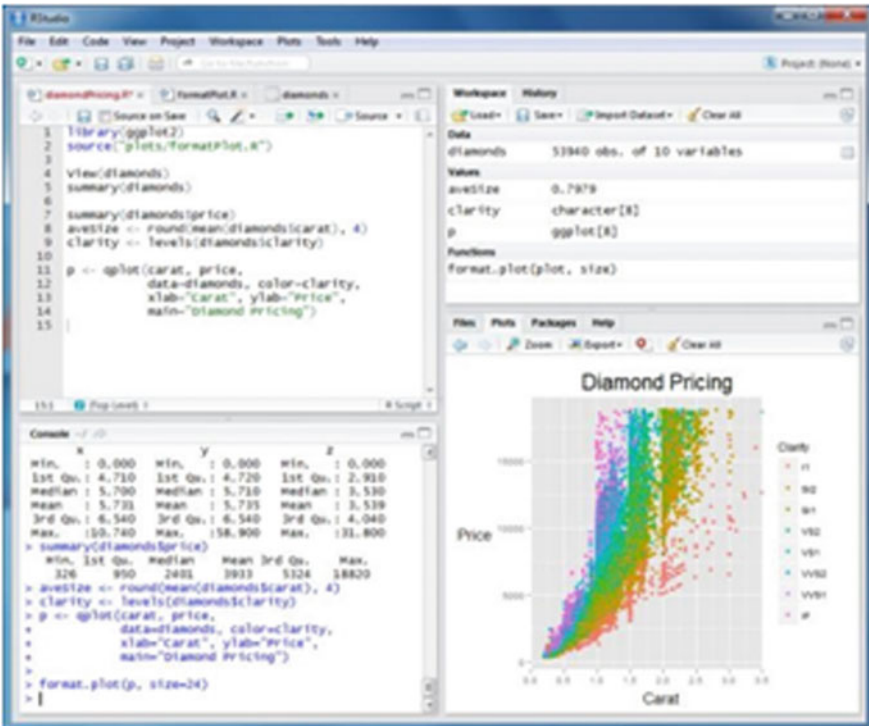


Fig. 2 R studio

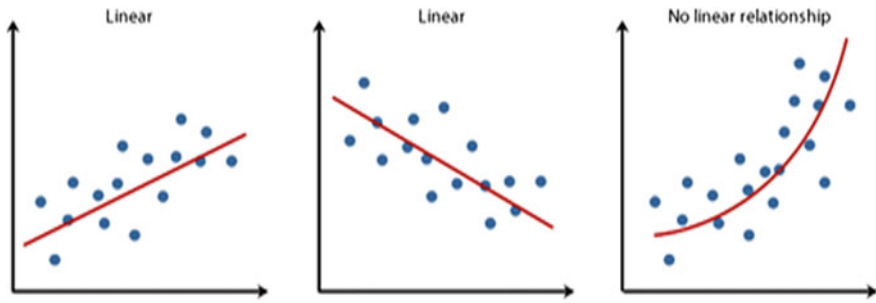


Fig. 3 X - Y plot

RStudio has been extensively used in all the analysis. It is very easy to use and for viewers it is very easy as an interface. It has many packages and inbuilt software like R Shiny Application, tidyverse, sparklyr etc. The RStudio has been preferred over Python or any other appropriate software due to the libraries and packages provided by R that are for the sole purpose of data analytics.

4 Mathematical Model

The X - Y plot is the main type of graph used to depict the regression analysis pp plot. The standard straight-line graph has the same equation $Y = mX + C$ (Fig. 3).

For any graph there must be a dependent variable and an independent variable. Similarly, for a pp plot, one of the axes must be independent variable. Any non-linear relationship cannot be described by linear regression.

5 Implementation

This paper has been developed from a series of codes written in RStudio for the data set of sticky ads and their attributes for its analysis. The data set contains over 500 different ads ranging over 10–15 different brands and categories. There are over 25 attributes for each advertisement. Once the data set was acquired, the first step was ordering the data set in terms of alphabetical order of ad category. In the RStudio the code for finding the beta-coefficients, the F-statistics value and the r -squared value are executed. Upon finding the r -squared value, the adjusted r -squared is also found (Fig. 4).

The adjusted r -squared value is a very important statistic. The r -squared measures the proportion of the variation in your dependent variable (Y) explained by your independent variables (X) for a linear regression model. Adjusted rsquared adjusts the statistic based on the number of independent variables in the model. With increasing

```
> ty$fstatistic
  value      numdf      dendf
39.96394    5.00000  549.00000
```

Fig. 4 F-statistics

number of independent variables, *r*-squared value tends to increase above 1, which is not desired. Thus, the adjusted *r*-squared value keeps its value constant with minimal variation. The *r*-squared value of the model is: 0.2668462 The adjusted *r*-squared value of the model is: 0.260169 There are 6 attributes among the 29 that influence the analytics of the data set the most. These are: ‘Seen’, ‘Tenure’, ‘Ad Location X’, ‘Ad Location Y’, ‘Usable rate’ and ‘Time To’. Once the important attributes are found, multicollinearity must be checked within these variables.

Seen:

See Fig. 5.

Time To:

See Fig. 6.

	vif.model.
Tenure	1.314518
Ad.location.y	1.287558
Ad.location.x	1.100369
Usable.rate	1.046794
Time.to	1.527807

Fig. 5 Seen

	vif.model.
Tenure	1.092656
Ad.location.y	1.212033
Ad.location.x	1.153066
Usable.rate	1.101336
SEEN	1.324293

Fig. 6 Time to

Fig. 7 Usable rate

	vif.model.
Tenure	1.352451
Ad.location.y	1.414991
Ad.location.x	1.141490
SEEN	1.296071
Time.to	1.573157

Fig. 8 Tenure

	vif.model.
Ad.location.y	1.401180
Ad.location.x	1.106893
Usable.rate	1.090403
SEEN	1.312199
Time.to	1.258350

Usable Rate:

See Fig. 7.

Tenure:

See Fig. 8.

Ad Location X:

See Figs. 9 and 10.

From the above multicollinearity comparison tables of attributes within each other, it is evident that none of the collinear statistics is more than 3. Thus, we can conclude that, the data set has no multicollinear attributes with each other, no data cleaning needs to be done. Since there is no multicollinearity among the data set, we can

Fig. 9 Ad Location X

	vif.model.
Tenure	1.308546
Ad.location.y	1.360246
Usable.rate	1.087980
SEEN	1.298538
Time.to	1.569839

	vif.model.
Tenure	1.350548
Ad.location.x	1.109048
Usable.rate	1.099602
SEEN	1.238842
Time.to	1.345391

Fig. 10 Ad location Y

proceed with the pp plot. The pp plot is the linear graph between expected probability and observed probability. The red line is the expected graph, and the dotted black line is the actual graph. Since there are no major variations between the two, we can conclude that the data set agrees with the expected output. This can be shown in the R Shiny application for the results. We can conclude from the implementation that, this paper has proposed a system, in which the comparison provides a very appreciable and an accurate result for the big data set of sticky ad analysis. Linear Regression model has been shown to be better than polynomial or RBF regression. It obviously follows due to Linear Regression’s simplicity in understanding that it is better than time-series analysis or any primitive Excel sheet analysis (Figs. 11, 12 and 13).

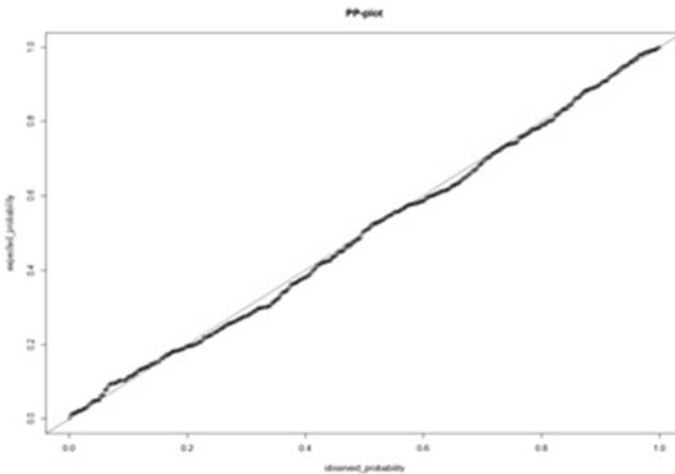


Fig. 11 PP plot

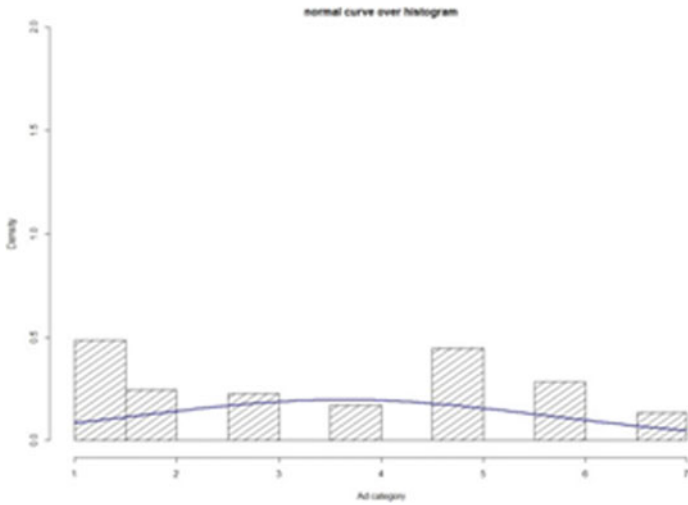


Fig. 12 QQ plot (histogram over normal curve)

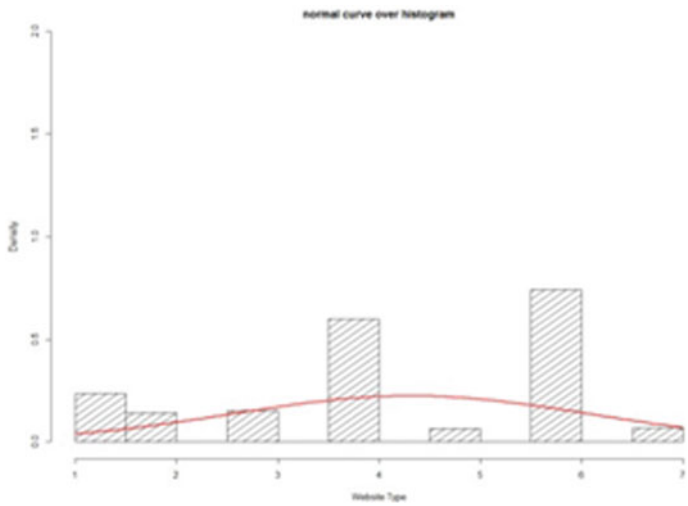


Fig. 13 QQ plot (histogram over normal curve)

6 Conclusion

Advertisements play an important role in everyone’s everyday life. The sticky ads are the new generation of ads in the Internet era. For any corporation, success of an ad means profits hitherto undreamt of. But for a sticky ad requires skill and precision. So, the success of an ad is imperative and for that success a template for a successful ad

will help any corporation in selling their products better. Linear regression analysis, using beta-coefficients, adjusted r -squared values, pp plot and histogram with normal curve has been done in this paper on the sticky ad data set. Multicollinearity issues has also been sorted in a simplistic way. The variation inflation factor or VIF values for the independent variables were found to be of acceptable range and thus correlation between the attributes was concluded to be little to nothing. We can conclude that this paper has proposed a system at par with all the available analysis which uses linear regression and predictive, exploratory analysis. The results were of expected accuracy and the pp plot showed that expected and observed probability were quite similar. Future enhancements can be made to this analysis with the help of other futuristic machine learning algorithms that could further improve the efficiency.

References

1. R. Saia, L. Boratto, S. Carta, A latent semantic pattern recognition strategy for an untrivial targeted advertising, in *2015 IEEE International Congress on Big Data*, (IEEE, New York, NY, 2015), pp. 491–498
2. D.U. Nandini, S. Divya, A literature survey on various watermarking techniques, in *2017 International Conference on Inventive Systems and Control (ICISC)* (IEEE, 2017), pp. 1–4
3. M. Huang, Z. Fang, S. Xiong, T. Zhang, Interest-driven outdoor advertising display location selection using mobile phone data. *IEEE Access* **7**, 30878–30889 (2019)
4. A.M. Posonia, D.V. Jyothi, Improving data access performance by reverse indexing. *Int. J. Eng. Technol. (IJET)* **7**(3) (2015)
5. L. Deng, J. Gao, An advertising analytics framework using social network big data, in *2015 5th International Conference on Information Science and Technology (ICIST)*, (Changsha, 2015), pp. 470–475
6. D. Tan, S. Liew, T. Tan, W. Yeoh, A feature selection model for binary classification of imbalanced data based on preference for target instances, in *2012 4th Conference on Data Mining and Optimization (DMO)*, (Langkawi, 2012), pp. 35–42
7. I. Bara, C.J. Fung, T. Dinh, Enhancing Twitter spam accounts discovery using cross-account pattern mining, in *2015 IFIP/IEEE International Symposium on Integrated Network Management (IM)*, (Ottawa, ON, 2015), pp. 491–496
8. Y. Yang, B. Padmanabhan, Segmenting customer transactions using a pattern-based clustering approach, in *3rd IEEE International Conference on Data Mining, Melbourne*, (FL, USA, 2003), pp. 411–418.
9. S.L. JanyShabu, C. Jayakumar, Multimodal image fusion using an evolutionary based algorithm for brain tumor detection (2018)
10. N. Vedulaet al., Multimodal content analysis for effective advertisements on YouTube, in *2017 IEEE International Conference on Data Mining (ICDM)*, (New Orleans, LA, 2017), pp. 1123–1128.
11. V. Ng, K-H. Mok, An intelligent agent for Web advertisements, in *Proceedings of the Third International Symposium on Cooperative Database Systems for Advanced Applications. (CODAS 2001)*, (Beijing, China, 2001), pp. 102–109
12. R. Yager, Ronald, Intelligent agents for world wide web advertising decisions. *Int. J. Intell. Syst.* **12**, 379–390 (1997)
13. G. Salton, *Term Weighting approaches in Automatic Text Retrieval*, Technical report COR-87–881, pp. 1–23, 1987.
14. B.W. Frakes, B.R. Yates, in *Information Retrieval: Data Structures and Algorithms*, (Prentice Hall PTR, 1992), pp. 102–160

15. D. Goldberg et al., Using collaborative filtering to wave an information tapestry. *Commun. ACM* **25**(12), 61–70 (1992)
16. T. Kahabka, K. Mari, G. Specht, GRAS: an adaptive personalization scheme for hypermedia databases, in *Proceedings of the Second Conference on Hypertext—Information Retrieval—Multimedia* (1997), pp. 279–292
17. H. He, E.A. Garcia, Learning from imbalanced data. *Knowledge Data Eng. IEEE Trans.* **21**, 1263–1284 (2009)
18. A. Pravin, S. Srinivasan, An efficient programming rule extraction and detection of violations in software source code using neural networks, in *2012 4th International Conference on Advanced Computing (ICoAC)* (IEEE, 2012), pp. 1–4
19. K. Pradeep, T.P. Jacob, Comparative analysis of scheduling and load balancing algorithms in cloud environment, in *2016 International Conference on Control, Instrumentation, Communication and Computational Technologies (ICCICCT)* (IEEE, 2016), pp. 526–531
20. G. Nagarajan, R.I. Minu, Wireless soil monitoring sensor for sprinkler irrigation automation system. *Wireless Pers. Commun.* **98**(2), 1835–1851 (2018)
21. S. Vigneshwari, SEFOS: semantic enriched fuzzy based ontological integration of web data tables, in *2015 International Conference on Circuits, Power and Computing Technologies [ICCPCT-2015]* (IEEE, 2015), pp. 1–4
22. N.N. Priyanka, N. Geetha, A.V.A. Mary, *Cross-Platform Recognition Of Unknown Identical Users In Multiple Social Media Networks* (2006)
23. S.P. Maniraj, P.S. Maran, Skin cancer-computer aided diagnosis by feature analysis and machine learning: a survey. *Indian J. Pub. Health Res. Dev.* **9**(6), 544–549 (2018)
24. P.S. Maran, A.B. Bing, *Wind Energy Location Prediction between Meteorological Stations Using ANN* (2014).

An Efficient Implementation of a Proposed Food Quality Ensuring Architecture Using Blockchain Technologies



P. Shiva Sujan, R. Ashok, Suja Cherukullapurath Mana, B. Keerthi Samhitha, and Jithina Jose

1 Introduction

In the late two decades, with the quick advancement of the economy and the constant improvement of individuals' expectations for everyday comforts, sanitation has progressively become the focal point of consideration and has been formed into an overall issue. Many disease outbreaks caused individuals to feel stressed. A few people even expected that all creature nourishment may have hormone and all plant nourishment may have poisons and colorant. This dread might be overcompensated; however, it likewise reflected numerous issues in the present nourishment generation, store network, and handling condition. Blockchain gives a useful answer for address a considerable lot of the confinements of customary IoT applications. Blockchain can guarantee IoT information trustworthiness without an outsider, while sparing transmission capacity and computational intensity of IoT devices. Besides, blockchain can give a protected and adaptable system for an IoT organization. Furnished with recognizable proof and confirmation capacities, blockchain can follow sensor information estimation and move information among IoT peers without a focal server. Moreover, blockchain can diminish the operational expense through the Internet of things. As, blockchain is risen as a regionalized open accord framework which keeps up the exchanged occasions which can be changeless, can't be distorted. Blockchain innovation is stood out past digital currency because of its capacity to give straightforward, secure, and dependable information in both private and open areas. The innovation depends on a disseminated record, which isn't possessed or constrained by a solitary substance. Information in the open record is noticeable freely and any

P. S. Sujan · R. Ashok · S. C. Mana (✉) · B. K. Samhitha · J. Jose
Department of Computer Science and Engineering, Sathyabama Institute of Science and Technology, Chennai, India
e-mail: cmsuja@gmail.com

© Springer Nature Singapore Pte Ltd. 2021
K. S. Sherpa et al. (eds.), *Advances in Smart Grid and Renewable Energy*,
Lecture Notes in Electrical Engineering 691,
https://doi.org/10.1007/978-981-15-7511-2_73

715

approved elements can present an exchange, which is added to the blockchain upon approval.

The benefit of blockchain innovation now is used in the food supply chain (FSC) for the improvement of computerized information trustworthiness that can be acquired as the product goes over various implementations of Food Safety Consortium and total nourishment item and perceptibility across various substances of the inventory network are being turned as the certainty through combination of BARCODE innovation infused with the blockchain built information the executives frameworks [1, 2]. Crucial advantages of infusing the information through blockchain involvement in FSC are: (1) ongoing following, detection nourishment items all through the FSC, and permitting distinguishing proof of key bottlenecks; (2) demoralizing contaminated of nourishment items and recognizing feeble connections on occurrence; (3) deciding the timeframe of realistic usability of nourishment items prompting diminished waste; (4) giving start to finish data to the purchaser; and (5) permitting explicit and focused on reviews. A test model of the BARCODE coordinated sensor is shown tentatively right now. The BARCODE coordinated sensor can be joined to a nourishment bundle to separate data with respect to the bundle along FSC.

Ongoing checking and nourishment value through and perceptibility of that high performing file, forestall flare-up and sustenance of ailments, financially propelled defilement, tainting, nourishment wastage because of misinterpretation of the marked expiry dates, and misfortunes because of deterioration, which impacts affect the nourishment security [3, 4]. So as to improve security and forestall wastage, present-day Internet of things built advances being used to screen the nourishment value then incrimination of perceptibility levels for obtained checked information. Now, we have various foundations of electronic observations (EAS), radio recurrence recognizable proof (BARCODE), and the code that is principally focused in programmed bundle. Be that as it may, the job of these advancements is restricted in distinguishing the nourishment bundle and does not give any data relating to the condition of the nourishment value. This restriction forestalls speedy expulsion of a blemished item from arriving at more elevated maximum values in FSC. Using the example, situation of value control slip can be recognized besides with FSC and organization to be compelled for the review of the nourishment items within a specific period of time, prompting the colossal financial misfortune that will be alleviated, accessibility nourishment bundle for individual value data coming through forthcoming focused reviews [5].

By writing, various detecting methods good with existing following and following foundation are proposed for checking nourishment items. BARCODEs may be obtrusive for checking the substantial assets in the nourishment [6].

In general, these sensors are expected to keep flawed items from arriving at the customers. Besides, BARCODEs can be useful for recognizing the ambiguity and improvements in FSC to achieve the maximum general proficiency [7]. Presently, efforts are being made to incorporate the BARCODEs to possible attributes. In addition, the gathered following just as detecting information is progressively unified and specifically utilized by explicit essentials used in Food Safety Consortium [8].

Purchasers should believe the behavior and nature of specific item through given date of expiry, with no extra information on its present value [9]. To move past a “pay-driven” to an “esteem-driven” production network, an increasingly decentralized methodology is required regarding information sharing [10]. In any case, a tradeoff exists between giving adequate data to the buyer about an individual item and simultaneously and following the fundamentals of the FSC.

2 Related Works

In numerous new inventions of the IoT, BARCODEs are being used prior because of its ease and little size to guarantee sanitation meeting the standards of the FSC [11]. As indicated by Food Safety Consortium, nourishment items that possess diminished time spans of usability show up out of the blue at a retailer, need ought to be given to offer those things to lessen the measure of nourishment wastage. In [12, 13], a point-by-point audit has been performed to talk about the capability of BARCODE innovation in calculated improvement of various parts for the FSC [14]. Be that as it may, the perceptibility of the nourishment items is constrained using measurement derived data distributed in between different production network level to the upcoming levels [15, 16]. Execution of blockchain innovations is giving non-modifiable advanced hint of the nourishment items in there specified living time along these lines matching through FSC unmistakable with everybody [17, 18]. The blockchain is introduced to build up the information board design to IoT gadgets. A deliberate review was acted in [19] to discover a computationally more affordable verification of work (PoW) for computationally lightweight IoT gadgets, for example, ease BARCODE labels. Be that as it may, bargaining the PoW would expand the weakness of the system design to noxious assaults [20]. For the discourse of this problem, a shrewd sharing and replacing contact controller framework are introduced in the gadget executives tending to problem of versatility [21, 22]. These gadgets do not connect with the blockchain organize legitimately yet through an administration center point, and hence, the information stockpiling and calculation undertakings are utilized to those administration center points [23].

This innovation is here to progress for a nourishment item in addition with production network utilizing diverse IoT-based innovation, for example, remote sensor organize (WSN), GPS, and BARCODE. Be that as it may, expansion of a solitary square in existing blockchain needs to experience broad calculation expending part of power. For instance, just Bitcoin’s yearly vitality utilization was tantamount to Ireland’s power utilization in 2014 [24]. Thus, executing the prevailing technology innovation to the standards of FSC is going to build working expense as well as the end nourishment item expense. The study of [25–27] don’t talk about how on keeping up the expense of nourishment items while executing the blockchain for FSC. The idea driving crypto technology reflects the shared faith dependent with the cryptographic Proof of Work procedure. A cryptographic proof for computing the PoW which is portrayed in [23] utilizing valuing capacities for controlled admission for

a mutual asset. This version with PoW is being enlarged using advanced marks with the record so as to maintain the chronicled reading morally sound using noxious onscreen characters in the system. The blockchain has numerous potential favorable circumstances, which made Bitcoin an effective electronic money or digital money. The essential preferences can be recorded as: (1) decentralized control and agreement; (2) exchange straightforwardness; (3) conveyed data; and (4) carefully designed as referenced in. A standard blockchain arrangement requires an accord calculation among the taking interest hubs to change over another data into a square and remember it for the current chain. There are various types of accord calculations separated from PoW, for example, evidence of-stake (PoS), assigned PoS (dPoS), verification of capacity among others. PoS utilizes accord dependent on the portion of partners instead of agreement of all hubs as in PoW.

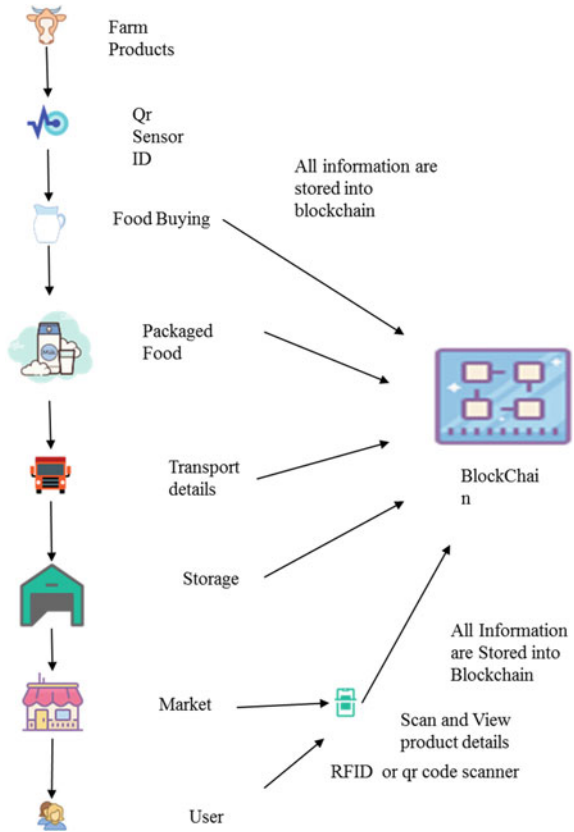
3 Existing System

In existing framework, the nourishment bundles do not contain the best possible subtleties like nourishment fixings, packers subtleties, bundle date, expiry date, and so forth. In this way, the end client or client does not have any familiarity with those item subtleties. That item has item id and shop data as it were. Ongoing observing of the nourishment value and perceptibility of that value record would forestall flare-up of nourishment-borne diseases, financially inspired debasement, pollution, nourishment wastage because of misguided judgment of the named expiry dates, and misfortunes because of decay, which affects the nourishment security.

4 Proposed System

So as to improve security and forestall wastage, present-day advanced IoT innovations must be screened to the nourishment value and increasing of perceptibility range of observed information. Detecting methods good with the existing following and the following foundation are proposed for observing nourishment items. These sensors can be obtrusive or non-intrusive in observing the physical or compound properties of nourishment, for example, pH, conductivity, and permittivity or the bundling condition, for example, temperature, stickiness, dampness or smell. By and large, these sensors are planned to keep flawed items from arriving at the customers. We should include all subtleties in blockchain like item purchasing spot and date, item fixings purchasing date, item bundling date, and so on. Blockchain innovation was proposed to improve the recognizability of a nourishment item. What is more, most significant we should utilize QR code scanner remote sensor for check the item and make sensor ID. Each bundled nourishment item with an installed sensor ID goes through various phases of exchanges at various terminals beginning from bundling through transportation, stockpiling lastly to a buyer for procurement. Information

Fig. 1 Overview of proposed system



square is made containing the data about the bundle at each substantial exchange. When the exchange is checked, the exchange of the sensor ID is changed over into a square of data and affixed to its prior information squares in this way shaping a chain of data squares and along these lines a blockchain (Fig. 1).

5 Functionality Descriptions

In the first module for every item, it contains the scanner tag number and its number will be going through nourishment API, and then fixings will be taken out by utilizing standardized identification number. First enrollment: The enrollment structure contains provider subtleties. At that point login, provider offers the items to all makes what the produce.

The maker at first makes the record. They will break down the crude materials and the maker will demand the amount of crude materials to the provider. At that point, providers will acknowledge the solicitation from producer and crude material

will be added to the maker stock. The assembling will send the item ID, expiry date, number of parcels, and so on, to the square chain, and afterward, the made item will be added to make shipment. From the square chain, the producer will recover the item.

In the distributor purchasing module, the enrollment part contains distributor subtleties. The distributor will be seeing the item in the producer truck and afterward purchasing item by the distributor will be added to the square chain. In the QR code verification and banking interface module the enrollment structure contains client subtleties. Buyer purchases the item from distributor. The shopper filter the QR examines by utilizing the portable application and afterward see the item in the versatile, for example, fabricating date, pressing date, etc. The buyer will check the item, and they will purchase the item by utilizing on the web exchange. At long last client exchange ID, item name and cost will be added to the square chain.

6 Results

This section shows some of the screen capture of actual implementation (Figs. 2 and 3).

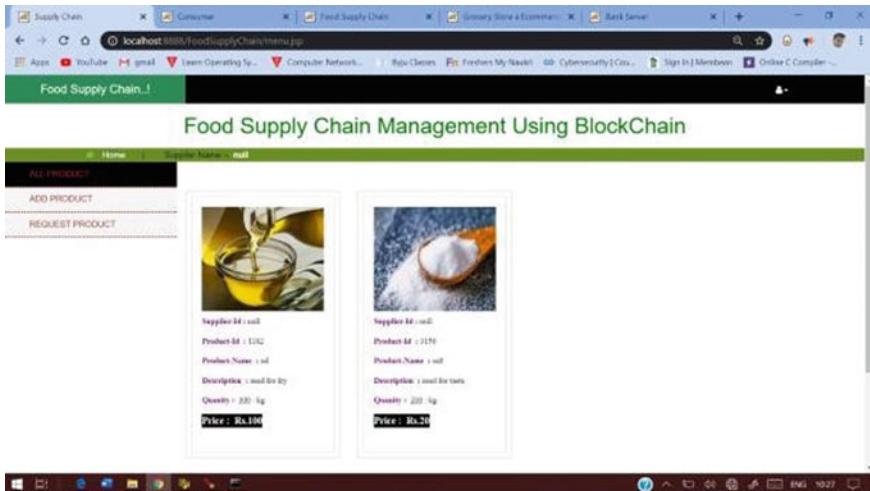


Fig. 2 Home page

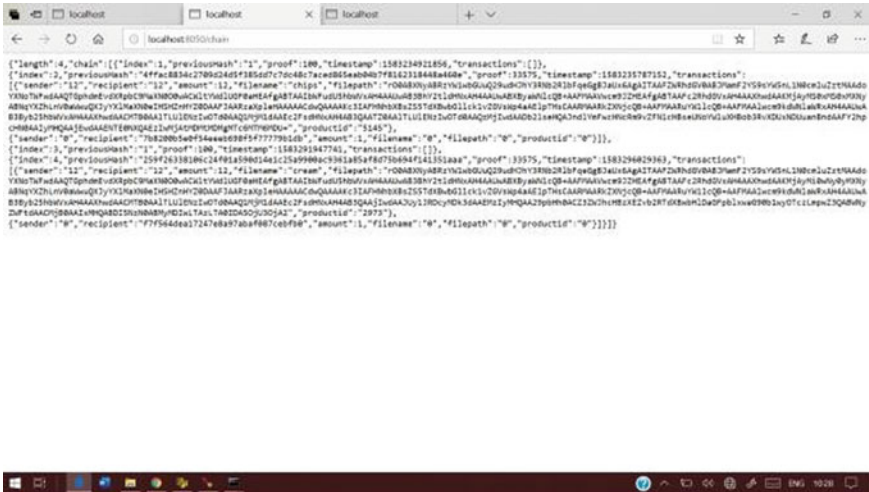


Fig. 3 Blockchain encrypted data

7 Conclusion

Blockchain innovation has been broadly applied in various administrations. The Internet of things (IoT) is getting universal in present-day life. Blockchain has given a down to earth answer for addressing huge numbers of the confinements of conventional IoT applications. The combination of the IoT and blockchain makes an undeniable and secure network. Thus, the primary point is to keep away from the nourishment debasement and make straightforward nourishment inventory network was accomplished effectively. An IoT-based FSC checking engineering has been proposed right now. Detecting methodology was incorporated with ID with a little impression for the following and value checking of the nourishment bundles. At the point when the nourishment bundles are examined at various retailers, co-ordinations, or capacity arrange inside the inventory network, the constant sensor information is refreshed in a blockchain giving a sealed advanced history. The security investigation demonstrated that the approval of a phony square is being reduced with a high range of hub cooperation with the system as well as different agreement phases. In any case, the security highlights will additionally be incremented with reinforcing of equipment security.

References

1. D.I. Ellis et al., Fingerprinting food: current technologies for the detection of food adulteration and contamination. *Chem. Soc. Rev.* **41**(17), 5706–5727 (2012)
2. Z. Pang, Q. Chen, W. Han, L. Zheng, Value-centric design of the Internet-of-Things solution for food supply chain: value creation, sensor portfolio and information fusion. *Inf. Syst. Front.* **17**(2), 289–319 (2015)
3. S. Herschdoerfer, *Value Control in the Food Industry*, vol. 2 (Elsevier, Cambridge, MA, USA, 2012)
4. J. Landt, The history of BARCODE. *IEEE Potentials* **24**(4), 8–11 (2005)
5. R. Saltini, R. Akkerman, Testing improvements in the chocolate traceability system: impact on product recalls and production efficiency. *Food Control* **23**(1), 221–226 (2012)
6. T.P. Jacob, A. Pravin, P. Asha, Arduino object follower with augmented reality. *Int. J. Eng. Technol.* **7**(3.27), 108–110 (2018)
7. W.-D. Huang et al., A passive radio-frequency pH-sensing tag for wireless food-value monitoring. *IEEE Sens. J.* **12**(3), 487–495 (2012)
8. E. Smits et al., Development of printed BARCODE sensor tags for smart food packaging, in *Proceedings of 14th Int. Meeting Chem. Sensors*, Nuremberg, Germany, 2012, pp. 20–23
9. K. Pradeep, T.P. Jacob, Comparative analysis of scheduling and load balancing algorithms in cloud environment, in *2016 International Conference on Control, Instrumentation, Communication and Computational Technologies (ICCICCT)* (IEEE, 2016), pp. 526–531
10. R.A. Potyrailo et al., Battery-free radio frequency identification (BARCODE) sensors for food value and safety. *J. Agricul. Food Chem.* **60**(35), 8535–8543 (2012)
11. C. Amador, J.-P. Emond, M.C.D.N. Nunes, Application of BARCODE technologies in the temperature mapping of the pineapple supply chain. *Sens. Instrum. Food Qual. Safety* **3**(1), 26–33 (2009)
12. S. Piramuthu, W. Zhou, *BARCODE and Sensor Network Automation in the Food Industry: Ensuring Value and Safety Through Supply Chain Visibility* (Wiley, Chichester, U.K., 2016)
13. C. Costa et al., A review on agri-food supply chain traceability by means of BARCODE technology. *Food Bioprocess Technol.* **6**(2), 353–366 (2013)
14. G. Nagarajan, K.K. Thyagarajan, A machine learning technique for semantic search engine. *Procedia Eng.* **38**, 2164–2171 (2012)
15. J. Virtanen, L. Ukkonen, T. Björninen, L. Sydänheimo, Printed humidity sensor for UHF BARCODE systems, in *Proceedings of IEEE Sens. Appl. Symp. (SAS)*, 2010, pp. 269–272
16. K.-H. Eom, K.-H. Hyun, S. Lin, J.-W. Kim, The meat freshness monitoring system using the smart BARCODE tag. *Int. J. Distrib. Sensor Netw.* **10**(7), 591812 (2014)
17. K.H. Eom, M.C. Kim, S. Lee, C.W. Lee, The vegetable freshness monitoring system using BARCODE with oxygen and carbon dioxide sensor. *Int. J. Distrib. Sensor Netw.* **8**(6), 472986 (2012)
18. S. Apte, N. Petrovsky, Will blockchain technology revolutionize excipient supply chain management? *J. Excipients Food Chem.* **7**(3), 76–78 (2016)
19. M. Conoscenti, A. Vetro, J.C. De Martin, Block chain for the Internet of Things: a systematic literature review, in *Proceedings of IEEE/ACS 13th International Conference on Computer Systems and Applications (AICCSA)* (2016), pp. 1–6
20. S. Vigneshwari, SEFOS: semantic enriched fuzzy based ontological integration of web data tables, in *2015 International Conference on Circuits, Power and Computing Technologies [ICCPCT-2015]* (IEEE, 2015), pp. 1–4
21. S. Underwood, Block chain beyond bitcoin. *Commun. ACM* **59**(11), 15–17 (2016)
22. O. Novo, Block chain meets IoT: an architecture for scalable access management in IoT. *IEEE Internet Things J.* **5**(2), 1184–1195 (2018)
23. F. Tian, An agri-food supply chain traceability system for China based on BARCODE and block chain technology, in *Proceedings of IEEE 13th International Conference on Network and Service Management. (ICSSSM)*, 2016, pp. 1–6

24. S.C. Mana, T. Sasiprabha, A study on various semantic metadata standards to improve data usability, in *2019 International Conference on Computational Intelligence in Data Science (ICCIDS)*, Chennai, India, (2019), pp. 1–4
25. F. Tian, A supply chain traceability system for food safety based on HACCP, blockchain and Internet of Things, in *Proceedings of International Conference on Service Systems and Service Management (ICSSSM)* (2017), pp. 1–6
26. S.C. Mana, B.K. Samhitha, J. Jose, V.S. Mydam, P.C.K. Reddy, Traffic violation detection using principal component analysis and viola jones algorithms. *Int. J. Recent Technol. Eng. (IJRTE)*. **8**(3) (2019). ISSN: 2277–3878
27. J. Jose, S.C. Mana, B.K. Samhitha, An efficient system to predict and analyze stock data using hadoop techniques. *Int. J. Recent Technol. Eng. (IJRTE)* **8**(2), (2019). ISSN: 2277–3878
28. S. Mondal, K.P. Wijewardena, S. Karuppuswami, N. Kriti, D. Kumar, P. Chahal, Block chain inspired RFID-based information architecture for food supply chain. *IEEE Internet Things J.* **6**(3), 5803–5813 (2019)

Fake Profile Detection in Facebook



S. Ranjana, Reshma Sathian, and Murari Devakannan Kamalesh

1 Introduction

In the present modern culture, web-based social networking assumes an essential job in everybody's life. The universally useful of web-based social networking is to stay in contact with companions, sharing news, and so on. The quantity of clients in online life is expanding exponentially. Instagram has as of late increased colossal prominence among online networking clients. With more than 1 billion dynamic clients, Instagram has gotten one of the most utilized online networking destinations [1]. After the development of Instagram to the web-based life situation, there has been gradual increase in the number of social media influencers. These Internet-based life influencers promote their business and products through social media [2]. Due to the broad utilization of Internet, it has become both an advantage and disadvantage for the public. Using social media for harming or bullying individuals, creating fake news is expanding rapidly. Counterfeit records are the significant wellspring of bogus data via web-based networking media. Business associations that put away immense sum of cash via web-based influencers must know whether the picked-up record is natural [3]. Thus, there is an across the broad requirement for a phony record recognition apparatus, which can precisely say whether the record is phony or not. Right now, use order calculations in AI to distinguish counterfeit records [4]. The way toward finding a phony record chiefly relies upon variables, for example, commitment rate and fake action.

These OSNs have rolled out an exceptional improvement in the manner, and we seek after our public activity [5]. Making new companions, staying in touch with them

S. Ranjana (✉) · R. Sathian · M. D. Kamalesh
Department of Computer Science and Engineering, Sathyabama Institute of Science and
Technology, Chennai, India
e-mail: ssranju1998@gmail.com

© Springer Nature Singapore Pte Ltd. 2021
K. S. Sherpa et al. (eds.), *Advances in Smart Grid and Renewable Energy*,
Lecture Notes in Electrical Engineering 691,
https://doi.org/10.1007/978-981-15-7511-2_74

725

and realizing their updates have gotten simpler. In any case, with the quick development of web-based life numerous issues like phony profiles, online pantomime has additionally grown [6]. There are no practical arrangements existing to control these issues. Fake records can be either human-produced, computer-generated (also alluded as “bots”), or cyborgs [7]. A cyborg is half-human, half-bot account [8]. Such a record is physically opened by a human; however, from that point onwards the activities are mechanized by a bot. To become individual from the OSN, the client needs to make his profile by entering data like name, photograph, date of birth, Email ID, graduation subtleties, work environment, old neighborhood, and interests. [9, 10]. A portion of the fields are required, and some are discretionary and it shifts from one OSN to the another. These sites are famous due to individuals’ enthusiasm for discovering companions, sharing pictures, labeling individuals in bunch photographs, sharing their thoughts and perspectives on normal themes, keep up great business relationship and general enthusiasm with others. Right now, thought of a structure in which programmed recognition of phony profiles is conceivable and is effective [11, 12]. This structure utilizes grouping strategies like support vector machine, random forest, and deep neural networks to characterize the profiles into phony or real classes [13]. As it is a programmed discovery strategy, it very well may be applied effectively by OSN which has a huge number of profile where profiles cannot be inspected physically [14]. We assess whether promptly accessible and designed highlights that are utilized for the fruitful identification, utilizing AI models.

2 Related Work

Informal organizations are getting increasingly famous in nowadays, and an ever-increasing number of individuals are speaking with companions, associates and family members. Individuals sharing their private data has been the reason for security and protection in social networks [15, 16]. Assailants and programmers are attempting in various manners to take and get the client’s qualifications and individual subtleties [17]. Intruders create fake accounts in order to illegally steal the users’ data, such accounts appear to be genuine. That is the principle perspective numerous analysts and associations are structuring various methods to shield the client from the assailants and spammers. Along these lines, Puttaswamy et al. [18] clarified the assaults of social crossing point were a productive and less exorbitant to get personal data of the any client [19]. Besides, Halim et al. [1] portrayed the technique to distinguish individuals those are engaged with malevolent exercises on Facebook. This method had two phases: In the first stage, semantic examination was performed to order the malevolent posts. In second stage, spatiotemporal examination was finished [20, 21]. At that point, the examination was done between the first companion diagram and the spatiotemporal chart [6, 22, 23]. In another examination, different social network stages like Facebook which give diverse protection settings to verify client’s close to home data in organize.

3 Problem Definition

Despite the fact that the majority of the interpersonal organizations have just included protection setting highlights for each post, notwithstanding, but any secured data can be stolen. Suppose a social media user has set e-security for an image to be viewed only by a set of selected companions and believe it to be secured. In any case, there is no assurance that the users' companion would not impart the image to any sort of group or individual without the knowledge of the user. The clients couldn't care less much about what they are sharing on interpersonal organizations and the security of their post, it tends to be very inconvenient for them. Overall advantages of online interpersonal organizations, there are numerous disservices data fraud which is probably the greatest worry of online informal communities. There are a great many phony profiles, which perniciously control or mischief others and the purpose behind this issue is that it is exceptionally basic and very quick to make and shape a phony profile by utilizing other's data or picture and utilize social designing methods to take data.

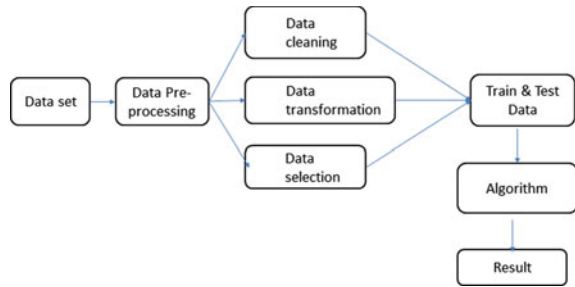
4 Existing System

The current system utilizes extremely less factors to choose whether a record is phony or not. The components to a great extent influence the manner in which dynamic happens. At the point when the quantity of components is low, the exactness of the dynamic is decreased altogether. There is an extraordinary improvement in counterfeit record creation, which is unrivaled by the product or application used to distinguish the phony record. Because of the progression in the production of phony record, existing techniques have turned out of date. The most widely recognized calculation utilized by counterfeit record recognition applications which is the random timberland calculation. The calculation has scarcely any drawbacks, for example, wastefulness to deal with the downright factors which have diverse number of levels. Likewise, when there is an expansion in the quantity of trees, the calculation's time proficiency endures a shot.

5 Proposed System

The proposed fake profile detection framework expects to locate the phony profiles in OSN dependent on information mining innovations that are exceptionally utilized. Here we can discover the phony profiles before we or anybody endure by the suspicious record. The application domain of the accompanying venture was community detection. Network recognition is vital to understand the structure of complex systems, and eventually extricating helpful data from them. Right now, thought of a

Fig. 1 Overview of the proposed system



structure through which we can recognize a phony profile utilizing AI calculations with the goal that the public activity of individuals becomes verified (Fig. 1).

6 Module Description

6.1 Data Collection and Preprocessing

Information assortment is the social event of assignment related data dependent on some focused on factors to break down and produce some important result. However, a portion of the information might be boisterous, for example, may contain off base qualities, inadequate qualities, or erroneous values. Hence, it is must to process the information before dissecting it and going to the results. Data pre-preparing should be possible by information cleaning, information change, information choice.

6.2 Data Cleaning, Transformation, and Selection

Data cleaning is the process of filling in the missing qualities, smooth boisterous information, distinguish or evacuate exceptions, and resolve inconsistencies. Data change may incorporate smoothing, conglomeration, speculation, change which improves the nature of the data. Data determination incorporates a few strategies or capacities which permit us to choose the valuable information for our framework.

6.3 Data Input

After finding the best algorithm, use that to predict the rate of fake profiles. Implement the algorithm and find the output.

7 Algorithm Implementation

7.1 Random Forest

Random forest is versatile method performing both classification and regression tasks [13]. It has nearly same hyperparameters as a decision tree or a bagging classifier. It creates multiple decision trees. The outcome with the highest vote will be used to predict identity deception. Each outcome from the classifier represents different section of a tree. The prediction which has higher number of votes is considered.

8 Results and Discussions

The algorithm is fed with a combination of fake user profiles and genuine user profiles for training. Then, a friend list is given as test data. The accuracy of the algorithm is calculated, and finally, the output is in the form of a heat map with the number of fake and genuine profiles in the given dataset (Figs. 2, 3, 4 and 5).

	id	name	screen_name	statuses_count	followers_count	friends_count	pages_like	followers
0	3610511	Davide Dellacasa	bradd	20370	5470	2385	145	52
1	5656162	Simone Economo	eKoeS	3131	506	381	9	40
2	5682702	tacone	tacone_	4024	264	87	323	16
3	6067292	alesaura	alesstar	40586	640	622	1118	32

Fig. 2 Uploading the training dataset

	statuses_count	friends_count	pages_like	followers	sex_code	lang_code
0	56	860	590	56	-2	1
1	33	1712	102	98	2	1
2	89	1569	890	45	-2	1
3	978	266	380	126	-1	2
4	38	193	10	85	0	1

Fig. 3 Selecting attributes and uploading test dataset

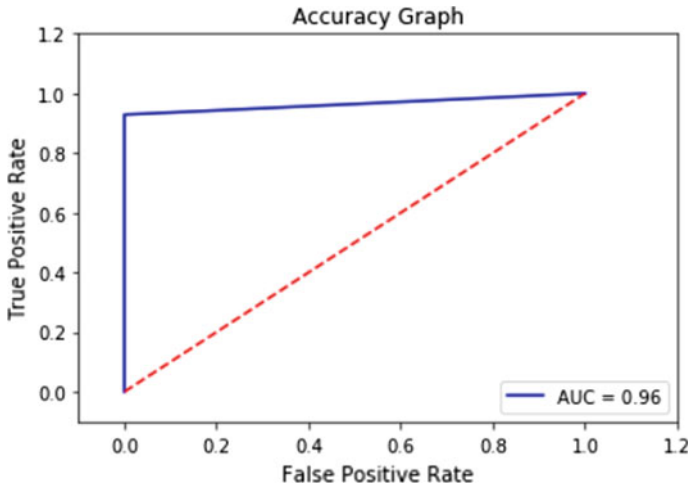


Fig. 4 Finding the accuracy of the algorithm

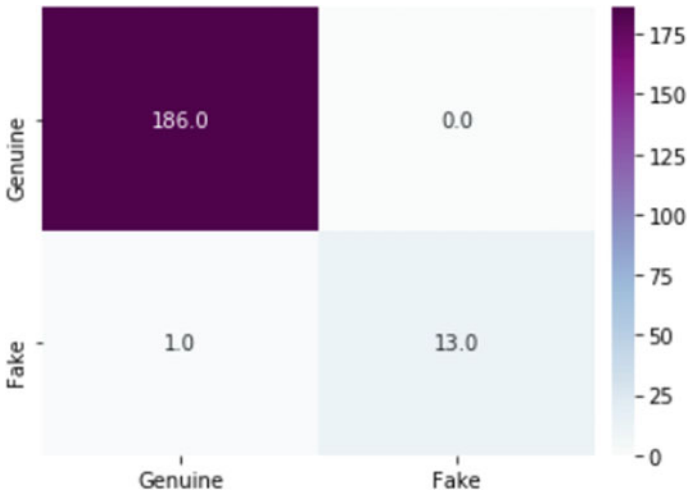


Fig. 5 Final output

9 Conclusion

In this research, we have presented a machine learning pipeline to detect fake accounts on online social networks by using random forest algorithm. Each profile in social network contains lot of information such as gender, friends, comments, education, work. The proposed fake profile detection system aims to find the fake profiles in Facebook based on data mining technologies that are highly employed. Random

forest algorithm is used to predict the fake profile rate in the given dataset. Based on that dataset, we can get the result using random forest algorithm to predict the result. Here we can also find out the accuracy rate of the prediction. It will be helpful for finding the fake profile rate.

References

1. Z. Halim, M. Gul, N. ul Hassan, R. Baig, S. Rehman, F. Naz, Malicious users' circle detection in social network based on spatiotemporal co-occurrence, in *2011 International Conference on Computer Networks and Information Technology (ICCNIT)*, pp. 35–390
2. T.P. Jacob, A. Pravin, P. Asha, Arduino object follower with augmented reality. *Int. J. Eng. Technol.* 7(3.27), 108–110 (2018)
3. K. Pradeep, T.P. Jacob, Comparative analysis of scheduling and load balancing algorithms in cloud environment, in *2016 International Conference on Control, Instrumentation, Communication and Computational Technologies (ICCICCT)* (IEEE, 2016), pp. 526–531
4. G. Nagarajan, R.I. Minu, Fuzzy ontology based multi-modal semantic information retrieval. *Procedia Comput. Sci.* **48**, 101–106 (2015)
5. S. Monisha, S. Vigneshwari, A framework for ontology based link analysis for web mining. *J. Theo. Appl. Inf. Technol.* **73**(2) (2015)
6. G. Nagarajan, R.I. Minu, A.J. Devi, Optimal nonparametric bayesian model-based multimodal BoVW creation using multilayer pLSA. *Circ. Syst. Sign. Process.* **39**(2), 1123–1132 (2020)
7. M. Fire, D. Kagan, A. Elyashar, Y. Elovici, Friend or foe? Fake profile identification in online social networks. *Soc. Netw. Anal. Min.* 1–23 (2014)
8. M.S. Rahman, T.K. Huang, H.V. Madhyastha, M. Faloutsos, Frappe: detecting malicious Facebook applications, in *Proceedings of the 8th International Conference on Emerging Networking Experiments and Technologies*, (ACM, 2012), pp. 313–324
9. S. Abu-Nimeh, T.M. Chen, O. Alzubi, Malicious and spam posts in online social networks. *Computer* **44**(9), 23–28 (2011)
10. Q. Cao, M. Sirivianos, X. Yang, K. Munagala, Combating friend spam using social rejections, in *IEEE 35th International Conference on Distributed Computing Systems*, (IEEE, 2015), pp. 235–244
11. K.P.N. Puttaswamy, A. Sala, B.Y. Zhao, Starclique: guaranteeing user privacy in social networks against intersection attacks, in *Proceedings of the 5th International Conference on Emerging Networking Experiments and Technologies, CoNEXT '09*. (ACM, New York, NY, USA, 2009), pp. 157–168
12. Y. Liu, K. Gummadi, B. Krishnamurthy, A. Mislove, Analyzing Facebook privacy settings: User expectations vs. reality, in *Proceedings of the 2011 ACM SIGCOMM Conference on Internet Measurement Conference*, (ACM, 2011), pp. 61–70
13. S. Mahmood, Y. Desmedt, Poster: preliminary analysis of google?'s privacy, in *Proceedings of the 18th ACM Conference on Computer and Communications Security*, (ACM, 2011), pp. 809–812
14. T. Stein, E. Chen, K. Mangla, Facebook immune system, in *Proceedings of the 4th Workshop On Social Network Systems*, (ACM, 2011), pp. 1–8
15. J. Kuzma, Account creation security of social network sites. *Int. J. Appl. Sci. Technol.* **1**(3), 8–13 (2011)
16. H. Kwak, C. Lee, H. Park, S. Moon, What is Twitter, a social network or a news media? in *International World Wide Web Conference Committee (IW3C2)*, (ACM, 2010), pp. 1–10
17. D. Debar, H. Wechsler, Using social network analysis for spam detection, in *Proceedings of the 3rd International Conference on Social Computing, Behavioral Modeling, and Prediction (SBP'10)*. (Springer, Berlin, Heidelberg, 2010), pp. 62–69

18. W.J. Cukierski, B. Hamner, B. Yang, Graph based features for supervised link prediction, in *IEEE International Joint Conference on Neural Networks (IJCNN)*, (IEEE 2011), pp. 1237–1244
19. G. Stringhini, C. Kruegel, G. Vigna, Detecting spammers on social networks, in *ACSAC '10: Proceedings of the 26th Annual Computer Security Applications Conference*. (ACM Request Permissions, 2012), pp. 1–9
20. M. Anwar, P.W. Fong, A visualization tool for evaluating access control policies in Facebook-style social network systems, in *Proceedings of the 27th annual ACM Symposium on Applied Computing*, (ACM, 2012), pp. 1443–1450
21. M. Rahman, T. Huang, H. Madhyastha, M. Faloutsos, Efficient and scalable socware detection in online social networks, in *Proceedings of the 21st USENIX Conference on Security Symposium 2012, USENIX Association*, pp. 32–32
22. M. Fire, G. Katz, Y. Elovici, Strangers intrusion detection detecting spammers and fake profiles in social networks based on topology anomalies. *ASE Hum. J.* **1**(1), 26–39 (2012)
23. F. Ahmed, M. Abulaish, An MCLBased approach for spam profile detection in online social networks, in *IEEE 11th International Conference on Trust, Security and Privacy in Computing and Communications* (2012), pp. 1–7

Intrusion Detection System Based on Secure Hashing Techniques



Obilineni Aparna, Padma Priyanka Kuncham, and A. Christy

1 Introduction

The sequence comparison rule of the algorithm that works to produce a convincing metric to demonstrate the degree of similarity between sequences of characters (i.e., strings) is currently thought in the main operations of written information of essential and very important strings. In recent decades, there are new technological advances in relation to the Internet business and distributed storage, which lead to large-scale information sets [1, 2]. Numerous cryptographic techniques, have the potential to preserve the key of the data, and therefore, the usability of the data is the only ones immediately different to obtain a secure outsourcing of the comparison of the sequences [3]. Character sequences are encrypted before outsourcing to the cloud service provider, and so on [4]. The comparison results are deciphered once sent by the cloud service provider. In an extremely fashionable period, companies and companies have already designed several encryption schemes, which constitute three categories: homomorphic coding, scattered circuits, and unconscious transfer [5]. The complicated machines of homomorphic coding techniques are prohibitively high, while the others simply divide a sequence of characters into two parts, so that they are sent individually to two servers within the cloud [6]. Presumably, these servers do not conspire with each other, and two-part secure PC protocols become transfer techniques in the other party's abuse. Security in an extremely multiserver

O. Aparna · P. P. Kuncham · A. Christy (✉)

Department of Computer Science and Engineering, Sathyabama Institute of Science and Technology, Chennai, India

e-mail: ac.christy@gmail.com

O. Aparna

e-mail: aparnaobilineni1999@gmail.com

P. P. Kuncham

e-mail: kunchampriyanka79@gmail.com

© Springer Nature Singapore Pte Ltd. 2021

K. S. Sherpa et al. (eds.), *Advances in Smart Grid and Renewable Energy*,

Lecture Notes in Electrical Engineering 691,

https://doi.org/10.1007/978-981-15-7511-2_75

model remains limited by the liability of the cloud service provider. A cloud server is working for the first time to produce a countable outsourcing service that preserves privacy to effectively resist collusion attacks from the cloud. With the preprocessing modules for artifacts, partitions, and extensions, it is not necessary to rewrite the subcontracted information throughout the comparison part of the non-interactive sequences [7]. The trusted authority sends the file to the type of cloud service provider for cloud storage. Subsequent key sets have been shown to have a range of fascinating properties that ensure the confidentiality of communication sessions against collusion attacks from different network nodes [8]. The nodes admitted to the universal public cloud outsourcing model, we tend to propose a general project for E-SC. This style is done by the superior user and, therefore, within the unqualified CSP. Its general system model, which has been indisputable for its security below the threat model, is simple and straightforward to implement [9].

2 Motivational Survey

Feng et al. [10] explained the reduction of the communication overload in the central trustee of the linear order of a series of users in the network who guarantee information, improve efficiency. They solved the problem of verifiable calculation of the outsourcing of sequence comparisons by integrating the confusion technique. Homomorphic cryptography circuit. He presented the formal analysis for the proposed construction [11, 12] a new secure outsourcing algorithm for modular exponential in first place in the single malevolent model. Compared to the latest generation algorithm, the proposed algorithm is fantastic both in terms of efficiency and verification capacity. Then, use this algorithm as a subroutine to obtain secure subcontracting encryption and signatures [13]. [14, 15] the development of applications that can only work on mobile devices without downloading calculations. The results show that applications based on Clone Clouds achieved a 21.2% improvement in performance over time. Wi-Fi-based connections offer high bandwidth and fewer delays than 3G. If both networks are available, the user uses Wi-Fi [16, 17]. Calculations distributed on a voluntary basis use additional processor cycles of Internet-connected personal computers. The resulting platforms provide computational power that is available only through the use of expensive clusters or supercomputers. They modified an algorithm that provides reasonable performance, most of the characteristics and, in many cases, all pairs of sequences that show statistically significant similarity according to the unmodified algorithm with reasonable levels of false positives [18].

Christy et al. [19] have proposed a keyword weighting function for document clustering. Each keyword in the sample is clustered based on the keyword weighting function. Experimental results were conducted with BBC news collection related to 5 domains and compared with K -means clustering and hierarchical clustering algorithms. It is shown that clustering followed by keyword weighting function has improved accuracy. Gandhi et al. described an interactive application analysis symptoms to diagnose, predict medical conditions, generate treatments and suggestions

based on the inputs provided by the user. In addition to that, the application tracks user's health activities like their step counts, sleep tracking, heart rate sensing, and other parameters and displays users their periodic health reports. It incorporates various fitness activities tracked and other factors like their age, gender, location, past medical records, and calories intake to perform a more accurate analysis [20, 21].

The microservice is a one of the service-oriented architecture that splits the monolithic architecture into small different services [22]. Prayla has come with novel monolithic architecture to design a pattern for biometric service. Here a biometric-based passport authentication system is generated wherein the physiological and biometric issues are collected and validated. All these services are treated as microservice and are interfaced with API [23]. Jesudoss et al. proposed an authentication model which protects against various number of security attacks. The main aim of the work is to provide unique authentication while satisfying security requirements [24]. Joseph Manoj et al. [25] proposed an access control model which provides the user with an effective means of preventing malicious users by calculating each user's trust value based on their behavior such as success rate, failure rate, access frequency, and transaction timeout. In web application, Roobini and Lakshmi [26] proposed a method by using algorithm such as ANN, naïve Bayes, KNN for the classification of Diabetes Mellitus.

3 System Architecture

The basic principle of this formula is the reallocation of characters compatible with the key auto-mutation. The useful life of a key is capable of the length of the key. This implies that any key state can only be responsible for encrypting a plaintext location equal to the length of that version of the key before the key is auto-mutated into a replacement version. This new edition may subsequently record a portion of the unencrypted text. The key entered by the user is divided into four separate "threads" of several perpetually mutant keys. These four totally different and completely different square keys are at the same time responsible for changing the plaintext letters one letter at a time to encrypted text in two different ways, for example, reallocation of the matrix and a form of "dynamic replacement encryption." This whole method is an eternity and, again, re-encodes a variety of times before the encrypted text is finished. The MD5 operation could be a cryptographic algorithm formula that accepts a discretionary length entry and produces a message of 128-bit long summary. The summary is also commonly known as the "hash" or "fingerprint" of the MD5 entry. It is used in various things wherever a doubtlessly long message needs to be processed and/or compared quickly. The common application is the creation and verification of digital signatures. The system architecture is depicted in Fig. 1.

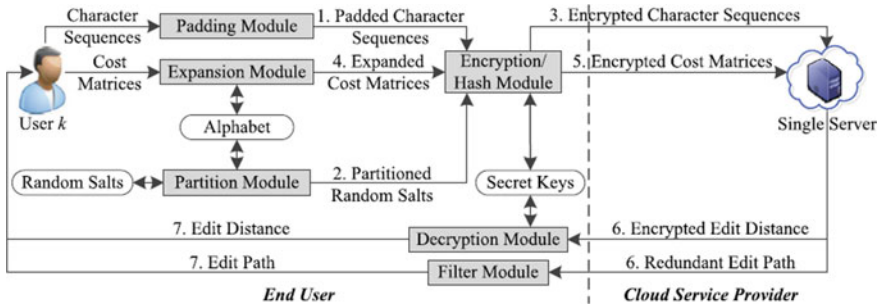


Fig. 1 System architecture

4 Modules

- Login Module
- Registration Module
- File Upload Module
- Intrusion Detection Module
- Detect Intruder Module.

Login Module This is the first activity, and the user must provide a correct contact number and password, which the user enters when registering, to access the application. If the information provided by the user matches the data in the database table, the user successfully accesses the application; otherwise, the login failed message is displayed and the user must reenter the correct information. It also provides a link to the registration activity for registering new users.

Registration Module A new user who wishes to approach the application must register before logging in. When you click the register button in the login activity, the registration activity opens. A new user registers by entering their full name, password, and contact number. A user must reenter the password in the password confirmation text box to confirm. When the user enters the information in all the text boxes, by clicking on the register button, the data is transferred to the database and the user is asked to log in again.

File Upload Module The owner of the data has no control over the data after uploading it to the cloud. In this form, the original data is encrypted in two different values. The data in each segment can be encrypted using the M3 encryption algorithm and the encryption key before storing it in the cloud.

Intrusion Detection Module In this module, receiver can find intrusion occurring or not using calculating a distance.

Detect Intruder Module In this module, the receiver can also detect the intruder. Intruder refers to another company that makes software for the original vendor’s product.

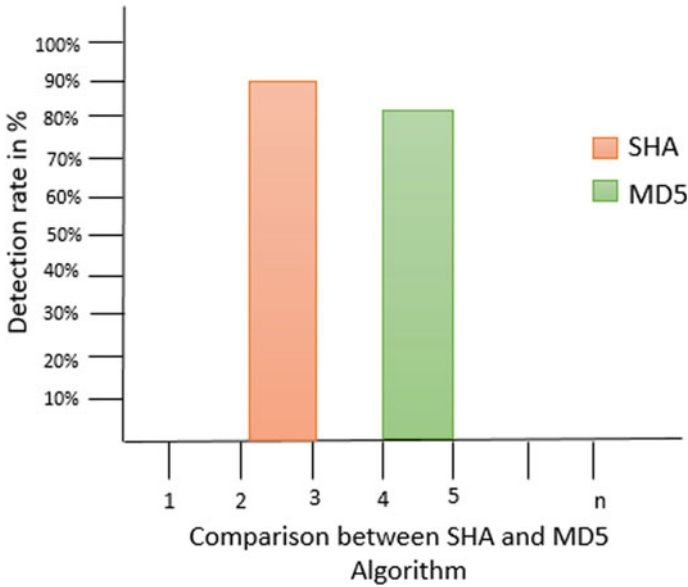


Fig. 2 Comparison between SHA and MD5 algorithm

5 Results and Discussion

Their experimental results using automatic learning of intrusion detection in the data show that the unlabelled samples belonging to low and high turbidity groups cause the main contributions to improve the accuracy of the intrusion detection system compared to the traditional one. The resulting key sets have been shown to have a set of preferable properties that ensure the confidentiality of communication sessions against collusion attacks from other nodes. The results are depicted in Fig. 2.

It is difficult to extend the work in our document to definite applications with multiple data sources. First, the two character sequences of different origins must be encoded with different keys, respectively. Second, three cost matrices need to be encoded together after being built by arbitration between the two parties. The goal of security is to accomplish the compare of sequences on an individual computer in the cloud to preserve privateness and assure that data written by the end user on both sides is not arbitrarily stolen by the other user or the CSP.

6 Conclusion

Through the above summary, due to trouble related to widespread collusion attacks in the secure outsourcing of sequential comparing algorithms, this document will present the reliable authority to authenticate users who have access to information

in the cloud. The trusted authority uses the SHA algorithm to generate the key and this key will be shared with the individual and the owner. The trusted authority module receives the file encrypted using the AES encryption algorithm from the data owner and calculates the hash value using the MD-5 algorithm. Stores the key in its database will be used during dynamic operations and to find out the part of the deception in the system. The trusted authority sends the file to the cloud service provider's form for cloud storage. The resulting key sets have been shown to have a set of desired properties that ensure the confidentiality of communication sessions against collusion attacks from other nodes in the network.

References

1. X. Chen, J. Li, J. Ma, Q. Tang, W. Lou, New algorithms for secure outsourcing of modular exponentiations. *IEEE Trans. Parallel Distrib. Syst.* **25**(9), 2386–2396 (2014)
2. R. Akimana, O. Markowitch, Y. Roggeman, Secure outsourcing of DNA sequences comparisons in a grid environment. *WSEAS Trans. Comput. Res.* **2**(2), 262–269 (2007)
3. M. Blanton, M.J. Atallah, K.B. Frikken, Q. Malluhi, Secure and efficient outsourcing of sequence comparisons, in *Proceedings of European Symposium on Research in Computer Security (ESORICS)*, Pisa, Italy, 2012, pp. 505–522
4. Y. Feng, H. Ma, X. Chen, H. Zhu, Secure and verifiable outsourcing of sequence comparisons, in *Proceedings of International Conference Information and Communication Technology-EurAsia*, Yogyakarta, Indonesia, 2013, pp. 243–252
5. S. Salinas, X. Chen, J. Li, P. Li, 'A tutorial on secure outsourcing of large-scale computations for big data.' *IEEE Access* **4**, 1406–1416 (2016)
6. X. Chen, J. Li, J. Weng, J. Ma, W. Lou, Verifiable computation over large database with incremental updates. *IEEE Trans. Comput.* **65**(10), 3184–3195 (2016)
7. R.J.R. Raj, Predicting the impact of climate change on Tidalzone Fishes using SVM approach, in *2nd International Conference on Intelligent Computing Communication and Convergence, ICCCC 2016*, Bhubaneswar, Odisha, India, 24–25 Jan 2016
8. T.P. Jacob, A. Pravin, P. Asha, Arduino object follower with augmented reality. *Int. J. Eng. Technol.* **7**(3.27), 108–110 (2018)
9. K. Pradeep, T.P. Jacob, Comparative analysis of scheduling and load balancing algorithms in cloud environment, in *2016 International Conference on Control, Instrumentation, Communication and Computational Technologies (ICCICCT)* (IEEE, 2016) (pp. 526–531)
10. Y. Feng, H. Ma, X. Chen, Efficient and verifiable outsourcing scheme of sequence comparisons. *Intell. Autom. Soft. Comput.* **21**(1), 51–63 (2015)
11. M. J. Atallah, J. Li, Secure outsourcing of sequence comparisons, in *Proceedings of International Workshop Privacy Enhancing Technology (PET)*, Toronto, ON, Canada, 2004, pp. 63–78
12. S. Jancy, C. Jayakumar, Pivot variable location-based clustering algorithm for reducing dead nodes in wireless sensor networks. *Neural Comput. Appl.* **31**(5), 1467–1480 (2019)
13. A.M. Poonia, D.V. Jyothi, Improving data access performance by reverse indexing. *Int. J. Eng. Technol. (IJET)* **7**(3) (2015)
14. M.J. Atallah, F. Kerschbaum, W. Du, Secure and private sequence comparisons, in *Proceedings of ACM Workshop on Privacy in the Electronic Society (WPES)*, Washington, DC, USA, 2003, pp. 39–44
15. D. Usha Nandini, R. Sathyabama Krishna, M. Nithya, R. Pavithra, A resourceful information collecting system using smart black box. *J. Comput. Theor. Nanosci.* **16**(8), 3346–3350 (2019)

16. D. Szajda, M. Pohl, J. Owen, B. Lawson, Toward a practical data privacy scheme for a distributed implementation of the Smith-Waterman genome sequence comparison algorithm, in *Proceedings of Network and Distributed System Security Symposium, NDSS*, San Diego, CA, USA, 2006, pp. 253–265
17. S.P. Maniraj, P.S. Maran, Skin cancer-computer aided diagnosis by feature analysis and machine learning: a survey. *Indian J. Pub. Health Res. Dev.* **9**(6), 544–549 (2018)
18. G. Nagarajan, K.K. Thyagarajan, A machine learning technique for semantic search engine. *Procedia Eng.* **38**, 2164–2171 (2012)
19. A. Christy, G.M. Gandhi, S. Vaithyasubramanian, Clustering of text documents with keyword weighting function. *Int. J. Intell. Enterp.* **6**(1) (2019). doi: <https://doi.org/10.1504/IJIE.2019.100029>
20. M. Gandhi, V.K. Singh, V. Kumar, IntelliDoctor—AI based medical assistant, in *2019 5th International Conference on Science Technology Engineering and Mathematics (ICONSTEM)*, Chennai, India, 2019, pp. 162–168
21. P.K. Rajendran, B. Muthukumar, G. Nagarajan, Hybrid intrusion detection system for private cloud: a systematic approach. *Procedia Comput. Sci.* **48**(C), 325–329 (2015)
22. Monisha, S., S. Vigneshwari, A framework for ontology based link analysis for web mining. *J. Theo. Appl. Inf. Technol.* **73**(2) (2015)
23. S. Prayla Shyry, Biometric-based three-tier Microservice architecture for mitigating the fraudulent behaviour, in eds. by S. Kundu, U. Acharya, C. De, S. Mukherjee, in *Proceedings of the 2nd International Conference on Communication, Devices and Computing, Lecture Notes in Electrical Engineering*, vol. 602. (Springer, Singapore, 2020).
24. A. Jesudoss, N.P. Subramaniam, EPBAS: Securing cloud-based healthcare information systems using enhanced password-based authentication scheme. *Asian J. Inf. Technol.* **15**(14), 2457–2463 (2016)
25. R. Joseph Manoj, M.D. Anto Praveena, M. Anvesh, M. Pujith, Secured user behaviour based access framework for web service. *IOP Conf. Ser. Mate. Sci. Eng.* **590**, 1–12 (2019)
26. M.S. Roobini, M. Lakshmi, Classification of diabetes mellitus using soft computing and machine learning techniques. *Int. J. Innovative Technol. Exploring Eng.* **8**(6S4) (2019)

Leveraging Affective Hashtags for Ranking Music Recommendations



M. Devi Priyanka, P. Renuka, and A. Christy

1 Introduction

The developing ubiquity of informal communities builds the accessibility of client conclusions, which has become a huge effect factor on purchasing choices, brand notorieties, and general suppositions [1]. Besides, prescribing relevant reports, records, and clients to follow has for quite some time been a most loved space for recommender frameworks inquire about [2]. A few new methodologies bridle ongoing small-scale blogging movement from administrations, for example, Twitter1, as the reason for recognizing client inclinations and separating significant substance to explicit individuals [3]. As of late, Twitter has become a fascinating wellspring of research movement because of the enormous measure of accessible client-created information [4]. Specifically Twitter licenses clients to share a sentence—called tweet—to the adherents, with a greatest length of 140 characters [5].

The awkward hushes, social attachment and correspondence, feeling guideline, and so forth [6]. From a full of feeling registering perspective, it is fascinating to examine the connection between a client's melodic inclination and the client's passionate state [7]. There have been numerous mental investigations on the job of

M. D. Priyanka (✉) · P. Renuka · A. Christy (✉)
Department of Computer Science and Engineering, Sathyabama Institute of Science and
Technology, Chennai, India
e-mail: priyankamalepati88@gmail.com

A. Christy
e-mail: ac.christy@gmail.com

P. Renuka
e-mail: renu17017@gmail.com

music in feeling guideline [8]. The passionate condition of an audience has additionally been considered as significant logical data in building recommender frameworks. A potential application is to manufacture a framework that screens individuals' feeling and predicts how to subliminally affect them by prescribing diverse music pieces [9]. However, as the enthusiastic condition of a client is difficult to catch in a huge scope study, most existing examinations are directed in a laboratory setting [10]. It stays hazy to which degree such discoveries can be summed up to the genuine use of music. Seeing the ubiquity of social smaller scale blogging sites, for example, opportunities to consider certifiable music listening conduct at scale [11]. Most curiously for our investigation, Twitter takes into consideration assembling purported now playing tweets, which tweets are portraying the track a client is presently tuning in to. One such model tweet is "now playing Crazy for You by Adele Happy." Right now, client not just distributes the music track and craftsman he/she is tuning in to, yet additionally includes a hashtag [12].

Seeing the notoriety of social microblogging sites, for example, Twitter1, we have new chances to consider real-world music listening conduct at scale. Most curiously for our investigation, Twitter takes into consideration assembling supposed #now playing tweets [13, 14], which are tweets portraying the track a client is right now tuning in to. One such model tweet is "#now playing Crazy For You by Adele #Happy" [15]. Right now, client not just distributes the music track and craftsman he/she is tuning in to, yet in addition includes a hashtag (i.e., watchwords or expressions beginning with the image depicting his/her simultaneous enthusiastic state. First, we propose to utilize, and look at the aftereffect of, two assessment errands to feature the significance of relevant data. For a given client and a unique situation, the principal task requires positioning the pertinence of a lot of tracks that are picked indiscriminately, while the subsequent errand requires positioning a lot of tracks that are known (from the preparation set) to be related with the client. While the principal task is chiefly about the general inclination of a client (i.e., which tracks a client might want), the subsequent assignment requires demonstrating the setting explicit inclination of a client for we definitely realize that all the up-and-comer tracks are enjoyed by the client yet just one of them can be positioned at top given that particular listening setting [16, 17]. A calculation cannot perform well on the off chance that it does not have the foggiest idea how a client's passionate setting influences their melodic inclination [14]. In correlation, existing work on setting mindful proposal for the most part centers around the calculations and essentially takes the full inventory of information in their assessment. Such an assessment technique does not recognize tracks that have been known to or not by clients, making it difficult to survey whether a calculation learns the general inclination or setting explicit inclination [18].

At long last, despite the fact that feeling-based music proposal is not new, existing work generally depends on client information gathered in a controlled situation and the scale is typically little [19]. Interestingly, our investigation depends on a huge assortment of Twitter information (around 560 K) that contain certifiable music listening data.

2 Related Work

Park et al. [20] By and enormous Web records, for instance, Google and Yahoo! Request, file significance for the given inquiry and thing master are two critical fragments of the situating system. Regardless, various information look for mechanical assemblies in Web business goals disregard thing expert in their situating systems. Somewhat, this may originate from the general difficulty of creating thing specialists due to the various characteristics of documents (or things) between Web business regions and the Web. Associations between reports in an online business site page routinely address relationship rather than proposition. For example, two chronicles (things) are related since both are made by a comparable association. We propose another situating procedure, which joins recommender systems with information check mechanical assemblies for better chase and scrutinizing. Our method uses a communitarian isolating count to deliver singular thing specialists for each customer and solidifies them with thing regions for better situating. To show our technique, we develop a model film Web crawler called MAD6 (Movies, Actors and Directors; 6 degrees of division).

Gediminas et al. [21] the importance of sensible information has been seen by researchers and experts in various requests, including Web business personalization, information recuperation, widespread and compact figuring, data mining, promoting, and the officials. While a noteworthy proportion of research has quite recently been acted in the region of recommender structures, most existing procedures revolve around endorsing the most appropriate things to customers without thinking about any extra sensible information, for instance, time, territory, or the association of others (e.g., for watching films or eating out). Right now, fight that material significant information makes a distinction in recommender systems and that it is imperative to think about this information while giving proposals. We look at the general thought of setting and how it might be exhibited in recommender systems. Besides, we present three particular algorithmic perfect models—important profiteering, post separating, and illustrating—for joining legitimate information into the recommendation system, inspect the possible results of combining a couple of setting careful proposition methodologies into a singular restricting together procedure, and give a logical examination of one such joined approach. Finally, we present additional capacities for setting careful recommenders and inspect indispensable and promising heading for future research.

Alena et al. [22] the essential drawback of any jargon-based idea examination system is the nonattendance of flexibility. Subsequently, right now, will depict procedures to normally make and score another end word reference, called Senti Ful, and develop it through direct synonymy relations and morphologic alterations with known lexical units. We propose to perceive four sorts of joins (used to decide new words) dependent upon the activity they play concerning feeling features: multiplying, exchanging, increasing, and crippling.

Adomavicius and Kwon [23] Recommender structures are twisting up dynamically crucial to particular customers and associations for giving redid proposals. In

any case, while the greater part of figurings proposed in recommender structures composing has focused on improving recommendation precision (as exemplified by the progressing Netflix Prize test), other indispensable pieces of proposition quality, for instance, the various assortment of proposition, have routinely been ignored. Right now, display and examine different thing situating techniques that can make recommendations that have altogether higher all out better than average assortment over all customers while keeping up comparative elements of proposition precision. Broad observational appraisal dependably shows the different assortment increments of the proposed methodology using a couple of genuine assessing datasets and unmistakable rating figure figurings.

Han et al. [24] Setting-based music recommendation is one of rapidly creating applications in the happening to ubiquitous time and requires multidisciplinary tries including low measurement feature extraction and music gathering, human inclination depiction and desire, cosmology-based depiction and proposition, and the establishment of relationship among them. Right now, contributed in three indisputable ways to deal with think about setting care in the music proposition field. Directly off the bat, we propose a novel inclination state progress appear to show human eager states and their advances by music. ESTM acts like an augmentation between customer condition information close by his/her inclination and low-level music features.

According to Christy et al. [25], feature selection plays an important role in knowledge discovery. Topic modeling plays a vital role in clustering documents. Clustering can be done by selecting good features obtained through Latent Dirichlet Allocation [14, 25]. Meeragandhi and Muruganantham proposed to estimate the influencers in a social media site using multi-criteria decision-making (MCDM) methods and compared the results. The proposed approach is more dynamic and capable of identifying the potential influencers preciously than using standard centrality measures, which are incapable to be applied in large-scale networks due to the computational complexity [19, 26]. Prayla et al. [27] have made an attempt to mitigate the botnet attacks by detecting the same in early stage. The real network is captured and they have used botminer algorithm with k -means and c -means clustering to detect the attacks. Their results have shown a remarkable result in the early detection [27, 28]. Jesudoss et al. proposed an image-based OTP for applications deployed in distributed environment. It protects Web applications against number of security attacks [29, 30].

3 Existing System

Existing framework utilizes manual intercession and utilization-based proposal. The suggestion of any assistance depends on the quantity of clients who previously mentioned comparable administrations on a similar segment. The outcomes were not constantly precise, as they are not considering the individual clients need on necessity. This framework expects that the mainstream music played by dominant part of individuals were useful for proposal.

4 Proposed Methodology

We propose a framework where the logical information of the client is considered for the suggestion. At the point when a client tweets about his intrigued music, as hashtag, he additionally expounds on his view. We attempt to dissect the estimation of the substance relating to the client. The opinion esteem and the melody the client is intrigued are viewed as together. The music is positioned dependent on the clients see and their assessment with architecture depicted in Fig. 1.

4.1 Data Collection and Preprocessing

We use Python language since it has tremendous assortment of AI libraries. First to peruse live tweet from Twitter, we have to utilize Twitter API for Python. To get to the Twitter server, we will utilize OAuth for verification. When we produce keys from Twitter server, we can utilize these keys to validate of program to get to Twitter server. We use search API to look through tweets dependent on relevant content.

4.2 Tweet Sentiment

We attempt to get the slant of the tweet. The tweets were cleaned for not English content and pictures. The hashtags were held in light of the fact that it will have some

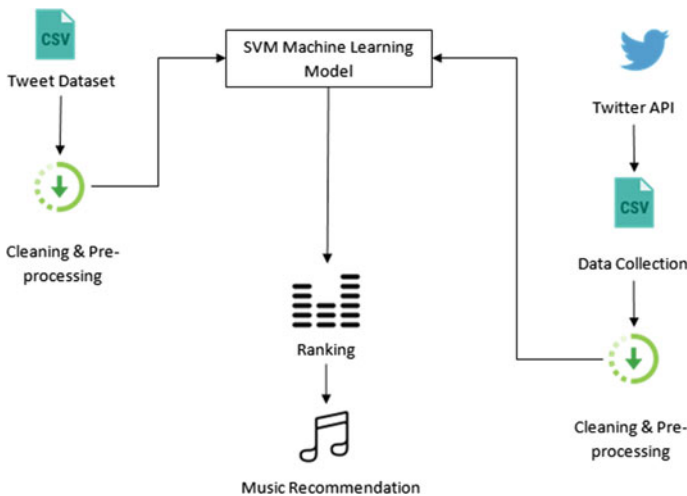


Fig. 1 System architecture

data. However, the hashtag might be a blend of more than single word. To part the words in the hashtag, we use word net as a lexicon and attempt to part the words part by part and examine with the word reference. When the hash labels were isolated, the conclusion examination is performed.

4.3 Ranking

The primary reason for positioning is to list the most appropriate tracks for the client on top. The primary structure hinders for figuring a positioning for a lot of suggestion up-and-comers are clients, tracks, and hashtags that are removed from the chart. We execute diverse positioning, like client-based positioning, track-based positioning, and Twitter labels-based positioning.

5 Conclusion

We have proposed another knowledge into music suggestion through an alternate methodology utilizing a clients feeling quanta. What we proposed depends on assessment scores dependent on the tracks, clients feeling through full of feeling hashtags like #nowplaying and the partner hashtags. We have proposed another knowledge into music suggestion through an alternate methodology utilizing a clients feeling quanta. What we proposed depends on feeling scores dependent on the tracks, clients feeling through emotional hashtags like #nowplaying and the buddy hashtags. Our technique is a novel strategy where we just utilize idle highlights from these hashtags. The fundamental procedure is positioning the tracks that are new to the client and furthermore doing likewise for the ones the client has tuned in to. For arbitrary tracks, we have discovered that looking at the idle highlights of the clients and errands has been fruitful. This is the general strategy that we propose. Also, our theory has been confirmed. For the last strategy, we have discovered that setting-based positioning, utilizing the outcomes widely prepared from the hashtags is all the more impressive and exact. Likewise, we have installed techniques for suggestions as per class. This generally builds the versatility of the procedure.

References

1. M. Schedl, The LFM-1b dataset for music retrieval and recommendation, in *Proceedings of ACM International Conference on Multimedia Retrieval*, (2016), pp. 103–110
2. G. Adomavicius, B. Mobasher, F. Ricci, A. Tuzhilin, Contextaware recommender systems. *AI Maga*. **32**(3), 67–80 (2011)

3. A. Karatzoglou, X. Amatriain, L. Baltrunas, N. Oliver, Multiverse recommendation: N-dimensional tensor factorization for context-aware collaborative filtering, in *Proceedings of ACM Recsys*, (2010), pp. 79–86
4. Y. Shi, M. Larson, and A. Hanjalic, “Collaborative filtering beyond the user-item matrix: A survey of the state of the art and future challenges. *ACM Comput. Surv.* **47**(1), 3:1–3: 45 (2014)
5. S. Rendle, Factorization machines with libFM. *ACM Trans. Intell. Syst. Technol.* **3**(3), 57:1–57:22, (2012)
6. B. Ferwerda, M. Schedl, Enhancing music recommender systems with personality information and emotional states: a proposal, in *Proceedings of Conference User Modeling, Adaptation, and Personalization*, (2014)
7. T.P. Jacob, A. Pravin, P. Asha, Arduino object follower with augmented reality. *Int. J. Eng. Technol.* **7**(3.27), 108–110 (2018)
8. R.L. Rosa, D.Z. Rodriguez, G. Bressan, Music recommendation system based on user’s sentiments extracted from social networks. *IEEE Trans. Consum. Electron.* **61**(3), 359–367 (2015)
9. D. Watson, R. Mandryk, An in-situ study of real-life listening context, in *Proceedings of Sound and Music Computing Conference*, (2012), pp. 11–16
10. D. Hauger, M. Schedl, A. Košir, and M. Tkalčič, The million musical tweets dataset: what can we learn from microblogs, in *Proceedings of the International Society for Music Information Retrieval Conference*, (2013)
11. M. Pichl, E. Zangerle, G. Specht, #nowplaying on #Spotify: leveraging Spotify information on Twitter for artist recommendations, in *Proceedings of the Workshop on Current Trends in WebEngineering*, (2015), pp. 163–174
12. K. Pradeep, T.P. Jacob, Comparative analysis of scheduling and load balancing algorithms in cloud environment, in *2016 International Conference on Control, Instrumentation, Communication and Computational Technologies (ICCICCT)*, (IEEE, 2016), pp. 526–531
13. E. Zangerle, M. Pichl, W. Gassler, G. Specht, #nowplaying music dataset: extracting listening behavior from Twitter, in *Proceedings of the International Workshop on Internet-Scale Multimedia Management*, (2014), pp. 21–26
14. B. Pang, L. Lee, Opinion mining and sentiment analysis. *Found. Trends Inf. Retrieval* **2**(1–2), 1–135 (2008)
15. G. Nagarajan, R.I. Minu, Wireless soil monitoring sensor for sprinkler irrigation automation system. *Wireless Pers. Commun.* **98**(2), 1835–1851 (2018)
16. T.V. Nguyen, A. Karatzoglou, L. Baltrunas, Gaussian process factorization machines for context-aware recommendations, in *Proceedings of ACM SIGIR*, (2014), pp. 63–72.
17. A. Neviarouskaya, H. Prendinger, M. Ishizuka, SentiFul: a lexicon for sentiment analysis. *IEEE Trans. Affect. Comput.* **2**(1), 22–36 (2011)
18. S. Vigneshwari, M. Aramudhan, An approach for ontology integration for personalization with the support of XML. *Int. J. Eng. Technol* **5**(6), 4556–4571 (2011)
19. E. Kouloumpis, T. Wilson, J. Moore, Twitter sentiment analysis: the good the bad and the OMG!, in *Proceedings of the Eighth International AAAI Conference on Weblogs and Social Media*, (2011), pp. 538–541
20. R.J.R. Raj, T. Sasipraba, Quality web services recommendation system based on enhanced personalised hybrid collaborative filtering approach, *Int. Rev. Comput. Software (I.R.E.C.O.S)*. **10**(3). ISSN 1828–6003 (2015). (Scopus Indexed)
21. G. Adomavicius, A. Tuzhilin, Context-aware recommender systems. Free University of Bozen-Bolzano. <https://doi.org/10.1609/aimag.v32i3.2364>
22. A. Neviarouskaya, H. Prendinger, M. Ishizuka, SentiFul: generating a reliable lexicon for sentiment analysis, in *2009 3rd International Conference on Affective Computing and Intelligent Interaction and Workshops*
23. G. Adomavicius, Y.O. Kwon, Improving aggregate recommendation diversity using ranking-based techniques, *IEEE Trans. Knowl. Data Eng.* **24**(5) (2012)
24. B.J.Han, S.Rho, S. Jun, E. Hwang, in *Music Emotion Classification and Context-Based Music Recommendation*. Published: 5 Aug 2009

25. A. Christy, A. Praveena, J. Shabu, A hybrid model for topic modelling using latent dirichlet allocation and feature selection method. *J. Comput. Theor. Nanosci.* **16**(8), 3367–3371 (2019)
26. G. Meeragandhi, A. Muruganatham, Potential influencers identification using multi-criteria decision making (MCDM) methods. *Procedia Comput. Sci.* **57**(2015), 1179–1188 (2015)
27. S.P. Shyry, A. Deepika, R. Subhashini, Efficient identification of bots by K-means clustering, in *Proceedings of the International Conference on Soft Computing Systems*, pp. 307–318, (2016)
28. R. Joseph Manoj, M.D. Anto Praveena, K. Vijayakumar, An ACO–ANN based feature selection algorithm for big data. *Cluster Comput.* **22**, 3953–3960 (2019)
29. A. Jesudoss, N.P. Subramaniam, EAM: architecting efficient authentication model for internet security using image-based one time password technique. *Indian J. Sci. Technol.* **9**(7), 1–6 (2016)
30. M.S. Roobini, Dr M. Lakshmi, Classification of diabetes mellitus using soft computing and machine learning techniques. *Int. J. Innovative Technol. Exploring Eng.* **8**(6S4) (2019). ISSN: 2278–3075

Awareness and Acceptability of Renewable Energy Products Across Demographic Factors



Rachana Rai, Neeta Dhusia, and Ajeya Jha

1 Introduction

Sikkim has been in news for being the first state in India to have officially announced adoption of organic farming [1] in the year 2003, where vegetables and fruits are grown without using pesticides. Globally, talks on healthy food, healthy air and healthy lifestyle have been taking rounds for the past years in a war-foot. Global citizens who are environmentally friendly have adopted altruism as a part of their lifestyle to make the world a better place to live. The need to adopt renewable energy pan globe is observed in the last few decades and Sikkim, which is the 22nd state of India with 610,577 [2] population; as of 2011, census has been adopting products of renewable energy. Various solar power plants are installed in government institutions in and around Sikkim, under the Jawaharlal National Solar Mission 2011–2012 [3].

Hence, researcher was keen on studying the current scenario surrounding the adoption of renewable energy in Sikkim even though its adoption in Sikkim is at nascent stage. Demographic factors are commonly used popular bases for segmenting people/groups while conducting research. Variables considered under demographic factors are age, gender, income, occupation, education, gender, nationality, race, religion and social class. It is believed that preferences of choice of product(s) differ with demographic factors.

R. Rai
Sikkim Central University, Gangtok, India
e-mail: rairach9@gmail.com

N. Dhusia · A. Jha (✉)
Sikkim Manipal Institute of Technology, Sikkim Manipal University, Gangtok, India
e-mail: ajeya.jha@smit.smu.edu.in

N. Dhusia
e-mail: neeta.s@smit.smu.edu.in

1.1 Literature Review

Any form of product awareness starts with effective promotional strategies adopted by companies. If the deciding factor of energy is not cost, then people may switch to renewable energy [4]. Variables such as image of the company and reliving childhood memories, consumption patterns of people and product characteristics may influence positive purchase attitude [5]. Young female(s) having high education and income were found to be more inclined towards green consumption and which, the researchers assumes, can be a new customer segment to sell green products [6]. Coming to adoption of environmental initiatives by tour operators, it was found that large tour operators were more willing to consider it as compared to self-catering tour operators [7]. Spreading information about products through word of mouth increases confidence while choosing product [8]. The literature review further helped the researcher to refine the study.

2 Methodology

Data for analysis were collected using structured questionnaire. Closed ended technique was used to remove errors from respondents. Collection of data took about 6 months. 600 filled and complete questionnaires were chosen for analysis. For segregating the data, Microsoft Excel Sheet was used, and for analysis, SPSS software version 20 was used.

2.1 Problem Definition

Awareness and acceptability related to renewable energy are negligible in the context of Sikkim. Though studies related to technical aspects of renewable energy have been consistent, awareness and reasons as to why people are not accepting are still at premature stage. Thus, researcher was motivated to find out the current state of awareness and acceptability of renewable energy in Sikkim which might further assist manufacturers and marketers to understand the underlying problems and maybe frame appropriate marketing strategies to enable its wide acceptance.

2.2 Objective

The main objective of the research is to find the current awareness level and acceptability related to solar water heater and solar lanterns in Sikkim.

2.3 Hypothesis

Based on the objective of the study, null hypothesis was generated.

H01: There are no significant differences across demographic factors vis-à-vis product awareness and acceptability.

A belief that people of Sikkim are aware and have accepted RE encouraged the researcher to find the actual scenario of the current period. Subsequently, to gain profound understanding and test the null hypotheses, subsidiary null hypothesis is generated.

H01_a: There are no significant differences in awareness of solar water heater across demographic factors.

H01_b: There are no significant differences in price awareness of solar water heater across demographic factors.

H01_c: There are no significant differences in rebuy intentions of solar water heater across demographic factors.

H01_d: There are no significant differences across demographic factors vis-à-vis product awareness of solar lantern.

H01_e: There are no significant differences across demographic factors in price range awareness of solar lantern.

H01_f: There are no significant differences across demographic factors in rebuy intentions of solar lantern.

3 Result and Discussions

Figure 1 shows that 531 respondents are aware of solar water heater, 159 respondents are interested to rebuy it, 47 respondents are aware of its price range and 17 respondents are aware of the brand name. Similarly, Fig. 2 shows that 501 respondents are aware of solar lanterns, 192 would rebuy it, 19 know where it is sold and the price range and only 6 are aware of the brand name. Brand names recalled by respondents are Sigma Solar, Rashmi, Jugnu Solar Lamps and Misotech. The following subsidiary null hypothesis discusses awareness of solar water heater across five demographic factors.

According to the data from Table 1, null hypothesis is rejected by demographic variables, such as marital status, area of residence, age of respondents and education level of respondents, whereas only monthly income of respondents as a demographic variable has accepted the null hypothesis.

Interpretation from Table 1 shows that respondents are aware of RE products which may be due to initiatives undertaken by the concerned state government as earlier solar water heater was distributed at subsidized rate. Awareness need not necessarily be very high as given by [9], stating that only 20% respondents were

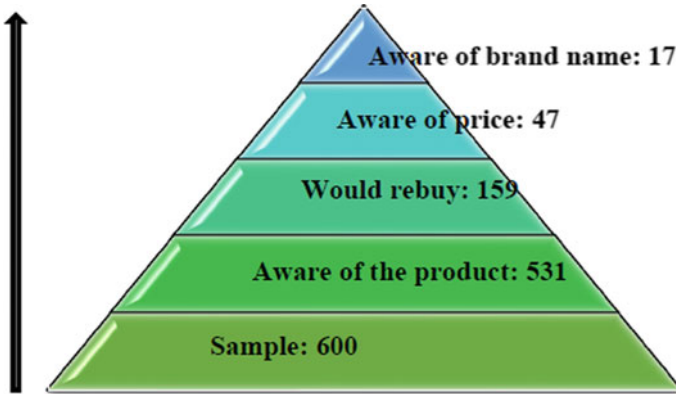


Fig. 1 Related to solar water heater



Fig. 2 Related to solar lanterns

aware of green building idea and 50% were aware of green building concepts. Result also shows that location influences product awareness; thus, manufacturers and policy makers may focus on both rural and urban sectors equally. Respondents from urban area are less aware of the product as compared to respondents from rural area as they may be comfortable using conventional energy due to easy availability. Results indicate that prospective buyers belong to age group of 15–45 years. Likewise, study based on Bhopal [9] inferred that potential buyers belonged to 18–35 years of age group. Hence, during product promotion and market segmentation, this age group may be considered. Subsequently, higher education is linked with higher health valuation [10]. But the result indicates that the income level has no association with respondents' awareness level. It is of utmost importance to spread awareness regarding the said products in order to convert potential users into actual users.

Table 1 Demographic factors and awareness level of solar water heater

Factors		Aware of SWH			Pearson chi-square	Asymp. sig	Null hypothesis				
		Aware	Unaware	Total							
Marital status	Unmarried	157	106	263	12.59	0	Reject				
		60%	40%	100%							
	Married	152	185	337							
		45%	55%	100%							
Area	Rural	71	104	175	16.21	0	Reject				
		41%	59%	100%							
	Sub-urban	144	94	238							
		61%	39%	100%							
	Urban	94	93	187							
		50%	50%	100%							
Age	15–25 year	95	78	173	18.41	0.001	Reject				
		55%	45%	100%							
	26–35 year	110	88	198							
		56%	44%	100%							
	36–45 year	54	49	103							
		52%	48%	100%							
	46–55 year	37	35	72							
		51%	49%	100%							
	Above 56 years	13	41	54							
		24%	76%	100%							
	Education	School level	91	73				164	15.63	0.001	Reject
			55%	45%				100%			
Graduate		87	94	181							
		48%	52%	100%							
Postgraduate		79	46	125							
		63%	37%	100%							
Others		52	78	130							
		40%	60%	100%							
Monthly income	Below ₹25,000	226	207	433	2.09	0.553	Accept				
		52%	48%	100%							
	₹25,001–₹50,000	61	64	125							
		49%	51%	100%							
	₹50,001–₹75,000	15	17	32							
		47%	53%	100%							
	₹75,001 and above	7	3	10							
		70%	30%	100%							

Null hypothesis is rejected by demographic variables, such as area of residence, age of respondents, education level of respondents and monthly income of respondents, whereas marital status as a demographic variable has accepted the null hypothesis. Solar water heater has merely captured domestic market in Sikkim, irrespective of subsidies provided by nodal agencies due to the cost being high. Thus, result based on Table 2 shows that there are no significant differences across marital status of respondents with being aware of price range of SWH. Researcher assumes that if nodal offices provide list of contingencies encountered while distributing renewable energy products, solutions may be suggested. Respondents believed that community must adopt more renewable energy sources. Diffusion of various benefits and incentives to customers might increase product acceptability of renewable energy. Researcher opines that convincing young people might be a challenging task, yet it might be workable with the help of appropriate policies. With a gradual technical advancement of such products, even urban population may be encouraged to use it;

Table 2 Demographic factors and awareness of price range of the product

Factors		Know price range of SWH		Total	Pearson chi-square	Asymp.sig	Null hypothesis
		Yes	No				
Marital status	Unmarried	26	237	263	2.73	0.098	Accept
		10%	90%	100%			
	Married	21	316	337			
		6%	94%	100%			
Area	Rural	10	165	175	14.03	0.001	Reject
		6%	94%	100%			
	Sub-urban	11	227	238			
		5%	95%	100%			
	Urban	26	161	187			
		14%	86%	100%			
Age	15–25 year	5	168	173	16.45	0.002	Reject
		3%	97%	100%			
	26–35 year	27	171	198			
		14%	86%	100%			
	36–45 year	8	95	103			
		8%	92%	100%			
	46–55 year	5	67	72			
		7%	93%	100%			
	Above 56 year	2	52	54			
		4%	96%	100%			

(continued)

Table 2 (continued)

Factors		Know price range of SWH		Total	Pearson chi-square	Asymp.sig	Null hypothesis
		Yes	No				
Education	School level	7	157	164	21.25	0	Reject
		4%	96%	100%			
	Graduate	10	171	181			
		6%	94%	100%			
	Postgraduate	22	103	125			
		18%	82%	100%			
Others	8	122	130				
	6%	94%	100%				
Monthly income	Below ₹25,000	28	405	433	28.51	0	Reject
		6%	94%	100%			
	₹25,001–₹50,000	9	116	125			
		7%	93%	100%			
	₹50,001–₹75,000	5	27	32			
		16%	84%	100%			
₹75,001 and above	5	5	10				
	50%	50%	100%				

thus, awareness of price may gradually increase. However, these products have not yet created a niche in Sikkim (Table 3).

Null hypothesis is rejected by demographic variables, such as marital status, area of residence, education level of respondents and monthly income of respondents, whereas only age of respondents as a demographic variable has accepted the null hypothesis. Respondent’s marital status has significant association with willingness to rebuy the product. The interest in buying the product needs to be supported by awareness of product benefits and place of purchase. Incentives, such as free trials, may be experimented in Sikkim in order to accelerate the acceptance of renewable energy technologies. The result shows that respondents from urban areas are more willing to buy RE products, whereas respondents from rural areas would prefer government subsidy. Respondents were not aware of the benefits of SWH as they preferred electric geysers and other sources of hot water. Focus must be on both users and non-users. Respondents, irrespective of their age, have no difference in repurchase of the products, which may be due to the ease of using conventional energy coupled with lack of interest in alternative clean sources of energy. Researcher found that more respondents were graduates, and result too indicated that their educational qualification had significant influence in repurchase decision. Researcher also assumes that similar economic and financial constraints are faced by respondents from Sikkim. 159 respondents were willing to rebuy SWH which is 26.5% of the

Table 3 Demographic factors and being interested to rebuy the product

Factors		Interested to rebuy		Total	Pearson Chi-Square	Asymp. sig	Null hypo thesis				
		yes	No								
Marital status	Unmarried	83	180	263	6.15	0.013	Reject				
		32%	68%	100%							
	Married	76	261	337							
		23%	77%	100%							
Area	Rural	36	139	175	74.81	0	Reject				
		21%	79%	100%							
	Sub-urban	31	207	238							
		13%	87%	100%							
	Urban	92	95	187							
		49%	51%	100%							
Age	15–25 year	51	122	173	9.46	0.051	Accept				
		29%	71%	100%							
	26–35 year	53	145	198							
		27%	73%	100%							
	36–45 year	30	73	100							
		30%	73%	100%							
	46–55 year	20	52	72							
		28%	72%	100%							
	Above 56 year	5	49	54							
		9%	91%	100%							
	Education	School level	16	148				164	70.31	0	Reject
			10%	90%				100%			
Graduate		50	131	181							
		28%	72%	100%							
Postgraduate		66	59	125							
		53%	47%	100%							
Others		27	103	130							
		21%	79%	100%							
Monthly income	Below ₹25,000	100	333	433	12.85	0.005	Reject				
		23%	77%	100%							
	₹25,001–₹50,000	42	83	125							
		34%	66%	100%							
	₹50,001–₹75,000	15	17	32							
		47%	53%	100%							

(continued)

Table 3 (continued)

Factors		Interested to rebuy		Total	Pearson Chi-Square	Asymp. sig	Null hypothesis
		yes	No				
	₹75,001 and above	2	8	10			
		20%	80%	100%			

total respondents. Considering the fact about lack of active promotional schemes, the number of rebuy still gives a promising figure for its acceptability.

Null hypothesis is rejected by demographic variables, such as marital status, area of residence, age of respondents and education level of respondents, whereas monthly income of respondents as a demographic variable has accepted the null hypothesis. Table 4 shows relation between respondent’s marital status and them being aware of solar lanterns, indicating that respondents are atleast aware of its existence. Researcher opines that being aware itself is a big leap towards the possible acceptance of RE. Solar lanterns may also be used in agricultural fields where farmers can cultivate vegetables early morning in order to sell it in the market as the demand for

Table 4 Demographic factor and being aware of solar lantern

Factors		Aware of solar lanterns		Total	Pearson chi-square	Asymp. sig	Null hypothesis
		Aware	Unaware				
Marital status	Unmarried	88	175	263	5.65	0.017	Reject
		33%	67%	100%			
	Married	83	254	337			
		25%	75%	100%			
Area	Rural	36	139	175	31.14	0	Reject
		21%	79%	100%			
	Sub-urban	98	140	238			
		41%	59%	100%			
	Urban	37	150	187			
		20%	80%	100%			
Age	15–25 year	51	122	173	31.64	0	Reject
		29%	71%	100%			
	26–35 year	75	123	198			
		38%	62%	100%			
	36–45 year	33	70	103			
		32%	68%	100%			
	46–55 year	6	66	72			

(continued)

Table 4 (continued)

Factors		Aware of solar lanterns		Total	Pearson chi-square	Asymp. sig	Null hypothesis
		Aware	Unaware				
Education	Above 56 year	8%	92%	100%	22.21	0	Reject
		6	48	54			
		11%	89%	100%			
	School level	24	140	164			
		15%	85%	100%			
	Graduate	64	117	181			
		35%	65%	100%			
Postgraduate	38	87	125				
	30%	70%	100%				
Others	45	85	130				
	35%	65%	100%				
Monthly income	Below ₹25,000	124	309	433	0.76	0.859	Accept
		29%	71%	100%			
	₹25,001–₹50,000	34	91	125			
		27%	73%	100%			
	₹50,001–₹75,000	9	23	32			
		28%	72%	100%			
	₹75,001 and above	4	6	10			
40%		60%	100%				

fresh vegetables are rising. Area of residence maybe considered as a possible market segmentation by marketers. If charging stations are set up, then it might attract people of Sikkim and may also provide the community with employment avenues, thereby instilling a desire to contribute in clean energy. Also, to further facilitate, if webinar and technical programmes are held periodically in Sikkim than the chances of spreading awareness may increase along with wide adoption of products of RE. Researcher infers that there is no significant difference across income of respondents and being aware of SL. But the result may vary with time and place of research.

Null hypothesis is rejected by demographic variables, such as age of respondents and education level of respondents, whereas marital status, area of residence and monthly income of respondents have accepted the null hypothesis. Products related to this sector must keep evolving with different pricing strategies which may be feasible in domestic market. Result from Table 5 shows no significant difference between area of residence with price awareness of SL and solar water heater. This is because solar lanterns have not yet set a firm ground in Sikkim, which makes it a less priority as there are other alternative products available. Involving all stakeholders is required. Respondents from Sikkim have significant difference between

Table 5 Demographic factor and being aware of price range of solar lantern

Factors		Know price range of SL		Total	Pearson chi-square	Asymp. Sig	Null hypothesis				
		Aware	Unaware								
Marital status	Unmarried	7	256	263	0.39	0.533	Accept				
		3%	97%	100%							
	Married	12	325	337							
		4%	96%	100%							
Area	Rural	7	168	175	3.91	0.142	Accept				
		4%	96%	100%							
	Sub-urban	10	228	238							
		4%	96%	100%							
	Urban	2	185	187							
		1%	99%	100%							
Age	15–25 year	0	173	173	29.25	0	Reject				
		0%	100%	100%							
	26–35 year	17	181	198							
		9%	91%	100%							
	36–45 year	2	101	103							
		2%	98%	100%							
	46–55 year	0	72	72							
		0%	100%	100%							
	Above 56 year	0	54	54							
		0%	100%	100%							
	Education	School level	1	163				164	8.96	0.030	Reject
			1%	99%				100%			
Graduate		9	172	181							
		5%	95%	100%							
Postgraduate		7	118	125							
		6%	94%	100%							
Others		2	128	130							
		2%	98%	100%							
Monthly income	Below ₹25,000	15	418	433	0.69	0.875	Accept				
		3%	97%	100%							
	₹25,001–₹50,000	3	122	125							
		2%	98%	100%							
	₹50,001–₹75,000	1	31	32							
		3%	97%	100%							

(continued)

Table 5 (continued)

Factors		Know price range of SL		Total	Pearson chi-square	Asymp. Sig	Null hypothesis
		Aware	Unaware				
	₹75,001 and above	0	10	10			
		0%	100%	100%			

price awareness and education level as shown in Table 5. Some of the respondents might have gained knowledge while they were pursuing their studies. Result shows that income level alone does not influence price awareness.

Null hypothesis is rejected by demographic variables, such as area of residence, age of respondents and education level of respondents, whereas monthly income and marital status of respondents as a demographic variable have accepted null hypotheses. Marital status of respondents has no significant difference with respondent's willingness to buy the product based on the result shown in Table 6. This enables researcher to assume that products of renewable energy might not be a priority for the respondents. Hence, promotion of this product can be done focusing on married couple assuming that they would eventually want a better and sustainable life for their family in future. The person who supports the idea of wind power opposes the construction of wind farm, thereby creating a 'gap' between public support and private behaviour. Similarly, irrespective of where respondents are residing, they have significant difference with the purchase intention of SL. As mentioned in the previous discussions, involving local community in the projects since inception may trigger the need of the product. It is recommended to have such projects in the areas where consumers reside. This may lead to greater acceptance of such products. Similar result from Table 6 shows that age of respondents affects their choice of buying products of renewable energy. This finding may help manufacturers and marketers to include young individuals as a protagonist in advertisements and entice potential customers to buy and use the product. Researcher assumes that the more educated an individual is, their perspective gradually widens in terms of adopting new lifestyle (adopting new products). Referring to Table 6, it is found that income level has no significant difference with purchase decision of respondents. Respondents earning between ₹50,001–₹75,000 have high mean value for not being interested in purchasing SL. Researcher during data collection observed that respondents do not associate any need for buying SL which requires in-depth reasons for future study. Respondents were upright ready to rebuy the product which directly shows the acceptability regarding solar lantern.

Table 6 Demographic factors and being interested to rebuy solar lantern

Factors		Interested to rebuy SL		Total	Pearson chi-square	Asymp.sig	Null hypothesis				
		Yes	No								
Marital status	Unmarried	43	220	263	1.04	0.308	Accept				
		16%	84%	100%							
	Married	66	271	337							
		20%	80%	100%							
Area	Rural	71	104	175	16.21	0	Reject				
		41%	59%	100%							
	Sub-urban	144	94	238							
		61%	39%	100%							
	Urban	94	93	187							
		50%	50%	100%							
	Age	15–25 year	95	78				173	18.41	0.001	Reject
			55%	45%				100%			
26–35 year		110	88	198							
		56%	44%	100%							
36–45 year		54	49	103							
		52%	48%	100%							
46–55 year		37	35	72							
		51%	49%	100%							
Above 56 year		13	41	54							
		24%	76%	100%							
Education		School level	91	73	164	15.63	0.001	Reject			
			55%	45%	100%						
	Graduate	87	94	181							
		48%	52%	100%							
	Postgraduate	79	46	125							
		63%	37%	100%							
	Others	52	78	130							
		40%	60%	100%							
Monthly income	Below ₹25,000	226	207	433	2.09	0.553	Accept				
		52%	48%	100%							
	₹25,001–₹50,000	61	64	125							
		49%	51%	100%							
	₹50,001–₹75,000	15	17	32							
		47%	53%	100%							

(continued)

Table 6 (continued)

Factors		Interested to rebuy SL		Total	Pearson chi-square	Asymp.sig	Null hypothesis
		Yes	No				
	₹75,001 and above	7	3	10			
		70%	30%	100%			

4 Implications and Recommendations

- i. Manufacturers along with policy makers and promoters may propose an attractive incentive to potential customers and choosing appropriate market intermediaries in selling renewable energy products.
- ii. The focus on demographic variables must be noted as it facilitates facts regarding possible adoption of products of renewable energy. Some result shows a positive purchase intention of respondents, which may be considered as battle half won by policy makers and manufacturers.
- iii. Concerned government needs to play an active role in sales promotion in order to convert potential customers into the existing customers. Researcher assumes that if testimony of satisfied customers is aired on television and on radio, then it may trigger curiosity and likeliness to adopt products of renewable energy.
- iv. Initial cost of RE products and banks providing financing schemes for the same may be taken seriously as this was pointed out even in other research as well, such as feed-in-tariffs and soft loans. Policy makers and manufacturers may work together with banks (private and public sector) by providing incentives to banks providing soft loan.

5 Conclusion

Understanding the problems and prospects of RE products might enable manufacturers, policy makers and marketers to attack on the root cause and further enhance the probability of converting prospective customers to present customers in Sikkim. When every household consciously starts using solar water heater and solar lantern, then the consumption of conventional energy might be under control. Demographic factors might enable manufacturers and policy makers to identify prospective customers and adequately frame an effective marketing strategy which might convert their awareness level into acceptance and adoption of solar water heater and solar lanterns. Awareness of the price might make respondents mentally ready to invest certain amount of their disposable income in RE products. Though product acceptance is at its nascent stage in Sikkim, there seems to be a wide scope for renewable energy. However, keeping in mind the erratic weather condition of Sikkim,

a hybrid connection of conventional and solar energy may contribute in reducing carbon emission, thereby using solar energy effectively and efficiently.

References

1. Anonymous. <https://www.fao.org/india/news/detail-events/en/c/1157760/>
2. Anonymous, Census reference tables-total population. Government of India (2011). Retrieved from <https://en.wikipedia.org/wiki/sikkim>.
3. R. Rai. N.D. Sharma, Renewable energy in Sikkim. *Int. J. Bus. Manage. Res.* **4**(6), 73–78 (2014). ISSN (Online):2249–8036, ISSN(Print):2249–6920, IC value:3.0,
4. S.H. Kulkarni, T.R. Anil, Status of rural electrification in India, energy scenario and People’s perception of renewable energy technologies. *Strat. Plan. Energy Environ.* **35**(1), 41–72 (2015)
5. H. Mobrezi, B. Khoshtinat, Investigating the factors affecting female consumers’ willingness toward green purchase based on the model of planned behavior. *Procedia Econ. Finan.* **36**, 441–447 (2016)
6. E. Rex, H. Baumann, Beyond ecolabels: what green marketing can learn from conventional marketing. *J. Clean. Prod.* **15**(6), 567–576 (2007)
7. G.J. Dalton, D.A. Lockington, T.E. Baldock, A survey of tourist operator attitudes to renewable energy supply in Queensland. Australia. *Renew. Energy* **32**(4), 567–586 (2007)
8. R.J. Blackwell, P.W. Miniard, J.F. Engel, *Consumer Behavior* (10th International ed.). (South Western-Thomson Learning, Cincinnati, OH, 2006)
9. Grover.P (2015), Analysing Market Feasibility of Residential Green Buildings in Tier-II Cities in India, *IOSR Journal of Business and Management (IOSR-JBM)*e-ISSN: 2278–487X, p-ISSN: 2319–7668. Volume 17, Issue 3.Ver. I (Mar. 2015), pp 62–69.
10. T.S. Reddy, R. Guleria, S. Sinha, S.K. Sharma, J.N. Pande, Domestic cooking fuel and lung functions in healthy non-smoking women. *Indian J. Chest Dis. Allied Sci.* **46**(2), 85–90 (2004)

Trusted and Preferred Sources of Receiving Information Related to Renewable Energy



Rachana Rai, Neeta Dhusia, and Ajeya Jha

1 Introduction

Renewable energy is defined as an energy which is naturally abundant, such as sunlight, wind, rain, tides, waves and geothermal heat. Sikkim has an autonomous agency named Sikkim Renewable Energy Development Agency (SREDA) which was constituted in 1999 by the State Government for endorsing and propagating renewable energy through various energy programmes and projects [1]. Though Sikkim is the second smallest State of India, but it has witnessed successful ventures related to renewable energy, such as Solar Power Plant at State Assembly Premises and Under Special Area Demonstration Programme (SADP). Solar water heating systems have been installed at Raj Bhawan Complex, Rongey Central Prison and biogas plant installations exist at various districts in Sikkim [2]. However, social acceptance of products of renewable energy needs more in-depth research, specially when it is related to Sikkim. Understanding peoples' needs and wants are always a challenge as taste and preferences of people keeps changing. Reasons may vary from time to time and from place to place and from situation to situation. Hence, this research is focused on understanding factors that people prefer and trust in relation to renewable energy.

R. Rai
Sikkim Central University, Gangtok, India
e-mail: rairach9@gmail.com

N. Dhusia · A. Jha (✉)
Sikkim Manipal Institute of Technology, Sikkim Manipal University, Gangtok, India
e-mail: ajeya.jha@smit.smu.edu.in

N. Dhusia
e-mail: neeta.s@smit.smu.edu.in

1.1 Literature Review

Salkin [3] stated that Government initiatives, such as Residential Renewable Tax Credit in 2005 provided up to 31% tax credit to owners for installing solar electric, small wind, solar water heating, fuel cell or geothermal heat pump generation system. Likewise, in South Africa, Renewable Energy Independent Power Producer Procurement Programme as mentioned by Lüdemann [4] that bidders had to meet minimum criteria and were also evaluated on the proposed bid price along with their objectives on economic development. Similarly, eco-taxes are levied in EU countries on electricity produced using non-renewable sources, CO₂ emissions and removal of subsidies on fossil and nuclear energy generation as stated by Haas et.al. [5]. Khare et.al. [6] mentioned that by installing solar applications in schools, malls and hospitals, Government is pursuing its use for social reasons. Lyon and Yin [7] stated that the US State Government has adopted Renewable Portfolio Standards (RPSs) to endorse generation of electricity along with ensuring its inclusion as one of the resources in the state's portfolio of electricity generation. In Sikkim, the installation of solar water heating system is done at Raj Bhawan Complex, Rongey Central prison and installation of biogas plant at various places in all districts of Sikkim [8]. Manufacturers must focus on the design of renewable energy products for ease of use and installations with minimal maintenance cost, additionally, various service centres must be operational with adequate spare parts for after sales services [9]. Thus, the role of Government and policymakers acts as a foundation for adoption of renewable energies.

How important is the trust on source on information source particularly in the case of renewable energy products and other green products? This question has invited attention of scholars across the world. Before discussing literature review in this respect it needs to be highlighted that *information search* is a critical step in purchase behaviour. Decision obviously needs to be made on the basis of perceived trustworthiness. This is true for purchase of any product. Renewable energy products are also expected to be approached in a similar manner. Kaenzig et al. [9] inferred that municipal utilities and public energy information centres appear to be by far the most trusted sources. This trustworthiness is in the context of green energy consumers. McDonald et al. [10] while comparing *sustainable consumption patterns across product sectors* also explored the trusted source of information for purchase. Momsen et al. [11] while exploring if nudges help consumers to choose renewable energy products concluded they do not all but some specific ones. Nudges, it may be emphasized, are change in information set that an individual faces when taking a decision and which can help people align intention and action. Wüstenhagen et al. [12] while investigating social acceptance of renewable energy innovation studied if the local community trust the information and the intentions of the investors and actors from outside the community? Moezzi et al. [13] concluded *that the most trusted information sources were friends, family and neighbours*. Implying that encouragement to purchase may be possible through such sources. Steg et al. [14] while exploring the factors motivating renewable energy found that *consumers information on costs and*

benefits will be particularly effective when such information is from a trusted source and offered at a time and place close to decisions. Testa et al. [15] while identifying factors that encourage/discourage energy consumers emphasized the role of trust in information as a contextual factor that influences the adoption of a pro-environmental behaviour. Wolske et al. [16] explored the role of consumer behaviour for limiting climate change and surmised that the **information** that consumers rely upon may also be influenced by the trustworthiness of the source. O'Shaughnessy et al. [17] and O'Reilly et al. [18] while ascertaining factors for bioenergy market development suggested that friends were the principal information source followed by family members. Trust on family and friends may be the driver in his study. Palm et al. [1] while studying residential solar electricity adoption established that the consumers wanted single-dimensional advice from a trusted independent source.

It may be summarized from the literature review that the trustworthiness of information source is a key factor in purchase of renewable energy product. The question that we answer through this study is that what is the hierarchy of the sources of information on trustworthiness in the context of purchase of renewable energy home products?

Methodology

Data for analysis were used from responses using structured questionnaire which included closed ended technique in order to remove respondents' error. Data collection from respondents was undertaken across 6 months. For analysis, 600 filled and complete questionnaires were selected. Friedman test was conducted as the procedure are based on mean rank of variables and it compares ranked values. Products of renewable energy undertaken for the study is solar water heater and solar lantern.

1.2 Problem Definition

Researcher desired to identify trusted sources and preferred sources of receiving information about products of renewable energy by the respondents from Sikkim. During data collection, it was observed that respondents were aware of products of renewable energy but adoption of it was questionable due to various factors. The main objective of this research is to identify various trusted and preferred sources of receiving information about renewable energy.

2 Result and Discussions

For the study, three factors were considered, namely initiative from the Government, friends' referral and advertisements on television and radio about renewable energy. Based on the data collected, these three factors were ranked accordingly as preferred sources of receiving information, which is shown in Table 1.

Table 1 Preferred sources of receiving information on products of renewable energy

Prefer to receive information about RE products	Total score	Ranking
1. Government promotional initiative	2396	1
2. Friends referral	2199	2
3. Advertisement on TV or radio	2045	3

From Table 1, researcher found that respondents preferred to receive information through Government followed by their friends’ referrals. Advertisements shown in television and aired on radio were also preferred. Hence, through this result, researcher finds the role of concerned Government on a priority basis while providing information related to products of renewable energy.

Friedman test was further conducted to verify the ranking given at Table 1.

Based on the statistics from Fig. 1, the chi-square value is 401.39 and significance level is 0.000, thereby showing that the ranking based on Table 1 matches with Friedman test ranking. Ranking based on trusted sources of information was also carried out and are identified in Table 2.

It was again found in Table 2 that respondents have trust and faith in Government promotional initiatives followed by friends’ referral and advertisements aired on television and radio. Thus, further strengthening the role that Government needs to

Fig. 1 Ranking of preference based on Friedman test

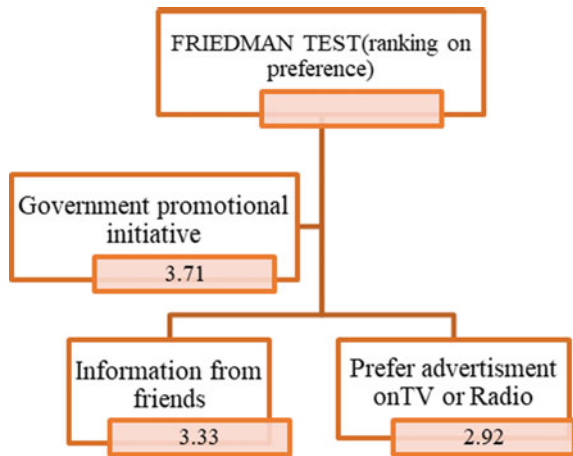
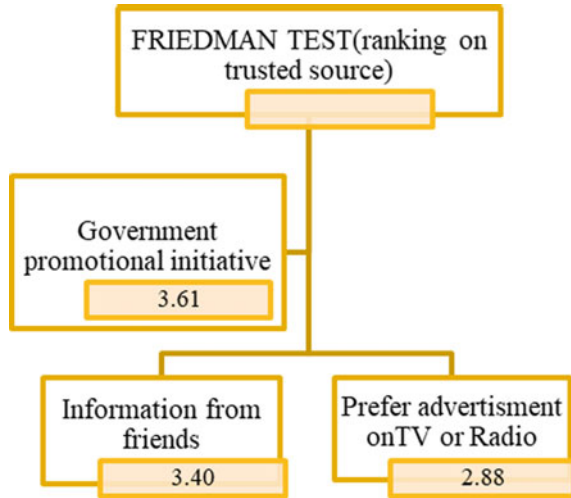


Table 2 Trusted sources of receiving information

Trust the most in order to receive information	Total score	Ranking
1. Government promotional initiative	2374	1
2. Friends referral	2231	2
3. Advertisement on television and radio	1961	3

Fig. 2 Ranking of trusted sources based on Friedman test



actively play in disseminating desired information related to products of renewable energy.

Friedman test was further conducted to verify the ranking given at Table 2.

Based on the statistics from Fig. 2, the chi-square value is 369.024 and significance level is 0.000, thereby showing that the ranking based on Table 2 matches with Friedman test ranking.

Additional correlation test was conducted based on the three factors mentioned in Tables 1 and 2 and the result revealed 0.789, 0.784 and 0.778, respectively, which are relatively high. This encouraged researcher to predict *preference* on the basis of *trust*. Thus, the regression analysis was conducted, and Table 3 depicts the result.

R (Table 3) represents simple correlation with value 0.855 and which indicates a high degree of correlation. Accordingly R² is 0.731 and which implies that this model Explains 73.1% of the variations of this relationship between preference (dependent variable) and trust (independent variable).

ANOVA test was further conducted to find whether the model is fit or not.

Table 4 indicates that the regression model predicts the dependent variable significantly as significance level is 0.000, which is less than 0.05, thus indicating that the regression model statistically predicts the outcome variable, it is a good fit for the data.

Coefficient table from Table 5 provides information to predict *preference* from *trust*. Significance value is 0.000 which is less than 0.05, thus, trust contributes

Table 3 Regression analysis on trust versus preference

Model summary		
R	R Square	Durbin-Watson
0.855	0.731	1.925

Table 4 ANOVA test: Predicting dependent variable, that is, preference

ANOVA					
model	Sum of squares	df	Mean square	F	Sig
Regression	4656.807	1	4656.80	1623.100	0.000
Residual	1715.711	598	2.869		
Total	6372.518	599			

Table 5 Coefficient table: To determine whether trust contributes to the preference of respondents

Coefficients				
model	Unstandardized coefficients		t	Sig
	B	Std. error		
(Constant) trust	4.186	0.334	12.525	0.000
	0.765	0.019	40.288	0.000

significantly to the model. The regression equation is as follows:

$$\text{Preference} = 4.186 + 0.765(\text{trust})$$

This model may or may not be generalizable but further research may determine the extent of generalizability.

- Conclusion and implications:** The study was undertaken to identify the trust-worthiness of various sources of information for purchase of renewable energy products. Results and discussion bring out the following conclusions

The following points were identified in this research:

- Preferred sources of receiving information about RE products are government initiative (2396), friends’ referral (2199) and advertisement on TV or radio (2045).
- Trusted sources of receiving information about RE products are government initiative (2374), friends’ referral (2231) and advertisement on TV or radio (1961).
- Active role of Government is required in sales promotion to attract potential customers and turn them into existing customers. Testimonies of satisfied customers on television and on radio may attract more customers.
- Policymakers and manufacturers may work with banks in order to plan attractive incentive to buyers of renewable energy.

These three factors identified in the study may be used with caution as it may differ from place to place and may change from time to time, as taste and preferences of people keeps changing.

References

1. Anonymous (2019). The Sikkim renewable energy development agency (SREDA). Retrieved from www.sreda.org
2. R. Rai, N.D. Sharma, Renewable energy in Sikkim. *Int. J. Bus. Manage. Res.* **4**(6), 73–78 (2014). ISSN (Online):2249–8036, ISSN(Print): 2249–6920, IC value: 3.0, Edition: DEC2014
3. P. Salkin, The key to unlocking the power of small scale renewable energy: local land use regulation. *J. Land Use Environ. Law* **27**, 339 (2011)
4. C. Lüdemann, Renewable energy promotion in South Africa-surrounding conditions and recent developments. *Verfassung und Recht in Übersee/Law and Politics in Africa, Asia and Latin America*, 315–323 (2012)
5. R. Haas, C. Panzer, G. Resch, M. Ragwitz, G. Reece, A. Held, A historical review of promotion strategies for electricity from renewable energy sources in EU countries. *Renew. Sustain. Energy Rev.* **15**(2), 1003–1034 (2011)
6. V. Khare, S. Nema, P. Baredar, Status of solar wind renewable energy in India. *Renew. Sustain. Energy Rev.* **27**, 1–10 (2013)
7. T.P. Lyon, H. Yin, Why do states adopt renewable portfolio standards? An empirical investigation. *Energy J.* 133–157 (2010)
8. R. Rai, N.D. Sharma, A. Jha, Identifying demographic determinants which might lead to the purchase of renewable energy products: a study based on Sikkim and Darjeeling. *Int. J. Manage. Soc. Sci. Res. Rev.* **1**(36) (2017), e-ISSN-2349-6746, ISSN-2349-6738
9. J. Kaenzig, R. Wüstenhagen, Understanding the green energy consumer. *Mark. Rev. St. Gallen* **25**(4), 12–16 (2008)
10. S. McDonald, C. Oates, M. Thyne, P. Alevizou, L.A. McMorland, Comparing sustainable consumption patterns across product sectors. *Int. J. Consum. Stud.* **33**(2), 137–145 (2009)
11. K. Momsen, T. Stoerk, From intention to action: can nudges help consumers to choose renewable energy? *Energy Policy* **74**, 376–382 (2014)
12. R. Wüstenhagen, M. Wolsink, M.J. Bürer, Social acceptance of renewable energy innovation: an introduction to the concept. *Energy Policy* **35**(5), 2683–2691 (2007)
13. M. Moezzi, A. Ingle, L. Lutzenhiser, B.O. Sigrin, *A Non-Modeling Exploration of Residential Solar Photovoltaic (PV) Adoption and Non-Adoption* (No. NREL/SR-6A20–67727). National Renewable Energy Lab. (NREL), Golden, CO (United States) (2017).
14. L. Steg, R. Shwom, T. Dietz, What drives energy consumers? engaging people in a sustainable energy transition. *IEEE Power Energ. Mag.* **16**(1), 20–28 (2018)
15. F. Testa, A. Cosic, F. Iraldo, Determining factors of curtailment and purchasing energy related behaviours. *J. Clean. Prod.* **112**, 3810–3819 (2016)
16. K.S. Wolske, P.C. Stern, Contributions of psychology to limiting climate change: opportunities through consumer behaviour, in *Psychology and Climate Change* (Academic Press, 2018), pp. 127–160
17. E.J. O’Shaughnessy, R.M. Margolis, *Solar Buyer’s Markets: Unlocking Lower Photovoltaic and Battery Prices on Online Quote Platforms* (No. NREL/TP-6A20–72172). National Renewable Energy Lab. (NREL), Golden, CO (United States) (2018)
18. P. O’Reilly, Factors for bioenergy market development. *Role Bioenergy Emerg. Bioecon. Resour. Technol. Sustain. Policy*, 320 (2018)
19. J. Palm, E. Eriksson, Residential solar electricity adoption: how households in Sweden search for and use information. *Energy Sustain. Soc.* **8**(1), 14 (2018)